2024 ISEK Virtual Congress Abstract Proceedings

International Society of
Electrophysiology and Kinesiology

CHUKYO UNIVERSITY

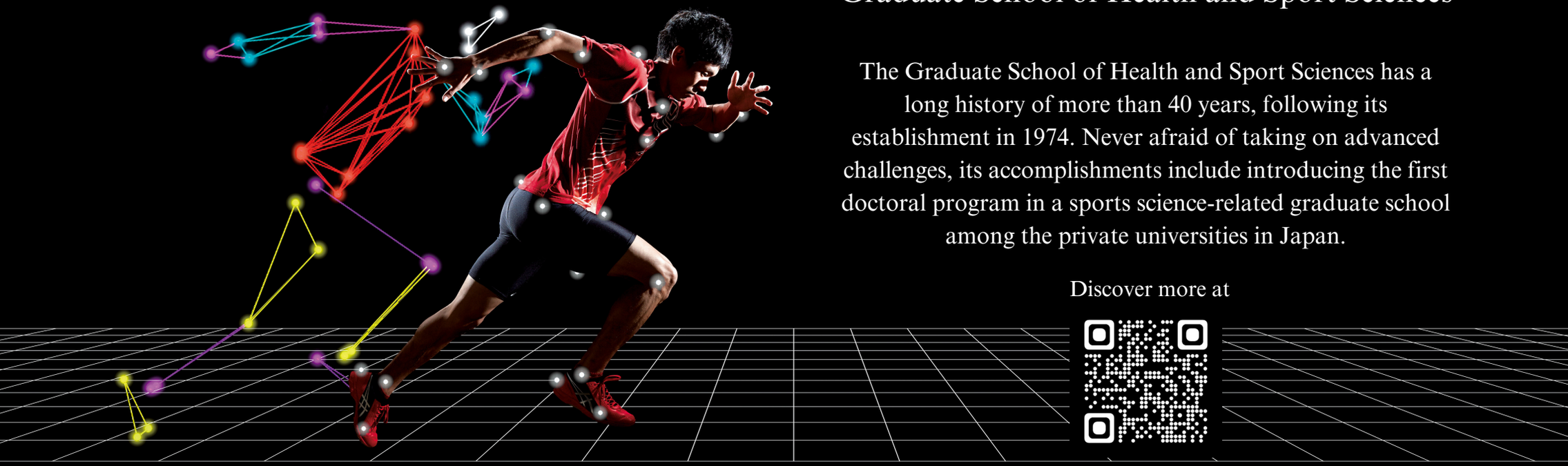

Graduate School of Health and Sport Sciences

The Graduate School of Health and Sport Sciences has a long history of more than 40 years, following its establishment in 1974. Never afraid of taking on advanced challenges, its accomplishments include introducing the first doctoral program in a sports science-related graduate school among the private universities in Japan.

Discover more at

https://sps.chukyo-u.ac.jp/graduate/

Contents

S.1: Estimating mechanical behavior of skeletal muscles using imaging and modeling modalities 3

S.2: Characterizing and targeting muscle stiffness to improve treatment and rehabilitation .. 7

S.3: Unique engineering approaches to modify neuromotor activity through human-robot intention and perception 10

S.4: Enhancing physical function in aging and hospitalized populations with neuromuscular electrical stimulation 12

S.5: enhancing physical function in aging and hospitalized populations with neuromuscular electrical stimulation 12

S.6: Motor unit analysis of surface EMG for precision rehabilitation: advances and challenges 16

S.7: Exoskeletons for health 18

S.8: International Motoneuron Society: non-invasive methods to understand human motoneuron physiology in health, disease, and training 22

S.9: From lab to living room - opportunities, challenges and potential using smart textiles and wearable solutions to facilitate self-administered home-based rehabilitation 26

S.10: Factors influencing neuromodulation of motoneurons and/or PICs: What do human studies tell us and what are the applications? 30

S.11: Neurorehabilitation pipeline for upper extremity motor paralysis after stroke: xR, non-invasive brain stimulation, and Constraint-induced movement therapy 34

S.12: Back in action: muscles, mechanics, and movement in adolescent idiopathic scoliosis 36

Oral Session 1 40

Oral Session 2 46

Oral Session 3 53

Oral Session 4 59

Oral Session 5 65

Oral Session 6 71

Oral Session 7 77

Oral Session 8 82

Oral Session 9 87

Oral Session 10 94

Oral Session 11 100

Oral Session 12 105

Oral Session 13 110

Back to Contents page

Oral Session 14 116
Oral Session 15 122
Oral Session 16 127
Oral Session 17 133
Oral Award Session 139
Poster Session 1 145
Poster Session 2 206
Poster Session 3 267

S.1: Estimating mechanical behavior of skeletal muscles using imaging and modeling modalities

S1.1: Skeletal muscle in vivo: unraveling mechanical behavior and detecting changes using ultrasound shear wave elastography

Filiz Ates, University of Stuttgart; Justus Marquetand, Department of neural dynamics and Magnetoencephalography, University of Tuebingen; Benedict Kleiser, Hertie-Institute for Clinical Brain Research, University of Tübingen, Tübingen, Germany; Manuela Zimmer, University of Stuttgart

BACKGROUND AND AIM: The mechanical behavior of muscles determines joint function and human movement. Characterizing muscle capacity and the length range of active force production in vivo is crucial for monitoring muscular changes. Ultrasound shear wave elastography (SWE), developed to assess local mechanical properties by measuring the shear wave propagation velocity within a tissue, emerges as a promising non-invasive approach in skeletal muscle mechanics [e.g. 1]. In this study, we explored the potential of SWE in detecting age-related and disease-induced muscular changes, contributing to a comprehensive understanding of muscle behavior. METHODS Biceps brachii muscle (BB) of healthy young (n=14; age: 28.1±5.1 years) [2] and older individuals (n=14;68.7±5.1 years) [3], and patients with myasthenia gravis (MG) (n=11; 47.6±15.7 years) [4] and facioscapulohumeral muscular dystrophy (FSHD) (n=8; 42.1±14.0 years) were studied during rest and isometric contractions at five elbow angles. SWE, electromyography, and joint moment were recorded simultaneously. RESULTS In the passive condition (Fig. 1A), the BB elastic modulus was significantly higher in the older and MG groups compared to the young group (e.g. up to 52.6% for the older group) [3,4]. However, there were no significant differences in the FSHD group. Substantial changes were observed in the exponential characteristics of the passive elastic modulus vs elbow angle curve due to aging and MG. In the active condition, the older (25.1%), MG (26.5%), and FSHD (15.8%) groups were slightly but significantly weaker in generating elbow moments compared to the young individuals. In comparison to the young group, the BB elastic modulus measured from the older (20.3%) and FSHD (20.4%) groups were significantly lower at 25% MVC, while the MG group was 8.9% lower at 75% MVC (Fig. 1B). CONCLUSIONS Our findings suggest that SWE is capable of detecting changes in BB muscle mechanics, holding promise for monitoring these changes in various settings, such as assessing muscles at different joint positions during rest or higher-level activities for MG, or low-level activities for aging and FSHD within community settings. While passive and active behavior of muscles deduced from SWE measurements offers insights into understanding muscular adaptation, it falls short of elucidating the underlying mechanism. To harness this information as an index of muscle force, it is imperative to develop muscle models for both healthy and diseased conditions. Additionally, the validation of these models will be a crucial step forward. These aspects will be further explored, laying the groundwork for future research in the field. REFERENCES[1] Nordez A. & Hug F. J Appl Physiol 108(5), 1389-1394, 2010[2] Zimmer M. et al., J. Mech.Behav. Biomed. Mat. 137: 105543, 2023[3] Ates F. et al., Nature Scientific Reports, 13(1): 20062, 2023[4] Zimmer M. et al., Diagnostics, 13(6), 1108, 2023ACKNOWLEDGMENTSThe BMBF - Federal Ministry of Education

and Research (3DFoot, 01EC1907B) and DFG - German Research Foundation (GRK 2198, 277536708).

S1.2: Image based model generation and optimisation for the human Achilles tendon

Alessia Furnaro, KU Leuven; Benedicte Vanwanseele, KU Leuven; Vickie Shm, University of Auckland

Background and Aim: The Achilles tendon is the largest and strongest tendon in the human body and plays a crucial role in human locomotion. Studies have shown that physical activity increases the cross-sectional area of a tendon, and this remodelling is driven by tendon cells called tenocytes. These cells are mechanosensitive in that they 'feel' the forces applied during daily activities and respond accordingly. However, the way that forces are transmitted from the body to the tenocytes is dependent on the intricate structures of tendon tissues, which modulate the force either in beneficial or detrimental ways. To truly understand Achilles tendon health in the context of degeneration and injury, it is vital to understand the tissue structure and its deformation patterns during activities of daily living. Interestingly, most Achilles tendon injuries are usually preceded by age-related degenerative changes in the tendon structure. This indicates that subtle changes in tissue microstructure from degeneration may lead to more severe tissue damage or failures. Since Achilles tendon structure is poorly understood in general, our understanding of the factors that drive age- or injury-related degenerative changes is still very limited. Methods: One intriguing feature of the Achilles tendon is that it is actuated by three muscles—the medial gastrocnemius, lateral gastrocnemius, and soleus. Bundles of tendon fascicles emanate from each of these muscles, all of these bundles fusing to form a single tendon. Although they are tightly fused, the fascicle bundles arising from these muscles are distinguishable units called subtendons. In recent years, the structure and function of these subtendons have received much attention, but this work has mainly involved tissue dissection of cadavers. Although they provided valuable insight into the tissue structure, it is still unknown how these three subtendons in the Achilles interact under physiological loading conditions and what role they play in tendon degeneration. Computational analysis can provide a solution to this problem as one can simulate how different loading conditions can affect tendon deformation patterns, hence might lead to tendon degeneration. Therefore, we have developed a robust pipeline that generates subject-specific finite element models of the Achilles tendon using 3D ultrasound images and speckle tracking and applied to both healthy and tendinopathy patients to identify the role of various rehabilitation exercises in tendon load transfer and healing. RESULTS: Our FE models show that degeneration and injury patterns are subject-specific, highlighting the need to include these factors in modelling studies. In particular, the subject-specific loading and the tendon geometry play a crucial role in load transfer and subsequent tendon healing from rehabilitation exercises. Conclusion: Our subject-specific FE models incorporating subtendon structures showed how strain is developed within the tendon during various rehabilitation exercises and which exercises are likely to induce tissue regeneration, providing insights into intricate structure/function relationships in the human Achilles tendon.

S1.3: Muscular connective tissues: do they only provide protective packaging, or are a determinant for muscle's active force production? Finite element and imaging analyses

Can Yucesoy, Bogazici University

Skeletal muscle is the motor for joint movement. It is comprised of force-producing components i.e., sarcomeres and protective packaging structures i.e., connective tissues. In terms of skeletal muscle mechanics, it is clear that the sarcomeres are responsible for active force production in a contracting muscle and the connective tissues are ascribable for the muscle's passive resistance to stretch. However, extrapolating this to a truly independent functioning of these two domains, hence implicitly making a linear system assumption in which the contributions of the sarcomeres and connective tissues to the muscle force can be superposed to establish muscle total force may be naïve. Or more directly speaking, assuming that no mechanical interaction occurs between these domains may not be comprehensive. In contrast, a unique consideration is to ascribe muscle related connective tissues a role in contractile force production in the active state. This is viable via muscle fibers' and intramuscular connective tissues' mechanical linkages along the full peripheral lengths of muscle fibers and taking into account the concept of myofascial loads. Also considering that connective tissues of different muscles are interconnected at the muscle belly (e.g., via neurovascular tracts and compartmental tissues), muscle relative position changes occurring during joint movement will stretch muscle related connective tissues leading to myofascial loads to develop. These loads acting along the length of muscle fibers can through the mentioned connectivity reach muscle fibrils and take part in the mechanical equilibrium that determines sarcomeres' lengths, which is the key determinant of sarcomere function. Therefore, a mechanical mechanism for muscle related connective tissues to indeed play a role in muscle force production in the active state is plausible. Animal experiments show unequal muscle forces measured at both ends of a muscle or changes in its muscle length-force characteristics in different experimental conditions despite the fact that identical measurements done on the target muscle. These findings do indicate that the mechanical mechanism described above must be effective. However, in animal experiments, there is no measurement done that can reveal how the forces measured at the tendons is produced. Yet, this can be done via a coupled finite element modeling, which is designed in a way to take mechanical interactions between muscle fiber and connective tissue domains into account. In addition, although it provides only a kinematic analysis, using magnetic resonance imaging (to calculate tissue strains) and diffusion tensor imaging (to determine along muscle fiber direction) techniques combined (to calculate the local length changes along muscle fibers) how this mechanical mechanism can manipulate sarcomere lengths also in human muscles, in vivo can be exemplified. The talk will describe this mechanism and show example cases illustrating effects of surgery, botulinum toxin type-A, titin's role and elastic therapeutic taping using finite element modeling and imaging.ReferencesYucesoy, CA., Exercise Sports Sci Rev 38, 128-134,2010Pamuk, U., Cankaya, OA. and Yucesoy, CA., Frontiers in Physiology 11, 789, 2020Cankaya, OA. and Yucesoy, CA., J Biomech 116, 110197, 2021Karakuzu et al., J Biomech 57, 69-78, 2017Yildiz, S., Arpak, A. and Yucesoy, CA., J Biomech 160, 111816, 2023Turkoglu, AN, Huijing, PA. andYucesoy, CA., J Biomech 47 (7), 1565-1571, 2014Yucesoy, CA., Koopman,BH.,Grootenboer,HJ. andHuijing,PA.Biomechanics and Modeling in Mechanobiology 7, 175-189, 2008

S1.4: Skeletal muscle architecture in 3D: insights from in vivo measurement with 3D ultrasonography and diffusion tensor MR imaging

Yasuo Kawakami, Waseda University

Among modalities to visualize and measure skeletal muscle architecture (fascicular/tendinous arrangements within the muscle-tendon unit), ultrasonography has often been used. Brightness-mode (B-mode) ultrasonography was first used in Japan to measure cross-sectional areas of skeletal muscles by Ikai and Fukunaga (1968) then the thickness of muscles as a measure of size (e.g., Weiss and Clark, 1985). The turning point of ultrasonography was when an ultrasonic probe was placed on the skin in a longitudinal direction of the underlying muscle, to visualize fascicular paths for the measurement of pennation angle and fascicle length (Kawakami et al 1993, 1998). There is particular advantage of ultrasonography in that it enables measurement of fascicle behavior in vivo, real-time, during movements (e.g., Kawakami et al. 2002). The disadvantage of ultrasonography however is the relatively limited scan area, and two-dimensional, planar information of fascicles and tendinous structures which in reality are three-dimensional. These drawbacks can be at least partly solved by a three-dimensional ultrasound system, in which multiple ultrasound images are reconstructed three-dimensionally (Kawakami et al 2000). But one issue with this, is that for the analysis of fascicles of interest, a plane must be cut out of the reconstructed volume of the muscle, i.e., the analysis is two dimensional. A recently emerging technique to visualize and analyze fascicle architecture along and across the whole human muscles in vivo, is the magnetic resonance diffusion tensor imaging (DTI) and tractography (Takahashi et al. 2022). This technique is based on the anisotropic diffusion of water molecules along the fascicular path, and visualizing the path in a three-dimensional space. We showed fascicle's architectural variation in three dimensions which was related with the muscle size. We also demonstrated fascicle rotation in the three-dimensional space that is associated with the passive gearing, enhancing muscle belly elongation (Takahashi et al. 2023). While there are issues and challenges to overcome with this methodology (inability to observe real-time fascicular dynamics for instance), but it has potential to substantially broaden the perspective on human muscle mechanics. In the symposium, the above findings will be reviewed to discuss insights intoskeletal muscle architecture in vivo, in three-dimensional space. References Ikai, M., Fukunaga, T. Intern. Zeitsch. f. Angew. Physiol., Einschl. Arbeitsphysiol. 26: 26-32, 1968.Weiss, L. W. and Clark, F. C. Phys. Ther. 65; 477-481, 1985.Kawakami, Y., Abe, T., Fukunaga, T. J. Appl. Physiol. 74: 2740-2744, 1993.Kawakami, Y., Ichinose, Y., Fukunaga, T. J. Appl. Physiol., 85: 398-404, 1998.Kawakami, Y., Muraoka, T., Ito, S., Kanehisa, H., Fukunaga, T. J. Physiol., 540: 635-646, 2002.Kawakami, Y., Ichinose, Y., Kubo, K., Ito, M., Fukunaga, T. J. Appl. Biomech. 16: 88-97, 2000.Takahashi, K., Shiotani, H., Evangelidis, P. E., Sado, N., Kawakami, Y. J. Anat. 241: 1324-1335, 2022.Takahashi, K., Shiotani, H., Evangelidis, P. E., Sado, N., Kawakami, Y. Med. Sci. Sports Exerc. 55: 2035-2044, 2023.

S1.5: Probing muscle and connective tissue structure in vivo with combined advanced MRI and computational modeling

Geoffrey Handsfield, University of North Carolina

BACKGROUND AND AIM: Skeletal muscle, fascia, aponeurosis, and tendon are the tissues involved in force generation and transmission. Much prior study of biomechanical force transmission focused on skeletal muscle and tendon, with conventional models frequently only giving tacit study to the aponeurosis, and fascia tissue often being absent from models altogether. Regarding fascia, it likely contributes significantly to the forces produced in the muscular system [1-3]. The inclusion of more high-fidelity connective tissue structures in computational models will benefit our understanding in the future. To undertake this challenge,

imaging and modeling techniques may be leveraged to create high-fidelity image based models of skeletal muscle, fascia, aponeurosis, and tendon. In this work, I present some of that work and the resulting models and results from this endeavor. Methods: We optimized dual-echo UTE (ultrashort echo time) MRI sequences [5,6] to image human fascia, aponeurosis, and tendon in vivo. Using a sub-millimeter resolution (0.7 x 0.7 mm2) and a slice thickness of 4mm, we resolved pixels containing deep fascia and aponeurosis, which have thicknesses on the order of 1.5-2 mm [4]. Longer echo times (TE = 2-10ms) captured skeletal muscle. Diffusion tensor imaging (DTI) was used to determine muscle fiber architecture so as to distinguish between aponeurosis and fascia. Using these protocols, we imaged the thigh and calf region of thirty adult participants on a 3T MRI scanner. Following image acquisition, segmentation was performed for deep fascia and lower limb muscles using ITK Snap software on axial images. Finite element models were developed from these image sets of a muscle-fascia system. Fiber directions were incorporated using data from DTI. RESULTS: Fascia thickness varied regionally on the muscle surface and spanned 1.5mm to 2.0mm, consistent with literature [4]. Our FE model of muscle and fascia (Fig. 1) explored the geometry and architecture of connective tissues interfacing with skeletal muscle, and we probed the mechanical contribution of fascia. In these models, we simulated the mechanical contribution of the presence of fascia, finding that models containing fascia presented greater longitudinal stresses on the tendon compared to models without. CONCLUSIONS: Using advanced MRI, we imaged fascia, aponeurosis, and tendon in humans in vivo and used these data to build computational models to explore force transmission. We demonstrate here novel non-Cartesian MRI that may be used to determine muscle and connective tissue architecture in vivo for new understanding and advanced model building. REFERENCES: Garfin et al. (1981) J Appl Physiol 51(2): 317-320.2. Maas et.al. (2010), J. Biomed. Biotechnol.5756723. Meijer et.al. (2007), J. Electromyogr.17, 698-7074. Bhansing et al. (2015), Muscle Nerve,52: 534-5395. Qian et al. (2008), Magn Reson Med.60: 135-1456. Ma et al. (2017), MR in Biomed.30: 3709.

S.2: Characterizing and targeting muscle stiffness to improve treatment and rehabilitation

S2.1: Exploring the dynamics of in vivo muscle shape change: integrating internal properties and the external environment

Nikki Kelp, University of Queensland; Taylor Dick, University of Queensland

BACKGROUND AND AIM: For centuries we have known that muscles bulge during a contraction. More recently, we have learned that 3-dimensional muscle shape changes [1] are intimately linked to muscle fibre rotations in pennate muscles [2]. These dynamic changes in architecture enable muscle fibres to undergo different length changes and velocities than the whole muscle belly (i.e., gearing), with implications for a muscles mechanical output. Yet our understanding of muscle deformations has originated from experiments on single muscles during controlled and maximally active contractions which fail to account for the complex mechanisms that underpin whole muscle behavior in vivo. The interplay between a muscle's active machinery (i.e., the contracting muscle fibres that shorten and expand radially) and

passive elements (i.e., the stiffness of the connective tissue within and surrounding a muscle) has been suggested to govern the dynamic gearing system of skeletal muscle [3]. However, in humans and animals, muscle's do not contract in isolation and thus should also be influenced by the contractile environment in which they are operating. To date, we have a limited understanding regarding how differences in internal muscle properties and the external contractile environment influence muscle shape change and gearing. Methods: We have performed a series of experiments, combining B-mode ultrasound, electromyography, and other imaging modalities, to explore the influence of internal muscle properties (muscle architecture, connective tissue stiffness, intramuscular fat) and the external contractile environment (theneuromechanical behaviour of surrounding muscles) on muscle shape change and gearing in younger and older adults. RESULTS: Our results have demonstrated that the relationship between muscle fibre rotation, shape change and fibre strain differs between synergists [4].We have also shown that stiffer muscles bulge less, muscles with greater amounts of intramuscular fat undergo less fibre rotation, and muscles with greater physiological cross-sectional area operate at higher gearing—suggesting that internal muscle properties play an important role in mediating in vivo muscle shape change and gearing, especially during high-force contractions [5]. Our most recent work has indicated that a complex interplay between passive muscle properties and spatiotemporal patterns of muscle activation likely governs in vivomuscle deformations when you experimentally manipulate a muscle's neuromechanical environment. CONCLUSIONS: Future investigations to quantify in vivo 3D muscle shape changes during dynamic tasks or in populations with increased stiffness as a result of neuromuscular disorders will yield important insights. REFERENCES Zuurbier CJ & Huijing PA (1992).J Biomech,25(9), 1017-1026.Azizi E et al. (2008).PNAS,105(5), 1745-1750.Eng, CM et al. (2018). Int Comp Biol,58(2), 207-218.Kelp, NY et al (2021).J Biomech 129, 110823.Kelp, NY et al (2023).J Appl Physiol 129, 1520-1529.

S2.2: Coupled micromechanical models and experiments reveal implications of collagen organization on passive muscle tissue properties

Ridhi Sahani, Northwestern University; Silvia Blemker, University of Virginia

BACKGROUND: Increased passive stiffness contributes to muscle dysfunction across numerous disorders. The extracellular matrix (ECM) surrounding (epimuscular) and within skeletal muscle (intramuscular) is a key contributor to passive muscle properties. Collagen fibers regulate the tensile properties of the ECM and increased collagen levels are often assumed to relate to increased passive muscle stiffness. However, previous studies show that collagen quantity and stiffness do not correlate, and such assumptions simplify the complex structure of the ECM, where unique collagen arrangements are reported across muscle groups and during diseases. We posit that variations in collagen microstructure regulate passive muscle properties and developed a novel framework combining experimental measurements of tissue microstructure and mechanical properties with finite element models to examine these structure-function relationships. Methods: The initial development, calibration, and validation of this framework focused on mdx (dystrophin null) and wildtype (WT) mouse diaphragm muscle, due to the devastating consequences of diaphragm muscle fibrosis in Duchenne muscular dystrophy. Intramuscular and epimuscular micromechanical models were developed to account for complex microstructure and predict stress within each region, and then coupled to predict bulk muscle tissue stress (Fig 1B). In vitro biaxial experiments were performed on

diaphragm muscle tissue samples to measure bulk tissue stresses in various loading states and calculate along- and cross-muscle fiber stiffness for model calibration and validation (Fig 1C). Imaging measurements were collected to determine tissue microstructure to initialize the intramuscular model geometries, and to couple the intramuscular and epimuscular model predictions (Fig 1A). RESULTS: The models suggest that collagen fibers primarily align in the cross-muscle fiber direction, with ~2x greater cross-muscle fiber alignment in mdx relative to WT models. During equibiaxial lengthening, greater cross-muscle fiber stiffness was predicted in mdx (690±30 kPa) compared to WT models (568±34 kPa), resulting in greater cross-muscle fiber stresses in mdx relative to WT ECM (Fig 1D). Additionally, the distribution of collagen fibers had a greater impact on tissue stiffness than the amount of collagen. CONCLUSIONS: These findings suggest that the orientation and distribution of collagen explains anisotropic tissue properties observed in the diaphragm muscle and discrepancies between measurements of collagen amounts and tissue stiffness. We also highlight the need to consider collagen microstructure and in vivo biaxial loads sustained by specific muscles to measure relevant stiffness values and to design and test treatments. Future applications of this framework include examining how collagen microstructure influences stiffness across skeletal muscles with distinct macroscopic architectures and during additional loading states.

S2.4: Quantification and modeling of whole muscle passive mechanics

Benjamin Binder-Markey, Drexel University

Computational musculoskeletal models are helpful in predicting muscle function. Whole muscle active length-tension properties can be accurately predicted by scaling fiber and sarcomere mechanics to the whole muscle level using the muscle's architecture. However, the passive mechanical properties in mammalian muscle do not scale linearly across muscles and size scales. Thus, traditional scaling methods used within musculoskeletal models do not accurately predict whole-muscle passive mechanics. We have used a combination of experimental mouse and human data and computational modeling to identify sources contributing to the non-linear scaling of passive mechanics. We found within our mouse studies that to model muscle passive mechanical properties accurately, the model must reflect the complexity of the muscle with surrogate parameters accounting for the intramuscular connective tissue (ICT) content variance among muscles. Furthermore, we have high-resolution data of directly measured muscle properties throughout the human gracilis muscle's anatomical range taken during a free-functioning gracilis surgical transfer. These data include isometric contractile force, passive force, passive sarcomere lengths, and muscle dimensions. As we moved the limb through its anatomical range, passive sarcomere lengths increased from an average of 3.2 μm to 3.5 μm. This equates to an increase in sarcomere length of only 13%. At the same time, measured in-situ muscle-tendon unit (MTU) length increased by 24%. Additionally, the measured active isometric forces increased and then decreased as the MTU was lengthened. Thus, the sarcomeres active operating range covered both the ascending and descending limbs of the force-length curve. Indicating sarcomere lengths operate around the optimal sarcomere length of 2.7μ, requiring significant shortening when activated from the measured passive sarcomere length. The discrepancies in passive length changes of MTU and sarcomere length and active sarcomere shortening indicate that significant intermuscular compliance is required to explain the data. However, these sarcomere dynamics are not observable when using a standard Hill muscle model in which bulk muscle is in series with bulk

tendon because of the stiff serial tendon. Only a more complex biomechanical model, in which a compliant parallel structure (likely again representing theICT) was added to the model, were the sarcomere length changes and muscle forces replicated. However, the precise structures these parallel elements in both the mouse and human models represent are the subject of ongoing investigations. These structural studies are required to define the ICT geometry and biomechanical properties and enable accurate predictions of the passive properties across muscles. With this understanding, we may be able to predict how following injury and disease changes in these ICT structures will affect muscle function.

S.3: Unique engineering approaches to modify neuromotor activity through human-robot intention and perception

S3.1: A new robotic rehabilitation paradigm: Controlling and embodying a detached robotic hand by synergistic torso muscle activity for limb function

Minoru Shinohara, Georgia Institute of Technology; Joshua Posen, Georgia Institute of Technology; Joshua Lee, Georgia Institute of Technology; Frank Hammond Iii, Georgia Institute of Technology

In neuromotor rehabilitation training, a voluntary effort to move the impaired limb may often not produce an intended functional movement. The frequent experience of such a mismatch between movement intention and production can negatively influence neural adaptation and training motivation. Mental practices such as motor imagery and action observation can intervene in the central nervous system without involving such a mismatch, but the mental tasks are not easy to perform or observe. We explored developing a new robotic rehabilitation paradigm to overcome these problems and facilitate neuromotor recovery of the upper limb impaired by stroke. The idea is to intervene in the central nervous activity without involving the upper limb muscles but activating the corresponding torso muscles that are synergistically involved in upper limb function. For example, to reach and grasp an object, stroke survivors would rotate the trunk inward and try to open the hand. To grasp and retrieve it, they would rotate the trunk backward and try to keep closing the hand. We incorporated these rotational synergies into the detached robotic hand system, in which a user activates the external oblique abdominal muscle to open the detached robotic hand and the latissimus dorsi muscle to close it, respectively. The user observes the opening and closing actions of the robotic hand and also listens to the modulated sounds associated with its movements. The repetition of the synergistic voluntary efforts and perceptual engagements can induce an embodiment of the detached robotic hand. This synergy-based human-robot interaction process may lead to the modulation of neuromotor activity and adaptations in the biological hand. We will introduce and discuss this unique robotic rehabilitation paradigm designed for stroke rehabilitation.
Supported by NIH/NINDS (1R21NS118435-01A1)

S3.2: Intention-driven strength augmentation: integration of an intelligent upper-limb exoskeleton with soft bioelectronics and deep learning

Jinwoo Lee, Dongguk University

The decline in musculoskeletal strength due to aging and stroke significantly impacts daily tasks involving the upper extremities. To address this, we present an innovative upper-limb exoskeleton system integrated with deep learning technology to anticipate human intention for strength augmentation. Incorporating soft wearable sensors, the system gathers real-time muscle activity data to interpret the user's intended movements. Cloud-based deep learning accurately predicts four upper-limb joint motions with an impressive average accuracy of 96.2% and a rapid response rate of 500–550 ms, indicating the exoskeleton's seamless operation based solely on human intent. Furthermore, a set of soft pneumatic actuators supports these intended movements, delivering a force of 897 newtons and a displacement of 87 mm at maximum capacity. Through this intention-driven approach, the exoskeleton reduces average human muscle activity by 3.7 times compared to its unassisted counterpart, offering promising implications for mitigating age and stroke-related musculoskeletal decline.

S3.3: Developing training support technology with simultaneous visual and force feedback using pneumatic gel artificial muscles

Yuichi Kurita, Hiroshima University

BACKGROUND AND AIM: Exercise is essential for all people to improve and maintain physical performance and health. Visual, auditory, and haptic feedback are being used to motivate people to engage in physical activity and exercise. It has been shown that providing feedback during a user's exercise can positively affect not only performance, but also sense of accomplishment. Self-awareness and task-orientation in exercise produce positive effects through intrinsic motivation for physical activity. Methods: We have developed a suit that provides force feedback assistance to the user's upper extremity. By attaching pneumatic gel muscles (PGMs) across the joints to the body, joint torque assistance can be provided by contraction of the PGMs. The prototype has two PGMs to assist wrist extension. A flexible LED band is also attached to the forearm, and the intensity of light emitted can be varied according to the contraction force of the PGMs. This allows force and vision to be controlled independently. We investigated how the perceived amount of force changed with the combination of greater or lesser force sensing intervention and greater or lesser visual display. The participants were seated in a chair with their upper arm relaxed on a desk, and when an extension force was applied to the wrist by the PGMs, the magnitude of the perceived force was investigated by a psychophysical experiment in which the force was reproduced against a force sensor in the same posture. RESULTS: Experimental results confirm that perceived force decreases when light intensity is less than the supporting force, and similarly, perceived force increases when light intensity is greater than the supporting force. CONCLUSIONS: We have conducted a study aimed at constructing a system that positively influences the human body and mind by independently controlling visual and force feedback. The training support technology with simultaneous visual and force feedback is expected to be used for exercise training and rehabilitation applications.

S.4: Enhancing physical function in aging and hospitalized populations with neuromuscular electrical stimulation

S4.1: Exploring the potential of sub-tetanic neuromuscular electrical stimulation for maintaining and improving physical function

Toshiaki Miyamoto, Kansai Medical University; Jun Umehara, Kansai Medical University; Satoshi Tagashira, Kansai Medical University; Takuya Fukushima, Kansai Medical University

In recent years, neuromuscular electrical stimulation (NMES) has been reported to maintain and improve physical function, including muscle strength, in various patient populations during hospitalization. However, due to the diversity in NMES settings, the optimal NMES protocol for maintaining and improving physical function remains unclear. Maffiuletti NA et al. have highlighted a lack of methodological considerations in the clinical application of NMES, emphasizing the need for establishing NMES protocols tailored to hospitalized patients based on their pathophysiological profiles. Generally, tetanic NMES, inducing strong muscle contractions, is considered as an alternative to resistance exercise, while sub-tetanic NMES is proposed as an alternative to aerobic exercise. Nevertheless, previous intervention studies have mainly focused on tetanic NMES, which might be insufficient for maintaining and improving physical function in hospitalized patients experiencing prolonged immobilization and the elderlies whose physical activity decreased. We have demonstrated that sub-tetanic NMES induces cardiorespiratory and metabolic responses comparable to walking, enhancing various systemic physiological responses. In this presentation, we report on the impact of sub-tetanic NMES on body composition, physical function, and biochemical responses, incorporating both past and recent data. Furthermore, we aim to deepen the discussion on the potential of sub-tetanic NMES for maintaining and improving physical function in hospitalized patients and the elderly.

S.5: enhancing physical function in aging and hospitalized populations with neuromuscular electrical stimulation

Symposium: Neuromechanical characterisation of muscles and their functional units using ultrasound imaging methods

S5.1: State-of-the-art and future perspectives

Robin Rohlén, Lund University / Imperial College London; Emma Lubel, Imperial College London; Christer Grönlund, Umeå University; Dario Farina, Imperial College London

Ultrasound imaging can be used to non-invasively assess muscle structure, musculoskeletal properties, and, more recently, neuromechanics in vivo. This technology can provide great spatial and temporal resolution, opening exciting avenues for investigating health, disease, and neural interfacing technology. This talk will build upon state-of-the-art ultrasound imaging technology and discuss future perspectives and translational capabilities of ultrasound imaging for the neuromechanical characterisation of muscle tissue. An ultrasound transducer on the skin parallel to the muscle fibres can be used to detect and analyse the muscle-tendon unit,

muscle thickness, pennation angle, fascicle length, aponeuroses and muscle gearing. This is usually performed using a clinical ultrasound scanner with B-mode (grayscale) imaging, making it accessible to researchers, clinicians, etc. On the other hand, these scanners operate at relatively low frame rates and do not enable access to raw data to calculate displacement fields. These displacement fields are important for identifying transient events like the subtle displacements of muscle fibres in response to the neural discharges of a single motoneuron. Thus, for these applications, a programmable ultrasound research system is used. Moreover, the ultrasound transducer is usually placed perpendicular to the fibres to increase the identification yield. The above cannot all be done simultaneously due to probe positioning. However, it would enable the study of the musculoskeletal structure and properties along with the neuromechanical properties and motoneuron spike trains. Here, I will present the advancements in 3D imaging that could be applied and how they could further enable the study of dynamic contractions. For some translational activities, these systems and probes are too bulky, leading to the incentives for the rise of wearable systems. Finally, I will discuss the feasibility of studying neuromechanics and identifying neural spike trains using a clinical system through an innovative post-processing method. Such a method would increase the accessibility of neural information since a programmable ultrasound research system is currently needed.

S5.2: Ultrafast ultrasound decomposition into individual motor unit contributions

Emma Lubel, Imperial College London; Robin Rohlén, Lund University / Imperial College London; Dario Farina, Imperial College London

When action potentials reach the muscle fibres of a motor unit, they result in a synchronised twitch of the innervated muscle fibres. This can be identified using ultrafast (high frame rate) ultrasound imaging perpendicular to the muscle fibres. The ability to detect and analyse these twitches can give insight into various neuromuscular diseases for research, diagnosis, and monitoring. Furthermore, identification of the precise times of these twitches could open avenues for neurorehabilitation and prosthesis control. Due to the high penetration depth of ultrasound, this could enable interfacing with deep muscle tissue which is currently inaccessible to alternative non-invasive techniques such as surface EMG. Recently, various methods to identify these twitches in voluntary contractions have been developed. This talk will provide a comprehensive overview of the current state of ultrafast ultrasound decomposition into individual motor unit contributions. We will discuss the evolution of these techniques and their relative merits, uses, and downfalls. First, a modified spike-triggered averaging approach will be presented. This relies on concurrent EMG recordings to provide motoneuron firing times. Using this method, motor units can be precisely located in the muscle cross-section, and their mean twitch profile can be obtained. Next, a method using spatiotemporal independent component analysis will be presented. Using this method, the same information can be derived with high repeatability. However, motoneuron firing times cannot be recovered accurately. Hence, the neural drive to the muscle cannot be estimated. Finally, convolutive blind source separation will be presented as a method for decomposing the ultrasound image series into motoneuron firing times. We show that using this method, high-accuracy motoneuron firing times can be extracted from a tissue velocity field derived from ultrafast ultrasound images. In a validation study on 10 participants, the units decomposed using ultrasound had a rate of

agreement with sEMG decomposition of 87.4 ± 10.3%. Over 50% of these motoneuron spike trains had a rate of agreement of greater than 90%. Furthermore, with ultrasound, we identified units more than 3 cm below the surface of the skin. In contrast, the mean depth of the EMG detected units was approximately 4 mm. To conclude, the proposed methodology can non-invasively interface with the outer layers of the central nervous system, innervating the muscle across its full cross-section.

S5.3: Neuromechanical characterization of muscles and their functional units – The basics of ultrafast ultrasound acquisition, processing and bio-mechanical source

Christer Gronlund, Umeå University

Ultrasound imaging is an established method to study skeletal muscle tissue. It can be used to study static and dynamic structure and function on the whole-muscle level. Recently, using ultrafast ultrasound imaging, it has been demonstrated that the rapid transient mechanics involved in the contraction of the fibres of single contracting motor units, can be detected in electro-stimulated as well as in voluntary skeletal muscle contractions. The key difference between the conventional ultrasound and ultrafast ultrasound is the images per second that can be recorded (~50 vs +1000 images per second). Thus, the ultrafast imaging has potential to study the transient mechanics involved in fibre twitch tetantic contractions. The aim of this talk is to cover the basics in ultrafast ultrasound image acquisition, image reconstruction and post-processing, required to access information of the complex deformation pattern during skeletal muscle contraction. The underlying biomechanical source of motor unit contraction will be discussed in relation to the bioelectrical source which is mediated by the excitation contraction coupling, action potential and motoneuron neural discharges. The influence of the fascia and the corresponding myofascial coupling for this task will also be discussed. Moreover, a brief description will be given on opportunities and limitations of other new methods to assess skeletal muscle contraction information on the motor unit level including e.g. magnetic resonance imaging and optical imaging techniques.

S5.4: Combining US imaging and High-Density EMG: applications, potentialities, and challenges

Alberto Botter, Politecnico di Torino - LISiN; Marco Carbonaro, Politecnico di Torino; Marco Gazzoni, Politecnico di Torino; Taian Vieira, Politecnico di Torino; Giacinto Luigi Cerone, Politecnico di Torino

Neural excitation triggers electrical and mechanical responses in the muscle, involving the depolarization and subsequent shortening of muscle fibers. These dynamic processes display distinct spatiotemporal characteristics, which can be non-invasively measured using electromyography (EMG) and ultrasound (US) imaging, respectively. EMG and US can be detected with varying spatial and temporal resolutions, influencing the informative content of the recorded data. Single-channel surface EMG is conventionally used to assess the overall degree and timing of muscle excitation. By increasing the number of detecting electrodes positioned over the muscle surface (High-Density EMG), it becomes possible to access the firing properties of individual motor units, enabling the study of how the central nervous system controls the activation of motor unit populations during force production. Similarly, standard frame rate US imaging is employed to characterize muscle anatomy and its changes throughout

a contraction. When detected with high frame rate devices, US has the potential to capture faster muscle tissue displacement allowing for the characterization of movements resulting from the excitation of single motor units. In this context, the combination of EMG and US emerges as a valuable tool, providing insights into both neural and mechanical variables and the way they interplay to generate force. The HDEMG-US integration has found applications in various areas of neuromuscular research. Standard frame rate US and HDEMG have been employed to: (i) investigate the association between common oscillations in motor unit spike trains and fascicle movements during constant force or force-varying contractions; (ii) non-invasively identify fasciculation potentials across a large muscle volume; (iii) study the electromechanical delay. More recently, the combination of HDEMG and US has been applied to the field of motor unit decomposition. Motor unit spike trains extracted from HDEMG were used to either enhance or validate innovative decomposition methods based on the processing of high frame rate US sequences. Additionally, quantifying architectural changes in the contracting muscle with US can enhance the tracking of motor unit action potentials during dynamic or force-varying isometric conditions. After providing an overview of these applications, this talk will focus on the technological challenges associated with the simultaneous detection of HDEMG and US from the same muscle region, with a specific emphasis on electrode technology. Possible technological solutions for the joint detection of high-quality HDEMG signals and US images will be presented, along with their advantages and disadvantages and their usability in various experimental contexts, including recordings from muscles with different sizes and architectures, during different motor tasks, and with various US techniques (e.g., 2D vs 3D imaging or panoramic US).

S5.5: Skeletal muscle ultrasound and the never-ending search for a link to function: beyond just static imaging

Martino Franchi, University of Padova; Marco Carbonaro, Politecnico di Torino; Alberto Botter, Politecnico di Torino - LISiN; Clarissa Brusco, Department of Biomedical Sciences, University of Padova

Martino V. Franchi 1, Marco Carbonaro 2, Alberto Botter 2, Clarissa M. Brusco 11Human Neuromuscular Lab, Department of Biomedical Sciences, University of Padua, Italy2LISiN, Dipartimento di Elettronica e Telecomunicazioni, Politecnico di Torino, Turin, Italy

Skeletal muscle is the largest adipose tissue-free mass in humans, crucial for locomotion and metabolic health. It's not surprising that muscle mass assessment holds importance in performance and clinical scenarios, from potential injury risks identification to the clinical diagnosis of sarcopenia or frailty. In this context, ultrasound represents an easily accessible option for examining skeletal muscle mass and its structure in-vivo. Two-dimensional ultrasound B-mode technique represents the most frequently applied technique to quantify skeletal muscle mass and evaluate architectural features to relate these parameters to muscle function in healthy, ageing, and clinical populations. The assessment of such properties is seen as fundamental to elucidate the mechanisms of how the muscle-tendon unit (MTU) functions as a whole system. In the last 15 years image quality has significantly improved and more refined methodologies, such as Extended Field of View (EFOV) and 3-D ultrasound, have been developed and implemented for the study of muscle architectural properties with the muscle relaxed or during contraction. Yet the link between MTU structure and function is still to

decipher, as well as how adaptations to increased loading (exercise) or unloading (muscle disuse, physical inactivity) impact on this structure-to-function relationship. The present talk will delineate the journey from old and novel static imaging possibilities to the use of ultrasound in dynamic scenariosemployed to characterize MTU behavior throughout muscle contraction, linking these structural properties to muscle force production and its efficiency. The concept of architectural changes during contraction (MTU gearing) in different context will be explained and unpublished data related to ageing populations will be presented. Moreover, the talk will present the current implementations on semi-automatic and automatic (deep learning based) approaches to measure MTU properties, discussing the pros and cons of such cutting-edge methodologies. Lastly, the main fields of application and the current challenges of MTU ultrasound assessment will be critically discussed, paving the way for the subsequent talk of Prof Botter, related to the integration of ultrasound-derived properties and motor unit features assessed by high-density electromyography.

S.6: Motor unit analysis of surface EMG for precision rehabilitation: advances and challenges

S6.1: Neuro-musculoskeletal modeling for online estimation of continuous wrist movements from motor unit activities

Xu Zhang, University of Science and Technology of China; Yunfei Liu, University of Science and Technology of China; Haowen Zhao, University of Science and Technology of China

Decoding movement intentions from motor unit (MU) activities remains an ongoing challenge. The cutting-edge data-driven approaches mainly employ a "black box" for mapping MU activities into body movements nonlinearly, thus constraining our comprehension of the intricate transition mechanism from microscopic neural commands to macroscopic movements. In contrast, model-based approaches can offer a series of explicit relationships to simulate this transition process, providing a foundation for strong physiological interpretability. However, several issues persist in the application of model-based approaches for resolving MU activities, e.g., incomplete utilization and inaccurate characterization of microscopic neural commands represented by the MU activities. This study presents an innovative neuro-musculoskeletal (NMS) model driven by MU activities for online estimation of continuous wrist movements. The proposed model employs a physiological and comprehensive utilization of MU firings and waveforms, thus facilitating the localization of MUs to muscle-tendon units (MTU) as well as the computation of MU-specific neural excitations. Subsequently, the MU-specific neural excitations were integrated to form the MTU-specific neural excitations, which were then inputted into a musculoskeletal model to accomplish the joint angle estimation. A global optimization algorithm was subsequently applied to obtain the model parameters that are challenging to measure in vivo. To assess the effectiveness of this model, high-density surface electromyogram and angular data were collected from the forearms of eight subjects during their performance of wrist flexion-extension task. Two pieces of 8 × 8 electrode arrays and a motion capture system were employed for data acquisition. Following offline model calibration, online angle estimation results demonstrated a significant superiority of the proposed model over two state-of-the-art NMS models (p < 0.05), yielding the lowest normalized root mean

square error (0.10 ± 0.02) and the highest determination coefficient (0.87 ± 0.06). This study provides a novel idea for the decoding of joint movements from individual MU activities. The results hold the potential to advance the development of NMS models towards the control of multiple degrees of freedom, with promising applications in the fields of motor control, biomechanics, and neuro-rehabilitation engineering.

S6.2: Muscle innervation zone estimation with surface EMG: a simulated comparison study using motor unit and overall muscle activities

Chengjun Huang, University of Health and Rehabilitation Sciences; Maoqi Chen, University of Health and Rehabilitation Sciences; Ping Zhou, University of Health and Rehabilitation Sciences

Background and Aim. Muscle innervation zones (IZs) are the site where the muscle fibers are innervated by the terminals of motor axons. Accurate estimation of muscle IZ location has important research and diagnostic value. The objective of this study was to investigate the performance of two different approaches to muscle IZ estimation using surface electrode array electromyography (EMG), based on motor unit and overall muscle activities, respectively. Methods. The study was performed by implementing a model simulating surface EMG signals. Three IZ distributions were simulated. Specifically, the first situation simulates the IZ distribution as a V-shape. The second situation simulates the IZ distribution as inclined lines with respect to muscle fiber direction. The third situation simulates that a muscle has two IZs. For each situation, electrode array surface EMG signals were simulated 10 times. Two approaches were applied and evaluated to estimate muscle IZs. The first approach was based on conventional interference surface EMG analyses. For the second approach, the simulated signals were decomposed by the progressive FastICA peel-off (PFP) method to extract multiple motor unit action potential (MUAP) trains. We then estimated individual motor unit IZ from its MUAP spatial distribution, and collectively estimated muscle IZ distribution from all extracted motor units. Results. For all the three situations, the IZ distribution estimated from decomposed motor unit activities was more consistent to the model input, compared with that derived from the interference surface EMG analysis. Conclusions. Advances in high-density surface EMG decomposition provide a useful approach to precise estimation of muscle IZ from collective individual motor unit activities, which has important value for neuromuscular investigation and clinical practice (e.g. guiding botulinum toxin injection for spasticity treatment).

S6.3: High-density surface EMG guided personalized botulinum neurotoxin injection in treating muscle spasticity

Yingchun Zhang, University of Houston

BACKGROUND AND AIM: Spasticity is commonly seen in about 1/3 of post-stroke survivors. It interacts with and amplifies other impairments, resulting in disabling consequences. Thus it imposes significant adverse impacts on patients, caregivers and society. As the first-line treatment for focal spasticity management, intramuscular botulinum neurotoxin (BoNT) injection has been proven as a relatively safe procedure; yet dose-dependent adverse effects may occur during treatment, such as excessive muscle weakness, atrophy, pain and spread blockage of off-target muscles and autonomic nerves. BoNT is a powerful inhibitor of synaptic transmission acting at neuromuscular junctions (NMJ), indicated by innervation zones (IZ). Therefore, BoNT injections directed to the proximity of NMJs can retain or even potentiate the

treatment efficacy, while simultaneously minimizing dosage-dependent adverse effects. Studies have demonstrated that increasing the injection distance by 1 cm from the IZ reduces the efficacy of BoNT by 46%. Unfortunately, current IZ localization technique is based on anatomical landmarks established in healthy muscles or cadavers. It is important to note that IZ locations in spastic muscles of stroke survivors are dramatically different from those from cadaver or healthy muscles. IZs are visually identified from EMG signals collected over the skin surface using evenly spaced linear sensor arrays or 2-dimensional grids. The application of these IZ localization methods at the skin level is intrinsically limited by their low spatial resolution and sensitivity to anatomic variations in patients, largely because the poor conducting subcutaneous fat tissues impose an electric blurring/distorting effect on the surface potential distribution. However, none of previous surface EMG techniques can tackle this electric blurring/distorting issue for an accurate IZ imaging. Methods: To bridge this technical gap, a 3-dimensional (3D) innervation zone imaging (3DIZI) technique has recently been developed by our group to image the 3D distributions of IZs in muscles from high-density surface EMG recordings. The developed 3DIZI technique has been utilized to guide BoNT injection in treating muscle spasticity in post-stroke survivors. RESULTS: Our pilot results achieved in both healthy and spastic muscle studies, and clinical trial studies have consistently demonstrated the superior IZ imaging accuracy and robustness of the 3DIZI, and its promising use in optimizing the therapeutic outcome of clinical BoNT injection. Patients (n=6) with muscle spasticity who received IZ imaging guided BoNT injections experienced superior therapeutic outcome compared to patients (n=6) who received standard ultrasound guided injections (non IZ imaging guided), evidenced by a larger and more stabilized reduction in supramaximal compound muscle action potentials (34.71±5.42% vs. 20.92±6.73%, p<0.01) and muscle activation volume (71.51±8.20% vs. 44.33±21.81%, p<0.05). CONCLUSIONS: Results demonstrated the feasibility of developing a personalized BoNT injection technique for the optimization of clinical treatment for post-stroke spasticity using the 3DIZI technique.

S.7: Exoskeletons for health

S7.1: Exoskeletons for more or better physical activity?

Pascal Madeleine, Aalborg University; Cristina-Ioana Pirscoveanu, Aalborg University; Lasse S Jacobsen, Aalborg University

BACKGROUND AND AIM: Exoskeletons can make activities of daily living easier. That goes for people with movement disorders, older adults, and asymptomatic workers (1,2). Exoskeletons are wearable mechanical structures divided in two categories: active and passive exoskeletons depending on whether these are motorized or not. Still the impact of exoskeletons on activities of daily living are just poorly understood (1,3). The aim of this abstract is to review the known physiological and biomechanical effects of using exoskeletons in both able-bodied and impaired adults. Methods: The electronic search was performed on PubMed-MEDLINE and Scopus. The search terms were combined and resulted in the following string: "exoskeleton" AND "biomechanics" AND "physiology". Additional searches were made based on the cited references of the retrieved papers. All abstracts were scrutinized, and the main findings were extracted. The studies assessed both physiological (e.g., oxygen consumption and surface electromyography) and biomechanical responses (e.g., kinetic and kinematics). RESULTS:

Ninety-one and 594 studies were retrieved in PubMed-MEDLINE and Scopus, respectively. Active exoskeletons have so far almost essentially been used in laboratory settings while passive exoskeletons have been used in both laboratory and field settings. There is evidence showing that exoskeletons can for instance reduce the energy cost of walking in both able-bodied and impaired adults, improve gait pattern of elderly adults and people with cerebral palsy, and diminish the biomechanical load of workers, i.e., decreasing the level of activation of low-back and neck-shoulder muscles. Most of these studies show that exoskeletons can augment physical performance while doing activities of daily living. CONCLUSIONS: Still the present studies do not access the long-term effects of using exoskeletons and fail to demonstrate and explain how and why some people adopt such devices. This underlines the current gaps in scientific literature concerning the use of active and passive exoskeletons and their long-term impact on activities of daily living. The presentation will open the invited symposium “Exoskeletons for Health” and will be followed by presentations from Ph.D. student C.I. Pirscoveanu, Professor D. Srinivasan, and Dr K Desbrosses. Poggensee and Collins. Sci Robot6: eabf1078, 2021Theurel and Desbrosses. IISE Trans Occup Ergon Hum Factors 7: 1–21.Nussbaum et al. IISE Trans Occup Ergon Hum Factors 3-4: 153–162.

S7.2: The effect of wearing a hip assistive exoskeleton on walking characteristics during dual-tasking

Cristina-Ioana Pirscoveanu, Aalborg University; Ernst Albin Hansen, University College Absalon; Jesper Franch, Aalborg University; Pascal Madeleine, Aalborg University

INTRODUCTION: Daily activities frequently entail undertaking multiple tasks related to mobility, cognition or decision-making which becomes increasingly difficult with age (1,2). Conventional walking aids can improve walking performance in the dual-tasking paradigms (3). Exoskeletons are a new assistive technology for the senior population (4), but the interplay between age, exoskeletons, and dual-tasking on walking characteristics remains unknown. Methods: Twenty-two senior adults (SA) (19 females and 3 males, 72.5±4.4 years, 1.67±0.07 m and 74.2±14.2 kg) and twenty-six young adults (YA) (9 females and 17males, 26.4±3.2 years, 1.78±0.12 m and 80.7±18.7 kg) walked at their preferred speed with an exoskeleton (Exo), without (noExo), and with placebo (Sham) during two types of walking: normal walking (NW) and dual-tasking (DT). During DT, participants had to do sequential subtractions of 7 from a randomly generated start number between 490 and 499. The exoskeleton used was a bilateral hip assistive exoskeleton (aLQ, IMASEN Electrical Ltd., Aichi, Japan). The gait pattern was recorded using mocap and force plates sampled at 1000 Hz. The recordings were made in a randomized and balanced order and repeated five times. Speed, cadence, double support time (DST), step length, and three-dimensional (X – flex/extension, Y- abd/adduction, Z- int/external rotation) hip range of motion (ROM) were extracted to characterize the gait pattern. Three-way MANOVA with age (SA vs YA), device (Exo vs noEXO vs Sham), and condition (NW vs DT) were conducted (p <.05, inferred significance). RESULTS: There was a main effect of condition for cadence (F1,275=11.4, p<.01), DST (F1,275=7.9, p<.01), and speed (F1,275=9.6, p<.01). There was a main effect of age for step length (F1,275=140.9, p<.01), speed (F1,275=39.9, p<.01), DST (F1,275=21.5, p<.01), ROMx (F1,275=5.5, p=.02), and ROMz (F1,275=6.6, p=.01). There was a main effect of the device only for ROMz (F1,275=3.1, p=.02). Lower cadence was seen during DT vs NW for SA during noExo (p=.02). Increased DST was seen for SA vs. YG during DT for all devices (p<.05). Shorter step lengths occurred for SA vs YA during both conditions (NW and

DT) and using all devices (Exo, noExo, Sham) (p<.01). Decreased speed was found for SA vs YA during DT (p<.01) and NW (p<.03) for all devices. Larger ROMz was found for SA for DT vs NW with Sham (p=.02). CONCLUSION: The present findings confirmed an age-related difference in gait patterns through decreased speed, shorter step length and increased DST in SA. Dual tasking and the exoskeleton did not influence the gait pattern of YG. However, the SA seemed more challenged by the DT, exemplified by decreased walking speed and increased DST. Wearing the exoskeleton mitigated the decline in gait patterns during DT of SA suggesting that this passive assistive hip exoskeleton could be used in more challenging activities of daily living. However, further research is needed to confirm this.(1). Brustio et al. PloS one 12(7): e0181698, 2017(2). Tramontano et al. Eur J Phys Rehabil Med 53(1): 7-13, 2017(3). Miyasike-daSilva et al. Gait & posture 37(2): 287-289, 2013(4). Chen et al. J Orthop Translat20: 4-13, 2020

S7.3: Muscle activities and kinematics during a shoulder flexion with the use of a physical assistance

Kévin Desbrosses, French National Institute of Occupational Health and Safety (INRS); Mathilde Schwartz, Working Life Department, National Institute of Occupational Health and Safety (INRS); Jean Theurel, Working Life Department, National Institute of Occupational Health and Safety (INRS)

BACKGROUND AND AIM: Manual handling tasks at work can induce mechanical strain and fatigue at the shoulder level and subsequently the development of musculoskeletal disorders. Upper-limb occupational exoskeletons could assist the workers in these tasks by reducing the activity of the main muscles involved in the shoulder flexion. Nevertheless, the majority of the shoulder tendinopathies, and more particularly subacromial impingement syndrome (SIS), depends on the muscle coordination and the kinematics of the joints composing the shoulder complex, and not just on an elevated activity of the shoulder flexor muscles. It therefore appears essential to ensure that the use of a physical assistive device, by reducing the activity of agonist muscles, does not lead to unexpected consequences on the functional behavior of the shoulder. Thus, the aim of the present study was to assess muscle activities and joint kinematics of the shoulder during an upper-limb elevation realized with and without a physical assistance. Methods: Twenty-five participants performed shoulder flexions from 0 to 100° of arm elevation without (FREE) and with a physical assistance of 50% (A50) and 90% (A90) of the required torque by the task (50% of the maximal voluntary torque). A homemade device provided the assistance. Movement speed was set to 15°/s using an isokinetic ergometer. The EMG activity of the anterior deltoid, posterior deltoid, medial deltoid, upper trapezoid, latissimus dorsi and triceps brachiimuscles was recorded. Kinematics of the shoulder was evaluated using an optoelectronic motion capture system and the subacromial space was measured using ultrasound imagery. RESULTS: EMG activity of anterior and medial deltoid muscles was reduced for A50 and A90 compared to FREE over the whole flexion (p<0.05). EMG activity of posterior deltoid and latissimus dorsi muscles was increased for A50 and A90 from 10 to 40° of flexion (p<0.05). The scapulohumeral rhythm was modified from 10 to 30° of flexion for A50 and from 10 to 60° for A90 (p<0.05). The subacromial space was larger for A50 and A90 as compared to FREE, respectively from 10 to 50° and from 10 to 70° of flexion (p<0.05). A tendency (p=0.08) was observed for a shorter subacromial space for A50 as compared to FREE for 90° of flexion. CONCLUSIONS: Our results shown a decrease in the EMG

activity of agonist muscles with the physical assistance, confirming the potential usefulness of exoskeletons. However, the increased EMG activity of antagonist muscles demonstrated a larger co-activation. These adaptations in muscles activity with the assistance could modify the kinematics of the shoulder as indicated by the evolution of the scapulohumeral rhythm. This could be problematic, especially for this joint that requires stability to avoid a SIS. Nevertheless, the subacromial space increased with the assistance for a large part of the movement, suggesting a lower risk for a SIS. Therefore, from 10 to 90° of shoulder flexion, the use of a physical assistance could limit the muscle stress and the mechanical strain at the origin of tendinopathies. For higher arm elevations (more than 90°), the subacromial space could decrease with the assistance. Future studies appear necessary to confirm these results.

S7.4: A comparative evaluation of passive vs. powered back-support exoskeletons for assisting load carriage

Divya Srinivasan, Clemson University; Rahul Narasimhan, Clemson University; Ananya Rao, Clemson University; Jangho Park, Clemson University

BACKGROUND AND AIM: The introduction of back-support exoskeletons (BSEs) is expected to reduce the risk of overexertion injuries to the back that are common in physically demanding tasks, such as lifting and load carriage. However, BSEs can be of several types, such as passive spring-based rigid devices, soft elastic exosuits, and even powered exoskeletons. These devices have significantly different design features, support torque profiles, and interfaces with the body, hence potentially affecting a user's movement kinematics and muscle coordination strategies quite differently. The aim of this study was to characterize the biomechanical effects of a variety of BSE designs during lifting and load carriage. Methods: Twenty-four healthy males and females, with no recent history of musculoskeletal disorders, were recruited from the local community. Participants performed a set of symmetric and asymmetric lifting and load carriage tasks in a control (no-exoskeleton condition) and using four different types of BSEs. Each BSE was set to provide a user-preferred level of assistance. Load levels and locations of load were manipulated, to realistically simulate industrially relevant tasks. Torso, hip, and knee kinematics, and muscle activity of the bilateral trunk flexors and extensors, were monitored during all tasks. Median and peak angles (from kinematic data), and median and peak amplitudes from the muscle activity data, were summarized and compared across experimental conditions. RESULTS: Preliminary results indicate that passive BSEs were associated with small but statistically significant reduction in trunk flexion angles, while no significant difference in trunk flexion angle was observed when using the powered exoskeleton, as compared to the control condition. All devices led to statistically significant reductions in trunk extensor muscle activity, as expected, however there were significant interactions between device type and task type, indicating that some devices were more effective in the asymmetric conditions than others. CONCLUSIONS: Several trade-offs between device type and task type were observed in our preliminary results, indicating that while there are many viable designs for BSEs, the optimal device choice may be best justified by the specific task characteristics, in order to maximally benefit from exoskeletons.

S.8: International Motoneuron Society: non-invasive methods to understand human motoneuron physiology in health, disease, and training

S8.1: Fatigue matters – force regulation and motor unit firing behavior in fatiguing contractions post stroke

Allison Hyngstrom, Marquette University; Zachary Kroll, Marquette University; Brian Schmit, Marquette University; Francesco Negro, Universita' degli Studi di Brescia; Matthew Durand, Medical College of Wisconsin

BACKGROUND AND AIM: Impaired firing behavior of motor units may limit motor performance during fatiguing contractions in people with chronic stroke. This study quantified stroke-related changes in estimations of common synaptic drive (CSD) and average discharge rates of motor units identified from high-density surface electromyography (HD-sEMG). Methods: In 11 chronic stroke survivors (5 female, average age= 58±10 yrs) and 10 people without stroke (4 female, average age=62±18 yrs), HD-sEMG measurements from the vastus lateralis were made during a sub-maximal, isometric fatiguing contraction on the paretic and the dominant legs, respectfully. HD-sEMG signals were decomposed using a multichannel convolutive blind source separation algorithm (Negro et al, 2016) to identify motor units and subsequently quantify discharge rates. The instantaneous motor unit discharge rates for each participant during the first and last 10% of the contraction were smoothed (Hann window 400ms, high-pass filter 0.75 Hz) and averaged together. A principal component analysis was performed and the coefficient of variation of the first common component (CV_FCC) was calculated to provide an estimate of the fluctuations in CSD to the motor neuron pool. The coefficient of variation of torque (CV_T) was calculated to quantify the relative magnitude of force fluctuations. RESULTS: On average, task duration was shorter for the paretic leg compared to the control (288±117s vs. 342±217s) and there was a larger relative decrease in discharge rates in the stroke versus control group (18.0±8%, vs. 5.9±19%). This was accompanied by the CV_FCC and CV_DR tending to be higher for the paretic leg versus control at the beginning and the end of the contraction. There was also a larger relative increase in the paretic CV_T versus control (205±150%, vs. 128±67%). For both the stroke and control group there was a positive correlation between the change in discharge rate and task duration (stroke r2=0.44, control r2=0.54). CONCLUSIONS: Greater declines in discharge rates and increased discharge rate variability may contribute to increased paretic muscle neuromuscular fatigability and impaired sub-maximal force regulation as compared to people without stroke.

S8.2: Sex matters – biological sex and hormonal effects on estimating motoneuron properties in humans

Sophie Jenz, Northwestern University; James Beauchamp, Carnegie Mellon University; Alex Benedetto, Northwestern University; Melissa Fajardo, Northwestern University; Colin Franz, Northwestern University; Tea Lulic-Kuryllo, University of Brescia; Francesco Negro, Universita' degli Studi di Brescia; CJ Heckman, Northwestern University; Greg Pearcey, Memorial University of Newfoundland

BACKGROUND AND AIM: Females have historically been excluded from research studies, due to the challenge of accounting for hormone fluctuations during the menstrual cycle in humans and the estrous cycle in other animals. Paradoxically, this is exactly why females should be studied. Their fluctuating hormones offer a fascinating model to better understand the roles and effects of these molecules in various areas of the nervous system, such as the neural control of movement. During this talk we will discuss several of our lab's studies using HDsEMG to identify mechanisms behind sex-related differences in human motor unit discharge. Sex-related differences motor unit discharge properties have been revealed in recent years, but the underlying mechanisms are unknown. A plausible mechanism that contributes to these differences is the magnitude of persistent inward currents (PICs). Methods: Using the paired motor unit technique to quantify the discharge rate hysteresis of motor units, we've shown that estimates of PICs in human lower limbs are higher in females than males. This suggests differences in monoaminergic signaling and/or local inhibitory circuits contribute to sex-related differences in discharge patterns. PICs are facilitated by monoaminergic signaling of serotonin and norepinephrine to spinal motoneurons and constrained by local inhibitory circuits. In reduced preparations, monoaminergic signaling is affected by female sex hormones in several areas of the nervous system. Our ongoing work investigates the motor unit discharge of eumenorrheic females across the menstrual cycle in comparison to females taking oral contraception, who subsequently have attenuated levels of endogenous sex hormones. RESULTS: Preliminary data suggest that estimates of PICs are reduced when levels of estradiol are high and progesterone are low (prior to ovulation in eumenorrheic females), suggesting elevated estradiol may influence the serotonin or noradrenergic signaling to spinal motor neurons. CONCLUSIONS: These novel findings help complete our understanding of motor physiology – one that includes all humans. They also emphasize the need to incorporate sex as a biological variable in neuromuscular studies. The overall goal of this talk is to shed light on the complex interplay between sex differences, endocrine function, and motor unit discharge patterns, of which our understanding just beginning to evolve.

S8.3: Behavioural context matters – motor unit discharge behavior during isolated and synergistic finger movements

Helio Cabral, Università degli Studi di Brescia; Caterina Cosentino, Università degli Studi di Brescia; Andrea Rizzardi, Università degli Studi di Brescia; Claudio Orizio, University of Brescia; Francesco Negro, Università degli Studi di Brescia

BACKGROUND AND AIM: The movement of the fingers requires a highly coordinated interplay between the hand extrinsic and intrinsic muscles, demanding complex control by the central nervous system. While the fingers do not flex in complete isolation, the opposable thumb exhibits a high level of individuation and control. This observation implies potential differences in neural control between the flexion of fingers (fingers flexion task), the flexion of the thumb (thumb flexion task) and the synergistic flexion of fingers and thumb (grasp task). In this study, we decomposed high-density surface electromyography (HDsEMG) signals from the hand extrinsic flexor muscles to investigate the control of motor units during these tasks. Methods: HDsEMG signals were recorded from the extrinsic flexor muscles in 17 healthy subjects, while they performed three tasks: fingers flexion task (simultaneous flexion of the four fingers); thumb flexion task (isolated flexion of the thumb); and grasp task (synergistic flexion of the four fingers and the thumb). Tasks were performed at 5% of maximal voluntary isometric contraction.

HDsEMG signals were decomposed into motor unit spike trains using a convolutive blind-source separation algorithm [1]. Motor units were tracked separately between fingers flexion and grasp tasks, and between thumb flexion and grasp tasks. Mean discharge rate of motor units and motor unit coherence within delta (1-5 Hz), alpha (5-15 Hz) and beta (15-35 Hz) bands were calculated. Linear mixed models were used to statistically compare these values between tasks. RESULTS: Results revealed significant changes in both motor unit mean discharge rate and motor unit coherence between fingers flexion, thumb flexion and grasp tasks. The grasp task showed a reduction of 0.7 ± 0.2 pps (mean ± standard error) in motor unit mean discharge rate compared to fingers flexion (P = 0.003), but an increase of 1.7 ± 0.4 pps compared to thumb flexion (P < 0.001). Due to the number of matched motor units, coherence analysis was performed only between fingers flexion and grasp tasks, revealing a significant decrease of 0.1 ± 0.03 in average z-coherence within the alpha band (P = 0.006), but not in delta or beta bands (P > 0.06 for both). CONCLUSIONS: Our findings indicate distinct neural control patterns between fingers flexion, thumb flexion and grasp contractions. Results suggest task-specific alterations in mean discharge rate of hand extrinsic flexors, with a decrease was observed between fingers flexion and grasp tasks and the opposite between thumb flexion and grasps tasks. Moreover, our study demonstrates a reduction in physiological tremor oscillations when comparing fingers flexion with synergistic grasp task. REFERENCES: [1] Negro et al., 2016.

S8.4: Training status matters – chronic training-induced plasticity of the human cortico-motoneuronal pathway

Duane Button, Memorial University of Newfoundland

BACKGROUND AND AIM: The corticospinal tract is an important pathway through which motor signals travel from the brain to the spinal cord in order to transmit voluntary motor commands to skeletal muscle. This pathway activates the motoneurones within the spinal cord and, in turn, the skeletal muscle. One way to increase the activation of this pathway is resistance training. During the acute (8-12 weeks) phase of resistance training, adaptions within the nervous system are the primary driver(s) for strength gains. In the longer term, or chronic resistance training, muscle adaptations are the primary driver(s) of strength gain. Because the acute phase of resistance training is of short duration and induces nervous system adaptation, the effects of acute resistance training on the nervous system dominates the literature. However, due to challenges involved in collecting data over long periods of time, the effect of chronic resistance training on the nervous system is rudimentary. Thus, the aim of this work was to determine the effect of chronic resistance training of thecortico-motoneuronal pathway. Methods: There were several methods employed to illustratechronic training-induced plasticity of the human cortico-motoneuronal pathway. Motor evoked potentials (MEP) arising from transcranial magnetic stimulation (TMS), cervicomedullary motor evoked potentials (CMEP) elicited via transmastoid electrical stimulation (TMES) and maximal muscle compound action potentials (Mmax) elicited by Erb's point electrical stimulation were used to assess supraspinal, spinal and muscle excitability, respectively. Paired-pulse TMS experiments were also employed to further examine changes in 'supraspinal' excitability. More specifically, paired-pulse stimulation was used to determine changes in motor cortex neurons and inhibitory networks via short-interval intracortical inhibition (SICI). RESULTS: Chronic resistance training alters thecortico-motoneuronal pathway of the biceps brachii. MEP and CMEP amplitudes and SICI of the biceps brachii were different between non-resistance trained and chronically trained groups indicating

nervous system changes both supraspinally (i.e. cortical neurons) and spinally (i.e. motoneurones). MEP and CMEP amplitudes of the biceps brachii were altered at higher contraction intensities (>50% of maximum voluntary contraction). It was argued that changes in MEP and CMEP amplitudes were due to altered motoneurone excitability. Furthermore, active motor threshold (i.e TMS intensity required to induce a MEP) and SICI of the biceps brachii were reduced during 25 and 40% MVC of the elbow flexors in the chronic-resistance trained individuals. CONCLUSIONS: There are few studies detailing the effects of chronic-resistance training on the cortico-motoneuronal pathway. Plasticity along thecortico-motoneuronal pathway to the biceps brachii has been shown tooccur supraspinally and spinally. This plasticity most likely includes changes in the intra-cortical circuitry leading to facilitation (i.e. reduced inhibition) of the upper motoneurons and greater firing frequencies of the motor units.

S8.5: Intensity matters – training and ageing-induced adaptations in the discharge behaviour of human motor unit populations

Jakob Škarabot, Loughborough University; Christopher D Connelly, Loughborough University; Haydn Thomason, Loughborough University; Tamara Valenčič, Loughborough University; James Beauchamp, Carnegie Mellon University; Greg Pearcey, Memorial University of Newfoundland

BACKGROUND AND AIM: Muscle contraction results from a non-linear transformation of motor commands via motor units (MUs). Ionotropic inputs provide excitation and inhibition whilst neuromodulatory inputs facilitate dendritic persistent inward currents (PICs) in motoneurons that generate non-linear MU discharge patterns allowing the estimation of motor command structure. It is currently unclear how these various inputs are shaped to support greater contraction forces, or whether these motor commands undergo adaptation with chronic training or ageing. We aimed to characterise the relative contribution of neuromodulation and the pattern of inhibition to human MU discharge with increased contraction force in three experiments: 1) across three different muscles (tibialis anterior, TA; vastus lateralis and medialis) of healthy individuals (n=15); 2) in TA of resistance (RT; n=23), endurance (ET; n=16), and untrained (UT; n=23) individuals; and 3) in TA of older (n=14; 71±4 years) vs. younger (n=14; 24±5 years) adults. Methods: In all experiments, participants performed isometric triangular contractions up to 30, 50, and 70% of maximal voluntary force (MVF) whilst high-density surface EMG signals were recorded, and decomposed into individual MU discharges that were then smoothed using support vector regression. Onset-offset hysteresis of pairs of MUs (ΔF) was calculated to estimate PIC magnitude. A quasi-geometric approach was used to garner insights into the neuromodulatory inputs (brace height) and the inhibition pattern (MU discharge acceleration, and post-acceleration [attenuation] slopes). RESULTS: Experiment 1. MU discharge patterns in all muscles were affected by contraction intensity, becoming more linear with lower slopes, but exhibiting greater discharge rate hysteresis. This suggests a reduced relative contribution of PICs to the increase in MU discharge and more reciprocal inhibitory patterns as a function of increased excitatory input. Experiment 2. RT exhibited greater discharge rates compared to ET and UT at 70% MVF. Both RT and ET exhibited more linear discharge patterns at 50 and 70% MVF compared to UT, though this appeared to be due to lower acceleration slopes in ET and lower attenuation slopes in RT. These results suggest modality-specific chronic training adaptations in the pattern of inhibition, with more reciprocal patterns associated with greater discharge rates and superior muscle force production in RT. Experiment

3. Older individuals exhibited reduced estimates of PICs at higher contraction intensities compared to sex-matched younger adults, suggesting modifications in the gain control of aged MUs. CONCLUSIONS: These experiments reveal that motor commands are uniquely shaped across contraction intensities, and that motor commands are modified with chronic training and ageing. The results also underscore the importance of contraction intensity when assessing the contribution of different components of motor commands to MU discharge.

S.9: From lab to living room - opportunities, challenges and potential using smart textiles and wearable solutions to facilitate self-administered home-based rehabilitation

S9.1: Co-creation of smart textile interventions for home-based rehabilitation after stroke – a case study

Leif Sandsjö, University of Borås; María Muñoz-Novoa, Gothenburg University; Peiman Khorramshahi, DaraLabs; Morten Kristoffersen, Center for Bionics and Pain Research; Margit Alt Murphy, University of Gothenburg; Li Guo, University of Borås

Background and Aim: About 80% of stroke survivors suffer from upper limb disorders. Shorter in-patient stays and limited access to rehabilitation programs puts a larger responsibility for functional recovery to the individual. In this context, technology-enabled, self-administered rehabilitation is presented as a way forward and biofeedback-based interventions using surface electromyography (sEMG) is a well-known candidate. However, current sEMG biofeedback methods are confined to the clinic, creating logistical hurdles which limit the training opportunities. This initiative aims to investigate the practicality, safety, and potential benefits of integrating smart textiles into post-stroke bio-feedback-based rehabilitation and explore if and how smart textiles solution(s) can improve the rehabilitation outcomes when performed by the patients themselves in their home environment. By introducing co-design of interventions, the study aims to harness insights from patients, healthcare professionals, and developers, ensuring user-centered and clinically relevant solution(s). Methods: The smart textile -based intervention(s) are formulated from a set of system components consisting of a) textile electrodes; b) sEMG acquisition system; c) biofeedback software app; d) data management and analysis platform. The co-design process focuses on optimizing these components for home-based self-administered interventions considering six distinct development aspects, i.e., i) targeted muscle(s); ii) textile electrode solution; iii) relevant training activities; iv) biofeedback measure(s); v) home-based training protocol; vi) user interface(s).The first stage of co-design involved technology developers working closely with healthcare professionals to understand the clinical and technical requirements and constraints related to home rehabilitation post-stroke to formulate a clinically viable prototype. At a second stage, the intervention will be further developed based on stroke survivors' input from testing the intervention at the clinic to co-design a training protocol for home use. RESULTS: Up to now (first stage) we have co-designed a system addressing (i) wrist flexors/extensors by means of (ii) a textile "sleeve" for the forearm comprising electrodes for wrist flexors and extensors to (iii) train wrist flexion/extension by (iv) providing feedback (bar graphs) when successfully activating or relaxing the targeted muscles. At the second stage it will be possible to test and provide users with individualized

training protocols (v) based on their preferences, encompassing various types of exercises designed for use with the textile electrode system in the home environment. The resulting intervention(s) will then be investigated focusing on feasibility, safety, functional recovery, usability (vi), user compliance, and overall benefits. Conclusion: By actively involving stroke survivors, healthcare professionals, and system developers in the co-design process, we feel confident that the resulting solution(s) will be user-centered and clinically relevant. It is essential to emphasize that this is an evolving study, and further testing and development are underway to refine and enhance the capabilities and usefulness of the system. Our overarching objective is to provide stroke survivors with a convenient and efficient home-based rehabilitation tool that has the potential to contribute significantly to recovery and overall quality of life.

S9.2: Phantom limb pain treatment at home facilitated by a textile electrode system – a case study

Li Guo, University of Borås; Anna Brjörkquist, University of Borås; Leif Sandsjö, University of Borås; Morten Kristoffersen, Center for Bionics and Pain Research; María Muñoz-Novoa, Gothenburg University; Max Ortiz-Catalan, Bionics Institute

BACKGROUND AND AIM: Phantom limb pain (PLP) is a common and frequently distressing condition affecting amputees, posing significant challenges in pain management and quality of life. Traditional approaches to managing PLP, such as mirror therapy, are not always effective, arguably because they can become tedious, leading to reduced patient engagement. Advanced treatments like biofeedback and VR/AR based interventions typically require continuous assistance from healthcare professionals, making independent, at-home management challenging due to the complex setup involved. This study aims to investigate the efficacy and user satisfaction of a novel textile-based solution, designed for PLP management, tested in home environments. The research focuses on evaluating the personalized textile electrode systems for rehabilitation techniques and deepening insights into the nuances of at-home PLP management. Methods: A qualitative study involving six participants with PLP was conducted. Each participant used a textile-based electrode system to perform phantom motor execution treatment over 3 to 6 months in their home environment. The study comprised two intervention phases: the initial phase, guided by the research team, aimed to validate the effectiveness of the textile electrode system. The second phase allowed participants independence in using the system, focusing on user compliance and satisfaction in a home setting. Qualitative data were gathered through semi-structured interviews following each intervention period, aiming to comprehensively document variations in type and level of pain, user experiences, and practical challenges encountered. The primary analysis of this data was conducted by the authors using Nvivo. Additionally, OpenAI's ChatGPT was employed as a supporting tool, offering supplementary insights into the qualitative analysis. RESULTS: Participants reported varying degrees of pain relief, with some experiencing significant reductions in PLP intensity. Main themes included improved pain management, positive impacts on daily activities, and overall life quality improvement. Challenges in system usability, particularly concerning cable management and difficulties with games, were highlighted; however, the textile prototype received positive feedback for its ease of use, reliability, and customizable treatment options. Additionally, the need for improvement to make the treatment more entertaining and challenging was identified, emphasizing their potential role in boosting user motivation and

compliance with the treatment regimen. CONCLUSIONS: The study highlights the importance of personalized rehabilitation, showcasing textile-based solutions as effective in managing PLP. The findings point towards a shift in rehabilitation practices, leaning more towards user-centered methods. AI's role in data analysis provided supplementary insights, enriching our understanding of participant experiences. Ultimately, the findings of this research open new possibilities for applying textile-based solutions in broader rehabilitation contexts, promoting their adoption in routine healthcare practices.

S9.3: Integrating textile electrodes into pants for transcutaneous electrical nerve stimulation in postoperative pain relief

Yohann Opolka, University of Borås; Courage Sundberg, Karolinska University Hospital; Robin Juthberg, Karolinska Institute, Department of Molecular Medicine and Surgery, Solna, 171 76 Stockholm; Amelie Olesen, University of Borås; Li Guo, University of Borås; Paul W. Ackermann, Karolinska University Hospital, Solna, 171 76 Stockholm; Nils-Krister Persson, University of Borås

BACKGROUND AND AIM: Patients undergoing hip surgery often face severe postoperative pain, which can significantly affect their recovery and quality of life. Traditional pain management methods, including medication, have their drawbacks. This study explores the use of Transcutaneous Electrical Nerve Stimulation (TENS) integrated into specially designed pants, aiming to provide an easy-to-use and effective pain relief option that also enhances mobility and comfort post-surgery. This approach also aims to address the need for more patient-centered and self-administered pain management strategies in post-surgical care. Methods: The study involved the design and development of a wearable solution - TENS pants. Special attention was given to the garment construction, ensuring flexible placement of TENS electrodes and overall ease of use for the pants. The iterative design process involved feedback from caregivers and users to maximize comfort, usability, and effectiveness in pain relief. A pilot study, a randomized single-blinded placebo-controlled trial (RCT) was conducted with thirty post hip surgery patients, to study the feasibility of using the TENS pants at a hospital. RESULTS: Results from the RCT study demonstrated a significant improvement in pain management compared to a placebo group in reducing postoperative pain and enhancing patient mobility. In addition, feedback from patients and healthcare professionals during the study resulted in the development of prototype pants for home use. This prototype, a tangible outcome of the study, addresses key aspects of usability and wearability and makes fully self-administrable pain relief possible in the home environment. CONCLUSIONS: The integration of TENS into textiles, as demonstrated by the TENS pants, has shown a promising direction in postoperative pain management for hip surgery patients. These pants have not only significantly reduced pain and improved mobility but also introduced an innovative and easy-to-use solution for self-administered pain management for home use. Future research will explore the long-term use and effectiveness of this home-use prototype, aiming to provide further insights into enhancing patient recovery and independence after surgery.

S9.4: Easy-to-use sEMG wearable device to monitor muscle activity at the clinic or at home

Elisa Romero Avila, Institute of Applied Medical Engineering; Catherine Disselhorst-Klug, Institute for Applied Medical Engineering, RWTH Aachen University

BACKGROUND AND AIM: The field of rehabilitation has observed, over the past years, an increase in the use of wearable devices for monitoring and assessing a person's movement performance. One of the methods used for this includes the recording of surface electromyography (sEMG). These wearables provide insights into a patient's condition and allow them to adjust their therapy, even at home. However, the quality and suitability of the recording may differ among the different devices. Accordingly, a 16-channel sEMG sensor system has been developed to be used autonomously and intuitively by patients with reduced arm function and without detailed knowledge about the exact positioning of the sEMG electrodes. This work aims to demonstrate the device's potential, including its feasibility and accuracy in identifying relevant sEMG channels, particularly in comparison to commercial sEMG systems that use pre-gelled electrodes. METHODOLOGY: The design includes a multichannel approach consisting of dry electrodes arranged in a circular form around the limb. The device is size-adaptive, and the 16 sEMG channels are distributed in eight modules, thus providing two sEMG channels per module to ensure correct localization and recording of muscles of interest. As a result, it increases the possibility that at least one sEMG channel is correctly positioned, and inexperienced users have more flexibility in electrode placement. Moreover, the sensor system ensures stable contact between the electrodes and the skin while compiling with the sEMG standards regarding electrode size and inter-electrode distance. The proof-of-principle of the device was proved during elbow flexion/extension movements by ten subjects. An algorithm was developed to identify the relevant channel recording the muscular activation of the biceps since it is one of the primary muscles involved in elbow flexion/extension movements. Then, the sEMG sensor system was repositioned before each trial, and the results were compared to those obtained using a conventional sEMG system with pre-gelled electrodes. RESULTS: The results indicate that even when placed by inexperienced users, the system adequately tracks muscular activation with sufficient accuracy and a signal quality comparable to conventional sEMG systems. The algorithm on the sEMG sensor system identified the relevant sEMG channel in more than 90% of the trials. Furthermore, the device was easily placed and removed by the subjects. CONCLUSION: These features enable the sEMG sensor system to be a promising instrument for tracking muscular activation and guiding the rehabilitation of patients with movement disorders in the clinic or at home. Besides enabling the monitoring by the medical staff and providing direct feedback to the patient, it may also be considered for future applications related to the control of smart prosthetics and orthotics.

S9.5: Gel-free textile-based electrodes for enhanced surface electromyography: towards efficient home-based health applications

Xi Wang, University of Borås; Yuqi Wang, The University of Manchester; Li Guo, University of Borås; Xuqing Liu, Northwestern Polytechnical University; Leif Sandsjö, University of Borås

Background and Aim: The development of easy-to-use surface electromyography (sEMG) in home-based health practices is increasingly recognized. Textile-based electrodes offer a promising approach for self-administered health monitoring due to their easy integration into everyday life, reducing barriers to practical use. However, textile-based electrodes, particularly in sEMG applications, still face challenges related to electrode-to-skin impedance, reliance on conductive gels, and, most importantly, the need to record from a well-defined position that prevents the electrode(s) from moving over the skin. This study aims to overcome these limitations of textile-based electrodes, particularly in enhancing electrode contact and

adhesion to the skin. Methods: The study employs Carbon Black (CB) encapsulated in one type of biocompatible elastomer, i.e. Ecoflex. Encased in an interphase layer, CB forms colloidal dispersions, facilitating quantum tunneling and percolation, with the quantum interfacial effect influenced by the distance between CB and the polymer inherent potential barrier, to maintain stable conductivity during movement. Additionally, a proportion investigation is applied to exhibit enhanced surface energy, due to silicon hydroxyl bonds, creating a skin-adhesive interface to improve skin-electrode contact and maintain a defined position over the muscle. The feasibility of the CB/Ecoflex electrodes was tested by comparing the myoelectric activity (sEMG) in relation to the signal recorded by standard Ag/AgCl electrodes. RESULTS: The developed electrodes exhibit good flexibility, stable electromechanical properties, and lower skin contact impedance. These electrodes, which do not require conductive gel, show a signal quality comparable to the standard Ag/AgCl electrodes during sEMG tests. Their efficacy was demonstrated by sEMG recordings from the wrist flexors and extensors while performing a series of hand/wrist activities. Conclusion: The gel-free, durable, and skin-conformable textile electrodes developed in this study show great potential in facilitating easier usage in home-based monitoring, treatment, and rehabilitation. They represent a more accessible and effective step forward in integrating soft electronics with biomedical engineering, promising the development of advanced, comfortable, and non-invasive health monitoring technologies in medical diagnostics, sports science, and rehabilitation applications.

S.10: Factors influencing neuromodulation of motoneurons and/or PICs: What do human studies tell us and what are the applications?

S10.1: Pharmacological manipulations of the serotonergic system reveal neuromodulatory effects at human motoneurons, but what do different tests of motoneuron excitability tell us?

Jacob Thorstensen, The University of Queensland; Tyler Henderson, Griffith University; Benjamin Goodlich, Griffith University; Justin Kavanagh, Griffith University

Descending motor pathways recruit spinal motoneurons to activate muscle fibres, whereby ionotropic and neuromodulatory inputs work in harmony to control the firing characteristics of pools of motor units. Ionotropic inputs such as the corticospinal system quickly bring motoneurons above their threshold for discharge. In contrast, motoneuron excitability is drastically altered by slower-acting metabotropic neuromodulators such as serotonin (5-HT) released from the brainstem raphe nuclei. Decades of animal work indicate that 5-HT has net faciliatory effects on motoneuron excitability, whereby more muscle force can be produced for the same excitatory input to motoneurons when 5-HT is released in the spinal cord. To enhance motoneuron excitability, amongst other mechanisms, 5-HT appears to strongly enhance the amplitude of voltage-gated persistent inward currents (PICs), which amplify and prolong excitatory synaptic input. In recent years, there has been an extended effort to translate the observed effects of 5-HT on motoneuron excitability in animals to humans. Specifically, several double-blinded, placebo-controlled drug studies involving drug interventions that either enhance 5-HT availability or antagonise its activity at the excitatory 5-HT2 receptor, have been paired with gold-standard tests of motoneuron excitability to provide insight into the

neurochemical effects of 5-HT at motoneurons in humans. Several different tests have been used to assess 5-HT drug effects at motoneurons, including transcranial magnetic stimulation (TMS) of the motor cortex to evoke electromyogram recorded motor evoked potentials (MEPs), cervicomedullary stimulation to evoke cervicomedullary motor evoked potentials (CMEPs), peripheral nerve stimulation to evoke F-waves, and high-density surface electromyography (HDsEMG) derived estimates of PICs. However, not all these tests detect changes in motoneuron excitability after 5-HT drug administration, and this could be due to subtle differences in the ways in which they assess motoneuron excitability. Likewise, 5-HT drug effects on measures of motoneuron excitability appear to be contraction-intensity dependent, whereby drug effects are more prevalent when more inputs to motoneurons are active. This presentation will discuss the effects of 5-HT drugs across several different measures of motoneuron excitability in humans, and what this tells us about the serotonergic control of motoneuron activity (with a particular focus on PICs). Specifically, we will compare 5-HT drug effects identified with HDsEMG estimates of PICs, to drug effects observed with neurostimulation of the motor system, and how outcomes associated with these techniques are affected by the magnitude of voluntary contraction that likely changes the magnitude of serotonergic drive to motoneurons.

S10.2: PICture this – an expansive analysis repertoire for unravelling the effects of persistent inward currents on the control of human motor output

Greg Pearcey, Memorial University of Newfoundland; James Beauchamp, Carnegie Mellon University; Jakob Škarabot, Loughborough University

BACKGROUND AND AIMHuman movement is achieved via activation of spinal motoneurons and their innervated muscle fibers, collectively known as motor units. Motoneuron discharge times are accessible in humans due to the one-to-one relationship between action potential discharges of the motoneuron and its innervated muscle fibers. Human motor unit recordings therefore provide valuable information about motor commands and biophysical properties of human motoneurons. It was once believed that motoneurons were passive integrators of net synaptic inputs, however, it is now clear that they possess active properties that can transform synaptic inputs to a great degree. During slowly increasing inputs, motoneuron discharge rates rapidly accelerate (secondary range), which reflects the onset activation of intrinsic persistent inward currents (PICs) in motoneurons. PICs further shape the discharge behaviour of motoneurons by producing sustained plateau potentials, which cause motoneuron discharge rates to increase linearly in response to an increasing intracellular current injection but with a much shallower slope. This lower-gain response, termed tertiary or rate attenuation range, reflects an increase in membrane conductance produced by the sustained opening of the Na and Ca channels mediating PICs. The tertiary range also exhibits a pronounced hysteresis whereby the sustained plateau potential mediated by PICs allows the motoneuron to discharge at inputs well below that needed to initially recruit the motoneuron. This hysteresis in discharge rate reflects the PICs contribution to self-sustained firing of the motoneuron and can be measured by the reduction in current injected into the soma at the offset of motoneuron discharge (de-recruitment) compared to the higher current required to initiate firing at recruitment. The number of studies estimating the effects of PICs on human motor unit discharge profiles has exploded in the last decade or so, but the analysis has primarily focused on hysteresis only. This has been achieved via the well-established paired motor unit analysis

technique. Further quantification of PIC-induced features of motor unit discharge rate profiles therefore provides great potential to understand human motor commands and biophysical properties of human motoneurons. METHODS Several emerging methods, that move beyond the well-established paired motor unit analysis technique (DF), will be discussed to facilitate further understanding of mechanisms contributing to changes in motor unit discharge behaviour. In particular, the assessment of non-linearities of motor unit discharge rate with respect to linear changes in behaviour (e.g., force or torque) will be used to provide insights about changes in motor commands that can contribute to changes in DF. Results Several experimental datasets will be discussed with regards to the amplitude, duration, and slope of the discharge rate acceleration (secondary firing range) and attenuation (tertiary firing range). In combination with realistic motoneuron models, these results allow unprecedented insights about changes in the patterns of neuromodulation and inhibition received by motoneuron pools during human behaviour. CONCLUSIONS Emerging methods for the analysis of human motor unit discharge profiles discussed in this presentation will facilitate a greater understanding of human motoneuron function in both heath and disease.

S10.3: Effect of experimental joint pain on estimates of persistent inward currents

Francois Hug, Université Côte d'Azur; Jacob Thorstensen, The University of Queensland; Manuela Besomi, The University of Queensland; Wolbert Van Den Hoorn, School of Biomedical Sciences, The University of Queensland, Australia; Kylie Tucker, The University of Queensland

BACKGROUND AND AIM. There is a series of studies reporting an overall decrease in motor neuron discharge rate during contractions with matched force when pain is induced experimentally in muscle or non-muscular tissue. Recent data show evidence of differential modulation of the activity across the motor neuron pool, with an increased discharge rate of some motor neurons. Possible mechanisms for these changes in motor neuron discharge characteristics involve persistent inward currents (PICs), which are activated by voltage-dependent ion channels and lead to a non-linear relationship between the net synaptic input received by a motor neuron and its output. The aim of this study was to assess the effect of experimental pain on the estimates of PICs and motor unit discharge characteristics. METHODS.10 participants (8 males, 2 females) performed triangular and trapezoid isometric knee extensions to a peak of 30% of their maximum voluntary contraction. Three conditions were tested: one control condition that preceded a condition where pain was induced in the knee fat pad by injection of hypertonic saline, and a washout condition performed after pain had completely ceased. We recorded high-density surface electromyography (HDsEMG) signals from the vastus lateralis (256 electrodes), and vastus medialis (128 electrodes) muscles. Signals were decomposed with convolutive blind source separation to identify motor units spike trains. A paired-motor-unit analysis was used to calculate ΔF, which is assumed to be proportional to PIC magnitude. RESULTS: Data are reported only for the Vastus lateralis muscle. An average of 26.6±15.1 (range: 8-58) motor units per participant were identified. When considering the trapezoid contractions, there was a significant decrease in motor unit discharge rate during pain (main effect; p<0.05 for both matched and unmatched motor units). However, the ΔF was not significantly affected by experimental pain (main effect p>0.05 for both matched and unmatched motor units). As we identified a relatively large number of motor units, we were able to run statistics for each participant separately. We observed large interindividual variability, with 5 participants exhibiting a significant decrease in ΔF during pain,

4 participants showing an increase and 1 participant showing no change. CONCLUSION. The effect of experimental pain onPICs appears to be individual-specific. Further work is needed to assess the robustness of these adaptations and to understand the reasons for this interindividual variability.

S10.4: Altered motor neurone firing patterns unravel impaired neuromodulatory and inhibitory effects on persistent inward currents in older adults

Lucas Orssatto, Deakin University

Muscle force production requires appropriate levels of synaptic input to the motor neurones, the final common pathway to muscle. Subsequently, the motor neurones are responsible for integrating and modulating excitatory synaptic input to evoke an appropriate motor unit firing output. Motor neurones can generate persistent inward currents (PICs), which are depolarising currents produced by specialised voltage-sensitive sodium and calcium channels within their dendrites. PICs increase cell excitability, accelerating, amplifying, and prolonging motor neurone output activity for a given synaptic input. Deteriorations observed within the function of aged motor neurones cause them to fire at lower frequencies, thereby reducing the ability of older motor units to produce high levels of force. Recent studies suggest that the lower firing frequencies observed in the older population could be partially explained by impairments in the ability of aged motor neurones to generate PICs. Studies tested various muscle groups, such as tibialis anterior, soleus, vastus lateralis, and biceps and triceps brachii. However, they relied solely on estimates of PIC contribution to motor neurone firing obtained from the paired-motor unit analysis method (to calculate Δ Frequency - ΔF). Although this method is considered the best current estimate of PICs in physiologically activated motor neurones, novel robust metrics have demonstrated the potential to provide a broader understanding of PICs when combined with ΔF data. A quasi-geometric approach has been developed and demonstrated validity in quantifying the neuromodulatory effects of PICs and inhibitory effects on PICs, influencing individual motor unit firing patterns. However, these metrics have not been explored in the aging context to date. This presentation will highlight: i) Recent work demonstrating that estimates of PIC contribution to motor neurone firing (estimated with paired-motor unit analysis to calculate ΔF) are reduced in older individuals;ii) Our novel data showing age-related changes to neuromodulatory and inhibitory input influencing PIC effects on motor neurone firing patterns. These were estimated with novel quasi-geometric metrics, such as brace height, acceleration and attenuation slopes, and angle.iii) Current evidence of PIC facilitation and inhibition impairments that could be contributing to reductions in general functional capacity in older adults. Collectively, data obtained from these metrics improve our understanding of age-related impairments in PIC contribution to reduced motor neurone firing, force production, and physical function in older adults. A better understanding of this motor neuronal mechanism can lead to the development of more effective strategies—whether through exercise, nutrition, and/or pharmacological interventions—to alleviate the debilitating effects of aging and improve the physical function and general quality of life of older adults.

S.11: Neurorehabilitation pipeline for upper extremity motor paralysis after stroke: xR, non-invasive brain stimulation, and Constraint-induced movement therapy

S11.1: Rehabilitation treatment package for optimal option adaptation to the stroke survivor's individual motor function

Fuminari Kaneko, Tokyo Metropolitan University

For post-stroke upper extremity (UE) motor paralysis, a multistep treatment strategy according to the functional status of individuals is significantly important. According to Liu et al. (2012), for individuals with UE paralysis after stroke, if electromyography (EMG) of finger extensors is not detectable, motor imagery-based training is an option (Level 1). If EMG of finger extensor muscles is detectable, functional electrical stimulation therapy is feasible (Level 2). Constraint-induced movement therapy may be selected as appropriate option if the patient is at a level where actual joint motion occurs, not just EMG (Level 3). As a treatment of motor imagery-based training, passively induced kinesthetic illusion with visual stimulation (Passive-KNVIS) is one option for people with Level 1 function. The seamless treatment strategy of applying the appropriate treatment option is called a "neurorehabilitation pipeline." In this presentation, I will propose a novel multistep treatment package as a neurorehabilitation pipeline. Kawakami et al. (2016) demonstrated that motor function improved when HANDS therapy, which is also included in our treatment package, was applied to individuals with improved finger extensor muscle activity following motor imagery-based training. However, there seemed to be a large gap in functional status between Levels 1 and 2. After finger extensor EMG activity was detectable during the hand movement, HANDS therapy could be performed even when extensor and flexor muscles were co-contracted. Therefore, we recently developed a novel EMG-feedback therapy (active-augmented body movement control with neuromuscular feedback system therapy [Active-AUMOC]) for individuals in whom the finger extensor muscle activity was detected after Passive-KINVIS, but co-contraction of the extensor and flexor muscles was observed (Level 1.5).In short, we propose to offer a novel multistep treatment package for individuals with severe motor paralysis after stroke in the chronic phase: Passive-KINVIS, Active-AUMOC, and HANDS therapy. To choose the appropriate approach for individuals, we used clinical assessments measuring motor function and EMG tests to determine whether to proceed to the next therapies in the treatment package or which therapies to apply for individuals with stroke. Let me first talk about Passive-KNVIS, which we developed. With KINVIS therapy, individuals with stroke can feel as if their paralyzed real body has been replaced by an artificial body with enhanced motor functions. Based on the results of our experimental studies and clinical trials, we will present the physiological and cognitive effects of Passive-KINVIS. The next step will be the results of application of our novel multistep treatment option package to individuals with severe motor paralysis after stroke in the chronic phase.

S11.2: Robotic rehabilitation for upper limb motor disorders after stroke

Takashi Takebayashi, Osaka Prefecture University

Stroke is the third leading cause of death worldwide, and it leaves residual effects, diminishing the quality of life (QOL) in later years. Many stroke survivors experience residual upper and lower limb motor deficits that manifest after the onset of stroke. Motor impairments in the upper limbs affect activities of daily living and are reported to significantly reduce patients' quality of life. Recently, robotic therapy has been reported as effective in treating upper limb motor impairments that arise after a stroke in guidelines from around the world. Robotic therapy is also noted for promoting functional recovery by ensuring an appropriate level of activity in the affected upper extremity when used as independent practice outside of therapist-provided rehabilitation time (Winstein et al., 2016).In our previous randomized controlled trial (RCT) investigating the effectiveness of robotic therapy as an adjuvant therapy using ReoGo-J (Teijin Pharma Limited, Tokyo, Japan), we observed no significant improvement in affected upper extremity function with robotic therapy used as a voluntary exercise compared to the group performing conventional voluntary exercise. However, there was no significant difference in the behavior (frequency of use) of the paralyzed hand in real life (Takahashi et al., 2016). Therefore, to transfer the functional improvement developed by robotic therapy to activities of daily living, we conducted a study using Constraint-Induced Movement Therapy (CIMT), recommended by international guidelines for improving the affected upper extremity use in daily life (Takebayashi et al., 2018).Based on the above hypothesis, an RCT was conducted to test the effects of robotic therapy and CIMT. The results suggested that the group receiving both robotic therapy and CIMT as independent practices significantly improved the behavior of paralytic hand use in daily life compared to the group receiving both conventional independent practice and conventional rehabilitation (Takebayashi et al., 2022). These results emphasize the importance of understanding the characteristics of robotic therapy and human-provided CIMT and integrating them into rehabilitation for the paralyzed hand after a stroke. Finally, we are currently developing an algorithm that will enable ReoGo to automatically recommend tasks of appropriate difficulty based on the severity of the patient's upper extremity motor impairment. The results have shown that, once the function of the paralyzed hand is assessed in the shoulder, elbow, and forearm categories of the Fugl-Meyer Assessment, it is possible to recommend appropriate exercises according to the patient's upper extremity function (Takebayashi, et al. 2023). This algorithm will be briefly discussed at the end of this lecture.

S11.3: Applications of transcranial magnetic stimulation in rehabilitation medicine

Michiyuki Kawakami, Keio University School of Medicine

Repetitive transcranial magnetic stimulation (rTMS) has long been used in clinical practice. rTMS is a method of changing the excitability of the cerebral cortex by varying the stimulus intensity, frequency, and frequency of repetitive stimulation. Recently, patterned form of rTMS has become more common as a more powerful stimulation method, and its representative stimulation methods are quadripulse stimulation (QPS) and theta burst stimulation (TBS). Both QPS and TBS have similarities in that they can induce LTP (Long-Term Potentiation)/LTD (Long-Term Depression)-like changes more powerfully than regular rTMS, and both have stimulation methods that produce a stimulatory effect and a suppressive effect. For example, when used to treat stroke patients, QPS and TBS are used to increase the excitability of the primary motor cortex of the injured side of the brain or to reduce the excess inhibition (interhemispheric inhibition) of the injured side of the brain by decreasing the brain activity of the non-injured side. TBS is easy to use in clinical situations because of its short stimulation time (90 to 190

seconds), and the number of research papers on TBS has increased. Several systematic reviews and meta-analysis studies have reported the efficacy of TBS in improving motor cortical plasticity, motor function, and daily functioning in stroke patients. Although the 30-minute stimulation time required for QPS is a hurdle to its clinical application, the relatively low inter-subject variability of its effects makes it easy to predict the effects that will be obtained. These magnetic stimulation techniques are expected to be used in combination with neurorehabilitation techniques. This presentation will focus on magnetic stimulation as a treatment for central motor paralysis in particular, and in combination with other rehabilitation techniques.

S.12: Back in action: muscles, mechanics, and movement in adolescent idiopathic scoliosis

S12.1: Quantifying full spine paraspinal muscle volume, intramuscular fat and fat-free muscle asymmetry in adolescent idiopathic scoliosis

Phoebe Duncombe, The University of Queensland; Taylor Dick, University of Queensland; Phoebe Ng, KK Women's and Children's Hospital/ The University of Queensland; Maree Izatt, Biomechanics and Spine Research Group, Centre for Children's Health Research, Australia; Robert Labrom, Biomechanics and Spine Research Group, Centre for Children's Health Research, Australia; Kylie Tucker, The University of Queensland

Adolescent idiopathic scoliosis (AIS) is characterized by an atypical 3D spinal curvature that develops/progresses between ages 10-18 years. Asymmetry in paraspinal muscle size and quality influences force-generation capacity and may contribute to asymmetrical vertebral growth. We aimed to quantify paraspinal muscle volume and intramuscular fat asymmetry in female adolescents with AIS and age-matched controls. Methods: T1-weighted and mDixon MRI scans were performed on 23 female adolescents with primary-right-convex thoracic scoliosis [Cobb angle: 38±16°; age: 13.7±1.5 years]; and 20 controls [age: 13.6±1.9 years]. Muscle volumes (multifidus and longissimus) were determined at vertebral levels T6 to L4. Fat-fraction maps from mDixon scans were co-registered with muscle volumes to determine intramuscular fat proportions. Muscle, intramuscular fat, and fat-free volume asymmetry indices [ln(concave/convex)] were determined. RESULTS: This work identified significant asymmetries in the AIS participants' paraspinal muscle volume, intramuscular fat and fat-free muscle along the full length of the scoliotic curve, which were greater than observed in control participants with symmetrical spines (p<0.05).Multifidus's volume was significantly greater on the concave-side of the spine near the thoracic scoliotic curve apex and greater on the convex-side in the lumbar spine for the AIS group (p<0.05, Fig 1A). For longissimus, only the volume at the 3rd vertebral level above the apex was greater on the concave side (p<0.05, Fig 2A).Both multifidus and longissimus intramuscular fat were significantly greater on the concave-side of the spine near the thoracic scoliotic curve apex (p<0.05, Fig 1B and 2B) and in the lumbar spine, greater on the convex-side for the AIS participants (p<0.05, Fig 1B and 2B).Multifidus fat-free muscle volume three vertebral levels above the apex was significantly greater on the concave-side and greater on the convex-side at the 5th vertebral level below the apex (p<0.05, Fig 1C). For longissimus, only at the 3rd vertebral level above the apex was the

fat-free muscle volume greater on the convex-side (p<0.05, Fig 2C).Discussion: Compared to the control group, participants with AIS have significant asymmetry in multifidus volume, intramuscular fat, and fat-free muscle across multiple vertebral levels around the thoracic curve apex and in the lumbar spine. Longissimus also has significant asymmetry in intramuscular fat levels around the apex of the thoracic curve and the lumbar spine. This provides evidence of an imbalance in the force-producing capacity of paraspinal muscles in AIS, particularly in the deep paraspinal muscle, which applies forces to the transverse and spinous processes of the vertebrae. The next step in this data collection is to determine if these asymmetries are correlated with curve severity, future progression of the curve, and bony asymmetries identified in our participants with AIS.

S12.2: Maximal and asymmetrical submaximal paraspinal muscle activation in adolescent idiopathic scoliosis during simple back extension tasks

Phoebe Duncombe, The University of Queensland; Andrew Claus, Royal Brisbane and Women's Hospital, Australia; Maree Izatt, Biomechanics and Spine Research Group, Centre for Children's Health Research, Australia; Peter Pivonka, Queensland University of Technology; Robert Labrom, Biomechanics and Spine Research Group, Centre for Children's Health Research, Australia; Wolbert Van Den Hoorn, School of Biomedical Sciences, The University of Queensland, Australia; Kylie Tucker, The University of Queensland

BACKGROUND AND AIMCurve progression in adolescent idiopathic scoliosis (AIS) is associated with three-dimensional wedging of spinal vertebrae and discs [1]. It is well known that muscle activity and morphology influence muscle force generation, and that the forces applied to bones and discs are substantial moderators of growth and adaptation [2]. There is growing evidence for asymmetrical force-generating capacity in paraspinal muscles in AIS [3,4]. However, data varies greatly between studies, and previous outcomes are highly dependent on the methodological approaches taken [5].The aim of this study was to determine if the symmetry of paraspinal muscle activation amplitude differs in adolescents with AIS compared to controls, during a voluntarily driven, symmetrical, submaximal task. METHODS Females with AIS (primary right thoracic curves, n=24, mean[SD] age: 13.8[1.5] years) and without AIS (n=20, 13.8[1.8] years) were recruited through a Spine outpatient clinic at the Queensland Children's Hospital and the local community. Six maximal trunk extensions were performed in lying: three in an unresisted pose, and three were manually resisted at the shoulders and thighs. The maximum activation recorded in any trial, for each muscle separately, was used for normalisation. Participants then performed a series of five (20-30s) submaximal trunkcontractions (Fig 1A), which was between 10-20% of their maximal activation (i.e. 10-20% MVC, from T9 left + right). Muscle activity was recorded using bipolar surface electrodes placed bilaterally atvertebral levels: T9 and T12 (Fig 1B, note that data from C7 and L5 were also recorded as part of a larger study but not reported as part of this study).The symmetry index of muscle activity was determined usingLn(right/left), which equates to Ln(convex/concave) in the AIS cohort. To assess the difference in muscle activation symmetry index between the groups, repetitions (1-5) and vertebral levels, a linear mixed model analysis was conducted. Participants were entered as random intercepts, with repetition, and interaction between group and vertebral level included as a fixed effects. RESULTS Greater paraspinal muscle activation asymmetry (convex>concave) was observed at the apex of those with AIS versus T9 of the control group (Estimate 0.36, 95%CI 0.05 to 0.80, p=0.002). There was no difference in

activation symmetry between groups at T12 (Estimate 0.27, 95%CI -0.04 to 0.58, p=0.12). CONCLUSIONS Compared to control participants, adolescents with AIS display greater asymmetry in paraspinal muscle activation at T9 during submaximal trunk extensions. This asymmetry was not observed at T12. Asymmetric paraspinal muscle activation may contribute to asymmetrical muscular forces for spines developing in children with AIS.REFERENCES[1] Negrini et al. Scoliosis Spinal Disord 13: 1-48, 2018[2] LeVeau et al. Phys Ther, 64: 1874-82, 1984.[3]Kennelly K and Stokes M. Spine 18: 913-7,1993[4] Meier MP et al. Spine 22: 2357-64, 1997.[5] Ng et al. J Electromyogr Kinesiol63: 1-11, 2022.

S12.3: Towards understanding paraspinal muscle activation asymmetry in idiopathic scoliosis – A pilot study

Juha-Pekka Kulmala, Helsinki University Hospital; Mikko Mattila, Helsinki University Hospital; Andrey Zhdanov2, Helsinki University Hospital; Jari Arokoski, Helsinki University Hospital

Background and Aims: Etiology of adolescent idiopathic scoliosis (AIS) is still unknown. Because adolescent spine is flexible, asymmetry in the paraspinal muscle activation may potentially play a role in the development of scoliosis. While some electromyographic (EMG) studies have reported higher activation in the convex side others have found no differences (1). Mixed findings may be due to fact that previous studies have analysed absolute rather than normalised EMG results, although latter is commonly recommended (1).Several normalisation procedures have been described, such as the reference to a maximal voluntary contraction (MVC) or sub-maximal (SubMax) voluntary contraction. We aimed to compare whether these methods provide a comparable results for muscle activation asymmetry in AIS. Methods: Paraspinal muscle activations at lumbar (L4 & L2) level and thoracic level (T11) were recorded during MVC and SubMax task. For aMVC, we used back extension task, and as a sub-maximal task, we used backward walking on a treadmill while pulling the ropes (Figure 1).EMG data were filtered with a bandpass filter (20-500Hz), and then rectified and low pass filtered using a 4th order Butterworth low-pass filter (10 Hz). We report absolute EMG values and asymmetry indexes of both methods from four AIS patients. We also report normalised EMG results during walking when using MVC and SubMax normalisation procedures. RESULTS: The absolute paraspinal muscle activations were about two times greater in MVC versus SubMax method (Fig 2). The mean asymmetry index showed relatively similar values between MVC versus SubMax method. However, at the individual level, notable differences between the two methods were observed especially at the T11 level: For the two participants (2 & 3), SubMax method provided greater activation on the right side whereas MVC method showed greater activation in the left side (Fig. 2). This results in a clearly greater side-to-side asymmetry in these participants during walking when analysed using MVC versus SubMax method (Fig 3). Discussion: We observed contracting results for between side paraspinal muscle activation level in some of the patients in the MVC versus SubMax measurements. It remains unclear to what extent these differences depends on patients' altered activation strategy in SubMax task, and on the other hand, the patients' ability to achieve maximum voluntary activation in the MVC task. To better understand paraspinal muscle function in AIS, we call for further research examining muscle activation strategies across different tasks and effort levels. ReferencesNg, P.T.T., Claus, A., Izatt, M.T., Pivonka, P. and Tucker, K. (2022).Is spinal neuromuscular function asymmetrical in adolescents with idiopathic scoliosis compared to those without scoliosis?: A

narrative review of surface EMG studies. Journal of Electromyography and Kinesiology, 63 102640, 102640. doi: 10.1016/j.jelekin.2022.102640

S12.4: Novel technology and methods for the assessment of deformity and function in Adolescent Idiopathic Scoliosis

Jessica Wenghofer, University of Ottawa; Kristen Beange, Carleton University; Wantuir, Carlos, Jr. Ramos, University of Ottawa; Mina Maksimovic, University of Ottawa; Matthew Mavor, University of Ottawa; Kevin Smit, The Children's Hospital of Eastern Ontario; Ryan Graham, University of Ottawa

Background and Aim: Adolescent Idiopathic Scoliosis (AIS) is a complex deformity that often requires early intervention to prevent the progression of the spinal curvature and, in many cases, a potential loss of function. This research highlights novel technologies for assessing AIS and spine function by presenting three studies: Study 1) the use of smartphones and deep learning (DL) to screen for AIS; Study 2) validation of an inertial measurement unit (IMU) based methodology to clinically assess spine motion in patients with AIS; and Study 3) development of a spine motion capture system using DL and a red-green-blue-depth (RGB-D) camera. Methods: In Study 1, 68 participants (53 AIS, 15 control) were recruited from the Children's Hospital of Eastern Ontario and were imaged with a smartphone containing a depth sensor. Participants were randomly divided into train and test datasets with an 80: 20 split. The training dataset was used to train a DL algorithm to classify participants based on diagnosis (AIS or control). The test dataset was used to assess model performance by measuring the model's accuracy, sensitivity, and specificity. In Study 2, spine kinematics of 10 participants performing dynamic trunk movements were simultaneously collected by optical (OPT) and IMU systems (equipment placed at C7, T12 and S1 vertebral levels) to assess concurrent validity and reliability of the IMU system to track absolute (C7, T12, and S1) and relative (thoracic, lumbar, and total) spine movement and range of motion (ROM). In Study 3, 15 participants performed repetitive flexion-extension while recorded with an RGB-D camera. ROM was controlled by adjusting targets in the sagittal midline to shoulder and knee height. Participants were divided into train and test datasets with an 80: 20 split. These data were used to train a DL algorithm to segment the posterior trunk into upper spine, lower spine, and pelvis segments. The corners of these segments were then used to create a 3D global coordinate system, enabling the measurement of spine kinematics and comparison to a gold-standard OPT system. The root means square error (RMSE) and intraclass correlation coefficients (ICC) were measured between the RGB-D and OPT systems. RESULTS: Study 1: An accuracy of 96% was achieved with a sensitivity and specificity of 99% and 82%, respectively. Study 2: The IMU method calculated kinematics within 2° RMSE of the OPT system and had excellent reliability for estimating ROM (ICC2,1 ≥ 0.950). Study 3: The algorithm achieved RMSE values <5° compared to the OPT system and was able to measure both lumbar and total spine kinematics. CONCLUSIONS: The results from these studies demonstrate that portable and inexpensive technology can be used to screen for AIS and measure spinal function through dynamic movements, making participation in research studies more accessible and demonstrating the potential for at home assessments and large-scale, multi-centre research studies.

Oral Session 1

O.1.1: Physical activity and body mass index are associated with skeletal muscle mass index after menopause

Emma Fortune, Mayo Clinic; Omid Jahanian, Mayo Clinic; Melissa Morrow, The University Medical Branch Texas; Michelle Mielke, Wake Forest University School of Medicine

Introduction: One in eight women have their ovaries removed before reaching natural menopause (premenopausal bilateral oophorectomy; PBO) for cancer prevention [1]. This may contribute to accelerated aging processes and is associated with a higher risk of multi-morbidity compared to women who undergo natural menopause [2]. A recent study reported that women who undergo PBO, particularly before 45 years old, have an elevated risk of sarcopenia (characterized by loss of skeletal muscle mass, strength, and function) compared to women who undergo natural menopause [3]. Physical activity is associated with a lower risk of sarcopenia in postmenopausal women [4]. However, there is limited information regarding physical activity and its relationship with low skeletal muscle mass in women with PBO. Therefore, we investigated the differences in daily step counts and skeletal muscle mass index (SMI; appendicular skeletal muscle mass (ASM) normalized to body weight [5]), and the association of daily step counts with SMI in women with PBO and referent women. We hypothesized that women with PBO would have lower daily step counts and poorer SMI, and that daily step counts would be positively associated with SMI. Methods: Fifty women with a history of PBO and 50 age-matched referent women (median ages: 66 and 65 years, respectively) received DEXA scans to estimate SMI and wore ankle accelerometers for 7 days. Daily step counts were calculated for each participant from acceleration data [6]. Differences between women with and without history of PBO were assessed using paired Wilcoxon Mann Whitney U-tests. Associations of daily step count with SMI were assessed using linear regression. Covariates included age, BMI, type of menopause (PBO or natural), age at menopause, and hormone replacement therapy (HRT; ever vs. never used). Results & Discussion: BMI was higher, and SMI was lower for PBO versus referent groups (p<0.04). Although the daily step count was lower for PBO versus referent groups, the difference was not statistically significant (p=0.22). The lack of significance was partly due to insufficient statistical power for the observed effect sizes. In addition, referent women with HRT use history had lower step counts and younger age at menopause compared to referent women with no history of HRT use, and also compared to PBO women with a history of HRT use. In the linear regression model, daily step count (β=0.125, ρ=0.014) and BMI (β=0.217, ρ=0.001) were significant predictors of SMI, explaining 51% of the variability (Fig. 1). Significance: Higher daily step count and lower BMI are associated with larger SMI. Larger sample sizes are needed to determine if PBO history results in lower daily step counts. Given the elevated risk of sarcopenia for women with PBO history, remote monitoring of daily step counts could provide a means to guide physical activity-based interventions for sarcopenia prevention. References: [1] Howe (1984), Am J Public Health; [2] Mucowski et al. (2014), Fertil Steril; [3] Karia (2021), Cancer Epidemiol Biomarkers Prev; [4] Keller (2019), Wien Med Wochenschr; [5] Kim (2016), J Intern Med; [6] Fortune (2014), Med Eng Phys.

O.1.2: The influence of workload on muscular fatigue, tissue properties, and postural stability in older and younger workers

Emile Marineau, Université du Québec à Trois-Rivières; Catherine Daneau, Université du Québec à Trois-Rivières; Janny Mathieu, Université du Québec à Trois-Rivières; Julien Ducas, Université du Québec à Trois-Rivières; Vincent Cantin, Université du Québec à Trois-Rivières; Stéphane Sobczak, Université du Québec à Trois-Rivières; Pierre-Yves Therriault, Université du Québec à Trois-Rivières; Jacques Abboud, Université du Québec à Trois-Rivières; Martin Descarreaux, Université du Québec à Trois-Rivières

Background: Most Western countries are currently facing numerous challenges linked to demographic aging. In Quebec, there is a noticeable increase in the workforce population aged over 55, accounting for nearly 20% of full-time employees in 2017. The presence of older workers may require adaptations in tasks to accommodate their physical capacities and limitations. Notably, aging involves a substantial decline in muscle mass, leading to decreased strength and muscle quality, impacting approximately 27% to 59% of women and 30% to 45% of men over 60. Furthermore, aging results in degenerative alterations of the musculoskeletal and sensorimotor systems (e.g., intervertebral disc height and postural stability). Despite these changes, job requirements and workloads, including both physical and cognitive aspects, are rarely tailored to the specific attributes of older workers. Despite the significant rise in the number of aging workers over the past 15 years, scientific data regarding the effects of physical and physiological changes accompanying aging in the workplace are lacking. Given the high prevalence of low back pain across all age groups, our study focuses on investigating the structure and functionality of the lumbar region. Objective: This research aimed to evaluate the impact of a workday involving physical exertion on tissue properties, the onset of muscular fatigue, and postural stability among both older and younger active workers. Methods: A total of 41 workers, 20 aged over 50 and 21 under 40 years old, engaged in working tasks requiring at least 50% of their work shift to be spent standing, were recruited for this study. To achieve our objective, three tests were conducted at the beginning and end of a standard work shift to assess the effects of the workday on tissue properties, muscle fatigue, and postural stability. Initially, disc height was measured using a stadiometer in a seated position. Then, muscle fatigue was assessed via an isometric contraction of the lumbar erector spinae muscles until exhaustion (Sorensen test). Electromyography was used to quantify a neuromuscular marker of fatigue (median frequency slope). Finally, participants' postural stability was evaluated using a force platform measuring root mean square, median frequencies, velocities in the anteroposterior and mediolateral directions, and displacement areas. Participants stood on the platform continuously for 30-second intervals under three conditions (eyes open, eyes closed, and on an unstable surface). Differences between older and younger worker groups were analyzed using repeated-measure ANOVAs. Preliminary Results: Initial findings indicated significant differences in postural stability (ML and AP velocities), endurance of the low back muscles, and stadiometer measurements (p<0.05) between the beginning and the end of participants' work shifts. Postural stability, endurance, and stadiometer measurements were deteriorated after the workday. Additionally, differences between older and younger workers were observed in postural stability (velocity AP, RMS AP) (p<0.05), with older workers demonstrating a decrease in postural stability than their younger counterparts. Research Implications: This study tends to understand the physical limitations and changes in older workers for adapting tasks and job requirements. The study's focus on the lumbar region and

could provide insights into preventive measures or interventions to reduce the incidence of low back pain.

O.1.3: Potential biomarkers extracted from multi-channel sEMG for sarcopenia early screening among community-dwelling Seniors

Haoru He, West China Hospital of Sichuan University; Na Li, West China Hospital of Sichuan University; Ning Jiang, West China Hospital Sichuan University; Jiayuan He, West China Hospital of Sichuan University

BACKGROUND AND AIM: : Sarcopenia is a clinical syndrome manifested as an age-related decline in muscle mass, muscle strength, and function. The incidence rate among the natural population ranges from 10% to 27% and usually leads to irreversible serious adverse health conditions if not treated early. Because of its insidious onset, it is often ignored until too late. Therefore, it is important to develop novel early screening tools for Sarcopenia in community settings. In this study, we hypothesized that biomarkers can be extracted from surface EMG (sEMG) for such a purpose. We investigated how multi-muscle coordination is altered by sarcopenia by symmetry analyses of sEMG data acquired during different levels of handgrip contractions. Methods: Ten senior individuals diagnosed with sarcopenia and ten age-matched healthy seniors were recruited for this study. The diagnosis was performed according to AWGS 2019. Participants performed handgrip tests for three trials to determine maximum voluntary contraction (MVC) with the dominant hand. Then they were asked to maintain a ten-second grasp at 20% and 50% of MVC randomly for four trials, respectively. EMG signals were acquired from brachioradialis (BRA), flexor carpi ulnaris (FCU), flexor carpi radialis (FCR), extensor carpi ulnaris (ECU), flexor digitorum superficialis (FDS), extensor digitorum (ED). Zero crossing (ZC) and median frequency (MDF) were extracted from the sEMG. Hexagon plots were based on the normalized values of six channels. Incenter-circumcenter distance (ICD) of the hexagon was used to measure its geometric symmetry. An unpaired t-test was used to compare group means with a significant level of 0.05. For nonparametric tests, the Mann-Whitney U-test was used for group comparisons. RESULTS: There were no differences between the two groups in age, calf circumference, BMI, and SMI. The duration of the 5-time chair-to-stand test was prolonged significantly in the patient group, which indicated that the lower limb function decreased more rapidly than the upper extremities. ICD of ZC had a statistically significant difference between the two groups ($p=0.015$) at 20% MVC, but no significance was found at 50% MVC ($p=0.105$). This result showed that the ZC differences between the groups are more pronounced at lower levels of contractions and suggested a potential relation to local muscle fiber changes or control strategies. There was no significant difference ($p=0.481$) in MDF at either contraction level. CONCLUSIONS: These results suggested that, at low contraction levels, the deviation from the maximal contraction patterns is larger in the healthy group. Conversely, the upper limb force generation pattern is more consistent across contraction levels. The difference observed in ZC indicates a potential biomarker for sarcopenia detection, and further research is warranted.

O.1.4: Impact of motor unit firing patterns on exercise pressor response in older hypertensive individuals

Ryosuke Takeda, CU; Tetsuya Hirono, Kyoto University; Taichi Nishikawa, Chukyo university; Tsubasa Amaike, Chukyo University; Kaito Igawa, Chukyo University; Rii Shinoda, Chukyo University; Shigehiko Ogoh, Toyo University; Kohei Watanabe, Chukyo University

Older hypertensive individuals exhibit significant variability in exercise pressor response (Delaney et al. 2010). Blood pressure (BP) increases with the activation of fast-twitch motor units (MUs) (Petrofsky et al. 1981). Since MU recruitment adheres to a hierarchical firing pattern, where low-threshold MUs (slow-twitch) discharge at a high frequency and high-threshold MUs (fast-twitch) discharge at a low frequency during submaximal exercise, an exaggerated exercise pressor response is less likely occur with relatively low-intensity exercise. However, this hierarchical MU firing pattern diminishes with aging (Watanabe et al. 2016). This study aimed to determine the relationship between the hierarchical MU firing pattern and exercise pressor response in older hypertensive individuals. We hypothesized exercise pressor response is exaggerated in hypertensive individuals without a hierarchical MU firing pattern.Fourteen older hypertensive [systolic BP (SBP≥130 mmHg), mean±SD, 74.7±5.5yr, 8 females] and 13 normotensive individuals (SBP<130 mmHg, 70.5±7.6yr, 8 females) were included in this study. High-density surface electromyography signals recorded during the ramp-up exercise until reaching 70% of their maximal voluntary contraction (MVC) were utilized to assess the MU firing pattern. This assessment involved evaluating the hierarchical MU firing pattern by analyzing “the slope” of the linear regression between firing rates of individual MUs and their recruitment thresholds. Forearm BP was measured before and during each intensity level of the incremental rhythmic isometric knee extension exercise (Ex) from 10 to 70% MVC.During Ex from 10 to 40% MVCs, the change in SBP from baseline (ΔSBP) was more pronounced in hypertensive group compared to the normotensive group (interaction, p=0.006). The hypertensive group also showed a higher variability in exercise pressor response than the normotensive group, especially at 30%MVC (hypertensive vs normotensive, 22±17 vs 10±5 mmHg, p=0.010). The slope was significantly different between the groups (p=0.030), but there was no difference in the post hoc test. Notably, within the hypertensive group, there was a positive correlation between ΔSBP and slope at 30%MVC (r=0.660, P=0.010).Restricted muscle blood flow associated with increased intramuscular pressure occurs during isometric exercise at 30-50% MVC (Osada et al. 2015). Hypertensive individuals with a steeper slope (indicating a significant disappearance of the hierarchical MU firing pattern) might require MUs with a high recruitment threshold discharge at a higher frequency. This scenario potentially prompts a quick restriction of muscle blood flow, leading to a more substantial elevation in SBP in contrast to hypertensive individuals with a less steep slope.In the hypertensive group, the increase in exercise pressor response during submaximal exercise is greater in individuals with a more pronounced loss of hierarchical MU firing pattern.

O.1.5: Modulation of motor unit discharge rate as a function of contraction intensity in young and older adults

Christopher Connelly, Loughborough University; Tamara Valenčič, Loughborough University; Haydn Thomason, Loughborough University; Mathew Piasecki, Nottingham University; Greg Pearcey, Memorial University of Newfoundland; Jonathan P Folland, Loughborough University; Jakob Škarabot, Loughborough University

Background and Aim: Older adults undergo alterations in the neuromuscular system ultimately leading to reduced muscle force generating capacity. The force exerted by a muscle is controlled by motor unit (MU) recruitment and discharge rate, with the latter having been shown to decrease with advancing age. However, less is known about MU discharge rate modulation with increased contraction intensity in aged compared to younger individuals with alterations in motoneuron structural integrity, ionotropic synaptic input, and neuromodulation indicating potentially greater age-related effects at higher contraction intensities. Therefore, we aimed to examine tibialis anterior (TA) MU discharge rate modulation across a wide range of contraction intensities in older compared to young adults. Methods: Fourteen young (6 female; 24±5 years) and 14 older adults (6 female; 71±4 years) matched for physical activity levels (3938 [2723, 6661] vs. 3431 [2068, 4795] MET.min/week, p=0.57) performed isometric dorsiflexion contractions both of a trapezoidal (10 s hold phase) and triangular shape (10 s ascending/descending phase) at 30%, 50% and 70% of maximum voluntary force (MVF). Multichannel electromyography signals were recorded from TA with a 64-channel array and were decomposed using Convolution Kernel Compensation algorithm into MU spike trains. From MU spike trains identified during trapezoidal contractions mean discharge rate during the hold phase was calculated. The MU spike trains during triangular contractions were smoothed with support vector regression, followed by the calculation of the onset-offset hysteresis of pairs of MUs (ΔF) to estimate the magnitude of persistent inward currents. Linear mixed effects models were used to determine if MU properties were predicted by age, contraction intensity and their interaction with MU recruitment threshold as a covariate. RESULTS: Dorsiflexion MVF was not significantly different between young and older adults (322 [278, 366] vs. 262 [222, 302] N; p=0.06). There was a significant interaction between age and contraction intensity for MU discharge rate (p=0.006). However, post hoc testing did not indicate any differences at individual contractions intensities (30% MVF: 14.5 [13.0, 16.0] vs. 12.7 [11.2, 14.1] pps, p=0.49; 50% MVF: 19.4 [17.9, 20.9] vs. 18.0 [16.5, 19.4] pps, p=0.71; 70% MVF: 26.0 [24.5, 27.5] vs. 25.3 [23.9, 26.8] pps; p=0.99). A significant age by contraction intensity interaction was also noted for ΔF (p<0.001), with greater ΔF noted for young compared to older adults at 70% (6.3 [5.7, 7.0] vs. 4.5 [3.8, 5.2] pps, p=0.006), but not 50% (5.8 [5.1, 6.4] vs. 4.4 [3.7, 5.1] pps, p=0.077) or 30% MVF (4.8 [4.1, 5.5] vs. 4.1 [3.4, 4.8] pps, p=0.6). CONCLUSION: : These findings demonstrate that MU discharge properties are differentially modulated from low to high contraction intensities between young and older individuals in the TA, suggesting alterations in the gain modulation of aged motoneurons.

O.1.6: Daily quercetin ingestion alters the effects of moderate-intensity resistance training on muscle strength and motor unit behavior in older adults

Taichi Nishikawa, Chukyo university; Ryosuke Takeda, CU; Kaito Igawa, Chukyo University; Saeko Ueda, Sugiyama Jogakuen University; Kohei Watanabe, Chukyo University

INTRODUCTION: As motor units are recruited according to the size principle, moderate-intensity resistance training cannot recruit motor units with a high recruitment threshold (Miller et al., J Strength Cond Res., 2020). Therefore, high-intensity resistance training is necessary to adapt to neurological factors in older adults and has been considered a viable strategy to prevent age-related muscle strength decline (Unhjem et al., J. Gerontol. A Biol. Sci. Med. Sci., 2021). Quercetin ingestion lowers the motor unit recruitment threshold and alters motor unit activity during a single session of resistance training (Nishikawa et al., Eur J Appl Physiol. in

press; Nishikawa et al., Appl Physiol Nutr Metab. in press). These results suggest that quercetin ingestion induces recruitment of motor units with high recruitment thresholds during moderate-intensity resistance training, which may enhance the adaptation of motor unit activity and muscle strength. This study investigated whether quercetin ingestion would improve adaptations in motor unit activity and muscle strength to moderate-intensity resistance training in older adults. Methods: Twenty-six older adults (72.2±4.4 yr, 11 males, 15 females) were assigned to either quercetin (QUE) or placebo groups (PLA). They participated in 6 weeks of isometric knee extension training and daily capsule ingestion intervention. Maximal voluntary contraction (MVC), motor unit firing properties and lower extremity muscle mass were measured before and after the intervention. As motor unit firing properties, motor unit firing rate, and the regression line between the recruitment threshold and firing rate were calculated by high-density surface electromyography and the Convolution Kernel Compensation method (Holobar et al., Clin Neurophysiol., 2009). Mixed-2way ANOVA (Time x Group) assessed statistical differences. RESULTS: There was significant interaction for MVC (QUE, 93.9±24.9 to 105.9±25.0 Nm; PLA, 111.2±46.5 to 117.1±48.9 Nm; p<0.01), and change in MVC was greater in QUE than PLA (QUE, +15.1%; PLA, +5.3%; p=0.01) (Fig.1A). There was significant interaction for motor unit firing rate (QUE, 14.1±3.4 to 16.0±4.4 pps; PLA, 13.9±3.7 to 14.2±4.7 pps; p=0.02), and post-hoc tests indicated motor unit firing rate increased in QUE (p=0.01), but not in PLA (p>0.99) (Fig.1B). Additionally, there were significant interactions for the intercept (QUE, 16.5±1.4 to 18.9±2.4 pps; PLA, 14.9±2.4 to 15.4 to 3.6 pps; p=0.04) and slope (QUE, -0.05±0.06 to -0.12±0.11 pps/%MVC; PLA, -0.05±0.01 to -0.03±0.03 pps/%MVC; p=0.01) from the regression line. There was no significant interaction (QUE, 12.5±2.0 to 12.3±1.9 kg; PLA, 14.1± 2.9 to 14.0±2.9 kg; p=0.61) and no main effects of Time (p=0.33) for muscle mass (Fig.1C). CONCLUSION: Daily quercetin ingestion altered motor unit firing properties and improved muscle strength by approximately 10% compared to placebo, through 6 weeks of moderate-intensity resistance training in older adults.

O.1.7: Vastus lateralis motor unit discharge characteristics in knee osteoarthritis

Jakob Škarabot, Loughborough University; Christopher D Connelly, Loughborough University; Tamara Valenčič, Loughborough University; Ales Holobar, University of Maribor, Faculty of Electrical Engineering and Computer Science; Mathew Piasecki, Nottingham University; Stefan Kluzek, University of Nottingham, United Kingdom; University of Oxford, United Kingdom; Jonathan P Folland, Loughborough University

Background and Aim: Knee osteoarthritis (OA) is a degenerative condition of the knee joint characterised by joint pain, stiffness, inflammation, and swelling leading to functional impairments. The latter are commonly underpinned by reduced knee extension strength and quadriceps voluntary activation (VA). In this study, we examined differences in vastus lateralis (VL) motor unit (MU) discharge properties in individuals with knee OA compared to age-matched controls as a potential basis for reduced VA. Methods: Fourteen individuals with confirmed knee OA (7 female; 72 ± 7 years, WOMAC score: 29 ± 14) and 14 controls (7 female; 71 ± 4 years, WOMAC score: 1 ± 2) performed unilateral maximal isometric knee extensions during which they received percutaneous nerve stimulation of the femoral nerve to quantify VA. Subsequently, participants performed trapezoidal contractions at 10, 20, 30, 50, and 70% of maximal voluntary force (MVF) with multichannel electromyography (EMG) recordings of VL. The EMG signals were decomposed using Convolution Kernel Compensation algorithm yielding

individual MU spike trains, from which discharge rate at recruitment and derecruitment, and the plateau phase of contractions were quantified. Additionally, coherence of MU spike trains obtained during 10% and 20% MVF contractions was calculated in the delta (0-5 Hz), alpha (5-12 Hz), and beta (12-30 Hz) bands. RESULTS: Both groups had similar MVF with no differences between legs (group by leg interaction: F=3.4, p=0.0668; OA: affected vs. less-affected leg, 339 [270, 407] vs. 382 [313, 450] N; Control: 401 [332, 470] vs. 396 [328, 465] N). A group by leg interaction was found for VA (F=6.1, p=0.0138) with differences between the legs detected for OA (82.7 [78.4, 87.0] vs. 90.2 [86.1, 94.4] N, p=0.0095), but not for controls (88.4 [84.1, 92.7] vs. 88.6 [84.4, 92.4] N). A significant group by contraction intensity interaction was observed for mean VL discharge rate (F=50.7, p<0.0001), suggesting a smaller relative increase in discharge rate with greater contraction force in OA individuals compared to controls. The between-leg discrepancy between groups was detected for MU discharge rate at recruitment (F=13.1, p=0.0003) and at derecruitment (F=13.1, p=0.0030) with the affected leg exhibiting lower initial discharge rate compared to less affected leg in OA (6.7 [6.3, 7.1] vs. 7.0 [6.6, 7.5] N, p<0.0001), but not in controls (6.9 [6.3, 7.1] vs. 7.0 [6.6, 7.5] N, p=0.0545). Greater coherence was found in OA individuals compared to controls in the alpha (z-score: 0.46 [0.42, 0.50] vs. 0.39 [0.35, 0.43], p = 0.0121), but not in the delta (p=0.8821) or beta bands (p=0.4189). CONCLUSIONS: The lower VA in the affected leg of knee OA individuals is accompanied by smaller VL MU discharge rate at recruitment and greater oscillations of MU discharges in the alpha band. These findings further our understanding of neural underpinnings of reduced VA levels in knee OA.

Oral Session 2

O.2.1: Muscle control strategies of the central nervous system (CNS) in terms of muscular coactivation and muscle synergies when performing unfamiliar tasks

Elisa Romero Avila, Institute of Applied Medical Engineering; Catherine Disselhorst-Klug, Institute for Applied Medical Engineering, RWTH Aachen University

The central nervous system (CNS) controls the coordination and execution of complex movements, regulates muscle activation via functional modules (synergies), acquires new motor skills, and supports joint stability. Particularly when acquiring new motor skills, modifications in the muscular activation patterns occur (i.e., increased coactivation of antagonist muscles), and even new muscle synergies may rise alongside alterations in the existing ones. Moreover, movement velocity seems to influence these modifications in muscular activation patterns and the appearance of new muscle synergies. AIM: The aim of this work is to investigate how muscle synergies and muscle coactivation change while performing unfamiliar elbow flexion/extension tasks with different movement velocities. METHODOLOGY: Twenty healthy subjects were recruited, and the muscular activation of the biceps, brachioradialis, and triceps was recorded during elbow flexion and extension movements in the sagittal and transverse planes. Movements in the transverse plane were selected to represent movements rarely used in daily life and, therefore, unfamiliar to the subjects. Additionally, a 3D motion capture system was used to determine elbow joint position, movement velocity, and movement direction. The resulting sEMG envelopes of both conditions were time-normalized and categorized based on the type of contraction (concentric/eccentric) and different angular

velocities. Finally, muscle synergies for each category were extracted using a non-negative matrix factorization algorithm. RESULTS: Regarding changes in muscle coactivation, the results showed statistically significant differences between both conditions, with an increase in the sEMG envelope of the three muscles when the measurements were performed in the transverse plane. Moreover, this increase was also detected for increasing angular velocity, with significant differences between slow and fast movements. Concerning muscle synergies, no differences between the sagittal and transverse planes were observed in the number of synergies. However, one muscle synergy was primarily found during elbow flexion on both conditions and during elbow extension, two muscle synergies were identified in half of the participants on both conditions. Additionally, the synergy weights in the transverse plane were higher than in the sagittal plane. These changes were also observed when moving with different angular velocities, where the synergy weights increased for all three muscles with increasing angular velocity. However, no effect of movement velocity on the temporal activation of the synergies was found in both conditions. CONCLUSION: Unfamiliarity with a task requires suitable neuromuscular coordination patterns. Since changes in functional modules are solely visible with increasing practice of a movement, when confronted with inexperienced tasks, the CNS only applied increased muscle coactivation to control posture and movement velocity.

O.2.2: The influence of contraction intensity on muscle activity of the triceps surae in males and females during isometric plantarflexion

Timothy Green, Andrew and Marjorie McCain Human Performance Laboratory, University of New Brunswick; Usha Kuruganti, University of New Brunswick

Introduction: Plantarflexion is pivotal in gait, balance, and activities of daily living (ADLs). The triceps surae muscle group is the prime mover for plantarflexion and is primarily comprised of the gastrocnemius and soleus muscle. Few studies have used surface electromyography (sEMG) to examine the triceps surae during plantarflexion and fewer have used high-density sEMG (HDsEMG) to examine muscle activation and synergies across a range of contraction intensities. Better understanding of the triceps surae muscle group during plantarflexion can provide valuable information to aid in training programs, injury rehabilitation plans, and lower leg muscular models. Aim: The purpose of this study was to compare HDsEMG spatial features and co-contraction indices (CCI) of the triceps surae muscles during low, moderate, high, and maximal plantarflexion contractions to examine muscle synergies. Methods: Ten participants (5 males, 5 females, mean age = age=22.6 2.2 years) completed ramped (trapezoidal) isometric plantarflexion contractions using an isokinetic dynamometer (Cybex, HumacNorm) with feedback at low, moderate, and high intensities. High-density sEMG electrode grids (HD10MM0804) were placed over the medial and lateral gastrocnemius (GM and GL respectively) and soleus (SM and SL respectively) of each leg and muscle activity was recorded wirelessly (OTBioelettronica, Turin, Italy). HDsEMG features including average rectified value (ARV) and median frequency (MF) along with CCI were compared between muscles and across intensities. Significant differences were determined using an Analysis of Variance (ANOVA). Tukey's post-hoc tests were completed when an ANOVA resulted in a p-value less than the alpha value, 0.05. Results: Preliminary results indicated no significant differences in amplitude between the four muscles (measured as ARV) regardless of leg and contraction intensity (p=0.999). However, for each leg, the four muscles produced significantly greater ARV values at 100% MVC compared to 25% MVC (p<0.05). Statistical tests indicated no significant

differences between CCI values. However, preliminary results suggest differences in synergistic muscle behaviour based on mean CCI values. CONCLUSIONS: While the triceps surae plays an important role in many ADLs, often the soleus muscle is omitted in sEMG studies. The present study explored both heads of the gastrocnemius and soleus during maximal and submaximal plantarflexion contractions. It was found that all muscles demonstrated greater ARV at 100% MVC than 25% MVC for both legs indicating that as contraction intensity increased, the muscle activation increased. However, the rate of increase was not examined, and this could provide greater insight regarding plantarflexor muscle synergies. While no significant differences were found, CCI mean values varied for muscle pairs. Specifically, CCI values that compared the medial and lateral soleus indicated high agreement between the two muscle heads across all contraction intensities. The CCI values that compared the gastrocnemius and soleus indicated less involvement from the soleus muscle as contraction intensity increased (Figure 1). Overall, CCI values indicated as plantarflexion contraction intensity increased the involvement of the soleus muscle decreased. Data collection is ongoing, and it is possible that with a larger data set, significant differences will be detected for CCI.

O.2.3: Neuromuscular control changes in Parkinson's disease after deep brain stimulation: insights from muscle synergy parameters

Marco Ghislieri, Politecnico di Torino; Fabrizio Sciscenti, Politecnico di Torino; MARCO KNAFLITZ, POLITECNICO DI TORINO; Laura Rizzi, University of Turin; Michele Lanotte, University of Turin; Valentina Agostini, Politecnico di Torino

BACKGROUND AND AIM: The bilateral Deep Brain Stimulation of the SubThalamic Nucleus (STN-DBS) was proven successful in alleviating the motor symptoms of patients suffering from Parkinson's Disease (PD). Although recent advances highlighted that muscle synergy analysis constitutes a powerful tool in the investigation of PD motor control changes after STN-DBS [1], a few quantitative parameters have been introduced so far in the literature, to be used as outcome measures. This work aims at presenting specific parameters extracted from muscle synergies for objectively evaluating the possible modifications of PD motor control strategies after STN-DBS neurosurgery. More specifically, the following parameters were computed: Full-Width at Half Maximum (FWHM) and its Coefficient of Variation (CoVFWHM) to assess the duration and the repeatability of the activation coefficients, respectively. Methods: A group of 20 PD patients underwent a 5-minute gait analysis (including sEMG recordings from 12 lower-limb and trunk muscles) at 3 different time points: before STN-DBS (T0), at 3 months after STN-DBS (T1), and at 12 months after STN-DBS (T2). A group of 20 age-matched controls was also tested, to have a reference dataset. Muscle synergies were computed from the sEMG envelopes as described in Ref. [1]. Then, FWHM was computed from the activation coefficients as the number of points exceeding half of the curve's maximum, after subtracting the minimum [2]. Results AND DISCUSSION: On average, FWHM is increased in PD patients compared to controls, at every time point (T0: p<10-5, T1: p<10-6, T2: p<10-4), revealing widened activation coefficients in PD patients due to pathology-related motor impairments. CoVFWHM is also increased in PD patients at T0 ($p=0.004$), but then it becomes not different from that of controls at T1 ($p=0.1$) and T2 ($p=0.2$), revealing more repeatable motor control strategies over task duration after STN-DBS. The preliminary results obtained revealed that FWHM and CoVFWHM, extracted from the muscle synergy activation coefficients, are appropriate outcome measures for assessing the changes in neuromuscular control due to pathology-related motor

impairments and STN-DBS neurosurgery, respectively.ACKNOWLEDGMENTS: This study was carried out within the «PD-DBS» project (protocol N° 2022KWSJJT) – funded by the Ministero dell'Università e della Ricerca – within the PRIN 2022 program (D.D.104 - 02/02/2022). This manuscript reflects only the authors' views and opinions and the Ministry cannot be considered responsible for them.REFERENCES[1] Ghislieri, M. et al. Muscle synergies in Parkinson's disease before and after the deep brain stimulation of the bilateral subthalamic nucleus. Sci Rep 13, 6997 (2023). doi: 10.1038/s41598-023-34151-6[2] Cappellini, G. et al. Immature Spinal Locomotor Output in Children with Cerebral Palsy. Front. Physiol. 7: 478. doi: 10.3389/fphys.2016.00478

O.2.3: Impact of electrode placement on muscle synergy extraction: insights from lower-limb sEMG signals

Marco Ghislieri, Politecnico di Torino; Taian Vieira, Politecnico di Torino; Valentina Agostini, Politecnico di Torino; Marco Gazzoni, Politecnico di Torino

BACKGROUND AND AIM: It is widely accepted that the central nervous system simplifies motor control by selecting and modulating a reduced number of motor modules, called muscle synergies. Muscle synergies are extracted from surface electromyographic (sEMG) signals through different factorization techniques. SEMG signals are typically collected through a bipolar electrode configuration, usually placing the pairs of electrodes on the muscle's belly. However, recent research has indicated that different muscle regions may contribute to distinct mechanical functions [1]. Therefore, this study tests the hypothesis that sEMG taken from different regions of individual muscles may affect muscle synergy compositions. Methods: Twenty healthy volunteers participated in the study at the Motion Analysis Laboratory of the PolitoBIOMed Lab of Politecnico di Torino (Turin, Italy). SEMG signals were acquired from 8 lower-limb muscles during a treadmill walking task. For six out of eight muscles (i.e., rectus femoris, vastus medialis, biceps femoris, semitendinosus, gastrocnemius, and soleus), sEMG signals were acquired considering two different electrode placements (i.e., proximal and distal placement). First, the sEMG envelopes calculated from the proximal and distal electrodes were compared to test differences in the muscle activation patterns between the two regions. Then, muscle synergies were extracted from the sEMG envelopes through the non-negative matrix factorization algorithm [2] and their compositions were assessed to test the influence of sEMG electrode placement on muscle synergies. Results AND DISCUSSION: Statistically significant differences were found in the sEMG envelopes of 4 out of 6 muscles (i.e., rectus femoris, vastus medialis, biceps femoris, and gastrocnemius) between proximal and distal placement, revealing that different muscle regions may show different muscle activation patterns and contribute to different biomechanical functions. Nevertheless, not all the differences observed in the sEMG envelopes between the proximal and distal placements had an impact on the muscle synergy composition. This result can be interpreted in two ways depending on the application context. On the one hand, the muscle synergy model may not be sensitive to the excitation of different muscle regions. On the other hand, at least for the condition we tested, the excitation of distinct regions of the leg muscles may be of limited relevance.REFERENCES[1] Watanabe, K. et al. Novel Insights into Biarticular Muscle Actions Gained from High-Density Electromyogram. Exerc Sport Sci Rev 49, 3 (2021). doi: 10.1249/JES.0000000000000254[2] Ghislieri, M. et al. Muscle synergies in Parkinson's disease before and after the deep brain

stimulation of the bilateral subthalamic nucleus. Sci Rep 13, 6997 (2023). doi: 10.1038/s41598-023-34151-6

O.2.4: Flexible and independent control of synergist muscles during standing balance

Christopher Thompson, Temple University; Martin Zaback, Temple University

Neural control of synergistic muscles is commonly thought to involve a shared synaptic drive to these motor pools. We demonstrate that the synergists within the human triceps surae can receive entirely opposite neural drives, enabling independent control of synergist muscles in a task-dependent manner. Ten healthy young adults participated in a series of dual and single-leg standing trials on independent force plates, during which high-density electromyography (EMG) was collected from the right soleus (SOL), medial gastrocnemius (MG), and lateral gastrocnemius (LG). Offline, the EMG data were decomposed into individual motor units and cleaned using a semi-automated algorithm. The center of pressure (COP) was calculated for each trial. A rotation matrix was iteratively applied at 5º increments to the 2-dimensional COP data, generating 72, 1-dimensional time series corresponding to COP movement about 360 degrees. Prominent peaks were identified in each COP time-series. EMG data were trigger-averaged to these peaks and the amplitude of event-related EMG was calculated to construct EMG tuning curves. During two-legged standing, active muscles of the triceps surae showed nearly identical EMG tuning curves, with maximal excitation oriented primarily along the sagittal plane. However, during one-legged standing, significant deviations in the tuning curves were observed, with the LG showing a nearly orthogonal activation pattern compared to the SOL and MG. In particular, LG was maximally excited with eversion but inhibited with inversion, whereas SOL and MG were maximally excited with inversion but inhibited with eversion. These findings were confirmed with peristimulus frequencygrams generated from the decomposed motor unit data. These results demonstrate that, depending on the nature of the balance task, muscles of the triceps surae can contribute to corrective ankle torques outside of the sagittal plane. The muscles of the triceps surae act as a functional unit during bipedal standing but can operate independently during single leg stance. This independent control allows muscles that normally function as synergists to act as antagonists, accommodating the biomechanical constraints of specific tasks.

O.2.5: Athletes with hamstring injuries exhibit lower EMG-EMG coherence of posterior chain coordination muscles during a single-leg postural lean

Amornthep Jankaew, National Cheng Kung University; Yih-Kuen Jan, University of Illinois at Urbana-Champaign; Cheng-Feng Lin, National Cheng Kung University

Background: Athletes with hamstring strains display activation deficits and poor motor control during functional tasks. However, there is limited evidence on how the strains affect coordinated activation of the hamstrings and associated muscles during postural control in the athletic population. Methods: 10 hamstring injured athletes (4 with LH and 6 with MH injuries; 22.20±3.26 years old with 8.40±5.48 months of injury) and 10 healthy-matched controls (21.60±1.35 years old) were recruited. Surface EMG electrodes were attached to the gluteus maximus (GM), lateral hamstring (LH), medial hamstring (MH), and medial gastrocnemius (MG). Participants completed three trials of single-leg postural stability, each lasting 15 seconds, with eyes-closed and eyes-open, while leaning forward and backward. EMG-EMG coherence was

assessed for five muscle pairs (LH-MH, LH-GM, LH-MH, MH-GM, and MH-MG) on the injured leg and matched leg, within the alpha (5-15Hz) and beta bands (15-45Hz). Concurrently, COP trajectories were analyzed for both directions. A two-way repeated measure ANOVA was employed to compare group and muscle pair differences in both directions, with a significant level set at 0.05. RESULTS: A significantly lower coherence was observed in the injured group, specifically in the α band for LH-MH during both forward and backward leans (F=19.928, p<0.001 and F=9.316, p=0.007, respectively). This trend was also observed for LH-MG during forward leans (F=18.050, p<0.001) and backward leans (F=7.456, p=0.014), as well as for MH-MG during forward leans (F=8.261, p=0.010) and backward leans (F=14.976, p=0.001) compared to the control group. Regarding the eye effects, the eyes-closed resulted in lower coherence in the β band for LH-GM (forward: F=6.277, p=0.022; backward F=11.571, p=0.003), MH-GM (forward: F=19.778, p<0.001; backward F=41.831, p<0.001), and MH-MG (forward: F=7.649, p=0.013; backward F=25.296, p<0.001). Deficits in muscle synchronization in the injured group led to a higher 95% sway area during backward leans (F=5.125, p=0.036). Furthermore, the eye conditions influenced the AP and ML sway range and the 95% sway area, with all p<0.001 except for the 95% sway area in the forward lean (F=17.065, p=0.001). CONCLUSION: : Athletes with hamstring injuries exhibited lower EMG-EMG coherence in the hamstrings and associated muscles compared to the control group. This indicated a decrease in the synchronous activation of the corticospinal inputs in athletes with hamstring injuries. Impairment in muscle synchronization resulted in poorer balance performance during challenging balance tasks in both forward and backward directions. Moreover, we found that the eyes-closed conditions had lower EMG coherence compared to the eyes-open condition. Therefore, our findings suggest that rehabilitation programs should focus on improving muscle synchronization to enhance postural stability by incorporating different eye conditions into training programs.

O.2.6: sEMG on muscle groups innervating the hand and fingers in hanging onto a thin hold in sport climbing.

Katsura Konishi, Keio University; Yuji Ohgi, Keio University

Sport climbing requires different grip techniques depending on the types of hold shapes. For a small and thin hold, crimp, half-crimp and slope grips are commonly used by climbers. Interestingly, the climber has their own strong and weak grip techniques. Previous studies have suggested that configuration of the wrist joint plays an important role in each grip technique.The purpose of this study was to clarify the influence of the wrist joint and fingers configuration on each grip technique by using surface electromyography measurements. An experimental climbing wall was settled up for this study. All thin hand holds were equipped with a single-axis load cell to measure vertical reaction forces. The subjects performed a hanging position and two sequential climbing motion with the left hand and the right hand in that order by three different grip techniques. Five male climbers aged 20 to 23 who are Japanese national team level were recruited. The Ag/AgCl surface electrodes (ϕ6) were affixed on the right arm at flexor digitorum superficialis (FDS), flexor digitorum profundus (FDP), flexor carpi ulnaris (FCU), flexor carpi radialis (FCR), extensor carpi ulnaris (ECU) and extensor carpi radialis (ECR). The sampling frequency was 1 kHz. The acquired data were smoothed using a Butterworth low pass filter, then the average rectified value (ARV) was calculated. The median of each muscle ARV in the crimp grip was used as a reference and compared to those in the half-crimp and slope grips. For

all subjects, their ARV amplitude of extensor carpi ulnaris (ECU) showed at least 20% greater in the crimp grip rather than those of the half-crimp and slope grips. Also, except one subject, their ARV amplitude of flexor digitorum superficialis （FDS) obviously larger than those of other five muscles. Especially, the difference between ARV of FDS and FCR was distinguished.

O.2.7: Neuromuscular control changes in Parkinson's disease after deep brain stimulation: insights from muscle synergy parameters

Marco Ghislieri, Politecnico di Torino; Fabrizio Sciscenti, Politecnico di Torino; Marco Knaflitz, Politecnico Di Torino; Laura Rizzi, University of Turin; Michele Lanotte, University of Turin; Valentina Agostini, Politecnico di Torino

BACKGROUND AND AIM: The bilateral Deep Brain Stimulation of the SubThalamic Nucleus (STN-DBS) was proven successful in alleviating the motor symptoms of patients suffering from Parkinson's Disease (PD). Although recent advances highlighted that muscle synergy analysis constitutes a powerful tool in the investigation of PD motor control changes after STN-DBS [1], a few quantitative parameters have been introduced so far in the literature, to be used as outcome measures. This work aims at presenting specific parameters extracted from muscle synergies for objectively evaluating the possible modifications of PD motor control strategies after STN-DBS neurosurgery. More specifically, the following parameters were computed: Full-Width at Half Maximum (FWHM) and its Coefficient of Variation (CoVFWHM) to assess the duration and the repeatability of the activation coefficients, respectively. Methods: A group of 20 PD patients underwent a 5-minute gait analysis (including sEMG recordings from 12 lower-limb and trunk muscles) at 3 different time points: before STN-DBS (T0), at 3 months after STN-DBS (T1), and at 12 months after STN-DBS (T2). A group of 20 age-matched controls was also tested, to have a reference dataset. Muscle synergies were computed from the sEMG envelopes as described in Ref. [1]. Then, FWHM was computed from the activation coefficients as the number of points exceeding half of the curve's maximum, after subtracting the minimum [2]. Results AND DISCUSSION: On average, FWHM is increased in PD patients compared to controls, at every time point (T0: p<10-5, T1: p<10-6, T2: p<10-4), revealing widened activation coefficients in PD patients due to pathology-related motor impairments. CoVFWHM is also increased in PD patients at T0 (p=0.004), but then it becomes not different from that of controls at T1 (p=0.1) and T2 (p=0.2), revealing more repeatable motor control strategies over task duration after STN-DBS. The preliminary results obtained revealed that FWHM and CoVFWHM, extracted from the muscle synergy activation coefficients, are appropriate outcome measures for assessing the changes in neuromuscular control due to pathology-related motor impairments and STN-DBS neurosurgery, respectively.ACKNOWLEDGMENTS: This study was carried out within the «PD-DBS» project (protocol N° 2022KWSJJT) – funded by the Ministero dell'Università e della Ricerca – within the PRIN 2022 program (D.D.104 - 02/02/2022). This manuscript reflects only the authors' views and opinions and the Ministry cannot be considered responsible for them.REFERENCES[1] Ghislieri, M. et al. Muscle synergies in Parkinson's disease before and after the deep brain stimulation of the bilateral subthalamic nucleus. Sci Rep 13, 6997 (2023). doi: 10.1038/s41598-023-34151-6[2] Cappellini, G. et al. Immature Spinal Locomotor Output in Children with Cerebral Palsy. Front. Physiol. 7: 478. doi: 10.3389/fphys.2016.00478

Oral Session 3

O.3.1: Effect of anticipation and sex on trunk and knee biomechanics during side-step cutting: implications for noncontact ACL injury

Mika Konishi, Universirty of Tsukuba; Nicholas C Clark, University of Essex; Masahiro Takemura, University of Tsukuba; Nelson Cortes, University of Essex

BACKGROUND AND AIM: Anterior cruciate ligament (ACL) sprains are among the most severe athletic knee injuries with an incidence 2-3 times higher in females than males. ACL injuries typically occur in rapidly changing, unanticipated, and noncontact athletic situations. Combined dynamic knee valgus, tibial internal rotation (IR), ipsilateral trunk tilt, and contralateral trunk rotation are considered the most common biomechanical characteristics for noncontact ACL injury, where all are exacerbated during unanticipated versus anticipated side-step cutting. We investigated the effect of anticipatory conditions and sex on these variables during side-step cutting. Methods: Thirty-two recreational athletes (16 males, 16 females) performed anticipated and unanticipated 45° side-step cutting tasks from a 30 cm high box using the dominant leg. In the unanticipated condition, a visual light stimulus was randomly triggered using a wireless sensor (Swift Neo wireless systems, Swift Performance, Australia) during the motion of hopping down from the box. Three-dimensional motion analysis and a force plate were used to quantify kinematics and kinetics (VICON, Oxford, England). Dependent variables included: trunk and knee biomechanics at initial contact (IC), the peak kinematic/kinetic values within 0-50% stance phase, and peak vertical ground reaction force (vGRF). We analysed variables using a two-way repeated-measures ANOVA to determine the effect of anticipation, sex, and any interactions. RESULTS: Significant interaction effects of anticipation and sex for peak trunk rotation angle toward non-dominant leg ($F_{1,32}=4.694$, $p=0.038$) and peak vGRF ($F_{1,32}=4.274$, $p=0.047$) were evident: peak trunk rotation angle toward the non-dominant leg was significantly lower in females versus males ($p=0.016$) and peak vGRF significantly increased in males (p<0.001) during unanticipated cutting compared with anticipated cutting. During unanticipated cutting, significant increases in peak knee valgus angle (KVA) ($F_{1,32}=4.543$, $p=0.041$), peak knee IR moment ($F_{1,32}=4.544$, $p=0.041$), peak trunk tilt angle toward dominant leg ($F_{1,32}=52.165$, p<0.001), and peak vGRF ($F_{1,32}=28.006$, p<0.001) occurred during unanticipated versus anticipated cutting in both males and females. Females showed significantly greater IC and peak KVA (IC: $F_{1,32}=8.846$, $p=0.006$; peak: $F_{1,32}=7.708$, $p=0.009$) and lower IC and peak trunk flexion angle (IC: $F_{1,32}=14.565$, p<0.001; peak: $F_{1,32}=23.681$, p<0.001) compared with males in both cutting conditions. CONCLUSIONS: Our findings suggest that trunk rotation in females contributes to absorbing landing impacts in unanticipated situations. In unanticipated cutting, both males and females demonstrated biomechanical features linked to increased risk for noncontact ACL injury. Furthermore, females demonstrated more trunk/knee features linked to noncontact ACL injury versus males. Improving trunk kinematics may reduce the risk of noncontact ACL injuries, especially in females.

O.3.2: Whole-body angular momentum during cross-slope walking in unilateral transfemoral prosthesis users

Genki Hisano, Arts et Metiers Sciences et Technologies; Helene Pillet, Arts et Métiers Sciences et Technologies; Xavier Bonnet, Arts et Métiers Sciences et Technologies

Background: Outdoor walking for transfemoral prosthesis users (TFPUs) is challenged by uneven terrain, including cross-slope (Villa C et al., 2017). To achieve the dynamic balance during walking, TFPUs are required to regulate the whole-body angular momentum (WBAM) about body center of mass (COM). In particular, the increase in the positive and negative integrated WBAM (iWBAM) reflect the increase in the body's counterclock- and clock-wise rotation about the body COM throughout the gait cycle. Thus, the integrated WBAM (iWBAM) is used to quantify the effect of perturbed conditions on the dynamic balance (Leestma et al., 2023). In this study, we aimed to evaluate the dynamic balance of the TFPUs during cross-slope walking by comparing iWBAM with level-ground. Methods: Five unilateral TFPUs performed walking along a level surface and a 6° (10%) inclined cross-slope surface at a self-selected speed. Three-dimensional kinematic data were collected using reflective markers and an optical motion capture system. For each of the three surface conditions (Level-ground, Cross-slope with bottom side prosthetic, and with top side prosthetic), four successful trials were selected. The sagittal, transverse, and frontal WBAM was calculated using a 15-segment model and normalized by body mass, height and walking speed. The positive and negative iWBAM per prosthetic gait cycle were calculated as the positive and negative area under the curve of WBAM, respectively. Further, net iWBAM was calculated as the sum of positive and negative iWBAM. One-way repeated measures ANOVA was performed to compare the variables among three surface conditions. If significant main effects of surface conditions were observed, Bonferroni post-hoc multiple comparisons were performed. Statistical significance was set to P < 0.05. RESULTS: No significant main effects of surface conditions were observed in the sagittal and transverse planes for the net, positive and negative iWBAM. In the frontal plane (refer to Figure 1), while the net iWBAM showed no significant main effect, significant main effects of surface conditions were observed for both positive (P = 0.008) and negative iWBAM (P = 0.001). Post-hoc analysis found no significant difference in the positive iWBAM. However, the negative iWBAM of cross-slope conditions are significantly smaller than that of level-ground condition (bottom side prosthetic: P = 0.005, top side prosthetic: P < 0.001). CONCLUSIONS: TFPUs exhibited greater negative iWBAM during cross-slope walking compared to level-ground, particularly in the frontal plane. This suggests that TFPUs experience more rotation about the body COM on cross-slope, indicating a need for advancements in prosthetic design and rehabilitation strategies. By addressing these specific dynamic balance challenges, we may significantly improve the mobility and safety of TFPUs in varied walking conditions.

O.3.3: Unilateral vs bilateral skipping gaits : symmetric limb functions lead to temporally more demanding and mechanically more loading

Genki Tokuda, Tokyo University of Science; Ryota Morishima, Tokyo University of Science; Hiroaki Hobara, Tokyo University of Science

Intro Skipping gait includes the double support phase and flight phase. Based on the step patterns, the skipping gaits are classified into two patterns: unilateral and bilateral skipping. Unilateral skipping is an asymmetrical pattern, where the trailing and leading limbs are fixed to either the left or the right limbs, respectively [1]. In contrast, bilateral skipping is a symmetrical pattern, with the trailing and leading limb exchanges bilaterally every stride [1]. While unilateral skipping gait is commonly adopted in many quadrupedal animals, bilateral skipping gait is prevalent in bipedal humans [2]. The strategic difference may be due to the biomechanical characteristics of each skip pattern, but it remains unclear. The present study

aimed to investigate the temporal and biomechanical parameters of unilateral and bilateral skipping gait at various speeds. METHODSEight healthy male subjects without musculoskeletal impairments in their lower limb performed unilateral and bilateral skipping gait at 9 speeds (2.0 – 10.0 km/h with increments of 1.0 km/h). Both skipping gaits were performed on an instrumented treadmill (FTMH-1244WA, Tec Gihan, Kyoto, Japan), where the ground reaction forces (GRFs) were collected at 1000 Hz. Then, we determined the cadence for both skipping gaits. Since both skipping gaits has multiple GRF peaks, we further determined the peak vertical GRFs (,), negative (,) and positive peaks of anteroposterior GRFs (,), respectively. The Shapiro–Wilk test was used in both data obtained from two skipping gaits to confirm data normality. To compare GRF variables between the bilateral and unilateral skipping gaits at each speed, we used two-way repeated measures ANOVA (9 levels) and a post-hoc comparison when the data were normally distributed. If the data were not normally distributed, the Friedman test (9 levels) and a Wilcoxon signed rank test were used. Statistical significance was set at p < 0.05. RESULTS Cadence increased with increasing speeds in both skipping gaits, but the cadence of bilateral skipping was significantly higher than those of unilateral skipping in a wide range of speeds. Further, we also found that the peak vertical GRF () stayed nearly constant, but peak vertical GRF () gradually increased with increasing speeds in both skipping gaits, respectively. However, there were no significant differences in and between two skipping gaits at all speeds. We also found that the peak anteroposterior GRF (, , , ,) increases consistently in unilateral skipping. In contrast, the increase of peak anteroposterior GRFs were observed only at lower or higher speeds in bilateral skipping. Additionally, unilateral skipping generally had a smaller peak anteroposterior GRFs (, ,) compared to bilateral skipping. **Discussion** We found that the cadence of bilateral skipping was significantly higher than unilateral skipping. And also, the braking and propulsive forces of bilateral skipping were more pronounced than those of unilateral skipping. These results suggest that the bilateral skipping may be temporally more demanding and mechanically more loading than unilateral skipping.

demanding and mechanically more loading. Reference[1] Alberto Minetti, Proc. R. Soc. Lond. B (1998)[2] Pieter et al. J Exp Biol, 216 (7): 1338–1349(2013)

O.3.4: Validation of a novel limb symmetry index to discriminate movement strategies during bilateral jump landing in individuals with ACLR with and without a history of ankle sprains.

Yuki Sugimoto, Northwestern University Feinberg School of Medicine; Anamaria Acosta, Feinberg School of Medicine, Northwestern University; Julius Dewald, Northwestern University Feinberg School of Medicine

BACKGROUND AND AIM: The Limb Symmetry Index (LSI), computed from kinetic parameters, tracks knee functionality post Anterior Cruciate Ligament Reconstruction (ACLR). However, LSI may lack accuracy in individuals with ACLR and ankle sprains, as it overlooks kinetic chain coordination across lower limb joints. Previous ankle sprains (AS) contribute to altered neuromuscular control in ACLR, emphasizing the need to evaluate within-limb coordination during bilateral tasks to prevent secondary ACL injuries. The effect of Energy Absorption Contribution (EAC) on joint work provides insight into the coordination between joints during observed movements. Thus, the purpose of this study was to validate a novel LSI based on EAC for discriminating movement strategies in bilateral drop vertical jump landing (DVJL) among

individuals with ACLR and ACLR-AS. Methods: 39 healthy athletes, including 13 ACLR-AS, 13 ACLR, and 13 healthy controls, were matched by age, height, weight, sex, sport, and limb dominance. Participants performed five DVJLs with kinematics and ground reaction forces recorded. Individual joint work (M) and EAC were calculated and averaged across the middle three trials to compute the LSI on individual joint work (LSIM) and EAC (LSIEAC). Negative LSI indicates asymmetry toward the unaffected-limb (UL), while positive LSI indicates asymmetry toward the affected-limb (AL). A 3x2x3 repeated measures analysis of variance was utilized to analyze interactions between groups, the LSI method, and joint. Tukey's LSD post-hoc analyses were used to examine within and between groups (alpha=0.05). RESULTS: There was a significant interaction between the group, LSI method, and joint (F4,72=5.297, P<.001). Both LSIM and LSIEAC revealed limb asymmetry at the hip (LSIM: P=.005; LSIEAC: P=.002), knee (LSIM: P=.005; LSIEAC: P=.017), and ankle (LSIM: P=.030; LSIEAC: P=.029) for the ACLR-AS group compared to healthy controls. For the ACLR group, LSIM revealed limb asymmetry at the knee (P=.039) while LSIEAC revealed limb asymmetry at the hip (P=.026) compared to healthy controls. Within the ACLR-AS, a significant difference in the degree of asymmetry at the hip (P=.011) was identified toward the UL with LSIM (-0.25) and LSIEAC (-23.23) toward the UL. Within healthy controls, both LSIM and LSIEAC revealed a significant difference in the degree of asymmetry toward AL at the hip (P=.030) and ankle (P=.037) and toward UL at the knee (P<.001). CONCLUSIONS: Only LSIEAC was able to distinguish group differences in asymmetry at the hip for individuals with ACLR-AS and ACLR compared to healthy controls, as well as at the knee and ankle for those with ACLR-AS. Moreover, LSIEAC identified asymmetry at the hip toward AL, which is supported by existing literature, implying the use of a hip strategy to unload the surgical knee. When taken as a whole, LSIEAC offers a more complete picture of movement strategies utilized during DVJL, especially for individuals with ACLR-AS. Therefore, LSIEAC is better suited for tracking the progression of rehabilitation following ACL-R to return to activity.

O.3.5: Effects of blood flow restriction and band tissue flossing technique on ankle stability and muscle control in athletes with chronic ankle instability

Hong Wei-Hsien, Department of Sports Medicine, China Medical University, Taichung, Taiwan; Wai-Hong Chin, China Medical University; Lin Shao-Jhen, Department of Sport Medicine, China Medical University

Ankle sprain is one of the most common lower extremity joint injuries and has a 20%-30% recurrence rate, and up to 75% of them will become chronic ankle instability (CAI). Blood flow restriction (BFR) training has emerged as a novel training approach for individuals with non-surgical musculoskeletal conditions. BFR training combines low-intensity exercise with the restriction of blood flow, achieving the effects of high-intensity training. However, the cost of BFR training system is on the high for individuals. Another technique to induce vascular occlusion is band tissue flossing (BTF), which provides a more affordable and have the similar effects to the benefits of BFR. However, to date, BTF has yet to be compared to the BFR in discerning differences in the efficacies of these methods. Therefore, the purpose of this study is to evaluate the effects of BFR and BTF training on ankle stability and muscle control in individuals with CAI.Thirty participants with unilateral CAI were recruited in this study, age between 20 to 40 years, and randomly allocated to 3 different groups: BFR, BTF, and non-training as control group (CON). A four-week intervention, 30 min per day, and three days per

week, the assessments were conducted pre- and post-training. A Vicon motion analysis system, AMTI force plate and Noraxon Electromyography (EMG) system was synchronously collected for joint angles of lower limb, ground reaction force (GRF), and EMG data during a single-leg jump landing. EMG electrodes was attached on medial gastrocnemius, tibialis anterior, tibialis posterior, and fibularis longus muscles of both sides. A repeated-measures ANOVA was conducted to determine the effects of groups and test times, and Bonferroni corrected were calculated and used in the post-hoc pairwise comparisons. p < 0.05 was considered statistically significant. Results showed larger ankle dorsiflexion (p < 0.05), peroneus longus and tibialis anterior muscle activations (p < 0.05), and lower GRFs (p < 0.05) during landing after training in BFR and BTF groups than those of control groups, but no significant differences between BFR and BTF groups. which peroneus longus and tibialis anterior muscles are activated to provide a dynamic defense mechanism. An increasing ankle dorsiflexion increases people absorb the landing force with the gastrocnemius–soleus complex. Conclusion, ankle mobility provides a buffer during landing, and peroneus longus activation inhibits ankle inversion; together, they can effectively minimize the risk of ankle inversion injuries. Results supported the use of BFR or BTF in treating CAI, which would in turn prevent ankle sprain and injury to neighboring joints.

O.3.6: Limb coordination in people with Parkinson's disease is differently modulated by dopamine medication and directional subthalamic deep brain stimulation

Marco Romanato, Sorbonne Université, Paris Brain Institute - ICM, Inserm, CNRS, APHP, Paris France; Saoussen Cherif, INSERM Delegation Paris IdF Centre Est / Paris Brain Institute; Edward Soundaravelou, Sorbonne Université, Paris Brain Institute - ICM, Inserm, CNRS, APHP, Paris France; Nathalie George, Sorbonne Université, Paris Brain Institute - ICM, Inserm, CNRS, APHP, Paris France; Carine Karachi, Sorbonne Université, Paris Brain Institute - ICM, Inserm, CNRS, APHP, Paris France; Brian Lau, Sorbonne Université, Paris Brain Institute - ICM, Inserm, CNRS, APHP, Paris France; Marie-Laure Welter, CHU Rouen, Brain Institute

IntroductionSubthalamic deep brain stimulation (STN-DBS) is an effective intervention to treat motor signs in people with Parkinson’s disease (PDD). However, no or less improvement in gait and freezing of gait (FOG) after STN-DBS has been reported in about 1/3 of patients, with better effects for STN-DBS localized in the STN central part, i.e. the FOG sweet-spot. FOG has also been related to a loss of limb coordination. Here, we aim to examine the effects of dopa and directional STN-DBS applied in different STN sub-territories on limbs coordination in freezers PPD.MethodGait kinematics of 10 freezers PPD (F/M=2/8, mean age=59.5±6.7 years and FOG-Q=25.7±5.3) were recorded using a motion capture system, before surgery both OFF and ON dopa, and 6 months after surgery in 6 STN-DBS conditions: 1) ring mode, or 2) directional sensorimotor-posterior area, 3) central-FOG sweet-spot, 4) falls sweet-spot (localized within the zona incerta), 5) outside the STN, and 6) OFF DBS. Sagittal joint angles of the trunk, lower and upper limbs were processed, and coupling angles were computed between each joint pair (i.e., trunk-pelvis, trunk-shoulder, etc.) by using vector coding techniques. As measurement of limb coordination, coupling angles variability (CAV) average over time was considered. Principal component analysis (PCA) was used to reduce the complexity of the results, and non-parametric tests applied to compare each treatment conditions. Ten age-matched healthy volunteers were also included for comparison. ResultsThe first two components explained 76% of the dataset variance (Figure 1A). The first PCA-1 (Figure 1B) positively correlated with all the

pairwise coupled joints angles and was considered as a global coordination index with higher scores indicating higher CAV and a lower limb coordination. The PCA-1 improved both with dopa and all STN-DBS conditions, with respect to OFF dopa, with better effects with FOG sweet-spot and outside STN-DBS conditions. PCA-2 (Figure 1C) positively correlated with trunk-pelvis and axial upper limb segments variability and negatively correlated with segmental inter-limb coupled joint angles. It was considered as an indicator of upper intra-limb coupling and segmental inter-limb coordination, with scores closest to zero indicating better coordination. PCA-2 was improved both with dopa, directional hotspot FOG and outside the STN-DBS conditions. Ring-mode and other directional STN-DBS conditions did not improve limb coordination. CONCLUSION: Limb coordination in PPD during walking is better restored by directional STN-DBS of the FOG sweet-spot, relative to posterior STN-DBS. This could reflect the preferential modulation of the STN-descending mesencephalic pathways when STN-DBS is applied in this central STN area. Further studies are needed to investigate neurophysiological implication of our findings, and propose directional STN-DBS of the FOG sweet-spot in PPD with residual FOG after STN-DBS.

O.3.7: The Influence of a stroke on reciprocal control of the stretch reflex during posture

Magdalene Mcdonough, Northwestern University; Daniel Ludvig, Northwestern University; Eric Perreault, Northwestern University

Introduction: Stroke is the leading cause of disability in the United States, disrupting neural pathways that contribute to smooth, controlled movement. The spinal stretch reflex is one such neural pathway, and evidence suggests its dysfunction is a contributor to ineffective muscle activations in post-stroke movement disorders. A hallmark of a healthy stretch reflex is the ability to modulate across tasks, and it was recently demonstrated that there is strong reciprocal control, or the effect of agonist and antagonist voluntary activation, of stretch reflex sensitivity during active tasks. We aimed to determine if and how stroke changes reciprocal control of the stretch reflex during various levels of voluntary muscle activation. Doing so is critical to understanding impaired motor control in people with stroke, improving our ability to create effective rehabilitation strategies. Methods: Stretch reflexes were measured from elbow muscles in 5 stroke survivors and 12 healthy controls at various levels of muscle co-activation (0-10% maximum voluntary contraction (MVC)). Reflexes were elicited in each subject's dominant arm (and paretic arm for stroke survivors) by imposing a continuous sequence of 0.03 rad perturbation about the elbow via a rotary motor. Electromyograms (EMGs) were recorded from the biceps brachii (a flexor) and the triceps long head (an extensor). Real-time EMG feedback guided subjects to maintain constant activation levels within each trial. Background EMG and reflex EMG were computed as the average rectified EMG 10-40 ms prior to and 20-50 ms following each perturbation, respectively. We determined the effect of agonist and antagonist background activity, referred to as gains, on biceps and triceps reflexes by fitting mixed-effects models with reflex EMG as the dependent variable, background EMG as continuous factors, subject group (control vs stroke) as a fixed factor and subject as a random factor. RESULTS: Across all levels of background activity, stretch reflexes were substantially greater in the stroke group. Our model fit the data well (R2=0.82 for biceps reflex, R2=0.77 for triceps reflex). Notably, agonist gains were 2 to 5 times higher in the stroke group when compared to the control group. Antagonist activity had no significant effect on the biceps reflex in either group but inhibited the triceps reflex in the stroke group only.Discussion: In both

groups, we see very little effect of antagonist and a large positive effect of agonist on the stretch reflex. This is consistent with our previous work in controls during posture. Contrary to previous findings, our results suggest that agonist gains increase after a stroke. Furthermore, it has been suggested that reciprocal inhibition, or antagonistic suppression of muscle activity, may diminish after a stroke, but our antagonist gains contradict this. Future work with more subjects is needed to validate our results and investigate the mechanisms behind this observed behavior.

Oral Session 4

O.4.1: Effects of 10 days of unilateral lower limb suspension followed by 21 days of retraining on motor unit conduction velocity

Giacomo Valli, Università degli Studi di Brescia; Fabio Sarto, Department of Biomedical Sciences, University of Padova Italy; Andrea Casolo, University of Padua; Martino Franchi, University of Padova; Elena Monti, Department of Biomedical Sciences, University of Padova Italy; Giovanni Martino, University of Padova; Sandra Zampieri, Department of Biomedical Sciences, University of Padova Italy; Francesco Negro, Universita' degli Studi di Brescia; Marco Narici, Department of Biomedical Sciences, University of Padova Italy; ,

BACKGROUND AND AIM: Motor unit conduction velocity (MUCV) is an EMG-derived physiological parameter related to muscle fibre membrane and contractile properties. In particular, because of its biophysical relation with muscle fibre diameter, MUCV is considered a ‘size principle parameter’. Furthermore, its non-invasive estimation provides an indirect window into the electrophysiological properties of the sarcolemma, which are known to be affected by a training stimulus. Conversely, at present it is unknown whether MUCV can be altered by short-term disuse or immobilization. Thus, in the present study we investigated adaptations of MUCV to 10 days of unilateral lower limb suspension (ULLS) followed by 21 days of active recovery based on resistance training (AR21), using high density surface electromyography (HDsEMG). Methods: All measures were performed at baseline (L0), after 10 days of ULLS (LS10) and after AR21. Ten healthy young male volunteers underwent to HDsEMG recording during linearly increasing trapezoidal isometric contractions executed at 25 and 50% of maximal voluntary contraction (MVC) using a 64 electrodes grid positioned over the VL muscle, aligned in the direction of muscle fibers. MUCV and action potential amplitude (MU RMS) were computed during the ascending phase of the trapezoidal contractions on the double differential derivation of MU action potential waveforms propagating along the electrode columns. At least three double differential channels from the same electrode column were selected, with a preference for channels exhibiting the highest cross-correlation coefficients (>0.8). A validated multichannel maximum likelihood algorithm was adopted to calculate MUCV, and MU RMS was computed on the same selected channels. In addition, biopsies from the vastus lateralis (VL) muscle were collected to estimate muscle fibers type and diameter. RESULTS: Average MUCV (m.s-1) was reduced at LS10, both at 25% MVC (from 4.36 ± 0.10 to 4.05 ± 0.11; P<0.001) and at 50% MVC (from 4.64 ± 0.12 to 4.28 ± 0.12; P<0.001). Nevertheless, it returned to LS0 values after AR21. In contrast, MU RMS did not change at any time point. Moreover, no differences were identified for both type I and type II muscle fibers diameter (ATPase staining) during the interventions, although type I muscle fiber percentage increased after AR21.

CONCLUSIONS: These novel findings revealed that 10 days of ULLS were sufficient to induce significant alterations in MUCV, which in turn could be reversed by 21 days of active recovery. Since MUCV adjustments were not associated with changes in muscle fiber size, our results suggest that 10 days of ULLS may lead to reversible alterations in the electrophysiological properties of muscle fiber membrane. These data can contribute to expand our understanding of the neuromuscular alterations that can be present in people exposed to a short-term disuse period. PRIN 2022 Cod. 2022T9YJXT "MOPLAST"

O.4.2: Cross-Education and motor unit adaptations: insights from high-density electromyography

Edoardo Lecce, University of Rome 'Foro Italico'; Stefano Nuccio, University of Rome "Foro Italico"; Alessandra Conti, University of Rome "Foro Italico," Italy; Paola Sbriccoli, University of Rome "Foro Italico"; Francesco Felici, University of Rome, Foro Italico; Ilenia Bazzucchi, University of Rome Foro Italico

Background and Aim: Cross-education, the phenomenon where untrained limbs exhibit increased strength following a training period of the contralateral limb, has been associated with increased excitability in ipsilateral corticospinal pathways and reduced short-intracortical inhibition, hypothesised to be linked to inter-hemisphere interactions facilitated by transcallosal projections. The aim of this study is to investigate the cross-education effect on motor unit (MU) behaviour by examining both trained and untrained limb MUs. Methods: High-density electromyography was used to analyse motor unit adaptations in the biceps brachii of twenty participants, randomly assigned to either an intervention or a control group. The intervention group completed an 8-week unilateral strength training protocol involving 4 sets by 6 repetitions of eccentric contractions of the elbow flexors thrice weekly. Participants were assessed at baseline (T0), after four weeks (T1), and after eight weeks (T2), performing maximal voluntary contractions to determine maximal voluntary force (MVF) and ramp contractions at 35% and 70% MVF. Raw HDsEMG signals were decomposed into individual MU discharge timings and identified MUs were tracked across experimental sessions (T0 vs T1 vs T2) for a robust comparison. RESULTS: In the intervention group, both the trained and untrained limbs showed significantly increased maximal voluntary force at T1 (+10%MVF, +8%MVF, respectively) and T2 (+18%MVF, +10%MVF, respectively). However, statistically significant differences between T1 and T2 were only observed in the trained limbs (p<0.0001). A significant decrease in recruitment threshold was observed at T1 (trained: from 35.9±12.8% to 28.0±11.6%; untrained: from 34.4±13.3% to 29.3±11.3%, p<0.0001) and T2 (22.9±9.2%; 29.1±12.1%, p<0.0001, respectively), with significant differences between T1 and T2 observed exclusively in the trained limbs (p<0.0001). Changes in the DRMEAN (estimated neural drive) were observed only in the trained limbs at T1 (from 17.0±3.47 pps to 19.15±4.22 pps, p=0.01) and T2 (21.28±3.60 pps, p<0.0001), with significant differences between T1 and T2 (p=0.002). The control group showed no significant differences. Discussion: These findings align with previous reports concerning resistance training adaptations, highlighting specific effects observed in the contralateral limb, likely mediated by the central nervous system modulating firing and recruitment strategies. Cross-education may be attributed to inter-hemisphere interactions, leading to increased excitability in the ipsilateral corticospinal pathways. The absence of direct stimuli likely accounts for the lack of neuromechanical enhancements between T1 and T2 in untrained limbs.

O.4.3: High density surface electromyographic (HDsEMG) technique to differentiate between coracobrachialis and short head of biceps activity

Roopam Dey, University of Cape Town; Kohei Watanabe, Chukyo University; Yumna Albertus, University of Cape Town; Jean-Pierre Du Plessis, Orthopaedic Research Unit (ORU), University of Cape Town; Stephen Roche, Orthopaedic Research Unit (ORU), University of Cape Town

Background: Arthroplasty surgeries of the shoulder, such as the reverse total shoulder arthroplasty and the Latarjet have been reported to alter the coracobrachialis (CB) and short head of biceps (SB) moment arms. There is a lack of evidence in the literature regarding the activity of both muscles during shoulder movement. Investigating healthy CB and SB muscle activity will allow us to better understand the post-operative changes due to surgical interventions. However, it is difficult to separate or identify the selective neuromuscular activation of CB muscle. We aimed to test whether CB and SB activate separately for different shoulder movements and whether CB muscle activity can be identified by high-density surface EMG mapping. Methods: For this case study, we recruited 3 healthy male volunteers. The mean (standard deviation) age, height, weight, and body mass index (BMI) of the cohort were 36 (5) years, 1.8 (0.1) meters, 79.1(9.8) kgs, and 24.7(1.9) BMI. To isolate CB and SB, the volunteers were supine on a bed with their dominant arm in the “banzai” position. Their arm was abducted to an angle of 135° with respect to the thorax. The shoulder was also positioned at maximum external rotation. The participants’ dominant arm axilla was shaved, and ultrasound measured of the underarm region, using a linear array probe. The border of the CB muscle was thus identified and marked. One 16-channel pin electrode was placed on the marked region of the CB muscle. Another 16-channel pin electrode was placed on the superior aspect of the SB muscle to avoid the innervation zones. The participants were asked to 6 perform isometric maximum voluntary contraction (MVC) during elbow flexion (EF) followed by shoulder adduction (SA). Muscle activation was recorded, as a differential signal, for 5 seconds where the first 3 seconds were used to ramp and the last 2 seconds for holding the MVC. The 16-channel electrodes were replaced by a 64-channel surface electrode with a 10mm inter-electrode distance, placed on the same outlined region as the two 16-channel pin electrodes. EF and SA were performed in the same order as before and the muscle activities were recorded as monopolar signals. For data analysis, the final 2 seconds of MVC were used to calculate the amplitude rectified value (ARV). Subsequently, EF/AD ARV was calculated for the two 16-channel electrodes and for the 64-channel, after calculating the differential signals for the latter. Results: The average EF/SA for the CB and SB muscles were 0.6 and 2.4 respectively and were significantly different (p<0.001). The ratio for each channel of the pin electrode suggests that the proximal channels might be better at detecting CB activity while the distal channels’ signal might be influenced by the SB activity. Only considering the proximal half of the sensors the EF/SA for CB and SB muscles were 0.3 and 2.3 respectively. EB/SA color map as presented in Figure 2 also suggests that the ratio was high for SB compared to CB. CONCLUSION: : This pilot research study provides conclusive evidence that CB muscle activity can be selectively detected using the HDsEMG technique.

O.4.4: Biomechanical changes in muscle length directly influence shared synaptic inputs to spinal motor neurons

J Greig Inglis, Università degli Studi di Brescia; Helio Cabral, Università degli Studi di Brescia; Alessandro Cudicio, Università degli Studi di Brescia; Marta Cogliati, Università degli Studi di Brescia; Claudio Orizio, University of Brescia; Utku S. Yavuz, University of Twente; Francesco Negro, Universita degli Studi di Brescia

BACKGROUND AND AIM: Alpha band oscillations in the shared synaptic input to the alpha motor neuron pool can be viewed as a source of common noise interfering with optimal force output control. Recent evidence has suggested that various factors can modulate this tremor frequency range in the common synaptic input to motor neurons [1-2]. This study investigated the impact of altering muscle length on the shared synaptic oscillations to spinal motor neurons and force steadiness. We also conducted a second set of experiments to explore how changes in muscle length affect the low-pass characteristics of the muscle twitches. Methods: Fourteen participants performed trapezoidal isometric dorsiflexion contractions at 10% of maximal voluntary contraction while the ankle joint was placed at 90° (shortened) and 130° (lengthened). For both conditions, high-density surface electromyography (HDsEMG) recorded from the tibialis anterior (TA) was decomposed into motor unit spike trains [3], and motor unit coherence within the delta (1-5 Hz), alpha (5-15 Hz) and beta (15-35 Hz) bands was calculated. Torque steadiness and torque spectral power within the tremor band were quantified. In a second set of experiments, evoked torque twitches were recorded in five participants with the ankle joint placed at 70° and 130°. Wilcoxon signed-rank tests were used to compare the torque steadiness and power between conditions. Linear mixed models were applied to compare motor unit coherence between conditions. RESULTS: There were no significant differences in torque steadiness between ankle joint positions (P = 0.715). In contrast, torque power within alpha band significantly decreased between 90° and 130° (P = 0.009). Similarly, z-coherence within alpha band significantly decreased as TA length changed from 90° to 130° (from 1.20 [0.95, 1.45] to 0.99 [0.73, 1.24]; P < 0.001), with no changes for delta or beta bands (P > 0.117 for both). Comparison of the evoked potentials between 70° and 130° revealed an 8.3-14.1 ms increase in twitch duration. These changes in twitch duration induced alterations in the TA low-pass filtering characteristics, as the cut-off frequency was found to be lower when the muscle was lengthened than shortened. A simple computational simulation supported these experimental results, demonstrating that similar excitatory drives arriving at motor neuron ensembles with different twitch durations resulted in distinct alpha band coherence between motor unit spike trains. CONCLUSIONS: Our experimental results, supported by a simplified computational simulation, suggested that the increase of motor unit twitch duration resulting from increased muscle length directly influences the translation of the alpha band (physiological tremor) oscillations to force output. Therefore, this study provides valuable insights into the interplay between muscle biomechanics and neural adjustments.REFERENCES: [1] Laine et al., 2014. [2] Yavuz et al., 2015.[3] Negro et al., 2016.

O.4.5: Changes in cortical beta inputs to spinal motoneurons during the acquisition and retention of a new visuomotor skill task

Eduardo Martinez-Valdes, University of Birmingham; David Jiménez-Grande, Centre of Precision Rehabilitation for Spinal Pain (CPR Spine), University of Birmingham, UK; Michail Arvanitidis, Centre of Precision Rehabilitation for Spinal Pain (CPR Spine), University of Birmingham, UK; Deborah Falla, University of Birmingham; Dario Farina, Imperial College London; Ned Jenkinson, University of Birmingham; Francesco Negro, Universita' degli Studi di Brescia

Background: The primary motor cortex (M1) plays a crucial role in acquiring and retaining new motor skills, yet the precise regulatory mechanisms of M1 on the motor unit pool during skill learning remain unclear. Corticomuscular coherence offers insight into the connection between brain oscillations from M1 and motor unit activity. However, conflicting evidence exists regarding the impact of motor skill acquisition and retention on the coupling between electroencephalographic (EEG) and electromyographic (EMG) signals.Purpose: This study aims to investigate the influence of visuo-motor skill acquisition and retention on the coupling between EEG activity recorded from M1 (Cz) and motor unit activity recorded from the triceps surae during the learning of a novel visuomotor plantar-flexion force-matching task. Methods: High-density surface electromyography (HDsEMG) was collected from the Gastrocnemius Medialis (GM), Gastrocnemius Lateralis (GL), and Soleus (SOL) muscles. Twelve healthy young adults (average age 29 (7) years, 7 males and 5 females) performed 15 trials of an isometric plantar-flexion force-matching task on two consecutive days (day 1: acquisition and day 2: retention). EEG and HDsEMG signals were recorded concurrently. The first and last three trials of each day, representing the beginning and end of skill acquisition and retention, were concatenated and decomposed into motor unit spike trains. The combined signal from the cumulative spike trains of the three muscles (GM, GL, and SOL) was used to assess corticomuscular coherence between triceps surae motor units and cortical oscillations from M1 (Cz). Results: Participants demonstrated improved learning performance, significantly reducing force matching error from the beginning to the end of acquisition (p<0.01). Retention day error levels (both beginning and end) resembled those at the end of acquisition (p=0.3). Coherence in the beta band (15-35 Hz) peaked at the beginning of acquisition and significantly decreased by the end of acquisition (p=0.008). This reduction in corticomuscular coherence persisted during the beginning and end of retention (p>0.05). CONCLUSIONS: The study reveals that cortical beta inputs to spinal motoneurons innervating the triceps surae group diminish after the acquisition and retention of a motor skill. This suggests dynamic evolution of cortical inputs to motoneurons during skill learning, requiring heightened cortical input initially, followed by a decrease once the skill has been learnt.

O.4.6: Effects of repeated bouts of split-belt walking on locomotor adaptation, physiological arousal, and cortical activation

Kaya Yoshida, Rehabilitation Research Program; Shannon Lim, University of British Columbia; Lara Boyd, University of British Columbia; Janice J. Eng, University of British Columbia; Amy Schneeberg, University of British Columbia; Courtney Pollock, University of British Columbia

Background & Aims: Data suggest anxious arousal modulated by the autonomic nervous system (ANS) affects how we adapt motor strategies during static balance tasks. This relationship has not been tested during adaptation to a continuous walking challenge. Split-belt treadmills allow the exploration of gait adaptation through measures of step length symmetry (SLS). Individuals adjust step length bilaterally to achieve a symmetrical gait pattern during split-belt walking despite differing belt speeds. This study aims to understand how anxious arousal, cortical activation associated with attentional demands, and motor adaptation co-modulate during repeated exposure to a single session of split-belt treadmill walking. Methods: Twenty (10F) healthy young adults (aged 26.8(+/-3.3) yrs) completed a single-session, repeated-block design on a split-belt treadmill, with three, 3.5-minute split-belt walking adaptation blocks (2: 1 speed ratio), interspersed with tied-belt blocks. Anxious arousal (electrodermal

activity (EDA), attentional demand (prefrontal cortex (PFC) activation from functional near-infrared spectroscopy oxyhemoglobin (HbO) response) and SLS (embedded force platforms) were measured. Data from early (first 30 strides) and late phases (last 30 strides) of each block was analyzed. Linear-mixed-effects models (LMM) and Spearman/Pearson's correlations explored trial effects on EDA, SLS, and HbO mean/variance of signals in the PFC for each block and phase. RESULTS: LMM revealed differences in SLS, EDA, and PFC mean activation between early and late phases in split block1 only. SLS increased while EDA and PFC activation decreased ($p \leq 0.05$) in the late phase of block1. Neural variability in the PFC increased from early to late phase within each block (1-3, $p \leq 0.05$). In block1, a moderate negative correlation ($r = -0.62$, p<0.001) was observed between early phase SLS and EDA. Weak correlations ($r = -0.25$, $p=0.06$) were found between SLS and mean PFC activation and between EDA and mean PFC activation ($r=0.15$, $p=0.29$). CONCLUSION: : The initial split-belt exposure induced significant changes in SLS, EDA, and PFC activation between early and late adaptation. Early exposure to split-belt walking showed a relationship between heightened anxious arousal response and more asymmetrical gait, suggestive of an association between error detection and ANS response in walking. Repeat exposures during blocks 2 and 3 of split-belt walking revealed that both levels of anxious arousal and SLS showed minimal further adaptation after block1. Interestingly, variability in activation increased in the PFC in each of the 3 blocks. The increase in neural variability from the early to late phases in all 3 blocks is suggestive of decreased attentional demands with each exposure. These findings inform our understanding of the co-modulation of anxious arousal and attentional demands during locomotor adaptation and provide novel insights into processes underpinning motor learning.

O.4.7: Associations between delayed onset trunk muscle soreness, altered EMG-torque relationships, and lumbar kinematics in dynamic contractions

Michail Arvanitidis, Centre of Precision Rehabilitation for Spinal Pain (CPR Spine), University of Birmingham, UK; David Jiménez-Grande, Centre of Precision Rehabilitation for Spinal Pain (CPR Spine), University of Birmingham, UK; Nadège Haouidji-Javaux, Centre of Precision Rehabilitation for Spinal Pain (CPR Spine), University of Birmingham, UK; Deborah Falla, University of Birmingham; Eduardo Martinez-Valdes, University of Birmingham

Background: People with chronic low back pain (CLBP) often show reduced trunk torque steadiness (TS). This finding is based on observational studies with a limited ability to draw causal inferences. As a pain model, delayed onset muscle soreness (DOMS) can help us better understand the effect of pain on trunk. Surface electromyography (sEMG) and force relationships are crucial in linking muscle activity to force output, given the correlation between the low-frequency component of force and rectified interference sEMG oscillations. Research on the lumbar erector spinae (ES), where decomposing high-density sEMG (HDsEMG) signals is challenging, can benefit from such approaches. To date, it remains unclear whether DOMS can influence dynamic trunk muscle control, potentially leading to alterations in EMG-torque relationships and patterns of thoracolumbar movement.Purpose: To evaluate the influence of DOMS on TS and HDsEMG features recorded from the lumbar ES muscle of asymptomatic people during concentric/eccentric submaximal (25%, 50% maximum voluntary contraction) trunk extension contractions. Methods: Twenty individuals attended three lab sessions (24h apart). HDsEMG signals were recorded unilaterally from the thoracolumbar ES with two 64-electrode grids and from the rectus abdominis and external oblique muscles using one 64-

electrode grid each. Torque was measured using an isokinetic dynamometer, and TS was quantified as the coefficient of variation (CoV) and standard deviation (SD) of torque. The interplay between HDsEMG signals and torque was explored via coherence (0-5Hz) and cross-correlation analysis. PCA was employed to reduce HDsEMG data dimensionality and improve HDsEMG-torque-based estimations. RESULTS: Muscle soreness and sensitivity in the thoracolumbar area, assessed using the visual analogue scale (VAS) and pressure pain threshold, increased 24h and 48h post-DOMS induction (VAS scores: 2.6 ± 2.1; 2.9 ± 1.8). For eccentric trunk extension, improved TS (SD) was observed after 24h and 48h, with greater flexion movement at higher forces. A decrease in δ band HDsEMG-torque coherence and cross-correlation was observed at 48h. Associations indicated that more flexion during eccentric trunk extensions correlated with better TS and higher levels of muscle soreness and that decreased TS was related to increased HDsEMG cross-correlation. During concentric trunk extension at 48h, improved TS (CoV, SD) was observed and was accompanied by reduced sagittal thoracolumbar movement, implying a preference for a more neutral lumbar spine position. Associations revealed that increased muscle soreness is associated with reduced improvements in TS and that minimal sagittal thoracolumbar movement is associated with better TS. CONCLUSIONS: In the presence of DOMS, individuals had better trunk concentric/eccentric TS. This improvement may be attributed to the observed adaptation of movement and recruitment strategies and a learning effect from the training exposure in the first session.

Oral Session 5

O.5.1: The decoding of extensive samples of motor units in human muscles reveals the rate coding of entire motoneuron pools

Simon Avrillon, Université Côte d'Azur; Francois Hug, Université Côte d'Azur; Roger Enoka, University of Colorado; Arnault Caillet, Imperial College London; Dario Farina, Imperial College London

Movements are performed by motoneurons transforming synaptic input into an activation signal that controls muscle force. The control signal is not linearly related to the net synaptic input, but instead emerges from interactions between ionotropic and neuromodulatory inputs to motoneurons. To advance our understanding of the neural control of muscle, we decoded the firing activity of extensive samples of motor units in the Tibialis Anterior (129±44 per participant; n=8) and the Vastus Lateralis (130±63 per participant; n=8) during isometric contractions of up to 80% of maximal force. From this unique dataset, we characterised the rate coding of each motor unit as the relation between its instantaneous firing rate and the muscle force, with the assumption that the linear increase in isometric force reflects a proportional increase in the net synaptic excitatory inputs received by the motoneuron. This relation was characterised with a natural logarithm function that comprised two phases. The initial phase was marked by a steep acceleration of firing rate, which was greater for low- than medium- and high-threshold motor units. The second phase comprised a linear increase in firing rate, which was greater for high- than medium- and low-threshold motor units. Changes in firing rate were largely non-linear during the ramp-up and ramp-down phases of the task, but with significant prolonged firing activity only evident for medium-threshold motor units.Contrary to what is usually assumed, our

results demonstrate that the firing rate of each motor unit can follow a large variety of trends with force across the pool. From a neural control perspective, these findings indicate how motor unit pools use gain control to transform inputs with limited bandwidths into an intended muscle force. We will show how these results can help to design linear or non-linear decoders that aim to predict muscle activation or muscle force from descending inputs recorded in supraspinal centres, with the will to generalise their performance across movements.

O.5.2: On time effectiveness of manual editing of motor unit spike trains

Nina Murks, University of Maribor, Faculty of Electrical Engineering and Computer Science; Jakob Škarabot, Loughborough University; Matej Kramberger, University of Maribor, Faculty of Electrical Engineering and Computer Science; Gašper Sedej, University of Maribor, Faculty of Electrical Engineering and Computer Science; Tamara Valenčič, Loughborough University; Christopher Connelly, Loughborough University; Haydn Thomason, Loughborough University; Matjaž Divjak, University of Maribor, Faculty of Electrical Engineering and Computer Science; Ales Holobar, University of Maribor, Faculty of Electrical Engineering and Computer Science; ,

BACKGROUND AND AIM: Automatic methods for motor unit (MU) spike train identification from HDEMG are extensively used, but segmentation of the MU spike trains into discharge patterns still requires manual editing. This represents one of the major bottlenecks in analysis. We explored how the time efficiency of manual editing depends on the quality of the identified spike trains (Pulse-to-Noise Ratio - PNR), the operator's level of experience, and muscle contraction levels. Methods: Experimental signals were acquired from the First Dorsal Interosseous, Tibialis Anterior, Vastus Lateralis, and Biceps Brachii (BB). Two male subjects performed isometric contractions for every muscle at 10, 30, 50, and 70% of MVC. The contractions were ~25 seconds long and were measured with a 13×5 electrode array. The same contraction levels were simulated in Soleus and BB with a 9×10 electrode array and 20 dB noise. All signals were decomposed using the Convolution-Kernel-Compensation method and manually edited by 9 operators (2 beginners with < 50, 2 intermediates with < 200, 3 advanced with < 1000, and 2 experts with > 1000 edited signals worth of experience). All operators underwent a tutorial to standardize the editing procedure. Results were analyzed with a linear mixed-effects model of editing_time ~ PNR * contraction_level * operator's _experience * signal_type + (PNR | muscle: subject). We only examined MUs with a PNR of 25 dB or higher. RESULTS: The editing time decreased with PNR (F=63.9, P<0.0001) with 55.9 ± 80.3 s and 8.1 ± 15 s spent for editing of MUs with PNR of 25-39 dB and 40-54 dB, respectively. Editing time increased with the contraction level (F=10.9, P<0.0001) as 42.6 ± 63.2 s, 54.2 ± 82 s, 57.8 ± 83.8 s, and 60 ± 82.9 s were spent editing the 10, 20, 30, 50 and 70% contraction level. The level of experience predicted the editing time (F=10.5, P<0.0001). Beginners required 65.9 ± 90.4 s, intermediates 55.1 ± 72.4 s, advanced operators 51.9 ± 90.9 s and experts 37.1 ± 40.6 s. Signal type (synthetic or experimental) did not influence editing time but was in significant interaction with contraction level (F=6.4, P=0.001), and operator's level of experience (F=4.7, P=0.003). There was also a significant interaction between PNR and contraction level (F=10.4, P<0.0001), PNR and operator's level of experience (F=7.1, P<0.0001), and contraction level and operator's level of experience (F=3.3, P=0.001). CONCLUSION: The time required for MU editing reduces almost linearly with the operator's level of experience and is dependent on the contraction level and PNR.FUNDING: This research was funded by the European Union's Horizon Europe Research and Innovation Program [HybridNeuro project, GA No. 101079392]. Views and

opinions expressed are however those of the author(s) only and do not necessarily reflect those of the European Union or Research Executive Agency. Neither the European Union nor the granting authority can be held responsible for them.

O.5.3: Quantifying the collective synchrony of motor units using multi-variate coherence

Lara Mcmanus, Trinity College Dublin; Sageanne Senneff, University College Dublin; Bahman Nasseroleslami, Trinity College Dublin; Madeleine Lowery, University College Dublin

BACKGROUND AND AIM: Synchronization in neuronal firing is widely studied as a potential mechanism supporting the encoding and transmission of information throughout the nervous system. Recent developments in multi-unit recording systems have enabled the activity of populations of neurons to be detected in both cortex and muscle (through motor unit recordings). This paper presents the multi-variate (MV) coherence estimate, a method of estimating both the collective synchrony of a neuronal sample and assessing the contributions of individual neurons to the total synchrony. Methods: The MV coherence estimate was tested and compared against the most widely used method of estimating motor unit coherence, described in [1], using both a computational model and experimental data. The model consisted of a biophysical motoneuron pool model based on the first dorsal (FDI) interosseous muscle [2]. Each motoneuron received some synchronous synaptic inputs, representing efferent cortical signals, in order to generate weakly correlated spike trains from the model. The MV coherence estimate was also applied to experimental motor unit firing data recorded from the FDI (N=18) during index finger abduction during forces ranging from 10% to 40% maximal voluntary contraction (MVC). Discriminable motor unit were extracted from the surface EMG using decomposition algorithms (Delsys, Inc.). RESULTS: Simulations from the computational model revealed that the MV method provides a more reliable and stable coherence estimate when compared with existing methods of estimating motor unit coherence, particularly for gamma-band coherence. Simulations demonstrated that the MV coherence method was less sensitive to the number of motor units included in the estimate, compared with existing methods that exhibit an approximately linear increase in coherence as the number of motor units is increased. When the synchronous inputs to the motoneurons were varied, the MV coherence was also able to estimate the change in the magnitude of these synchronous inputs more accurately. When the MV coherence estimate was applied to experimental motor unit data from the FDI muscle, it revealed an increase in gamma-band coherence with force level. A distinct coherence peak at ~40 Hz (piper rhythm) was also observed during the contractions at 40%MVC. CONCLUSIONS: This is the first time that the Piper rhythm has been detected in a study correlating activity between single motor units. The method enabled the detection of an increase in gamma-band coherence at higher muscle contraction forces, which was not identified using the cumulative spike train coherence method. Multi-variate coherence enables the effective detection of beta- and gamma-band synchronization in neuronal firing, which will be essential for future studies investigating the functional role of neural synchrony in both brain and muscle.[1] Farina D et al. (2014) J Physiol 592: 3427-3441.[2] Senneff, S. et al. (2019). 41st Annual International Conference of the IEEE EMBC (pp. 2293-2296). IEEE.

O.5.4: Activity index outperforms cumulative spike train and amplitude envelopes in surface EMG coherence analysis

Leon Kutoš, Faculty of Electrical Engineering and Computer Science, University of Maribor, Maribor, Slovenia; Matjaž Divjak, University of Maribor, Faculty of Electrical Engineering and Computer Science; Ales Holobar, University of Maribor, Faculty of Electrical Engineering and Computer Science

BACKGROUND AND AIM: Coherence is frequently used to study functional coupling between two motor neuron pools. Decomposing surface electromyograms (sEMG) into spike trains of individual motor units (MUs) and summing them into cumulative spike train (CST) [1] may improve the coherence estimates provided by sEMG amplitude envelopes (AE), mainly due to removal of MU action potentials (MUAPs). However, the coherence estimation in CST depends on the number of MUs and reaches optimal values at several tens of detected MUs. Such a high number of MUs cannot always be guaranteed. Conversely, activity index (AI), which constitutes the first step of the CKC algorithm [2], compensates the MUAPs and combines contributions of all the MUs active in the detection volume of sEMG electrodes. In this study we compare coherence calculations using AE, AI and CST in synthetic and experimental sEMG. Methods: 10 biceps brachii muscles were simulated with 500 MUs each. 20 s of 9×10 sEMG channels were simulated and sampled at 2048 Hz. Excitation levels of 10%, 30% and 50% of MVC were simulated with superimposed 10 Hz sinusoidal modulation with amplitude of 5% MVC. Experimental sEMG was acquired by 5×13 electrode array from gastrocnemius medialis (GM) and lateralis (GL) muscles of 5 healthy subjects during 20 s long 30% MVC contraction. All sEMG signals were decomposed by CKC algorithm [2], yielding MU spike trains and AI. MU spike trains with pulse-to-noise ratio > 25 dB were summed into CST and spatial average of rectified sEMG was used as AE. Coherence was calculated between all pairs of sEMG signals from two different simulated muscles and between simultaneous recordings of GL and GM. We evaluated the coherence values at 10 Hz (synthetic signals) and at the coherence peak on the 8-30 Hz interval (exp. signals). RESULTS: 14.2±6.1 and 26.1±16.7 MUs were identified from synthetic and exp. sEMG. In synthetic case, the AI yielded significantly higher (P<0.001) coherence values at 10 Hz (0.97±0.01) than the AE (0.83±0.07) and CST (0.78±0.23). In exp. signals coherence peaks were significantly (P<0.05) higher in the AI (0.48±0.20) than in the AE (0.35±0.26) or CST (0.24±0.07). CONCLUSION: : The AI yielded higher coherence values than the AE and CST, likely due to the larger number of MUs (compared to the CST) and MUAPs compensation (compared to the AE).FUNDING: This research was funded by the European Union's Horizon Europe Research and Innovation Program (HybridNeuro project, GA No. 101079392). Views and opinions expressed are however those of the author(s) only and do not necessarily reflect those of the European Union or Research Executive Agency. Neither the European Union nor the granting authority can be held responsible for them.[1] Farina et al. The effective neural drive to muscles is the common synaptic input to motor neurons. J. Physiol. 2014.[2] Holobar et al. Multichannel blind source separation using convolution kernel compensation. IEEE Trans. Sig. Proc. 2007.

O.5.5: Interfacing with motor unit activity using high-density thin-film electrodes following targeted muscle reinnervation

Laura Ferrante, Imperial College London; Deren Y. Barsakcioglu, Imperial College London; Silvia Muceli, Chalmers University of Technology; Anna Bösendorfer, Medical University of Vienna; Benedikt Baumgartner, Medical University of Vienna; Oskar Aszmann, Medical University of Vienna; Dario Farina, Imperial College London

Background: Targeted Muscle Reinnervation (TMR) involves the surgical transfer of peripheral nerves, originally innervating muscles of the missing limb, into targeted muscles above the amputation level (Kuiken et al., 2009). After TMR, these muscles are probed using non-invasive electromyographic (EMG) or intramuscular EMG electrodes to record the myoelectric activity triggered by the rerouted nerves. Classic methods to estimate the human motor intent typically extract global features from recorded EMG signals. However, Farina et al. (2017) introduced a paradigm shift in human-machine interfacing where the neural activity of individual motor neurons was decoupled from high-density surface EMG signals and used for prosthesis control in TMR patients. Muceli et al., 2018, proposed multi-channel epimysial EMG electrodes to overcome the limitations of non-invasive sensing and to establish a high-throughput neural interface for detecting single motor neuron spiking activity in animal models of TMR. Our current study is the first exploration of this human-machine interface paradigm in TMR patients. Methods: In contrast to classic TMR and prior investigations, which measure from spacially distinct myoelectric sites to minimise the signal interference, we used 40-channel thin-film electrodes (Muceli et al., 2015) to obtain a single highly dense sample of EMG activity from ten muscles where peripheral donor nerves with large cognitive control were redirected through TMR. Each volunteer performed isometric contractions at 10-20% of the maximum voluntary contraction while thinking about different movements ranging from single Degree of Freedom (DoF) tasks (e.g., pinky flexion) to a combinationof DoF tasks (e.g., tripod). Firstly, we investigate how changes in the neuromuscular morphology following TMR impact the morphology of motor units (MU) by examining the MU action potential amplitude, duration, and MU territories. Secondly, we examine the MU firing characteristics during the entire task execution. Finally, we provide a comparative discussion of the characteristics of MUs active fordifferent tasks. RESULTS: We demonstrate that the TMR muscles exhibit high compartmentalisation likely due to hyper-reinnervation following TMR (Bergmeiste et al., 2019). This muscle compartmentalisation corresponds to a functional heterogeneous innervation: the probed muscle fibres are innervated by clusters of motor neurons associated with different functional tasks. Thus, decomposition methods can be used to unmix EMG signals and extract neural activity uniquely associated with motor functions. CONCLUSIONS: Our results indicate that TMR offers an efficient biointerface for prosthesis control. Additionally, our observations on the functional heterogeneity of active motor units indicate that common synaptic input is shared across the motor neurons that have the same functional role (Hug et al, 2023).

O.5.6: Estimating low-threshold motor unit twitch responses in high-force trials: towards real-time estimation of neuromusculoskeletal function through motor unit-driven approaches

Antonio De Jesus Gogeascoechea Hernandez, Universiteit Twente; Utku Yavuz, The University of Twente; Massimo Sartori, University of Twente

BACKGROUND: Interfacing with motor units (MUs) in intact humans in vivo is key for understanding the interaction between alpha motor neurons and the innervated muscles. Recent advancements in high-density electromyography (HD-EMG) decomposition techniques allow the non-invasive identification of MU firing and contractile properties. In combination with musculoskeletal modeling, this enables decoding the individual contribution of MUs to muscle force generation [1]. However, due to MU action potential (MUAP) amplitude cancellation and the volume conductor effect, it remains challenging to decode low-threshold MUs in high-force

tasks. In this study, we combine a peel-off decomposition approach [2] with the refinement of MU filters obtained from low-force trials to enrich the estimation of MU-specific activation dynamics in high-force tasks. Methods: Experimental protocol: Four healthy subjects performed isometric dorsi-plantar flexion contractions across different levels of force, during which HD-EMGs and torque measurements were collected. Decomposition procedures: The HD-EMGs were decomposed offline into MU firing events using a convolutive blind source separation technique [3]. For the high-force trials (>50% MVC), we estimated MUAP waveforms from the HD-EMGs [2]. Subsequently, we employed the found MUAPs to obtain EMG residuals. For the peel-off approach, we further decomposed the EMG residuals by refining MU filters found in low force. We eliminated duplicates and spike trains with low silhouette values.MU-specific activation dynamics: We estimated discharge rates and recruitment thresholds. We computed a linear combination of these firing features through principal component analysis and projected them onto their eigenvector [1]. We linearly mapped the firing features with twitch properties found in humans. We employed the estimated contraction times and peak amplitudes to design twitch responses for each MU. The total MU-specific activation was defined as the sum of the individual twitch responses. RESULTS: Preliminary results on the tibialis anterior showed that the activation estimated from spike trains of the peel-off approach provided a higher correlation with force than the activation derived from the conventional decomposition (0.55 ± 0.14 and 0.70 ± 0.06, respectively). CONCLUSIONS: We proposed a framework that integrates a peel-off decomposition approach, refinement of MU filters, and characterization of MU properties for decoding a more diverse subset of MUs from HD-EMGs, with a wider range of recruitment characteristics. This not only improved the estimation of muscle activation but also opens avenues for designing highly efficient neuro-modulative strategies. Future work will further integrate this framework with musculoskeletal modeling to achieve optimal control neuro-rehabilitation devices in real-time. REFERENCES: [1] A. Gogeascoechea et al, IEEE TNSRE, 2023.[2] M. Chen et al, IEEE TNSRE, 2016.[3] F. Negro et al, J. of Neu. Eng. 2016.

O.5.7: Magnetomyography can provide new insights into motor units in living humans

Thomas Klotz, University of Stuttgart; Francesco Negro, Universita' degli Studi di Brescia; Justus Marquetand, Department of neural dynamics and Magnetoencephalography, University of Tuebingen; Oliver Röhrle, University of Stuttgart

BACKGROUND AND AIM: Magnetomyography (MMG) measures the magnetic field induced by the activation of muscle fibers and is a complementary method to well-established electromyographic (EMG) recordings. Although MMG was scarcely explored in the past, mainly due to technological limitations, the MMG's physical properties motivate the investigation of the method. Most importantly, the magnetic permeability of the human body is (nearly) the same as in free space. Thus, MMG can be measured contact-free, and the MMG signal is potentially less affected by the body properties and anatomy than EMG. In this contribution, we explore whether these theoretical advantages can be leveraged to obtain new insight into motor unit (MU) physiology in living humans. Methods: We use a biophysical model of EMG and MMG to perform MU decompositions in a controlled environment. To focus on the physical properties of the signal (and not the performance of the decomposition algorithm itself), we derive an in-silico trial framework integrating the biophysical model into the spike estimation step of blind source separation-based MU decomposition algorithms. MUs with a silhouette score higher

than 0.9 are considered identifiable. First, the performance of MMG-based and surface EMG-based MU decompositions are compared. Further, the influence of the magnetometer properties (e.g., noise, bandwidth, vector field components, and density) is explored. As proof of concept, blind source separation-based MU decomposition is applied to experimental data, i.e., isometric contractions (5%, 10%, 20%, and 30% MVC) of the abductor digiti minimi muscle. All experiments were conducted in a magnetically shielded room (ak3b) of the MEG center in Tübingen. The MMG is measured with 15 commercially available optically pumped magnetometers (OPMs) (FiledLine Inc.) arranged through a custom-made 3D-printed sensor holder. The simultaneous measurement of high-density EMG was only possible through a specifically designed new high-density EMG electrode (OT Biolelectronica). RESULTS: The in-silico trials show that MMG-based MU decomposition is theoretically superior to surface EMG-based MU decomposition. The number of decomposable MUs increases by 76%. Decomposing MMG can identify MUs with depths higher than 2 mm that are typically not identifiable through surface EMG. In detail, the MMG detects 88% of the superficial MUs (i.e., up to 2 mm in depth) and 41% of the deep MUs (more than 2 mm in depth). In contrast, the EMG identifies 67% of the superficial MUs and 4% of the deep MUs. Through two-source validation, the proof-of-concept in-vivo experiments illustrate that it is possible to decompose MUs from high-density MMG data. However, the performance of MMG-based decompositions is currently limited by the performance of the detection system. The in-silico experiments revealed that the most relevant limitation is the bandwidth and the noise level of the utilized magnetometers. DISCUSSION: The presented research provides new insights into methods to study MUs in living humans. Unlocking the full potential of MMG-based MU decomposition requires further developments of the detection system.

Oral Session 6

O.6.1: The process of filling of the sEMG signal with motor unit potentials as force is gradually increased in the quadriceps

Javier Rodriguez-Falces, Public University of Navarra; Javier Navallas, Public University of Navarra; Armando Malanda, Public University of Navarra; Cristina Mariscal Aguilar, Universitary Hospital of Navarra

BACKGROUND AND AIM: : As the force of an isometric contraction is gradually increased, the number of active motor unit increases, larger units are progressively recruited, and already recruited units increase their firing rate. However, several questions related to this increase remain unresolved: (1) Does the increase in sEMG amplitude occur gradually and smoothly or does it occur in steps? (2) Is the sEMG activity at low force levels “pulsatile” (composed of a few large-amplitude spikes) or “continuous” (formed by many small-amplitude MUP spikes)? (3) What is the force level at which the sEMG signal is completely filled up? There is no complete understanding of the way in which the surface EMG signal progressively fills with MUPs as force increases. We sought to investigate this sEMG filling process. Methods: Surface EMG signals were recorded from the quadriceps muscles of 33 healthy subjects as force was gradually increased from 0 to 40% MVC in 60s (see Fig. 1a). The sEMG filling process was analyzed by measuring the EMG filling factor, calculated from the non-central moments of the rectified sEMG signal. RESULTS: (1) As force was gradually increased, one or two prominent abrupt

jumps in sEMG amplitude appeared between 0 and 10% of MVC force (mean 2.5% MVC) in all the vastus lateralis and medialis muscles (Fig. 1b).(2) The jumps in amplitude were originated when a few large-amplitude MUPs, clearly standing out from the previous sEMG activity or from noise, appeared in the sEMG signal (Fig. 1b).(3) Every time an abrupt jump in sEMG amplitude occurred, a new stage of sEMG filling was initiated (Fig. 1b).(4) The filling factor decreased significantly every time an abrupt jump in sEMG amplitude occurred, and this index increased progressively as additional MUPs are successively incorporated to the sEMG signal (Fig. 1c). CONCLUSIONS: It has been found that, as force was slowly increased in the vastii muscles, prominent abrupt jumps in sEMG amplitude occurred at low force levels (<10% MVC). Thus, the filling process of the sEMG signal occurred one or two stages in these muscles, with the sEMG being almost completely filled at very low forces (2-12% MVC).SIGNIFICANCE: The filling factor is a useful promising tool to analyse the EMG filling process.

O.6.2: Asymmetry in the onset of paraspinal muscles activity during rapid arm movements differs in adolescents with idiopathic scoliosis compared to those with a symmetrical spine.

Frederique Dupuis, Université Laval; Phoebe Ng, KK Women's and Children's Hospital/ The University of Queensland; Phoebe Duncombe, The University of Queensland; Wolbert Van Den Hoorn, School of Biomedical Sciences, The University of Queensland, Australia; Maree Izatt, Biomechanics and Spine Research Group, Centre for Children's Health Research, Australia; Robert Labrom, Biomechanics and Spine Research Group, Centre for Children's Health Research, Australia; Kylie Tucker, The University of Queensland

BACKGROUND Adolescent idiopathic scoliosis (AIS) occurs in ~2-4% of adolescents globally.1 The 3D spinal deformation is associated with progressive wedging, translation, and rotation of multiple vertebrae.1 The curvature typically begins between 9-12 years of age, develops rapidly, and has no known cause or cure. There is growing evidence of altered muscle activation in AIS however many previous studies are limited by insufficient clarity on tasks performed, and data recording and processing techniques.2 Muscle activation is one of the factors that contribute to muscle force generation. If an asymmetry in paraspinal muscle activation is present in AIS, it may contribute to an asymmetry in forces applied to the spine, and curve progression. OBJECTIVE To determine if symmetry of paraspinal muscle activation differs in those with AIS compared to controls during a simple, highly repeatable movement task. METHODS Girls with AIS [n=24; primary right thoracic curve; Cobb angle 39.5(16.4)°, age 13.8(1.5) years], and matched controls [n=20, age 13.1(1.8) years] participated. Surface electrodes were placed bilaterally on anterior deltoid, and erector spinae adjacent to C7, T9, T12 and L5 vertebrae. In response to a visual (light) signal, participants performed a bilateral rapid arm flexion while holding a small wooden rod (in both hands to aid movement symmetry). Muscle activation onsets were manually selected while blinded for group, from 6 trials for each participant. Activation symmetry (i.e. onset left – right) was calculated for each muscle pair. To compare between groups, a linear mixed model with group and muscle as fixed factors and participants as random intercepts was used. Results Right anterior deltoid onset was earlier than the left in 65% of trials, however there was no difference in this asymmetry between groups (χ^2 p=.22). There was a significant Group×Muscle interaction (p<0.01) for activation asymmetry, with the difference between groups identified at T9 (mean difference 14ms; 95%CI: 4-25ms, post hoc p<0.01). Activation was 6ms (95%CI: 6-12ms) earlier on the right (convex) side of the curve in

AIS. In contrast activation was 8ms (95%CI: 1-15ms) earlier on the left side in controls (Fig 1). There were no group differences at other vertebral levels (all post hoc p>0.44). CONCLUSION: The result of this study provides evidence of a difference in paraspinal muscle activation onset at the level of the curve apex in AIS during a well-controlled symmetrical upper limb movement task. It is likely that the longissimus muscle contributes the greatest to the recorded muscle activation at T9. The longissimus is a powerful extensor and lateral flexor that attaches to the transverse processes and the lower rib angles. These bony structures are known to present with deformation in AIS. Future studies are now justified to investigate the underlying mechanisms for this difference in activation, and its potential consequences on spine deformity. 1.Negrini S et al. Scoliosis and Spinal Disorders. 2018.2. Ng P et al. Journal of Electromyography and Kinesiology. 2022.

O.6.3: Long-term effects of ACL reconstruction with a hamstring tendon autograft on neural control of the vastii muscles at different knee-joint angles

Tamara Valenčič, Loughborough University; Jakob Škarabot, Loughborough University; Stefan Kluzek, University of Nottingham, United Kingdom; University of Oxford, United Kingdom; Ales Holobar, University of Maribor, Faculty of Electrical Engineering and Computer Science; Jonathan P Folland, Loughborough University

BACKGROUND AND AIM: After anterior cruciate ligament reconstruction (ACLR), the ability to activate and contract the knee-extensor muscles in the injured leg often fails to recover for months or even years after surgery despite exercise rehabilitation. Furthermore, evidence suggests potential for greater quadriceps inhibition at extended compared to flexed knee-joint positions. Whilst long-term muscle inhibition post ACLR has been demonstrated on the whole muscle level, adjustments at the motor unit (MU) level remain largely unexplored. This study examined MU discharge properties of the vastii muscles at different knee-joint angles and compared individuals 1-5 years post ACLR and healthy controls. Methods: Twelve participants 3.1 ± 1.3 (range: 1.2-5.1) years post a primary, unilateral ACLR with a hamstring tendon autograft and twelve sex-, body mass- and physical activity-matched controls performed unilateral trapezoidal isometric knee-extension contractions at 30, 50, and 70% of their maximal voluntary torque (MVT) at 25, 55, and 85° of knee flexion (full extension: 0°). High-density surface electromyography signals were recorded from the vastus lateralis and medialis muscles and decomposed into discharge timings of individual MUs. Discharge rate during the contraction plateau (DRplat), and at recruitment (DRrec) and derecruitment (DRderec) were quantified for individual MUs. Linear mixed models were constructed to examine whether the outcome variables were predicted by group, leg, knee-joint angle, and contraction intensity, with MU recruitment threshold included as a covariate in the statistical models. RESULTS: In the ACLR group, MVT was similar for both legs at all knee-joint angles, with no differences compared to the control group (ACLR, injured vs contralateral leg: 246 [216, 275] vs 246 [216, 276] Nm, respectively; control: 229 [199, 259] vs 226 [196, 256] Nm; all interactions: $p \geq 0.5042$). A group*leg interaction for DRplat ($p = 0.0447$) suggested lower DRplat in the injured compared to the contralateral leg in the ACLR group; however, post hoc testing did not indicate any side-to-side differences in either group (ACLR: 12.2 [11.3, 13.2] vs 12.9 [11.9, 13.8] pps; $p = 0.0596$; control: 12.8 [11.8, 13.7] vs 12.9 [11.9, 13.8]; $p = 0.964$). No significant group*leg interactions were observed for DRrec (ACLR: 8.1 [7.3, 8.8] vs 8.4 [7.6, 9.2] pps; control: 8.4 [7.7, 9.2] vs 8.6 [7.9, 9.4] pps; $p = 0.6026$) or DRderec (ACLR: 6.1 [5.7, 6.5] vs 6.2 [5.8, 6.7] pps;

control: 6.0 [5.6, 6.5] vs 6.2 [5.8, 6.6] pps; p = 0.5498). For DRplat, DRrec, and DRderec, no group*leg interactions with knee-joint angle and/or contraction intensity were detected (p ≥ 0.1594). CONCLUSION: : These results suggest that despite having successfully restored their knee-extensor strength, ACLR individuals may exhibit subtle long-term deficits in MU discharge properties of the vastii muscles of the injured compared to the contralateral leg.

O.6.4: Characterization of spinal circuits with high density surface electromyography (HDsEMG)

Alejandro Pascual Valdunciel, Imperial College London; M. Gorkem Ozyurt, Department of Neuromuscular Diseases, Institute of Neurology, Queen Square, University College Londo; Filipe Nascimento, Department of Neuromuscular Diseases, Institute of Neurology Queen Square, University College Londo; Marco Beato, Neuro, Physiology & Pharmacology (NPP), Division of Biosciences, University College London; Robert Brownstone, Institute of Neurology, UCL; Martin Koltzenburg, University College London, Clinical and Movement Neurosciences; Dario Farina, Department of Bioengineering, Imperial College London

Spinal circuits are fundamental in the control of movement, with spinal interneurons defining motoneuron excitability and shaping the patterns of motor output. Local spinal networks are affected in many neuromuscular disorders, such as Amyotrophic Lateral Sclerosis (ALS) or dystonia. For instance, ALS changes the synaptic wiring contributing to motor dysfunction that might appear before denervation. Standard neurophysiological techniques used to assess spinal circuits in clinics are based on the use of surface EMG, which has a poor temporal resolution to identify circuit features, such as latency or duration; or needle electrodes, which are invasive and allow identification of only a few motor units (MUs) (typically < 3 MUs per needle). HDsEMG allows non-invasive identification of a pool of MUs at a time and more accurate study of motor pool properties. Only two studies have previously proposed the use of HDsEMG to study reciprocal inhibition through the decomposition of individual MUs. Latest advances on HDsEMG acquisition and decomposition methods have allowed sampling larger proportion of the motor pool even at low force levels; while new protocols have been proposed to study recurrent inhibition based on stimulation of motor axons and recording MUs using intramuscular electrodes. In this study, we propose to use the state-of-the-art HDsEMG technique to characterize spinal circuits, particularly recurrent and reciprocal inhibition, in large population of MUs.HDsEMG grids of electrodes were placed on the Tibialis Anterior (TA) and Soleus (SOL) muscles of healthy participants. Individuals had their foot strapped to a dynamometer and were to produce isometric contractions at low force levels (5% and 10%) of MVC. During the steady contractions, inhibitory responses were activated by nerve stimulation with single pulses at an interstimulus interval (ISI) of 1s or 2s to silence the ongoing muscle activity. Essentially, recurrent or reciprocal inhibitory circuits to inhibit SOL activity were evoked by nerve stimulation of the tibial nerve to stimulate SOL motor axons to antidromically activate recurrent inhibition (SOL-to-SOL); or the antagonist common peroneal to stimulate TA Ia fibres to orthodromically activate reciprocal inhibition (TA-to-SOL). A similar approach was followed for TA muscle activity: antagonist SOL Ia fibres (for reciprocal, SOL-to-TA) and TA motor axons (for recurrent, TA-to-TA) were stimulated. Individual MUs were decomposed with a blind source separation algorithm and their stimulus-triggered responses were investigated to determine the inhibition latency and duration using peristimulus histograms based on their instantaneous firing rate or occurrence. For the first time, we non-invasively estimated the latency and duration

of recurrent inhibition in the TA and SOL muscles in a large population of MUs. At the same time, we characterized optimal experimental conditions (contraction level and ISIs) to measure both spinal circuits.The technique and results derived from this study will allow to develop neurophysiological biomarkers which might contribute to early diagnosis or monitoring the progress of neuromuscular diseases, such ALS. In addition, this study aimed at favouring the translation of HDsEMG into clinical practice and neurophysiological research as a technological advancement.

O.6.5: Modulation of subthalamic nucleus activity during gait initiation in parkinson's disease patients: a biomarker for freezing

Mathieu Yèche, Sorbonne Université, Paris Brain Institute - ICM, Inserm, CNRS, APHP, Paris France; Antoine Collomb-Clerc, Sorbonne Université; Katia Lehongre, Sorbonne Université, Paris Brain Institute - ICM, Inserm, CNRS, APHP, Paris France; Saoussen Cherif, INSERM Delegation Paris IdF Centre Est / Paris Brain Institute; David Maltête, Department of Neurology, Rouen University Hospital and University of Rouen, France; David Maltête, Department of Neurology, Rouen University Hospital and University of Rouen, France; David Maltête, Department of Neurology, Rouen University Hospital and University of Rouen, France; Edward Soundaravelou, Sorbonne Université, Paris Brain Institute - ICM, Inserm, CNRS, APHP, Paris France; Déborah Ziri, Sorbonne Université, Paris Brain Institute - ICM, Inserm, CNRS, APHP, Paris France; Brian Lau, Sorbonne Université, Paris Brain Institute - ICM, Inserm, CNRS, APHP, Paris France

BACKGROUND: Freezing of gait is a major debilitating motor symptom in people with Parkinson’s disease (PPD). While increased beta band (12-35Hz) oscillatory activity in the subthalamic nucleus (STN) has been linked to motor symptom severity, identifying a clear biomarker for gait disorders and FOG in PPD remains elusive. In this study, we recorded STN neuronal activity in PPD experiencing FOG during walking, particularly focusing on gait initiation, a phase significantly affected in these patients. Our goal was to uncover the relations between STN neuronal activity modulation and gait and balance disorders, aiming to identify a potential biomarker for FOG. Methods: We simultaneously recorded STN neuronal activity and gait kinetics and kinematics parameters in 31 PPD who underwent STN deep brain stimulation (23M/8F, age = 58 ± 9 yrs, disease duration = 11 ± 4 yrs), using a force plate, motion capture system, and an embedded EEG amplifier. Patients were recorded both in the OFF and ON-dopa states (UPDRS-III score OFF-dopa = 38 ± 13 and ON-dopa = 8 ± 6). STN neuronal activity and gait recordings were subsequently analyzed offline. RESULTS: OFF-dopa, 10 patients experienced FOG episodes during gait recordings, while 21 did not. In non-FOG patients OFF-dopa, we observed beta desynchronization alongside alpha and gamma hypersynchronization at gait initiation. Beta desynchronization primarily occurred in the posterior-motor part of the STN. Conversely, in FOG patients, beta desynchronization was more widespread across the posterior and central parts of the STN during gait initiation. During trials with FOG, this desynchronization was predominant in the central part with relatively less desynchronization in the posterior part. DISCUSSION AND CONCLUSION: In PD patients with FOG, beta desynchronization is broadly distributed within the STN during successful gait initiation trials, indicating higher central-associative modulation but reduced posterior-motor involvement when a FOG episode will occur. This potentially reflects the activation of executive networks to compensate for the motor function loss during successful gait trials and a failure of this compensatory mechanism during

FOG episodes. These findings could potentially serve as a biomarker for FOG, crucial for the development of closed-loop adaptive DBS systems. ACKNOWLEDGEMENTS: We are deeply thankful to the patients for their participation and implication. Study supported by Boston Scientific, Agence Nationale de la Recherche.

O.6.6: Feasibility of high-density surface electromyography for the detection of neuromuscular disorders in children

Eduardo Martinez-Valdes, University of Birmingham; Francesco Negro, Universita' degli Studi di Brescia; Ignacio Contreras, University of Birmingham; Andrew Lawley, Department of Neurophysiology, Birmingham Children's Hospital, Birmingham, UK.

Background: The diagnosis of neuromuscular disorders in children is challenging. Concentric needle electromyography (CNEMG) is the current standard for electrophysiological examinations; however, this technique has multiple limitations that may compromise the assessment of neuromuscular function in children. First, these assessments are invasive and can be uncomfortable. Second, limited muscle sampling can be performed due to small recording area of electrodes and lack of tolerance in small children. High-density surface electromyography (HDsEMG) might overcome these limitations as it is non-invasive and better tolerated than CNEMG, and has higher spatial resolution, allowing the identification of a greater number of motor units (MUs) from different muscle regions. Purpose: To assess the feasibility of HDsEMG MU decomposition in children referred to Birmingham Children's Hospital (BCH) for electrophysiological examination and determine potential MU firing parameters allowing discriminating between children with diagnostic impression of neuropathy, myopathy, and normal examination. Methods: Fifty-four children (8.9 (5.2) y, range 0 to 16 y) that attended to BCH for electrophysiological examination underwent a CNEMG study followed by a HDsEMG assessment using a 64-channel electrode grid on tibialis anterior or biceps bracchi. Participants were requested to contract for 15s at 20% of the maximal EMG or perform a spontaneous contraction (depending on age). EMG signals were then decomposed into individual MU spike trains by convolutive blind source separation. The total number of MUs identified per participant and, the association between the number of identified MUs and age were assessed. In addition, MU firing properties were compared between groups of children with a diagnostic impression of neuropathy, myopathy, or normal electrophysiological examination (according to CNEMG results). Results: MUs could be reliably identified in 87.0% of the children. On average, 5 (4) MUs, with a complete firing pattern could be identified per child. The number of identified MUs did not depend on the diagnostic impression (p=0.129), nor sex (p=0.211), but was dependent on age (r=0.504, p<0.001), as the MU yield increased in older children. Mean discharge rate was similar across groups (p=0.734), however, discharge rate variability (quantified as the coefficient of variation for the inter-spike interval, CoVisi) was significantly higher in children with a diagnostic impression of myopathy (p=0.036). Conclusions: The results of the present study demonstrate the feasibility of HDsEMG MU decomposition in children with neuromuscular disorders, enabling the examination of full MU firing patterns in this population. This can potentially open the door for the identification of new biomarkers allowing an improved diagnosis and monitoring of neuromuscular disorders in children.

O.6.7: On the origin of short and medium latency soleus stretch reflexes: how do the amount and speed of ankle joint rotation relate to the spinal stretch reflexes in humans?

Yukiko Makihara, International University of Health and Welfare; Natalie Mrachacz-Kersting, University of Freiburg; Thomas Sinkjær, Aalborg University; Aiko Thompson, Medical University of South Carolina

Stretch reflexes are thought to contribute to various motor functions. To better understand how stretch reflexes may contribute to plantarflexor force generation, in this study, we aimed to examine how different amounts and speeds of ankle joint rotation relate to the spinal components (M1 and M2) of soleus stretch reflexes. For this, we varied only the amount and speed of ankle joint rotation. Unlike previous stretch reflex-related studies, in the present setup, the participant remained seated with a fixed joint posture for all measurements, so that we would be able to control for and maintain factors that could influence the spinal reflex excitability such as joint position and muscle contraction level.Twelve adults with no known neurological conditions participated. All measurements were made while the participant sat in a custom-made chair. The amplitude and onset latency of M1 and M2 reflexes were measured in 2 experiments; experiment 1 in which 6-12 degrees of dorsiflexion rotations were tested at a single speed (≈200deg/s), and experiment 2 in which 6 degrees of dorsiflexion rotations were tested at five different speeds (≈75–225deg/s). To characterize different rotation speed conditions, the time to reach the initial 2deg of dorsiflexion (TR2deg) and the rotation speed over the initial 2deg were calculated. The stretch reflexes were elicited while the participants maintained ≈10% MVC level of soleus background EMG.The experiment 1 results show that the amount of rotation did not affect the M1 and M2. When the rotation speed increased (experiment 2), the M1 and M2 amplitudes increased (p<0.05); the M1 latencies did not change across the speeds; the M2 latencies and TR2deg progressively shortened with increasing speeds from 63.1±5.0 to 54.1±3.2ms, and 33.6±0.9 to 10.6±0.3ms, respectively (p<0.05). To further quantify the speed dependency, the correlations between the rotation speed in the initial 2deg and the M1 and M2 amplitude, and TR2deg and M1 and M2 latency were examined. The M1 amplitude was highly correlated with the rotation speed (r=0.86±0.08), but the speed did not affect the M1 latency (r=0.19±0.20). The M2 amplitude was moderately speed dependent (r=0.55±0.16), and the M2 latency was moderately correlated with the assigned speed (r=0.60±0.12).The present results confirm past studies that the origin of M1 is likely the velocity sensitive Ia afferents from the muscle spindles. We speculate that the length-sensitive afferents (group II) may importantly contribute to the M2 having their own unique threshold muscle lengths. The longer latency of M2 with a slower speed would reflect this threshold length because a slower joint rotation would delay the timing for the group II afferents to reach the thresholds. The M1 and M2 responses can, together with intrinsic properties of the contracted muscles, be interpreted as a fist line of neural response to stabilize the joint position to an unexpected external event.

Oral Session 7

O.7.1: Respiratory sEMG measurements for quantitative comparison of bipolar electrode leads

Andra Oltmann, Fraunhofer IMTE; Jan Graßhoff, Fraunhofer IMTE; Nils Lange, Fraunhofer IMTE; Philipp Rostalski, Fraunhofer IMTE / Institute for Electrical Engineering in Medicine, Universität zu Lübeck

Surface electromyography (sEMG) of respiratory muscles has applications in assisted mechanical ventilation. It has been proposed as an approach to quantifying spontaneous breathing activity and monitoring patient-ventilator interaction by recording the diaphragm and accessory muscles. Due to the anatomy of these muscles and the presence of crosstalk respiratory sEMG usually has a small signal-to-noise ratio (SNR). To date, there is no consensus on acquisition procedures and electrode positions. The current study contributes to the standardization of respiratory sEMG measurement by conducting a quantitative comparison of bipolar leads.Measurements of respiratory sEMG were performed using the SAGA 64+ (TMSi, Oldenzaal, Netherlands) amplifier with 64 electrodes. Electrodes were placed bilaterally on the midaxillary line (MAL), anterior axillary line (AAL), midclavicular line (MCL), and parasternal line (PSL). Subjects performed a baseline measurement of muscle relaxation, 300s of quiet breathing, 5 maximum inspiratory maneuvers (MIP), and resistance breathing at 20% of maximum MIP. Cardiac artifacts were suppressed using wavelet denoising, and differential sEMG envelopes were calculated. Three metrics were determined to quantify the SNR, namely the ratio between the sEMG amplitude reached during inspiration and (1) tonic muscle activity (SNR_tech), (2) expiratory muscle activity (SNR_cross), (3) ECG interference.The current study included 11 healthy subjects (female=5 / male=6, age=25.64±3.04 years, BMI=24.30±3.58 kg/m^2), leading to the following preliminary results. Regarding the diaphragm, we evaluated the performance of bilateral electrode pairs at the standard position (costal margin). The MCL and PSL attained the highest SNRs (SNR_tech: 7.04±5.26 dB and 5.78±2.85 dB, SNR_cross: 3.05±1.15 dB and 3.00±0.97 dB, resistance breathing), outperforming the MAL and AAL. On the MCL, superior placement 2.5cm above the costal margin attained higher SNRs (SNR_tech: 9.63±8.16 dB, SNR_cross: 3.53±1.21 dB, resistance breathing) than the standard and inferior position. Regarding the intercostal muscles, we compared bilateral electrode pairs at the 2nd and 3rd intercostal space (ICS). Differences were less pronounced than for the diaphragm. On the MCL and PSL, both the 2nd (SNR_tech: 4.10±2.99 dB and 3.42±2.33 dB, SNR_cross: 2.08±0.61 dB and 2.40±0.56 dB, resistance breathing) and 3rd (SNR_tech: 3.71±2.77 dB and 3.30±2.44 dB, SNR_cross: 2.06±0.50 dB and 2.01±0.46 dB, resistance breathing) performed similarly. ECG generally was highest for positions closer to the heart, reaching up to -27.64±2.86 dB on the MCL 5cm above the costal margin and up to -24.97±5.58 dB on 3rd ICS (for quiet breathing).The presented study enables a comparison of different electrode pairs for recording respiratory muscle activity, thus providing important evidence for standardization. In the future, we intend to evaluate further electrode combinations and resistance levels.

O.7.2: Muscle activity mapping by 3-dimensional localization of motor unit action potentials from high-density surface electromyography

Jonathan Lundsberg, Lund University; Nebojsa Malesevic, Lund University; Anders Björkman, University of Gothenburg and Sahlgrenska University Hospital; Christian Antfolk, Lund University

Background: The spatial activity pattern of muscle contractions can provide information required to quantitatively assess individual muscles recovering from injuries such as stroke. Patients recovering after lost motor function may compensate the impairment of individual muscles with increased synergistic contractions of other muscles, which changes the activity pattern. Furthermore, distinguishing the activity of individual muscles may provide a path for direct translation between prosthetic control and user intent. A robust non-invasive tool for the

mapping of distinct muscle contractions is therefore in high demand. High-density surface electromyography (HDsEMG) provides a large amount of information on muscle activity, which can be used to estimate the spatial origin of motor unit action potentials (MUAPs).Method: In a new approach, we identified MUAPs and estimated their positions and fibre directions using a custom surface fit and a cylindrical volume conductor model. The surface fit was applied to the to the distribution of each MUAP signal across the HDsEMG grid. The estimated parameters from each surface fit were used to directly calculate the spatial origin of each signal. By localizing thousands of action potential firings, substantial robustness is achieved in muscle discrimination. To test the method, HDsEMG data was recorded with two 5-by-13 electrode grids, from the posterior forearm during isolated isometric low force contractions of the wrist and finger extensors. RESULTS: The MUAP activity of all finger and wrist extensors was consistently separated into distinct regions and motor unit paths in a cylinder model. MUAPs from wrist extensions with radial and ulnar rotation were localized at the radial and ulnar edges of the model respectively. MUAPs from finger extensions were localized in between the estimated regions of the carpi muscles. Furthermore, clear medial-lateral discrimination was observed between index, ring, and little finger extensions, while proximal-distal discrimination was observed between middle finger extension and all other movements. We generate 3-dimensional and cross-sectional plots of the estimated positions for clear visualization. Lastly, an energy estimate for each muscle is generated, taking muscle position into account. CONCLUSIONS: With this method, assessments of individual muscles can identify and account for compensatory synergistic contractions of other muscles. Furthermore, the nuances of individual finger movements could be used in a real-time application to improve the intuitive control of prosthetic devices.

O.7.3: Identification of mutual motor unit expression in two independently decomposed HDsEMG signals

Subaryani Soedirdjo, UT Southwestern Medical Center; Ales Holobar, University of Maribor, Faculty of Electrical Engineering and Computer Science; Yasin Dhaher, Northwestern University and The Shirley Ryan AbilityLab

Background. High-density surface electromyography (HDsEMG) systems have been used to identify the activities of motor units (MUs) during voluntary contraction. Adaptation of the neuromuscular system to interventions, injuries, or diseases may affect the behavior and properties of MU. To evaluate changes in a specific set of MUs during intervention or disease progression, identification of the expression of the same MUs is required. This study aimed to propose an algorithm to identify mutual motor unit expressions across testing visits. METHODS. Fourteen healthy subjects (26 ± 4 yr., BMI 24.1 ± 3.3 kg/m2, mean ± SD) were tested on a number of visits within a span of 30 days. They were placed in a pronate position, their knees fully extended, and their ankle joint was secured in a boot attached to a load cell. After skin preparation, a 64-channel HDsEMG grid (13 rows, 5 columns, 8 mm inter-electrode distance) was placed on the anterior tibialis with columns parallel to the proximal-distal muscle axis. The monopolar HDsEMG signals and torque were recorded at a sampling rate of 2000 Hz while the subjects performed isometric dorsiflexion following a trapezoidal torque trajectory: 10 s sustained torque at 10% of the maximal voluntary contraction (MVC) and 2% MVC/s torque increment and decrement rate.HDsEMG signals from two random visits separated by 12–16 days were selected. After independent MU decomposition in a monopolar configuration using

the Convolution Kernel Compensation algorithm, column-wise single differential MU action potential (MUAP) shapes were calculated using spike-triggered averaging. MUs with a pulse-to-noise ratio (PNR) <28 dB were discarded. Mutual MU expression was then identified using the MUAP image registration method. The performance of the proposed algorithm was evaluated by comparing the PNR, precision, and sensitivity of the firing patterns with reinforcement before and after the application of the algorithm. Results. The Wilcoxon paired test showed no significant difference in MVC (31.7 ± 8.0 Nm and 32.4 ± 8.1 Nm, p = .71), number of identified MUs (16 ± 7 and 14 ± 5, p = .11), and average PNRs (34.2 ± 3.5 dB and 35.2 ± 4.9 dB, p = .85) between the two visits. On average, the proposed algorithm could identify the mutual expressions of 61% of the identified MUs in 11 participants and failed in 3. There was a significant improvement in the average PNR from 25.9 dB to 34.1 dB (p < .001), an increase in the average sensitivity from 59% to 92% (p < .001), and an increase in the average precision from 64% to 92% (p < .001). CONCLUSION: . We proposed an algorithm to identify the expression of mutual MUs in two testing visits. This approach will help expand our understanding of the characteristics of MUs across testing visits.Funding. S.D.H.S. and Y.Y.D. are supported by NIAMS (1R01AR069176-01A1). A.H. is supported by the Slovenian Research Agency (J2-1731 and P2-0041).

O.7.4: Is spinal motion preserved following vertebral body tethering for adolescent idiopathic scoliosis? A prospective study

Kristen Beange, Carleton University; Kevin Smit, The Children's Hospital of Eastern Ontario; Holly Livock, The Children's Hospital of Eastern Ontario; Ryan Graham, University of Ottawa

Purpose: Adolescent idiopathic scoliosis (AIS) is a 3D structural deformity of the spine, characterized by abnormal curvature and rotation of the vertebral column, often requiring early intervention to stop or slow curve progression, or surgery in severe cases. The gold-standard surgery is posterior spinal fusion and instrumentation (PSF); however, significant loss of range of motion (ROM) has been reported, which can lead to long-term complications. Vertebral body tethering (VBT) is a novel minimally invasive surgical technique that has shown preservation of ROM in computer-simulated and animal models. Results from pilot work retrospectively evaluating ROM suggest that spinal motion is preserved in the transverse plane (Maksimovic et al., 2023); however, the effect on spine ROM has not been explored prospectively. The purpose of this work is to prospectively compare spine ROM in 4 groups: 1) VBT; 2) PSF; 3) untreated/braced AIS; and 4) controls (CTRL). Methods: 51 participants (8 PSF, 11 VBT, 13 AIS, 19 CTRL) have completed a baseline assessment, and 16 participants (1 PSF, 7 VBT, 7 AIS, 1 CTRL) have completed 1-year follow-ups. Aligning with our previously validated protocol (e.g., Beange et al., 2023), 3 inertial measurement units were placed over C7, T12, and S1 vertebrae (locations confirmed via ultrasound imaging to ensure sensor placement reliability between visits). Participants performed 2 repetitions each of spine forward flexion, and bilateral lateral bending, axial rotation, and circumduction to their end ROM in 2 conditions: constrained (at the hip) and unconstrained. Fused quaternion data were extracted and converted to rotation matrices. Relative thoracic (C7 relative to T12), lumbar (T12 relative to S1), and total (C7 relative to S1) orientation was computed and converted to Euler angles using a transverse-frontal-sagittal rotation sequence. Orientation was zeroed to a standing position, and axial ROM was calculated by computing the maximum orientation (for bilateral movements, right and left ROM were averaged). Box plots were constructed to evaluate between-group and between-visit

differences. RESULTS: Results for constrained lateral bending are presented, as previous pilot work showed significant differences between groups for this task. Total ROM (Figure 1c) decreased between baseline and follow-up visits, and there is a slight increase in lumbar ROM, which is likely a result of compensatory movement to offset decreased ROM in the thoracic region (most commonly affected region). Conclusion: While it is difficult to draw conclusions from all groups (e.g., N=1 in PSF and CTRL follow-up groups), ROM estimates in the current study align with results from pilot work. Results for the remaining tasks and 1 year follow-up visits will be presented at the conference. It is expected that spine ROM will be preserved in VBT patients compared to PSF, and that post-treatment ROM will assume the following order: CTRL > AIS > VBT > PSF.

O.7.5: Continous knee dynamics monitoring: combining inertial measurement units and multichannel electromyography

Nebojsa Malesevic, Lund University; Ingrid Svensson, Lund University; Gunnar Hägglund, Lund University; Christian Antfolk, Lund University

The assessment of human joint kinematics and muscle activity is crucial for understanding movement and function, particularly in diagnosing and treating musculoskeletal conditions. This research focuses on Cerebral Palsy (CP), a common childhood motor impairment syndrome characterized by a variety of movement and posture disorders. CP arises from brain lesions or abnormal development, especially in motor control regions, leading to symptoms like spasticity, muscle weakness, and impaired postural control.This paper introduces a novel multimodal approach that synergizes inertial measurement unit (IMU) sensors with electromyography (EMG). Except for the precise measurement of knee angles in individuals suffering from CP, the use of EMG provides valuable complementary data, offering insights into the patterns of muscle activation which are essential in understanding the complexities of CP-affected gait. This hardware features a minimal design for seamless integration into clothing, ensuring user comfort during extended periods. It employs two IMUs placed on the thigh and shank for precise, non-intrusive knee angle measurements, overcoming the drawbacks of traditional mechanical sensors. The system also includes an 8-channel EMG amplifier to monitor muscle activity. An embedded ARM M7 microcontroller manages sensor communication, real-time signal processing, and data storage. For continuous, all-day knee activity monitoring, the device is powered by a 5000 mAh external battery pack, conveniently carried in the user's trouser pocket. In this paper, our focus was on examining the efficacy of this integrated approach, particularly the accuracy of IMU sensors in tracking knee joint movements, EMG signal quality, and synchronous data acquisition suitable for further analysis. This angle accuracy was benchmarked against an optical motion-tracking system, a standard in the field. The EMG signal quality was estimated during self-paced walking on a treadmill. The results show that the knee angle estimation error of the presented device falls within the state-of-the-art devices (mean RMSE of 6°) while the signal-to-noise ratio of the 8 EMG channels exceeded 100 dB. The synchronization between knee angle and muscle activity was qualitatively evaluated using observed perturbations in the gait cycles. While the primary aim of developing and evaluating this system was its inclusion in an ongoing clinical CP study, the design of both the hardware and algorithms is not limited to CP patients. This allows the device to be applicable in measuring joint activity across various human joints and in different protocols.

O.7.6: Design and validation of a versatile and flexible electrode grid for US-transparent acquisition of HD-sEMG signals

Giacinto Luigi Cerone, Politecnico di Torino; Taian Vieira, Politecnico di Torino; Maurizio Martinez, ReC Bioengineering Laboratories S.r.l.; Marco Gazzoni, Politecnico di Torino; Alberto Botter, Politecnico di Torino - LISiN

BACKGROUND AND AIM. High Density EMG (HD-EMG) and ultrasound (US) imaging provide complementary information about the physiological mechanisms underlying force generation. Their combination can reveal how neural and mechanical variables interplay during a muscle contraction. Although different approaches have been proposed, the use of US-transparent electrode grids seems the most suitable way to implement this integration. Despite the progresses made in this field[1], current US-transparent electrodes have two limitations: 1) the minimum inter-electrode distance (IED) achievable with the current manufacturing technology (10 mm), limiting electrodes' density and recordings from small muscles; 2) the 50 Hz/60 Hz common mode voltage injected by the US probe, leading to power line interference in HD-sEMG signals. While the latter factor was minimized by ground-floating and miniaturized amplifiers[2], the first one still requires technological improvements. The aim of this work is to design, develop and test a highly-conformable and US-transparent HD-sEMG grid. METHODS. The electrode grid is composed by a thin silicone substrate integrating a flexible silver electrode grid. Two 8x4 grids with 5 mm and 10 mm IED were prototyped (Fig 1.a) and characterized with electrical and functional tests. The electrical characterization included an impedance analysis performed though a custom-made impedance meter. The electrode-skin impedance (ESI) was measured on the biceps of six subjects and compared with that of standard HD-sEMG electrodes. Afterwards, HD-sEMG signals and US images were concurrently acquired during isometric elbow flexions at 5%, 10% and 30% MVC. MEACS system (LISiN and ReC Bioengineering Laboratories, Italy) and ArtUs (Telemed, LT) were used to collect HD-sEMG and US images respectively. Signal quality was assessed through visual inspection and quantified through the SNR. HD-sEMG decomposition was applied to verify the possibility of identifying the activity of single motor units. RESULTS. The magnitude of the ESI at 50Hz was 89kΩ±23kΩ and was comparable to that of standard electrodes for HD-sEMG[3]. The SNR was always higher than 46dB. HD-sEMG decomposition allowed to extract the firing pattern of 5.8±2.3 MUs per contraction (PNRR=29.3±5.2). The comparison between the US images detected with/without the presence of the grid between the US probe and the skin showed no alterations in the image quality (Fig 1.b). CONCLUSIONS. The developed detection system represents an improvement of the current technology for the concurrent acquisition of HD-sEMG and US images opening the possibility to use denser grids and to investigate smaller muscles. Its characteristics in terms of conformability and electrode-skin interface makes the proposed solution a valid option for the collection of high-quality HD-sEMG signals also in general-purpose scenarios.REFERENCES[1] Botter et al. 2013 JAP[2] Cerone et al. 2029 IEEE TBE[3] Piervirgili et al. 2014 Phys. Meas.

Oral Session 8

O.8.1: Statistical and physiological variations in single motor unit reflex amplitude estimation

Laura Schmid, University of Stuttgart; Thomas Klotz, University of Stuttgart; Oliver Röhrle, University of Stuttgart; Francesco Negro, Universita' degli Studi di Brescia; Utku Yavuz, The University of Twente

BACKGROUND AND AIM: The peri-stimulus time histogram (PSTH) and peri-stimulus frequency-gram (PSF) are two common methods for analyzing reflex responses of motor units (MU). In both methods, it is assumed that the size of synaptic input to MU is correlated with the size of its reflex response. However, the variation in MU reflex response is multi-factorial. For example, the size of reflex amplitude changes with the discharge rate and membrane noise. These phenomena complicate using measured reflex responses to estimate the size of the input current and the input-output gain. In the present study, we aim to investigate factors correlated with reflex size among a MU population. We hypothesized that the numerical discrepancies between PSTH and PSF can be sources of uncertainty that influence the estimation of synaptic input among a MU population, each sensitive to different discharge properties of MUs.METHOD: We analyzed Hoffmann (H-) reflex amplitude variability among a MU population using experimental and simulation data. In-vivo MUs were identified by decomposing high-density surface EMG signals from tibialis anterior muscles. The reflex is elicited by stimulating the common peroneal nerve during sustained dorsiflexion contraction (10% and 20% of maximum voluntary contraction). In the simulation, we created 200 motoneurons using a model with soma and dendrite compartments. To obtain a motoneuron pool, the membrane resistance and compartment size were exponentially distributed across motoneurons. The supraspinal neural drive was modelled with common and independent noise, while the monosynaptic reflex input (EPSP) was kept the same for the entire pool. The reflex amplitude was measured using the cumulative sum of PSTH and PSF for experimental and simulation data. RESULTS: For experimental data, we found a significant positive linear correlation between reflex amplitude measured from PSF and background discharge rate in 4 of 6 subjects (R = 0.40-0.72, P <0.05). The slope of the regression between background discharge rate and reflex amplitude was correlated with the amount of total membrane noise computed as the coefficient of variation of the inter-spike interval (R=0.50 and P=0.04). PSTH did not confirm the same relation. This discrepancy between PSTH and PSF was further investigated using a computational model. The simulations confirmed that the reflex amplitude is nonlinearly influenced by the discharge probability (discharge rate and variability of inter-spike intervals). However, the effect differs between PSTH and PSF. The PSF was sensitive to the distribution of the soma resistance (MU type) that was induced in the simulation, while the PSTH method was not particularly responsive to that. CONCLUSION: These results can be interpreted in such a way that the choice between PSF and PSTH depends on the specific research question and the level of analysis. For example, the PSF can be a better method to analyze the distribution of reflex size among a motor unit population with different phenotypes.

O.8.2: Comparsion of FES induced muscle fatigue during isometric and isotonic forearm muscle contractions

Sascha Selkmann, Ruhr-Universitaet Bochum; Christian Sure, Ruhr-Universitaet Bochum; Marc Neumann, Ruhr-Universitaet Bochum; Beate Bender, Ruhr-Universitaet Bochum

Background: Fatigue limits the practical applicability of Functional Electrical Stimulation (FES). As fatigue is not avoidable, the classification and management becomes a priority. An effective

implementation of this strategy requires an understanding of the current state of fatigue and the fatigue behavior of the muscles. Previous studies on fatigue have focused on the lower extremities and investigated the forces and torques generated. However, when applied to the hands forces and movements are of importance. It is therefore crucial to identify indicators of fatigue that consider force and movement aspects. The aim of the present study is to compare the dependence of fatigue on the stimulation parameters during isometric and isotonic contractions and to collect data for a future fatigue management system. Methods: In our study, we examined nine healthy volunteers (8M,1F; Age: 38.1±11.9y; Ht: 1.78±0.07m; Wt: 76.6±9.4kg) who each completed 16 stimulation sessions of 20 minutes one week apart. We separately measured the movements and forces of the flexor digitorum superficialis (FDS) and extensor digitorum (ED) muscles under four different stimulation conditions (15 Hz 70 µs, 15 Hz 300 µs, 30 Hz 70 µs, 30 Hz 300 µs) and 70% of the max. tolerable stimulation current. We choose a stimulation cycle (SC) with a ratio of 12 seconds stimulation and 4 seconds pause. Muscle activity was recorded using sEMG, force and motion measurements were performed with self-developed devices. We classified fatigue into four levels based on amplitude decay: none (NF): up to 10%; light (LF): up to 25%; moderate (MF): up to 50%; and high (HF): over 50%. RESULTS: The force and movement measurements on the ED and FDS showed significant differences under all conditions (p < 0.05). In isometric contractions, LF occurred after an average of 9±6 and MF after 24±8 SC, while in isotonic contractions LF was observed after 16±9 and MF after 35±12 SC. HF was observed in isometric contractions in five cases after 43±10 cycles and in isotonic contractions only in one case after 59 cycles. At 15 Hz (36±12 SC) MF occurred under all variations up to twice as late as at 30 Hz (17±8 SC). The two pulse lengths show little difference 70 µs (27±8) vs 300 µs (25±14). Due to the small sample size, a trend is recognizable, but without statistical significance. Conclusion: Fatigue manifests differently under isometric and isotonic contractions. LF and MF occur sooner in isometric contractions compared to isotonic ones, indicating a quicker onset of muscle fatigue in the former. HF was less frequently observed and appeared later, particularly in isotonic contractions. At 15 Hz, the time until MF was almost double compared to a higher frequency of 30 Hz, suggesting that lower frequencies may be more beneficial for delaying fatigue. However, the difference in pulse lengths (70 µs and 300 µs) showed minimal impact on fatigue. A larger group of participants is necessary to validate these trends.

O.8.3: Modulation of spinal motor neuron excitability by transcranial electrical stimulation

Prakarsh Yadav, PhD student; Douglas Weber, Carnegie Mellon University; Mats Forssell, Postdoctoral researcher; Jeehyun Kim, Electrical & Computer Engineering; Vishal Jain, Electrical & Computer Engineering; Pulkit Grover, Electrical & Computer Engineering

Neuromodulation of corticospinal excitability can be achieved through transcranial electrical stimulation (TES) and may be used to promote motor rehabilitation. The stimulation site and waveform parameters can be tuned to target spinal motor neurons of specific muscle groups. Most studies of TES measure motor evoked potentials (MEPs), which are compound muscle action potentials generated by the synchronous activation of motor neurons in response to stimulation of corticospinal neurons. While MEPs represent clear and direct effects of TES on corticospinal activity, the threshold for evoking MEPs by TES is typically very high, requiring high amplitude stimulation that is uncomfortable or even painful. For TES to be suitable as a rehabilitation tool, it is necessary to develop stimulation protocols that avoid causing extreme

discomfort in patients. In this study, we hypothesized that TES could be used to modulate the excitability of spinal motor neurons at stimulation intensities below the threshold for evoking MEPs. We used high-density electromyography (HDEMG) and motor unit decomposition to measure the spontaneous discharge of motor units recorded in flexor muscles of the forearm of participants performing isometric wrist flexion tasks. TES was applied over the contralateral motor cortex, targeting the wrist flexor muscles. MEPs were recorded to confirm the target location for the anode, which was found to be at C3 and the cathode was located at CZ.We estimated motor neuron excitability using the delta-F method on the motor unit spiking data. Participants performed isometric wrist flexion as a ramping force contraction by following a force trace prompt. The force profile was monotonically increasing for 30 seconds and then monotonically decreasing for 30 seconds. During wrist flexion and relaxation, TES was delivered to evoke MEPs. We also repeated the experiment with sham stimulation applied at a different location, 5 cm posterior to the forearm flexor representation, to control for persistent inward current (PIC) modulation as a response to the pain of stimulation. We decomposed the isometric wrist flexion HDEMG data to get motor unit (MU) firing information. The MU decomposition was performed through the Convolution Kernel Compensation (CKC) algorithm. From the motor unit firing information we identified test and reporter MUs for the delta-F method of motor neuron excitability. This early finding can provide insights to improve the design of TES protocols for motor rehabilitation and future studies to unravel the mechanism of modulation of spinal motor neuron excitability.

O.8.4: Caffeine attenuates discharge rate reduction during maximal sustained contractions

Karen Mackay, Torrens University Australia; Lucas Orssatto, Deakin University; Gabriel S Trajano, 3

INTRODUCTION: Caffeine is a methylxanthine with proved ergogenic effects on exercise performance and known to influence the central nervous system by increasing the release of monoamines. Recent research shows that repetitive sustained maximal contractions reduced PIC contribution to motoneuron discharge rates, despite the consumption of caffeine. Yet, caffeine consumption attenuated torque loss during repetitive fatiguing contractions. This suggests an effect of caffeine on intrinsic motoneuron properties that might contribute to torque production during repetitive fatiguing contractions.PURPOSE: To investigate if caffeine consumption would change motor unit discharge rates during maximal repetitive sustained contractions. Methods: In a crossover, double-blind design, six individuals performed four isometric maximal contractions and sustained them until torque production dropped to 60% of maximum capacity after consuming either 6 mg· kg-1 of caffeine (CAF) or placebo (PLA). Tibialis anterior motor unit discharge rates were recorded from a 64-channel electrode and analysed from high-density surface electromyograms (HD-EMG). HD-EMG signals were decomposed into single motor unit discharge events and then converted into instantaneous discharge rates. Motoneuron discharge rates were recorded at the beginning and end of each contraction. Total torque-time integral was measured during the repetitive sustained maximal contractions. RESULTS: No differences in discharge rates were observed between CAF and PLA at the beginning of the contractions [P= 0.99; mean difference 0.15 Hz (95%CI: -0.82,1.14)], but were 2.7 Hz (95%CI: 1.7, 3.7) higher during CAF at the end of the contractions (p<0.001; d = 1.1). Overall, discharge rates reduced 5.4 Hz (95%CI: 4.4, 6.5) for CAF and 8.0 Hz (95%CI: 7.1, 8.8)

for PLA from the beginning to the end of the contraction (p<0.001, CAF: d= 2.2 and PLA: d= 3.3). Participants produced 337 Nm.s (95%CI: 49.9,624) (d=0.63) more torque integral during the repetitive sustained maximal contractions after caffeine consumption. CONCLUSION: : Caffeine-attenuated the reduction of discharge rates during repetitive maximal sustained contractions. This allowed participants to endure maximal torque production for longer.

O.8.5: Changes in recruitment and motor unit firing patterns with deep brain stimulation for Parkinson's disease

Jérémy Liegey, UCD; Richard Walsh, Tallaght Hospital, Mater Misericordiae University Hospital; Ben O'callaghan, University College Dublin; Madeleine Lowery, University College Dublin

Deep Brain Stimulation (DBS) and dopaminergic medication are well-established therapies for reducing the symptoms of Parkinson's disease. The manner in which they influence motor unit and muscle activation patterns, however, are not well-understood. The aim of this study was to gain insight into the underlying mechanisms through which DBS and medication improve motor function and , specifically, how they influence motor unit firing and recruitment patterns. High density electromyography (HD-EMG) signals were recorded in 14 participants with bilateral DBS for Parkinson's disease under four different conditions representing all combinations of Medication ON and OFF, and DBS ON and OFF. Data were recorded from the first dorsal interosseus muscle during submaximal isometric index finger abduction at 10 %, 20 % and 30 % of maximum voluntary contraction (MVC). HD-EMG were decomposed into individual motor unit spike trains using convolutive blind source separation [1], [2]. Individual motor units were tracked across conditions using methods based on multi-dimensional representations of motor unit action potentials and surface EMG features, motor unit firing and action potential properties estimated and compared across conditions. A total of 1,822 units were decomposed from the steady state of the contraction in 252 trials and 495 motor units tracked across conditions. Both medication and DBS led to a significant increase in MVC force (p << 0.01 and p = 0.031). In parallel to the increase in force, DBS led to a significant increase of the mean firing rate of the tracked motor units when participants were off medication (p = 0.043). Simultaneous application of DBS and medication led to a significant decrease in mean firing rates when compared to single-treatment conditions (p = 0.039 and p = 0.005). Both the peak-to-peak amplitude of the decomposed motor unit action potentials and the median frequency of the HD-EMG signal increased with this reduction in firing rate, consistent with the recruitment of higher threshold motor units.The results indicate that DBS leads to an increase in motor unit mean firing rate when medication is OFF but alters the relative contribution of firing rate and recruitment in favor of recruitment when on dopaminergic medication. The results provide insights into the way in which motor unit firing and recruitment patterns are altered by DBS resulting in increased force generating capacity.[1] F. Negro, S. Muceli, A. M. Castronovo, A. Holobar, and D. Farina, "Multi-channel intramuscular and surface EMG decomposition by convolutive blind source separation," J. Neural Eng., vol. 13, no. 2, p. 026027, Feb. 2016, doi: 10.1088/1741-2560/13/2/026027.[2] A. Holobar and D. Zazula, "Multichannel Blind Source Separation Using Convolution Kernel Compensation," IEEE Trans. Signal Process., vol. 55, no. 9, pp. 4487–4496, Sep. 2007, doi: 10.1109/TSP.2007.896108.

O.8.6: Serotonergic modulation of lower and higher threshold motoneurones via 5-HT2 receptors in humans

Tyler Henderson, Griffith University; Janet Taylor, Neuroscience Research Australia (NeuRA); Jacob Thorstensen, The University of Queensland; Justin Kavanagh, Griffith University

Introduction: Recent human work has utilised pharmacological interventions to influence 5-HT activity within the central nervous system and assessed the effects of 5-HT2 receptor antagonism on motoneurone excitability. The results of these studies suggest that reduced activation of 5-HT2 receptors can influence the excitability of the motoneurone pool and reduce motor unit firing rates during voluntary efforts, primarily through the modulation of persistent inward currents (PIC). During voluntary muscle contractions, a proportion of the motoneurone pool is recruited, made up of smaller and larger threshold neurones, which are differently affected by PICs. The contribution of PICs to the firing characteristics of smaller motoneurones is greater than larger motoneurones due to the prolonged firing characteristics of smaller motoneurones. Currently, it remains unclear whether different motoneurones within a pool are affected differently by 5-HT2 modulation, as most assessments of motoneurone activity encompass a large proportion of the pool including low- and high-threshold neurones. Methods: Eight healthy individuals (aged 24 ± 3yr) participated in two testing sessions, where either a placebo, or 5-HT2 antagonist cyproheptadine (8mg) was administered. All measures were obtained pre- and post-pill ingestion for the placebo and cyproheptadine condition. Participants performed low-intensity elbow flexions to 10%, 20% and 30% of their maximal torque capacity with cervicomedullary motor evoked potentials (CMEP) measured from the biceps brachii during each contraction. Two stimulation intensities (low and high) were used to produce CMEPs. Low intensity stimulation would likely recruit a small portion of the motoneurone pool, and only motoneurones which are active or close to firing during the voluntary contraction. During low intensity contractions, this proportion of neurones recruited into the CMEP response would be lower threshold due to low descending drive. High intensity stimulation recruits a large portion of the motoneurone pool, and this portion of the motoneurone pool would probably include both low- and high-threshold neurones. All CMEP responses were normalised to relevant Mmax values. RESULTS: For the placebo condition, there were no differences (p > 0.05) in maximal force production or CMEP amplitude following ingestion of the placebo. However, cyproheptadine reduced maximal torque production by ~5% (p = 0.008), and increased CMEP amplitude for low intensity stimulation (~20%) and high intensity stimulation (~15%) across each contraction intensity. The change in CMEP amplitude from baseline was greater in the cyproheptadine condition compared to placebo for low intensity stimulation (p = 0.001) and high intensity stimulation (p = 0.042) at all contraction intensities. Conclusion: Antagonism of 5-HT2 receptors provide insight to the effects of serotonergic neuromodulation. Our results suggest that 5-HT2 receptors modulate both lower and higher threshold motoneurones, and these effects may be greater on lower threshold motoneurones. In addition, it appears that greater descending drive to the motoneurone pool is required to achieve submaximal torque targets when activation of 5-HT2 receptors is reduced. This project provides further insight to the role of serotonin in regulating motoneurone activity during voluntary muscle contractions.

Oral Session 9

O.9.1: Uncertainty aware hand posture classification for better assistive devices in spinal cord injury patients

Raul Sîmpetru, Friedrich-Alexander-Universität Erlangen-Nürnberg; Daniela Souza de Oliveira, Friedrich-Alexander University Erlangen-Nürnberg; Dominik Braun, Friedrich-Alexander-Universität Erlangen-Nürnberg (FAU); Matthias Ponfick, Krankenhaus Rummelsberg GmbH, Querschnittszentrum Rummelsberg; Alessandro Del Vecchio, Friedrich-Alexander Universität, Erlangen-Nürnberg

Individuals with motor-complete spinal cord injuries (SCI) (Rupp et al., 2023) experience a complete loss of hand motor control, significantly impacting their ability to perform daily tasks. Recent findings from surface electromyography (sEMG) studies (Ting et al., 2019) indicate that certain motor units (MUs) located below the injury site remain unaffected. Based on this discovery, we hypothesize that the signals from the preserved MUS could be utilized to predict the desired hand posture. However, while it is known that the sEMG signal exhibits variability within the same task, existing classification algorithms do not offer any means to measure uncertainty. This limitation often results in undesired movements being executed.We utilized two datasets comprising 13 healthy individuals and 8 subjects with complete motor impairment (C4-C6) due to chronic SCI for our analysis. Each participant imitated hand movements—finger flexions, grasps, and pinches—displayed digitally on a screen. During these actions, sEMG data from the forearm was captured using 320 electrodes. We employed our previously published AI model (Sîmpetru et al., 2023), capable of real-time prediction of hand kinematics, which we trained for each subject (Fig. 1A). To use the model for classification, we projected its high-dimensional latent space using the Uniform Manifold Approximation and Projection technique (McInnes et al., 2022) into 2D representations (Fig. 1B). We classified the movements using the 2D projections by employing a support vector classifier (SVC). To gauge the certainty of classification, we adopted the Regularized Adaptive Prediction Sets (RAPS) conformal calibration technique. This method provided prediction sets with a 95% guarantee of containing the true class. The quantity of classes within the set enables us to assess uncertainty levels: one class represents certainty, while the maximum number of classes (in this case, 8) indicates uncertainty and lack of reliability (Fig. 1C). We found that the AI system could make proportional hand kinematic predictions for healthy individuals, but when applied to SCI patients it could, as expected, only predict a subset of movements (p < 0.001, n = 60480 predictions; 2880 per subject). When used for classification, we achieved 99.8% accuracy for the healthy subjects and 98.2% for SCI using the SVC on its own. The sets predicted using RAPS have been used in two ways. First, if we found an uncertain prediction (Fig. 1B & C, more than one prediction in set), we used prior certain predictions to guess the best solution. This improved the accuracy to 99.3% for SCI. The other way, which may be of higher benefit for real-life, is to not output an uncertain prediction at all. This attempt brought the accuracy to 99.7%, showing that in some cases the AI model was certainly wrong in its prediction.Although the results have been tested on offline data and online assessment is now in progress, we believe that uncertainty aware classification can provide valuable rehabilitation prospects for patients and could help mitigate unwanted gesture switches. Further, the uncertain regions could provide insight into whether a motor command is recoverable or not, as uncertain areas might be a sign of damage.

O.9.2: Conditional generative models to simulate motor unit action potentials during dynamic contractions

Shihan Ma, Imperial College London; Alexander Clarke, Imperial College London; Kostiantyn Maksymenko, Neurodec; Samuel Deslauriers-Gauthier, Neurodec, Inria Centre at Université

Côte d'Azur; Xinjun Sheng, Shanghai Jiao Tong University; Xiangyang Zhu, Shanghai Jiao Tong University; Dario Farina, Imperial College London

BACKGROUND AND AIM: Forward modelling of volume conductors provides a fundamental tool to study the generation process of surface electromyogram signals. Current state-of-the-art models use numerical methods, which describe anatomically accurate geometries but are computationally consuming to simulate dynamic contractions. We propose that an alternative approach to modelling realistic volume conductors during dynamic movement is to combine transfer learning with conditional generative models. METHODS We propose BioMime, a conditional generative model that aims to capture the underlying distribution of the motor unit action potentials (MUAPs) by distilling knowledge from the limited outputs of an advanced numerical model. BioMime takes the form of a semi-supervised deep latent generative model with an encoder-decoder structure and is trained in an adversarial manner. This allows the model to embed the states of MUAPs into the latent representations and then generate new data by applying a dynamic change to the embedded states. By minimising the Kullback-Leibler divergence between the predicted distribution of the latent and a prior distribution, BioMime can also be used to generate new data by sampling from the prior distribution. BioMime was trained on the MUAP waveforms generated by an advanced numerical model. The dataset includes the waveforms of 1,500 MUs from eight superficial forearm muscles under 256 conditions, which capture the variance of motor unit locations, fibre density, current source propagation velocity, muscle fibre length, and innervation zone position. RESULTS We demonstrate that BioMime is accurate to generate MUAPs that are consistent with the ground truth (normalised root mean square error less than 2.0% on the held-out test dataset). When we feed BioMime with a sweep of continuously changed conditions, BioMime outputs MUAPs that change smoothly and match the ground truth waveform when the ground truth exists in the dataset. This indicates that the model is able to generalise the system states and could be used to simulate dynamic MUAPs. Lastly, we show that generating new data using BioMime is ultra-fast. It takes BioMime less than 0.3 seconds to generate MUAPs within one muscle under one condition. This effectiveness allows BioMime to be used for simulating MUAPs during dynamic contractions. CONCLUSIONS The proposed BioMime model is an example of a conditional generative model that embeds the volume conductor system into the weights of a neural network. The accuracy and efficiency provided by BioMime allow the generation of dynamic MUAPs during a voluntary movement with high temporal resolution. We anticipate the promise offered by BioMime will stimulate research in such dynamic simulations and biophysiological system designs.

O.9.3: Development of an adaptive and generic model to forecast ankle motion based on EMG signals during walking at different speeds and inclines

Homayoon Zarshenas, The University of Auckland; Andreas Kempa-Liehr, The University of Auckland; Bryan Ruddy, The University of Auckland; Thor Besier, The University of Auckland

Background and AimPredicting the motion intention of individuals accurately and reliably is critical to provide an intuitive interaction between humans and assistive robots. For this, electromyography (EMG) signals alongside the kinetics/kinematics information can be used as inputs for neuromusculoskeletal [1] or data-driven models [2]. However, creating a generic EMG-based motion predictor to match a broad range of activities for a wide population is

challenging. Here, we propose a task- and subject-independent adaptive model without the need for prolonged calibration phases and evaluate its performance to predict ankle angles. METHODSAnkle angles in the sagittal plane measured via a motion capture system, and EMG signals from five muscles in each of the left and right legs were collected from 10 individuals walking at four speeds (1, 1.5, 2, and 2.5m/s) on a treadmill at three different inclines (-10%, 0%, and +10% slope). The study was approved by the local ethics committee. Training of the model was performed on the data of one participant walking at 1 m/s at 0 % slope, while the model's performance when predicting ankle angle was assessed from the whole dataset. The model was developed to predict the ankle angle 30 ms in the future (at 100 Hz) based on a 1 s window of EMG signals and ankle kinematics (Fig. 1). Data fusion of the raw input time series was performed before frequency- and time-based features were extracted and the best 50 features to predict ankle angles were selected using the Python library "tsfresh" [3]. A polynomial regression model then predicted the ankle angle. To build the adaptive model, the error between the forecasted ankle angle and the actual value was used in a feedback loop to update the model parameters if the error was more than 3°. Finally, the model performance in adaptive mode (with feedback loop) was compared to non-adaptive mode (without feedback loop). ResultsThe adaptive model predicted the ankle angles for unseen data at the various walking speeds and inclines with a root mean square error (RMSE) between 1.66° to 5.06° (coefficient of determination (R2) between 0.820 to 0.964), demonstrating its generic use across individuals and walking parameters. The adaptive model outperformed the conventional model by reducing the RMSE by ~70%. CONCLUSIONSThe proposed model is responsive to walking speed changes, anatomical differences among people, and terrain diversity and achieved continuous and accurate predictions of joint kinematics. It paves the way for a stable and reliable control for wearable assistive robots for the ankle joint, where ankle angle measurements can be achieved with simple strain gauge goniometers.References1. Lloyd D.G et al., J. Biomech. 36: 765-776, 20032. Zhang L et al., IEEE Trans. Auto. Sci. Eng. 18: 564-573, 20213. Christ M et al., Neurocomputing 307: 72-77, 2018

O.9.4: Automated movement screen: using smartphone videos to objectively appraise low back motor function

Shawn Beaudette, Brock University; Carl Alano, Brock University

Introduction: Low back disorders (LBDs) are the leading cause of disability, affecting >500 million people annually across the globe [1]. Through the biopsychosocial model, there are many intersecting phenomena related to the disproportionately high chronicity of LBDs [2]. Using lab-based motion capture, studies have identified limitations in motor function associated with LBDs, leading researchers to emphasize the need to stratify LBDs based on motor control outcomes [3]. Recently, advancements in computer vision allow for the analysis of human pose using commercially available video. It is possible that kinematic data, derived from a smartphone (or similar) may have utility in objectively discriminating those with LBDs to streamline diagnoses or track rehabilitation outcomes. The purpose of the current work was to explore the ability of human pose data, derived from consumer-grade video cameras during the completion of common activities of daily living (ADLs), in the objective scoring of participant reported outcome measures (PROMs) related to low back function. Methods: A sample of 448 participants from across the globe completed the current study. After providing informed consent, all participants completed six PROMs related to perceived disability, kinesiophobia,

pain catastrophizing, physical activity, and pain/discomfort. In addition, participants filmed their completion of four ADLs: (1) body weight squat, (2) small object pickup, (3) spine flexion/extension, and (4) sit-to-stand transitions. Following normalization to z-scores, PROM data were summed to calculate a composite index (CI) of low back function. Further, ADL videos were analyzed using an open-source pose estimator, MediaPipeTM whereby 33 body-referenced landmarks were obtained for all recorded video frames. Pose data from all videos were subsequently interpolated, filtered, cropped, and aligned using custom MATLAB script prior to input into Principal Components Analysis (PCA). PC scores explaining ≥99% variance within the dataset were retained and input as predictors into a stepwise linear regression model to predict CI. RESULTS: Preliminary data from the body-weight squat movement suggest that PCs derived from video recordings with high quality (n = 359) maintain a significant multivariate linear relationship (p < 0.0001, R2 = 0.351, RMSE = 0.542) with CIs. Aggregate PCA reconstruction (Figure 1) depicts functionally relevant differences related to lower body joint range-of motion, trunk inclination angle, and movement velocity. CONCLUSIONS: Features derived from open-source pose estimators show moderate-strong relationships to PROM-referenced CIs of low back function. The data-driven approach explored with this work is novel for the use of computer vision algorithms to objectively track LBDs. References: [1] Wu, A et al. (2020). Ann Transl Med 8(6): 299; [2] O'Sullivan, P. (2005). Man Ther, 10(4), 242–255; [3] van Dieën et al., (2019). J Orthop Sports Phys Ther 49(6): 370-9.

O.9.5: The use of artificial intelligence and accessible smartphone technology for predicting the degree of spinal curvature in adolescents with adolescent idiopathic scoliosis

Jessica Wenghofer, University of Ottawa; Holly Livock, The Children's Hospital of Eastern Ontario; Andrew Tice, The Children's Hospital of Eastern Ontario; Kevin Smit, The Children's Hospital of Eastern Ontario; Ryan Graham, University of Ottawa

Introduction: Adolescent Idiopathic Scoliosis (AIS) is a spine deformity, characterized by three-dimensional curvatures of the spine. The current gold-standard for diagnosing AIS and monitoring curve progression is the measurement of the Cobb angle of the spine from posterior-anterior (PA) standing radiographs. The Cobb angle is defined as the angle between the endplates of the two most tilted vertebrae. Despite being the gold-standard, radiographs should be used conservatively as adolescents are particularly vulnerable to excess radiation exposure. Therefore, adolescents should not be prescribed a radiograph unless there is reason to suspect an underlying spine deformity. The purpose of this research is to use accessible smartphone technology to create a deep learning (DL) algorithm that can screen for AIS and predict the Cobb angle of the spine, enabling at home assessments and radiation free monitoring of spinal curvatures. Methods: 68 participants (53 AIS, 15 control) were recruited from the Children's Hospital of Eastern Ontario. Prior to study participation, all participants received their normal standard of care, which included a PA spinal radiograph and Cobb angle measurement. Participants were imaged in standing and forward bending positions with a smartphone containing a depth sensor. The resultant red-green-blue-depth (RGB-D) images were then labelled according to Cobb angle and were separated into train and test datasets with an 80: 20 split. Two DL algorithms with a Resnet-34 architecture were developed: 1) A binary classification algorithm that classified the images according to diagnosis (i.e., AIS or control); and 2) a regression algorithm that was trained to predict the largest Cobb angle of the spine. The

performance of these algorithms was assessed on the test dataset of 'unseen' participants (participants not used in training). The binary classification algorithm was assessed by measuring the accuracy of the classifications, as well as the sensitivity and specificity of the models' predictions. The regression algorithm was assessed by measuring the root mean squared error (RMSE) between the predicted and ground truth Cobb angles. RESULTS: Data collection and analysis is ongoing; however, preliminary results indicate that the developed algorithm can identify Cobb angles >10° with an accuracy of 96% from RGB-D images captured with a smartphone. The sensitivity and specificity were found to be 99% and 82%, respectively. The algorithm was able to predict the Cobb angles within 8° of the ground truth Cobb angles, which is comparable to the degree of error seen with manual measurements from spinal radiographs. CONCLUSIONS: These results demonstrate that accessible and inexpensive technologies, such as modern smartphones, can be used to predict the degree of spinal curvature in adolescents with AIS. This has the potential to make health care more accessible to patients, allowing at home screening and monitoring.

O.9.6: Prediction of upper limb function from simple activity of daily living using deep learning in patients with stroke

Dain Shim, Yonsei University; Joong-On Choi, Yonsei University College of Medicine; Juntaek Hong, Yonsei University College of Medicine; Jehyeon Yoo, Yonsei University College of Medicine; Taeyoung Choi, Yonsei University College of Medicine; Jeuhee Lee, Yonsei University; Yebin Cho, Yonsei University College of Medicine; Dong-Wook Rha, Yonsei University College of Medicine

IntroductionClinical measurements are most widely used to measure upper limb function in stroke patients. However, these methods are time-consuming and require trained clinicians. An objective method for measuring upper limb function in stroke patients is the 3D computerized motion analysis test. However, this method can only obtain massive joint kinematic data, making it difficult to interpret upper limb function and required experts to conduct complex post-processing after examination to obtain results. With the development of artificial intelligence, simpler methods to quantitatively measure the impairment of body function are expected.Objectives The aim of this study was to predict the clinically measured upper limb function from 3D coordinate data during simple activity of daily living using deep learning in stroke patients.Materials & Method We collected Fugl-Meyer Assessment - Upper Extremity (FMA-UE) score and Box and Block Test (BBT) score in 265 stroke patients. And we collected the temporospatial parameters including Movement Time (MT), Index of Curvature (IC) and Number of Movement Units (NMU) and Arm Profile Score (APS) calculated from 3D motion capture during Reach & Grasp Cycle. The number of data was 624 for FMA-UE, 621 for BBT, 575 for temporospatial parameters, and 575 for APS. The input data for deep learning to predict upper limb function consisted of 3D coordinates of 10 markers: C7, T10, Clavicle, Sternum, Shoulder, Elbow, Wrist (2). and Finger (2). And time normalization was performed using TimeSeriesResampler to set all data frames to 2000. A Convolutional Neural Network was used to classify the patients into 3 groups according to the severity of upper limb dysfunction measured by FMA-UE and BBT and to estimate temporospatial parameters and APS. 80% of data was assigned for training & validation, and 20% for test. Results The accuracy, precision, recall, and f1-score of FMA-UE classification were 0.91, 0.90, 0.90 and 0.90 and BBT classification were 0.79, 0.72, 0.73 and 0.73, respectively. (Fig. 1) The correlation coefficient

between the predicted MT, IC, NMU and APS and the true values were 0.54, 0.75, 0.60 and 0.78, respectively. (p<0.01)Conclusion The deep learning method gave highly promising results in predicting upper limb function of stroke patients using coordinate data obtained from 3D motion capture during simple activity of daily living: reach and grasp the cup. The upper limb dysfunction could be classified according to its severity measured by FMA-UE and BBT. Also, temporospatial parameters and APS showed moderate to strong correlation between the predicted values and true values.

O.9.7: Planting the CEDE: Co-designing and co-developing knowledge translation strategies to implement current expert-based recommendations on electromyography – bridging evidence to practice

Manuela Besomi, The University of Queensland; Lisa Anemaat, The University of Queensland; Emmah Doig, The University of Queensland; Madeleine Lowery, University College Dublin; Paul Hodges, The University of Queensland

While electromyography (EMG) technology rapidly develops, its application faces frequent errors in use and interpretation. Over the past 5 years, the Consensus for Experimental Design in Electromyography (CEDE) project has developed matrices to guide planning, performance, and interpretation of EMG studies. Their implementation requires planning and involvement with end-users. Without targeted knowledge translation, CEDE recommendations may not reach the intended researchers, clinicians and patients. This project aims to co-design and co-develop strategies for optimal CEDE recommendation implementation.The project followed three phases (Figure 1). Phase 1 assessed awareness, interest, and/or use of CEDE recommendations through an online survey (n = 105) and explored perspectives of researchers (including ~50 EMG users from early to senior career levels) during a workshop held at the 2022 ISEK Congress. 60% of survey participants reported being “aware of CEDE matrices but not tried” or “preparing to use but haven't yet”. Common challenges included the length of the tables, formatting issues, lack of understanding of some methods, and general difficulty in using EMG. Participants during the ISEK workshop proposed various alternatives to disseminate these resources, including having a webpage, utilizing social media, and developing graphical content. To enhance the uptake and use of these matrices, researchers recommended implementing a decision-tree algorithm to guide the navigation process of the matrices. They also emphasized the need to develop a clinician-specific resource. In Phase 2, we employed a modified Experience-Based Co-Design approach to co-design and co-develop a strategy for implementing the “CEDE Amplitude Normalization matrix”. This involved ten researchers with a diverse range of expertise in EMG, and the strategy was informed by their views and needs through an iterative process. Following consensus meetings, a decision-tree algorithm was collaboratively agreed upon as the focal point for co-design workshops. Design principles were then applied to the development of the decision-tree via a series of questions/answers. Co-design focused on determining the elements of the decision-tree (i.e., entry points and key questions), design principles to address the development of the tool and the improvement of the content delivered. Phase 3 will involve a usability test of the decision-tree algorithm among co-design collaborators and extended end-users, utilizing user experience design principles. The implementation and evaluation of this co-designed tool may promote and facilitate the uptake and use of the CEDE recommendations in research, adhering to best practices when using EMG in research projects.

Oral Session 10

O.10.1: Differences in the muscle activity pattern of the superficial trunk extensor muscles to the onset of the rectus femoris in the active straight leg raising score in the functional movement screen

Tomoya Kitamura, Saitama Prefectural University; Hiroshi Takasaki, Saitama Prefectural University

Introduction: Active straight leg raising (ASLR) is a common test for multisegmental control in the trunk and lower limbs and is included in the Functional Movement Screen (FMS). The FMS is a valid and reliable system for grading movement competency with 4 grades (score 0–3) in each of the seven screening tests. In the FMS, a subgroup of those with a score of 1 due to limitations in the ASLR but not in the passive straight leg raising (PSLR) is considered to have a stability or motor control dysfunction (SMCD). This study investigated whether there is a difference in the relative latency between the onset of the superficial trunk extensor muscles and the rectus femoris (RF) during ASLR depending on the ASLR score in the FMS. Methods: A total of 30 participants were recruited; 10 in the FMS-ASLR score group 1 (FMS-ASLR1), 10 in the FMS-ASLR score group 2 (FMS-ASLR2), and 10 in the FMS-ASLR score group 3 (FMS-ASLR3). Inclusion criteria for participants were as follows: (1) ≥18 years of age without neck pain, back pain, or lower extremity pain and (2) PSLR > 70°. The FMS-ASLR scores were evaluated by the author, an international certified qualification holder. A surface electromyography system synchronized with the promotion inertial sensor system was used. Surface electrodes were applied to the left- and right-longissimus thoracis (L-LT and R-LT), left- and right-iliocostalis lumborum (L-IL and R-IL), left- and right-multifidus (L-MF and R-MF), and right RF; EMG signals were recorded during ASLR. The onset of muscle activity for each muscle was identified by using a manual onset detection method after blinding the participant's FMS-ASLR score and the muscle type. As outcomes, the relative latency of the onsets of L-LT, R-LT, L-IL, R-IL, L-MF, and R-MF to the onset of the right RF during the right ASLR was calculated, and a one-way analysis of variance was performed. RESULTS: The statistical analysis showed no significant difference in the relative latency of the trunk superficial extensor muscles to the right RF during right ASLR depending on the ASLR score in the FMS ($P \geq 0.05$). As a post hoc test, Pearson's correlation coefficients (r) were calculated for combinations (15 combinations) of the relative latency of the six superficial trunk extensor muscles in each FMS-ASLR group.Significant positive correlations were observed in 12 of 15 muscle combinations in FMS-ASLR1, 8 of 15 muscle in FMS-ASLR2, and 1of 15 muscle combinations (L-MF and R-MF) in FMS-ASLR3. CONCLUSION: : This study showed that there was no statistically significant difference in the relative latency of the trunk superficial extensor muscles to the right RF during right ASLR depending on the ASLR score in the FMS.

O.10.2: Modulation of activity and synchrony of ankle muscles during quiet standing by emotional intervention

Ryogo Takahashi, The University of Tokyo; Naotsugu Kaneko, University of Tokyo; Naoki Tsukamoto, The University of Tokyo; Atsushi Oshima, The University of Tokyo; Bowen Liu, The

University of Tokyo; Inhyeok Jeong, The University of Tokyo; Mayu Dohata, The University of Tokyo; Kimitaka Nakazawa, The University of Tokyo

BACKGROUND AND AIM: Quiet standing is influenced by emotion. In quiet standing, the balance is maintained by mainly regulating ankle torque. Center of pressure (COP) is often used as an index reflecting ankle torque. While previous studies have shown that aroused emotions increase the frequency of COP, indicating increased ankle stiffness, the neuromuscular mechanisms underlying the COP frequency changes remain unclear. This study aimed to investigate effects of emotional intervention on ankle muscle activities during quiet standing. Because COP is controlled by the combined contribution of ankle plantar/dorsiflexor muscles, we focused on individual muscle activity and inter-muscular synchrony in these muscles. Methods: Twenty-four healthy males (24.5±2.4 yr) participated. Emotional states can be represented as a two-dimensional model of arousal and valence. We set four conditions composed of two valences (Pleasant and Unpleasant) and two arousals (High and Low). The participants stood on a force plate, viewing a monitor 1 m ahead. Each of the four blocks began with a 30 s preparatory phase followed by a 72 s intervention phase, displaying 12 condition-specific pictures for 6 s each. During the task, ground reaction forces and moments were measured from the force plate and COP was calculated. Electrodermal activity (EDA) was measured to quantify autonomic nervous activity. Electromyogram (EMG) was recorded from tibialis anterior (TA), soleus (SOL), medial (MG), and lateral gastrocnemius (LG) muscles, and then root mean square (RMS) of EMG was calculated. Inter-muscular coherence (IMC) of SOL-MG, SOL-LG, and MG-LG pairs was calculated at 0–4 and 8–12 Hz bands to quantify inter-muscular synchrony. The former and latter bands are linked to muscle activity associated with postural sway, and with physiological tremor to enhance ankle stiffness, respectively. RESULTS: High arousal showed a significantly higher mean EDA amplitude (p < 0.001, Aligned rank transformed ANOVA) than Low arousal, indicating sympathetic activation and successful arousal intervention. Also, High arousal showed a significantly higher mean power frequency of COP (p < 0.001) than Low arousal, indicating greater ankle stiffness. RMS of SOL was significantly lower in High arousal (p = 0.015) than in Low arousal, while other muscles showed no significant difference. Mean IMC at 0–4 Hz of all muscle pairs was not significantly different among the conditions. In contrast, mean IMC at 8–12 Hz of SOL-MG (p = 0.036) and MG-LG (p = 0.049) were significantly higher in High arousal than in Low arousal. CONCLUSIONS: Our results indicate that aroused emotion with sympathetic activation would increase ankle stiffness during quiet standing. Notably, while aroused emotion decrease SOL activity, the coherence between plantarflexor muscles. Our findings would lead to a better understanding of the association between emotion and postural control.

O.10.3: Distribution of forearm SEMG amplitude during isolated and combined activation of extrinsic hand and finger muscles

Christian Sure, Ruhr-Universitaet Bochum; Sascha Selkmann, Ruhr-Universitaet Bochum; Marc Neumann, Ruhr-Universitaet Bochum; Beate Bender, Ruhr-Universitaet Bochum

Background: Distinguishing activity of individual forearm muscles during hand and finger movement is generally considered a difficult task. Due to their size and layered arrangement, combined activation of multiple muscles often results in significant crosstalk. Common setups for surface electromyography (SEMG) with only a few hand-placed electrodes can therefore only

provide a rough overview of flexor and extensor activity. Applications like SEMG biofeedback therapy could benefit from the ability to better distinguish between forearm muscle activity. Feeding characteristics of amplitude maps measured across the forearm into a fuzzy classifier might be a possible approach. To generate the necessary design data and assess feasibility, we conducted a preliminary study. METHODSSeven healthy subjects performed isometric contractions of extrinsic hand and finger muscles under varying complexity and intensity while SEMG signals were measured across a wide portion of the forearm. A custom hand force meter was used for measuring resulting hand and finger forces. Subjects performed simple contractions, where only few muscles were active, as well as more complex contractions, where several muscles were activated simultaneously. Electrodes were applied using a custom forearm sleeve, equipped with 6 rings of 16 equally spaced dry electrodes. With a total length of 10 cm, the electrode matrix covered a section of the forearm from approx. 25 % to 65 % of the distance from the lateral epicondyle to the ulnar styloid process. Using measuring technology from DeMeTec, the monopolar SEMG signal was sampled at 1024 Hz and filtered with a band-pass between 10 and 500 Hz and a notch at 50 Hz. For signal quantization, root-mean-square was calculated in a moving window of 1 s. Results: Individual contractions of the hand and fingers generally resulted in the formation of distinct activity hotspots across the measured section of the forearm. While hotspots could generally be correlated to extrinsic hand and finger muscle activation based on anatomical and kinematic considerations, some contractions (e.g. flexion of the thumb) did not produce hotspots in the relevant part of the matrix. Peak amplitudes at the hotspots correlated with the applied force in an approximately linear fashion, though gradients differed substantially between muscles. Amplitudes on the dorsal forearm appeared generally higher than on the ventral forearm. Distinctiveness of hotspots during combined activation varied between muscles, depending on their proximity and degree of overlap. Hotspot locations between subjects showed similarities while not being identical. CONCLUSION: : The study reinforces our assumption, that position, shape and amplitude of activity hotspots across the forearm hold sufficient information to distinguish between activity of several forearm muscles during combined contraction. A suitable approach for converting the findings into a classifier is currently being developed.

O.10.4: Volitional muscular activation alters cortical processing of ankle joint proprioceptive afference

Alessandra Giangrande, Politecnico di Torino; Giacinto Luigi Cerone, Politecnico di Torino; Alberto Botter, Politecnico di Torino - LISiN; Harri Piitulainen, University of Jyväskylä

INTRODUCTIONCortical processing of proprioceptive stimulation can be assessed by means of corticokinematic coherence (CKC), and evoked and induced EEG responses to continuous and intermittent joint rotations. CKC quantifies the degree of cortical processing of proprioceptive afference [1], whereas evoked and induced responses reflect the strength of cortical activation and excitability. The effect of a maintained voluntary muscle activation on the cortical proprioceptive processing is still unclear. Thus, we used proprioceptive stimulation in active and passive conditions to evaluate respective modulation of CKC, evoked and induced EEG responses by muscular activity. METHODS25 healthy adults (14 males; 28.8 ± 7 y.o.) were recruited. A custom-made movement actuator delivered 2-min of continuous (2 Hz) or 100 intermittent (ISI 4 ± 0.25 s) rotations of the ankle joint, while 30-EEG signals were recorded with (active condition) and without (passive condition) isometric voluntary activation of the plantar

flexors (5 Nm torque) [2]. CKC was computed between EEG and foot angular displacement, and it was defined as the maximum coherence value at the movement frequency [3]. Evoked responses were obtained by averaging EEG epochs with respect to the movement onset. Induced responses in the cortical sensorimotor beta rhythm were quantified through the temporal spectral evolution method [4]. A Wilcoxon signed rank test was used to evaluate between-conditions differences for (i) CKC strength, (ii) evoked response amplitude and (iii) induced beta suppression and rebound amplitudes. RESULTSProprioceptive stimuli during the active condition elicited significantly stronger (i) CKC (~333%), (ii) evoked responses (~26%) and (iii) beta suppression (~38%), but weaker (~–42%) beta rebound amplitudes than the passive condition (p < 0.05) at the Cz-EEG electrode corresponding to the foot area of the sensorimotor cortex SM1 (Figure 1).DISCUSSIONResults indicated (i) intensified cortical proprioceptive processing, (ii) enhanced cortical activation (evoked response and beta suppression) and (iii) weaker cortical inhibition (beta rebound) of the SM1 cortex during the active muscle activation. Therefore, we demonstrated that the cortical processing of the proprioceptive afference from the ankle joint is altered when a maintained volitional muscular activation is performed compared to a passive condition. The mechanisms could involve both peripheral (i.e. sensitization of the proprioceptors) and central (i.e. altered functional cortical state or stronger intra- and inter-hemispheric inhibition) factors. These findings may extend the use of the adopted metrics to assess the motor efference-proprioceptive afference relationship in various scenarios.REFERENCES[1] Piitulainen et al., Neurosci. 238: 361-370,2013. [2] Cerone et al. IEEE TNSRE 30: 61-71, 2022. [3] Halliday et al., Prog. Bio. Mol. Biol., 64: 237-278, 1995.[4] Salmelin and Hari, Neurosci. 60: 537-550, 1994.

O.10.5: Center of pressure displacements during gait initiation in healthy children : Temporal and positional analysis

Atsushi Yamasaki, Bunkyo Gakuin University; Kazuyuki Mito, The University of Electro-Communications

[Objectives] Gait initiation must be transitioned from a bipedal standing position to a one-legged standing position. The shift of the body center of gravity (COG) to the support leg at gait initiation involves the displacement of the center of pressure (COP) to the swing leg. Such a reverse reaction phenomenon (RRP) are anticipated laterally and backward movements and are known as anticipatory postural adjustments (APAs). The aim of this study was to quantitatively characterize the strategy of children during gait initiation using parameters obtained from the COP track. [Methods] A total of 13 healthy children aged 6–12 years (3 females, 10 males ; height 1.31 ± 0.12 m) participated in this study. Measurements were taken using a force platform (UM-BAR; Unimec Co. Ltd., Tokyo, Japan) and recorded at 100 Hz. In the starting position, each foot was grounded in the center of the two platforms. COP plots were the coordinates of the most outward displacement of the COP to the swing leg (APAs1) and the COP to the support leg (APAs2). Statistical analysis was performed using SPSS Ver. 28.0.1.1 (IBM Co. Ltd., Amonk, USA) to analyze the relationship between each parameter.[Results] A positive correlation was observed between the time taken from the start of operation to APAs1 and the time taken from APAs1 to APAs2 (r = 0.956, p<0.001). When the COP coordinates were examined in relation to the start of movement, a positive correlation was observed both externally (r = 0.791, p<0.001) and posteriorly (r = 0.965, p<0.001) in APAs1. In APAs2, a positive correlation was observed only in the posterior direction (r = 0.593, p<0.045). The

relationship between APAs1 and APAs2 showed a positive correlation only in the posterior direction (r = 0.641, p<0.018).[Conclusions] Lateral and posterior displacement of the point of COP to the swinging leg is important for APAs at gait initiation. APAs1 depended on the COP at the start of operation, but the influence of the anterior-posterior direction was significant. In contrast, APAs2 showed a significant correlation with COP at the beginning of operation only in the antero-posterior direction. In addition, it is characteristic that the correlation between APAs1 and APAs2 was found only in the anterior-posterior direction. Therefore, it is suggested that the travel time and distance of the COP in the front-back direction have a significant effect on the reverse response phenomenon of gait initiation. Similarly, the lateral and posterior location of the COG of the swinging leg in the gait initiation posture may also be involved. In the present study, healthy children, who are less affected by lifestyle and disease, were the subjects. Future experiments will be conducted on healthy adults and patients with joint diseases to compare the results.

O.10.6: Changes in electromyographic signals of the prime movers during sustained submaximal isometric bench press

Kentaro Chino, Kokugakuin University

In sustained submaximal tasks, neural drive for recruitment of additional motor units is generated to compensate for the reduced contractile force caused by the fatigued motor units, resulting in the increase in the root mean square (RMS) amplitude of the EMG signals. The median power frequency (MPF) of the EMG signals is particularly sensitive to local metabolic disturbance and strongly associated with the muscle fiber conduction velocity which decreases in sustained submaximal tasks. Therefore, the RMS amplitude and MPF of the EMG signals are considered to be well suited for monitoring the progression of fatigue in sustained submaximal tasks. In this study, the changes in the RMS amplitude and MPF of the EMG signals was examined for the prime movers of the bench press during submaximal isometric bench press until exhaustion. Sixteen healthy males performed an isometric bench press in which the bar with 70% of the one-repetition maximum load was held at the elbow joint at 90 degrees until exhaustion. Surface EMG signals during the bench press was recorded from the pectoralis major (PM) , anterior deltoid (AD), and long head of the triceps brachii (TB). The RMS amplitude and MPF of the EMG signals was calculated for 1.0 second at 0%, 25%, 50%, and 75% of the time to exhaustion (TTE). The RMS amplitude was normalized by the RMS amplitude during the maximal voluntary isometric bench press (MVI), and the MFP was normalized by the MFP at 0% of the TTE. Significant increase in the RMS amplitude was observed from 0% to 75% of the TTE in the PM and AD and from 0% to 25% of the TTE in the TB. This finding suggests that the neural drive reached a maximum before exhaustion in all prime movers, especially in the TB. There was no significant difference between the prime mover muscles in the RMS amplitude at 0% of the TTE (PM, 71.1 ± 18.4%; AD, 56.6 ± 22.9%; TB, 61.7 ± 30.0% of the MVI), and no significant difference between the muscles in the RMS amplitude at 100% of the TTE (PM, 113.5 ± 30.0%; AD, 108.4 ± 32.2%; TB, 89.0 ± 39.6% of the MVI). This finding indicates that prime movers were similarly recruited at the beginning of the bench press and similarly fatigued at exhaustion. Significant decrease in the MPF was observed from 0% to 50% of the TTE in the PM and from 0% to 100% of the TTE in the AD and TB , which indicates that the PM fatigued the earliest of all prime movers. Taken together with the above findings, all prime movers of the bench press were

fatigued during sustained submaximal isometric bench press, but it could not be clear which prime movers were most fatigued.

O.10.7: Effect of inclined and declined slopes on postural balance and ankle muscle activity

Siripatra Atsawakaewmongkhon, Paris Saclay University; Annabelle Couillandre, Univeristy of Orléans; Alain Hamaoui, Paris Saclay University

Sloped surfaces are frequently encountered in everyday life. They alter the function of the ankle joint, which plays an essential role in postural control, by modifying its flexion/extension angle and the tension of the muscles controlling its mobility. However, few previous studies have examined the combination of postural control and ankle muscle activity while standing on sloped surfaces. The study aims to evaluate the effect of sloped surfaces on postural balance and ankle motor muscle function. It is hypothesized that these changes induce an alteration in balance that varies with the direction and extent of surface inclination. Fifteen healthy subjects underwent five posturographic examination conditions, where the inclination of the support surface was varied in the sagittal plane: the horizontal control condition (H0, reference condition), dorsal flexion at 7° (DF7), and 15° (DF15), and plantar flexion at 7° (PF7) and 15° (PF15). These measurements were coupled with electromyography (EMG) recordings of the Tibialis Anterior, Soleus (Sol), and Gastrocnemius Medialis muscles. The repeated measures ANOVA, with a simple contrast test compared to H0, was used in our study. Analysis of the posturographic indices shows that the mean position of the center of pressure (CP) is significantly influenced by the amplitude and direction of inclination of the support surface, with a posterior shift in dorsal flexion (DF7 and DF15) and an anterior shift in plantar flexion (PF7 and PF15). It also appears that dorsal flexion induces a significant increase in mean CP deviation along the anteroposterior (P < 0.01 between H0 and DF15) and mediolateral (P < 0.05 between H0 and DF15) axes, as well as an increase in mean speed (P < 0.01 between H0 and DF7, and between H0 and DF15). Conversely, plantar flexion induced no significant increase in these indices and even decreased mean CP deviation along the anteroposterior axis in the PF7 condition compared with H0. Analysis of the EMG data revealed that the activity level of the three muscles tested was significantly increased when they were placed in a shortened position and significantly decreased when they were placed in an extended position.In line with previous studies, the inclination of the ground support surface alters postural balance and the function of ankle motor muscles. More specifically, this study shows that inclinations placing the ankle in dorsal flexion induce the most significant disturbances, probably due to the lower joint mobility in dorsal flexion, which limits compensation capacities and due to an altered sensory-motor mechanism. On the other hand, that postural balance can be improved by slight ankle plantar flexion, similar to that associated with wearing low heels. The factors behind these changes could be related to biomechanics, neurophysiology, and muscle physiology, which could guide management strategies for people at risk of balance loss when standing on sloped surfaces.

Oral Session 11

O.11.1: Association between trunk rotation sequence and pitching velocity in college baseball pitchers using inertial measurement units

Shiu-Min Wang, National Taiwan University; Wei-Li Hsu, National Taiwan University; Jyh-How Huang, National Taiwan University of Sport; Yuh-Renn Wu, National Taiwan University

Introduction: The trunk rotation sequence during pitching involves sequential rotation of multiple segments. Previous studies found that achieving peak pelvic rotation velocity before peak upper torso axial rotation velocity is crucial for efficient pitching. Understanding this sequence is vital for performance enhancement. However, previous studies used motion analysis systems to detect the trunk rotation sequence, none have examined this sequence on the baseball court using inertial measurement units (IMU).The purpose of this study was to explore the association between the trunk rotation sequence detected by IMUs and pitching performance in college baseball pitchers. We hypothesized that the proper trunk rotation sequence has better pitching velocity.Materials and Methods: Pitchers aged 18 to 25 with no surgery history were recruited. Four IMU were attached to the pitching arm, thigh of stride leg, sternum, and pelvis. Each subject threw 10 maximal effort fastballs. IMU measured pelvis and upper trunk angular velocities, while the thigh IMU detected foot contact (FC), and the pitching arm IMU detected maximal internal rotation (MIR). Trunk rotation sequence was determined by the difference in percentage of peak pelvis rotation velocity (PPRV) and peak sternum rotation velocity (PSRV) between events. Pitching velocity was recorded by a radar gun, and parameters were computed using MATLAB R2022a.The top 5 pitches were classified as high velocity (HV), while the remaining 5 were classified as low velocity (LV). Differences of trunk rotation sequence between HV and LV were analyzed using the Wilcoxon signed-rank test. A p-value < 0.05 was considered statistically significant. PASW Statistics 18 for Windows (SPSS, USA) was employed for the analysis. Results: Eight college baseball pitchers were recruited (age: 22.38 ± 1.60 years; height: 173.25 ± 5.63 cm; weight: 65.13 ± 9.31 kg). Differences of trunk rotation sequence between HV and LV was significantly different ($z = -2.52$, $p = 0.01$) (Fig. 1).Discussions: The results supported our hypothesis that a proper trunk rotation sequence is linked to higher pitching velocity. Pitchers with a larger difference in timing between PPRV and PSRV tended to achieve higher pitching velocity. IMUs on the baseball field can help measure the trunk rotation sequence, aiding pitchers and coaches in optimizing training and improving performance.Acknowledgement: This work was supported by Ministry of Science and Technology (NSTC 112-2425-H-028-002) awarded to Dr. Wei-Li Hsu.

O.11.2: Kinematic comparisons of taiwanese and japanese university baseball pitchers

Yen-Wei Chiu, National Sun Yet-Sen University; Keizo Takahashi, Biwako Seikei Sport College; Wen-Fan Chen, Institute of Medical Science and Technology, National Sun Yat-sen University, Kaohsiung, Taiwan; Hao-Yuan Hsiao, National Sun Yat-sen University; Yuan-Kun Tu, Department of Orthopedics, E-Da Hospital; Zhi-Yan Wang, Department of Orthopaedics, E-Da Hospital, I-Shou University, Kaohsiung, Taiwan; 靜玉 陳, National Sun Yat-Sen University; Yi-Jung Tsai, E-Da Hospital; Chih-Kun Hsiao, Department of Medical Research, E-Da Hospital; ,

INTRODUCTIONTaiwanese collegiate baseball players have high level skills by world standards. Studies regarding the throwing motion of Taiwanese pitchers are very few. The training methods

depends on the culture of the country, resulting in a difference in pitching behavior, and it is considered that the results of survey by other pitchers cannot be applied perfectly to Taiwanese pitchers. To compare Taiwanese and Japanese collegiate baseball pitchers, it is thought possible to research and clarify the pitching motion characteristics of Taiwanese baseball pitchers. The purpose of this study was to clarify the characteristics of the pitching motion of Taiwanese baseball pitchers by using three-dimensional motion analysis method. METHODSTen Taiwanese right-handed over-throw pitchers participated in the experiment as subjects. Each participant performed 10 fastball pitches with full effort. The trials that showed the highest ball velocity were used for analysis. Three high-speed cameras (GC-L20B, Sports sensing Co, LTD, Japan) were used to collect movies at a rate of 240 Hz. Frame Dias IV (DKH Corp, Japan) was used to digitize 24 body segment points and ball manually, and calculated three-dimensional coordinates of these measuring points using the Direct Linear Transformation (DLT) method. Matlab (The MathWorks, Natict, MA) was used for data processing. The coordinate data were digitally filtered in the X, Y, and Z directions, respectively. Kinematic parameters such as the rotation angle and angular velocity of trunk and hip, as well as ball velocity were calculated and compared with Japanese baseball pitchers. RESULTSThe ball velocity thrown by Taiwanese baseball pitchers was slower than that thrown by Japanese baseball pitchers. Upper trunk rotation angle at ball release (define as REL) of Taiwanese has a larger angle then Japanese varsity baseball pitcher. However, the pelvis rotation angle of Taiwanese at REL was smaller than that of Japanese varsity baseball pitchers. Maximum trunk rotation angular velocity of Taiwanese was smaller than that Japanese collegiate baseball pitchers. Maximum pelvis rotation angular velocity of Taiwanese was the fastest compared with Japanese baseball pitchers. CONCLUSION: To optimize the desired speed and direction in the crucial final throwing stage, coaches are recommended to employ targeted drills and exercises focused on enhancing torso rotation. The vital role of incorporating tailored drills and exercises designed to enhance torso rotation among Taiwanese college baseball pitchers. Coaches are strongly encouraged to prioritize refining power transfer during the final throwing stage, offering a pragmatic approach to enhance the overall performance of players.

O.11.3: Muscular demand associated with three different techniques for moving patients vertically in a hospital bed

Wayne Albert, University of New Brunswick; Luke Kell, University of New Brunswick; Elnaz Roudi, University of New Brunswick; Samantha Gaboury, Université de Moncton; Cynthia Dion, Univerity of New Brunswick; Puneet Singh, Université de Moncton

IntroductionSafe patient handling (PH) programs have been developed based on biomechanical principles to help reduce the physical strain of repositioning patients in their beds. In New Brunswick (Canada) two PH programs have been developed, Back in Form (BiF) and All the Right Moves (ATRM). There is limited research quantifying whether these PH programs actually succeed in reducing physical strain of the caregiver as they reposition a patient. This research study assessed the activity of eight muscles bilaterally when using patient handling techniques to move a patient vertically in the bed. The muscle activity was assessed in two phases: the preparation to repositioning the patient (PRP phase) and the repositioning of the patient (RP phase). MethodsTwenty-six university aged students between the ages of 19 and 35 and who did not suffer from low back pain or shoulder disorder during the study period (or 3 months prior volunteered for this study.The BiF program has two techniques for repositioning a patient

vertically in their bed and are referred to as Hammock 1 and Hammock 2, respectively. The ATRM program has one technique referred to as Up in Bed. Participants performed each of the techniques twice while neuromuscular activity was monitored bilaterally on eight muscles using a Bortec Octopus AMT-8. The eight muscles of interest were: anterior deltoid [AD], trapezius descendens [TD], biceps brachii [BB], thoracic erector spinae [TES] located at the level of the T9 spinous process, lumbar erector spinae [LES] located at the level of the L3 spinous process, external oblique [EO], rectus femoris [RF], and biceps femoris [BF]. A ground electrode was placed on the right and left collarbone. Results/Conclusion The raw EMG signal was rectified, and Butterworth low passed filtered (RMS converted) using MATLAB. Peak activity was determined for each muscle during a maximum voluntary contraction protocol (MVC) and used to normalize all subsequent EMG data. Differences in maximum muscle activity were determined through a series of ANOVAs with corrections. In the RPR phase the participant braces for the repositioning technique and places themselves in a balanced position. Lower muscle activity was found for the AD, BB and BF on both sides and the LES on the right side only for the Hammock 2 technique; UT was lowest for the Hammock 1 technique. In the RP phase, there was significantly lower muscle activity in all muscles associated with the Hammock 1 technique, except for the LE on the right-hand side. The Hammock 1 requires distributing the weight equally into a squat position with a 45º counterbalance movement; this technique heavily relies on gravity. This technique has as the lowest risk of injury compared to the other two, with the least favourable outcome being that the patient does not move. The limitation of this technique is that there is a weight limit between the caregiver and the patient.

O.11.4: The role of biarticular muscles during squat-to-stand task: a consideration of bimodal ground reaction force-time curves

Shinichi Kawamoto, Graduate School of Medicine Kyoto University

Background/Purpose: The bimodality of ground reaction force (GRF)-time curves during closed kinetic chain lower limb extension (CKE) have been predominantly discussed for countermovement jumps. The authors observed similar bimodality of GRF during the squat-to-stand task, which has no relevant study. Scrutinizing the history of research for CKE, the hypothesis occurs that the variations (bimodality) of GRF-time curves during squat-to-stand tasks reflect the extent to which each actor utilizes the function of biarticular muscles. Therefore, the aim of this study was to examine the relation between the bimodality of GRF during squat-to-stand tasks and lower limb biarticular muscle function. Methods: Nine female students without knee problems (20.9±2.1years, 1.58±0.08m, 54.9±5.8kg) participated in this study. Squat-to-stand tasks were executed on the force plates to stand from a deep squat position as quickly as possible. GRF-time curves are recorded with 3D motion capture to establish initial joint angles and peak net joint moments. Surface EMG electrodes were placed on gluteus maximus (GMax), rectus femoris (RF), vastus lateralis (VL), vastus medialis (VM), and biceps femoris (BF) to measure muscle activity (EMG) synchronization between monoarticular muscles and biarticular muscles. As a continuous variable representing the bimodality of GRF a depression area was defined between the two (fictitious for the second peak in some cases) peaks using the derivative of the GRF curves. EMG synchronization was expressed by the cross-correlation coefficient (R-value) between the two EMG signals during the propulsion phase. Furthermore, isokinetic maximum hip/knee extension torques were measured using the dynamometer as muscle strength. Results: The main findings were that the depression area

(bimodality) had a strong correlation with initial knee flexion angle, an inverse correlation with R-value between VM and BF, a weak correlation with propulsion duration, and a weak inverse correlation with isokinetic maximum knee extension torque.Discussions: The strong influence of the initial posture on the shapes of GRF-time curves indicates that motor control during squat-to-stand tasks with deep knee bending is governed by the geometrical (biomechanical) constraints rather than the neurally based constraints, at least for young healthy women. The primary mechanical demand in the squat-to-stand task is to rotate the femur segment upright. Segment-based conception by Cleather et al.(2015) advocates that considering the relative sizes of moment arms suggests biarticular hamstrings cause an extension of the femur segment (towards leg extension direction) with the aid of quadriceps femoris. EMG synchronization between VM and BF in subjects with more unimodal GRF and shorter propulsion duration in the current study supports the theoretical proposition. CONCLUSIONS: Young healthy women with bimodality of GRF-time curves during squat-to-stand tasks tend to underuse biarticular hamstrings.

O.11.5: Neuromuscular control at the ankle joint when completing a proprioceptive task wearing textured foot orthoses

Kelly Robb, Wilfrid Laurier University; Daniel Schmidt, Technische Universitat Chemnitz; Andresa Germano, Technische Universitat Chemnitz; Stephen Perry, Wilfrid Laurier University

TITLE: Neuromuscular control at the ankle joint when completing a proprioceptive task wearing textured foot orthosesAUTHORS: Kelly A. Robb, Daniel Schmidt, Andresa Germano & Stephen D. PerryABSTRACT: BACKGROUND AND AIM: Degraded functioning of the somatosensory system, including reduced feedback from cutaneous inputs of foot sole skin [1] and proprioception inputs from the ankle joint [2], are known factors impeding balance control. It remains unknown if targeted interventions to facilitate cutaneous feedback from the foot sole can improve body position accuracy (proprioception) from the ankle joint to counteract or improve these motor performance declines. Thus, the purpose of this study was to assess the neuromuscular and proprioceptive control of the ankle joint, in healthy young and middle-aged adults, and to investigate if ankle joint position sense (AJPS) accuracy improves when increasing sensory feedback under the foot sole (using textured orthoses). Methods: Forty-eight participants were divided into two groups: healthy young (n=31, 23.8±2.1 years) and healthy middle-aged (n=17, 43.3±10.5 years). All participants completed an ankle proprioception task, defined as ankle joint position sense (AJPS) reproducibility, while standing on a custom-built proprioceptive device in standardized footwear and wearing two different foot orthoses: a smooth non-textured orthosis and a textured orthosis. Starting in a neutral ankle position (90o), two trials of AJPS were tested per orthosis condition which manipulating both the a) target angle (5o or 10o), or b) target angle direction (ankle plantarflexion or ankle dorsiflexion). Orthotic device exposure and experimental conditions were block randomized across participants.The study's primary outcome measures include the absolute target angle error (o), medio-lateral and antero-posterior center of pressure data (mm) (SF=100Hz, Pedar, Novel, USA), and root mean square of the tibialis anterior and medial gastrocnemius muscles (N) (SF=1000Hz, Trigno Wireless EMG System, Delsys, USA) at the start, middle, and end of the proprioceptive task. RESULTS: Preliminary results of this study demonstrate that accuracy in completing the proprioceptive tasks is modulated according to the direction of the task, target angle direction, and foot orthoses worn by participants of both age groups (Table 1). CONCLUSIONS: While this

research fills an important gap in academic research and increases knowledge pertaining to sensory and proprioceptive impairments, preliminary results suggest that textured orthoses may provide a low-cost and effective conservative treatment option to improve balance control and reduce fall risks in young and older adults.REFERENCES: [1] Perry, SD (2006). Neurosci Lett 392: 62-67. [2] Chen, X & Qu X (2019). Hum Factors 61: 702-711.

O.11.6: Functional connectivity between muscle pairs decreases in the final stage of a 2000-meter all-out kayak ergometer test

Mathias Kristiansen, Aalborg University; Matthew Flood, Luxembourg Institute of Health; Mark De Zee, ExerciseTech, Department of Health Science and Technology, Aalborg University,; Pascal Madeleine, Aalborg University; Kent Klitgaard, ExerciseTech, Department of Health Science and Technology, Aalborg University,

BACKGROUND AND AIM: Optimal performance in flatwater sprint kayak requires high power output of the upper body musculature combined with technical proficiency. Technical proficiency is heavily related to muscle coordination which can be defined as the interplay between the onset/offset and activation level of the involved muscles. Normalized mutual information (NMI) has previously been used to assess functional connectivity between muscle pairs using surface electromyography (sEMG) recordings. The aim of this study was to assess changes in NMI values of upper body muscle pairs during a 2000m kayak ergometer test. Methods: Fifteen elite kayak paddlers (11 males and 4 females) volunteered to participate in the study. sEMG was recorded using a bipolar configuration from eight muscles of the upper body on the dominant side during a 2000m all-out kayak ergometer test. Kinematics of the upper body were recorded using an Xsens Awinda motion capture system and synchronized with the sEMG recording. Based on the kinematics, the sEMG data was then divided into two separate stroke phases throughout the trial, with one phase representing the pulling motion and one phase representing the forward motion of the left hand, respectively. NMI between muscle pairs of the eight upper body muscles were then computed for each phase. Lastly, the NMI values of the entire 2000m trial were segmented into ten non-overlapping epochs and averaged, with each epoch representing the muscle coordination for one tenth of the trial. A one-way ANOVA with repeated measures was used to assess changes in NMI values between the ten epochs for all muscle pairs. RESULTS: For all combinations of muscle pairs, and for both the pulling and forward motion phase, the NMI values of the last epoch were significantly lower than the nine preceding epochs ($p \leq 0.05$). No significant changes were found between NMI values of the other epochs for any of the muscle pairs. DISCUSSION: The fact that NMI values decreased in the final epoch may be explained by the large amount of fatigue experienced during this period of the 2000m all-out kayak ergometer test. It is therefore possible that the functional connectivity between the investigated muscle pairs were altered in response to fatigue and that this in turn may have influenced the technical proficiency during this part of the test. The decrease in NMI indicating lowered functional connectivity between most of the studied muscle pairs may also be explained by decreased muscle stabilization among kayak paddlers. CONCLUSIONS: NMI values of muscle pairs of the upper body are significantly decreased in the final stage of a 2000m all-out kayak ergometer test.

Oral Session 12

O.12.1: Surface electromyography thresholds as a measure for performance fatigability during incremental cycling in patients with neuromuscular disorders

Nicole Voet, Radboudumc/ Klimmendaal

Neuromuscular disorders (NMD) affect 1 in 625 individuals worldwide. Patients with NMD do not always detect fatigability in real-time. As a result, for patients, it is difficult to cope with performance fatigability in daily life, which often leads to overuse and, in the end, a vicious circle of inactivity and a further decline in (muscle) performance. Valid measures for fatigability could help people with NMD find the right intensity of daily life activities and exercise. Previous research described that surface electromyography (sEMG) has excellent reliability for assessing signs of performance fatigability during a cycle test in healthy subjects. In healthy persons, there is an excellent relation between the timing of the (two) surface electromyography (sEMG) thresholds and the (two) ventilatory thresholds during exercise. The primary aim of this study was to determine the relative timing of both sEMG and ventilatory thresholds in patients with neuromuscular disorders (NMD) compared with healthy subjects during a maximal ergospirometry cycling test. We hypothesized that in patients with NMD, the sEMG thresholds would occur relatively earlier in time than the ventilatory thresholds, compared to healthy subjects, because performance fatigability occurs more rapidly. In total, 24 healthy controls and 32 patients with a neuromuscular disorder performed a cardiopulmonary exercise test on a bicycle using a 10-min ramp protocol, during which we collected ergospirometry data: power at both ventilatory and sEMG thresholds, and sEMG data of lower leg muscles. In line with our hypothesis, normalized values for all thresholds were lower for patients than for healthy subjects. These differences were significant for the first ventilatory ($p = 0.008$) and sEMG threshold ($p < 0.001$) but not for the second sEMG ($p = 0.053$) and ventilatory threshold ($p = 0.238$). Most parameters for test–retest reliability of all thresholds did not show any fixed bias, except for the second ventilatory threshold. The feasibility of the sEMG thresholds was lower than the ventilatory thresholds, particularly the first sEMG threshold. As expected, the sEMG thresholds, particularly the first threshold, occurred relatively earlier in time than the ventilatory thresholds in patients compared with healthy subjects. A possible explanation could be (a combination of) a difference in fiber type composition, disuse, and limited muscle-specific force in patients with neuromuscular disorders. sEMG measurements during submaximal dynamic exercises are needed to generalize the measurements to daily life activities for future use in prescribing and evaluating rehabilitation interventions. Further research is required to address a multi-model approach to measure performance fatigability in NMD to differentiate performance fatigability developed from the disease itself compared to normal physiological and aging processes, understand the concomitant nature of performance fatigability and perceived effort, identify appropriate therapeutic interventions to minimize performance fatigability in patients with NMD.

O.12.2: Dynamic networks of cardio-muscular interactions during exercise

Sergi Garcia-Retortillo, Wake Forest University; Maddie Sayre, Wake Forest University; Maddie Davis, Wake Forest University; Fidanka Vasileva, IDIBGI Girona Biomedical Research Institute; Plamen Ivanov, Boston University

BACKGROUND A fundamental question in cardiovascular and muscle physiology revolves around how the heart operates in concert with distinct muscles to maintain cardiovascular homeostasis, facilitate movement, and adapt to exercise demands and fatigue. However, the precise mechanisms by which autonomic regulation of heart rate variability facilitates coordination with distinct muscle fibers within muscles remain unknown. Here we investigate how cardio-muscular coordination evolves in time and respond to fatigue during a maximal squat test. Methods: Thirty healthy young adults performed two maximal body weight squat sets until exhaustion. During the protocol, a Biopac MP150 unit (Biopac Systems Inc, Goleta, CA, USA) was used to collect synchronized electrocardiogram (EKG Lead II; BN-RSPEC2-T), and electromyogram (EMG; BN-EMG2-T) signals from the following muscles: left and right vastus lateralis (LegL, LegR); left and right erector spinae (BackL, BackR). EKG and EMG raw data were recorded at a sample frequency of 2000 Hz, and filtered online using a 0.5-150 Hz (EKG) and 5–500 Hz (EMG) band-pass filter. We first obtained instantaneous heart rate (IHR, representing heart rate variability) derived from the EKG signal (Pan-Tomkins QRS detection), and decompose the EMG recordings in ten frequency bands [F1-F10], which may represent the activation of distinct muscle fiber types. We next quantified pair-wise coupling (cross-correlation C; amplitude-amplitude coupling) between the time series for IHR and all EMG spectral power frequency bands in each Leg and Back muscle. RESULTS: During Set 1, low [F1-F5] EMG frequency bands, associated with type-I slow muscle fibers, exhibited stronger coupling with IHR (CMEAN = 0.35: SD = 0.03) compared to intermediate/fast frequency [F6-F10] EMG bands (CMEAN = 0.20: SD = 0.02). With progression of fatigue in Set 2, a significant overall decline in coupling strength between IHR and all EMG frequency bands was observed (~50%; p = 0.02). Notably, while the probability of positive-correlations significantly decreased (15%) with fatigue in Set 2, the probability for anti-correlations (negative) significantly increased (40%) . CONCLUSION: The overall stronger coupling between IHR and slower muscle fibers underscores the potentially vital role of heart rate variability in supporting the endurance-oriented function of these fibers, which rely on a steady supply of oxygen. The overall decline in cardio-muscular coupling with fatigue in Set 2, as well as the transition from positive to anti-correlated behavior, reflects the complex impact of exhaustion on cardiac and muscle function. This dynamic network approach introduces new avenues for the development of novel network-based biomarkers to characterize cardio-muscular interactions during exercise, assess fitness status or the effectiveness of cardiovascular and muscle injury rehabilitation.

O.12.3: Quantitative estimation of maximum isometric torque and muscle fatigue on forearm supination-pronation

Hao-Yuan Hsiao, National Sun Yat-sen University; Wen-Fan Chen, Institute of Medical Science and Technology, National Sun Yat-sen University, Kaohsiung, Taiwan; Yuan-Kun Tu, Department of Orthopedics, E-Da Hospital; Yi-Jung Tsai, E-Da Hospital; Chih-Kun Hsiao, Department of Medical Research, E-Da Hospital; 靜玉 陳, National Sun Yat-Sen University

Quantitative Estimation of Maximum Isometric Torque and Muscle Fatigue on Forearm Supination-PronationHao-Yuan Hsiao1,2, Wen-Fan Chen1*, Yuan-Kun Tu2, Yi-Jung Tsai3, Chih-Kun Hsiao3*, Jing-Yu Chen1,31 Institute of Medical Science and Technology, National Sun Yat-sen University, Kaohsiung, Taiwan2 Department of Orthopedics, E-Da Hospital, I-Shou University, Kaohsiung, Taiwan3 Department of Medical Research, E-Da Hospital, I-Shou University, Kaohsiung, TaiwanEmail: m8571409@yahoo.com.twINTRODUCTIONContinuous

intense muscle contraction or performing a submaximal isometric contraction could lead to muscle fatigue or muscle damage. In several literatures, muscle fatigue is considered to be closely related to MSD, especially for muscle-related disorders. Although it is not difficult to know when one is fatigued, few principles have emerged to characterize the phenomenon of muscle fatigue. This study measured the pronation/supination torque and the EMG activity in forearm muscles during an isometric contraction in which a maximal isometric force was kept for as long as possible. The findings might provide valuable insights for scientifically-based fatigue management and prevention of forearm diseases. METHODS: Twelve adults participated in this study, a 90-second fatigue test was performed on who exerted maximum isometric pronation and supination on their dominant and non-dominant forearms. EMG signals were captured on the biceps (Bic.), brachioradialis (Bra.), flexor carpi radialis (F.C.R.), extensor carpi radialis (E.C.R.), and extensor carpi ulnaris (E.C.U.) muscles. The time to failure, maximum isometric torque and reduction rate of EMG activation patterns were measured and compared as an indicator of muscle fatigue. RESULTS: In the dominant side forearm pronation, the F.C.R. muscle displayed the highest fatigue rate, with both EMG signal amplitude and torque values decreasing after 20 seconds, hitting below 50% torque value at 30 seconds. Similarly, during dominant supination, the E.C.U. muscle showed the highest fatigue, with both signals declining after 15 seconds, hitting below 50% torque value at 55 seconds. For the non-dominant forearm pronation, the F.C.R. muscle again exhibited the highest fatigue, with signals dropping after 20 seconds, reaching below 50% torque at 30 seconds. In non-dominant forearm supination, the E.C.U. muscle displayed the highest fatigue, with signals decreasing after 20 seconds, falling below 50% torque value at 55 seconds. CONCLUSION: The first 20-30 seconds of continuous maximum isometric force on the forearm sends a signal of rapid muscle fatigue. This emphasizes the importance of scheduling breaks or interventions to prevent strain, reduce injury risk, and maintain performance during prolonged forearm tasks. High-intensity movements result in rapid onset of muscle fatigue, with the F.C.R. and E.C.U muscles experiencing the fastest decline in muscle strength and could yield fatigue faster than other muscles.

O.12.4: Assessment of forearm muscle strength and performance fatigue during orthopedic spine surgery for bone screw fixation

Zhi-Yan Wang, Department of Orthopaedics, E-Da Hospital, I-Shou University, Kaohsiung, Taiwan; Hao-Yuan Hsiao, National Sun Yat-sen University; Yen-Wei Chiu, National Sun Yet-Sen University; 靜玉 陳, National Sun Yat-Sen University; Yuan-Kun Tu, Department of Orthopedics, E-Da Hospital; Yi-Jung Tsai, E-Da Hospital; Chih-Kun Hsiao, Department of Medical Research, E-Da Hospital

INTRODUCTION Orthopedic surgeons engaged in prolonged, repetitive operations at either high or low intensity, coupled with unfavorable hand postures, may experience forearm fatigue, leading to the development of chronic musculoskeletal disorders. In the event of injuries to orthopedic surgeons, the quality of surgical treatments may be affected, potentially contributing to a shortage of medical professionals. Given the limited research on occupational injuries specific to orthopedic surgeons, this study focuses on quantitatively assessing forearm muscle strength and muscle performance characteristics during the clavicle screw insertion process in orthopedic surgery. METHODS Eight right-handed surgeons participated in the experiment, which was conducted in three stages. In Stage 1, measurements of pre-surgery

maximal isometric force (MIF) were taken, including maximal isometric grip force (MIGF), maximal isometric driving torque (MIDT), and maximal isometric push force (MIPF). Each test was performed three times, with a 30-second rest between trials and a 5-minute break between different tests. Stage 2 involved performing surgery with the insertion of 10 bone screws. In Stage 3, post-surgery measurements of MIF (MIDT, MIPF, MIGF) were conducted. Each participant was required to insert 10 bone screws into a pig thoracic vertebra specimen (approximately 6 months old), and the testing platform was pre-adjusted to an appropriate level according to each participant's requirements. During the surgery, a digital handgrip dynamometer measured the maximal isometric gripping force (MIGF) before and after the screwing tasks. A six-dimensional load cell, synchronized with electromyographic (EMG) signals, captured experimental data, enabling the assessment of maximal driving torque (DT), sub-cycling forces, and the evaluation of muscle responses and fatigue levels in designated muscles (Medial Deltoid：MD, Biceps brachii：BB, Brachioradialis：BR, and Extensor carpi ulnaris：ECU). Results Under pre- and post-fatigue conditions, the post-test results for MIGF, MIDT, and MIPF were lower than the corresponding pre-test values. In both the MIPF and MIDT tests, the electromyographic (EMG) amplitude variations (ΔEMG %) for MD, BB, BR, and ECU were reduced in the post-test compared to the pre-test. Notably, the EMG amplitudes of these four muscles were lower at the 4th, 7th, and 10th screw insertions than at the 1st screw insertion. CONCLUSION The primary findings of this study underscore the influence of forearm muscle strength and fatigue on surgeons during bone screw operations: (1) There was a significant decrease in grip strength, driving torque (DT), and push force (PF) after the insertion of 10 bone screws. (2) Comparisons of MIGF, MIPF, and MIDT, as well as the ΔEMG % at screws 1, 4, 7, and 10, indicate that surgeons performing operations with more than 10 inserted bone screws may encounter muscle fatigue.

O.12.5: EMG biomarkers for fatigue prediction during isometric wrist flexion

Martín Durán-Santos, Universidad de las Americas Puebla, Mexico; Cristina Romero, University of Alicante, Spain; Rocío Salazar-Varas, Universidad de las Americas Puebla, Mexico; Andres Ubeda, University of Alicante

The identification of neuromechanical biomarkers can be a key factor for knowing a patient's physical status during a motor rehabilitation procedure. In this ambit, monitoring of muscle fatigability is essential to safely track physical improvement and can be a guide for therapist to evaluate the rehabilitation effectiveness. Some previous efforts have already classified discrete fatigue levels by analyzing surface electromyography (sEMG). The underlying aim of this study is to identify potential biomarkers for fatigue prediction, considering only isometric muscle contractions tasks in a more quantitative way using Multiple Linear Regression. To achieve this goal, ten subjects were involved in the experiment, where each participant seated comfortably in a chair and performed a wrist flexor movement to push a 6-axis force sensor, while locking the dominant wrist with a velcro strap. The muscle activity of flexor and extensor carpi radialis were recorded while the participant performed 3 isometric contractions at 40% maximal voluntary contraction (MVC) until muscle failure, with pauses between repetitions to recover from exhaustion. A preprocessing step was performed for noise filtering and features selection. In addition, the optimization of the window size and overlap to extract features was found at 1 second and 0.83 seconds, respectively. The proposed solution is a Multiple Linear Regression model, where the input corresponds to a selected features matrix (containing features from

both flexor and extensor muscles), and the output (labeled signal) assumes 0% fatigue at the beginning of the contraction and then 100% at the end. To validate the proposed model, the second isometric contraction was used to train the model, and the third isometric contraction to test it, using the correlation between the predicted signal in the test process and the control fatigue labelled (0% - 100%) as performance metric. From a group of 18 different features, our results suggest that the best features (hence, possible potential biomarkers) can be found at the Mean frequency, Median frequency, RMS, Integral EMG, Average Amplitude Change, Difference absolute standard deviation value, Zero-Crossing, Frequency Ratio, and 4th-level daubechies-2 wavelet, reaching 93.1331% ± 3.2229 averaged correlation among individuals. This work has the potential to deeply understand muscle fatigue, allowing its application in several field of motor rehabilitation, sport and optimal control of exoskeletons.This study has been developed within project MYOREHAB (PCI2023-143405), funded by MCIN/AEI/10.13039/501100011033 and the European Union.

O.12.6: Recovery of muscle endurance and muscle fibres conduction velocity after intensive care unit discharge

Giacomo Valli, Università degli Studi di Brescia; Marco Benedini, University of Brescia; Marta Cogliati, Università degli Studi di Brescia; Simone Piva, Università di Brescia; Nicola Latronico, Universita' degli Studi di Brescia; Claudio Orizio, University of Brescia; Francesco Negro, Universita' degli Studi di Brescia

Introduction: Following discharge from the intensive care unit (ICU), patients face several neuromuscular consequences, including reduction in muscle force and endurance, which can persist for up to 1 year or more [1]. This impairment has noticeable consequences on quality of life and life expectancy [2]. The conduction velocity (CV) of action potentials proved to be a valid estimator of muscle endurance and fatigue, whether examined from single motor units or the interference EMG signal [3]. The aim of this study was to investigate the changes in CV during isometric fatiguing contractions subsequent to ICU discharge. Methods: Ten patients (8 males and 2 females, average age of 61.3±7.8 years) underwent High-Density Surface EMG (HD-sEMG) recordings at 6 (T6) and 12 (T12) months post-ICU discharge. HD-EMG was recorded during sustained contractions at 50% of the maximum voluntary contraction up to exhaustion from the tibialis anterior muscle. Muscle fibres CV was estimated via a newly developed algorithm that takes advantage of the relation between spatial and temporal spectra of the multichannel EMG signals induced by the propagation velocity of the action potentials [4]. CV reduction during the sustained contraction was estimated via the slope of its linear regression and the maximum change in CV was estimated as the difference between the maximum and minimum CV values (usually at the beginning and at the end of the contraction, respectively). RESULTS: MVC increased between T6 and T12 by 31% (from 14.9±2.1 to 19.5±2.1 Kg, p=0.002) and the time to task failure by 70% (from 117±24 to 202±26 seconds, p=0.003). During the same period, the slope of the regression line describing the CV adaptation was reduced by 42% (from -0.081±0.0013 to -0.047±0.0013 (m/s)/min, p=0.038) and both maximum and minimum CV values decreased. Specifically, maximum CV was reduced by 16% (from 4.58±0.29 to 3.83±0.29 m/s, p=0.086), while minimum CV was reduced by 19% (from 4.37±0.27 to 3.53±0.27 m/s, p=0.042), with a similar maximum change in CV (from 0.24±0.12 to 0.29±0.14 m/s). Discussions: Our findings indicate that, between 6 and 12 months post-ICU discharge, patients undergo a substantial improvement in muscle force and endurance. The increase in muscle

endurance aligns with a slower decline of muscle fibres CV and, on average, with lower CV values required to sustain the same relative contraction intensity, suggesting a potentially more efficient excitation-contraction coupling.References: 1) Huang L, et al. 1-year outcomes in hospital survivors with COVID-19: A longitudinal cohort study. Lancet. 2021.2) Cooper R, et al. Objectively measured physical capability levels and mortality: systematic review and meta-analysis. BMJ. 2010.3) Del Vecchio A, et al. Associations between motor unit action potential parameters and surface EMG features. J Appl Physiol (1985). 2017.4) Farina D, Negro F. Estimation of muscle fiber conduction velocity with a spectral multidip approach. IEEE Trans Biomed Eng. 2007.

Oral Session 13

O.13.1: Shar wave tensiometry for the evaluation of Achilles tendon loading: a cross-sectional study on conservatively treated tendons after rupture

Alessandro Schneebeli, University of Applied Sciences and Arts of Southern Switzerland; Corrado Cescon, University of Applied Sciences and Arts of Southern Switzerland; Giuseppe Filardo, Service of Orthopaedics and Traumatology, Department of Surgery, EOC, Lugano, Switzerland; Enrique Testa, Service of Orthopaedics and Traumatology, Department of Surgery, EOC, Lugano, Switzerland; Alessandro Sangiorgio, Service of Orthopaedics and Traumatology, Department of Surgery, EOC, Lugano, Switzerland; Deborah Falla, University of Birmingham; Marco Barbero, University of Applied Sciences and Arts of Southern Switzerland; Martin Riegger, Service of Orthopaedics and Traumatology, Department of Surgery, EOC, Lugano, Switzerland

Background and Aim: Achilles Tendon rupture (ATR) is a frequently occurring musculoskeletal injury, with an annual occurrence rate ranging from 5 to 50 cases per 100,000 individuals, potentially leading to significant disability. To date, clinical outcomes at 12 months post-injury appear to be comparable between those who undergo surgery and those who receive conservative treatment. Shear wave tensiometry is a recently described technology that uses accelerometers to measure wave propagation along the tendon in order to define tendon mechanical properties. This technology is based on the concept that the axial stress within the tissue affects the squared tendon wave speed. The aim of this study was to evaluate differences in shear wave speed (SWS) between a conservatively treated Achilles tendon after rupture and the unaffected contralateral tendon. Methods: Twenty-nine participants that underwent conservative treatment following ATR between 1 and 7 years ago were recruited. Participants were divided in two groups depending on the location of the rupture. Tendon loading was measured using a shear wave tensiometer consisting of four accelerometers fixed on the tendon. The accelerometers were placed on the tendon following an ultrasound imaging procedure to ensure proper positioning. The wave propagation along the tendon was manually elicited using a reflex hammer. Five repeated measurements were taken during isometric contractions of increasing intensity (0-35 Nm ankle plantar flexion torque) on both the left and right AT of each participant. The SWS was calculated based on the time delay between the different waves detected by the accelerometers and the mechanical wave propagation on the tendon. SWS between the ruptured and the unaffected side was evaluated using Friedman test. Results: The group with a mid-tendon rupture showed a significant SWS difference between sides but only at 3.5 Nm and 7 Nm (p=0.001 and p=0.020). No significant difference in SWS

were found between the ruptured and unaffected side for those with a myotendinous rupture. Conclusion: The Achilles tendon treated conservatively following ATR appears to have restore its mechanical properties. The relationship between SWS and clinical features should be further investigated. An instrument capable of detecting changes in tendon loading over time has the potential to improve our understanding of tendon behavior during the healing process and aid clinicians in tailoring rehabilitation protocols for individual patients.

O.13.2: In vivo non-invasive assessment of skeletal muscle behavior using shear wave elastography: Active and passive force-length characteristics of the triceps surae muscle group

Manuela Zimmer, University of Stuttgart; Filiz Ates, University of Stuttgart

Background and Aim Characterizing skeletal muscle behavior is crucial for deciphering human movement and muscle adaptation. The understanding of muscle mechanics is built upon the force-length characteristics. Measurement of muscle forces directly from its tendon would be ideal; however, such data collection is limited due to its invasiveness [1]. Shear wave elastography (SWE) is a non-invasive method that offers insights into passive muscle stiffness [2,3] and active characteristics [3], assuming linear elastic, transversely isotropic material properties. Though relating muscle shear elastic modulus to its force production is challenging. Presently, we characterized the triceps surae muscle group in passive and active states, hypothesizing that SWE reveals the muscles' length and activity-dependent mechanical characteristics. METHODS Gastrocnemius medialis (GM), lateralis (GL), and soleus (SOL) muscles of ten volunteers (24.7±1.7 years, 5 males) were studied during rest, maximal voluntary contraction (MVC), and submaximal isometric contractions (25%, 50%, 75% of MVC) at four ankle angles from 30° plantarflexion (PF) to 15° dorsiflexion (DF). SWE, electromyography, and ankle moment were recorded simultaneously. The lengths of the muscles were assessed sonographically. Results At rest, muscle length (p<0.05), passive shear elastic modulus (p<0.001, Fig. 1), and ankle moment (p<0.001) increased from PF to DF. Although muscle resistance is not the only source of passive ankle moment, the increase in muscle stiffness indicates the passive force-length characteristics, hence increasing muscle force from shorter to longer lengths. MVC moment increased from 75.21±25.53 Nm at 30° PF to 159.15±43.88 Nm at 15° DF (p<0.001). At submaximal levels, the active shear elastic modulus increased with increasing level (p<0.001), demonstrating the potential of SWE for force estimation, and was unchanging for GL and SOL, and decreasing maximally 59.5% for GM (p<0.001) from PF to DF (Fig. 1). Interpreting these results as muscle stiffness-strain characteristics, i.e. the first derivative of the stress-strain characteristics, this indicates that the muscles operate at optimal or shorter than optimal lengths. CONCLUSIONS Supporting our hypothesis, the derived passive and active muscle stiffness-strain characteristics may serve as a surrogate for in vivo force-length characteristics, contingent on validation through direct force measurements. This suggests the potential of SWE as an index of individual muscle force and together with mathematical modeling, it holds promise for establishing links between muscular adaptation and joint function. Acknowledgments The DFG - German Research Foundation (GRK 2198, 277536708) and BMBF - Federal Ministry of Education and Research (3DFoot, 01EC1907B).References1.Brendecke E, et al., Front. Physiol. 14: 1143292, 20232.Ates F, et al., Eur. J. Appl. Physiol., 118: 585–593, 20183.Zimmer M, et al., J. Mech. Behav. Biomed. Mat. 137: 105543, 2023

O.13.3: Supraspinatus tendon thickness changes following therapeutic exercises for patients with rotator cuff-related shoulder pain; secondary analyses of two randomised controlled trials

Marc-Olivier Dubé, La Trobe University; Kim Gordon Ingwersen, Lillebaelt Hospital; Jean-Sébastien Roy, Université Laval; Centre for interdisciplinary research in rehabilitation and social integration; François Desmeules, Université de Montréal; Maisonneuve-Rosemont Hospital Research Center; Jeremy Lewis, Finchley Memorial Hospital; University of Nottingham; University of Limerick; Birgit Juul-Kristensen, University of Southern Denmark; Jette Vobbe, Lillebaelt Hospital; Steen Lund Jensen, Aalborg University; Karen Mccreesh, University of Limerick; ,

Background: The mechanistic response of rotator cuff tendons to exercises within the context of rotator cuff-related shoulder pain (RCRSP) remains a significant gap in current research. A greater understanding of this response can shed light on why individuals exhibit varying responses to exercise interventions. It can also provide information on the influence of certain types of exercise on tendons. The primary aim of this article is to explore if changes in supraspinatus tendon thickness (SSTT) ratio differ between exercise interventions (high load vs. low load). The secondary aims are to explore if changes in SSTT ratio differ between ultrasonographic tendinopathy subgroups (reactive vs. degenerative) and if there are associations between tendinopathy subgroups, changes in tendon thickness ratio, and clinical outcomes (disability). Methods: This study comprises secondary analyses of the combined dataset from two randomised controlled trials in patients with RCRSP. In those trials, different exercise interventions were compared: 1) progressive high-load strengthening exercises, and 2) low-load strengthening with or without motor control exercises. In one trial, there was also a third group that was not allocated to exercises (education only). Ultrasound-assessed SSTT ratio, derived from comparing symptomatic and asymptomatic sides, served as the primary measure in categorizing participants into tendinopathy subgroups (reactive, normal and degenerative) at baseline. RESULTS: Data from 159 participants were analysed. There were significant Group (p<0.001) and Group X Time interaction (p<0.001) effects for the SSTT ratio in different tendinopathy subgroups, but no Time effect (p=0.63). Following the interventions, SSTT ratio increased in the "Degenerative" subgroup (0.14 [95% CI: 0.09 to 0.19]), decreased in the "Reactive" subgroup (-0.11 [95% CI: -0.16 to -0.06]), and remained unchanged in the "Normal" subgroup (-0.01 [95% CI: -0.04 to 0.02]). There was no Time (p=0.21), Group (p=0.61), or Group X Time interaction (p=0.66) effect for the SSTT ratio based on intervention allocation. Results of the linear regression did not highlight any significant association between the tendinopathy subgroup (p=0.25) or change in SSTT ratio (p=0.40) and change in disability score. CONCLUSION: : Findings from this study suggest that, over time, SSTT in individuals with RCRSP tends to normalise, compared to the contralateral side, regardless of the exercise intervention. Different subgroups of symptomatic tendons behave differently, emphasizing the need to potentially consider tendinopathy subtypes in RCRSP research. Future adequately powered studies should investigate how those different tendinopathy subgroups may predict long-term clinical outcomes.

O.13.4: Development and validation of a MIMU-based wearable device for telerehabilitation: a reach-to-grasp protocol study

Gregorio Dotti, Politecnico di Torino; Marco Ghislieri, Politecnico di Torino; Marco Caruso, Politecnico di Torino; Daniele Fortunato, Politecnico di Torino; Andrea Cereatti, Politecnico di Torino; MARCO KNAFLITZ, POLITECNICO DI TORINO

BACKGROUND AND AIM: Telerehabilitation has been found to be an effective alternative to in-person therapy sessions. It reduces costs and transportation-related challenges for patients and improves rehabilitation outcomes [1]. Magneto-Inertial Measurement Units (MIMUs) are commonly used for kinematic assessments in various pathological conditions. However, current MIMU solutions often work as data loggers and rely on external units for data processing. This study aims to introduce and validate an innovative MIMU-based wearable device for hand trajectory estimation during telerehabilitation protocols. Methods: The newly proposed device (size: 63 × 35 × 16 mm) was designed and developed at the BIOLAB of Politecnico di Torino (Turin, Italy). It consists of a MIMU (LSM9DS1, STMicroelectronics), a Bluetooth Low Energy module, a floating-point microcontroller (SAME70, Microchip) to easily install and run custom algorithms onboard, a micro-SD card to store raw and processed data, and an 800 mAh battery. Twenty-five healthy volunteers (age: 22.5 ± 2.1 years; height: 1.7 ± 0.1 m; weight: 62.6 ± 10.2 kg) were enrolled to test the device during a reach-to-grasp protocol and to validate the algorithm for orientation estimation. The device was fixed to the subjects' wrist (dominant side) through adhesive tape and volunteers were asked to perform the reach-to-grasp movement 75 times following the experimenter's instructions (7 task repetitions per minute). Four reflective spherical markers were placed on the device to obtain the orientation reference through 12 infrared stereophotogrammetric cameras (Vicon T20, Vicon Motion Systems). The orientation estimation was performed in MATLAB® by applying the complementary Madgwick filter to the gyroscope and accelerometer readings (acquired at 119 Hz) [2]. To minimize the convergence time, the orientation was initialized by means of an algebraic quaternion obtained with the algorithm proposed by Valenti et al. [3]. The heading and attitude orientation errors were estimated considering different values of the filter's parameter β in the range between 10-5 and 1 by using a grid search approach [4]. RESULTS AND DISCUSSION: The minimum orientation error was obtained considering β equal to 0.06 rad/s and 0.025 rad/s for the heading and attitude errors, respectively. The average orientation error of 2.3 ± 1.2 deg in heading and 2.1 ± 0.7 deg in attitude revealed the high performance of the sensor fusion algorithm in estimating device orientation during the reach-to-grasp movements [4]. Future studies will focus on embedding the sensor fusion algorithm on board and on validating the device in patients affected by neurological disorders. REFERENCES [1] Ostrowska, P.M., et al. Healthcare (2021), doi: 10.3390/healthcare9060654 [2] Madgwick, S.O.H. et al. IEEE ICORR, (2011), doi: 10.1109/ICORR.2011.5975346 [3] Valenti, I. et al. Sensors, (2015), doi: 10.3390/s150819302 [4] Caruso, M. et al. Sensors (2021), doi: 10.3390/s21072543

O.13.5: Effect of the ultrasound frame rate and beamforming method on fascicle tracking during dynamic contractions

Kristen Meiburger, Politecnico di Torino; Elena Cesti, Politecnico di Torino; Marco Carbonaro, Politecnico di Torino; Silvia Seoni, Politecnico di Torino; Marta Boccardo, Politecnico di Torino; Alberto Botter, Politecnico di Torino - LISiN

BACKGROUND AND AIM. The ultrasound (US) tracking of fascicle length (FL) and pennation angle (PA) is a fundamental tool to investigate mechanical phenomena underlying force generation in healthy and pathological subjects. Several algorithms have been proposed to automatically quantify and track these parameters throughout the contraction. Regardless of the tracking approach, the image quality and the temporal resolution of the image sequence seem to play a crucial role in fascicle tracking, particularly during dynamic tasks where muscle architecture undergoes significant and rapid changes. Recent US devices enable access to radiofrequency (RF) data at high frame rates, opening up possibilities to apply different beamforming approaches for improving the image quality in terms of image contrast and resolution. In this study we assess the impact of different frame rates and beamforming techniques on the performance of a fascicle tracking algorithm. The analyzed beamforming methods are the traditional delay-and-sum (DAS) algorithm and the filtered delay multiply and sum (FDMAS) [1]. METHODS. High frame rate US videos were acquired from longitudinal scans of the medial gastrocnemius muscle during two dynamic tasks (heel rise and walk). Starting from the raw RF signals, the DAS and FDMAS beamforming methods were applied to generate B-mode images. For each beamforming method, the original video at 1000 fps was downsampled to obtain four different frame rates (25, 50, 125, 250 fps). FL and PA were tracked with a modified version of a tracking algorithm [2]. The quality of the tracking was evaluated through the root mean square error (RMSE) and the correlation coefficient (CC) between the results of the automatic and the manual tracking. RESULTS. Overall, the DAS tracking results for heel rise (CC>0.85) showed higher correlations when compared with walking (CC>0.38). However, the CCs of the FDMAS walk video significantly increased (CC>0.7). The RMSEs of the FL and PA tracking on the heel rise DAS video were 3.74 mm and 1.73° for 25 fps, 2.69 mm and 1.11° for 50 fps, 2.92 mm and 1.53° for 125 fps, and 3.70 mm and 1.91° for 250 fps. Considering the walk task, the mean RMSEs using FDMAS (FL=6.11 mm, PA=1.98°) were significantly lower than using DAS (FL=15.54 mm, PA=3.97°). CONCLUSIONS. The results obtained suggest that the superior resolution and contrast obtained by means of the FDMAS beamforming method can improve the result of the automatic tracking. As for the effect of the frame rate, preliminary results show that frame rates higher than 50 fps do not lead to an improvement in the tracking quality. However, the effect of the velocity of the task (e.g. faster walk) needs to be further investigated. [1] Seoni S et al. (2023) Ultrasonics, 2023 May: 131: 106940[2] Drazan JF et al. (2019) PeerJ. 2019(7)

O.13.6: Three-dimensional shape of skeletal muscle determines muscle strength in older adults

Jun Umehara, Kansai Medical University; Masashi Taniguchi, Kyoto University; Masahide Yagi, Kyoto University; Ganping Li, Nara Institute of Science and Technology; Mazen Soufi, Nara Institute of Science and Technology; Yoshito Otake, Nara Institute of Science and Technology; Yoshinobu Sato, Nara Institute of Science and Technology; Yoshihiro Fukumoto, Kansai Medical University; Tetsuya Hirono, Kyoto University; Momoko Yamagata, Kansai Medical University

Skeletal muscle varies in size and shape across individuals. While a large body of literature has shown that the muscle size (e.g., volume) determines the muscle strength, whether muscle shape influences muscle strength has not been sufficiently investigated. Our study found that the three-dimensional shape of the vastus medialis muscle was associated with knee extension torque in young adults, with the possibility that muscle shape contributes to its force exertion

even in older adults. However, it is unclear how well the analogy between young and older adults holds because muscle shape substantially changes with aging. Therefore, we explored whether the three-dimensional muscle shape determines strength exertion even in older adults using statistical shape modeling.T1-weighted images of the right lower limb were obtained from 86 older adults using a 3.0-T magnetic resonance imaging system. The heads of the quadriceps femoris muscle were classified on the image based on automatic segmentation, and the muscle shape model of each head was then created. Taking shape correspondence among individual models of each head using free-form deformation, the statistical shape model, which consists of mean shape and shape vectors encoding shape variations, was constructed by applying principal component analysis. An individual feature of muscle shape was defined as the representation in the shape vector space (i.e., the principal component score). Maximum isometric knee extensor torque was measured for the muscle strength using a dynamometer. To probe the association between muscle shape and muscle strength, stepwise regression was used specifying the knee extensor torque as a dependent variable and the principal component score and muscle volume as independent variables in each muscle.The statistical shape model was constructed for each muscle, where 80% of the individual variation in muscle shape was accounted for by less than four principal components for all muscles. Stepwise regression showed that only muscle volume was the dependent variable for the rectus femoris and vastus intermedius. Interestingly, not only the muscle volume but the principal component score was identified as the dependent variable for the vastus lateralis (R2 = 0.56) and medialis (R2 = 0.57) muscles. Specifically, significant principal components of both muscles represented the shape difference in the anterior-posterior direction, suggesting that this muscle shape might lead to efficient torque exertion by constraining the muscle force vector during muscle contraction. The shape of the vastus muscles is one of the determinants of the knee extension torque in older adults, similar to our previous findings in young adults. Taken together, because the analogy between young and older adults holds for the association between muscle shape and strength, the idea that skeletal muscle geometry is closely linked to its function can be generalized.

O.13.7: Identifying motor unit spike trains in ultrasound images comprised of varying successive twitch-like shapes and degrees of fusion in isometric contractions

Robin Rohlén, Lund University / Imperial College London; Emma Lubel, Imperial College London; Dario Farina, Imperial College London

Ultrasound can detect the activity of a large population of motoneurons, which may be used for neural interfacing purposes. Detecting motor unit (MU) spike trains from ultrafast ultrasound (US) images was first introduced using a linear blind source separation (BSS) method focused on instantaneous mixtures to provide an optimal spatial filter. Although this approach can accurately identify the location and average twitch of MUs, it has low spike train detection accuracy because it does not include the temporal evolution in the separation process.A solution was to use convolutive BSS, which has shown a very high spike train agreement for a large population of MUs in superficial and deep muscle parts. However, the assumption of equal successive twitches may not be fully accurate, as previous studies showed. Therefore, how the accuracy of the BSS algorithm is affected by varying twitch shapes needs to be clarified. In addition, a related question is whether the degree of fusion of the tetanic contraction reflects the accuracy of the decoding algorithm.In this work, we aimed to investigate the accuracy of the convolutive BSS method in estimating MU spike trains in US

images comprised of varying twitch-like shapes in response to neural discharges of each MU and a varying degree of fusion of the tetanic contraction. For these purposes, we performed 30-second in-silico experiments based on a MU recruitment model using current knowledge about the experimental spatial distributions and twitch characteristics of MUs.We found that we could identify a large population of MU spike trains across different excitatory drive and noise levels, even when the individual MU had varying twitch-like shapes. The identified MU spike trains with varying twitch-like shapes resulted in varying amplitudes of the estimated sources, as opposed to equal twitch-like shapes, which resulted in estimated sources with similar amplitudes, and these varying amplitudes were correlated with the ground truth amplitudes of the twitches. The identified spike trains had a wide range (up to 35 Hz), i.e., the method is not selective to a higher degree of fusion. The spike train of MUs with larger twitch amplitudes was easier to identify than small amplitude ones unless the relative twitch amplitudes were not too large. Finally, we explored the consistency of the findings from the in-silico experiment with an in-vivo experiment on the TA muscle using thin-film intramuscular EMG as a reference for MU detection. We found a high spike train agreement between MU spike trains from US and EMG, as well as many spike trains not matched with EMG from 5% of maximum voluntary isometric force (MVIC) up to 40% MVIC. These identified MU spike trains showed features consistent with those in the in-silico experiments. These findings suggest the robustness of the BSS method for identifying MU spike trains under varying successive twitch-like shapes, degrees of fusion, and force levels.

Oral Session 14

O.14.1: Sensorimotor control of quadriceps muscles after anterior cruciate ligament reconstruction: a case-control study

Wanutchaya Yawichai, Buddhist Tzu Chi University; Chich-Haung Yang, Tzu Chi University; Kuan-Lin Liu, Department of Orthopedics, Hualien Tzu Chi Hospital

Introduction: The incident of anterior cruciate ligament reconstruction (ACLR) is commonly found in musculoskeletal patients. Furthermore, one of the major problems is weakness in the quadriceps muscle, which can affect their movement. The number of motor units (MU) and mean firing rate (MFRs) were recorded using a recent high-density surface electromyography (HDsEMG) device to determine the motor unit behaviors in the vastus medialis (VM), rectus femoris (RF) and vastus lateralis (VL) in injured and uninjured knees, Additionally, quantitative sensory testing (QST) and pressure pain threshold (PPT) were used to investigate the alteration of sensorimotor control. However, limited research has studied the change in sensorimotor control after surgery mechanism. Objective: This study aimed to evaluate QST, PPT, average peak torque, the number of MUs, and MU firing rates in the VM, RF, and VL muscles and whether it measured the alteration of sensorimotor function and motor units in individuals with ACLR. Methods: We explored data from eleven patients with ACLR and thirteen healthy for QST, PPT, and maximal isometric contraction (MVIC). Furthermore, bilateral quadriceps muscles with 50% MVIC as a trapezoidal contraction (30 s) were tested while using a Biodex dynamometer. The ACLR participant was asked to perform all processes after reconstruction. The EMG data were analyzed using Neuromap software version 1.2.1 (Delsys Inc., Boston, USA), and the independent T-Test was calculated to demonstrate the difference between limbs and groups of the outcomes. RESULTS: Our finding revealed that ACLR-affected individuals had a lower

average peak MVIC torque in the injured knee compared to the uninjured knee (p = 0.030) and groups (p < 0.000). There were no significant differences in PPT and QST between the limbs (p > 0.05) and between the groups (p > 0.05). Except for CS and WS in the medial area compared to the lateral area on injured and uninjured knees in individuals with ACL reconstruction (p = 0.041, p = 0.08, respectively). Similar to control outcomes. The WS threshold was lower in the medial area compared to the lateral area (p = 0.002, p = 0.045, respectively) in both limbs. A total of 1,601 MU (VM = 544: ACLR = 264, control = 280; RF = 530: ACLR = 219, control = 311; VL = 527: ACLR = 223, control = 304) were analyzed in this study. There was no significant difference between muscles, limbs, and groups (p > 0.05). Furthermore, the RF MFRs of the injured knees were slower in the injured limbs in individuals compared to match-injured limbs in control (p = 0.005). VM and VL did not show significant difference between limbs and the groups. CONCLUSIONS: Our finding suggested that the incline of MU recruitment could limit activated motor unit firing rates, contributing to the deficit in quadriceps muscle activation. Furthermore, QST and PPT have inadequate accuracy in determining the alteration of afferent input excitability due to the variety in an individual's perception.

O.14.2: Predicting lateral perturbation-induced stepping leg with electromyography of the lower limb muscles

Vicki Gray, University of Maryland School of Medicine; Shabnam Lateef, Physical Therapy and Rehabilitation Science; Nathan Frakes, Physical Therapy and Rehabilitation Science; Marcel Lanza, University of Maryland Baltimore

BACKGROUND AND AIM: Impaired lateral weight transfer and reactive stepping from a loss of balance are associated with falls after stroke. A mediolateral loss of balance loads the limb (ipsilateral) in the direction of the potential fall while unloading the opposite limb (contralateral). A lateral protective step requires unloading the ipsilateral leg. In contrast, the unloaded contralateral leg responds with a crossover or medial step without a transfer of body weight. Contralateral stepping responses are less biomechanically stable, require multiple steps, and are associated with falls in older adults. Understanding the muscle activation patterns underlying protective stepping is essential for developing interventions for reducing falls in stroke. The study aimed to characterize muscle activation patterns during mediolateral protective stepping in chronic stroke. The second aim was to determine whether the lower limb muscle activation patterns could predict the leg used to recover balance. Methods: Twenty-nine individuals >6 months post-stroke and ten controls participated in the study. Participants performed 24 trials of randomly ordered lateral waist-pull perturbations at four magnitudes. The perturbation magnitude where participants transitioned from single to multiple steps, called the balance tolerance limit (BTL), was used for analysis. Surface electromyography (EMG) was measured bilaterally from the soleus (SOL), tibialis anterior (TA), rectus femoris (RF), biceps femoris (BF), gluteus medius (GM), and adductor longus (ADD) muscles. The outcome measures were initiation time of the muscle activity relative to the pull and rate of activation (RoA) of the lower limb muscles. EMG signals were processed according to ISEK standards. Group differences (paretic, non-paretic, controls) were determined for a right and left pull with multivariate analysis, adjusting for differences in BTL. Discriminate function analysis determined whether EMG initiation time or RoA could predict the leg used to step. EMG initiation time and RoA were used to predict the step leg by discriminant function analysis

(DFA). RESULTS: No significant group differences were found in the EMG initiation time ipsilateral to the pull direction. However, the contralateral paretic RF (p=0.007) and ADD (p=0.03) muscles were delayed, and the TA (p=0.03) initiation time was earlier compared to controls after adjusting for BTL. The paretic GM RoA ipsilateral and contralateral to the pull was reduced compared to controls. The DFAs revealed that the contralateral RF and TA EMG initiation time could classify the leg used to step 68% of the time. CONCLUSION: The muscle initiation times in the contralateral limb may be more crucial for protective stepping responses in mediolateral balance disturbances after stroke. The RF and ADD may be more important for stabilizing the leg before the transfer of weight occurs, with the GM important for controlling the lateral weight transfer after stroke.

O.14.3: Differences in ground reaction forces between the intact and prosthetic limbs during sit-to-stand task in individuals with unilateral transfemoral amputation

Yukihiko Mizuno, Tokyo university of science; Genki Hisano, Arts et Metiers Sciences et Technologies; Haruki Tomita, Tokyo University of Science; Hiroaki Hobara, Tokyo University of Science

1. INTRODUCTION Sit-to-stand is a crucial task for individuals with unilateral transfemoral amputation (uTFA). Although a previous study demonstrated that peak vertical ground reaction force (GRF) during the sit-to-stand task was greater in the intact limb than prosthetic limb [1], time-series GRF profiles between the limbs were not evaluated. Therefore, the aim of this study was to investigate GRFs in both intact and prosthetic limbs during the sit-to-stand task in individuals with uTFA.2. METHODS We recruited 8 individuals with uTFA (7 females and 1 male, 45.0 ± 16.3 years old, 1.7 ± 0.1 m, 69.9 ± 16.6 kg). All participants were instructed to perform the sit-to-stand task three times as naturally as possible with their daily-use prosthesis (6 microprocessor-controlled knees and 2 non-microprocessor-controlled knees). The sit-to-stand task was performed on two force platforms (TF-40120-CL and TF-40120-CR, Tec Gihan, Kyoto, Japan), which recorded GRFs at a sampling rate of 1000 Hz. GRF data were normalized to participant's body weight. We used a statistical parametric mapping (SPM) to assess the time-course difference of the anteroposterior and vertical GRFs during GRF development between the intact and the prosthetic limb. The sit-to-stand task initiation was determined when the derivative of the total anteroposterior GRF exceeded 2.5% of the peak-to-peak value [2]. The endpoint was defined as the peak value of vertical GRF of the intact limb. Furthermore, the force development was time-normalized to 0-100%. Statistical significance was set at p < 0.05.3. Results There was no significant difference in the anteroposterior GRF profiles between the intact and prosthetic limb. However, as shown in figure.1 , we found a significant difference in the vertical GRF profiles from 78% to 100% of the% GRF development.4.DISCUSSIONIn the sit-to-stand task for the individuals with uTFA, the vertical GRF plays a dominant role, while the anteroposterior GRF applies relatively less force. There was no significant difference in anteroposterior and vertical GRF in the earlier phase, suggesting symmetric force exertions between the intact and prosthetic limbs (including residual limb and prosthetic components). However, beyond 78% of the %GRF development, the vertical GRF exerted on the intact limb was greater than that on the prosthetic limb. The results of the present study suggest that sound-limb reliance for daily activities [3] and potential functional limitations (e.g. the prosthetic knee buckling risk) [4] may influence the asymmetric force exertion in the latter part of the sit-to-stand task. ACKNOWLEDGEMENTS We appreciate all subjects who participated in

the study.REFERENCES[1] Highsmith et al, Gait Posture, 34: 86-91, 2011.[2] Kralj et al, J Biomech, 23: 1123-1138[3] Gailey et al, J Rehabil Res Dev, 45: 15-30, 2008[4] Fanciullacci et al, J. Neuroeng. Rehabilitation, 18: 168, 2021

O.14.4: Effect of acute increase in estradiol level on cutaneous silent period in young healthy females

Yu-Chen Chung, University of Texas Southwestern Medical Center; Subaryani Soedirdjo, UT Southwestern Medical Center; Yasin Dhaher, Northwestern University and The Shirley Ryan AbilityLab

Background. It has been shown that both classical and non-nuclear estrogen receptors are expressed in the spinal cord. Therefore, fluctuation in estradiol (E2) concentrations may affect the spinal network and modulate the control of movement. Herein, we assessed the neuro-modulatory effect of acute increase of estradiol on sensorimotor integration at spinal and supraspinal levels by using cutaneous silent period as a model system. Methods. Ten healthy eumenorrheic females (25 ± 4 yr., BMI 25.5 ± 3.3 kg/m2, mean ± SD) were tested every other day for one menstrual cycle. They were placed in a pronate position, their knees fully extended, and their ankle joint was secured in a boot attached to a load cell. A pair of stimulating electrodes (5 x 5 cm) were placed on the arch of the foot and over the area between the first and second metatarsal. The tibialis anterior surface electromyogram (sEMG) was recorded using a bipolar electrode (inter electrode distance 10 mm, dimension 10 × 1 mm). Cutaneous silent period (CSP) was elicited by delivering 10 trains of five electrical pulses (1 ms width, 200 Hz) separated by a 15-20 s random interval, while the subjects performed dorsi flexion at 10% of their maximal voluntary contraction. The intensity of stimulus was set to 1.1 x motor threshold (lowest stimulus intensity that generated flexion reflex in relax condition). The sEMG envelope was then obtained using a 4th order zero-lag Butterworth low-pass filter on the rectified sEMG. CSP was defined as the sEMG envelope with amplitude ≤ 80% of the baseline activity and duration ≥ 15 ms. Baseline activity was obtained by calculating the average sEMG envelope 100 ms before the onset of the stimulus. To quantify the magnitude of inhibition, the inhibition index was computed as 1 – (mean of sEMG envelope during CSP / mean baseline sEMG). E2 and progesterone (P4) levels were obtained from blood samples. Data collected during menses and periovulatory periods were used in this study. Hormone levels and average CSP properties (latency, duration, and the inhibition index) were compared using the Wilcoxon paired test. Results. The E2 concentrations between menses and periovulation were significantly different (34.5 ± 13.5 pg/mL and 287.9 ± 109.9 pg/mL, p = .002), whereas the P4 concentrations remained low (0.6 ± 0.4 ng/mL and 0.8 ± 0.4 ng/mL, p = .286). An increase in E2 levels did not affect CSP latency (p = .695), duration (p = .492), or inhibition index (p = .492). CONCLUSION: . CSP has protective role to avoid injury and may involve either inhibition of spinal motoneurons, interneurons, corticospinal tract, or a combination of these mechanisms. Our results suggest that acute fluctuation of estradiol concentrations during the follicular phase of the menstrual cycle did not associate with latency, duration, and inhibition index of CSP. Funding. This study is supported by NIAMS (1R01AR069176-01A1).

O.14.5: Non-invasive brain stimulation effects on dual-task performances in patients with Parkinson's disease: A meta-analysis

Hajun Lee, Incheon National University; Nyeonju Kang, Incheon National University

BACKGROUND AND AIM: Parkinson's disease (PD) is a neurodegenerative disease leading to progressive motor and non-motor symptoms. Dual-tasking requiring simultaneous controlling motor and cognitive functions frequently occurs in daily life so that patients with PD experiences more impairments in successfully performing various dual-tasks (e.g., talking while walking). Given that non-invasive brain stimulation (NIBS) techniques may improve motor and cognitive performances by modulating neural activations across key regions, we investigated potential effects of NIBS on dual-task performances in patients with PD using meta-analytic approaches. Methods: Ten studies were included in this meta-analysis. We extracted a total of 85 comparisons from the included studies: (a) motor performance = 73 comparisons from 10 studies, (b) cognitive performance = 12 comparisons from four studies. Effect sizes were calculated using standardized mean difference (SMD) by comparing changes in motor and cognitive performances during the dual-task between active and sham stimulation conditions. A moderator variable analysis additionally determined whether changes in the dual-task performance were different based on specific stimulation areas. Finally, we conducted meta-regression analyses to identify potential relationship between demographic characteristics and changes in performances after receiving NIBS techniques. RESULTS: Random-effects model meta-analyses found that NIBS significantly improved motor and cognitive performances during the dual-task: (a) motor performance (SMD = 0.143; P = 0.001; prediction interval = -0.022 to 0.308) and (b) cognitive performance (SMD = 0.375; P = 0.001; prediction interval = -0.174 to 0.925). Moderator variable analyses reported that NIBS on the dorsolateral prefrontal cortex (DLPFC) significantly advanced motor performance (SMD = 0.211; P < 0.001) and cognitive performance (SMD = 0.283; P = 0.004; prediction interval = -0.112 to 0.679). Finally, meta-regression analyses revealed that decreased age and greater proportion of female in total participants were associated with improved motor performances. CONCLUSION: These findings suggest that applying NIBS on the DLPFC may be an effective option for improving both motor and cognitive functions in patients with PD facilitating more independent activities of daily living.

O.14.6: Bilateral lower limb force control deficits in patients with Parkinson's disease

Hanall Lee, Incheon National University; Nyeonju Kang, Incheon National University

BACKGROUND AND AIM: Parkinson's disease (PD) is the neurodegenerative disorder inducing abnormal movements such as bradykinesia, limb rigidity, gait and balance deficits. Moreover, asymmetrical motor control between more affected and less affected side is often observed in patients with PD presumably interfering with coordinative actions in the lower limbs. Thus, we examined bilateral motor control capabilities in lower limbs of patients with PD using isometric force control paradigm. Methods: Twenty patients with PD and 20 age-matched controls participated in this study. They performed bilateral ankle dorsiflexion force control tasks at two targeted force level (i.e., 10% and 40% of maximum voluntary contraction: MVC) with and without visual feedback. Force control capabilities were estimated by quantifying force accuracy, variability, and interlimb force coordination using the uncontrolled manifold (UCM) analysis. For all outcome measures, we used three-way mixed (Group × Vision × Force Level; 2 × 2 × 2) ANOVAs. RESULTS: The findings revealed that patients with PD showed significantly lower force accuracy at 40% of MVC for all vision conditions and produced greater force variability collapsed across vision and force level conditions. For interlimb force coordination, patients with PD showed significantly lower bilateral motor synergies in vision condition for all force

levels. CONCLUSION: These findings suggested that patients with PD may have deficits in bilateral lower limb force control potentially influencing postural control and locomotion performances.

O.14.7: Influence of a subject's level of technology acceptance on muscular coactivation during usage of an assistive robotic system

Maximilian Siebert, Institute of Applied Medical Engineering; Catherine Disselhorst-Klug, Institute for Applied Medical Engineering, RWTH Aachen University

BACKGROUND: The effect of coactivation of agonistic and antagonistic muscles (short: coactivation) has been described in the literature for a considerable time, while the specific reasons leading to coactivation have been debated. Coactivation appears as a neural control strategy for fine movement patterns but can be observed in patients with chronic pain and fatigue as well. Earlier studies analysing the effect of assistive robotic systems on subjects' movement patterns suggested that a subject's level of technology acceptance might correlate with muscular coactivation during human-robot interaction. AIM: The objective of this study is to investigate, how a subject's level of technology acceptance influence muscular activation and the occurrence of muscular coactivation during a simulated robotic assisted caregiving task. METHODOLOGY: 30 healthy subjects were recruited (15 male, 15 female). To simulate a caregiving task, subjects lay in supine position, while a lightweight robotic arm (KUKA lbr med) or a caregiver held the subject's leg for 60 seconds with knee and hip flexed in the sagittal plane and the shank in a height of 25 cm. The task was performed in four conditions: 1. low robotic assistance, 2. mid robotic assistance, 3. high robotic assistance, 4. caregiver. The order of conditions was randomized. After each condition, subjects had a break for 60 seconds. Each subject indicated the condition they individually preferred. All subjects answered a standardized questionnaire based on the Technology Acceptance Model (TAM) to determine their level of technology acceptance. Here, a lower TAM value indicates lower technology acceptance. The muscular activation of two groups of muscles was recorded with surface electromyography (sEMG) according to SENIAM recommendations. Mind the position of the subject, muscle group 1 regarded muscles acting against gravity (gastrocnemius, biceps femoris, semitendinosus) and muscle group 2 considered muscles working in the direction of gravity (vastus lateralis, rectus femoris, tibialis anterior). The normalized sEMG envelopes were calculated and the root mean square (RMS) was used to characterize the amount of muscular activation. RESULTS: RMS of all muscles increased significantly when the TAM value was decreased. This effect was more pronounced in muscles of group 1 compared to muscles of group 2. Additionally, RMS of all muscles decreased during preferred conditions compared to non-preferred, with a higher effect for subjects with a lower TAM value. DISCUSSION and CONCLUSION: The results showed that muscular activation of all muscles of both groups increased when the TAM value decreased. Since muscles of group 1 and group 2 oppose each other, it can be assumed that coactivation of antagonistic muscles is increased when the technology acceptance is low. This supports the assumption that in human-robot-interaction muscular coordination is affected by psychological factors like technology acceptance.

Oral Session 15

O.15.1: Prediction of the distribution of muscle damage among hamstring heads during Nordic hamstring and stiff-leg deadlift exercises

Titouan Morin, Laboratory Movement Interactions Performance, University of Nantes; Antoine Nordez, University of Nantes; Arnault Caillet, Imperial College London; Lilian Lacourpaille, University of Nantes

Thanks to Calibrated Electromyography Informed Neuromusculoskeletal Modelling (CEINMS), a recent study suggests that the effectiveness of rehabilitation exercises can be classified the relative muscle force. Unfortunately, this model does not take into account that muscle contractions at long muscle length induced larger alterations (i.e., muscle damage) and larger adaptations (i.e., muscle hypertrophy) while the relative muscle force decreases compared to intermediate length. We have developed a neuromusculoskeletal modelling (patent FR2308074) considering that the longer the muscle length the larger the contraction intensity (index of muscle stress), even beyond the optimal length, for a given excitation and contraction speed. The aim of this study was to compare the ability to predict the distribution of muscle damage among hamstring muscles between CEINMS and our neuromusculoskeletal modelling after the Nordic hamstring and the stiff-leg deadlift exercise. A total of 28 participants where splitted in equivalent two groups: Nordic hamstring exercise (23.6+/-3.4 years; 174.4+/-7.6 cm; 67.1+/-8.2 kg) and Stiff-leg deadlift exercise (23.0+/-2.5 years; 176.2+/-8.2 cm; 76.2+/-11.2 kg). They performed three experimental sessions. After a first familiarization session, the second evaluation assessed maximal knee flexion torque (before exercise), resting shear modulus (a proxy of muscle damage; before and 30 min after exercise) of the three main hamstring (semimembranosus (SM), semitendinosus (ST), biceps femoris long head (BF)). The excitation of the aforementioned muscles was assessed with surface EMG. Ground reaction forces were measured for calibration purposes of CEINMS. Lower limb kinematics was assessed using IMU. For both exercises, participants performed eight sets of eight unilateral eccentric repetitions at the pre-established 10 maximal repetitions. The third session was performed 24 hours after the exercise to quantify the strength loss. We found a significant strength loss at 24h after the exercises (-9.9+/-7.7% and -8.9+/-11.2% for Nordic hamstring and Stiff-leg deadlift exercise, respectively); without differences between exercises (P=0.677). According to our hypothesis, the increase in shear modulus was larger for ST (25.6+/-25.4%) after Nordic hamstring compared to Stiff-leg deadlift exercise (-7.1+/-11.2%; P<0.001), respectively), while the increase in shear modulus was larger for SM (12.4+/-18.8%) after Stiff-leg deadlift compared to Nordic hamstring exercise (-2.5+/-11.7%; P<0.001). We are still processing the data of the distribution of muscle force and stress through CEINMS and our approach, respectively. Nonetheless, our approach has been already applied on previously published data. Briefly, after a damaging seated leg curl session, we found that the distribution of damage was 70.8% and 50.3% larger in ST compared to SM and BF, respectively. The distribution of stress estimated through our approach was 50.7% and 35.0% larger in ST compared to SM and BF. Accordingly, we found a strong correlation (R = 0.77) between the distribution the increase in shear modulus and the distribution of muscle stress (figure 1). This provides the first impetus of our ability to predict the distribution of damage. A future study will determine whether these approaches predict the distribution of muscle hypertrophy after a training program.

O.15.2: Scapular kinematics and associated muscle activity in scapular-focused closed and open kinetic chain exercises

Chon Kio Wong, College of Medicine, National Taiwan University; Shu-Chi Wu, College of Medicine, National Taiwan University; Yu-Jen Chen, Department of Physical Education, Fu Jen Catholic University; Wei-Li Hsu, National Taiwan University; Jing-Lan Yang, Department of Physical Medicine and Rehabilitation, National Taiwan University Hospital; Jiu Jenq Lin, College of Medicine, National Taiwan University

Background: Scapular motor control deficits could contribute to subacromial pain syndrome (SAPS). The scapula and humerus work as a chain during scapular-focused exercises. Although these exercises have been proved to be effective in clinical symptoms of SAPS, effects on scapular motor control during exercises are inconclusive. Objectives: To compare the effects of scapular-focused closed and open kinetic chain exercises on scapular kinematics and associated muscle activity in individuals with SAPS and healthy controls. Methods: Twelve patients with SAPS and 12 healthy controls performed two closed kinetic exercises: horizontal row (HRC) and push-up plus (PUP), and two open kinetic exercises: horizontal row (HRO) and serratus punch (SP). Three-dimensional scapular kinematics and surface electromyography on upper trapezius (UT), middle trapezius (MT), lower trapezius (LT) and serratus anterior (SA) were collected during exercises. Comparisons between SAPS and healthy controls as well as closed and open chain exercises were conducted. Also, the characteristics of selected exercises were investigated through principal component analysis (PCA). RESULTS: There were no significant differences in scapular kinematics and muscle activity between SAPS patients and healthy controls during exercises. In HR exercise, higher UT activity (9.91±2.06%, p<0.001) was observed during open compared to closed chained exercise. Moreover, subjects showed higher SA (5.52±1.47%, p<0.001) and less UT (1.75±0.56%, p=0.007) activities in eccentric phase of PUP compared to SP. In scapular kinematics of HR, all participants performed more external rotation (10.2±2.0 degrees, p<0.001) and upward rotation (11.2±2.2 degrees, p<0.001) in concentric phase during open compared to closed chained exercises. Moreover, there was more upward rotation (10.3±2.6 degrees, p<0.001) during PUP compared to SP. In PCA of closed and open HR exercises, MT and LT muscle activities exhibited higher loadings of PC1 (0.84-0.94) throughout the entire phase. External rotation and upward rotation of the scapula demonstrated higher loadings of PC1 (0.74-0.93) during the concentric phase. In PCA of both PUP and SP exercises, MT and LT as well as upward rotation and posterior tipping of the scapula played dominant roles based on the PC1 results (0.67-0.94). CONCLUSIONS: Either closed or open kinetic chain HR and PUP exercises may be suggested to selectively activate specific scapular muscles to enhance scapular motor control. While HR is recommended for activating MT and LT, supported by PCA results, PUP is recommended for activating SA without excessive UT activation. As decreased external rotation and upward rotation of the scapula are related to winging scapula and shoulder impingement, respectively, restoring normal scapular kinematics is crucial. Based on our study, open kinetic chain HR is recommended for increasing external rotation, while PUP is recommended to induce more upward rotation.

O.15.3: Consensus for experimental design in electromyography (CEDE) project: Application of EMG to estimate muscle force matrix

Taylor Dick, University of Queensland; Francois Hug, Université Côte d'Azur; Kylie Tucker, The University of Queensland; Manuela Besomi, The University of Queensland; Paul Hodges, The University of Queensland

The neural system modulates the force generated by a muscle via two mechanisms: recruitment (activating additional motor units) and rate coding (changing the rate at which active motor units fire). However, the interpretation of muscle force directly from electromyographic (EMG) recordings can be problematic. Here, we provide a matrix developed by the Consensus for Experimental Design in Electromyography (CEDE) project, to suggest the appropriateness of global and motor unit-based EMG features to estimate the force generated by skeletal muscle during isometric and dynamic contractions.Consistent with previous CEDE matrices, the steering committee and the lead investigator prepared a draft of the matrix, which was then sent to the other CEDE members to reach consensus on the content following a Delphi process. Consensus was reached when >70% of contributors provided scores between 7–9 (appropriate) and <15% of contributors provided scores between 1–3 (inappropriate), with an interquartile range < 2 units. From the 19 CEDE experts who agreed to participate in the Delphi process, 18 (95%) replied to the first- and second-round questionnaires, after which consensus was reached.The matrix is organized according to the most common approaches to record and/or represent muscle activation: interference EMG which considers the interference pattern of summated action potentials separately for three electrode types: (i) bipolar surface EMG; (ii) high-density surface EMG and (iii) intra-muscular EMG and (iv) decomposition of motor units (from any electrode type). For each approach, the content was arranged into four tables that each consider a different application of EMG to estimate force. These were the use of EMG to: (1) identify the onset and (2) offset of muscle force during isometric contractions, (3) identify force fluctuations during isometric contractions, and (4) estimate force during dynamic contractions and in combination with muscle models. For each combination of EMG approach and application, we provide a recommendation regarding the appropriateness of using EMG to estimate force, as “yes”, “caution”, or “no” along with a detailed justification for the recommendation. This matrix is intended to facilitate the appropriate interpretation of EMG data in relation to muscle force, and more broadly to drive innovation, discovery, and translation in human movement studies.

O.15.4: Movement specific beta-band modulation during movement cancellation in EMG

Ciaran Mcgeady, Imperial College London; Dario Farina, Imperial College London

Cancellation of volitional movement has been shown to synchronise neuronal firing in the sensorimotor cortex, manifesting as an increase in spectral power within the beta band (15—30 Hz) of local field potentials [1]. Despite having no bearing on motor generation, this synchronisation is also reflected in the spectral content of EMG [2]. Whether this phenomenon is functionally relevant for motor control is not yet understood. To further characterise the projection of cortical dynamics to peripheral muscles we aimed to determine whether movement cancellation elicited spectral modulation in all active muscles or whether modulation was movement specific.In nine able-bodied participants, muscle activity was recorded from bilateral wrist extensors using EMG. Participants performed bimanual isometric wrist extensions at 10% maximum voluntary contraction. At the beginning of each trial participants were instructed to anticipate performing either a left or right ballistic wrist

extension contingent on the appearance of an imperative go cue halfway through the trial. In 50% of trials the go cue did not appear at the expected moment. Participants maintained a steady contraction until the end of the trial in the absence of a go cue. There were 100 repetitions for each type of ballistic extension.EMG data from trials where no go cue was delivered were isolated for analysis. Trials that showed excessive deviation from the target force were excluded. EMG was high pass filtered at 10 Hz, rectified and decomposed into a time-frequency representation with Morlet wavelets (–2 to 2 s, relative to pre-stimulus interval; 10 to 60 Hz). The spectral power from the beta band range (15—30 Hz) was taken from 0 – 1 s relative to stimulus onset and normalised with respect to the mean of the pre-stimulus interval (–1 to 0 s). Laterality of beta band modulation was considered during movement cancellation for the two cancellation conditions. A two-way ANOVA was performed to compare the effect movement anticipation and muscle location had on beta-band power.Time-frequency decomposition showed that beta-band power was elevated during the no-go condition with respect to the pre-stimulus interval. Although an elevation in beta-band power was noted bilaterally, there was a lateralisation in power towards the side relevant to the movement task. During left wrist motor cancellation, the left wrist showed a 42% increase in beta-band power and the right wrist showed a 20% increase, with respect to the pre-stimulus interval. Further, right wrist movement cancellation resulted in the inverse: A 28% increase in the left side and a 43% on the right side. The results of a two-way ANOVA demonstrated a significant interaction effect between movement cancellation type and recording location (p=0.028), revealing a lateralisation of the effect.This study demonstrates that beta-band modulation following movement cancellation does not extend to peripheral muscles in a non-guided way but is specific in its projection to muscles. Future work will explore whether this specificity is directed from the cortical or spinal level.References[1] Wessel (2017)[2] Zicher et al. (2022)

O.15.5: A myoelectric pattern recognition method against electrode shifts with adaptive feature sampling

Xinhui Li, Anhui University

Background and Objective: Myoelectric pattern recognition can decode human movement intents and is widely used in rehabilitation robotics, prosthetic control, and other fields. Although the current myoelectric pattern recognition technology has achieved satisfactory performance under ideal circumstances, it still faces more difficult problems in practical applications. Among them, the electrode shift that occurs when repeatedly wearing the signal acquisition device is one of the more common interference factors, which will make the data feature space change, thus leading to the degradation of recognition performance. In this paper, we proposed an adaptive feature sampling method for robust myoelectric pattern recognition. Methods: A sampling grid generator was used to generate feature sampling locations for each input sample adaptively. By jointly training the sampling grid generator and classifier on samples with different shifts, the proposed methods can sample features that are invariant to the electrode shift. The proposed method enjoys two merits. First, it can be applied on different methods because it can be achieved by adding an extra sampling grid parameter estimator on existing methods. Second, different from previous methods that are designed to improve classification accuracy, the proposed method can explicitly estimate the electrode shift parameters, which makes it more explainable. The performance of the proposed method was evaluated via experiments of classifying six hand gestures using high-density myoelectric data

recorded from ten intact-limbed subjects at six electrode positions. RESULTS: The average classification accuracies of the proposed method were 97.01 ± 3.84%, outperforming the state-of-the-art baselines with statistical significance (p <0.05). Conclusion: This study provides a promising solution to mitigate the negative effect of the electrode shift, improving the performance of myoelectric pattern recognition. It can help build more robust and natural human-computer interfaces and promote the application of myoelectric pattern recognition in prosthetic limb control, consumer electronics, and rehabilitation engineering.

O.15.6: Enhance the robustness of myoelectric control in the presence of low-signal-quality electrodes

Ge Gao, University of Science and Technology of China; Xu Zhang, University of Science and Technology of China

Background and Objective: Myoelectric control technology holds immense promise for developing neuromuscular interfaces, intelligent prostheses, and human-machine systems. However, in surface electromyography (EMG) signal acquisition, interferences such as friction between electrodes and the skin, electrode doffing, and hardware damage can lead to abnormal data recording in certain channels, significantly diminishing the robustness of myoelectric control. While previous studies have found that abnormal channels can be accurately detected, there remains substantial room for enhancing the quality of reconstructed data. This study aims to address this problem by constructing a deep-learning-based EMG data reconstruction model that alleviates the impact of abnormal channels on the robustness of myoelectric control. Methods: An autoencoder network (AEN) was developed to reconstruct the EMG feature map, and a support vector machine (SVM) was adopted for pattern classification. During the training phase, 1-3 channels in the feature map were randomly masked before being input into AEN. The mean square error between the output of AEN and the unmasked original feature map was calculated, optimizing the parameters of AEN to enable the model to learn the ability to reconstruct the original feature map. In the testing phase, feature data from abnormal channels was masked and input into the pre-trained AEN to obtain the reconstructed EMG feature map. For performance evaluation, both user-dependent and user-independent testing experiments were conducted (considering six different electrode abnormal conditions: one channel, two non-adjacent channels, two adjacent channels, three non-adjacent channels, two adjacent channels with another non-adjacent channel, and three adjacent channels) with ten subjects performing six gestures by wearing an 8-channel EMG armband on the forearm. RESULTS: The average classification accuracies of the proposed method were 94.40 ± 4.74% and 81.77 ± 10.42% under user-dependent and user-independent testing conditions, respectively, and outperformed those of the existing interpolation-based data reconstruction method (85.73±9.24% and 73.07±8.20%) with statistical significance (p <0.05). Conclusion: The proposed method is demonstrated as a useful tool for reconstructing the EMG feature map in the presence of abnormal data in several channels, thereby enhancing the robustness of myoelectric control for practical clinical applications.

O.15.7: Effects of percussion massage therapy on exercise-induced muscle damage

Xin Ye, University of Hartford

BACKGROUND AND AIM: Percussion massage therapy (PMT) is a type of massage therapy that uses a device called a massage gun to deliver rapid blows to the soft tissue. This type of intervention is thought to increase blood flow and reduce muscle soreness, thereby assisting post-exercise muscle recovery. Interestingly, limited data supports the efficacy of this intervention. The purpose of the project, therefore, was to determine if PMT is effective in muscle recovery after a session of intensive elbow flexion eccentric exercise. Methods: Twenty healthy adults (PMT group: n =10, age = 23 ± 2 years, height = 175.9 ± 8.4 cm, body mass = 80.1 ± 15.1 kg; Control group: n =10, age = 24 ± 5 years, height = 169.5 ± 10.6 cm, body mass = 78.2 ± 20.5 kg) completed this 5-visit study. After the first visit served as the familiarization, all subjects performed a session of unilateral (nondominant) elbow flexion eccentric exercises (six sets of 10 repetitions at 80% of the concentric 1-repetition maximum, with 2 minutes rest between sets) during the second visit to the laboratory. Before, immediately after, one day, two days, and seven days after the exercise intervention, indirect muscle damage markers from the exercised muscle (muscle soreness through visual analogue scale, elbow joint range of motion, upper arm circumference, elbow flexion isometric strength, biceps brachii muscle voluntary activation, and resting twitch) were measured. The PMT group received two, 2.5 minutes of percussive massage via a percussion massage gun (2800 RPM) at the end of the second, third, and fourth visits; and the Control group did not receive any treatment. Two-way (group × time) mixed factorial analysis of variance (ANOVA) tests were used to examine the potential changes in the indirect muscle damage markers through time between groups. RESULTS: There were no significant differences for all baseline characteristics and the 1-repetition maximum between the groups (p > 0.05). Additionally, ratings of perceived exertion (RPE) after each eccentric exercise set significantly increased (p < 0.001) throughout the exercise sets, but did not differ between groups (p = 0.966). For all the indirect muscle damage markers, the two-way ANOVAs indicated significant main effects for time (p < 0.05) but not for group (p > 0.05). A small treatment effect of PMT (Cohen's d = 0.3) was observed one day post-exercise for muscle soreness when compared to the Control group. CONCLUSIONS: The results from this study do not support that PMT can improve muscle recovery and performance following an intensive session of exercise.

Oral Session 16

O.16.1: Influence of temperature on motor unit activity during ballistic contraction

Kazutaka Ota, The University of Tokyo; Hikaru Yokoyama, Tokyo University of Agriculture and Technology; Kazushige Sasaki, The University of Tokyo

BACKGROUND AND AIM: Temperature is known to influence motor performance, especially the rate of torque development (RTD) which has been shown to depend strongly on neural rather than muscle contractile properties. However, the temperature effects on motor unit activity (e.g. discharge rate and recruitment speed) during ballistic contractions remain largely unknown. This study aimed to clarify the influence of local limb temperature on motor unit activity, RTD, and their association during ballistic contractions in humans. We hypothesized that a decrease in temperature would decrease RTD via a reduction in motor unit discharge rate and/or recruitment speed. Methods: Ten healthy males rested in a sitting position while immersing their right lower leg in water of different temperatures (Cold: ~10°C, Neutral: ~33°C, Hot:

~43°C) for 20 minutes each. Participants then completed three types of voluntary isometric contractions of dorsiflexors while maintained on water immersion in each temperature condition. Specifically, they were instructed to perform maximal voluntary contraction for 3 s (MVC), to develop joint torque as fast as possible to reach at least 75% of MVC torque (ballistic contraction), and to linearly increase torque for 10 s from rest to 20% MVC and sustain the torque for 20 s (ramp-and-hold contraction). Surface electromyography was recorded from the tibialis anterior muscle with grids of 64 electrodes (interelectrode distance of 8 mm) and decomposed into individual motor unit spike trains using the fast independent component analysis with the convolution kernel compensation algorithm. RESULTS: Compared to Neutral, MVC torque was lower in Cold ($p = 0.02$) but not in Hot. During ballistic contractions, the temperature had no significant influence on the “early” RTD (from 0 to 50 ms after the torque onset), but the “late” RTD (from 0 to 150 ms) was lower in Cold than in the other two ($p < 0.001$) even when normalized by MVC torque. On the other hand, the motor unit discharge rate at the time of recruitment was higher in Cold than in Hot (Figure A, $p = 0.03$), while the recruitment threshold decreased with the temperature (Figure B, $p < 0.05$). Moderate-to-strong correlations were found between the changes in recruitment threshold and the late RTD ($r = −0.77$, $p = 0.01$) and between those in discharge rate and the early RTD ($r = 0.41$, $p = 0.09$), although the latter was not statistically significant. During ramp-and-hold contractions, no significant change with temperature was observed in the discharge rate or recruitment threshold. CONCLUSIONS: We provide evidence that the decrease in local temperature due to cold water immersion leads to the decrease in recruitment threshold and the increase in discharge rate during ballistic contractions. These changes may act as a compensatory mechanism against the cold-induced impairment in contractile function, since the larger changes in motor unit activity were associated with the smaller reduction in RTD.

O.16.2: Voluntary co-contraction of ankle muscles alters motor unit discharge characteristics and reduces estimates of persistent inward currents

Matheus Gomes, Universiy of São Paulo; Sophia Jenz, Northwestern University; James Beauchamp, Northwestern University; Francesco Negro, Universita' degli Studi di Brescia; CJ Heckman, Northwestern University; Greg Pearcey, Memorial University of Newfoundland

BACKGROUND AND AIM: Voluntary co-contraction training, which involves voluntary and simultaneous contraction (i.e., co-contraction) of antagonistic pairs without requiring external apparatuses for loading, has shown promise for promoting strength gain and hypertrophy. The impact of voluntary co-contraction on intrinsic properties of motoneurons, such as persistent inward currents (PICs), key intrinsic properties that contribute to motoneuron function, are unknown. During co-contraction, motoneurons receive competing excitatory and inhibitory inputs, both of which affect PICs. Reciprocal inhibition from antagonist muscles are likely to attenuate PICs, while increased neural drive may counteract these effects on PICs. To study the underlying neural control of co-contraction, we estimated PICs from motor unit (MU) discharge patterns during voluntary co-contraction of ankle muscles. Methods: Sixteen adults (7 females) performed triangular co-contraction (simultaneous dorsiflexion and plantarflexion) and isometric dorsiflexion ramps (10s up and down) to a peak of 30% of their maximum muscle activity achieved during a maximal voluntary contraction. We decomposed MU spike trains from high-density surface electromyograms recorded from the tibialis anterior (TA) using a blind source separation algorithm. To estimate PIC magnitude, we quantified discharge rate

hysteresis (ΔF) by comparing the onset and offset of a higher-threshold MU in relation to the discharge rate of lower-threshold MUs. To garner insights into individual MU discharge behavior, we used a quasi-geometric approach to analyze non-linearities in MU discharge rates with respect to rectified EMG amplitude. We used linear mixed effects models to determine if outcome variables were predicted by the fixed effect of contraction type. RESULTS: Estimates of PICs were lower during co-contraction [χ2(1)=72.66, p<0.001] compared to isometric dorsiflexion (4.5 vs. 5.6 pps, respectively). Brace height (χ2(1)=19.65, p< 0.001), a quantification of non-linearity of discharge rate with respect to rectified EMG amplitude, and the angle between the acceleration and post-acceleration attenuation slopes (χ2(1)=18.12, p< 0.001) were both reduced during co-contraction compared to isometric dorsiflexion (45.9 vs. 51.0%; 229 vs. 237 degrees, respectively), indicating a more linear increase in discharge rate in the co-contraction condition. CONCLUSIONS: These findings suggest that, during voluntary co-contraction, the inhibitory input from the antagonist muscle overcomes the additional excitatory drive induced by the antagonist muscle contraction. The novelty of our approach, which concurrently considers both inhibitory and excitatory inputs arising from voluntary co-contraction, enhances our comprehension of the intricate coordination of motor commands that govern MU behavior.

O.16.3: The influence of low-intensity vibration on motor unit firing rate and muscle fatigue

Zuyu Du, Shanghaitech University; Yaodan Xu, Shanghaitech University

Background: Force-modulated vibratory stimulation (FVS) has demonstrated positive effects on strength training, primarily studied in the context of high-intensity muscle contractions, such as 80% maximal voluntary contraction (MVC) [1]. However, the impact and mechanisms of FVS on low-intensity contractions remain unclear. This study aims to investigate the effects of low-intensity vibration (LIV) on motor unit (MU) synchronization and muscle fatigue.Method: Ten healthy right-handed subjects used a previously established FVS system [1]. We measured each subject's biceps brachii isometric MVC with a load cell embedded in the FVS system, maintaining a 90-degree elbow angle. Subjects then performed multiple 60-second LIV trials with a baseline force set at 30% MVC, maintaining the same elbow angle. The vibration amplitude was set at 50% of the baseline force, with vibration frequencies ranging from 0, 15, 25, 35, to 45 Hz in various trials. Two 64-channel high-density electrode grids measured surface electromyography (sEMG) on each subject's biceps brachii. EMG data were decomposed into MU spike trains using the CKC algorithm, followed by manual editing to ensure a pulse-to-noise ratio exceeding 30 dB. For each FVS frequency, a firing rate histogram was generated from MU spike trains across all subjects. The synchronization index (SI) of MU was quantified as the ratio of firing rates within the vibration frequency and its subharmonics to the entire histogram. Additionally, muscle fatigue for each FVS trial was estimated by the slope of a linear regression applied to muscle fiber conductive velocity (CV) on manually identified channels using a 1-second sliding window. One-way ANOVA assessed the effects of vibration frequency on SI and CV slope. Result: All vibration trials exhibit significantly larger SIs than the control condition (0 Hz). The 15-Hz FVS trial's firing rate histogram displays a distinct peak at the vibration frequency, while other conditions show dominant peaks at the second, third, and fourth subharmonics. There is no significant difference in the CV slope across various vibration frequencies.Discussion: Prior studies suggest FVS superimposed on 80% MVC to produce a significantly larger degree of fatigue than the control condition [1]. However, in the present

study, no significant effect can be observed when FVS is superimposed on 30% MVC, suggesting the effects of FVS on muscle fatigue depend strongly on the initial contraction level of the muscle. Yet, such low-intensity FVS yields significant MU synchronization at the vibration frequency and/or its subharmonics. The observed subharmonic synchronization may be because the maximum firing rate of the biceps brachii is below 30 Hz.[1] Xu, L., Cardinale, M., Rabotti, C., Beju, B., & Mischi, M. (2016). Eight-week vibration training of the elbow flexors by force modulation: effects on dynamic and isometric strength. The Journal of Strength & Conditioning Research, 30(3), 739-746.

O.16.4: Exploring motor unit modes in repetitive isometric tasks

Helio Cabral, Università degli Studi di Brescia; J Greig Inglis, Università degli Studi di Brescia; Elmira Pourreza, Università degli Studi di Brescia; Caterina Cosentino, Università degli Studi di Brescia; Milena Santos, Università degli Studi di Brescia; Francesco Negro, Universita degli Studi di Brescia

BACKGROUND AND AIM: The covariation in discharge rates can be used to estimate the motor unit (MU) modes (or common synaptic input components) underlying the activity of neuronal ensembles. Previous evidence suggested a principal component explaining fluctuations in MU discharge times within individual muscles [1], highly correlated with force output. Other findings proposed the existence of more than one factor, particularly in synergistic muscles [2]. This study used principal component analysis (PCA) and factorization analysis (FA) to investigate the consistency of MU modes during repetitive isometric tasks involving the same force output oscillations. Methods: Two muscles, tibialis anterior (TA; 11 participants) and first dorsal interosseous (FDI; 7 participants), were assessed while participants completed 15 trials of an isometric force-matching task. Each trial involved following oscillations of a random signal for 30 s. The three consecutive trials with the smallest error between the force and target were selected. High-density surface electromyograms were decomposed into MU spike trains and MUs were tracked between trials. The number of components to be retained was determined using PCA with parallel analysis [3]. Subsequently, we applied PCA and FA (unrotated) to the standardized MU smoothed discharge rates. To explore the correlation between extracted MU mode fluctuations and force output, cross-correlation between these signals was calculated. Additionally, the cross-correlation between trials was computed to assess the consistency of the extracted MU modes. Linear mixed models (LMM) were used to compare main and interaction effect of trials and extracted MU modes on cross-correlation values. RESULTS: Parallel analysis revealed that one MU mode explained most of the variance of MU discharge rate in 11 out of 18 participants. In the other participants, two MU modes were extracted. We then opted to use two modes for subsequent analyses. For both muscles, the first MU mode was significantly more correlated with force output (~0.6 ± 0.1) than the second MU mode (~0.2 ± 0.1), regardless of the trial (LMM, P < 0.001 for all). Moreover, the first MU mode presented significantly greater correlation across trials (~0.5 ± 0.1) than the second MU mode (~0.1 ± 0.2; LMM, P < 0.001 for all). These results were consistent for both PCA and FA. CONCLUSIONS: Our main results demonstrated that the first MU mode showed high consistency across repetitive isometric tasks with similar force output, whereas the second mode did not. These findings suggest that motor units in individual muscles are mainly controlled by one low-frequency control synaptic input highly resembling the output force oscillations. In upcoming research, we aim to extend our methodology to synergistic muscles and examine how changes

in the parametrization of PCA and FA might impact the results.REFERENCES: [1] Negro et al., 2009[2] Del Vecchio et al., 2023[3] Hayton et al., 2004

O.16.5: Motor unit firing properties of knee extensors immediately after repeated static stretching of rectus femoris in healthy males

Tetsuya Hirono, Kyoto University; Masahide Yagi, Kyoto University; Zimin Wang, Kyoto University; Haruka Sakata, Kyoto University; Shogo Okada, Kyoto University; Kaede Nakazato, Kyoto University; Noriaki Ichihashi, Kyoto University; Kohei Watanabe, Chukyo University

Introduction: Static stretching (SS) immediately affects various neuromusculoskeletal components, including neuromuscular physiological alterations. Immediately after repeated SS of the triceps surae, the motor unit (MU) firing rate (FR) increased during low-intensity contraction (Mazzo et al. J Physiol. 2021), thus SS may alter MU firing properties. However, the impact of SS on the neural drive in both the stretched muscle and unstretched synergists is not well understood. Our motivation of this study was to clarify the differences in the neural drive strategies among synergist muscles after SS. Specifically, this study investigated alterations in MU firing properties of rectus femoris (RF) and vastus lateralis (VL) immediately after selective SS which reduced only RF stiffness. We hypothesized that MU FR increased or MU recruitment threshold (RT) decreased in RF or VL to compensate for the reduction of RF stiffness. Methods: Twelve healthy males (23.8±2.4 yrs) visited the laboratory on two separate days; SS or rest (control condition; CON) was performed each day. Maximal voluntary isometric contraction (MVC) torque of knee extension was measured, and high-density surface electromyography of RF and VL was evaluated to assess individual MU firing during 10% of MVC and ramp-up to 35% of MVC, and same MUs were tracked before and after each intervention. Before and after SS or CON, shear elastic moduli of RF and VL were measured using ultrasound shear wave elastography. SS was performed for 1 min with maximal hip extension and knee flexion where the participants could tolerate, and was repeated for six sets. In CON, the participants rested for 6 min. Mixed-model analyses of variance were performed. RESULTS: The shear elastic modulus of RF significantly decreased only after SS (interaction: $p = 0.032$). However, the shear elastic modulus of VL did not change after either condition (interaction: $p = 0.497$). At 10% of MVC, MU FR of RF did not change in either condition (interaction: $p = 0.192$), while the MU FR of VL after CON significantly increased, but not after SS (interaction: p < 0.001). There were no interactions in MU FR in either RF ($p = 0.809$) or VL ($p = 0.203$) at 30-35% of MVC, but main effects of time were observed in both muscles, revealing MU FRs significantly increased (both p < 0.001). There were no interactions in MU RTs in either RF ($p = 0.673$) or VL ($p = 0.204$), but a main effect of time was observed, revealing MU RTs decreased (both p < 0.001). The MVC torque significantly decreased in both conditions (p < 0.001) without interaction ($p = 0.444$). CONCLUSION: : The 6-min repeated SS with hip extension and knee flexion could decrease the stiffness of RF, but not VL. The MU firing properties of RF and VL were not affected by the selective SS of RF. When a selective muscle stiffness only decreased among the synergist muscles, it was suggested that MU firing pattern did not necessarily compensate for the change in muscle compliance.

O.16.6: Common neural input to deltoid segments: preliminary findings on control

Wolbert Van Den Hoorn, Queensland University of Technology; Francois Hug, Université Côte d'Azur; Ella Hill, The University of Queensland, School of Biomedical Sciences, Australia;

Frederique Dupuis, Université Laval; Ashish Gupta, Queensland Unit for Advanced Shoulder Research, Queensland University of Technology, Australia; Kenneth Cutbush, The University of Queensland; Kylie Tucker, The University of Queensland

Introduction: Functional outcomes following total reverse shoulder replacement surgery vary. Our overall goal is to understand how the central nervous system controls shoulder muscles in health and disease, and if this control impacts recovery from surgery. To this end, our initial aim was to determine the complexity of neural drive to the deltoid muscle at the spinal motoneuron level in individuals with healthy shoulder function. The deltoid comprises of three main segments, the anterior, middle, and posterior deltoid. Each segment comprises of many individual muscle fibres, each innervated by a single spinal motoneuron, together grouped as a motor unit. By measuring the correlated activity of multiple single motor units, we gain direct insight into the common drive of a motoneuron pool. This approach has been used to reveal the control signals for other large skeletal muscles but not the deltoid muscles. Methods: Three high-density electromyography grids (GR08MM1305, OT Bioelettronica, Italy) were used to record deltoid activity during force-matched abduction tasks (45-degree shoulder abduction) in 10 participants with healthy shoulder function [1 female, age: 29 (10) yrs, height: 1.76 (0.09) m, weight: 73 (11) kg]. Signals were decomposed into motor unit spike trains using blind source separation, edited with MUedit software, and smoothed with a 400ms Hanning window. Cross-correlation analysis extracted common dynamics among multiple motor units (when at least 4 motor units were decomposed for a muscle segment). A significance threshold (95th percentile) was determined for each motor unit pair using bootstrapping. Common drive within and between muscles was estimated as the percentage of significantly correlated motor unit pairs. Activation level was determined from bipolar derivation of monopolar signals (2 x 5 channels, ied 24mm) and normalized to a maximum voluntary contraction. RESULTS: Too few motor units were detected in two male participants; findings are therefore reported from n=8 participants. Smoothed firings were concatenated from two 8s contractions. During the plateau, participants activated their deltoid at (mean(SD)): anterior 11 (5) %MVC, middle: 15 (6) %MVC, posterior: 7 (4) %MVC. We identified: anterior: 8.4 (3.3), middle: 7.3 (3.6), posterior: 5.5 (3.9) motor units per participant. Estimated common drive was typically very high within a deltoid segment (anterior: 69 (22)%, middle: 76 (27)%, posterior: 76 (26)%, and low between deltoid segments (anterior-middle: 12 (13)%, anterior-posterior: 9 (16%), middle-posterior: 41 (20%)). Individual data is reported in Table 1.Discussion: Preliminary findings suggest complex and variable neural control of the deltoid muscles between individuals, with common neural input to each and across deltoid heads. This likely relates to force production and stabilization functions, offering crucial insights into the neural control of healthy deltoid muscles.

O.16.7: Changes in discharge properties of longitudinally-tracked motor units after four weeks of isometric strength training in older adults

Andrea Casolo, University of Padua; Stefanie Del Vecchio, Neurology, Nurnberg Hospital, Germany; Bastian Schrader, Department of Cardiology, University of Oldenburg, Klinikum Oldenburg, Germany; Stefano Nuccio, University of Rome "Foro Italico"; Edoardo Lecce, Department of Movement, Human and Health Sciences, University of Rome “Foro Italico”, Rome, Italy; Joachim Schrader, Department of Cardiology, University of Oldenburg, Klinikum Oldenburg, Germany; Alessandro Del Vecchio, Friedrich-Alexander Universität, Erlangen-Nürnberg

Background and Aim: Aging is accompanied by significant losses of muscle mass and ability to produce muscular force. These dysfunctions could be partly underpinned by alterations within the nervous system, particularly at the motor neuron level, which in turn could be partly reversed by resistance training. Previous evidences in young adults showed that 4 weeks of strength training are sufficient to evoke changes in motor unit (MU) discharge rate, in turn mediating the increase in force. Nevertheless, the specific motor unit adaptations after strength training in older adults remain elusive. Thus, this study investigated the effects of 4-week strength training intervention on the behavior and properties of the same tracked motor units in older adults. Methods: Twenty-three participants were randomly assigned to either a strength training (INT, n = 13; 71.2±4.7 yr) or to a control group (CON, n = 10; 69.0±2.7 yr). ST group completed a 4-week combined strength training protocol involving ballistic (4 x 10) and sustained (3 x 10) isometric ankle dorsiflexions. Measurement sessions involved the recording of voluntary maximum (MVF) and submaximal isometric forces during ramp contractions up to 70% MVF. Concurrently, myoelectrical activity from tibialis anterior muscle was recorded with high-density surface EMG (HDsEMG). HDsEMG signals were decomposed into individual MU discharge timings and MU were tracked across experimental sessions (pre vs post), allowing a robust comparison of properties of the same motor units. RESULTS: The total number of identified MU across participants, contractions and measurement sessions was 2672, of which 406 (~15%) were tracked across sessions. Maximum voluntary force increased in the INT group (+18%, P = 0.003). Similarly, average MU discharge rate increased at recruitment (+9%, P = 0.036) and plateau (+12%, P = 0.004) of the ramp contractions after the training, but it did not change at derecruitment. Interestingly, changes in MU discharge rate both at recruitment (P = 0.027) and plateau (P = 0.004) were observed mainly in lower threshold MU. On the other hand, normalized MU recruitment/derecruitment thresholds did not change with the training. CONCLUSIONS: Unlike what was observed in young adults, the increase in maximum voluntary strength was accompanied by increases in initial motor neuron discharge rate and absence of changes in MU recruitment threshold. However, similar to what observed in young adults, the training intervention increased the maximum muscular force and this was accompanied by an increase in MU discharge rate during the plateau phase of contractions. These findings may indicate different adjustments in the behavior and discharge properties of MU between young and older adults exposed to the same strength training protocol. Our results provide further evidence of the adaptability of the nervous system and particularly of motor neuron discharge rate to short-term exercise in older adults.

Oral Session 17

O.17.1: Effects of subthreshold electrical stimulation with pink noise on treadmill walking

Momoko Yamagata, Kansai Medical University; Kei Maekaku, Kobe University; Ryota Tanoue, Kobe University; Tetsuya Kimura, Kobe University

BACKGROUND AND AIM: : Falling during walking is a serious problem in various populations. As a way to reduce the risk of falling, this study focused on the stochastic resonance (SR). SR is a phenomenon in which subthreshold noise enhances the detection and transmission of a weak signal in sensory systems. Previous studies have revealed that electrical noise stimulation improved postural control during standing via SR, and such SR effects were further enhanced by

the stimulation of pink noise structure. However, the effects of pink-noise stimulation on walking remains unclear. Thus, we aimed to explore whether pink-noise stimulation improves walking ability. Methods: Ten healthy young adults walked on a treadmill for 15 minutes, and the imposed speeds were 4.5 km/h and 2.7 km/h. Two noise conditions were employed for each speed. In the control (CONT) condition, no stimulation was applied during walking; whereas in the pink-noise (PINK) condition, pink-noise stimulation was applied to both knee joints 3-4 minutes after participants started walking. A triaxial accelerometer was attached to the low back (L4-L5 region) and body accelerations in mediolateral (ML), vertical (V), and anteroposterior (AP) directions were extracted for the last 10 minutes. For every minute, stride-to-stride variabilities of acceleration were computed to evaluate the walking ability. We also evaluated the average and coefficient of variation of stride time. For each speed, two-way ANOVAs with the factors Noise (CONT, PINK) and Time (10 levels) were performed to evaluate the noise effects over time ($\alpha = 0.05$). When the interaction effect was significant, post-hoc analysis with Bonferroni correction ($\alpha = 0.005$) was performed for differences between CONT and PINK conditions. RESULTS: At a normal speed (4.5 km/h), a significant interaction in the average stride time was found, and at the first two intervals, there was a tendency to increase the average stride time in the PINK condition (0-1 minutes: $p = 0.022$, 1-2 minutes: $p = 0.007$). At a slow speed (2.7 km/h), we found significant interactions in variabilities of ML and AP accelerations, but such an effect was not found in V acceleration. At the last time interval (9-10 minutes), AP variability was significantly lower in the PINK condition than in the CONT condition ($p = 0.004$). Similarly, ML variability tended to decrease during 9-10 minutes in the PINK condition ($p = 0.020$). There were no significant effects in the other indices. CONCLUSION: : This exploratory study suggested that pink-noise stimulation may be beneficial in walking. Specifically, pink-noise stimulation tended to increase the average stride time in the early phase of noise application. Moreover, pink-noise stimulation decreased the variability of acceleration at the last phase of the 15-min walk, indicating that noise stimulation might improve walking ability after walking for a certain amount of time.

O.17.2: Effect of Neuromuscular electrical stimulation on the humeral adductors in patients with rotator cuff tear

Yang-Ting Chien, National Taiwan University; Che-Yuan Chang, School and Graduate Institute of Physical Therapy, College of Medicine, National Taiwan University; Yi-Hsuan Weng, National Taiwan University, College of Medicine; Chung-Hsun Chang, Department of Orthopedic Surgery, National Taiwan University Hospital; Jing-Lan Yang, Department of Physical Medicine and Rehabilitation, National Taiwan University Hospital; Po-Tsun Chen, School of Physical Therapy, Master Program in Rehabilitation Science, Chang Gung University; Jiu Jenq Lin, College of Medicine, National Taiwan University

Introduction: In symptomatic patients with rotator cuff tear, MRI and radiographic studies have recognized the pain symptom to insufficient humeral head depression during arm elevations. The application of Neuromuscular Electrical Stimulation (NMES) to the lower trapezius and anterior serratus enhances AHD in addition to improving scapular kinematics. Humeral adductors such as the teres major (TM) or pectoralis major (PM) may assist in humeral head depression during arm elevation. The effect of neuromuscular electrical stimulation on the humeral adductors is still unknown. This study investigated the effects of NMES application on humeral adductors in AHD and scapular kinematics.Method: A cross-sectional study of NMES

of the teres major and pectoralis major was conducted on 30 symptomatic subjects with rotator cuff tear. We employed a cross-over strategy to randomly stimulate the TM or PM to account for order effects. The acromiohumeral distance and scapular kinematics during arm elevation were measured by ultrasonography and a three-dimensional motion tracking system, respectively. RESULTS: For the acromiohumeral distance, there was a significant increase during NMES on TM (0.43-0.88mm, p< 0.001) and a significant decrease during NMES on PM (0.78 mm, p< 0.001) compared to no NMES. However, the scapular kinematics of scapular upward rotation was greater with NMES on TM compared with those when NMES on PM (1.32-3.36°, p≤ 0.001). In addition, scapular external significantly decreased with NMES on PM than that with NMES on TM (p= 0.003). CONCLUSION: : NMES of the TM can increase acromiohumeral distance and scapular upward rotation during arm elevation. However, the decreased upward and external rotation of the scapula during arm elevation with NMES of the PM may be associated with subacromial impingement.

O.17.3: Novel brace with neuromuscular electrical stimulation in patients with full-thickness rotator cuff tear: a randomized controlled trial

Yi-Hsuan Weng, National Taiwan University, College of Medicine; Yang-Ting Chien, National Taiwan University; Chon Kio Wong, College of Medicine, National Taiwan University; Jing-Lan Yang, Department of Physical Medicine and Rehabilitation, National Taiwan University Hospital; Chung-Hsun Chang, Department of Orthopedic Surgery, National Taiwan University Hospital; Jiu Jenq Lin, College of Medicine, National Taiwan University

Introduction: A full-thickness tear of the rotator cuff can lead to subacromial pain, diminished abducted force, limited range of motion, and functional impairment. Rotator cuff deficits can result in the decentralization and augmented translation of the humeral head during arm elevations. Teres major (TM) is believed to play a compensation role in adducting, depressing, and centralizing the humeral head during arm elevations. However, limited studies have explored the impact of TM training in patients with full-thickness rotator cuff tear. This study aims to investigate the effects of a novel brace with neuromuscular electrical stimulation (NMES) plus exercise for 6 weeks in comparison with control therapy. Methods: Sixteen participants with full-thickness rotator cuff tears were split into the brace with an NMES group (BNMES) and an exercise control group. Characteristics, tear size, and location were recorded using ultrasonography or MRI. Humeral head migration was gauged at 0°, 60°, and 90° of shoulder abduction using ultrasonography. Shoulder muscle strength (upper trapezius, lower trapezius, serratus anterior, and TM), pain levels, and self-reported shoulder function (FLEX-SF questionnaire) were evaluated. Both groups underwent a 6-week intervention consisting of scapular-focused exercises, including scapula row, serratus punch, and adduction exercises performed at 10 repetitions per set for 3 sets daily. The BNMES group received additional NMES during exercises. Measurements were taken at the beginning, weeks 3, and weeks 6, and analyzed via a two-way mixed analysis of variance with group (BNMES and control) and time (beginning, weeks 3, and weeks 6) factors. Results: There was no significant time-group interaction, but the main effect was on time. Following the intervention, participants exhibited significant improvements in pain (2.2±0.5, p<0.005; 3.1±0.6, p<0.001) and function (2.8±1.0, p=0.048; 6.4±1.3, <0.001) at weeks 3 and 6, but no difference between weeks 3 and 6. Shoulder muscle strength also increased in the serratus anterior (3.5±1.1kg, p=0.021; 8.1±2.0 kg, p=0.004) and TM (2.5±0.9kg, p= 0.021; 4.6±.1.1kg, 0.004) at weeks 3 and 6. Lower trapezius

strength only increased from weeks 3 to 6 (1.9±0.6kg, p= 0.026). However, the humeral head migration did not reveal significant differences post-intervention. CONCLUSION: : Scapular-focused exercises plus shoulder adductor training demonstrated the potential to alleviate pain and enhance function in patients with full-thickness rotator cuff tears. The improvements may be attributed to increased strength in serratus anterior and TM. Six weeks of exercise can further improve lower trapezius strength with concurrent improvement in pain reached clinical difference. Notably, humeral head superior migration remained unchanged. Clinical practitioners could consider introducing these exercises to patients with full-thickness rotator cuff tears as a safe and promising option.Keywords: brace, teres major, neuromuscular electrical stimulation, full-thickness rotator cuff tear

O.17.4: The effect of femoral strapping on excessive hip internal rotation and pain response in females with patellofemoral pain

David Selkowitz, MGH Institute of Health Professions; Richard Souza, University of California, San Francisco; Christopher Powers, University of Southern California

Introduction: Excessive hip internal rotation has been theorized to affect patellofemoral joint mechanics and contribute to patellofemoral pain (PFP). The SERF (Stability through External Rotation of the Femur) strap was designed to provide hip stability by pulling the thigh into external rotation during weight-bearing activities. The effects of the strap have not been assessed in persons with PFP who have excessive amounts of hip internal rotation during tasks when not wearing the strap. Thus, the purpose of our study was to evaluate the effects of the SERF strap on hip internal rotation (IR) and pain response during dynamic, weight-bearing activities in females with PFP who have excessive amounts of hip internal rotation.Method: Nineteen females with a diagnosis of PFP were tested while wearing the strap and not wearing the strap. Three-dimensional motion analysis was performed to obtain hip kinematic data, and a 10-cm visual analog scale was used to assess pain. Each subject performed 3 tasks, with and without the SERF strap: drop-jump, unilateral step-down, over-ground running. The stance phase of each task was identified, and 15 subjects who demonstrated 4 degrees or more of hip IR during at least 2 of the tasks while not wearing the strap were retained in the study for further analysis between strap conditions. Two-way (strap condition by task) ANOVAs were used to analyze the hip IR and pain data. RESULTS: Significant main effects revealed reductions in peak hip IR (p<0.001) and pain scores (p=0.03) across tasks when wearing the SERF strap. Conclusion: When it is necessary to limit hip internal rotation during weight-bearing activities, the SERF Strap may be a useful treatment adjunct for persons with PFP who have excessive amounts of hip internal rotation.

O.17.5: Changes in tonic vibratory reflex after visually induced kinesthetic illusion therapy in post-stroke patients with spasticity

Kenya Tanamachi, Tokyo Metropolitan University; Megumi Okawada, Keio University School of Medicine; Wataru Kuwahara, Tokyo Metropolitan University; Takayuki Kamimoto, Keio University School of Medicine; Yuka Yamada, Keio University School of Medicine; Michiyuki Kawakami, Keio University School of Medicine; Fuminari Kaneko, Tokyo Metropolitan University

[Background and aim]Visually induced kinesthetic illusion (V-KI) is a psychological phenomenon in which a resting person feels as if a body part is moving or feels the desire to

move a body part while watching film footage of a moving body part (Kaneko et al. Neuroscience, 2007). Miyawaki et al. (Front Syst Neurosci, 2021) showed that V-KI therapy combined with therapeutic exercise reduced the modified Ashworth scale (MAS) score, improving motor assessment scores. However, the MAS score largely reflects muscle degeneration due to long-term spasticity. Therefore, it is necessary to consider that the MAS score is influenced by the musculature components in addition to the degree of spasticity.Vibrating the flexor digitorum tendon at the appropriate location induces firing of Ia fibers owing to muscle spindle activity, generating an afferent input. Moreover, the firing frequency of Ia fibers is known to adjust to the vibratory stimulation frequency (Brown MC et al., J Physiol, 1967). The reflex triggered by vibration is known as the tonic vibration reflex (TVR). This study aimed to apply vibrations of different frequencies to a post-stroke patient with hemiplegia and spasticity and to clarify the relationship between TVR-induced surface electromyography (sEMG) and motor function changes following V-KI therapy.[Method]Fourteen post-stroke patients underwent a 15-day V-KI therapy, evaluated through vibratory stimulation before and after treatment. The participants were instructed to relax their wrist and finger muscles which were fixed on a table. Vibratory stimulation (eyes open) was applied three times for 3 s to the paralyzed finger flexor digitorum tendon. Frequencies of 40, 60, 80, and 100 Hz were utilized with sEMG recordings of the extensor digitorum communis and flexor digitorum profundus. Analysis was performed by applying a 5–500 Hz bandpass filter and calculating and normalizing the RMS mean values during stimulation by the maximum RMS mean value. The minimum RMS mean value served as the reference, and the slope of the maximum change in the RMS with frequency (RMS slope) was determined.[Result]In all participants, the RMS mean value during stimulation was lowest at 40 Hz. The RMS slope negatively correlated with motor function change after V-KI therapy. Although MAS improved significantly after V-KI treatment (Mann–Whitney U test, p<0.001), it was not correlated with improved motor function[Discussion]The TVR-induced sEMG signal originated from the stretch reflex arc. V-KI therapy may have affected stretch reflex gains, thereby affecting motor function. MAS and motor function were not correlated; however, the small sample size of this study compared with those of prior studies should be considered.TVR induction is straightforward and enables the investigation of neurological factors associated with the improvement of motor function. Thus, it is a clinically useful assessment in post-stroke patients.

O.17.6: Characteristics of electromyographic activity during yoga-applied lunge exercise

Kazuma Uebayashi, Suzuki Clinic Orthopaedic River City; Emi Motohashi, General incorporated association, Educate Movement Institute; Yu Okubo, Saitama Medical University; Kiyokazu Akasaka, Graduate School of Medicine, Saitama Medical University

Introduction: Benefits of yoga for lower back pain have been reported. (Anheyer D et al, 2022.) Yoga lunge exercises (YLE) involve similar trunk and arm movements as general lunge exercises (GLE) and are used to improve thoracic spine mobility and trunk stability. We aimed to compare the muscle activity associated with GLE and YLE to clarify characteristic muscle activity patterns during YLE. Methods: Fourteen healthy men with no previous yoga experience were recruited. They performed GLE including front and side lunge. They also performed YLE including front lunge with arm elevation, 3 types of twist YLE with trunk rotation to stepping side (twist lunge, twist lunge with praying hands, twist lunge with arm elevation), and 4 types of warrior YLE with trunk rotation to non-stepping side (warrior, warrior with trunk side bend,

warrior with arm elevation, and warrior with hand behind back) on both sides. Electromyographic (EMG) data was recorded for upper and lower trapezius (UT and LT), internal oblique (IO), Erector spinae, gluteus maximus, gluteus medius (Gmed), rectus femoris, and biceps femoris on the right side using surface electrodes. EMG activities were compared using Kruskal-Wallis tests between each exercise for each muscle. RESULTS: UT and LT activities were significantly higher with YLE than with GLE. Gmed (twist lunge: 24.0±8.3% MVIC, twist lunge with praying hands: 23.9±10.7% MVIC, twist lunge with arm elevation: 22.6±1.5% MVIC) and IO activity levels (twist lunge: 19.2±7.8% MVIC, twist lunge with praying hands: 15.2±6.5% MVIC, twist lunge with arm elevation: 18.0±11.1% MVIC) on stepping side during twist YLE were significantly higher than those recorded during GLE. On the non-stepping side, the %MVIC value of Gmed activities in the twist YLE (twist lunge with praying hands: 15.1±15.3% MVIC, twist lunge with arm elevation: 32.5±26.2% MVIC), and IO activities in the warrior YLE (warrior: 19.4±10.8% MVIC, warrior with trunk side bend: 14.2±6.7% MVIC, warrior with arm elevation: 20.0±13.8% MVIC, warrior with hand behind back: 22.5±11.1% MVIC) were significantly higher than that in GLE. Discussion ： UT and LT activities were increased by upper limb elevation in YLE. The twist YLE on the stepping side involves ipsilateral trunk rotation, which increased IO activity. Twist YLE also resulted in hip flexion and internal rotation on the step side, increasing Gmed muscle activity due to increased hip internal rotation moment arm in the hip flexor position (Neumann DA. 2010). The Gmed, a hip rotator, on the non-stepping side also showed higher activity during twist YLE including hip rotation with trunk rotation. Additionally, warrior YLE on the non-stepping side increased IO activity due to trunk lateral flexion against the forward center of gravity. Thus, YLE is a promising trapezius activating exercise. Twist YLE also activates bilateral Gmed and IO on the stepping side, and warrior YLE activates IO on the non-stepping side.

O.17.7: Influence of diaphragm and breathing on shoulder kinematics and associated muscle activity

Kuan-Yun Liu, College of Medicine, National Taiwan University, Taipei, Taiwan.; Hsing-Ni Lai, School and Graduate Institute of Physical Therapy, College of Medicine, National Taiwan University; Jing-Lan Yang, Department of Physical Medicine and Rehabilitation, National Taiwan University Hospital; Kwan-Hwa Lin, School and Graduate Institute of Physical Therapy, College of Medicine, National Taiwan University; Yung-Shen Tsai, Department of Physical Therapy, National Cheng Kung University, Tainan City, Taiwan, ROC; Jiu Jenq Lin, College of Medicine, National Taiwan University

Background: Diaphragmatic breathing training is widely used clinically. However, relationship between diaphragm function and shoulder pain is lack of evidence. Studies indicated that impaired diaphragm breathing function can increase activation of breathing accessory muscles. As these muscles are direct or indirect attached to shoulder girdle, they may affect the shoulder kinematics and muscle activities. Additionally, the diaphragm's role in postural stabilization might influence shoulder function. Further investigation is needed to know if diaphragm stabilization affects the shoulder kinematics and stability through kinetic chain. Purpose: (1) to characterize the kinematics, and muscle activations of the scapula in 3 breathing conditions during arm elevation task (2) to investigate the influence of diaphragm challenge on shoulder kinematics, and muscle activation during arm elevation in healthy adult. Methods: It's a cross-

sectional study. 30 healthy adults were recruited. Participants were assessed for maximal inspiratory pressure (PImax), diaphragm ultrasonography and core stability test, then the shoulder kinematics and associated muscle activation were collected during weighted arm elevation in three breathing conditions, including quiet breathing, breath-holding at the end of inspiration (Apnea-I) and breath-holding at the end of expiration (Apnea-E). After 30-minutes rest, the inspiratory resistance loading protocol was applied to challenge their diaphragm function. Then the shoulder kinematics and associated muscle activation during weighted arm elevation in quiet breathing were collected. Finally, the first three tests were assessed again. Statistical analysis: Two-way repeated ANOVA was used to compare shoulder kinematics and associated muscle activation among 3 breathing conditions as well as the effect of diaphragm challenge. Statistical analysis was calculated by SPSS 22.0 with significant level set as 0.005 after the Bonferroni correction. Results: Comparing Apnea-I to quiet breathing, there was significant increase in scapular upward rotation (1.2°-1.7°±9.84) and internal rotation (1.3°±4.83) as well as increased UT (0.5%±14.2) and SCM (1.0-1.2%±3.5) muscle activities. Conversely, Apnea-E condition showed significant decrease in scapular internal rotation (1.1-5°±6.04) along with increase SA (3.0-5.8%±13.61) and LT (4.5%±23.65) as well as decrease UT (1.9%±19.1) and SCM (0.4-0.8%±3.59) activities. In addition, increased scapular upward rotation (0.8-2.38°±6.37) was found after diaphragm challenge. Conclusion: The differences between Apnea-I and Apnea-E may be caused by rib cage diameter and thoracic movement. We suggest Apnea-E as a more effective strategy to maintain ideal scapula kinematics and muscular activities. Though increased scapular upward rotation was found after diaphragm challenge protocol, the clinical relevance of the effect of high intensity breathing training in scapular kinematics still requires further research.

Oral Award Session

Oral.Award.1: Site-specific assessment of the mechanical properties of each hamstring muscle in human cadavers using shear wave elastography

Gakuto Nakao, Sapporo Medical University; Taiki Kodesho, Japan Institute of Sports Sciences (JISS); Kazuma Yamagata, Sapporo Medical University; Kota Watanabe, Sapporo Medical University; Yuki Ohsaki, Sapporo Medical University; Masaki Katayose, Sapporo Medical University; Keigo Taniguchi, Sapporo Medical University

Background and Aim: Hamstring strain, primarily caused by increased tensile stress, frequently manifests in the proximal long head of the biceps femoris muscle (BF) and the proximal and distal semimembranosus muscle (SM). Recent elasticity measurements using ultrasonic shear wave elastography (SWE) have revealed that the mechanical stress that increases with elongation differs among various muscles and sites. However, the inter- and intramuscular regional disparities in mechanical stresses related to muscle elongation remain unclear. This study aimed to investigate whether the mechanical stresses associated with increased elongation differ among hamstring muscles and multiple sites within the muscle using a soft-embalmed Thiel cadaver. Methods: BF, Semitendinosus (ST), and SM muscles were dissected from eight cadavers. The proximal and distal hamstring tendons were affixed to a mechanical testing machine. Slack length (L) denoted the initial muscle length upon the application of a tensile load (P). Muscle length was measured using a tape measure, and the anatomical cross-

sectional area (ACSA) of the muscle was determined at two sites—the proximal (33%) and distal (67%) using B-mode ultrasonography. For the loading protocol, the muscle underwent elongation from its slack length to a maximum of 8% strain at a rate of 20 mm/min, and the amount of displacement (ΔL) and tensile load, as well as shear modulus, were measured for each muscle. Strain (%, ΔL/L) and stress (kPa, P/ACSA) were calculated to evaluate mechanical properties. The shear modulus was measured using SWE at the same sites as ACSA measurements. For data analysis, the shear modulus and stress relationship was compared between each tested muscle region and analyzed using a least-squares regression line. Three-way analysis of variance was used to compare the changes in shear modulus with increasing strain among muscles and sites. RESULTS: A linear correlation between the shear modulus and stress was evident for all the hamstring muscles in each region (P<0.01). The mean coefficient of determination (R2) for all muscles and sites was 0.98±0.02 (0.84–0.99). A significant interaction (muscle × site × strain) was observed in the shear modulus. Post-hoc tests revealed higher shear modulus in BF and SM than that in ST after 3% strain. Moreover, proximal BF exhibited higher values after 4% strain, whereas distal SM showed higher values after 6.5% strain compared with other sites within the same muscle (P <0.01). The average shear modulus at 8% strain, where the most substantial differences were observed, was ST (proximal: 26 kPa, distal: 25 kPa) compared with BF (proximal: 65 kPa, distal: 56 kPa) and SM (proximal: 44 kPa, distal: 58 kPa). CONCLUSIONS: The mechanical stresses applied to the three muscles at similar strains might be higher in the proximal BF and distal SM. Our findings indicate that elastic alterations in the proximal BF and distal SM during elongation elucidate the heightened incidence of muscle strain in these regions.

Oral.Award.2: Antagonism of 5-HT2 receptors attenuates self-sustained firing of human motor units

Benjamin Goodlich, Griffith University; Greg Pearcey, Memorial University of Newfoundland; Alessandro Del Vecchio, Friedrich-Alexander Universität, Erlangen-Nürnberg; Sean Horan, Griffith University; Justin Kavanagh, Griffith University

Activation of 5-HT2 receptors on motoneurones play a critical role in facilitating persistent inward currents (PICs). Although facilitation of PICs can enhance self-sustained firing after brief periods of excitatory input to motoneurones, the relationship between 5-HT2 receptor activity and self-sustained firing in human motor units (MUs) has not been resolved. Therefore, this study examined how 5-HT2 receptor activity contributes to self-sustained firing of MUs in humans. MU activity was assessed from tibialis anterior in 10 healthy adults (24.9 ± 2.8 yr) during two contraction protocols. Both protocols featured steady-state isometric contractions with constant descending drive to the motoneuron pool, however one protocol also included an additional phase of superimposed descending drive during the steady-state contraction. Adding and then removing descending drive in the middle of steady-state contractions altered the MU discharge behaviour across the motor pool, where newly recruited units in the superimposed phase were unable to switch off due to their self-sustained firing (P = 0.0002), and units recruited prior to the additional descending drive reduced their discharge rates (P < 0.0001, difference in EMM (Δ) = 2.24 pulses/s). The 5-HT2 receptor antagonist, cyproheptadine, was then administered to determine if changes in MU discharge behaviour were mediated by serotonergic mechanisms. 5-HT2 receptor antagonism caused reductions in MU discharge rate (P < 0.001, Δ = 1.65 pulses/s), recruitment threshold (P = 0.00112, Δ = 1.09% MVC), and self-

sustained firing duration (P < 0.0001, Δ = 1.77s) after the additional descending drive was removed in the middle of the steady-state contraction. These findings indicate that serotonergic neuromodulation plays a key role in facilitating MU discharge and self-sustained firing of human motoneurones, where adaptative changes in MU recruitment must occur to meet the demands of the contraction.

Oral.Award.3: Neuroplastic alterations in common synaptic inputs and synergistic motor unit clusters controlling the vastii muscles of individuals with ACL reconstruction

Stefano Nuccio, University of Rome "Foro Italico"; Carina Germer, Universidade Estadual de Campinas; Andrea Casolo, University of Padua; Riccardo Borzuola, University of Rome "Foro Italico"; Luciana Labanca, Physical Medicine and Rehabilitation Unit, IRCSS – Istituto Ortopedico Rizzoli, Bologna, Italy.; Jacopo Emanuele Rocchi, Villa Stuart Sport Clinic – FIFA Medical Centre of Excellence, Rome, Italy; Pier Paolo Mariani, Villa Stuart Sports Clinic - FIFA Medical Centre of Excellence; Francesco Felici, University of Rome, Foro Italico; Dario Farina, Imperial College London; Deborah Falla, University of Birmingham

Background. Restoration of knee extension strength and control is a priority for the rehabilitation process after anterior cruciate ligament reconstruction (ACLR). This emphasis is due to the fact that, despite extensive rehabilitation, persistent quadriceps dysfunction is common post-ACLR, leading to severe consequences such as an increased risk of reinjury and knee osteoarthritis.1 Volitional force modulation is primarily governed by common synaptic inputs (CSIs) that are shared across motor neurons. Recent evidence has shown that, rather than projecting only to muscle-specific pools of motor units (MUs), CSIs are distributed across functional clusters of MUs that can change plastically to provide a flexible control of motor output.2-3Aim. This cross-sectional study aims to elucidate the neural strategies adopted by the central nervous system to coordinate the activation of vastus lateralis (VL) and vastus medialis (VM) muscles for the control of knee extension forces in individuals with ACLR. Methods. Eleven soccer players with ACLR (age: 24.8 ± 3 years; BMI: 23.3 ± 0.6 kg*m-2) and nine control players (age: 25.7 ± 2.5 years; BMI: 22.9 ± 0.5 kg*m-2) performed unilateral isometric steady knee extensions at 10% and 30% of their maximum voluntary force. Simultaneous recordings of high-density surface electromyography and force output were conducted to examine the discharge properties of VL and VM MUs and to estimate the CSI delivered to each muscle through intramuscular coherence analyses. A factorization analysis was adopted to investigate the neural strategies underlying the control of synergistic clusters of MUs. Results. MUs identified in the VL of the reconstructed side exhibited lower magnitude and proportion of CSI at low-frequency bandwidths (< 5 Hz), compared to those governing the VL in unaffected lower limbs (P < 0.05). Furthermore, the reconstructed side demonstrated a higher proportion of MUs identified in the VM muscle that were correlated with the neural input common to the synergistic VL muscle, compared to unaffected lower limbs (P < 0.01). CONCLUSIONS. The lower magnitude and proportion of CSI projecting to motor neurons of the VL muscle suggest an increased contribution of independent synaptic inputs to force control in the reconstructed side, compared to unaffected lower limbs. Additionally, the output of the factorization analysis indicated a plastic rearrangement in the neural input for the synergistic activation of VL and VM clusters of MUs that control knee extension forces in the reconstructed side. Further studies are needed to confirm and extend our findings. A comprehensive understanding of these neural adaptations could aid in designing targeted neurological

rehabilitation approaches, often neglected in clinical practice.References1. Buckthorpe et al. Int J Sports Phys Ther. 2019;14(1): 159. 2. Del Vecchio et al. J Neurosci. 2023;43(16): 2860-2863. 3. Hug et al. J Physiol. 2023;601(1): 11-20.

Oral.Award.4: Motor unit activity and muscle contractile properties during rapid contractions in long-term resistance trained and untrained individuals

Haydn Thomason, Loughborough University; Jonathan P Folland, Loughborough University; Jakob Škarabot, Loughborough University

Background and Aim: Maximal rate of force development (RFD) is determined by neural (motor unit [MU] recruitment speed and discharge rate) and muscular properties. Though resistance trained (RT) individuals typically exhibit greater absolute RFD, the findings are equivocal regarding relative RFD (i.e., normalised to maximal voluntary force [MVF]), with studies reporting greater, similar, or even lower relative RFD in RT individuals. Nevertheless, chronic resistance training may confer neural adaptations including greater spinal cord output in RT compared to untrained individuals (UT), that facilitates faster RFD. Here, we assessed MU discharge characteristics and intrinsic muscle contractile properties within RT and UT individuals during maximal rapid contractions. Methods: Twenty-two RT and 22 UT (6 females per group) individuals produced maximal and rapid voluntary isometric dorsiflexion force (up to ~80% of MVF), to determine MVF and RFD (maximal slope of the force-time curve from force onset), respectively. Percutaneous nerve stimulation (25 pulses at 100 Hz and 8 pulses at 300 Hz) was administered to the common peroneal nerve at rest to record maximal evoked force (MEF) and RFD. A 64-channel grid electrode was placed on the tibialis anterior muscle of the dominant leg to assess myoelectrical activity (EMG). The EMG signals were decomposed into individual MU spike trains using Convolution Kernel Compensation algorithm. Discharge rate in the initial (first five spikes) and plateau period (20 spikes) of rapid contractions, and recruitment speed of the identified MUs were calculated. RESULTS: MVF and MEF were significantly larger in RT (393 [337, 449] N and 245 [212, 278] N) compared to UT (296 [260, 331] N, p=0.014, and 174 [151, 198] N; p<0.001), respectively. Greater absolute RFD was observed in RT compared to UT during voluntary (1792 [1550, 2035] vs 1307 [1064, 1550] N/s; p=0.007) and evoked (2001 [1751, 2252] vs 1492 [1247, 1736] N/s; p=0.005) contractions. However, when normalised to MVF, there were no differences between groups for either voluntary (454 [429, 480] vs 420 [394, 445]%MVF/s, p=0.056) or evoked RFD (513 [447, 579] vs 493 [429, 557]%MVF/s, p=0.665). Compared to UT, RT exhibited greater discharge rate in the initial period of rapid contractions (73 [68, 79] vs 65 [59, 71] pps; p=0.022), but not during the contraction plateau (31 [28, 34] vs 28 [26, 31] pps; p=0.176). Both groups displayed similar MU recruitment speed (302 [203, 401] vs 281 [170, 392] MU/ms; p=0.767). Conclusion: RT individuals exhibited greater maximal strength and absolute RFD. However, despite greater initial MU discharge rate, relative RFD was similar between groups. The lack of differences in relative RFD likely stems from between-group similarity in intrinsic contractile properties and MU recruitment speed, two key determinants of maximal RFD.

Oral.Award.5: Ischaemic block of large-diameter axons increases motor unit discharge rate non-linearity and hysteresis

Nikki Bonett, Loughborough University; Tamara Valenčič, Loughborough University; Christopher Connelly, Loughborough University; Haydn Thomason, Loughborough University; Greg Pearcey, Memorial University of Newfoundland; Jakob Škarabot, Loughborough University

Background and Aim: Persistent inward currents (PICs) provide gain control of motoneuron output and are influenced by both diffuse neuromodulation and local inhibitory inputs. However, if feedback from large diameter axons is lost, as is the case in some neurological impairments, amplification and prolongation of synaptic inputs by PICs is likely to be facilitated. Here, we tested the hypothesis that reduced Ia afferent transmission from lower limb muscles would increase tibialis anterior (TA) motor unit (MU) discharge rate hysteresis and result in greater non-linearity of MU discharge patterns, indicating a greater contribution of PICs to MU discharge. Methods: 10 neurologically intact adults (4 female) performed triangular shaped isometric dorsiflexion to 30% of maximum voluntary force (MVF) at the beginning of the experiment (PRE1), and after 20 minutes of rest (PRE2; control condition). A sphygmomanometer cuff was then inflated to 200 mmHg just above the knee to induce an ischaemic nerve block. Soleus H-reflex was monitored every 2 mins to assess when Ia afferent transmission was abolished (<10% original value; 15±4 mins per participant) after which the triangular contractions were repeated whilst the participant's leg remained occluded (POST condition). Myoelectrical (EMG) activity of the TA was measured using a 64-electrode array and EMG signals were decomposed into individual MU spike trains using a Convolution Kernel Compensation algorithm. From smoothed MU discharges (support vector regression), discharge rate hysteresis (ΔF) and non-linearity in the ascending modulation of MU discharge rate (brace height) were quantified. RESULTS: Occlusion did not affect maximal M-wave (Mmax; 4.37 [3.41, 5.33] vs 4.76 [3.81, 5.71] mV; p=0.092), whereas H-reflex was lower at POST compared to pre-occlusion (3.21 [-6.21, 12.60] vs 42.08 [32.66, 51.50] %Mmax; p<0.001), indicating reduced Ia afferent input. Peak discharge rate at POST (28.3 [24.8, 31.7] pps) was greater compared to PRE1 (19.8 [16.3, 23.3], p<0.001) and PRE2 (20.9 [17.4, 24.4], p<0.001), with no differences between PRE1 and PRE2 (p=0.199). Discharge rate hysteresis at POST (5.14 [4.11, 6.18] pps) was greater than at PRE1 (4.65 [3.61, 5.68] pps, p=0.038) and PRE2 (4.55 [3.52, 5.58] pps, p=0.007), with no differences between PRE1 and PRE2 (p=0.869). Brace height, indicating the extent of non-linearity during the ascending discharge rate modulation, was greater at POST (39.8 [35.0, 44.7]%) than at PRE1 (32.5 [27.9, 37.1]%, p<0.001). CONCLUSION: : An ischaemic block of large-diameter axons led to greater MU discharge rate hysteresis, and more non-linear discharge patterns, suggesting increased PIC contribution to discharge rate modulation in conditions of reduced inhibitory input. These findings provide insight into the role of Ia afferent input on MU discharge patterns and offer a possible explanation for spasticity in some neurological impairments.

Oral.Award.6: The neuromuscular control of the shoulder muscles in healthy individuals: a TMS study

Yuyao Ma, The University of Queensland

Introduction: Coordination between the shoulder muscles is critical to maintain dynamic stability of the glenohumeral joint. This involves coactivation of the rotator cuff muscles to control glenohumeral translation and rotation during shoulder movements, e.g., activation of the rotator cuff such as subscapularis (SS) to control cranial glenohumeral translation when the

middle deltoid (MD) abducts the shoulder. How this coordination is controlled by the motor cortex is poorly understood. Emerging evidence has proposed the concept of "functional somatotopy" of the primary motor cortex (M1), indicating its role in coding task-specific motor strategies. It is suggested that individual muscles are controlled by multiple brain regions that might each serve different functions, and that multiple muscles involved in a task are controlled by a common region. Based on this proposal we hypothesized that: 1) cortical representation of MD (and SS) would differ when the muscle performs different tasks, 2) the representation of MD and SS would overlap when are active in the same task, and 3) the representation would have little overlap when MD and SS are active in different tasks. Methods: The left-side motor cortex representations of MD and SS were mapped with transcranial magnetic stimulation (TMS) in seven right-handed healthy adults. MD and SS electromyography (EMG) was recorded with intramuscular electrodes. In separate trials, participants performed isometric shoulder abduction (ABD) and internal rotation (IR) in 90° abduction at 2% of maximal voluntary contraction. We identified the hotspot and active motor threshold (aMT) for each muscle. Using rapid TMS mapping we generated maps for MD or SS during ABD or IR. For each of the 4 maps, ~100 stimuli were delivered pseudorandomly over a 6x7cm grid at 120% aMT of the target muscle. After map interpolation, we calculated 1) area of map with intensity above 60% the peak amplitude for each map, 2) the area of overlap between the maps (as a proportion of summed total area) of MD or SS during ABD and IR (same muscle different tasks), MD and SS during ABD (different muscles same task) and MD during ABD and SS during IR (different muscles different tasks). RESULTS: Figure 1 shows data for a representative participant. Preliminary analysis shows that: 1) the cortical representation for each muscle differs between tasks – MD 87(10)% and SS 80(15)% of the total map area did not overlap between tasks; 2) the cortical representations of MD and SS overlap when they are both active in ABD (9(7)%); and there is little overlap between cortical maps for MD in ABD and SS in IR (6(4)%). Discussion: These preliminary results suggest that the cortical representation for a muscle differs based on the task being performed (some overlap, but with a majority non-overlapping), the maps of two muscles overlap when they are both active in a single task, and the maps of two muscle have limited overlap when performing different tasks.

Poster Session 1

P1.1-A: Changes in mid-thigh muscle and adipose tissue cross sectional areas in older people: a seven years study

Kosuke Kano, The University of Electro-Communications; Rie Tomiga, Fukuoka University; Mizuki Sudo, Meiji Yasuda Life Foundation of Health and Welfare; Yujiro Kose, National Institute of Fitness and Sports in Kanoya; Yasuki Higaki, Fukuoka University; Yoichi Hatamoto, National Institute of Biomedical Innovation, Health and Nutrition; Soichi Ando, The University of Electro-Communications; Hiroaki Tanaka, Fukuoka University

Introduction: Aging is defined as a gradual decline in physical capacity, which results in a progressive decline in the performance of multiple organs. It has been suggested that habitual exercise prevents muscle mass reductions in older people. However, it is less clear how once-a-week exercise influences mid-thigh muscle mass and adipose tissue in older people. The purpose of this study was to examine the changes in mid-thigh muscle and adipose tissue cross sectional areas (CSAs) in community-dwelling older people.Method: The present cohort study (Fukuoka Island City Study: UMIN Clinical Trials Registry, registration number: 000036659) was conducted in 2015, 2017, 2018, and 2022. We used data from 20 participants (14 females, age: 70.3 ± 7.5 yr., height: 153.9 ± 8.2 cm, weight: 52.4 ± 11.1 kg, at the initial measurement) who completed all four measurements. The participants joined exercise class once a week. Quadriceps muscle and adipose tissue CSAs at the mid-thigh (50% of the femur) region were collected using magnetic resonance imaging (MRI). Muscle and intramuscular, intermuscular, and subcutaneous adipose tissue CSAs were analyzed using the sliceOmatic program (Tomovision, Montreal, Canada). We performed a repeated measures correlation analysis to examine the relationship between age and muscle/adipose tissue CSAs. RESULTS: Repeated measures correlations revealed that the quadriceps muscle CSA (r = -0.623, confidence interval (CI) [-0.756, -0.440], p < 0.001) was negatively correlated with age. This indicates that muscle CSA decreased as a function of age. There were no significant correlations between age and intramuscular (r = 0.216, CI [-0.037, -0.444], p = 0.094), intermuscular (r = 0.180, CI [-0.075, 0.413], p = 0.165), subcutaneous (r = 0.121, CI [-0.135, 0.362], p = 0.353) adipose tissue CSAs. However, when expressed relative to muscle CSA, intramuscular adipose tissue CSA was positively correlated with age (r = 0.302, CI [0.054, 0.514], p = 0.018). CONCLUSION: : The present findings suggest that once-a-week exercise did not prevent muscle atrophy in older people. Aging appears to affect mid-thigh muscle and intramuscular, intermuscular, and subcutaneous adipose tissue in a different manner.

P1.2-A: Novel approach to highlight differences in balance control in young and older adults

Mateus Souza Silva, Federal University of Bahia; Jeanfrancois Daneault, Rutgers University; Nathan Wages, Rutgers University; Jose Garcia Vivas Miranda, Federal University of Bahia

INTRODUCTION: Balance is a complex perceptual-motor capacity that relies on multiple systems and, as these systems undergo gradual declines related to aging, it makes it more

difficult to maintain balance. It is imperative to identify and characterize important features associated with this decline in balance control to develop targeted interventions. Understanding both linear and nonlinear dynamics is key to fully characterizing postural control. Linear measures like sway path length and range assume balance operates through proportional, predictable responses to perturbations. However, balance is adaptive and complex, involving nonlinear interactions between sensory systems, muscles, limbs, and the environment. Small changes in one element can lead to large unpredictable effects overall. Nonlinear analysis can capture this complex variability in postural sway patterns over time, while linear approaches cannot. Here, we examine the control of balance of young and older adults during both simple and dual tasks using a method developed by our group that provides insights into nonlinear dynamics of human movement. The method uses simple algorithms to decompose movements into one-dimensional sub-movements within a Cartesian coordinate system. Methods: We recruited 22 healthy young adults (23.4±5.6 years) and 23 healthy older adults (64.04±7.18 years). Anteroposterior and mediolateral movements were captured from an overhead camera during a simple bipedal standing task, with and without the simultaneous performance of a cognitive task (listing words starting with a specific letter). Each participant performed a total of X trials of 30s. Movement data was extracted from the video and segmented into the sub-movements. Several features of those sub-movements were then compared statistically between groups and tasks. RESULTS: The proportion of sub-movements that matched the theoretical model (homogeneous set) varied across groups and tasks. The average percentage (±SD) of sub-movements included in the homogeneous set was 46.0±6.0% and 44.4±8.0% for the young group during the simple and dual tasks, respectively. For the older group the distribution was 50.3±7.8% and 43.2±6.7% for the simple and dual tasks, respectively. A two-way mixed model ANOVA showed that the percentage of sub-movements in the homogeneous set was statistically larger for the simple task than for the dual task when groups were pooled ($p=0.005$) but that there was no difference between groups when both tasks were pooled ($p=0.306$). There was also a statistically greater percentage of sub-movements in the homogeneous set during the simple task than in the dual task in the older group ($p=0.008$). Additionally, specific features, including the number of sub-movements and the nonlinear factor between velocity and displacement, were significantly different between groups.DISCUSSION: These results highlight that both linear and nonlinear approaches to the evaluation of balance are important as they provide complementary information and nonlinear metrics were the most sensitive to changes in balance. Furthermore, our results show that the complexity of balance increases during the dual task, especially in the older group, highlighting the impact of the task on underlying control structures. Future work will focus on identifying how these linear and nonlinear features respond to interventions and if we can use those to personalize treatments.

P1.3-A: Comparison of differences in arterial stiffness gradient according to the degree of unilateral arm exercise participation

Do-Yeop Kim, Incheon National University; Ruda Lee, University of Iowa; Moon-Hyon Hwang, Incheon National University

Comparison of differences in arterial stiffness gradient according to the degree of unilateral arm exercise participationDo-Yeop Kim, Ruda Lee, Moon-Hyon HwangINTRODUCTIONPulse wave velocity (PWV), a validated measure of arterial stiffness, is a clinical indicator to evaluate cardiovascular disease risk. Arterial stiffness gradient, a novel marker of cardiovascular morbidity and mortality, is the ratio of central (aortic or carotid to femoral, cf) PWV to peripheral (arm or leg) PWV. Regular physical activity reduces central arterial stiffness in various populations including chronic cardiometabolic disease patients. But its effect on peripheral PWV is still controversial. In addition, there are a handful of studies to investigate alterations in peripheral PWV in response to unilateral exercise. Therefore, the purpose of this study was to compare the differences in arterial stiffness gradient according to the degree of unilateral arm exercise participation.METHODTwenty-six young women participated in this study; eight elite-level badminton players (ELIT), ten club-level badminton players (CLUB), and eight age-matched sedentary participants (CONT). Carotid-femoral PWV (cfPWV) as the central stiffness was measured using SphygmoCor Xcel system. Brachial-radial PWV (armPWV) as the peripheral stiffness was measured using Doppler Flowmeters and the associated data was collected and analyzed by PowerLab data acquisition system including Labchart Pro V8 software. Arterial stiffness gradient was calculated as the ratio of cfPWV to armPWV at both dominant and non-dominant arm, respectively. RESULTSIn the dominant arm, the arterial stiffness gradient of ELIT and CLUB were significantly higher than CONT (0.73 vs. 0.46, ELIT vs. CONT, P<0.001; 0.59 vs. 0.46, CLUB vs. CONT, P=0.04). The arterial stiffness gradient of ELIT was also significantly higher than CLUB (0.73 vs. 0.59, ELIT vs. CLUB, P=0.03).In the non-dominant arm, the arterial stiffness Gradient of ELIT was significantly higher than CONT (ELIT: 0.59 vs. CON: 0.44 P= 0.007), but there was no significant difference between ELIT and CLUB, and CLUB and CONT (0.00 vs. 0.00, ELIT vs. CLUB, P=...; 0.53 vs. 0.44, CLUB vs. CONT, P=0.09). CONCLUSION: The more unilateral arm exercise accumulated in the dominant arm, the higher the arterial stiffness gradient. The transfer effect of training regarding arterial stiffness gradient is only seen in the ELIT. In active young adults, increased arterial stiffness gradient may be associated with reduced cardiovascular disease risk.

P1.4-B: Sign language recognition system based on multi-channel surface electromyography

Yuanxi Wang, Tokyo Institute of Technology; Yasuharu Koike, Tokyo Institute of Technology

This study introduces a novel Sign Language Recognition (SLR) system based on Surface Electromyography (sEMG) signals, designed to address the communication barriers faced by approximately 466 million people worldwide with hearing loss. Traditional SLR methods, mainly camera-based, face limitations such as dependence on lighting conditions, restricted detection range, and computational expense. Sensor-integrated gloves also present the inconvenience of usage.The sEMG sensors can overcome these problems, offering a more versatile and user-friendly approach. Wearable device is one of the current trend and focus of technology. Such sEMG-based devices can be utilized in many applications, including sign language recognition systems, gesture recognition, and prosthesis control.The primary objective of this research is to develop a sign language recognition system using a 32-channel EMG sensor, capable of estimating surface and deeper muscle activities through Independent Component Analysis

(ICA). This system aims to accurately identify several alphabets and gestures from American Sign Language (ASL).Methodologically, the research involves data collection using a 32-channel electrode sleeve for EMG signals from participants performing sign language gestures. The preprocessing of this data involves filtering raw EMG signals to eliminate noise and artifacts, followed by ICA to extract a few components, allowing for the differentiation of surface and deeper muscle activities. The IC components with noise were removed, and the remaining clean components were used to reconstruct the original signal. The reconstructed signal was then rectified and processed with a lowpass filter to acquire the envelope. These preprocessing methods aim to remove noise and minimize input signals.Four features were calculated from the processed IC components, including root mean square, variance, integrated EMG, and mean absolute value. For the classification process, features were input into a Support Vector Machine (SVM) classifier, and five-fold cross-validation was performed to check the accuracy. With five stationary American Sign Language gestures, the SVM classifier achieved 96.6% accuracy on the raw EMG signal, and the accuracy improved to the highest 98.4% with the processed signal.

P1.6-C: Comparing of lower limbs kinematics between 3D motion analysis and Inertial measurement unit during countermovement jump in healthy adults

Chuanpis Boonkerd, Thammasat University

Background: Jumping is a crucial sporting skill that provides valuable information for treatment and rehabilitation assessments. Inertial measurement units (IMUs) have emerged as an alternative tool for evaluating joint kinematics during movement analysis. However, comparative data supporting the use of IMUs during countermovement jumps (CMJs) is lacking.Objective: To compare lower limb kinematics between 3D motion analysis and IMU during CMJs in healthy adults. Methods: Thirteen healthy individuals (9 males, 4 females; age 21.85 ± 0.66 years) participated in the study. Kinematic data were collected using 16 retroreflective markers and eight IMU sensors attached to anatomical landmarks according to the lower limb Plug-in gait model. Participants performed three CMJs while kinematic data were recorded using 3D motion analysis and IMU systems. Paired t-tests were employed to compare peak ankle, hip, and knee joint angles between the two measurement methods. Bland-Altman plots were used to assess the agreement between the two methods. RESULTS: No statistically significant differences were observed in peak hip, knee, and ankle angles (p > 0.05) between the two measurement methods, except for left hip abduction/adduction, right knee abduction/adduction, and both ankle dorsiflexion/plantarflexion angles (p < 0.05). Of the total measurements conducted between the two methods, 100% (1/19) of hip motion measurements fell within the limits of agreement, while 7.6% (1/13) of knee and ankle motion measurements did not fall within the limits of agreement. CONCLUSION: : This study suggests that IMUs provide acceptable agreement with 3D motion analysis for assessing kinematics during CMJs. Further research is warranted to validate these findings in larger and more diverse populations.

P1.8-C: Role of the upper trapezius muscle on clavicular kinematics: an exploratory study

Chunkai Tang, National Yang Ming Chiao Tung University; Yi Fen Shih, Department of Physical Therapy and Assistive Technology, National Yang Ming Chiao Tung University

Background: The role of upper trapezius (UT) muscle in scapular kinematics demonstrated inconsistent findings in previous studies. One possible reason for the conflicts might arise from the influence of clavicular movement. The purposes of this study were firstly to establish the measurement reliability of clavicular kinematics, and secondly to explore the effect of the UT stimulation on clavicular kinematics. Methods: Eleven asymptomatic healthy adults between 20-30 y/o were recruited. Three-dimensional scapular and clavicular kinematics were collected using the Polhemus Liberty electromagnetic tracking system with the clavicular mini-sensor (CS) and the scapular sensor (SS). Scapular and clavicular kinematics were recorded with the subject's arm rest by side, and at scaption angles of 120, 90, 60, 30 degrees while the neuromuscular stimulation (NMES) of the UT was delivered. The NMES intensity was the maximal intensity that produced UT activation without activating the levator scapulae based on the real-time musculoskeletal ultrasonography. The between-day measurement reliability of clavicular kinematics was assessed using the intraclass correlation coefficients (ICC3,2). Paired t-tests were used to compare kinematics before and after ES. RESULTS: Our results showed that the test-retest reliability coefficients of measuring clavicular kinematics were similar for CS and SS (CS: 0.62-0.91, SS: 0.63-0.98) with smaller standard errors of measurements (CS: 0.59-5.23, SS: 0.48-7.08) and minimal detectable changes (CS: 1.07-3.2, 0.97-3.73) for CS. With CS, smaller clavicular elevation (CS: -3.38±4.54 to -6.31±6.66, SS: 0.14±9.64 to -8.77±11.38) and retraction (CS: -21.13±6.72 to -35.59±10.5, SS: -22.22±6.51 to -15±15.48) were observed during arm elevation, which was similar to data reported previously using the bone-pin sensor. NMES of the UT resulted in significant clavicular retraction at scaption 0, 30 and 60 degrees and posterior rotation at 30, 60, and 120 degree (p<0.05), and scapular upward rotation at 0, 30, and 60-degree of scaption (p<0.05). CONCLUSIONS: Using a clavicular sensor to record clavicular kinematics is recommended for it was a reliable and had smaller measuring errors when compared with the scapular sensor. Activation of the upper trapezius produced scapular and clavicular movement under 60 degrees of scaption; but only produced clavicular movement up to 120 degrees of scaption.

P1.9-C: Robot-assisted weight relief for prevention of musculoskeletal pain among bronchoscopists

Pernille Knudsen, Odense University Hospital; Rikke Jepsen, University of Southern Denmark; Anders Sørensen, University of Southern Denmark; Amanda Juul, Odense University Hospital; Jeppe Andersen, University of Southern Denmark; Malte Deleuran, Odense University Hospital; Tina Dalager, University of Southern Denmark; Karen Søgaard, University of Southern Denmark

IntroductionMusculoskeletal disorders (MSDs) are a common challenge among endoscopists due to prolonged awkward postures during procedures [1]. A study involving clinicians performning pulmonary endoscopic procedures, specifically bronchoscopists, revealed that 50.6% of survey respondents reported musculoskeletal pain [2]. Among endoscopists, the most severe regions of pain reported are the back, neck, and shoulders [2, 3]. This study investigated the effects of a robotic weight relief system for alleviating the physician’s arm during simulated bronchoscopy to reduce MSDs. METHODSSix experienced bronchoscopists from the

Department of Respiratory Medicine at Odense University Hospital participated in the study using a repeated-measures design. They each conducted two 40-minutes bronchoscopies on a GI-BRONCH Mentor endoscopy simulator, one conventional procedure and one using the robotic weight relief system, which was attached to the arm holding the bronchoscope. Bipolar surface electromyography (EMG) recordings were collected from the forearm and shoulder, and an Amplitude Probability Distribution Function (APDF) was calculated to find the static (10), median (50), and peak (90) levels of muscle activity. Changes in arm movement patterns were investigated using accelerometer data. Results and discussionThe APDF indicated increased forearm muscle activity during the weight-relieved bronchoscopy compared to the conventional procedure (see Table). This increase in muscle activity was likely due to the attachment of the robotic system to the wrist, requiring the subject to make ulnar deviation to maintain a stable and vertical position of the scope. For the shoulder, the APDF showed reduced muscle activity when performing the weight-relieved bronchoscopy, with statistical significance observed for the peak level for anterior deltoid and the static level for medial deltoid (see Table). Overall, the EMG analysis indicated that the robotic system was more demanding on the forearm and less demanding on the shoulder compared to the conventional procedure.The study found an average increase in arm elevation angle of 5.9 degrees during the weight-relieved bronchoscopy. This increase along with the decrease in shoulder muscle activity suggests that the robotic system may be effective in preventing MSDs in procedures that require elevated arm positions and allow for better flexibility and variation without increasing the shoulder load. ConclusionThe decrease in shoulder muscle activity along along with the changes in arm movement pattern indicated a positive impact of the robotic system. This provides an incentive for further development of the system to improve its effectiveness in reducing musculoskeletal pain among bronchoscopists.ReferencesKamani L, Kalwar H, Clin Endosc 54(3): 356-362, 2021 Gilbert CR, et al., J Bronchology Interv Pulmonol 20(2): 113-20, 2013Yung DE, et al., Expert Rev Gastroenterol Hepatol 11(10): 939-947, 2017

P1.10-C: The laterality of the postural stability and the shock attenuation on legs: a comparison of dancers and non-dancers

Tomoha Ogawa, Ochanomizu University; Mayumi Kuno-Mizumura, Ochanomizu University

PurposeA number of studies have been done regarding postural stability and the shock attenuation ability in dancers because of their superior skills to non-dancers. However, the effect of dance experience on the laterality of these abilities between legs is still controversial. Therefore, this study aims to identify whether the dance experience affects the lateral bias by using questionnaires and kinetic measurements.MethodThirty-two Japanese female university students participated in this study. They were divided into two groups according to their dance experience regardless of the genre: a dancer group (D) with more than 5 years of dance experience and continuing that at least once a week (n=15) and a non-dancer group (ND) with less than 5 years of experience (n=17). They were asked to answer the Japanese version of the Waterloo Footedness Questionnaire (WFQ-R) (Elias et al., 1998) to evaluate their foot preference with numerical values from -20 to 20. After that, they performed a single-leg stance and single-legged drop landings on a force plate (frequency of 1000 Hz) under three conditions: eyes-open, eyes-open with a mirror and eyes-closed (not for the drop landing). Then, the center

of pressure (COP) and the ground reaction force (GRF) were used for calculating the sum of COP displacement, the rectangular area of COP, the peak vertical GRF, the time to stabilization (TTS) (Scott et al., 1999) and the shock attenuation ability. The laterality ratio (LR score) was generated by dividing data from the left leg by data from the right leg. Then, the LR score was compared between two groups and among three conditions. Results and DiscussionThere were no differences in the result of the WFQ-R between groups, resulting in the dance experience did not influence foot preference. For the force plate experiments, the shock attenuation ability under the eyes-open condition showed a difference in the LR score between groups ($p=0.044$); specifically, group ND tended to have left-leg dominance, whereas group D was equal or right-leg dominance. However, no other significant difference was observed between groups or among conditions. Therefore, it might indicate that the dance experience influences the shock attenuation ability but not the postural stability, which contradicts previous studies. Based on this, the influence of dance experience on postural stability might be applied only to professional or pre-professional ballet dancers. CONCLUSION: In this study, the difference in the laterality between groups was observed in the shock attenuation ability, meaning that might be an element that the dance experiences across genres and training levels have influences on. In contrast, the effect on the postural stability might vary depending on the dance genre or intensity of the training. Further research on these skills in dancers would contribute to the usage of dance in clinical settings.

P1.12-E: The persistence of F-wave does not change with stimulus intensity from submaximal to supramaximal stimulation, but the shape of the F-wave waveform is completely different

Toshiaki Suzuki, Graduate School of Kansai University of Health Sciences; 真理奈 東藤, Graduated School of Kansai University of Health Sciences; Yuki Fukumoto, Graduated School of Kansai University of Health Sciences; Makiko Tani, Graduated School of Kansai University of Health Sciences; Naoki Kado, Kobe College of Rehabilitation and Health; Fumiaki Okada, Senreikai Harima Hospital; Masaaki Hanaoka, Graduate School of Medicine, Shinshu University

IntroductionF waves are one of the indicators of spinal cord anterior horn cell excitability, and the test of F wave is somewhat painful for subjects because it involves electrical stimulation of the alpha motor nerve with supramaximal stimulation. Therefore, we investigated whether it is possible to obtain results similar to those of the usual F wave test by decreasing the stimulation intensity. Stimulus intensity was 90-120% of the intensity at which the maximum amplitude of the M wave is obtained. In order to examine the reproducibility of the F wave data for each stimulus intensity, these trials were performed five times with an interval of at least one day, and the variability of the results was examined. As a result, no obvious changes in the persistence of F wave. In the present study, we limited the stimulus intensity to 90-120% and examined the persistence of the repeater F wave using F wave waveform analysis software developed by Hanaoka et al. MethodsF wave was recorded from the abductor pollicis brevis muscle during median nerve stimulation in five healthy subjects. For stimulus conditions of median nerve stimulation, frequency was 1 Hz, duration 0.2 ms, and number of times of stimulation 64 times. The stimulation intensity was 90 to 120% of intensity at which the maximum amplitude of M wave was obtained, and F wave was recorded 4 times at 10% intervals. For recording

conditions, the probe electrode was placed on the belly of the left abductor pollicis brevis muscle, reference electrode on the left basal phalanx of the left thumb, and the ground electrode at the center of the palmar side of the left forearm. F wave analysis items were the persistence of F wave and repeater F wave, and types of repeater F wave in all 5 trials of stimulation using F-wave waveform analysis software developed by Hanaoka et al. The coefficient of variation of F-wave data with the different stimulus intensity was obtained. We also examined whether repeater F waves appeared on different days at same intensity. This study was approved the Research Ethics Committee at Kansai University of Health Sciences (Approval No. 21-06). RESULTSThe variation in persistence of the F-wave with changes in stimulus intensity had a coefficient of variation of less than 0.08. The coefficient of variation of the frequency and types of repeater F wave with changes in stimulus intensity was 0.25 in one subject, while the coefficient of variation was greater than 0.6 in the four subjects. Repeater F waves appeared between trials with different testing dates in 3 subjects for 90% stimulation and in only 1 subject for 120% stimulation. No repeater F waves appeared with different testing date for 100% and 110% stimulation. DiscussionIn this study, we examined five trials of F waves with varying stimulus intensity from 90% to 120% on different days. Persistence of F wave was similar with varying stimulus intensity, but the frequency and types of repeater F wave differed significantly. From the result in this study, the excitability of anterior horn cells in the spinal cord was similar, but types of anterior horn cells to make up F wave was different with changes in stimulus intensity. And the type of spinal cord anterior horn cells to make up the F wave with the same stimulus intensity may result in completely different on different inspection dates.

P1.13-E: A comparison of techniques to determine active motor threshold from lower limb transcranial magnetic stimulation (TMS)

Jonathan Beausejour, University of Central Florida; Matt Stock, University of Central Florida; Jason DeFreitas, Oklahoma State University; Jay Rusch, University of Central Florida, USA; Kevan Knowles, University of Central Florida, USA; Jason Pagan, University of Central Florida, USA

The determination of active motor threshold (AMT) is a critical step in transcranial magnetic stimulation (TMS) research protocols involving voluntary muscle actions. Defined as the lowest stimulator output intensity necessary to evoke reliable responses of the target muscle, AMT is frequently determined using an absolute electromyographic (EMG) threshold (i.e., 200μV peak-to-peak amplitude). However, absolute EMG values acquired during voluntary contractions vary greatly across participants, muscles, days, and recording systems. To overcome these limitations, TMS researchers have proposed using a relative threshold when quantifying AMT (i.e., 2× background EMG during the voluntary contraction), but these approaches have never been systemically compared in the lower limbs. PURPOSE: We sought to investigate the test-retest reliability of two methods commonly used to determine AMT in lower limb TMS, as well as compare these approaches (absolute = 200μV vs. relative = 2× background EMG). Methods: Eighteen young adults (9 males and 9 females; mean ± SD age = 23 ± 2 years) visited the laboratory on two occasions. All testing was conducted on the dominant knee extensors. During each laboratory visit, isometric maximal voluntary contraction (MVC) peak torque was measured, with all subsequent TMS procedures conducted as participants maintained 10% of

MVC peak torque. AMT values were determined for each method using motor evoked potentials recorded from the vastus lateralis (VL). TMS pulses were delivered at a predetermined hotspot location while participants briefly activated their knee extensors at 10% MVC peak torque (~3-4 seconds), with ~10 seconds between TMS pulses. AMT was defined as the lowest stimulator output (%) needed to meet the specified criteria in ≥5/10 pulses. The order of the methods (i.e., absolute vs. relative) was randomized and counterbalanced. Intraclass correlation coefficients (ICC3,1), standard errors of measurement (SEMs), and the minimal difference (MD) score were calculated to assess test-retest reliability of each AMT determination method. A dependent samples t-test was used to compare mean differences in acquired AMT values obtained during the second laboratory visit. RESULTS: Both the absolute and relative methods demonstrated good-to-excellent test-retest reliability (ICC3,1 = .887 and .893, respectively), and the SEM/MD values were similar (absolute SEM = 7.9%, MD = 10.4%; relative SEM = 6.9%, MD = 8.9%). Differences between AMT methods were small and not statistically significant (absolute mean = 48.9%, relative mean = 47.4%; p = .309, Cohen's d = 0.247) (Figure 1). CONCLUSION: Quantifying AMT with an absolute threshold of 200μV peak-to-peak amplitude and 2× background EMG resulted in similar values for the VL. Lower limb TMS researchers can expect good-to-excellent reliability with both AMT determination methods. Given our findings, the use an absolute or relative AMT method may be considered on a case-by-case basis.

P1.14-E: Estimates of persistent inward current magnitude may predict upper limb function in people with incomplete cervical spinal cord injury

Alex Benedetto, Northwestern University; Sophie Jenz, Northwestern University; Bradley Heit, Northwestern University; James Beauchamp, Carnegie Mellon University; Sina Sangari, Shirley Ryan Ability Lab; CJ Heckman, Northwestern University; Monica Perez, Shirley Ryan AbilityLab; Greg Pearcey, Memorial University of Newfoundland

Motor commands are comprised of excitatory, inhibitory, and neuromodulatory components, and disruptions in descending inputs caused by spinal cord injury (SCI) affects all three of these components. The aim of this study was to determine if these disruptions alter motor unit discharge patterns in the upper limb muscles following cervical SCI, and whether motor unit properties were associated with upper limb function. Experiments were performed on twenty-one people with chronic, incomplete SCI at the cervical level, and fifteen non-injured control participants. High-density surface electromyographic arrays were placed over the biceps and triceps brachii and participants were seated with their arm secured to a force transducer. Elbow flexion and extension maximal voluntary isometric contractions (MViC) were used to normalize subsequent contractions. SCI participants were categorized into high-functioning and low-functioning groups based on MViC values. Participants performed submaximal isometric triangular ramps up to 30% MViC. Blind source separation was used to identify spike times of biceps and triceps motor units and persistent inward currents were estimated using the paired-MU analysis technique, which quantifies discharge rate hysteresis (ΔF). Preliminary results revealed that estimates of PICs were lowest in the low-functioning SCI participants and highest in the high-functioning SCI participants. This suggests that PICs are impaired in low-functioning, but enhanced in high-functioning, SCI participants, and that enhanced motoneuron excitability may augment function in some people with incomplete SCI in the presence of disrupted motor

commands. These findings may help inform therapeutic strategies to enhance function in people living with chronic incomplete SCI.

P1.15-E: Effects of operant conditioning of the motor evoked potential (MEP) on the tibialis anterior MEP and silent period in people with chronic incomplete SCI

Aiko Thompson, Medical University of South Carolina; Roland Cote, Medical University of South Carolina; Alli Lewis, Medical University of South Carolina; Blair Dellenbach, Medical University of South Carolina; Alan Phipps, Medical University of South Carolina

Background: After spinal cord injury (SCI), corticospinal excitability diminishes, resulting in weak voluntary activation of muscles below the injury and impaired motor control. However, such deficits are reversible at least partially, and an intervention that increases corticospinal excitability may enhance motor function recovery. Thus, operant up-conditioning of the motor evoked potential (MEP) to increase corticospinal excitability may improve the activation of the targeted muscle and improve motor functions in which that muscle participates. Previous studies indicated that up-conditioning of the ankle dorsiflexor MEP can improve locomotion in individuals with incomplete SCI (J Neurophysiol 2018: 120: 2745-60; 2019: 121: 853-66). As the first step in investigating the mechanisms of corticospinal plasticity and therapeutic effects associated with MEP up-conditioning, we are currently examining changes in MEP size and silent period (SP) after MEP, which reflects cortical inhibition at least partly, in ankle dorsiflexor tibialis anterior (TA) of people with chronic incomplete SCI. Methods: Adults with chronic (>1 yr post SCI) stable incomplete SCI are exposed to an MEP up-conditioning or control protocol that consists of 6 baseline and 24 up-conditioning or control sessions over 10 wk. In all sessions, 225 MEPs are elicited at ~10% above active threshold in the TA while the participant maintains ~30% maximum voluntary contraction (MVC) level of TA EMG activity. During baseline and control sessions, MEPs are simply measured. During conditioning trials of the conditioning sessions, the participant is encouraged to increase MEP size and is given immediate feedback as to whether MEP was larger than a criterion. Over the course of study, MVC, MEP size, and SP (measured as the period from the end of MEP to the recovery of EMG activity to the prestimulus level) are measured, and all values are compared between the 6 baseline sessions and the last 6 conditioning/control sessions. Results & Discussion: Over the course of 24 up-conditioning sessions (N=12), MVC changed by +11±6%, MEP by +44±6%, SP by -23±6%, and 10-m walking speed by 0 to +50%; whereas over the 24 control sessions (N=5), MVC changed by +25±9%, MEP by +23±19%, SP by +12±18%, and walking speed by -30 to +50%. These initial observations suggest that MEP up-conditioning increases MEP size and decreases SP duration, while MEP control protocol may increase MVC and MEP in some while producing no reduction of SP. Most striking observation is that SP-to-MEP ratio (indicating the balance between corticospinal inhibition and corticospinal excitation) decreases very clearly and persistently (-45±5%) with up-conditioning, whereas such changes are not obvious with control (-2±12%), indicating MEP up-conditioning specific effects on corticospinal inhibition. To understand the potential link between SP changes and function improvements, further studies and analyses are currently underway.

P1.16-F: The increase in spinal excitability is modulated by NMES frequency in the flexor carpi radialis but not in the soleus muscle

Riccardo Borzuola, Università di Roma "Foro Italico"; Valerio Caricati, Università di Roma "Foro Italico"; Martina Parrella, Università di Roma "Foro Italico"; Martina Scalia, University of Rome "Foro Italico"; Andrea Macaluso, University of Rome "Foro Italico"

BACKGROUND AND AIM: Superimposing neuromuscular electrical stimulation (NMES) on voluntary contractions has proven to be highly effective for improving muscle strength and performance (Borzuola et al. 2022). These beneficial effects might be related to specific adaptations occurring at cortical and spinal level. Some authors suggested that the effects of NMES on corticospinal activation could strongly depend on the stimulation frequency and significantly differ between upper and lower limb muscles (Mang et al. 2011; Blazevich et al. 2021). The aim of this study was to investigate acute responses in spinal excitability, as measured by H-reflex amplitude of flexor carpi radialis (FCR) and soleus (SOL) muscles, after a single bout of NMES superimposed on voluntary contractions (NMES+) of FCR and triceps surae (TS) muscles, delivered at low and high pulse frequencies (40 and 80 Hz). Methods: Twelve healthy young adults took part in a single experimental session which involved four experimental conditions: 1) NMES+ of FCR at 40Hz; 2) NMES+ of FCR at 80Hz; 3) NMES+ of TS at 40Hz; 2) NMES+ of TS at 80Hz. Each experimental conditions consisted of fifteen intermittent contractions (6s contraction/6s rest) at submaximal force level. Participants performed an assessment of the maximal voluntary isometric contraction (MVIC) of the wrist flexor and ankle plantar-flexor muscles. The intensity of the stimulation was set to achieve the 20% MVIC for each contraction. Surface electromyography (sEMG) was used to record the amplitude of H-reflex and motor waves from the FCR and the SOL muscles, following percutaneous stimulation of the posterior tibial nerve and the median nerve, respectively. A small motor wave was kept constant throughout the experiment, to accurately compare H-reflexes (Zehr et al. 2002) before and after the conditioning contractions. Each condition was preceded by assessments of a baseline H-reflex and followed by a post-treatment H-reflex assessment and MVIC. RESULTS: In the FCR, H-reflex amplitude increased after both NMES at 40 Hz (+43.2%, $p = 0.001$) and 80 Hz (+24%, $p = 0.003$) compared to baseline. Similarly, in the SOL, H-reflex amplitude increased following both NMES at 40 Hz (+11.3%, $p = 0.003$) and 80 Hz (+9.9%, $p = 0.001$) compared to baseline. Notably, in the FCR, the H-reflex amplitude was significantly greater in response to the 40 Hz compared to the 80 Hz condition ($p = 0.02$), whereas there were no differences in post-assessment H-reflex amplitudes between low and high frequency NMES ($p = 0.435$) in the SOL. CONCLUSIONS: These findings indicated that superimposing NMES on voluntary isometric contractions has an excitatory effect on spinal motoneurons in both upper and lower limb muscles with the largest response after low frequency NMES in the FCR. Such facilitation could be associated to enhanced somatosensory stimuli conjunctly with higher supraspinal downward commands. These findings provide novel information on the neurophysiological mechanisms underlying electrical stimulation and offer new perspectives on exercise-induced adjustment in spinal excitability, which could be valuable in designing rehabilitation and training protocols.

P1.17-F: Neuromuscular electrical stimulation superimposed on voluntary contractions increases force steadiness by modulating the neural drive to the tibialis anterior muscle

Riccardo Borzuola, Università di Roma "Foro Italico"; Stefano Nuccio, University of Rome "Foro Italico"; Ilenia Bazzucchi, University of Rome Foro Italico; Alessandro Del Vecchio, Friedrich-Alexander Universität, Erlangen-Nürnberg; Francesco Felici, University of Rome, Foro Italico; Andrea Macaluso, University of Rome "Foro Italico"

BACKGROUND AND AIM: Neuromuscular electrical stimulation (NMES) has become increasingly popular for its ability to preserve, restore, or enhance muscle mass and function in healthy individuals and those with injuries (Vanderthommen and Duchateau 2007). Evidence indicates that superimposing NMES on voluntary contractions (NMES+) promotes further improvements in muscle performance through specific neuro-physiological adaptations (Lagerquist 2016). Specifically, NMES+ seems to modulate motor unit (MU) discharge characteristics (Borzuola et al. 2023), potentially affecting the capacity to generate and sustain muscle force. However, the neural mechanisms underlying NMES+ need to be fully explored to provide key insights into the methodological aspects of NMES. The aim of this study was to investigate the changes in motor unit discharge characteristics and force steadiness following three acute experimental conditions: NMES superimposed to voluntary isometric contractions of the ankle plantar-flexor muscles (NMES+ISO); passive NMES; and voluntary isometric contractions only (ISO). Methods: Ten healthy young adults participated in this study. They were instructed to maintain an ankle plantar-flexor torque of 20% of their maximum voluntary isometric contraction (MVIC) for 15 contractions (6s contraction/6s rest) during each experimental condition. NMES was delivered over the tibialis anterior (TA), while the intensity of stimulation was adjusted to achieve the 20% MVIC for each contraction. High-density surface electromyography (HDsEMG) was used to record myoelectric activity in the TA during steady force-matching contractions at 10% MVIC. The motor unit discharge rate (DR) was calculated from the decomposition of the HDsEMG signal. A coherence analysis was performed on the decomposed signals and the proportion of common synaptic input (pCSI) received by spinal motoneurons was estimated by computing the rate of change of the relation between average coherence values in the delta frequency band (< 5 Hz) and the number of identified MUs. Moreover, the coefficient of variation of the force (CoVF) was computed during the steady contractions to assess force steadiness. Linear mixed effect models were used to analyse and compare the evaluated parameters before and after the experimental conditions. RESULTS: NMES+ induced a significant increase in DR and pCSI compared to baseline levels (DR, p=0.001; pCSI, p=0.002), as well as compared to post-intervention values of NMES (DR, p=0.007; pCSI, p=0.027) and ISO (DR, p=0.005; pCSI, p=0.028). Moreover, CoVF was reduced following NMES+ compared to baseline (p=0.005) and post-NMES values (p=0.014). CONCLUSIONS: These findings suggest that superimposing NMES to voluntary contractions can enhance the neural drive to the muscle by acutely modulating DR and pCSI, at low force levels. These adaptations in response to NMES+ seem to positively contribute to force steadiness, likely by engaging filtering mechanisms which minimize the independent synaptic noise affecting motor control. Among the possible mechanisms, NMES+ could promote the recruitment of additional motor units which plays a key role in reducing synaptic noise and improve force steadiness. These findings provide new perspectives on the adaptations induced by NMES exercise and shed light on the intricate neuro-physiological mechanisms involved,

enriching our knowledge of how the neuromuscular system responds and adapts to NMES-based interventions.

P1.18-G: A new look in Electromyographic Fatigue Threshold - an approach based on firing stability alteration

Klaus Becker, Faculty of sports of University of Porto; Marcio Fagundes Goethel, Faculty of Sport Science of University of Porto; João Paulo Vilas-Boas, Faculty of Sport Science of University of Porto; Ulysses Fernandes Ervilha, University of São Paulo

Electromyographic (EMG) signals can provide access to physiological processes that cause the muscle to generate force, i. e. when contractions are sustained, the EMG signal suffers a change in it amplitude and frequency, this have been called EMG fatigue threshold (EMGft) [1], this indicative have considerable application, since that the signal displays time-dependent changes prior to any force modification [2]. A current of thought has tried to correlate the EMGft with physiological thresholds as anaerobic threshold [3], since the increase in EMG could be due to the fact that type II muscle fiber are thicker and produces a higher action potential [4], despite its resemblance in time, to the date no paper found a good match on these variables. Which means that the changes in the EMG signal is not due to some biochemical change or selection of muscle fibers, the phenomenon is better explained by the synchronicity of motor units [5, 6], our hypothesis is that we can find a marker in the stability curve of MU firings, exacerbating the changes in EMG pattern, interpreted as EMGft, and that this occurs due to some changes in the motor drive events and by consequence alterations in the rhythm of firings. Since EMG signals are the result of a set of events of motor units (MU) firing, this means that the same output can be achieved with superposition of different MU and becomes indistinguishable with naked eyes. To overcome this issue De Luca & Cols created an algorithm of decomposition of EMG (dEMG) [7, 8]. Our proposal is to evaluate the stability threshold using an non-linear approach to evaluate stability in the signal. So, we calculated the largest Lyapunov exponent in a moving window of 1s with 0.9995 overlap window, achieving a resolution of 0.0005s, determining the instant at which the standard deviation of the stability curve changed abruptly [9, 10]. We further decompose the signal into individual MU to analyze its firing rate (MUFR), and calculate the median frequency of EMG (EMGfreq) and mean envelope (ENVm), to compare those variables before and after the EMGft. To induce fatigue, 10 male volunteers performed 30 isokinetic maximum concentric/eccentric contractions at 60º/s for knee extensors on dynamometer isokinetic. The signal recording consisted of a dEMG Galileo sensor electrode placed on the dominant lower limb, on vastus lateralis. The EMGfreq before EMGft was 85.64 ± 21.69 Hz compared to 75.36 ± 16.33 Hz after (p = 0.0129). The ENVm was 0.0465 ± 0.0211 mV before the EMGft, compared to 2.104e-7 ± 1.595e-6 mV after (p < 0.001). And regarding MUFR the average before was 11.91 ± 2.722 Hz and decreasing to 10.36 ± 2.429 Hz (p=0.0104). Conclusion: Our proposal shows that it's possible to find the point of critical changes in the firing pattern, which can be interpreted by some changes in the rhythm of motor drive firings, mainly showed by the alterations in EMGfreq and MUFR.Bibliography1. Moritani T, Takaishi T, Matsumoto T. Determination of maximal power output at neuromuscular fatigue threshold. J Appl Physiol. 1993;74(4): 1729-1734.2. De Luca CJ. Myoelectrical manifestations of localized muscular fatigue in humans. Crit Rev Biomed Eng. 1984;11(4): 251-

279.3. Lucía A, Sánchez O, Carvajal A, Chicharro JL. Analysis of the aerobic-anaerobic transition in elite cyclists during incremental exercise with the use of electromyography. Br J Sports Med. 1999;33(3): 178-85.4. Crozara LF, Castro A, De Almeida Neto AF, Laroche DP, Cardozo AC, Gonçalves M. Utility of electromyographic fatigue threshold during treadmill running. Muscle Nerve. 2015;52(6): 1030-1039.5. Yao W, Fuglevand RJ, Enoka RM. Motor-unit synchronization increases EMG amplitude and decreases force steadiness of simulated contractions. J Neurophysiol. 2000;83(1): 441-452.6. Zhou P, Rymer WZ. Factors governing the form of the relation between muscle force and the EMG: a simulation study. J Neurophysiol. 2004;92(5): 2878-2886.7. De Luca CJ, Adam A, Wotiz R, Gilmore LD, Nawab SH. Decomposition of surface EMG signals. J Neurophysiol. 2006;96(3): 1646-1657.8. Nawab SH, Chang SS, De Luca CJ. High-yield decomposition of surface EMG signals. Clin Neurophysiol. 2010;121(10): 1602-15.9. Killick R, Fearnhead P, Eckley I. Optimal detection of changepoints with a linear computational cost. Journal of the American Statistical Association, 2012;107(500), 1590-1598.10. Lavielle M. Using penalized contrasts for the change-point problem. Signal Processing. 2005;85(8): 1501-1510.

P1.19-G: Regional neuromuscular modulation of the hamstring muscles during muscle fatigue tasks

Nobuhiro Aoki, Sapporo Medical University; Keigo Okuyama, Sapporo Medical University; Masaki Katayose, Sapporo Medical University

The semitendinosus (ST) and biceps femoris (BF) muscles of the hamstrings coordinate knee flexion movement. The hamstring muscles are susceptible to muscle injury during sports activities, and one of the risk factors is muscle fatigue. Recent reports have investigated the differences in activity between different regions of the hamstring using multi-channel surface electromyography. Our research focused on the fact that the ST is a biventricular muscle with a tendinous intersection, and the differences in muscle function between the ST and BF were investigated. Detailed characterization of muscle activity during muscle fatigue may provide basic data for estimating the changes in neuromuscular activity that occur under muscle fatigue conditions during sports activities, and for diagnosing affected individuals and preventing injury. This study aimed to characterize the region-dependent muscle activity of ST and BF during sustained knee flexion contraction.Ten healthy men participated in this study. The participants were placed in a supine position, and the maximum knee flexion torque (maximal voluntary contraction [MVC] torque) during maximal voluntary isometric contraction was measured in both legs. Next, the participants performed a submaximal voluntary isometric contraction task in which 50% of the MVC torque was maintained as a muscle fatigue task. The muscle fatigue task was defined as one that resulted in muscle fatigue at a 5% decrease relative to the target force. The measurement items were ST and BF site-specific surface electromyograms of the right lower limb, which were measured using a multichannel surface electrode. The electrodes were placed in a series, and surface electromyography was measured using monopolar induction from each electrode. During the application of the electrodes to the ST, the position of the muscle edges and the tendinous intersection at rest were confirmed using an ultrasound imaging system. The electrodes were applied to the BF so that the midpoint of the line connecting the sciatic tuberosity and the head of the fibula was at the center of the multichannel electrode. The electromyograms measured by 15 channels were obtained for all

participants and were time normalized with the point at which muscle fatigue was achieved set at 100%. Root mean square (RMS) and median frequency (MDF) for each channel were calculated every 25% from the start of the exercise. Next, mean RMS and MDF values of all channels were calculated were calculated by dividing the electromyography electrodes into proximal, central, and distal regions. Friedman tests were performed to compare the results for different regions at each time point. The results showed that RMS tended to increase during the muscle fatigue task; however, no significant differences between the regions were observed. In contrast, MDF tended to decrease during the muscle fatigue task; no significant differences between the regions were observed. These results suggest that site-specific muscle activity in ST and BF may not occur during the knee flexion task in both legs.

P1.20-H: Fast and Stable Decomposition of Unwhitened Surface EMG Signal by Random Projection [Poster Award]

Alexander Clarke, Imperial College London; Agnese Grison, Imperial College London; Irene Mendez Guerra, Imperial College London; Dario Farina, Imperial College London

The decomposition of surface electromyography (sEMG) signal into its constituent motor unit (MU) activity offers a non-invasive method of directly accessing the neural drive to muscles, providing an extremely clean control signal for human machine interfacing (HMI) applications. However, in practice, decomposition algorithms invoke a high computational burden, which can introduce an unacceptable latency in real-time HMI. A major contributing factor is that incoming sEMG signal must be whitened prior to source separation, which requires an expensive singular value decomposition (SVD) on an extended version of the time series. Current methods try to mitigate this by retaining and applying the whitening matrix used originally to estimate the separation vectors, but this will quickly begin to fail due to signal non-stationarities, eventually requiring expensive recalculation.We propose to sidestep the need for data-driven whitening entirely by using a convolution operation to output a generalised Achlioptas random projection of the signal. We demonstrate that this simple operation has a strong decorrelating effect on spatio-temporal windows of sEMG, allowing for efficient discovery of separation vectors without the associated preprocessing costs. The projection is then combined with an optimized convolutional independent component analysis procedure to create an extremely fast projection pursuit algorithm for sEMG decomposition. By tuning the dimensionality of the random projection, we demonstrate that source separation can be easily focused on either MU yield or speed. Finally, we show that ICA optimization on sEMG has an extremely high tolerance to the distortion introduced by a low-dimensionality random projection. We hypothesise that this is due to the sparsity of neurophysiological data, which reduces the distortion that might otherwise be expected for a given number of samples under the Johnson–Lindenstrauss lemma.The effectiveness of the proposed sEMG decomposition algorithm is robustly examined experimentally using paired intramuscular recordings for two-source validation. For both overall yield and rate of agreement with decomposed intramuscular data, no significant difference was found between the proposed method and a state-of-the-art decomposition algorithm which used data-driven decorrelation. Furthermore, by artificially perturbing the signal in a way that would normally require recalculation of the whitening matrix, we show that a random projection maintains its decorrelation capability without affecting the

viability of a learned separation vector.In conclusion, we show that a computationally-expensive preprocessing step considered critical in the decomposition pipeline, SVD whitening, can be bypassed completely. We present a novel method of decorrelating sEMG signal in a data-independent way, removing a critical barrier to the use of spinal motor neurons as a control signal in non-invasive HMI applications.

P1.21-I: Investigating the muscular activation of healthy subjects using an end effector robot-based assistive system during a simulated daily task.

Sybele Williams, Institute of Applied Medical Engineering / AME, RWTH Aachen University; Catherine Disselhorst-Klug, Institute for Applied Medical Engineering, RWTH Aachen University

BACKGROUND AND AIM: The organization and control of human movement is managed by the brain's reciprocal perception-action loop. It unifies the proprioceptive and exteroceptive feedback systems with the neuronal interfacing to functional modules and reflects its sensitivity to external stimuli. The effect of the contextual environment e.g. person-robot interaction on this loop is vital for understanding movement performance, muscular activation and motor learning. This study investigated the changes in muscular activation due to the use of an end-effector robot-based assistive system during movement tasks. METHOD: 20 healthy subjects were recruited to exclude the effects of pathology (avg. age: 32.55 ± 12.66 yrs.). Subjects performed a simulated movement task: Cup to Box, Cup to Mouth (CBCM) with and without robot-assistance. The assistive system centered on an Iiwa 14 robotic arm (KUKA Robotics). While seated before the robotic system, subjects were connected to the robotic arm via a wrist splint (BORT Medical) with a bespoke magnetic connector. The investigator led the robot through the movement task with the subject connected to the robot. The robotic system, having saved the task's movement trajectories, could then assist subjects as they autonomously performed that task. The joint stiffness of the robotic arm was varied to provide 2 robot-assisted scenarios: partially supported (PS) and fully supported (MS). The third task was the free, unassisted CBCM task (FM). The task order was randomized to minimize fatigue or familiarization effects. Surface electromyography (sEMG) signals were collected according to SENIAM recommendations from M biceps brachii, M triceps lateralis and M. brachioradialis. DATA ANALYSIS: The SEMG data was sampled at 2000 Hz and bandpass filtered (range: 1 - 500 Hz). The data was then rectified, smoothed and a normalized SEMG envelope was determined. The root mean square (RMS) value of each muscle was determined for each scenario of CBCM. RESULTS: For all 3 muscles, the RMS values for FM were the lowest when compared with the scenarios PS and MS. Additionally, PS consistently showed the highest RMS values among the scenarios. DISCUSSION: It is to be expected that performance of the movement task while fully supported by the robot arm would result in the lowest level of muscular activation. However, the unfamiliar robot-assisted task presented new exteroceptive stimuli, which possibly modified existing functional models of the task and challenged both the learning and performance of the task. This resulted in higher RMS values than for FM. The highest RMS values were observed for PS. This may reflect subjects' greater uncertainty when executing tasks under PS. The RMS values suggest possible coactivation of the muscles during task performance. CONCLUSION: An end-effector robot-based assistive system has a marked effect on the muscular activation of healthy subjects and thus impacts motor control and motor learning.

P1.22-I: Rhythmic galvanic vestibular stimulation modulates sensorimotor synchronization to auditory syncopation

Ryoichiro Yamazaki, Keio University; Junichi Ushiyama, Keio University

Sensory inputs from multiple modalities are integrated for better performance. Such multimodality sensory integration is reported to improve synchronized movements to rhythmic auditory inputs. Vestibular inputs are known to be involved in the spatial and temporal processing of auditory information. In addition, afferent signals from the vestibular system project to subcortical structures included in neural networks generating rhythmic movements. Although rhythmic vestibular inputs are reported to modulate auditory meter perception, it is unclear whether such vestibular inputs affect the quality of sensorimotor synchronization to rhythmic auditory inputs. The present research used galvanic vestibular stimulation (GVS) in a sensorimotor synchronization task to examine the involvement of the vestibular system in the neural basis for sensorimotor synchronization. Participants flexed their index fingers in the dominant hand to the beats in syncopated auditory sequences. In the real GVS condition, square-wave GVS pulses lasting 10 ms were applied at the intensity below the individual cutaneous thresholds. The train of GVS synchronized with the auditory beats. In the sham GVS condition, on the other hand, no GVS was applied. The participants were informed that they were under the GVS application in all experimental trials. At the same time, none of them perceived the stimulation in the real GVS condition. For quantifying the synchronization errors, asynchrony was defined by calculating the temporal gap between the timings of the meters and those of maximal flexion in the dominant index finger. The stability and accuracy of synchronization were assessed by calculating the standard deviation and the absolute value of the asynchrony. These three indices, asynchrony, the standard deviation of asynchrony, and the absolute value of asynchrony, were compared between the real GVS condition and the sham GVS condition. As a result, compared to the sham GVS condition, the asynchrony shifted toward negative values in the real GVS condition, i.e., finger flexion occurred earlier than the auditory beats. This result might be associated with the asynchronous perception of auditory and vestibular inputs: the subjective perception of vestibular sensation is known to occur earlier than the auditory one when these two sensory inputs are provided simultaneously. This study provides a new perspective on the involvement of the vestibular system in the neural basis for sensorimotor synchronization.

P1.23-I: Validation of a Novel Motor Learning Task: Does Grip Force Tracking Induce Peripheral Muscle Fatigue?

Hailey Tabbert, Ontario Tech Univeristy; Nicholas Antony, Ontario Tech Univeristy; Paul Yielder, Ontario Tech Univeristy; Bernadette Murphy, Ontario Tech Univeristy

Previous work has examined motor skill acquisition using motor tracing tasks, simple typing tasks, and more recently tasks that require force modulation. The latter is more heavily reliant on proprioception and serves as a valuable tool to evaluate motor acquisition in populations with impaired proprioceptive processing. However, recent work using this task reported minimal improvements in motor performance from pre- to post-acquisition with no capacity for skill

retention. This is likely due to a lack of complexity and the discrete nature of the task used. The purpose of this research was to develop and validate a complex and continuous, force-based motor learning task. 11 right-handed, healthy participants(6F) aged 22.6±2.5 had bipolar surface electromyography(EMG) recorded from the right extensor carpi radialis(ECR) and flexor carpi ulnaris(FCU) throughout the duration of a novel hand-grip force matching tracking task(FMTT). The FMTT was delivered in 6 phases: pre-acquisition, 3 acquisition phases (acq1, 2, 3), and post-acquisition completed on day one and retention 24 hours later. Task performance was measured as absolute error(AE) and standard deviation of error(SdE). EMG signals were bandpass filtered (20-500Hz) and mean power frequency(MnPF) and EMG amplitude (RMSa) were computed to measure fatigue. MnPF was calculated using a Fast Fourier Transform computed in a 0.5 second window with a 50% overlap across filtered signals. RMSa was calculated using a 250ms root mean square smoothing window across filtered signals. Repeated measures ANOVAs compared EMG variables and performance accuracy normalized to baseline. Relative to baseline performance, there was a significant effect of time post-acquisition where AE decreased by 21.1% (p<0.001) and SdE decreased by 23.9% (p<0.001). At retention, AE decreased by 3.04% (p=0.009) relative to post with no effect of time for SdE (p=0.73). ECR: Relative to baseline, there were no fatigue effects of time for MnPF at: acq1 (p=0.1), acq2 (p=0.1), acq3 (p=0.09), or post (p=0.08) or RMSa at: acq1 (p=0.16), acq2 (p=0.33), acq3 (p=0.31), or post (p=0.13) when compared to baseline. FCU: There was a significant effect of time from pre to acq2 where MnPF increased by 6.38% (p=0.03), however there were no significant effects at acq1 (p=0.55), acq3 (p=0.12), or post (p=0.23). There were no significant effects for RMSa at acq1 (p=0.27), acq2 (p=0.3), acq3 (p=0.71), or post (p=0.21). Significant improvements in motor performance from pre-post indicate this task facilitated motor skill acquisition. Further improvements in absolute error from post-retention demonstrates that this task also facilitates retention of the acquired motor skill in healthy young adults. The absence of change in EMG variables in both muscles is evidence that this task does not induce muscle fatigue in healthy controls. This new FMTT can be used in future work to evaluate how motor skill acquisition is impacted in different clinical populations.

P1.24-I: A systematic review of electromyographic activity of trunk and pelvic floor muscles in pregnant women

Yu Okubo, Saitama Medical University; Saki Matsuno, Saitama Medical University

Introduction: Most of pregnant women experienced low back pain and pelvic girdle pain. (Colla et al., 2017) Some previous studies have reported that activity pattern of trunk and pelvic floor muscles (PFM) in the pregnant women was changed with the pain. (Hatami, 1961; Kim et al., 2022) However, there are controversy issues how change muscle activity of trunk muscles and PFM in prenatal and postpartum. Therefore, the purpose of this systematic review was to investigate change in muscle activity of trunk and PFM during pregnancy period and post parturition, and suggest optimal exercise therapy for pregnant women. Methods: A systematic literature search was performed using PubMed and ICHUSHI. (Japan medical abstract database) Search phrases were (pregnancy or pregnant or parturition) AND (electromyography or muscle activity) AND (trunk or pelvic). Inclusion criteria was studies which measured electromyographic (EMG) activity of trunk muscles or PFM in pregnant women. The exclusion

criteria were: 1) studies which did not show EMG amplitudes, 2) studies with subjects who delivered by C-section, 3) studies which used subjects with orthopaedic or medical disease, 4) review articles, 5) intervention studies. Two reviewers selected studies by 2 screenings of the title, abstract and full text independently. Selected studies were grouped into measurement muscles, and systematically organized by change in muscle activity for each muscle. RESULTS: Sixteen studies were extracted by 2 screenings. These studies were grouped into measurement muscles as follows: 6 studies for the PFM, 5 studies for the internal oblique (IO), 4 studies for the rectus abdominis (RA) and external oblique (EO), 3 studies for the erector spinae (ES), and 3 studies for the anal sphincter and levator ani. Five out of 6 studies demonstrated that PFM activity in pregnant was significantly lower that in controls. (women without childbirth experience) Three out of 5 studies showed significantly lower activity in the IO during late pregnancy and postpartum than controls, while there were no significant differences in the RA and EO between pregnant and controls. Two out of 3 studies showed highest activity in the ES during late pregnancy. The muscle activity of the AS and LA significantly decreased in postpartum. Discussion: Most studies have shown decrease of the activity of the PFM and IO in pregnant women. The results suggest that pregnant women decrease the function for co-contraction of the PFM and deep abdominal muscles while controls have enough ability of co-contraction of the PFM and IO. (Larissa et al., 2013) In contrast, some studies showed that ES activity was higher during late pregnancy. Increase of lumbar lordosis with expansion of abdominal volume might result in hyper-activation of the ES in pregnant women. This systematic review implies that exercise therapy such as draw-in maneuver which enhance co-contraction of the PFM and deep abdominal muscles and inhibit the ES activity may be effective for pregnant women.

P1.25-I: The effects of central sensitization on motor unit properties in the upper limb

Nicholas Antony, Ontario Tech Univeristy; Hailey Tabbert, Ontario Tech Univeristy; Imran Khan Niazi, New Zealand College Of Chiropractic; John Srbely, University of Guelph; Fredy Rojas, New Zealand College of Chiropractic; Paul Yielder, Ontario Tech Univeristy; Heidi Haavik, New Zealand College of Chiropractic; Bernadette Murphy, Ontario Tech Univeristy

One in five Canadian adults live with chronic pain, 50% of which have lived with the condition for over ten years. The International Association for the Study of Pain defines chronic musculoskeletal (MSK) pain as persistent pain that lasts beyond the normal tissue healing time, typically at least 3 months duration. This implies that chronic MSK pain is mediated through the spinal cord and higher levels. Central sensitization (CS) is the increased responsiveness of nociceptors in the central nervous system (CNS) to normal or subthreshold afferent input. The least invasive method of inducing CS experimentally is through the use of topically administrated capsaicin cream. This method has been utilized to detail the underlying mechanisms in the development of chronic pain and investigate the maladaptive neuronal plasticity occurring within the spinal cord and supraspinal centers. Previous research suggests that CS may directly impact the ventral root of the spinal cord or motor unit (MU) excitability. Our current study uses capsaicin-induced CS methods to investigate the changes in MU excitability of subjects during a gripping task. CS was induced by applying Zostrix 0.075% capsaicin cream, while the control group has a placebo cream of similar consistency applied.

Participants (n=13,7F) were divided into CS and control groups and were required to trace a ramp by gripping a force transducer up to 10% MVC. Either capsaicin or control cream was applied over the participant's neck and shoulder during the study. HDsEMG was recorded from the flexor carpi ulnaris muscle (FCU), a wrist flexor, and extensor carpi radialis (ECR), a wrist extensor using a 64-channel HDsEMG electrode over each muscle belly, being careful to avoid the motor point. Muscle activity was recorded prior to, and 10-, 20-, 30- and 40-minutes post cream application. At each time point, the participant performed 4 blocks of 3 grips each. The purpose was to compare changes in HDsEMG properties relative to baseline. All EMG data was band pass filtered between 10 and 500 Hz, with 250 ms window, 0 ms gap. The Centroid of the root mean square (RMS) of EMG activity and sample entropy for the plateau phase of each grip were calculated and averaged for the pre, 10-, 20-, 30- and 40-minute time point and compared between groups. The centroid represents the spatial distribution of the EMG signals across the electrode array. Differences between CS and healthy were found in the forearm extensor muscles at 10- and 20-minutes post cream application for both RMS and sample entropy, with no difference between groups for the flexor muscles. These results can provide insight into the neural mechanisms which may initiate chronic pain, and their effect on MU recruitment properties. This information could be valuable in both understanding and detailing the subsequent effects of CS, and chronic pain, on neuromuscular control.

P1.26-I: Transcutaneous Spinal Random Noise Stimulation Facilitates Motor Memory Consolidation in Healthy Individuals

Mitsuhiro Nito, Yamagata Prefectural University of Health Sciences; Daisuke Kudo, Yamagata Prefectural University of Health Sciences; Tadaki Koseki, Yamagata Saisei Hospital; Shigeo Tanabe, Fujita Health University; Tomofumi Yamaguchi, Juntendo University

Motor skill training transiently increases in the corticospinal excitability and the functional oscillatory coupling of the corticospinal drive to motoneurons. The change is thought to reflect changes in neuronal connectivity associated with improvements in sensorimotor performance, and also associated with consolidation of motor skills. We have reported that transcutaneous spinal random noise stimulation (tsRNS) over the cervical level can enhance corticospinal drive to spinal motoneurons in healthy individuals, and it could be induced by increasing ascending afferent input via the somatosensory cortex to pyramidal cells in primary motor cortex. We hypothesized that tsRNS can enhance motor skill acquisition process and facilitate motor memory consolidation. Here, we investigated the effect of tsRNS over the cervical level on motor performance in 40 healthy volunteers. Motor performance was assessed by visuomotor accuracy tracking task with rapid shifts in pinch force levels are required, and measured as the average percentage time on target. Motor performance was tested just before and after training (Day 1), 1 (Day 2) and 7 days after motor training (Day 8). During motor training, participants received real or sham tsRNS with maximum current of 3 mA for 20 min or 0.5 min, respectively. Electroencephalography and electromyography from the first dorsal interosseous (FDI) muscle were measured during tonic isometric contraction of thumb and index finger (pinch) for 2 min to quantify corticomuscular coherence (CMC). Motor training improved motor performance, but no significant difference was observed between real and sham tsRNS groups, suggesting that tsRNS did not affect motor performance in Day 1. A significant increase in beta-band CMC after

training both groups, the changes tended to be larger in tsRNS group compared to sham group. Investigating the retention effects, tsRNS group maintained higher performance on days 2 and 8 compared to sham group. These findings suggest that tsRNS combined with motor training facilitates consolidation of motor skills.

P1.27-I: Peak torque variability in the MVCs of the plantar flexors is associated with the resting systolic blood pressure

Chinami Taki, Setsunan university; Naruhiro Shiozawa, Ritsumeikan university; Tetsuya Kimura, Kobe University

BACKGROUND AND AIM: Variations in the peak torques often occur among multiple MVC trials and these variations would affect several motor performances. It has been suggested that there is a direct connection between motor control system and autonomic nervous system. Especially, higher motor output may be achieved by increased sympathetic nervous activity. The aim of the present study was therefore to investigate whether higher MVC peak torque is obtained when blood pressure is deliberately raised by the modulation of respiration. Methods: Eight healthy young participants volunteered for this study. Surface EMG (bipolar Ag/AgCl electrodes, pick-up diameter 4 mm, inter-electrode distance 20 mm) were obtained from the medial gastrocnemius (MG), lateral gastrocnemius (LG), and soleus muscles (SOL). The reference electrode was located on the lateral malleolus. Blood pressure was measured at the same time. The participants repeated 2-s isometric MVC of plantar flexors 14 times with sufficient rests (>4 min). The MVC trials involved two types of breathing pattern for 30 s just before the muscle contraction: (1) normal respiration and (2) rapid respiration. During the rapid respiration, the participants were instructed to breathe in time with a metronome at 1 Hz. Each breathing pattern was performed seven times at random order. For each MVC trial, the EMG RMS value (1-s window) at peak torque was computed in each muscle. The averages of the peak torque, EMG RMS for each muscle, and mean resting systolic blood pressure (SBP) for 30 s just before the MVC were calculated for each breathing condition in each participant, and they were compared between the breathing conditions. RESULTS: In the rapid respiration condition, peak torque and resting SBP were significantly higher than those in the normal respiration condition (P<0.05). Additionally, EMG RMS values in the MG and LG tended to be larger in the rapid respiration condition (P=0.05). CONCLUSIONS: The intentional modulation of SBP would achieve higher MVC peak torque in the plantar flexors.

P1.28-J: High-frequency firing of erector spinae motor units during arm-raised sitting in patients with subacute stroke

Hiroki Hanawa, University of Human Arts and Sciences; Keisuke Hirata, Tokyo Kasei University; Taku Miyazawa, University of Human Arts and Sciences

Stroke-induced motor paralysis extends from the patient's limbs to the trunk. Patients are unable to hold their trunk upright, which accounts for half of their body weight. Approximately 25% of patients are unable to sit without assistance one month after stroke (W.C. Chen, 2022). In the present study, we investigated 1) the effect of electrical stimulation on the erector spinae,

which acts in trunk extension during sitting. However, we could observe little activity in the erector spinae when simply sitting, and they relied on other tissues for support. Therefore, we investigated 2) whether erector spinae activity could be observed by voluntary arm movements from a sitting position and how the motor units were firing.Subjects in both experiments were patients with subacute stroke; 1) 13 and 2) 12 patients. Measurements were taken on average 1) 19 and 2) 20 days after onset of stroke. A High-Density surface ElectroMyoGraphy (HDsEMG, OT-Bioelettronica) was used as the research instrument; 64 electrodes were attached to the erector spinae (longissimus). The subjects were seated on the edge of a bed in a resting posture, leaning with their arms on the table in front of them. The subjects then 1) underwent electrical stimulation in the task posture with their hands floating off the table; 2) in the task posture with their arms raised above their heads or reaching forward without electrical stimulation.RESULT 1: The criterion for action potential detection was defined as the mean amplitude + 3 times the standard deviation for 3 seconds in the resting posture. Although 64 channels of each subject were investigated, the criterion was exceeded in 2/13 subjects in the task posture. These subjects showed activity both before and after electrical stimulation. The other subjects did not meet the criteria for activity before and after electrical stimulation.RESULT 2: Activity of the erector spinae was observed in the task posture. This was evident in the arm-raised posture, where 10/12 subjects were able to decompose the motor unit. In the arm-forward posture, 6/12 subjects were able to decompose the motor unit. In any case, only 1-2 motor units could be decomposed in each subject. Their average firing rate was 21.9 [fps] (range 11.8 - 42.9).Comparing results 1) and 2), we found that voluntary arm movements activated the erector spinae more than electrical stimulation while sitting. The number of motor units that could be decomposed from the erector spinae activity of each patient was small. On the other hand, the average firing rate of motor units was higher than in previous studies. In the previous study, it was 5.4 [fps] in healthy adults during sitting (L.R. Lothe, 2015) and 15.8-23.9 [fps] during maximum extension (M.F. Silva, 2017). CONCLUSION: : Patients with subacute stroke do not rely on muscle contractions to hold a sitting position. When moving their arms from a seated position, a small number of their erector spinae motor units may increase the firing rate to produce adequate force.

P1.29-K: Assessing intrinsic properties of human motoneurons during slow lengthening and shortening contractions

Ben Nazaroff, Memorial University of Newfoundland; Riley Pike, Memorial University of Newfoundland; Sophie Jenz, Northwestern University; James Beauchamp, Carnegie Mellon University; Greg Pearcey, Memorial University of Newfoundland

It is unknown whether intrinsic motoneuron properties that regulate human motor unit discharge patterns are altered under dynamic conditions. Work in the decerebrate cat preparation have shown that movement of the limb can influence persistent inward currents (PICs) via activation of local inhibitory circuits. In humans, however, estimating intrinsic properties of motoneurons (i.e., PICs) have primarily been done under isometric conditions. The aim of this study was to explore the effects of slow isokinetic ramp contractions on estimates of PIC magnitude in healthy, young adults. Participants first performed dorsiflexion MVCs at 80°, 90°, and 100° of ankle flexion to establish a predictive algorithm, which was used to transform

the torque feedback throughout the contraction and ensure relative efforts remained constant across joint angles. Next, using this transformed feedback, they performed triangular (5s up/down) dorsiflexion contractions to a peak of 30 and 50% MVC while the isokinetic dynamometer moved their ankle through plantarflexion (i.e., 80° to 100°) or dorsiflexion (i.e., 100° to 80°). High-density surface electromyograms were recorded and decomposed into motor unit spike trains. We then used a paired motor unit analysis technique to calculate discharge rate hysteresis (estimate of the magnitude of PICs; delta frequency [DF]) from smoothed discharge rate patterns. Discharge rates were higher during concentric contractions (22.7 [20.1, 25.4] pps) compared to eccentric (21.1 [18.5, 23.8] pps), and during 50% contractions (24.8 [22.2, 27.5]) compared to 30% (19 [16.4, 21.7] pps). There was also a reduction in DF during concentric contractions (3.93 [2.78, 5.08]) compared to eccentric (5.46 [4.31, 6.61]), and this effect was exemplified at higher contraction intensities. Since PICs are affected by local inhibitory circuits, and concentric actions necessitate lengthening of the antagonist muscle, which is likely to impart Ia reciprocal inhibition, these findings suggest that, even during slow length changes during concentric contractions, local inhibitory circuits can have profound effects of intrinsic motoneuron excitability in humans.

P1.30-K: Noradrenergic perturbations modulate human motor unit discharge behavior and attenuate motor impairments in chronic stroke

James Beauchamp, Carnegie Mellon University; Sophie Jenz, Northwestern University; Thomas Plaisier, Northwestern University; Margaret Sereika, Northwestern University; Sebastian Urday, Northwestern University; Farzaneh Sorond, Northwestern University; CJ Heckman, Northwestern University; Julius Dewald, Northwestern University Feinberg School of Medicine

Persistent inward currents (PICs) augment excitatory synaptic input to motoneurons and are facilitated by monoamines (e.g., norepinephrine), setting a motoneuron's state. While the monoaminergic dependence of PICs is thought critical for human motor function, this dependence may facilitate motor impairments in chronic hemiparetic stroke where monoaminergic dysfunction is theorized. To investigate this interplay, we performed a series of experiments using single-dose noradrenergic pharmacological probes, high-density surface electromyography (HDsEMG), and novel mechatronic devices in both neurologically intact and chronic hemiparetic stroke populations.In the first experiment, eleven neurologically intact participants performed isometric elbow flexion, shoulder abduction (SABD), and index finger abduction contractions before and after taking tizanidine, yohimbe, atomoxetine, or a placebo. The isometric paradigms were designed to highlight PIC behavior, with motor units (MUs) decomposed from HDsEMG of the biceps brachii, deltoids, and first dorsal interosseus.In the second experiment, individuals with chronic hemiparetic stroke were interfaced with a novel robotic device and asked to generate isometric elbow flexion and SABD torque profiles. To highlight independent joint control, an additional task required simultaneous isometric elbow flexion while generating a dynamic SABD load. All tasks were performed before and after tizanidine, with MUs decomposed in the biceps brachii and deltoid muscles.Initial analysis indicates that noradrenergic probes modulate MU discharge profiles in both experiments. Furthermore, preliminary findings from the second set of experiments in chronic hemiparetic stroke suggest a potential decrease in estimates of PICs post tizanidine, with estimated

decreases of 0.42 pps (d = 0.23) in deltaF and 5.01 %rTri (d = 0.26) in brace height. Overall, these findings provide insights into the acute effects of noradrenergic perturbations on human MUs in a neurologically intact population and highlight the potential noradrenergic dependence of motor impairments in chronic stroke.

P1.31-K: Simulating Motor Neuron Diseases in Synthetic Muscles

Cathrine Nayrouz, University of Guelph; Andrew Hamilton-Wright, University of Guelph

Title: Simulating Motor Neuron Diseases in Synthetic MusclesCathrine Pierre Nayrouz, and Andrew Hamilton-WrightIntroduction: Motor Neuron Diseases (MNDs) are a wide range of diseases that can be split into three major classes, upper motor neuron diseases, lower motor neuron diseases (LMN), and diseases that contain both UMN and LMN degeneration, like Amyotrophic Lateral Sclerosis (ALS). These diseases are part of the same family where neuronal damage leads to the slow progression of muscle weakness, stiffness, and loss of control. The symptom presentation, areas of damage, as well as general disease progression can vary between the various classes, however, there is a commonality in their underlying mechanisms. Using muscle simulation, we can create synthetic muscles, and model diseases, such as MNDs, in order to better study, understand, and test varying hypotheses in a way that is simply not possible in a clinical setting. Using a muscle simulator would allow us to explore the linkage between cellular disease involvement and the effect on the signal produced by the model so that EMG-based diagnostic algorithms can be better utilized. Furthermore, there are obvious problems with performing an invasive, and mildly uncomfortable procedure to gain a better understanding of the signals released. This presents another valuable use case of having a simulated muscle model, where we can generate the interference pattern using the same firing rate, with exact needle positioning, however with restructuring due to disease – which of course is simply not possible in real life. By using a synthetic muscle, various hypotheses regarding interference patterns obtained under potential restructuring strategies may be explored. The resulting improved understanding of how a given disease state manifests opens up the potential for earlier diagnosis and a deeper understanding of the cellular reconfigurations occurring throughout the disease progression. Methods: A disease model is created that takes in a healthy muscle, and gradually increases the level of involvement of the disease as time progresses, modelling the removal of motor units from the muscle, forcing their fibres to either be adopted by nearby motor units, or in the case that no neighbouring motor units are available to take on fibres they gradually start to die off. As the fibres die off, a muscle compaction algorithm 'tucks in' the muscle towards the centre – both to make sure there are no 'holes' in the muscle, but also to simulate the atrophy that occurs over time. Since for some of these processes, the literature is not conclusive on how they occur in the human body, the results of several comparative experiments are presented, to test which method produced results closest to reality as described in the literature. RESULTS: As seen in Table 1 we can see plots of the muscle as it progresses through the disease (0% to 50% motor unit involvement). As seen in the first graph (0 involvement) each motor unit centre is shown as a uniquely coloured square, with its attached fibres shown as dots of the same colour. If the fibre gets readopted by a surviving motor unit, it becomes a star with the colour of its new parent motor unit, but shown as a black triangle. The resulting signals of the diseased muscle are then compared to those collected in a

clinical setting, as well as validating that the fibre density and CMAP are comparable to real patients at that same stage in the disease as described in the literature. CONCLUSION: The tool presented, while not perfect, is a first step towards a new model to explore potentially available diagnostic information related to these vicious diseases and will allow scientists and researchers to test hypotheses in a way that is novel for MNDs, based on this cellular level physiological model.

P1.32-K: A Particle Swarm Optimised Nonlinearity for High Yield Surface EMG Decomposition

Agnese Grison, Imperial College London; Alexander Clarke, Imperial College London; Irene Mendez Guerra, Imperial College London; Jaime Ibanez, Imperial College London; Dario Farina, Department of Bioengineering, Imperial College London

Methods that can accurately decompose surface electromyographic (sEMG) signals into their constituent neural activity are critically important for motor neuroscience research as well as human-machine interfacing applications such as prosthetics, neurorehabilitation, and wearable consumer devices. The introduction of advanced high-density surface electrode arrays has made the simultaneous collection of hundreds of channels of neurophysiological time series possible, motivating the need for a new class of automated blind source separation algorithms that capitalize on the superior spatial resolution these arrays provide. However, whilst the theory of independent component analysis (ICA) presents a strong theoretical base for these algorithms, practical implementation challenges frequently lead to imperfect outcomes, especially with sparse sources. In particular, the non-linearity used to estimate independence is often sub-optimally selective for a given source. In this study we show that the most efficient non-linearity can vary per source in a recording, posing a significant challenge to the separation process if a high source yield is desired. We go on to demonstrate how the correct design of the contrast function can allow for the separation of sources with very similar motor unit action potential (MUAP) waveforms. Our findings indicate that employing a single non-linear optimization function in the ICA process for identifying spiking sources can adversely affect the process, hindering the effective isolation and accurate separation of all spiking sources within the signal. Using these insights, we propose a particle swarm methodology for sEMG decomposition, adaptively traversing a polynomial family of non-linearities that approximate the asymmetric cumulants of the sources. We robustly investigate the utility of the resultant algorithm experimentally using two-source validation between high-density sEMG (12x5 grid) signal and intramuscular EMG (2 bipolar wires) signal recorded concurrently from the Tibialis Anterior (TA) muscle. We processed the sEMG data using both the current gold standard in automatic decomposition, namely convolutive Blind Source Separation (cBSS), and the proposed algorithm, Swarm Contrastive Decomposition (SCD). For both methods, we refined the outputs automatically by eliminating duplicate units and filtering out units with either a coefficient of variation exceeding 40 or a firing rate surpassing 35Hz. Across 90 recording sessions, the cBSS and SCD methods identified 226 and 474 units, respectively. Additionally, we applied SCD to decompose the iEMG data, which led to the identification of 313 unique units. A significant number of the motor units identified from the iEMG were also detected from the independent decomposition of the corresponding sEMG signal. The presence of matching

units between the two decomposition modalities serves as a reliable indicator of decomposition accuracy. In conclusion, we present a method for the decomposition of HD-sEMG data that improves on the current state-of-the-art by leveraging a source-specific independence estimator to separate it from the sEMG mixture.

P1.33-K: Tracking motor units across wrist joint angles: characterisation of motor unit action potentials under muscle fibre shortening and lengthening

Irene Mendez Guerra, Imperial College London; Deren Y. Barsakcioglu, Imperial College London; Dario Farina, Imperial College London

Objective.Understanding the modulation motor units (MUs) undergo during dynamic contractions is essential to develop more accurate and robust neuromechanical models and neural interfaces.Approach.Here, we propose a novel sequential assignment algorithm that condenses spatial, temporal, and amplitude features to track MUs across different levels of muscle shortening and lengthening based on their motor unit action potentials (MUAPs).First, the algorithm compares two sets of MUAPs based on their normalised mean squared error (NMSE) after automatic temporal alignment and spatial channel selection. Then, the assignment process is carried out as a minimisation of the NMSE of the tracking paths for the MUAPs whose NMSE is below a predefined threshold. This process is sequentially repeated across consecutive and disjoint angles to track the full MUAP representation. To validate this, MUAPs detected at multiple wrist joint angles (every 10° from -40° wrist flexion to 40° wrist extension) were tracked with respect to the reference position at 0°, computed from high density EMG signals concurrently recorded from the forearm and the wrist during isometric contractions (individual and combined finger flexions at 15% maximum voluntary contraction) from 9 participants. Main results. Results showed that overall, more MUs were tracked at the wrist than at the forearm (178 vs 130 MUs, respectively) and over more angles (4 ± 2 vs 3 ± 1 count of tracked angles, respectively, mean ± std). This was explained by lower changes with muscle fibre shortening and lengthening in the non-propagating far-field potentials at the wrist than in the propagating components of the MUAPs at the forearm (up to 0.18 ± 0.09 n.u. and 0.26 ± 0.13 n.u. NMSE at -40° flexion, respectively).Furthermore, the NMSE between the tracked MUs was significantly lower than the NMSE between their respective second-best alternatives (0.08 ± 0.04 n.u. vs 0.57 ± 0.26 n.u., respectively, p<0.001). This shows that the selected tracking paths were outliers in the MU's (dis)similarity distributions and supports the notion that modulated MUAPs retain their uniqueness within the MU population in both locations.Significance.These findings showcase the effectiveness of the proposed assignment algorithm to track MUAPs across a wide range of motion, revealing physiological insights about their modulation during muscle shortening and lengthening. Furthermore, by matching the MUAPs across conditions (in this case, joint angles), the tracking approach also links the spike trains used to compute the MUAPs at each angle and their corresponding decomposition models, providing a non-invasive validation set for decomposition adaptation algorithms.

P1.34-K: Developing a Stimulation-Free Remote Motor Unit Number Estimate in Motor Neurone Disease (REMUNE)

Judith Bilgorai, King's College London

Background: Motor Neurone Disease (MND) affects the motor neurones responsible for transmitting movement-related signals towards the muscles to produce movements. The current method used for monitoring disease progression and diagnosis is called Motor Unit Number Estimate (MUNE) and involves electrical stimulations to accurately estimate the number of functional motor units. However, this approach can cause extreme discomfort for some participants. These assessments also require individuals with MND to come to a clinical environment every 2-months. Developing a stimulation-free MUNE would enable more comfortable assessments leading to a greater amount of data collected, eliminate the need for specialised staff, and save time. Overall, it represents a first step in making these assessments remote and home-based in the future. Methods: This study involves people with MND (n ≥24), and healthy age-matched controls (n ≥12) attending six assessments over 12-months. During these assessments, 64-channels surface EMG sensors will be applied bilaterally over the thumb, index finger, little finger, and shin for a duration of 16-minutes. While recording their muscle activity, the participants will perform several muscle contractions at different force levels. Additionally, MUNIX (Motor Unit Number Index), a gold-standard MUNE, will be performed on the same muscles as a comparative measure of motor unit loss. Objectives: To reliably identify the active motor unit pool at varying force levels by combining HD-sEMG with an advanced motor unit decomposition technique. To seek physiological correlations between motor unit parameters, muscle power and MUNIX over time and across body regions in MND and control patients. To define a novel stimulation-free MUNE. To this date, the data from 14 participants (both healthy and MND) have been recorded over 3 visits resulting in approximately 11-hours of recording.

P1.35-K: Antagonist vibration affects force output and underlying motor unit discharge behaviour

Kaitlyn Sutton, Memorial University of Newfoundland; Ben Nazaroff, Memorial University of Newfoundland; Riley Pike, Memorial University of Newfoundland; Nicholas Maher, Memorial University of Newfoundland; Ethan Kean, Memorial University of Newfoundland; Greg Pearcey, Memorial University of Newfoundland

Gain control of muscle force output is mediated by motoneuronal persistent inward currents (PICs), which are facilitated by diffuse monoaminergic inputs and highly sensitive to local inhibitory inputs. Recent work has shown that estimates of PICs in humans are dampened in the presence of Ia reciprocal inhibition via electrical stimulation of mixed nerves innervating the antagonist muscle, and vibration of the antagonist muscle tendon. A direct link between PIC magnitude and voluntary force control, however, has not yet been established. Thus, the goal of the present work was to determine if force control and underlying motor unit discharge behaviour is modified under conditions of reduced PIC magnitude. We recorded 64 channels of high-density EMG from the tibialis anterior while participants performed two subsequent isometric contractions with their ankle dorsiflexors per trial. In the first, they received visual feedback and were instructed to produce and hold torque at ~25% of their maximum for 5 seconds; and, in the second, we asked them to match the same level of effort required to produce torque in the first contraction while we blinded them to their actual torque output.

Vibration to the Achilles tendon was applied during the first, second, or neither of the contractions in separate trials. We hypothesized that 1) vibration in the first contraction would reduce PICs, and cause participants to produce more torque in the subsequent contraction without vibration, and 2) vibration in the second contraction would reduce PICs, and cause participants to produce less torque when matching the effort required previously without vibration. We implemented mixed effects models to determine if the vibration predicted mean torque. Preliminary data (3 females; 5 males) indicate that compared to trials without any vibration (mean torque = 26.9% [23.2, 30.7]), vibration in the second contraction (without visual feedback) reduced voluntary torque output (22.4% (18.6, 26.1]), whereas voluntary torque was increased (28.7% [25, 32.5]) when vibration was applied in the first contraction. Our behavioural data support our hypothesis that implicates PIC magnitude as an important gain control mechanism that contributes to the perception of muscle force output in humans. Decomposition of EMG signals into motor unit spike trains and analysis is ongoing, and data will be presented at the congress.

P1.36-K: Flexible High-Density Electromyography Microneedle Electrode Arrays

Jérémy Liegey, UCD; Thomas Lijnse, University of Calgary; Kevin Krieger, University College Dublin; Kazim Haider, University Of Calgary; Colin Dalton, University of Calgary; Eoin O'cearbhaill, University College Dublin; Madeleine Lowery, University College Dublin

High-density surface electromyography (HD-sEMG) enables detection of EMG signal distribution across the skin surface and, when combined with decomposition methods, bridges the gap between the information which can be extracted from surface and intramuscular EMG. Despite its advantages, care must be taken with skin preparation and electrode placement. Decomposition accuracy can also be affected by movement or shifting of the electrodes. Here, we propose and demonstrate the efficacy of a novel dry microneedle array electrode (MNEA) for HD-sEMG. The MNEA yielded high-quality sEMG signals comparable to signals recorded using conventional flat surface electrode arrays, while providing better coupling between the electrode and tissue and without requiring prior skin preparation.A dry-use flexible microneedle array electrode (MNEA) was fabricated comprising of a flexible backing layer with embedded microneedle electrode contacts made of biocompatible conductive materials integrated on-top of a flexible PCB backing. Functionality of the MNEA was assessed by examining EMG activity recorded from the biceps brachy during isometric contraction at a range of force levels, without prior skin preparation. The experiments were repeated using a conventional surface electrode array with the addition skin preparation. HD-sEMG signals detected using the MNEA exhibited low baseline noise, high signal to noise ratio and high signal spatial selectivity. Surface EMG amplitude intensity maps were generated from the MNEA data which also enabled motor unit decomposition and localization of the innervation zone. The signal to noise ratio and decomposition yield was similar or higher than standard electrodes without the need for any skin preparation or the use of an electrolyte gels. In conclusion, the developed dry-use MNEA can record high quality HD-sEMG without requiring skin preparation or electrolyte gel. MNEAs have the potential to expand the range of application areas of HD-sEMG by improving signal quality and ease of application, for example in clinical applications where stable and consistent

placements are required and in protocols which call for consistent high-quality recordings for an extended period of time.

P1.37-K: Effects of neuromuscular electrical stimulation on motor unit behavior during voluntary muscle contractions: A high-density surface electromyogram (HDsEMG) study

Atsushi Sasaki, University of Miami Miller School of Medicine; Hikaru Yokoyama, Tokyo University of Agriculture and Technology; Naotsugu Kaneko, University of Tokyo; Tatsuya Kato, Sony Computer Science Laboratories Inc; Matija Milosevic, University of Miami Miller School of Medicine; Kimitaka Nakazawa, The University of Tokyo

Neuromuscular electrical stimulation (NMES) can be used to generate muscle contractions without central commands and while doing so modulate the excitability of cortical and spinal neural circuits by activating sensory and motor pathways. While the application of NMES has been successfully used to enhance motor function in the clinical population, the underlying neurophysiological mechanisms are yet to be fully understood. Specifically, the impact of NMES intervention on motor unit activity, a key determinant of neuromuscular control, remains largely unexplored. Therefore, the purpose of our current study was to investigate the effect of a single-session NMES intervention on motor unit behavior using high-density surface electromyography (HDsEMG) techniques. Ten able-bodied individuals participated in this study. During the intervention, NMES at the frequency of 25 Hz was intermittently applied (800 msec on / 800 msec off duty cycle) over the right common peroneal nerve to activate the tibialis anterior (TA) muscle and induce ankle dorsiflexion for a total of 10 min. NMES intensity was set to evoke 50% of the maximum M-wave response (Mmax) elicited by single-pulse common peroneal nerve stimulation. Motor unit behavior of the TA muscle was assessed by recording 64-channel HDsEMG during isometric ramp contractions targeting 35% of maximal voluntary contraction force. Assessments were conducted at baseline and immediately, 10 min, and 20 min after the NMES intervention. In offline analysis, HDsEMG signals were decomposed into single motor unit activity using blind source separation algorithms based on FastICA and the convolutional kernel compensation approach. Motor unit firing rate and recruitment and de-recruitment threshold were then computed from the identified motor unit activity. Results showed that the motor unit firing rate was significantly increased immediately after NMES intervention, and the effect lasted for at least 20 min (p<0.05). Specifically, the firing rates during the plateau and de-recruitment phase of the submaximal isometric contraction were increased after NMES intervention (p<0.05). Moreover, results showed that the de-recruitment threshold decreased 10 min after the NMES intervention, lasting at least 10 min, while the recruitment threshold was not affected. These findings suggest that even a short-duration / single-session NMES intervention can induce changes in motor unit activity, reflected in altered firing rate and de-recruitment threshold. Since NMES activates the sensory and motor nerves, it is possible that NMES-induced repetitive motoneuron activation through reflex circuits and/or direct motoneuron activation contributed to the observed modulation of motor unit activity after the intervention. Overall, our results proposed that alterations in the motor unit activity may underlie the mechanisms driving NMES-induced plasticity.

P1.38-L: Neck Intermuscular Coherence in Chronic Neck Pain During Dynamic and Static Tasks

David Jimenez Grande, University of Birmingham

BACKGROUND AND AIM: Chronic neck pain (CNP) often involves neuromuscular impairments, as observed in clinical settings [1]. This study extends the existing knowledge by hypothesizing that CNP affects the interconnectivity of neck muscles. Our aim is to examine how muscle coordination varies in individuals with CNP compared to asymptomatic individuals during dynamic neck movements and static tasks, including smartphone use. Through the use of intermuscular coherence analysis, this study seeks to shed light on how multi-muscle coordination in CNP patients differs during these activities. Methods: Twenty asymptomatic individuals and 20 people with CNP participated in the study. Each participant performed three consecutive neck flexions followed by a standing task while using a smartphone to watch a 3-minute video. Electromyography (EMG) signals were collected from key neck muscles: the upper trapezius (UT), splenius capitis (SC), anterior scalene (AS), and sternocleidomastoid (SCM) bilaterally. Intermuscular coherence, measured through magnitude squared coherence (MSC), enabled the analysis of functional interactions and connectivity strength between muscles. This methodology produced weighted adjacency matrices for each participant, emphasizing significant connections while filtering out less relevant ones [2]. The study analyzed four frequency bands (δ, θ, α, β) to construct and compare functional muscle networks based on strength (ST) and betweenness centrality (BC), the last indicating crucial points of information flow within the network. RESULTS: The cervical flexion task showed significant differences in both BC and ST in the δ band between CNP and asymptomatic participants ($p = 0.01$ and $p = 0.03$, respectively). However, during the static task, no significant differences were observed in any frequency band or parameter ($p = 0.97$ and $p = 0.90$). Additionally, neck muscle networks during dynamic tasks revealed distinct graphical differences in the δ band, with CNP participants exhibiting reduced connectivity and localized activation in the SCM and SC muscles with a less symmetrical network, unlike the control group (Figure 1A). On the other hand, these differences were less evident in the static task networks (Figure 1B). CONCLUSIONS: Our findings indicate altered muscle synergies in individuals with CNP, particularly during cervical flexion and predominantly in the δ frequency band [3], known for its importance in force generation and control [4]. This study contributes to a deeper understanding of neuromuscular adaptations in CNP and highlights the potential impact of common activities like smartphone use on muscle coordination in this population.

P1.39-L: Reconsideration of exercise trainings for the stair descent: A study using muscle synergy analysis

Ryotaro Araki, Hiroshima university; Yoshitaka Iwamoto, Hiroshima University Hospital; Masanosuke Mizutani, Hiroshima university; Kaho Yamamoto, Hiroshima university; Hikaru Yokoyama, Tokyo University of Agriculture and Technology; Makoto Takahashi, Hiroshima University

Stair ambulation is a common activity of daily living, but one of the most challenging tasks for older people. Because 75% of falls on stairs occurs during descent, stair descent exercises are

frequently conducted in rehabilitation. Stair descent exercises with stairs and steps may be difficult and risky of falling. Therefore, in some cases, exercise trainings such as squatting and lunging are introduced at a preparatory stage before attempting stair descent. However, it is unclear whether these activities are similar to stair descent in terms of muscle coordination. Exercise trainings with similar coordinated muscle activity may be effective. This study aimed to identify the similarity of muscle coordination between stair descent and exercise trainings, and to help develop programs for improving the ability of stair descent.Ten healthy adults (age: 21.5±0.5 years) were recruited in this study. Stair descent (DS) trials were performed on three-step stairs (step height: 20cm). In addition, double leg squat (DLS), single leg squat (SLS), and forward lunge (FL) were performed. During DLS, SLS, and FL, participants flexed their knee to approximately 60 [°]. The kinematics data were obtained using a three-dimensional motion analysis system, and the muscle activity data of 13 lower muscles of the dominant leg were measured using surface electromyography (EMG). A non-negative matrix factorization was applied to the EMG data to extract muscle synergies. The similarities between muscle weightings extracted from DS and exercise trainings were evaluated using cosine similarity. A pair of muscle weightings was considered similar if the cosine similarity were ≥ 0.8.The maximal knee joint flexion angles during tasks were 95.0 ± 3.1 [°] for DS, 59.6 ± 5.3 [°] for DLS, 60.7 ± 3.6 [°] for SLS, 58.4 ± 5.2 [°] for FL. Three modules were extracted from DS, two modules were extracted from DLS and SLS, and one module was extracted from FL. DS1 showed main contribution of rectus femoris (RF), vastus lateralis (VL), vastus medialis (VM), and soleus (SOL) during mid-stance. DS2 showed main contribution of adductor magnus, biceps femoris, semitendinosus (ST), and tibialis anterior during late-stance. DS3 showed main contribution of gluteus max, gluteus medial (Gmed), and gastrocnemius medial (GM) during late-swing. DLS1 and SLS1 showed main contribution of RF, VL and VM during descent phase. DLS2 showed main contribution of tensor fascia latae, ST, and GM, and SLS2 showed main contribution of Gmed and GM during start and end of squatting. FL1 showed contribution of almost all muscles during forward transition. The pair of muscle synergies similar to DS1 were DLS1, SLS1, and FL1. In addition, DS3 was similar to DLS2 and SLS2. Muscle synergies similar to those found in stair descent were also identified in DLS, SLS, and FL. Exercise trainings such as DLS, SLS, and FL may be effective at a stage before stair descent in terms of muscle coordination.

P1.40-M: Differences in Neuromechanical Factors Affecting Explosive Torque Production During Knee Extensions: A Preliminary Comparative Study of Males and Females.

Marcel Lanza, University of Maryland Baltimore

Background & Aim: The ability to generate explosive force is influenced by different neuromechanical factors. Prior research, mainly involving males, has shown that muscle activation (measured with surface electromyography-EMG), contractile properties (assessed by electrical stimulation), and morphology (determined by muscle size) are key determinants of torque production. Additionally, muscle quality, gauged by echo intensity in ultrasound images, and muscle stiffness, measured with shear-wave elastography, may also impact torque generation. It is yet to be clarified if these factors vary between sex. Thus, this preliminary study aims to investigate whether the neuromechanical factors underlying explosive force differ between males and females. Methods: Twelve young adults (5 males; 27±2y; 1.68±0.7m;

69±21kg; X±SD) who did not consistently perform exercise visited the laboratory for a single session. Upon arrival, participants rested for 10 minutes before undergoing ultrasound measurements. B-mode and shear wave ultrasound images were taken from the vastus lateralis (VL) and rectus femoris (RF) muscles, with two images for each muscle while the participant was seated on an Isokinetic Dynamometer (HUMAC). EMG sensors were placed on the same muscles, following SENIAM guidelines for both the ultrasound probe and EMG placement. Electrical stimulation at rest was administered through femoral nerve stimulation to record maximal M-waves (MMAX) and twitch torque. EMG signals were processed according to ISEK standards. Participants performed three maximal isometric contractions of the knee extensors at a knee flexion of 90 degrees, and the highest contraction was selected for analysis. The rate of force development (RFD) was calculate from force onset to peak force, while VL and RF rate of activation (RoA) were calculated from EMG signal onset to EMG peak. An independent t-test was employed to compare sex differences in muscle thickness, stiffness, quality, MMAX, RFD (%MVIC), time to force peak, RoA (%MMAX), twitch force (%MVIC). Statistical analyses were conducted using SPSS software, with the significance threshold set at P≤0.05Results: RFD was not different between males and females. Muscle thickness in the rectus femoris (RF) (P=0.039) and vastus lateralis (VL) (P=0.047) was found to differ between males and females, with males exhibiting 30% (RF) and 44% (VL) greater muscle thickness than females. However, no other measured outcomes showed significant differences between males and females (P≥ 0.052). Although not statistically significant, MMAX was observed to be 46% and 55% higher in males than in females. Similarly, RFD, twitch force, RoA were 17% to 34% higher in males. CONCLUSION: : This preliminary study showed that muscle thickness was the only variable that differed significantly between males and females. However, it is important to note that other variables were generally higher in males, although these differences were not statistically significant. Given the small size of the present cohort, the inclusion of more participants could potentially alter these findings.

P1.41-M: Modulation of spinal and tendon reflex excitabilities of the soleus muscle during and after static stretching

Akira Saito, Kyushu Sangyo Univeristy; Takamasa Mizuno, Nagoya University

Static stretching induces neural changes in spinal reflex excitability and sensitivity of muscle spindles. These changes can be tested in the soleus muscle by evoking the Hoffman-reflex (H-reflex) and the tendon reflex. The H-reflex and tendon reflex are depressed during static stretching. After stretching, the H-reflex returns immediately to the state before stretching, but the tendon reflex remains depressed. These suggest that spinal reflex excitability is inhibited during static stretching, and long-lasting inhibition of muscle spindle sensitivity occurs with stretching. However, the effects of repeated static stretching on modulation of spinal and tendon reflex excitabilities are unclear. This study examined changes in the H-reflex and the tendon reflex of the soleus muscle during and after static stretching. Eleven healthy men were recruited. The participants were in the prone position with their hips and knees fully extended, and the foot in the anatomical position was attached to an isokinetic dynamometer. Static stretching involved five repetitions of 1-min stretching with a 1-min interval between repetitions at the maximal dorsiflexion angle. The H-reflex and the tendon reflex were recorded from the

soleus muscle before and during stretching, at intervals between stretching, and 0, 2, 5, 10, and 20 min after static stretching. The H-reflex was evoked by transcutaneous electrical stimulation of the posterior tibial nerve, and stimulation intensity was adjusted to 5% of the maximal M-wave. The tendon reflex was evoked by a reflex hammer that was dropped on the Achilles tendon from a constant height. Peak-to-peak amplitudes of five responses of the H-reflex and of the tendon reflex were averaged, and time course changes of these responses from baseline (i.e., before stretching) were calculated. Measurements of the H-reflex and the tendon reflex were done on different days. Dorsiflexion angles during stretching were significantly increased with repeated stretching trials in both measurements. H-reflex amplitudes during stretching were 54.0-57.8% depressed (p < 0.05), and these depressions returned to baseline in the interval immediately following. Tendon reflex amplitudes during stretching were 74.2-78.8% depressed (p < 0.05), and these depressions were maintained in the interval immediately following. The recovery of significant depressions of tendon reflex amplitudes was observed at least 2 min after stretching. These results suggest that depression of spinal reflex excitability during static stretching disappears immediately after stretching, but long-lasting inhibition in muscle spindle sensitivity is induced by static stretching. Furthermore, there was no significant repetition effect on H-reflex and tendon reflex amplitudes during stretching. Repeated static stretching appears to have no modulating effect on spinal and tendon reflex excitabilities of the soleus muscle.

P1.42-M: Influence of vibration therapy on the spinal reflex excitability of multiple lower limb muscles in able-bodied subjects

Yohei Masugi, Tokyo International University; Matija Milosevic, University of Miami Miller School of Medicine; Takashi Inomata, Tokyo International University; Misono Sakai, Tokyo International University

Whole-body vibration (WBV) and local vibration are widely used as therapeutic interventions for individuals with central nervous system injuries. Although these vibration methods are shown to strongly suppress H-reflex excitability of the soleus muscle, the broader effects on various homologous and non-homologous muscle groups remain unexplored. Recently, a novel method using transcutaneous spinal cord stimulation (tSCS) was developed to evaluate spinal reflex excitability in multiple lower limb muscle groups. Using this method, the present study examined the effects of WBV on the spinal reflex circuits of the flexor and extensor muscles of the thigh and lower leg. The participants were seven healthy men who underwent assessments before, during, and after WBV and a control condition that included standing without vibration. Surface electromyography signals were unilaterally recorded in the right leg throughout the experiments. In the WBV condition, the intervention was applied for 1 min. In the control condition, the participants stood still for 1 min. Posterior root muscle (PRM) reflexes were elicited by tSCS and measured in four lower extremity muscles, including the tibialis anterior (TA), soleus (SOL), vastus medialis (VM), and biceps femoris (BF) before, during, and after the interventions. The effects of local vibration to the right Achilles tendon on the spinal reflexes were investigated in one participant in the sitting position. PRM reflexes were measured in the lower limb muscles before, during, and after the interventions. Our results showed that the peak-to-peak amplitudes of PRM reflexes of the TA, SOL, and BF muscles decreased

significantly during the WBV intervention but returned to baseline after the intervention. The control condition has no effects. These results indicate that WBV has widespread inhibitory effects on reflex circuits in homologous and non-homologous muscles, excluding the SOL during WBV, but this effect is not sustained following a short-duration intervention. The characteristics of the suppression due to WBV were similar to those during local vibration. Overall, our results suggest that WBV and local vibration can be used effectively to temporarily decrease spinal excitability, which is relevant for treatment of spasticity in neurological disorders. Further studies are required to optimize the duration and frequency of these interventions to enhance and prolong their benefits in individuals with central nervous system injuries.

P1.43-M: A new modular neurocontroller recombines synergies for stand-to-walk simulations [Poster Award]

David Muñoz, University College Dublin; Donal Holland, University College Dublin; Giacomo Severini, University College Dublin

Predictive neuromuscular models are a powerful tool for decoding the underlying architecture of the sensorimotor control and its neural activity. Applied to gait, these models can be categorised in CPG-based models (central pattern generators), which are good at modulating motor behaviours (i.e., gait speed), but lack neurophysiological representation in humans, and reflex-based models, which represent the principles of the legged mechanics, but the control of motor behaviour is a multidimensional problem. Also, these models are generally task-specific and mapping completely the skill space of a motion requires the tuning of all the parameters of the system. We here propose a modular model for posture and locomotion (MPL model). This model presents a modular architecture where synergies, coactivated muscle responses, are recombined by internal models (IMs) to display different motor tasks. The IMs are controlled by a hypothetical volitional signal generated by a higher structure, the mesencephalic locomotor region (MLR). The tuning of this signal allows to switch between IMs and, consequently, motor tasks. Specifically, we applied this architecture to a stand-to-walk motion. At a specific time of the simulation, the MLR switches the controlling signal, the controller breaks the upright posture, and the musculoskeletal model starts walking. The displayed gait matches human-like walking and the kinematics, ground reaction forces and muscle activation patterns are consistent to human data. Also, the modulation of the controlling signal has been shown capable of speed transition during walking. Once the model reaches steady walking at 1.3 ms-1, the MLR was able to map a new neural pathway and raise or lower the speed to 1.6 and 0.8ms-1, respectively. We hope that this preliminary implementation of the MPL model could be the first step to achieve a standardization of the modular representation of the human motor system. Thus, further development is needed to unblock the potential of the MPL model. As a start, we are developing an extension of the model to a walk-to-stand capability.

P1.44-M: Effect of side dominance on lumbar muscle activation patterns: high-density electromyography insights

Julien Ducas, Université du Québec à Trois-Rivières; Jacques Abboud, Université du Québec à Trois-Rivières

BACKGROUND AND AIM: Previous research has indicated that the global activation of the lumbar erector spinae (ES) muscle is influenced by the trunk side dominance, determined with hand dominance [1]. Nevertheless, contemporary understanding acknowledges that the activation of ES muscles does not exhibit uniform spatial distribution across the cranio-caudal and medio-lateral axes. Recent studies have revealed distinctive side patterns of spatial activation in the lumbar ES muscles without a clear explanation in existing literature [2-3]. Therefore, it is hypothesized that the observed asymmetrical patterns of lumbar muscle activity may be partially attributed to the effects of side dominance. This study aims to investigate the impact of the trunk side dominance on the spatial distribution of muscle activation. Methods: 43 participants (10 left-handed and 33 right-handed) took part in this study. The dominant side of the back was determined using the manual preference questionnaire [4]. A 20 second isometric back extension submaximal contraction was conducted. During the contraction, muscle activation strategies of the left and right lumbar ES were recorded using high-density surface electromyography (two grids of 8x8 electrodes). Spatial distribution was measured using the location of the centroid coordinates (medio-lateral and cranio-caudal) on both grids. The centroid represents the average position of the channels that had RMS values higher than 70% of the maximum value across all channels. A pairwise t-test was used to evaluate differences between the dominant and non-dominant sides of the ES muscle. Additionally, an independent t-test was performed to assess disparities between left-handed and right-handed participants. RESULTS: Dominance significantly influenced centroid location, indicating a more cranial activation on the dominant side ($p=0.016$). No medio-lateral differences were observed ($p=0.224$). Additionally, no distinctions were found between left- and right-handed subjects. CONCLUSION: Side dominance may induce uneven ES demands during daily tasks, potentially causing morphological adaptations over time. Such adaptations may result in heightened activation of the ES muscle on the dominant side, predominantly located in the cranial region, which could explain the more cranial activation observed on the dominant side [5]. Given these findings, we recommend that future studies assessing spatial distribution of ES muscle consider (I) evaluating both sides of the ES muscle and (II) assessing ES dominance.[1] PS Sung et al., Spine 29 (17), 1914 (2004).[2] Z Hao et al., Pain Research and Management 2020 (2020).[3] J Abboud et al., European journal of applied physiology 114, 2645 (2014).[4] G Dellatolas et al., Revue de psychologie appliquée (1988).[5] JE MACINTOSH and N BOGDUK, Spine 12 (7), 658 (1987).

P1.45-M: Relationship Between Joint Angle and Patterns of Hamstrings Activation After ACL Reconstruction

Ava Schwartz, University of Central Florida; David Sherman, Boston University; Justin Rush, Ohio University; Moein Koohestani, University of Central Florida; Grant Norte, University of Central Florida

BACKGROUND/AIM: Individuals who have undergone anterior cruciate ligament reconstruction via hamstrings tendon autograft (ACLR-HT) exhibit persistent hamstrings weakness. Despite muscular deficits, biceps femoris (BF) and semitendinosus (ST) facilitation is reported during

sub-maximal tasks (e.g., gait, stair ambulation). However, relative activation of the medial (ST)-to-lateral (BF) hamstrings has not been investigated during maximal effort, particularly as a function of joint angle. Therefore, we aimed to compare the magnitude and ratio of medial and lateral hamstrings activity during maximal effort at different muscle lengths between limbs of individuals with ACLR-HT. Methods: Electromyographic (EMG) activity of the BF and ST was recorded during a series of randomized maximal voluntary isometric contractions (MVICs) at 20°, 40°, 60°, and 80° of knee flexion in twenty-three individuals with primary, unilateral ACLR-HT (age=23±3.1 years, sex=14 females, time from surgery=46.9±26.3 months). Average root mean square amplitudes of raw EMG signals were recorded from the middle 1-second of MVIC plateaus and averaged across trials for each muscle and joint angle. The ratio of medial (ST)-to-lateral (BF) hamstrings activity was calculated using processed EMG signals and quantified at each joint angle. Separate 2x4 repeated measures ANOVAs were used to investigate isolated or interactive effects of muscle and joint angle for each limb, using Holm-Bonferroni correction for post-hoc testing where applicable. Paired samples t-tests were used to compare muscle activity between limbs at each joint angle. Cohen's d effect sizes with 95% confidence intervals were used to quantify magnitudes of observed differences. Results are reported as percentage difference (%) in EMG activity. RESULTS: EMG activity differed by joint angle, but not muscle, for both limbs. In the involved limb, collapsed EMG activity was higher at 60° than 20° (26.2%, p<.001, d=0.71 [0.19, 1.23]). In the uninvolved limb, collapsed EMG activity was higher at 40° (16.6%, p=.043, d=0.29 [-0.6, 0.06]), 60° (44.7%, p<.001, d=0.79, [0.32, 1.27], and 80° (30.2%, p<.001, d=0.54 [0.14, 0.94]) than 20°, and at 60° than 40° (20.1%, p<.001, d=0.5 [0.11, 0.89]). Medial-to-lateral hamstrings activation ratios and BF EMG activity did not differ between limbs or joint angles. ST EMG activity was lower in the involved compared to uninvolved limb at 60° (-18%, p=.044, d=-0.45 [-0.87, -0.01]). CONCLUSIONS: Activation patterns were similar for the medial and lateral hamstrings across joint angles, with higher activation of both muscles observed at greater knee flexion angles. Lower ST activation of the involved limb near optimal fiber length may reflect a reduced neuromuscular capacity of the medial hamstrings at maximal effort, potentially due to this muscle serving as the graft donor. Thus, interventions targeting maximal effort medial hamstrings activation may be warranted in individuals with ACLR-HT.

P1.46-N: Investigation of the mechanism behind corticomuscular communication based on bursts of neural activity

Takuya Ideriha, Keio University; Junichi Ushiyama, Keio University

Our nervous system achieves movement control and sensory information processing by appropriately sending and receiving electrical signals. Phase synchronization has been proposed as a mechanism that enables such efficient information transmission. Phase synchronization refers to the phenomenon where the rhythms of neural activity (neural oscillations) between different neural regions synchronize. Such phase synchronization is known to occur not only between brain regions but also between the sensorimotor cortex and muscles, which is called corticomuscular coherence (CMC). However, there are many unclear points regarding how such phase synchronization occurs and what specific benefits (functional significance) it brings to the nervous system. CMC is the optimal system for examining the mechanisms of phase synchronization and its functional significance because it is observed in

a relatively simple system of sensorimotor cortex and muscles that is easy to measure and shows clear individual differences; CMC is not observed in about half of the participants. Therefore, our study focused on CMC to investigate the mechanisms of phase synchronization and its functional significance. We recorded scalp electroencephalograms over the sensorimotor area and surface electromyograms from the tibialis anterior muscle while human participants carried out ankle dorsiflexion. As a new analytical method, signals of the electroencephalogram were averaged on the timing of hundreds of electromyographic bursts. This indicates that bursts of muscle activity were used as events for event-related potentials in the electroencephalogram. As a result, a clear rhythmicity in the beta band (15–35 Hz), where CMC has traditionally been observed, was observed in the averaged waveforms (Figure 1). This result intuitively shows that the electromyographic bursts are strictly phase-locked to the beta oscillations of the sensorimotor cortex. Advantages of this method include the ability to examine the pattern of signal transmission from muscle to brain in participants where CMC is not observed, and the ability to examine how CMC occurs over time from the start of movement. Our presentation will discuss in detail the methodology and the signal transmission mechanism it suggests. Figure 1: (Left) An averaged electroencephalographic waveform relative to 240 electromyographic bursts. (Right) Time-frequency map for the waveform.

P1.47-N: Femoral cartilage cross-sectional area in collegiate Archery, Badminton, Taekwondo, and Tennis players, and non-athletic individuals: a 12-month follow-up study

Seunghun Lee, Kyung Hee University; Junhyeong Lim, Kyung Hee University; Seonggyu Jeon, Kyung Hee University; Jaewon Kim, Kyung Hee University; Jinwoo Lee, Kyung Hee University; Sanghyup Park, Kyung Hee University; Dongkyun Seo, Kyung Hee University; Jihong Park, Kyung Hee University

BACKGROUND: While most weight bearing sports activities accompany joint pressure loading, a cross-sectional comparison in sports with or without rotational joint loading would provide insight into early detection in joint degeneration. While time (aging) is the contributing factor, an interval assessment (e.g., 12 months) would be a surrogate of a process of an adaption of cartilage morphology. PURPOSE: To prospectively compared femoral cartilage cross-sectional area (CSA) morphology across Archery, Badminton, Taekwondo, Tennis players and non-athletic individuals over two years. Methods: A total of 139 individuals, categorised by four groups (30 Archery, 42 racquet sport—Badminton and Tennis, 36 Taekwondo players, 31 non-athletic individuals) were studied between the first- and second-year measurements. After taken demographic information (age, height, weight, body mass index—BMI, dominant leg, and athletic careers) and functional outcomes of knee, subjects had a 20-min unloading period (seated with knees fully extended) to minimise effects of preceding weight bearing on the femoral cartilage CSA. Femoral cartilage CSA images on each side were obtained at the first- and second-year measurements using ultrasonography, then manually segmented to calculate the femoral cartilage CSA. Femoral cartilage CSA were nomalised by BMI (mm2/kg/m2). To test femoral cartilage CSA between groups over time, a two-way (group × time) analysis of variance and Tukey-tests were performed on each side separately (α=0.05). Cohen's d (d) was calculated where statistical differences existed. RESULTS: The right side of the femoral cartilage CSA was different (group × time: F3,135=20.05, p<0.0001). At first year, racquet sport players (3.81

mm2) had a greater femoral cartilage CSA than Archery players (3.03 mm2, p<0.0001, d=0.6) and non-athletic individuals (3.09 mm2, p<0.0001, d=0.6); Taekwondo players (3.83 mm2) had a greater femoral cartilage CSA than Archery players (3.03 mm2, p<0.0001, d=0.7) and non-athletic individuals (3.09 mm2, p<0.0001, d=0.6). At second year, Taekwondo players (3.88 mm2) showed a reduction in femoral cartilage CSA relative to the first year (3.44 mm2, p=0.001, d=0.7). The left side of the femoral cartilage CSA was different (group × time: $F_{3,135}=3.88$, p=0.011). At first year, racquet sport players (3.68 mm2) had a greater femoral cartilage CSA than Archey players (3.01 mm2, p=0.002, d=0.7) and non-athletic individuals (3.09 mm2, p=0.01 d=0.6); Taekwondo (3.63 mm2) players had a greater femoral cartilage CSA than Archey players (3.01 mm2, p=0.0001, d=0.8) and non-athletic individuals (p=0.001, d=0.7). At second year, Taekwondo players (3.63 mm2) reduced to relative the first year (3.36 mm2, p=0.001, d=0.6). CONCLUSIONS: A femoral cartilage CSA reduction at both sides in Taekwondo at the second year might also be attributed to sports-specific characteristics (e.g., contact combat sport) relative to Archery and racquet sports.

P1.48-O: Investigating regional flexion relaxation phenomenon changes in lumbar muscles under delayed onset muscle soreness

Julien Ducas, Université du Québec à Trois-Rivières; Alvaro Pano-Rodriguez, Department of Human Kinetics, Université du Québec À Trois-Rivières, Trois-Rivières, Canada.; Guillaume Vadez, Department of Human Kinetics, Université du Québec À Trois-Rivières, Trois-Rivières, Canada.; Jacques Abboud, Université du Québec à Trois-Rivières

BACKGROUND AND AIM: The flexion relaxation phenomenon (FRP) refers to the reduction of muscle activity in the lumbar erector spinae muscles when the trunk is fully flexed. Some individuals with chronic low back pain have shown altered FRP, indicating its potential as a biomarker for this condition. However, there is considerable variability in reported results, likely stemming from chronic low back pain confounding factors and assessment methods (bipolar EMG at different vertebral level). To mitigate this variability, experimentally induced pain can reduce variability by controlling those confounding factors, while high-density surface electromyography (HDsEMG) enhances precision and enables spatial mapping for a more comprehensive understanding of lumbar erector spinae muscle behavior. Notably, using HDsEMG, delayed onset of the FRP in the cranial region of the erector spinae muscle in individuals with lower back pain compared to healthy participants was observed [1]. Despite this observed regional delay in FRP onset, the impact of pain on the magnitude of FRP within different lumbar regions remains unknown. The aim of this study is to investigate how lumbar pain, induced with delayed onset muscle soreness (DOMS), influences the magnitude of the FRP regionally. Methods: This study involved twenty healthy adults. Participants underwent five trunk flexion relaxation contractions in two sessions. The first session occurred without DOMS, while the second occurred 24-36 hours after inducing DOMS. To evaluate DOMS induction, pain, soreness, maximal voluntary contraction, and pressure pain threshold in the lumbar muscle were assessed. During the flexion-relaxation contractions, muscle activation strategies of the left and right lumbar erector spinae were recorded using HDsEMG (two grids of 8x8 electrodes). The flexion/relaxation ratio characterized the magnitude of FRP, calculated on each channel of both grids using 1 second of maximal root mean square muscle activity during

flexion and relaxation. Contraction phases were identified using 3D kinematics markers on the lumbar and hip regions. Repeated measure ANOVA was conducted to assess the extent of FRP occurrence (mean ratio for all channels) and its location using centroid coordinates (spatial distribution of FRP ratio values on the grid) between the two sessions. RESULTS: Preliminary findings (n=10) found a cranial shift in FRP with DOMS on the left side only (Left p=0.049; Right: p=0.272). However, no significant difference was observed on the extent of FRP occurrence (Left: p=0.710, Right: p=0.879). CONCLUSION: These preliminary findings suggest that DOMS-induced pain did not increase overall FRP in the erector spinae. Rather, it prompted a shift of FRP toward cranial areas, while reducing its caudal presence. Yet, these findings are still preliminary and require further confirmation with the complete sample size (n=20).[1] C Murillo et al., Scientific reports 9 (1), 15938 (2019).

P1.49-O: Evaluation of Muscle Electrical Activity in Patients with Myofascial Pain Syndrome Using Surface Electromyography

Na Li, West China Hospital of Sichuan University; Qian Wang, West China Hospital of Sichuan University; Chenqi He, West China Hospital of Sichuan University; Jiayuan He, West China Hospital of Sichuan University; Ning Jiang, West China Hospital of Sichuan University

Subject: Myofascial pain syndrome (MPS) is a common health problem characterized by the presence of myofascial trigger points (MTrP). However, the changes in neuromuscular functions incurred by MPS are still well-understood. The purpose of this study was to compare the differences in muscle electrical activity between the painful (P) and non-painful (NP) sides in patients with unilateral MPS and to verify the feasibility of surface electromyography (sEMG) for assisting in MPS assessment. Methods: Forty patients with unilateral lumbar MPS were recruited via the outpatient department of West China Hospital Sichuan University from October 2022 to October 2023. A sEMG system was used to record the sEMG signals of both sides of the erector spinae muscles. Then, the subjects conducted six trunk extension trials. Each trial was a 5-second maximal voluntary contraction with a 5-second rest period in between. Six time-domain features of sEMG were extracted, namely, root mean square (RMS), mean absolute value (MAV), integrated EMG (iEMG), and waveform length (WL). Additionally, the frequency domain features used are the median frequency (MDF) and mean power frequency (MPF). RESULTS: The time-domain features on the painful side were significantly higher than those on the non-painful side (RMS, P: 75.4 ± 34.1, NP: 63.4 ± 24.9, p < 0.001; MAV, P: 59.3 ± 26.8, NP: 49.6 ± 19.5, p < 0.001; iEMG, P: 11854.6 ± 5352.0, NP: 9923.6 ± 3898.9, p < 0.001; WL, P: 8809.9 ± 4161.9, NP: 7613.6 ± 3421.0, p = 0.001). Additionally, there was no difference in the frequency-domain features between the painful side and the non-painful side (MPF, P: 111.4 ± 21.2, NP: 113.0 ± 22.7, p = 0.478; MDF, P: 91.8 ± 20.8, NP: 92.5 ± 22.3, p = 0.758). CONCLUSION: : Our results indicated that MPS likely leads to abnormal time-domain features of sEMG, while not in frequency-domain features. These preliminary results demonstrated the potential feasibility of using sEMG as a tool for assessing the neuromuscular function of MPS.

P1.50-P: Gait analysis for support in diagnostics in neuromuscular disorders

Nicole Voet, Radboudumc/ Klimmendaal

In rehabilitation medicine, instrumented gait analysis was developed to assist in clinical decision-making to optimise treatment to improve walking in patients with neuromuscular diseases (NMD) and complex gait problems. In instrumented gait analysis, quantitative data of the gait cycle is collected: kinematics, kinetics and electromyography.We recently applied gait analysis in two cases to assist the neurologist in the diagnostic process: a patient with nemaline myopathy and polyneuropathy, respectively. In both patients, an accurate diagnosis could not be found based on the symptoms they reported, despite a thorough analysis by the neurologist. Instead, the symptoms were caused by the compensations patients used to optimise walking and not directly by the health condition itself. Through instrumented gait analysis, the direct impact of a health condition on the gait pattern can be distinguished from compensations. This can be an asset in finding the correct diagnosis, especially in NMD patients with complex gait problems or multiple health conditions. In patients with abnormal gait patterns, the complaints are not always the direct result of the primary problem; they may also result from compensations, secondary problems or a yet undiagnosed underlying condition. When there are complaints during walking, it may be valuable to have the rehabilitation physician perform a gait image analysis in the diagnostic phase. This can identify the primary problem, shorten diagnostics and optimise treatment.

P1.51-P: Exploring the Biomechanical Impact of Chronic Ankle Instability on Cutting Movements: a systemic review

Teerapat Laddawong, Waseda University, Japan; Hiromi Saito, Graduate School of Sport Sciences, Waseda University, Japan; Toshiaki Soga, Graduate School of Engineering and Science, Shibaura Institute of Technology, Saitama, Japan; Norikazu Hirose, Faculty of Sport Sciences, Waseda University, Japan

This review investigates lower limb biomechanics during side-cutting movements in individuals with chronic ankle instability (CAI). Studies from PubMed, Scopus, Web of Science, and SPORTDiscus up to 2023 were examined, focusing on case-control studies with subjects exhibiting CAI or recurrent ankle sprains. Inclusion criteria comprised chronic, functional, or mechanical instability, with primary outcomes including joint angle, ground reaction force (GRF), and muscle activation during cutting. Fourteen articles met the criteria, assessed for quality using a modified Downs and Black Checklist. CAI individuals exhibited distinct biomechanical alterations, including joint angle deficits, increased ankle inversion, abnormal sagittal motion, and altered kinetics and muscle activities during cutting tasks. These findings highlight the intricate biomechanical adaptations in CAI individuals, suggesting potential compensatory mechanisms and neuromuscular compromise.

P1.52-P: Relationship between fibula motion characteristics and knee joint during walking.

Akihiro Yamashita, The University of Electro-Communications; Tsutomu Fukui, Bunkyo Gakuin University; Kazuyuki Mito, The University of Electro-Communications

INTRODUCTIONDue to its position and structure in the body, the fibula has almost no role in compressive stress on the physiological axis and is said to be unrelated to load. But the lower leg transmits the impact of walking ground above the knee joint. Since a shock-absorbing effect occurs throughout the lower limb when grounded, it may have a similar function between the tibia and fibula. The position of the fibula relative to the tibia affects the knee joint and ankle joint, but its dynamics are still largely unknown. Therefore, in this study, by measuring the fibular dynamics during walking in relation to the tibia, we will elucidate a part of the fibula function by examining the movement of the fibula relative to the tibia during walking and examine whether intervention on the fibula is useful for knee joint treatment because of the influence of the fibula function on the joint movement of the knee joint. METHODSThe subjects were 16 healthy adult males aged 18 to 40 who had a history of lower limb surgery, orthopedic disease within the past 1 year, and no pain. The measurement operation was a stationary standing and walking, and the subject was instructed to step on the floor reaction force meter on the fourth step on a 10 m straight road. The measurement instrument used a 3D motion capture system consisting of 12 MX cameras, and the measurement sampling frequency was 100 Hz. A total of 45 infrared reflective markers with a diameter of 14 mm were affixed to the subjects' bodies. Segments were created using the arithmetic processing software Body Builder, and the angles of the femur, tibia, and fibula in absolute space were calculated. Correlation analysis was performed using the amount of angular change of the fibula with respect to the tibia and the amount of angular change of the tibia relative to the femur as output variables. Results AND DISCUSSIONThe fibula changed position relative to the tibia when walking. We also found that the phenomenon during the loading response correlated with the knee joint of the coronal plane and the horizontal plane at the same time. Since the time when the fibula moves during walking is like the time when the ankle joint moves, it is expected to be affected by talus pulleys. Previous studies have shown that when the lower leg muscle was resected and then dorsiflexed from the median position with a load applied, the malleolus was displaced backwards. The movement of the fibula is thought to change its position due to joint structure and muscle contraction because the anterior displacement of the outer malleolus was also observed in this experiment. CONCLUSIONSIt was predicted that the fibula moves independently of the tibia to absorb the impact applied to the knee joint by performing a combination of coronal, sagittal, and horizontal planes. These results suggest that the observation of peroneal dynamics can be used as an index to predict knee joint rotation during walking.

P1.53-P: High-density surface electromyography feedback improves the recruitment of the peroneus longus muscle in individuals with chronic ankle instability

Guillermo Mendez-Rebolledo, Universidad Santo Tomás; Eduardo Martinez-Valdes, University of Birmingham

Context: People with chronic ankle instability (CAI) have inhibition of the posterior compartment of the peroneus longus. However, it is unknown if any intervention can restore regional activation of this muscle. One possible solution is high-density surface electromyography (HD-sEMG) feedback.Purpose: This study aimed to determine whether individuals with CAI can activate the peroneus longus compartments with HD-sEMG feedback to the same extent as those without CAI and HD-sEMG feedback use. Methods: Sixteen

volunteers were involved in the CAI group, and another 16 volunteers were part of the healthy group (No-CAI). All Participants were given 20 minutes to learn HD-sEMG feedback (familiarization protocol) and instructed to shift the center of gravity in the peroneus longus muscle. They performed ankle eversion at 30% and 70% maximum voluntary isometric contraction (MVIC), with adjustments to activate specific muscle compartments (Figure 1). After 5 minutes of rest, the HD-sEMG feedback training protocol was executed. The center of mass (COM) and the sEMG amplitude at each compartment (anterior and posterior) of the peroneus longus were recorded during ankle eversion at 30 and 70% of their MVIC, both with and without visual feedback on the spatial distribution of peroneus longus (Figure 1). Each participant completed 8 randomly eversion movements to mitigate learning bias. A thwo-way ANOVA (group x feedback condition) with repeated measures was applied. RESULTS: A significant interaction effect between group and feedback condition was observed ($F1, 31 = 12.54$; $P = 0.0013$) during ankle eversion only at 70% MVIC. The posterior compartment sEMG amplitude in the CAI group trained with HD-sEMG feedback was significantly higher than without HD-sEMG feedback ($P = 0.0010$) and was similar to the No-CAI group without HD-sEMG feedback ($P = 0.9935$). The COMx in the CAI group trained with HD-sEMG feedback was significantly shifted in the anteroposterior direction compared to the group without HD-sEMG feedback ($P = 0.0012$). CONCLUSION: : The use of HD-sEMG feedback during ankle eversion allows activation of the posterior compartment of the peroneus longus to the same extent as healthy people not using feedback devices. HD-sEMG-based topographic maps can be used as a feedback training tool to restore motor control, although their long-term effectiveness needs to be investigated through longitudinal and prospective studies.LeyendFigure 1: Representation of high-density surface electromyography electrode (13 x 5 electrodes; 1 mm diameter electrode; 8 mm interelectrode distance) placement over participants' peroneus longus muscle. Surface electrodes arranged in 5 columns which represented the anterior (columns 1/2) and posterior (columns 4/5) compartments. Representation of the testing setup. Participants were instructed to shift the position of the center of gravity of the HD-sEMG map towards the posterior compartment of peroneus longus. For this, a researcher palpated the posterior region of the electrode mesh to induce an artifact in the sEMG signal –represented by hot colors in the activation map– that would allow the participant to recognize the activation of posterior compartment of the peroneus longus.

P1.54-P: The intervention combining motor imagery of knee extension and transcranial magnetic stimulation facilitates corticospinal excitability of the tibialis anterior muscle, but not the rectus femoris muscle.

Keiichi Ishikawa, The University of Tokyo; Naotsugu Kaneko, University of Tokyo; Kimitaka Nakazawa, The University of Tokyo

Introduction Motor imagery (MI) is the mental simulation of movement and can modulate corticospinal excitability (CSE). MI is used in rehabilitation, but its effects have been suggested to vary depending on the MI task and target muscle. Our recent study found that MI of knee extension facilitates CSE of the rectus femoris muscle (RF), which is the agonist muscle, and tibialis anterior muscle (TA), which is not recruited in the knee extension. As a continuation of the study, we propose the intervention combining MI with transcranial magnetic stimulation

(TMS) to induce neuroplastic changes. This study aimed to investigate the effects of the intervention (MI+TMS) on CSE of the lower limb muscles. Method Twenty healthy individuals participated in this study. Participants were seated on a chair and electromyographic (EMG) activity was recorded from the right side of the RF, biceps femoris (BF), TA, and soleus (SOL) muscles. CSE was evaluated by motor evoked potential (MEP) amplitudes obtained by TMS to the primary motor cortex. The stimulation position was the hotspot of RF, and the intensity of TMS was set at 1.2 times the resting motor threshold of RF for both intervention and evaluation. In MI+TMS, participants were instructed to avoid any muscle contraction and to repeat the resting and MI states every 4 seconds. In the resting state, they were asked to relax without internal imagery. In the MI state, they performed MI of maximal effort knee extension, and TMS was applied during MI. MI and TMS were repeated 120 times, and the duration of MI+TMS was 16 minutes. Evaluations of CSE at rest were performed before the intervention (Pre), immediately after the intervention (Post 0), 15 minutes later (Post 15), and 30 minutes later (Post 30). The average peak-to-peak amplitude of 12 MEPs at each time point was calculated. The Friedman test and Steel post hoc test were used to compare MEP amplitudes between Pre and Post MI+TMS. Results MEP amplitudes of RF, BF, and SOL after MI+TMS were not significantly different from those at Pre at any time point (p > 0.05). On the other hand, MEP amplitude for TA was significantly larger at Post 0 and Post 15 than at Pre (p < 0.05). Discussion The MI task in this study was a knee extension movement and expected to facilitate CSE of RF, which mainly acts for knee extension movement. However, there was no significant change in CSE of RF after MI+TMS. On the other hand, the intervention enhanced CSE of TA at Post 0 and Post 15. Although our previous study indicated that MI of knee extension facilitated CSE of RF and TA, in this study, the effect of MI+TMS was apparent only in the TA muscle. These results suggest that CSE of TA is more susceptible to neuroplastic changes than that of RF. Our findings may contribute to the development of neuro-rehabilitation methods to restore motor function by inducing plastic changes in the central nervous system.

P1.55-P: Motor Imagery then Action Observation as a Treatment for Stroke Patients with Distal Upper Limb Flaccidity- Preliminary Results in Normal Adults

Hsin-Min Lee, I-Shou University; Chen Wen Yen, Department of Mechanical and Electro-mechanical Engineering, National Sun Yat-sen University; Jia Yuan You, Department of Physical Therapy, I-Shou University; Hung Chia Wu, Department of Physical Medicine and Rehabilitation, E-Da Hospital

Introduction: Poor motor recovery in the upper extremity (UE) following a cerebral stroke significantly compromises the independence of the patient's life and places a substantial burden on both the patient and their caregivers. Recent scientific evidence indicates that action observation (AO), motor imagery (MI), and mirror therapy (MT) can effectively enhance UE motor function in stroke patients. These interventions can be applied even when patients have limited or no ability to move their limbs, making them suitable for individuals with flaccid hands post-stroke. However, these treatments have not been classified as essential; rather, they are often regarded as adjuvant therapies for improving hand flaccidity following a stroke. One key reason for this might be their limited bidirectional influences on both the central and peripheral components of the motor system (Figure 1 illustrates the distinctions among these training

modes concerning the direction of influences over the peripheral and central components of the motor system).Aim& Methods: To address this gap, we have developed an integrated treatment platform capable of delivering AO, MI, and a novel training mode (MI then AO) that establishes a connection between central motivation and peripheral visual stimulation. These modes can also be adjusted to tune the velocity and range of movement videos, making them adaptable to the specific training needs in clinical settings. In the preliminary study, we recruited 20 healthy participants to record EEG signals from the sensorimotor cortex (C3, Cz, and C4). We analyzed the event-related desynchronization (ERD) of the mu rhythm under a carefully designed paradigm to evaluate the effects of these three distinct training modes. RESULTS: The initial findings revealed a noticeable increase in the overall ERD area in the C4 channel compared to C3 and Cz channels across all three modes (all P < 0.001). During the P3 phase (2-4 seconds), we identified a significantly higher activation in the C4 ERD area during the MI then AO mode (P<0.01), which suggests that the novel training mode induces a greater level of brain activity. Conclusion: Our findings demonstrate that the novel training mode enhances cortical activation in specific brain areas in normal participants. Moving forward, we aim to extend the implementation of our treatment strategy to clinics, with the hope that our innovative approach will prove beneficial for patients experiencing distal UE flaccidity.

P1.56-P: Development of an Integrated Digital Movement Therapy Platform for Mirror Therapy, Action Observation and Motor Imagery

Stroke can have a profound impact on an individual's motor function, often leading to muscle weakness and limited mobility. However, a cognitive treatment approach, which includes motor imagery, action observation, and mirror therapy, has shown promising results in improving the motor function of stroke patients. Motor imagery involves mentally visualizing movements and actions, activating neural pathways associated with physical tasks. Stroke survivors can mentally rehearse movements they struggle to perform, effectively retraining their brains to regain motor skills. Action observation complements this by having patients observe others performing tasks, enhancing their understanding and motivation to relearn movements. Mirror therapy uses a reflective surface to create the illusion of a functional limb, encouraging the affected limb to mimic the movements of the unaffected one. This visual feedback stimulates brain activity and promotes the recovery of motor function.Together, these cognitive techniques harness the brain's neuroplasticity, fostering the rewiring and strengthening of damaged neural connections. Stroke patients can regain muscle strength, coordination, and mobility, ultimately regaining independence and enhancing their quality of life. This holistic approach to rehabilitation offers hope and tangible progress for those on the journey to recovery.

P1.57-P: Relationship between rotational movement patterns of the pelvis and each thoracic vertebral level during gait in healthy adults

Kai Iida, Bunkyo Gakuin University; Tsutomu Fukui, Bunkyo Gakuin University; Kazuyuki Mito, The University of Electro-Communications

Background and aimsDuring gait, the thorax exhibits a coordinated movement pattern with pelvic rotation, resulting in rotation in the opposite direction of the pelvis to maintain

equilibrium. However, we speculate that not all thoracic vertebrae rotate identically in the opposite direction to the pelvis during gait; instead, the direction of rotation differs at each thoracic vertebral level. Therefore, we aimed to examine the relationship between pelvic rotation during gait and the rotational movement patterns at each thoracic vertebral level. Clarifying these relationships will improve the current understanding of trunk motor control necessary for efficient gait and will serve as an indicator for gait evaluation. MethodsThe participants were 17 healthy adult males (age 23.0 ± 1.5 years, height 1.72 ± 0.05 m, weight 65.2 ± 8.7 kg). The measurement device used was a VICON system, a three-dimensional motion analyzer, and the Visual 3D software was used for analyses. A total of 46 markers were attached to the participants by modifying an IOR gait model. The trunk was divided into four segments: T2, T4, T7, and T10; a marker was attached to each thoracic spinous process (T2, T4, T7, and T10), along with two other markers that formed a triangle under the spinous processes. The measurements were averaged over five runs of barefoot gait at the optimal speed, and the measurement interval was 100% normalized to a total of three steps from the right heel contact to the second left heel contact. Time series data of the pelvic and thorax segments, T2, T4, T7, and T10 rotation angles (+; left rotation) during the normalized gait cycle were calculated, and the relationship between the pelvic and thorax segments and T2, T4, T7, and T10 was examined using cross-correlation coefficients. The significance level was set at <5%. ResultsThe time series waveform of the rotation angle (Fig.1) showed a different waveform trend at each thoracic vertebral level. The correlations between the pelvic segment and each segment were as follows: thorax segment (r = -0.507), T2 (r = -0.345), T4 (r = 0.290), T7 (r = 0.931), and T10 (r = 0.813). The correlations between the thorax segments and each thoracic spine were as follows: T2 (r = 0.976), T4 (r = 0.657), T7 (r = -0176), and T10 (r = 0.053). CONCLUSION: The lower thoracic vertebral levels (T7 and T10) had ipsilateral and similar rotation patterns to the pelvis, whereas the upper thoracic vertebral level (T2) had contralateral and different rotation patterns; however, T4 showed no consistent relationship to the pelvis. The thorax and upper thoracic vertebrae levels (T2 and T4) exhibited similar rotation patterns. These findings suggest that the lower thoracic vertebral level rotates ipsilaterally in coordination with the pelvis and that counter-rotational motion to the pelvis may occur at the upper thoracic vertebral level. The upper and lower thoracic vertebral levels may have different motor controls during gait in healthy adults.

P1.58-P: The effect of Scapulothoracic Motion Restriction on Glenohumeral Muscle Activation: Implications to Injury

Vassilios Vardaxis, Des Moines University; Angela Palant, Des Moines University; Taylor Alexander, Des Moines University; Royal Cole, Des Moines University; Micah Thatcher, Des Moines University; Traci Bush, Des Moines University

Background and Aim: The shoulder joint is highly complex, requiring coordinated motion at the glenohumeral (GH), scapulothoracic (ST), acromioclavicular (AC), and sternoclavicular (SC) joints. Prior research has proposed that scapular dyskinesia can lead to injury by disrupting the scapulohumeral rhythm (SHR). The scapula can be restricted by endogenous pathology, through nerve injuries or muscle dysfunction, or by exogenous factors, such as body positioning, PPE, tight or restrictive clothing, and the use of some tools (e.g., backpacks, harnesses, hosing). These restrictive scenarios are commonly encountered in the workplace or

during activities of daily living. The aim of this project was to investigate the effect of scapular dyskinesia, imposed by applying antero-inferior compression to the scapula, on both task-specific and overall muscle activation profiles. Methods: Fifteen right-handed adult males without history of shoulder pathology performed activities of daily living (ADLs) using their dominant arm, with and without a custom-made scapula restriction device. The selected ADLs performed by each subject were: straight-arm scaption, flexion, and abduction (simple), and combing hair front-to-back, pouring water from a pitcher, and removing and replacing an object from a shelf using an anterior and a cross-body reach (complex). Surface electromyography (sEMG) data was recorded on 11 muscles; anterior, middle, and posterior deltoid (ADel, MDel, PDel), upper and lower pectorals (UPec, LPec), upper and lower trapezius (UTrap, LTrap), latissimus dorsi (LDor), infraspinatus (InSp), biceps brachii (BiBr), and triceps long head (TrLh). Infrared motion-capture technology was simultaneously used to track 3-D movement of the subject's trunk, scapula, and dominant arm. Muscle activation patterns were demeaned, band-pass filtered (10-450 Hz), and RMS processed using MATLAB and normalized to percent maximum voluntary contraction (%MVC) produced during isometric/isokinetic tasks on a Cybex dynamometer. MANOVAs were used to assess differences in level of sEMG activation between restriction conditions, followed with post-hoc univariate F tests. Results and Discussion: There was significantly higher sEMG muscle activation in the restricted condition across tasks (simple p<0.003, η2>0.83; complex p<0.024, η2>0.68). The post-hoc univariate test indicated higher sEMG activation: for MDel, PDel, and LDor during abduction (p<0.009; partial η2>0.39); for UPec and LDor during flexion (p<0.009; partial η2>0.21); for MDel and LDor during scaption (p<0.019; partial η2>0.33); for ADel, MDel, UPec and ADel, UPec during anterior (p<0.017; partial η2>0.35) and cross-body (p<0.002; partial η2>0.50) object removal and replacement, respectively; for MDel, LDor, and BiBr for hair combing (p<0.025; partial η2>0.50); and for Adel and UPec for water pouring (p<0.005; partial η2>0.34). Interestingly the InSp showed a statistically significant decrease in activation during cross-body object placement and water pouring (p<0.01). CONCLUSIONS: Restriction of ST motion causes a compensatory increase in activation of several muscles crossing the GH joint, which may predispose individuals to increased rates of shoulder pathology when performing tasks in the upper extremity workspace. These findings can provide a predictive foundation for injury risk determination and medical management in individuals with scapular dyskinesia or exogenous ST motion restriction.

P1.59-P: Closed-loop transcutaneous vagus nerve stimulation (tVNS) approach for facilitating motor learning and rehabilitation with neuromodulation [Poster Award]

Joshua Posen, Georgia Institute of Technology; Milka Trajkova, Georgia Institute of Technology; Nathaniel Green, Georgia Institute of Technology; Koki Asahina, Georgia Institute of Technology; Chanyeong Choi, Georgia Institute of Technology; Woon-Hong Yeo, Georgia Institute of Technology; Minoru Shinohara, Georgia Institute of Technology

Applying afferent vagus nerve stimulation via implanted electrodes during motor training can either enhance or impair motor recovery after stroke and motor learning in rodents, depending on the timing of stimulation. The stimulation modulates neurotransmitters in the cortex, such as acetylcholine and norepinephrine, due to the resultant activation of the brainstem. In a

translational study employing noninvasive stimulation of the auricular branch of the vagus nerve in humans, random application of transcutaneous vagus nerve stimulation (tVNS) during training slowed motor adaptation in healthy adults (St. Pierre & Shinohara, J Neurophysiol, 2023), as reported in healthy mice. Rodent studies also suggest that motor learning or recovery enhancement can be expected if brief (500 ms) vagus nerve stimulation is applied immediately after only successful motor trials. No commercially available system can replicate such a closed-loop operation of brief tVNS and movement quality. Moreover, the effectiveness of brief tVNS on acutely inducing neuromodulation is unknown. Additionally, the available surface electrodes for tVNS on the outer ear are bulky and unsuitable for training involving whole-body or head movement. Our objective was to develop a closed-loop tVNS system for human motor training and explore the improvement of associated electrodes and procedures. A commercially available tVNS device was customized to be preprogrammed for an appropriate set of stimulation parameters and triggered by an external voltage input. By creating an Android app and a relay unit between the phone and the tVNS device, we enabled the tVNS device to be triggered wirelessly via Bluetooth. It allowed assessors to wirelessly send and record a tVNS trigger cue by tapping on the phone when they recognized a successful movement trial. We also developed a software toolkit for automated movement classification from markerless videos using machine learning, which identified successful backward walking steps with 88% accuracy in 28 older adults (73-93 years old) with and without Parkinson's disease. To improve tVNS electrodes, we developed thin film-like electrodes, which reduced the mass by 75% (from 0.29 g to 0.07 g) and the uncomfortableness of wearing electrodes while maintaining acceptable impedance (44k ohm vs. acceptable 500k ohm). To assess the effectiveness of brief tVNS in acutely inducing neuromodulation, we used a screen-based eye-tracker to analyze the pupil size, which is known to be increased with activation of the locus coeruleus in the brainstem. In our preliminary assessment, brief (500 ms) tVNS caused a transient increase in pupil size by 6.5% (4.8% - 8.3%), on average, in four young adults. Collectively, the study successfully created a closed-loop tVNS system and an acute neuromodulation assessment procedure and demonstrated their proof of concept and feasibility.Funding: McCamish Parkinson's Disease Innovation Program at Georgia Tech and Emory University

P1.60-Q: Decoding Prime Mover Motor Units Enables the Intuitive Control of the Paralyzed Hand after Spinal Cord Injury

Dominik Braun, Friedrich-Alexander-Universität Erlangen-Nürnberg (FAU); Daniela Souza de Oliveira, Friedrich-Alexander University Erlangen-Nürnberg; Matthias Ponfick, Krankenhaus Rummelsberg GmbH, Querschnittszentrum Rummelsberg; Jonas Walter, Friedrich-Alexander-Universität Erlangen-Nürnberg (FAU); Nico Weber, Friedrich-Alexander-Universität Erlangen-Nürnberg (FAU); Maria Pozzi, University of Siena; Leonardo Franco, University of Siena; Gionata Salvietti, University of Siena; Jörg Franke, Friedrich-Alexander-Universität Erlangen-Nürnberg (FAU); Domenico Prattichizzo, University of Siena; Alessandro Del Vecchio, Friedrich-Alexander Universität, Erlangen-Nürnberg,

The intricate movements of the human hand are governed by a neural network involving large number of neurons in the brain and spinal cord. Surface electromyography (sEMG) records electrical currents generated by muscle fiber contractions. Recent advancements in high-

density sEMG (HD-sEMG) analysis allow precise identification of motor unit firing activities. Individuals with motor complete spinal cord injuries (SCI, AIS A & B) exhibit residual motor units responsible for finger movements. Our research aims to decode prime mover motor unit ensembles using online decomposition and connect these ensembles to mechatronic systems to assist individuals living with motor complete SCI in their daily lives in real-time. This study aimed to investigate the performance of our approach in achieving precise and intuitive control over rehabilitative systems with the goal of restoring grasp functionality.In our study, we have applied 128 channels of HD-sEMG on the forearms of individuals with motor complete SCI (n=4, injury level C5-C6). Using our software NeurOne, we performed real-time digitalization of motor unit activity. The HD-sEMG signals were decomposed into individual motor units using convolutive blind source separation. The decoded motor units were classified into the prime mover motor unit ensembles afterwards. NeurOne converted the decoded spiking activity of the prime mover motor units into smooth activation signals by utilizing a physiologically driven motor unit twitch. The resulting smoothed activation signals for each prime mover ensemble were then used to control different mechatronic and virtual systems. The first experiment was to enable paralyzed individuals to track the movements of a virtual hand with a second virtual hand under their control. In addition, in a second experiment, the NeurOne output enabled control of an artificial sixth finger attached to the paralyzed user's wrist and facing the palm for simple grasping movements. In addition, the NeurOne system was connected to a neuroorthosis covering the thumb and index finger in a third experiment, which was attached to the paralyzed hand equipped with HD sEMG electrodes. Task-specific protocols were created for both mechatronic systems, in which the test subjects had to perform various tasks with different objects. The performance assessments were carried out with and without the support of the respective systems to enable a comparative analysis.Paralyzed individuals were able to use the control signal provided by NeurOne to follow a virtual hand intuitively and accurately. In combination with mechatronic systems, NeurOne enabled people with complete motor SCI to grasp and lift objects. Some of these tasks were impossible without mechatronic support, such as removing the lid from a bottle, demonstrating NeurOne's potential as an intuitive assistive device control to enhance the independence of the paralyzed.

P1.61-Q: The Effects of Combined Use of Robotic Control on the Ankle Joint and Electrical Stimulation Therapy

Ayaka Hanaki, Hiroshima University Graduate School of Biomedical and Health Sciences; Shunpei Kishida, Hiroshima University Graduate School of Biomedical and Health Sciences; Nozomi Maeda, Hiroshima University Graduate School of Biomedical and Health Sciences; Makoto Takahashi, Hiroshima University; Eiichiro Tanaka, Waseda University; Louis Yuge, Hiroshima University; Kei Nakagawa, Hiroshima University

One of the causes of abnormal gait in patients with cerebrovascular disorders is dorsiflexion impairment of the ankle joint. Electrical stimulation therapy (ES) is often used for the treatment of gait impairment. On the other hand, the use of robots has been advanced (i.e., an ankle assisted walking robot, RE-Gait®). It was hypothesized that combining ES and robotic control on the ankle joint may enhance the treatment effectiveness compared to each intervention alone. Therefore, this study investigated the combined effects from the perspectives of ankle joint

angle, minimum toe clearance (MTC), and electromyogram (EMG) of TA muscles.Ten healthy adults participated in this study. They performed gait training (GT) under 4 conditions with wearing RE-Gait® on the right lower limb as follows; RE-Gait® and ES both inactive (OFF), ES only active (ES), RE-Gait® only active (RG), and both RE-Gait® and ES active (RG+ES). Measurements were taken following a protocol; barefoot walking (PREBF), RE-Gait® wearing only (PREGT), gait training under each condition (15 minutes after intervention, DURINGGT), and barefoot walking again (POSTBF). Kinematic data were measured at all time points, and EMG data were measured at PREBF and POSTBF. Each intervention time was 20 minutes, and the measurements were taken on four separate days with an interval of at least one day between each measurement. Short-term intervention effects before and after intervention were verified by comparing PREBF and POSTBF. The effects during intervention were examined by comparing PREGT and DURINGGT.Comparing PREGT and DURINGGT, RE-Gait® intervention (RG and RG+ES conditions) showed a significant increase in dorsiflexion angle and MTC. Comparing PREBF and POSTBF, no changes were observed in ankle joint angle under all conditions. However, in the three conditions except of the OFF condition, there was a significant increase in MTC. In the ES condition, peak amplitude of TA activity was significantly decreased, and peak latency was significantly decreased. In the RG+ES condition, there was a trend of decreased peak latency.Significant increases in kinematic data were observed during intervention in the RG condition, and EMG changes were observed in the ES condition. These results may suggest distinctive changes with each intervention alone, indicating different therapeutic effects. Additionally, in the RG+ES condition, the significant increase in kinematic data suggests a treatment effect similar to the RG condition, and the changes in TA activity indicate a therapeutic effect similar to the ES condition. These findings may suggest that combining ankle joint dynamic control and ES may exhibit the respective effects and potentially achieve a higher therapeutic effect.

P1.62-Q: Intramuscular coherence of the lower flexor muscles during robotic ankle-assisted gait training

Kei Nakagawa, Hiroshima University; Akari Ikeda, Hiroshima University; Eiichiro Tanaka, Waseda University; Louis Yuge, Hiroshima University; Makoto Takahashi, Hiroshima University

From the terminal stance to the pre-swing phase of the gait, the forefoot rocker function plays a crucial role in smooth energy utilization by generating plantar flexion torque. Subsequent dorsiflexion torque occurs in the swing phase to prevent toe dragging. These movements are essential for efficient walking; however, it is difficult to provide enough assistance using manual support or static orthoses alone. To address this issue, robotic walking rehabilitation devices have been developed. A robotic-controlled ankle-foot orthosis (rAFO) designed to support ankle dorsiflexion and plantarflexion movements has the potential to be effective in acquiring a proper gait pattern throughout the entire gait cycle. However, there is currently insufficient neurophysiological evidence to support its therapeutic effect. When assessing the function of the sensory-motor loop during gait, intramuscular coherence (IMC) in each frequency band from two parts of the tibialis anterior muscles is often used to determine if a common synaptic drive is present. Therefore, this study investigated whether the functioning of the sensorimotor loop was enhanced during the utilization of the rAFO from the pre-swing to the initial swing

phase.Seventeen healthy volunteers participated in this study. They engaged in a 15-minute session of robotic-assisted gait training using the rAFO on a treadmill at their comfortable speed. Robotic assistance was administered to facilitate rapid plantar-flexion during the pre-swing phase (after the heel offset) to generate push-off movement. Additionally, dorsiflexion assistance was provided during the initial swing phase to enhance toe clearance. Gait parameters and IMC of proximal and distal parts of the tibialis anterior muscles were measured before (pre), during, and immediately after (post) a 15-minute intervention.As a result, the trailing limb angle and step length were significantly enhanced during and post the session compared to the pre-session. In addition, the values of IMC in the beta frequency band were significantly different in the initial swing phase (F(2,32)=3.40, p<0.05, η2=0.18), and post-hoc tests revealed that the rAFO session significantly enhanced the IMC in the beta band compared with the pre-session (p<0.05). Comparing the behavioral and neurophysiological data, a significant correlation was found between IMCs in the beta and low-gamma frequency bands and the enhancement ratio of step length.These findings suggest that implementing robotic ankle assistance, incorporating both plantar flexion and dorsiflexion from the pre-swing to initial swing phase, may improve gait function with an enhancement of the functioning of the sensorimotor loop.

P1.63-R: Strength training and magnetomyography – a controlled study using optically pumped magnetometer [Poster Award]

Tim Brümmer, Hertie-Institute for Clinical Brain Research, University of Tübingen, Tübingen, Germany; Justus Marquetand, Department of neural dynamics and Magnetoencephalography, University of Tuebingen; Hongyu Lu, Hertie-Institute for Clinical Brain Research, University of Tübingen, Tübingen, Germany; Lukas Baier, Hertie-Institute for Clinical Brain Research, University of Tübingen, Tübingen, Germany; Haodi Yang, Hertie-Institute for Clinical Brain Research, University of Tübingen, Tübingen, Germany; Thomas Middelmann, Department of Biosignals, Physikalisch-Technische Bundesanstalt (PTB), Berlin, Germany; Christoph Braun, Hertie-Institute for Clinical Brain Research, University of Tübingen, Tübingen, Germany; Markus Siegel, Hertie-Institute for Clinical Brain Research, University of Tübingen, Tübingen, Germany

Muscle strength training induces neuromuscular adaptations, typically assessed through electromyography (EMG). Magnetomyography (MMG) captures these signals by quantifying the circular and concentric magnetic fields generated by the muscle's electrical currents, adhering to the Biot-Savart law. This study investigates the potential of MMG as a new contactless modality for recording neuromuscular signals, utilizing miniaturized quantum sensors, more specifically optically pumped magnetometers (OPM). The employed zero-field-OPM are based on a zero-field resonance caused by the Zeemann-effect and utilize laser light absorption of vaporized and spin-polarized alkali metal atoms to measure the magnetic field. The primary objective of this study is to test whether MMG can detect neuromuscular adaptations comparable to those, which are measurable using EMG.This study investigates the potential of MMG as a new contactless modality for recording neuromuscular signals, utilizing miniaturized quantum sensors known as optically pumped magnetometers (OPM). OPM are based on the Zeemann-effect and utilize laser spectroscopy to measure the wavelength changes of vaporized and spin-polarized alkali metals induced by the changing magnetic field. Simultaneous EMG

and OPM-MMG recordings were conducted on the right biceps brachii muscle in 12 healthy, untrained subjects during maximal voluntary contraction (MVC) and a 40% MVC muscle fatigue paradigm, lasting three minutes. Data collection encompassed three time points: pre-training, mid-training, and post-training over a 30-day strength training program, with six subjects undergoing training and an equivalent control group. Results revealed anthropometric enlargements of the biceps muscle of the trained, but not the non-trained control cohort. Both EMG and MMG revealed increasing signal amplitude (here, root-mean-square (RMS)) over the training period during the MVC- and fatigue-paradigms, with no concurrent alteration in frequency (here, Center of gravity, COG). A strong correlation could be determined between the RMS and COG of EMG and the three axes OPM-MMG-signals (Bx, By, Bz). Furthermore, three-dimensional visualization of time-series data was possible using a single OPM, a capability that is impossible using a single bipolar EMG.This study pioneers the first-ever performed longitudinal MMG, providing insights into the potentials and hurdles of OPM-MMG. The robust correlation between EMG and MMG suggests the capability of MMG in measuring the increasing neural drive resulting from training-induced neuromuscular adaptations. Our study paves the way for future longitudinal MMG studies, potentially enabling monitoring of physiological and pathological changes in sport science or neuromuscular diseases. The integration of OPM introduces a novel modality, showcasing their potential for three-dimensional visualization and potentially also enabling a complementary view of neuromuscular physiology.

P1.64-R: The Effect of Sporting Expertise on Motor Strategies under the influence of muscle fatigue

Emile Marineau, Université du Québec à Trois-Rivières; Julien Ducas, Université du Québec à Trois-Rivières; Jacques Abboud, Université du Québec à Trois-Rivières; Martin Descarreaux, Université du Québec à Trois-Rivières

Background: Lately, the performance of athletes, both novice and expert, has garnered significant attention by researchers, especially to explore the boundaries of human performance and the risk of musculoskeletal injury. Sporting expertise leads to the development of motor strategies within an athlete's motor system, which either enhance performance and/or minimize functional costs. On the other hand, an increased injury risk has been consistently reported among novice athletes. Consequently, it is plausible that the motor strategies used by experts may also have injury prevention potential. Motor strategies in sports performance is commonly assessed by the concept of motor variability (MV). MV refers to the fluctuations observed in motor performance across multiple repetitions of the same task. It can be assessed through muscle activity, motion, or forces generated during tasks. In sports, several investigations have assessed the impact of expertise on MV in different activities. Recently, we have conducted a scoping review about the effect of expertise on MV in sports gesture which included 53 studies (unpublished results). This review concluded that higher-skilled athletes tend to use less MV than lower-skilled ones while performing their sports without any constraint. Despite the recurring presence of muscle fatigue while practising multiple sports and the well-known alteration of fatigue on MV, to our knowledge, no studies have explored the effect of expertise in sport on VM in the presence this constraint. Objective: The aim of this study is to assess the impact of expertise on MV in the presence of muscle

fatigue in cycling. Methods: To answer this objective, 40 cyclists, including novices and experimented, will be recruited to pedal on a smart stationary bike. The MV of their lower limbs will be assessed during submaximal pedalling in two different contexts: without constraint, and with lower limbs muscle fatigue. Two instruments will be used to quantify participants' motor strategies: a 3D motion analysis system (OptiTrack) and a bipolar wireless surface electromyography system (Delsys). To quantify MV, metrics such as the coefficient of variation and muscle synergy, will be calculated on different biomechanical variables. These variables include kinematic parameters (range of motion, linear velocity, linear acceleration, angular velocity, and angular acceleration) and muscular activity parameters (amplitude and median frequency of the signal). Repeated-measures ANOVAs will be used to compare the effect of levels of expertise (novice and expert) and muscle fatigue on the MV metrics. Special attention will be given to strive for gender-balanced athlete groups, as our literature review reveals a significant gap in the study of female athletes.Research implications: By integrating muscle fatigue into this research protocol, it enables a deeper comprehension of how experienced athletes adapt their motor strategies to surpass their novice counterparts, even when faced with sub-optimal performance conditions. Future studies should investigate the effect of other constraints in sports like pain.

P1.65-R: Anaerobic power and kinematic characteristics during sliding are associated with performance in long-track speed skating.

Tomoki Iizuka, Kurosawa Hospital; Yosuke Tomita, Takasaki University of Health and Welfare; Koichi Irisawa, Department of Physical Therapy, Graduate School of Health Care, Takasaki University of Health and We

Background: Long-track speed skating requires significant mechanical output. Previous studies highlighted the importance of physical functions, including vertical jump height and anaerobic power. Studies also reported the significance of techniques like knee and hip joint angles. However, there has been no study that has comprehensively investigated the relationship between performance, physical function, and technical aspects. This study aimed to investigate factors influencing skating performance, considering both technical aspects and physical functions.Method: Participants were 23 high school and college speed skaters (13 males, average height 167.4±8.0 cm, weight 63.2±8.0 kg). Physical functions were evaluated with the vertical jump height, anaerobic power test using Power Max V III, and the Wingate test. Technical aspects were assessed during ice skating. Skaters started from a stationary position. Short-distance skaters (n=11) covered 500 m, and middle- and long-distance skaters (n=12) skated 1500 m at maximum power. The first lap was used as the performance indicator. The Inertial Measurement Unit (myoMOTION, Noraxon) was used for technical analysis, measuring hip and knee joint angles, and pelvic orientation. Pearson's correlation coefficient determined the correlation between lap time and physical function/technique. In Model 1, a single regression equation was created with the physical function variable showing the highest correlation coefficient as the independent variable and lap time as the dependent variable. In Model 2, multiple regression equations were developed, with lap time as the dependent variable and the physical function and technique variables with the highest correlation coefficients entered one by one as independent variables. The statistical significance level was

set at 5%. RESULTS: The physical function exhibiting the highest significant negative correlation coefficient with lap time was anaerobic power (r=-0.835, p<0.01). The technical outcome exhibiting the highest negative correlation coefficient with lap time was hip abduction angle at push-on (r=-0.623, p<0.01). The regression equation of the Model 1 was “lap time = 36.584 - 0.006 * anaerobic power” (R2=0.697, F=30.946, p<0.01, Figure 1 A). The regression equation of the Model 2 was “Lap time = 36.292 - 0.005 * anaerobic power - 0.084 * hip abduction angle (R2=0.809, F=42.393, p<0.01, Figure 1 B), where the standard partial regression coefficients were -0.700 (p<0.01) for anaerobic power and -0.361 (p<0.01) for hip abduction angle.Discussion: Model 2, which integrated both physical function and skating technique, showed superior predictive ability (R2=0.809) compared to Model 1 (R2=0.697). These findings underscore the significance of technique in skating performance. The highest correlation coefficient for technique in this study indicates that the hip abduction angle might be a crucial factor influencing speed skating time, independently of anaerobic power.

P1.66-R: The relationship between shank angular acceleration, hamstring muscle activation, and maximum speed during treadmill sprinting

Thiet Le, Niigata University of Health and Welfare

Purpose: Hamstring muscle strain injury (HSI) stands as the most prevalent non-contact muscle injury in sports involving sprinting. Previous research has suggested motion-dependent torque (MDT), arising from lower limb segment movements and their mechanical interactions, as a significant risk factor for HSI. MDT places increased demand on the hamstring muscles, particularly in the late swing phase of the running cycle. Notably, the shank angular acceleration (SAA), the largest component of MDT at both the hip and knee joints, has been suggested as a potential factor contributing to excessive strain and an overloading of the hamstring muscles during this phase. Consequently, enhancing control over SAA during the late swing could be instrumental in reducing the risk of HSI. However, the relationship between SAA and hamstring muscle activation remains unclear, and improving control over SAA may pose a challenge to maximum running speed. Therefore, the aim of our study was to clarify the pattern of SAA and examine its relationship with both hamstring muscle activation and the maximum speed within the swing phase of the running cycle in sprinting. Methods: Eighteen recreational players of various sports were recruited and gave their written informed consent to participate in this study. Each participant was instructed to perform a minimum of three successful treadmill sprints with maximum speed. Hamstring muscle activation and SAA were collected by employing wireless electromyography and inertial measurement units (IMU). Spearman’s rank correlation coefficient (r) was employed to determine the relationship between SAA during the swing phase, hamstring muscle activation, and maximum speed, using a significant level of 0.05. RESULTS: During the swing phase of the running cycle in maximum speed sprinting, SAA exhibited a pattern of alternating between flexion and extension. SAA reached its initial peak of flexion value shortly after toe off (at approximately 20% of the swing duration), before attaining maximum extension value (at approximately 60% of the swing duration). Towards the end of the swing phase, SAA again reached the peak flexion value at foot strike. Strong positive relationships between SAA and the peak activation of semitendinosus (ST) were identified, while no significant correlation between SAA and the peak activation of bicep femoris long head

(BF) was found. In addition, significant positive relationships were also discovered between the activation of BF at toe off and SAA. Meanwhile, no significant relationship between SAA and maximum speed was observed, even when considering stride length and frequency. CONCLUSION: : Based on these results, the mitigation of SAA during the swing phase may serve to reduce loading demand on the hamstring muscle in the late swing phase, without compromising maximum speed. Additionally, the effect of SAA varies among different muscles and clinically it may indicate the development of training methods focusing on individual muscles to prevent injury. These insights could be valuable in informing clinical decision making for coaches and players when developing training programs.

P1.67-R: Muscle Activation During Ankle Machine and Thera-Band Training in The Individuals with Chronic Ankle Instability

Yong-Hsiang Yang, China Medical University; Hsiu-Chen Lin, Department of Physical Therapy, China Medical University; Chih-Wei Chen, The Ph.D Program for Medical Engineering and Rehabilitation Science, China Medical University; Chia-Ming Chang, Department of Physical Therapy, China Medical University

Background: Chronic ankle instability (CAI) is a long-term symptom that often occurs after an ankle sprain. The most common type of ankle sprain is inversion sprain that usually damage and weaken the peroneal longus and brevis. Strength training is an important part of the therapeutic approaches for athletes suffering from CAI. Traditionally, the training of ankle muscular strength practically utilizes elastic bands. A new type of ankle training machine was designed to provide multi-directional training and allow the subjects to be trained with stable trails in sitting position.Objective: The purpose of this study is to investigate the effectiveness of the ankle machine training by comparing the electromyographic (EMG) signals between Thera-band and ankle machine training in individuals with CAI. Methods: The study is expected to recruit 10 college students, who are regularly participated in sports at least three times a week. All participants should have not experienced severe lower-limb injuries or surgery in the past 3 months. They will be allocated into the CAI or control group by using Cumberland Ankle Instability Tool (CAIT). The participants in the CAI group should have a history of at least one severe ankle sprain that affect his sports participation. The experimental process begins with the use of the BIODEX System 3 to obtain the maximum voluntary isometric contraction (MVIC) and determine the intensity of the strength training. At the same time, EMG from tibialis anterior, peroneal longus, and medial gastrocnemius are also collected to establish the baseline data for normalization. Then, two training programs were implemented by a randomly assigned order for Thera-band and the ankle machine, while the EMG signals are measured during the exercises. The raw EMG data of four movements were collected at sampling rate of 2000Hz. Subsequently, a bandpass filter with a range of 20-450Hz is applied, followed by the use of the root mean square (RMS) with 10-ms moving window to obtain the amplitudes of muscle recruitment data. The two-way ANOVA was used to examine differences in muscle recruitment levels between the two types of training and between two groups. Levels of significance was set at p<0.05. Results: Until now, six individuals have completed the experimental program in this study (CAI=3, control group = 3). There is no statistical difference between two training programs in EMG activation level during dorsiflexion, plantarflexion and inversion movement. However,

during eversion movement, the EMG activation level showed significantly higher in the ankle machine group (109.83 vs. 46.80 %MVIC, p=0.011). CONCLUSION: : This study confirmed that the training in eversion with the ankle machine is more effective than training with Thera-band. The well-trained peroneal longus muscle is able to prevent the ankle joint from recurrent inversion ankle sprain in athletes.

P1.68-R: A comparison of neuromechanical latencies between karate practitioners and general population during gyaku tsuki executions

Paola Rodríguez, University of Alicante; José M. Sempere, University of Alicante; Desirée I. Gracia, Miguel Hernández University, Spain; Andres Ubeda, University of Alicante; Eduardo Iáñez, Brain-Machine Interface Systems Lab, Miguel Hernández University of Elche, Elche, Spain

Electromechanical delay (EMD) is defined as the latency between neuromuscular activation and exerted force during a muscle contraction. The evaluation of EMD is an important field of interest in sport science. However, only a few preliminary studies have dealt with how EMD behaves in karate practitioners. The main objective of this study is to analyze the EMD in a karate-specific movement of the upper limb, the gyaku tsuki. The gyaku tsuki is a movement consisting of a straight punch executed from a front stance when the advanced leg and fist are on opposite sides. Three karate athletes and three people with no experience in karate participated in the study. 10 gyaku tsuki executions were performed by each participant. During the movements, several recordings were performed: kinematics (with an inertial measurement unit); electromyographic activity (EMG) activity of the deltoid, pectoralis major, triceps and biceps muscles (1500 Hz sample frequency, Noraxon MiniDTS system); and the contact force of the punch (arm full extension) with a flat force sensor placed on a self-made makiwara (punching cushion). To compute the delays, the envelope of the EMG signal for every muscle has been obtained to extract muscle onsets. The onset of the first active muscle has been compared to the movement onset and the force onset. Results show that the biceps muscle is the one that activates first during the movement. A significant difference is present between karate practitioners and general population during gyaku tsuki execution in terms of EMG to Contact Force delay (402±18 ms for karate y 512±26 ms for the control group), EMG to Movement Onset delay (320±17 ms for karate y 349±35 ms for the control group) and Movement Onset to Contact Force delay (82±8 ms for karate y 163±25 ms for the control group). These results show that all delay components are significantly lower for the karate practitioners, meaning that a decrease in EMD components is present after specific training. This is coherent with the way karatekas are trained to increase punching velocity and precision and with a decrease of EMD with increased force, as previously proven in literature. Still remains to be estimated how the different EMD components are affecting these delays, so future studies should focus on evaluating if these changes are due to neural adaptations or improvements in the muscle and tendon properties due to specific training. In the future, this setup will also allow the analysis of different isometric and isotonic movements.This study has been developed within project MYOREHAB (PCI2023-143405), funded by MCIN/AEI/10.13039/501100011033. This research has also been supported by the Valencian Graduate School and Research Network on Artificial Intelligence (ValgrAI), Generalitat Valenciana and the European Union.

P1.69-S: Differences in sit-to-stand motion between older people with and without frailty using sensors embedded chair

Haruki Toda, The Hyogo Institute of Assistive Technology; Kiyohiro Omori, The Hyogo Institute of Assistive Technology; Katsuya Fukui, The Hyogo Institute of Assistive Technology; Takaaki Chin, The Hyogo Institute of Assistive Technology

Background: Sit-to-stand (STS) motion is frequently used to evaluate physical function in older adults. Frail older people take a longer time to perform STS than healthy people. In addition, the trunk lean angle in older adults was smaller than that in younger adults. These parameters were measured using an optical motion capture (MoCap) system and stopwatches. Thus, operators of these devices were necessary for the evaluation. However, we believe that evaluations of the physical functions of older adults via STS motion should be performed in daily life. Our developed chair: We developed laser range finders-embedded chair to easily evaluate the STS motion. This chair has two laser range finders, which measure the distance between the seat and the right thigh, and the backrest and trunk. The sensors were controlled using microcontrollers. Trunk and thigh angles were calculated using the distances assumed in the two-link model. Purpose: This study aimed to examine differences in trunk kinematic parameters during STS motion between older people with and without frailty. Methods: Ninety-five community-dwelling older adults participated in this study. The participants were instructed to stand up at a comfortable speed with their hands folded in front of their chest. The STS motion was measured five times. The noise of the distance data was removed using a fourth-order low-pass Butterworth filter with a cut-off frequency of 6 Hz. We calculated trunk flexion angle, angular velocity, angular acceleration, and STS time. Angle-related parameters were extracted from the peak values during the flexion phase. We defined the start and end of the STS motion as a change of at least 1 °in the trunk angle and a change of at least 1 °in the thigh angle. Frailty was assessed using physical strength-related items from the Kihon Checklist. Participants with a score ≥ 3 on that item were considered frail. STS-related parameters were compared between participants with and without frailty using unpaired t-tests. RESULTS: Older adults with frailty had significantly smaller trunk flexion angles, angular velocities, and angular accelerations, and longer STS times than healthy adults. CONCLUSION: : Our developed sensor-embedded chair could measure the STS motion of frailty in older people. This chair can realize to assess the physical function of older adults in their daily lives.

P1.70-S: Validation of a digital dynamometer for assessing the cranio-cervical flexion test in volunteers with neck pain

Daniele Lonati, supsi; Corrado Cescon, University of Applied Sciences and Arts of Southern Switzerland; Alessandro Bonafine, University of Applied Sciences and Arts of Southern Switzerland; Tiziano Negrisolo, Fisioterapia Kinesis; Emanuele Falzone, Fisioterapia Emanuele Falzone; Samuel Pedrucci, FisioRehab, Manno; Erik Cattrysse, Experimental Anatomy Research group (EXAN),; Deborah Falla, University of Birmingham; Marco Barbero, University of Applied Sciences and Arts of Southern Switzerland,

Introduction: The Cranio-Cervical Flexion Test (CCFT) is a clinical test designed to evaluate the activation of the deep cervical flexor muscles, particularly the longus capitis and longus colli,

pivotal for optimal motor control and postural function in the craniocervical region. The test involves incremental stages of cranio-cervical flexion, facilitated by a pressure biofeedback unit, gauging muscle activation as the patient progresses through the incremental levels of the test. The CCFT's primary objectives are to assess the activation and endurance of these muscles, to determine the need for training the cranio-cervical flexor muscles. Despite its established construct validity and widespread clinical recognition, the application of the CCFT with a customized digital dynamometers has not been investigated.The aim of this study is to validate the use of the Neuromuscular Cranio-cervical Device (NOD, OT Bioelettronica, Italy) during the execution of the CCFT by conducting a comparative analysis with the Stabilizer (Chattanooga, USA), the established reference standard. Methods: A strong positive correlation was hypothesized between CCFT scores obtained using the two devices: the NOD and the Stabilizer. Sixty-two volunteers with neck pain were recruited across five outpatient clinics. Each was scheduled for a CCFT session involving both devices during their treatment plan. To counteract order effects, the sequence of device use was randomized. A Mantel-Haenszel test of trend was run to determine whether a linear association existed between the CCFT scores obtained using Stabilizer and NOD; afterwards, a Pearson's product-moment correlation was run to estimate the strength and direction of the association. Video motion analysis assessed the upper cervical spine's range of motion during all completed CCFT stages, and results from both devices were compared via two-way ANOVA. RESULTS: The distribution of CCFT scores revealed a pronounced skewness towards scores higher than the “normal response” threshold, limiting the definitive assessment of the NOD's validity, especially at lower scores. However, among the 62 volunteers enrolled, only four (6.45%) failed to achieve equivalent test scores across the devices. The Mantel-Haenszel test of trend showed a statistically significant linear association between the scores (X2(1) = 45.295, p < .001) and Pearson’s correlation procedures supported a strong positive relationship (p < .001, r = .862). The range of motion analysis showed no significant differences during the execution of the CCFT using the two devices. The observed mean difference of -0.77 degrees falls within the instruments' sensitivity threshold of 1 degree, indicating that the devices did not influence cranio-cervical flexion movement during the CCFT. CONCLUSION: : The study findings endorse the NOD's validation for evaluating CCFT performance in patients experiencing neck pain. Additional research involving individuals with greater impairment of the deep cervical flexor muscles is recommended. The NOD emerges as a valuable tool for assessing the CCFT in clinical and research settings.

P1.71-S: Temporary tattoo for high-density electromyography

Antonello Mascia, University of Cagliari; Andrea Spanu, University School for Advanced Studies IUSS Pavia; Tiffany Hamstreet, Chalmers University of Technology; Piero Cosseddu, University of Cagliari; Silvia Muceli, Chalmers University of Technology

High-density surface electromyography (EMG) is used in a range of applications, including identification of motor unit discharge patterns and myoelectric control. Conventional technology relies on materials that are relatively stiff and therefore prone to lift-off, preventing long-term use. Soft electrodes that can conform with the curved skin surface are crucial for overall wearability.To this end, we have designed and manufactured flexible high-density tattoo

electrodes that can be temporarily applied to the skin for EMG recordings.The electrodes feature 64 detection sites in gold (3 mm diameter) arranged in a rectangular configuration (13x5 electrodes with one missing at one of the corners) with 8 mm inter-electrode distance. Gold is sandwiched between two layers of parylene C. The total thickness is less than 2 microns. Electrodes were clean-room manufactured (Myfab Chalmers).Due to the constituent materials and their minimal thickness, the electrode grids are extremely flexible ensuring conformal adhesion to the skin and high-quality EMG signals.

P1.72-S: Non-linear measures of postural control in the low back, mobile phone technology versus gold standard. BackMeUp project

Edith Elgueta-Cancino, Universidad Andres Bello; Ririka Fujiwara, School of Sport, Exercise and Rehabilitation Sciences, University of Birmingham, Birmingham, United; Angeli Bassi, School of Sport, Exercise and Rehabilitation Sciences, University of Birmingham, Birmingham, United; Luis Eduardo Cofre-Lizama, The University of Melbourne

Low back pain (LBP) individuals are shown to have altered postural control compared to healthy individuals yet research in linear measures have not provided valuable indicators to distinguish between healthy and LBP populations. Nonlinear analyses have been able to identify those alterations and discriminate between pathological populations, for instance, risk of fall in elderly population or the degradation of motor skill in Parkinson disease. Force plates and motion capture systems are the gold standard to measure postural control but mobile phones could be a cheaper alternative in combination with non-linear methods such as multiscale entropy (MSE) to provide a greater insight into the complex nature of postural control.The aim of this study was to investigate the concurrent validity of nonlinear measures of postural sway derived from a smartphone against the gold standard 3D motion capture system. METHODSTwenty healthy adults (age: 21.1 ± 3.36) completed four static balance tasks in a random order. The data were simultaneously collected by the smartphone (Samsung Galaxy A3, Samsung, Seoul, South Korea) fixed on the sternum at 100 Hz and by an eight-camera SMART-D Motion Capture System (BTS S.p.A., Milan, Italy) at 250 Hz using twenty-five passive reflective markers. Concurrent validity was examined by comparison (Spearman's rank correlations) of nonlinear measures, quantified as complexity indexes of Multiscale entropy (MSE) of postural sway acceleration derived from the two systems. ResultsThere were significant correlations between MSE from the smartphone and the motion capture system during tandem stance (rho=0.535, p =0.018) and single leg stance (rho=0.698, p =0.001), but not during double leg stance with eyes open (rho=0.165, p =0.448) and closed (rho=0.142, p =0.481). Conclusions These preliminary results demonstrated that smartphones are valid to assess nonlinear measures of postural sway during challenging static stance with the small base of support. Smartphones have potential to provide accessible, objective postural sway measures, to identify people at risk of LBP, which may have an impact on clinical practice, the development of mobile digital health, accessible (self-)assessment, and implementation of LBP preventive strategies.

P1.73-P: Analysis of Upper Limb Movement during Equine-Assisted Therapy for Super Low-Birthweight Children: Insights from EMG and 3D Motion Analysis

Kenichi Kaneko, Fuji University; Hitoshi Makabe, Juntendo University; Kazuyuki Mito, The University of Electro-Communications; Kiyoshi Yonemoto, Iwate Prefectural University; Yoshiya Kawanori, Doho University

Equine-assisted therapy stands out as a promising rehabilitation method for individuals with spinal injuries and/or brain damage. In recent years, a substantial number of studies have been conducted to investigate the effects of equine-assisted therapy. The results obtained in this present review demonstrate the potential benefits of equine-assisted therapy in enhancing gross motor function among children with cerebral palsy (CP). We investigated differences in the activity patterns of trunk and cervical muscles during equine-assisted therapy between super low-birthweight children with CP and healthy children using electromyogram (Trigno Wireless System, USA) and 3D motion analysis (Xsens MVN and MVN Animate, Netherlands). In children with CP, the muscle activity pattern in the lumbar region exhibited reduced activity during horseback riding compared to that of healthy children. In children with CP, EMG activity in the cervical region for the overall muscle activities of trunk muscles was observed to be greater than that in the lumbar children with CP exhibited improved trunk posture control during horseback riding, primarily in the engagement of cervical muscles. The EMG activities with the low-frequency band (62.5-20 Hz) was smaller than that for the healthy group within the muscles of the lumbar region. The chi-square test for independence revealed a statistically significant difference of 1% for the muscles of the lumbar region. In contrast, there was no statistical difference for the muscles of the cervical region. In addition, the trajectory of upper limb movement during horseback riding, analyzed through motion capture, was found to be larger in children with CP healthy children. The trajectory of chest movement during horseback riding was larger in individuals with CP than in healthy children as shown in the figure. These results suggest that the characteristics of trunk muscle activities and the strategy for controlling trunk posture during horseback riding differ between children with CP and their healthy counterparts. It is hypothesized that the spectral properties of surface EMG are influenced by the volume conductor effects of muscle fibers and the number of activated motor units (MUs). The recruitment strategies of the lumbar region in children with CP may involve higher MUs activities compared to healthy children during equine-assisted therapy. The lower-frequency EMG activity within the lumbar region may serve as a suitable physiological index for evaluating gross motor function and the effectiveness of equine-assisted therapy.

P1.74-P: Asymmetry of intermuscular coherence during static and dynamic standing tasks in sub-acute patients after stroke

Eiji Yamanaka, Tokyo Bay Rehabilitation Hospital; Ryosuke Goto, Tokyo Bay Rehabilitation Hospital; Michiyuki Kawakami, Keio University School of Medicine; Takaki Tateishi, Musashigaoka Clinical Research Center, Musashigaoka Hospital; Kunitsugu Kondo, Tokyo Bay Rehabilitation Hospital; Ippei Nojima, Nagoya City University

Introduction: Sub-acute patients after stroke often experience balance disability during both static and dynamic standing tasks, significantly increasing their risk of falls. Previous studies

have reported that asymmetrical neuromuscular control due to hemiparesis is an essential characteristic in observed balance deficits during static standing in patients after stroke. Dynamic standing activities are believed to demand more complex modulations of postural muscle control by the motor cortex compared to static standing activities, to cope with increasing task difficulty. However, neuromuscular control during dynamic balance tasks in stroke patients remains largely unclear. Therefore, the present study aimed to elucidate the neuromuscular control mechanisms of the motor cortex through intermuscular coherence analysis in dynamic standing tasks among sub-acute patients after stroke. Methods: Twenty patients after stroke within their sub-acute phase (< 3 months) participated in the study. The participants performed the static and dynamic standing tasks without prosthetic devices or physical assistance. The dynamic standing tasks consisted of maintaining the maximum leaning posture for twenty seconds each in the forward and backward directions. Surface electromyography of the bilateral tibialis anterior (TA), soleus (SL), and medial gastrocnemius (MG) muscles was acquired during the tasks. Intermuscular coherence was calculated using the Fourier transform of surface electromyography in the pairs of unilateral synergistic (SL-MG), antagonistic (TA-SL and TA-MG) of paretic and non-paretic sides. The area under the z-transformed coherence curve of the 95% confidence interval in the beta bands (15-35 Hz), reflecting the descending common input from the motor cortex, was calculated. Two-way [task condition (static, dynamic forward, and dynamic backward) and muscle type (paretic or non-paretic)] repeated measures ANOVA was performed in each pair of the intermuscular coherence area to investigate the modulation of cortical muscle control and its asymmetry. RESULTS: Two-way repeated measures ANOVA revealed a significant main effect of muscle type (paretic or non-paretic) on intermuscular coherence area across all pairs, indicating that intermuscular coherence area in non-paretic muscles was larger compared to the paretic ones during both static and dynamic standing tasks. On the other hand, two-way repeated measures ANOVA indicated that task condition did not significantly influence the intermuscular coherence area for any muscle pairs. CONCLUSIONS: The study shows the inherent asymmetry in cortical muscle control during static and dynamic standing tasks among sub-acute stroke patients. It also suggests that the adaptation of neuromuscular control in response to varying task difficulties is limited, indicating the mechanisms and potential areas for therapeutic intervention in the dynamic balance disability.

P1.75-P: The Association Between Motor Unit Firing Rate and Deformity and Pain Severity in Patients with Knee Osteoarthritis

Masahide Yagi, Kyoto University; Yuichi Nishikawa, Kanazawa University; Tetsuya Hirono, Kyoto University; Masashi Taniguchi, Kyoto University; Shogo Okada, Kyoto University; Sayaka Okada, Kyoto University; Masashi Kobayashi, Kobayashi Orthopaedic Clinic; Kyoseki Kanemitsu, Kanemitsu Clinic; Noriaki Ichihashi, Kyoto University,

IntroductionInterest in neural factors has grown due to their contribution to the decline of muscle function in patients with knee osteoarthritis (OA). Previous studies have demonstrated that patients with experimental knee pain or who have undergone anterior cruciate ligament reconstruction show a lower firing rate (FR) of motor units (MU) during muscle contraction. Because various factors can influence neural changes, the association between these changes

and knee joint deformity or pain severity is not fully understood in knee OA. This study aims to investigate the relationship between MUFR and knee joint deformity and pain in patients with knee OA. MethodForty-six older women were evaluated for knee joint deformity severity using the Kellgren-Lawrence (KL) grading scale, which assesses the severity of OA based on radiographic findings, and for knee pain using the Knee Society Score (KSS) symptom score, which evaluates knee pain and function. High-density surface electromyography signals were recorded from the vastus lateralis (VL) during isometric knee extension at 20% of maximum voluntary contraction (MVC) and were decomposed into individual MU firings. The average FR of all detected MU was calculated for each participant. The normalized amplitude during 20% MVC (20%EMGamp) was calculated using the amplitude during MVC, and MVC torque was normalized to each participant's body weight. From B-mode ultrasound images, muscle echo intensity (EI) and muscle thickness (MT) in the VL in the supine position were assessed. Participants were categorized based on knee joint deformity severity into non-OA (KL grade 0,1), mild OA (KL grade 2), and severe OA (KL grade 3,4) groups, and based on knee pain severity into asymptomatic (KSS≥23), moderate symptom (KSS≥18), and severe symptom (KSS<18) groups. Indicators were compared using one-way analysis of variance with the Holm-Sidak post hoc test. The significance level was set at p<0.05. ResultAn average of 7.9 ± 4.9 of MU was detected per individual. When comparing groups based on knee joint deformity severity, only EI showed a significant difference, with the mild OA group having significantly higher EI values than the non-OA group (p<0.05). Analysis based on knee pain severity revealed significant main effects in MVC, EI, and average FR (p<0.05). FR was lower in the moderate symptom group compared to the asymptomatic group (p<0.05). Both moderate and severe symptom groups had lower MVC values than the asymptomatic group, and EI was higher in the severe symptom group compared to the asymptomatic group (p<0.05). No differences were observed in MT and 20%EMGamp. ConclusionAnalysis of knee pain severity showed no differences in 20%EMGamp between groups, but FR was lower in the moderate symptom group compared to the asymptomatic group. When comparing groups based on deformity severity, no differences in MUFR were found. These findings suggest that in patients with knee OA, the lower MUFR in the VL is more closely related to the severity of knee pain rather than to deformity severity.

Poster Session 2

P2.1-A: Investigation of the association between swallowing problems and jaw kinematic movements in the elderly

Chen-Fu Hung, Master Program of Long-Term Care in Aging, College of Nursing ,Kaohsiung Medical University, Taiwan; Min Hsu, Kaohsiung Medical University; Hsiu-Yueh Liu, Department of Oral Hygiene, College of Dental Medicine ,Kaohsiung Medical University, Taiwan; Lan-Yuen Guo, Kaohsiung Medical University

Background and Purpose: Videofluoroscopy (VF) and videoendoscopy (VE) are both widely used as the gold standard for diagnosis of swallowing disorders despite that the limitations related to their radiation exposure or invasive procedure. There is a growing emphasis and emerging trend on using non-invasive/non-radiation assessment tools for swallowing disorders. This study aimed to identify swallowing difficulties using the repetitive saliva swallowing test (RSST), and to determine if observation of jaw kinematic movements could be a non-invasive means of screening for swallowing problems. Methods: One hundred community dwelling elderly people (74 females and 26 males; 41 aged between 65-74 y/o, 40 aged between 75-84 y/o and 19 aged between 85-94 y/o) were recruited in this study. The criterion for swallowing problems was RSST<3. The Kinovea software was used to analyze jaw kinematics, maximum mouth opening distance, maximum mouth opening angle, opening velocity, closing velocity, opening angular velocity and closing angular velocity were calculated. In addition, the study designed diadochokinetic (DDK) tasks, participants must finish 10, 15 repetitions and in one breath to pronounce /pa/, /ta/, /ka/ sound respectively. Audacity audio software was used to calculate the pronunciation rate in Hz to represent the agility of tongue movement. RESULTS: The results showed that swallowing problems with a notable increase in the 75-84 y/o (60%) and 85-94 y/o (61%) groups compared with 65-74 y/o (36%). A moderate correlation (r=0.302-0.377, p<0.01) between maximum mouth opening distance/angle and DDK performance were found. There was significantly different for females in closing velocity (p<0.05) and closing angular velocity (p<0.05) between subjects with swallowing problems or not. Meanwhile, there was significantly different for males in mouth opening velocity (p<0.05) and opening angular velocity (p<0.05) between subjects with swallowing problems or not. Subjects with swallowing problem showed slower mouth opening or closing velocity as well as smaller mouth opening or closing angular velocity compared with those without swallowing problem. Conclusion: Image analysis of jaw kinematic movements shows considerable potential as a non-invasive and rapid screening tool for identifying swallowing problems. It is recommended that the focus on future community screening should be on individuals aged over 75 years old.

P2.2-A: Motor unit discharge characteristics in post-menopausal females and the effects of hormone replacement therapy

Jessica Piasecki, Nottingham Trent University; Mollie O'hanlon, Nottingham Trent University; Elisa Nédélec, Nottingham Trent University; Tom Inns, Nottingham Trent University; Paul Ansdell, Northumbria University; Mathew Piasecki, Nottingham University

Oestrogen and progesterone are the predominant female sex hormones which potentially influence neuronal activity via excitatory and inhibitory effects (Ansdell et al., 2019; Piasecki et al., 2023). The menopausal transition marks the cessation of the female reproductive cycle and is characterised by a rapid decline in these sex hormones. This significant hormonal shift is not observed in males and may contribute to sex-based disparities in the development of frailty (Piasecki et al., 2024). Hormone Replacement Therapy (HRT) has been shown to have beneficial effects on physical function in post-menopausal females (Ronkainen et al., 2009), however, the effects of HRT on individual motor unit (MU) characteristics have not yet been fully investigated. Eight post-menopausal females aged 59.5 yrs (±7.4) were recruited according to NICE guidelines, and all participants reported ≥ 12 consecutive months without menstruation. HRT users (n=4) were taking combined hormone therapy for a minimum of 6 months, and control females (n=4) were not using any form of hormone therapy. Maximum isometric dorsiflexor force was recorded from the right leg. High-density surface electromyography (HD-sEMG) signals were recorded from the tibialis anterior (TA) during trapezoid contractions (3s ramp up, 12s hold, 3s ramp down) normalised to 25% of maximum force, and decomposed into individual MU spike trains. The mean number of TA MUs recorded from these older individuals was 15 ± 5. Non-HRT users had a maximum dorsiflexion strength of 94.8N, compared to 117.2N in the HRT group. Mean MU discharge rate (MUDR) at the point of recruitment was 9.23Hz in the non-HRT group, and 9.01Hz in the HRT. At de-recruitment, mean MUDR was 7.58Hz in the non-HRT, and 7.84Hz in the HRT. During the sustained phase held at 25% of maximum force, mean MUDR was 12.94Hz in the non-HRT and 13.41Hz in the HRT group. Although the current pilot data preclude definitive outcomes, there are indications muscle strength may differ across these hormonally distinct groups, with little difference between MU characteristics at this single contraction intensity. The current data and the accompanying ongoing study highlight the plausibility of exploring the effects of exogenous hormone administration in older humans and help alleviate the minimal MU data available in older females. This has the potential to identify clinically relevant interventional targets to help address sex-based differences in sarcopenia and frailty. REFERENCES: Ansdell, P et al, 2019. Menstrual cycle-associated modulations in neuromuscular function and fatigability of the knee extensors in eumenorrheic women. Journal of Applied Physiology.Piasecki, J et al., 2023. Menstrual Cycle Associated Alteration of Vastus Lateralis Motor Unit Function. Sports Medicine - Open.Piasecki, J., Škarabot, J., Spillane, P., Piasecki, M., Ansdell, P., 2024. Sex Differences in Neuromuscular Ageing: The Role of Sex Hormones. Exerc Sport Sci Rev. Ronkainen, P.H.A, et al., 2009. Postmenopausal hormone replacement therapy modifies skeletal muscle composition and function: a study with monozygotic twin pairs. Journal of Applied Physiology.

P2.3-B: Asymmetry in Children with Cerebral Palsy and Healthy Controls Performing Fine-Motor Tasks, as Measured by Machine Learning Models

Stephen Macneille, Rutgers University; Aleksandra Kostic, Rutgers University; Mara Rao, Rutgers University; Matthew Weintraub, Rutgers University; David Ahn, Rutgers University; Nathan Wages, Rutgers University; Jean-Francois Daneault, Rutgers University; Alice Chu, Rutgers University

Introduction: Cerebral palsy can lead to impaired bimanual function and heightened preference for the dominant hand, hindering performance of activities of daily living (ADLs). We used 3D motion analysis, submovement decomposition, and machine learning models to assess dominance along the upper extremity in cerebral palsy patients and healthy controls during a block-stacking task. Methods: We recorded the movements of 25 healthy subjects and 3 with cerebral palsy while stacking six blocks using the Vicon Vero motion capture system. Participants performed the task with their dominant and non-dominant hand three times each. We then processed data to remove noise and segmented each trial into submovements using joint velocity zero-crossings, and extracted features from each submovement. We discarded highly correlated features, retaining between 30 and 60 features per joint marker. We then trained machine learning models to predict hand dominance at each joint. For the best performing models, we used SHAP feature importance to identify the most influential features. Results: Tree-based models, like RandomForest, were most accurate for estimating dominance, with a 95% score at the hand and 78% at the shoulder. Accuracy for cerebral palsy patients was 90% at the same markers. For healthy patients, proximity of a joint influenced predictability, with accuracy decreasing sequentially from the hand to shoulder. Cerebral palsy patients showed less of a proximal-distal pattern. The most important features also differed. In healthy patients, horizontal velocity, vertical change in acceleration (jerk), and late peak (i.e. accelerative) submovement velocity had strong relationships with dominance at proximal and distal markers. The relevant features for cerebral palsy patients varied with location. Proximal features such as skewness, entropy, and absolute maximum velocity fell in importance at distal locations, where top features more closely resemble those of healthy subjects. Conclusion: Our findings suggest that machine learning models can expose differences in features of dominance between healthy individuals and cerebral palsy patients during upper-limb motor tasks—particularly between distal and proximal joint movements. Significance: Cerebral palsy often presents with asymmetric hand motion and upper extremity dysfunction, leading to challenges in ADLs. These results present potential measures to assess improvement or deterioration.
Keywords: Cerebral palsy, handedness, machine learning, fine motor tasks

P2.4-B: Possibility of Measuring Skills by Operating Experience of a Surgical Simulator Using Multi-Channel Surface EMG

Hideo Nakamura, Osaka Electro-Communication University; Tatsuro Fujie, Morinomiya University of Medical Sciences

With the increase in the number of robot-assisted surgeries in recent years, many studies have been reported that are interested in skill evaluation in the training of surgeons. In our previous report, the authors showed the data suggesting that it is possible to quantitatively evaluate surgical skill relatively based on statistics of amplitude information from time-frequency analysis and a machine learning method. However, the authors have not been able to identify the reason why those statistics can reflect the degree of surgical skill. In this study, the authors record four channels of the radial and ulnar sides of the forearm EMGs during two trials of a specific procedure on a surgical simulator in non-skilled persons. This study aims to evaluate the difference in skill level between the first and second trials based on the statistics of EMG amplitude and to clarify the dependence of skill level on learning experience. All participants

were young, healthy adults with no previous surgical simulator experience. They stood in front of the surgical training box and held forceps in both hands. Inside the box was monitored by a camera, and they could confirm their own operation on the monitor in front of them. Many rods stand in the box, and elastic rings are threaded through the rods. The participants are asked to pick up a ring with the left forceps, change to the right forceps, and pass the ring through a rod other than the original rod 20 times in one trial.The EMG amplitude in the time-frequency domain is calculated by applying CDM to the filtered EMG. The extracted amplitude distribution was divided into several analytic durations with frequencies ranging from 50-250 Hz, and the standard deviation, skewness, and kurtosis were calculated. Logistic regression was applied to the statistics as input to evaluate the degree of skill. Test data were selected from one of the participants, and data from the remaining participants were used as training data. The training was performed 12 times between two trials. Our results showed that there was no clear trend in the difference in proficiency between the first and second trials. It is clear that the second trial was more successful than the first trial, as evidenced by the significant reduction in operation time. Our previous study was an evaluation of skills among highly trained specialists in real surgical settings, whereas the present study is not easy to compare because of its short analytical duration. In other words, the analysis duration was shorter than before, which may have caused instability in the statistics. When the operation time was significantly different between the first and second trials, a trend toward a significantly higher skill level on the second trial was obtained. In conclusion, our results suggest that the analytic duration may contribute significantly to the statistics.

P2.5-C: Importance of weight bearing on the affected side in gait of hemiplegic stroke patients: A Cyclogram analysis of the unaffected Side

Jehyeon Yu, Yonsei universitiy; Juntaek Hong, Yonsei University College of Medicine; Taeyoung Choi, Yonsei University; Taekyung Lee, Yonsei university; Jeuhee Lee, Yonsei university; Yebin Cho, Yonsei University College of Medicine; Dong-Wook Rha, Yonsei University College of Medicine

IntroductionGait disturbance is common in hemiplegic stroke patient due to weakness, spasticity and motor incoordination. Especially in hemiplegic stroke, muscle weakness could limit the ability to transfer weight to the affected side. Previous studies have shown that weight bearing on the hemiplegic side plays a crucial role in stroke patients' locomotion. However, quantifying the amount of weight bearing on the hemiplegic side remains a challenge. While measuring ground reaction forces using force plates is the gold standard, its high cost and limited accessibility pose significant barriers. We propose utilizing cyclogram-based analysis of the unaffected side to estimate the ground reaction force on the affected side and identify potential correlations with gait quality and balance, as assessed by the Berg Balance Scale (BBS) score. MethodsWe retrospectively enrolled 208 hemiplegic stroke patients who were able to walk independently indoors (FAC 4,5) and conducted instrumented gait analysis. We derived the cyclogram parameters from the kinematic data of a single gait cycle using the result of gait analysis. Additionally, we collected spatio-temporal data and ground reaction force data during the gait analysis. We compared the peak vertical ground reaction force on the affected side with the cyclogram parameter on the unaffected side, spatio-temporal parameters, and the Berg

Balance Scale (BBS) score. To assess the significance of these relationships, we computed Spearman rank correlation coefficients. ResultsWe found the correlation between ground reaction force on affected side and cyclogram's area of swing phase of unaffected side. (ρ = 0.62, p<0.01) Swing phase area of cyclogram of unaffected side was correlated with gait speed (ρ = 0.76, p<0.01) and BBS (ρ = 0.49, p<0.01). Ground reaction force on the affected side is also directly correlated with gait speed (ρ = 0.62, p<0.01) and BBS (ρ = 0.33, p<0.01). ConclusionOur study found that the swing phase area of the hip-knee cyclogram on the unaffected side correlated with amount of weight-bearing on the affected side measured by force plate during gait. The swing phase area of the cyclogram of the unaffected side correlated with gait speed and balance control ability as well.

P2.6-C: Relationship between neural drive of the lower trapezius and serratus anterior and scapular motion

Masahro Kuniki, Hiroshima International University; Rei Konishi, Hiroshima International University; Daisuke Kuwahara, Hiroshima International University; Daiki Yamagiwa, Hiroshima International University; Nobuhiro Kito, Hiroshima International University

BackgroundMuscle weakness of the lower trapezius and serratus anterior is associated with alterations in scapular motion. Morphological and neurological factors contribute to muscle weakness. The importance of neurological factors rather than morphological factors in scapular motor control has been suggested, but the details are unclear. The purpose of this study was to investigate the relationship between neural drive of the lower trapezius and scapular motion, and neural drive of the serratus anterior and scapular motion, respectively. METHODSThree scapular motions (upward (–) /downward (+) rotation, external (–) /internal (+) rotation, anterior (–) /posterior (+) tilt) during scapular plane upper limb elevation in 50 healthy young subjects (25 males/25 females) were recorded with an electromagnetic tracking device (Liberty, Polhemus, Colchester, VT, USA). From the data obtained, the scapular motion angle at 120° of upper limb elevation was extracted. Next, a trapezoidal contraction task at 70% maximum voluntary contraction of the lower trapezius and serratus anterior was performed, and surface electromyography (sEMG) waveforms (Delsys Inc., Natick, MA, USA) were collected during the task. The obtained sEMG waveforms were decomposed into motor unit action potential amplitude (MUAPAMP), mean firing rate (MFR), and recruitment threshold (RT). Motor units with a decomposition accuracy of ≥85% were used in the analysis, and the average MUAPAMP, average MFR, slope and y-intercept of the regression of MUAPAMP and MFR with RT were used as indicators of neural drive. Pearson product-moment correlation coefficient or Spearman rank correlations were used to examine the relationship between the three extracted scapular motion angles and indices of neural drive. ResultsSignificant correlations were found between scapular posterior tilt angle and average MUAPAMP of the lower trapezius (r = 0.466, p = 0.001), MUAPAMP-RT slope of the lower trapezius (ρ = 0.459, p = 0.001), MFR-RT y-intercept of the lower trapezius (r = 0.369, p = 0.009), and average MFR of the serratus anterior (r = 0.367, p = 0.009) (Figure 1a).Significant correlations were found between scapular upward rotation angle and average MFR of the serratus anterior (r = –0.309, p= 0.030) and MUAPAMP-RT slope of the serratus anterior (r = –0.330, p = 0.021) (Figure 1b). CONCLUSION: Neural drive of the lower trapezius affects the angle of scapular posterior tilt and angle of upward rotation, and neural

drive of the serratus anterior affects the angle of scapular upward rotation. In correcting abnormal scapular motion, it may be necessary to improve the neural drive (size and firing rate of the motor units) of the lower trapezius and serratus anterior.

P2.7-C: The effects of speeds on EMG profiles of Tibialis posterior detected by multiple fine wire electrodes

Pornsuree Kuvijitsuwan, Chiang Mai university; Siam Tongprasert, Department of Rehabilitation Medicine, Faculty of Medicine, Chiang Mai University, 110 Intaravaroros; Kristen Hollands, University of Salford; Richard Jones, University of Salford

IntroductionThe tibialis posterior (TP) has important roles in controlling the subtalar joints and other joints within the foot. Fine-wire (FW) electrodes are the only method for detecting EMG in TP due to their location. There are two common approaches and positions for FW insertions in TP. The EMG profiles detected by them are similar at the normal self-selected speed, but the performance of these insertions is unknown at different speeds. This study aims to examine the differences in dislocation rate and detected EMG profiles between two common sites of FW in TP at different speeds.Participants and method11 healthy volunteers (age 35 ± 6 years, 7 males, height 1.67±0.10 m, weight 71±12 kg) who were self-reported to be free from any neurological or musculoskeletal disease gave consent to participate in the study. Using two methods under the guidance of ultrasonography, FW electrodes detected EMG at two locations in the TP that were each 2 cm apart from one another [1, 2]. The participants were instructed to walk at different speeds: self-selected speeds, 25% slower, 50% slower, 25% faster, and 50% faster. The processing of EMG data involved time normalization to 100% of the gait cycle, the removal of movement artifacts, full wave rectification, and envelope detection. Then they were normalized from peak amplitude at self-selected speed and averaged from six gait cycles for comparison between participants.ResultTheir average walking speed was 1.18 ± 0.15 m/s. The detected average speeds are slowest (0.64 ±0.15 m/s), slower (0.94 ±0.14 m/s), self-selected speed (1.18 ±0.15 m/s), faster (1.46 ±0.19 m/s), and fastest (1.86 ±0.24 m/s). The dislocation of the distal electrodes occurred at 'faster' speed in 1 case and at 'fastest speed' in 4 cases, whereas the dislocations of the proximal electrodes occurred at the 'fastest' speed in 3 participants. The amplitude of EMG increased, and the timing of the peak normalized EMG occurred earlier in the gait cycle during the active phases as the speed increased. The magnitude of the normalized EMG at the distal electrodes tended to be higher than that at the proximal electrodes.DiscussionThe dislocation rate of the distal electrode was higher than that of the proximal one. This may be due to closer contact with the other limb. The increase in muscle activity is not directly proportional to the increase in speed. There is a slight difference between the two EMG peak values at the faster speed, which may require further investigation. CONCLUSION: EMG detected by two FW sensors at different speeds in TP tended to be similar: an increase in peak magnitude and a change in timing of peak. However, the distal electrodes had a higher dislocation rate than the proximal electrodes. The walking speed or task stated in the protocol for EMG data collection should be considered when selecting the appropriate location of the electrode in TP.

P2.8-C: Study of the floor pressing force with the hallux and metatarsals during walking for hallux valgus.

Iori Arisue, Kansai University of Welfare Sciences; Yuto Konishi, Butsuryo College of Osaka; Ayako Hisari, Osaka Kawasaki Rehabilitation University; Naoko TAKEUCHI, Graduate school of Science, Osaka Prefecture University; Fujinaga Takeshi, Yamato University; Tamaki Katsuya, Neurosurgery Nipponbashi Hospital; Iwashita Atsushi, Yamato University

[Background and aim] We have been measured for the floor pressing force (FPF) vector with the toes (1st toe, 3rd toe, 5th toe) and metatarsal head (1st metatarsal head, 5th metatarsal head) during gait. (Arisue et al. 2018,2022) How pressing on the floor in three axes force vector has not been studied, when hallux valgus people walking. The purpose of this research is to measure the floor pressing force with the hallux and metatarsals during walking for hallux valgus, and use this as basic data for walking.[Participants and Methods] Two hallux valgus students that did not affect daily life participated. The participants walked on a flat straight road of about 20m. We measured the FPF vector for right toes (1st toe, 3rd toe) and right metatarsal head (1st metatarsal head, 5th metatarsal head), right heel. We used the sensors, attached the acrylic plates (100mm × 100mm × 20 mm) to 3-axis force sensor (Tec Gihan Co., Ltd.), for measuring the FPF vector of each toe. We set the sampling frequency of the sensors to 100 Hz. We specified a walking cycle from the right heel contact to next right heel contact. We normalized with the time taken for a walking cycle as 100%. In order to examine whether the waveforms are similar from the first step to the stop, we used a cross-correlation function to calculate the value (Rxy(0)) when there is no time lag (lag 0). The analysis was performed using SPSS (ver.28).[Results] A low correlation was observed in the waveforms of the first 2 to 3 steps. A similarly low correlation was seen for 2 to 3 steps before stopping. In other steady walking sections, the correlation coefficients for 1MP tended to be high, and the same was true for 5MP (r=0.6 to 0.9). In addition, the correlation between the vertical and anteroposterior components of the big toe in the steady walking section was high (r=0.6-0.99), and the correlation between the left and right components was low (r=0.28-0.4).[Conclusion] Based on the results of this study, it was thought that the correlation was high because even for hallux valgus, loads are applied in the vertical direction depending on the state of deformation. The above results are similar to those of healthy subjects, indicating that it is possible to evaluate the degree to which hallux valgus people press their toes against the floor when walking.

P2.9-C: Preferred direction of muscle activities in the hip adductors varies with hip flexion angles

Hironoshin Tozawa, Graduate School of Health and Sports Science, Doshisha University, Kyoto, Japan; Raki Kawama, Faculty of Health and Sports Science, Doshisha University, Kyoto, Japan; Taku Wakahara, Faculty of Health and Sports Science, Doshisha University, Kyoto, Japan

INTRODUCTION: Hip adductors (adductor longus [AL], gracilis [Gra], and adductor magnus [AM]) have moment arms of hip flexion and extension as well as that of hip adduction (1). We can exert force in various directions around the hip joint (e.g., between the hip flexion and adduction). However, little is known about the direction in which the muscle activity of the hip adductors is highest in the transverse plane (preferred direction: PD). The electromyographic

(EMG) activity of AL and AM during hip flexion significantly decreased as the hip flexion angle increased (2), suggesting that the PDs of muscle activities may also change with the hip flexion angle. This study aimed to investigate the effects of hip flexion angle on the PDs of muscle activities of the hip adductors in the transverse plane. Methods: Eighteen males performed maximum voluntary isometric contractions (MVIC) in five directions (hip flexion, flexion + adduction, adduction, extension + adduction, and extension) at three hip flexion angles (at 0°, 45°, and 90°). The direction of the force was measured as the angle of a load cell with respect to the horizontal line. The electrode positions of AL, Gra, and AM were carefully determined using ultrasonography (3). Root mean square (RMS) of EMG and force direction during MVICs were plotted in a polar coordinate system. The angle of the vector connecting the centroid of the five MVICs and the pole with respect to the polar axis was defined as the PD of muscle activity. The Friedman test was used to analyze the differences in PDs between different hip flexion angles. Data were presented as median (interquartile range). RESULTS: The PDs of AL at 45°[15.3 (11.0 to 21.4)°] and 90° [8.8 (4.8 to 13.6)°] of hip flexion were significantly inclined to extension compared with that at 0° of hip flexion [19.2 (17.1 to 27.3)°]. The PD of Gra at 90° of hip flexion [13.0 (6.8 to 16.5)°] was significantly inclined to flexion compared with that at 0° of hip flexion [−2.0 (−9.0 to 4.3)°].The PD of AM at 90° of hip flexion [−20.7 (−36.4 to −7.8)°] was significantly inclined to flexion compared with that at 0° of hip flexion [−37.8 (−49.0 to −32.8)°].DISCUSSION: The PD of AL was significantly inclined to extension as the hip flexion angle increased. This result is in line with the previous findings that AL acts as a hip flexor in the hip extended position and acts as a hip extensor in the hip deeply flexed position. Meanwhile, the PDs of Gra and AM were significantly inclined to flexion as the hip flexion angle increased. These results is inconsistent withthe anatomical findings (1). These results suggest that the changes in the PD with the hip flexion angle are likely to be attributed to possible changes in the role within the synergistic muscles rather than changes in the moment armREFERENCES: Dostal et al., Phys Ther, 1986 Kato et al., Eur J Appl Physiol, 2019Watanabe et al., Eur J Appl Physiol, 2009

P2.10-C: Muscle activity required to turn patients in their bed: an assessment of four techniques

Wayne Albert, University of New Brunswick; Elnaz Roudi, University of New Brunswick; Luke Kell, University of New Brunswick; Alex Cameron, University of New Brunswick; Puneet Singh, Université de Moncton; Michelle Cardoso, Université de Moncton

IntroductionPatient handling (PH) is a leading cause of musculoskeletal injury among health care providers. In New Brunswick (Canada) there are two competing PH programs developed to reduce the biomechanical and muscular strain associated with PH tasks. This research assessed the activity of eight muscles bilaterally when using the Back in Form (BiF) and All The Right Moves (ATRM) PH techniques developed to reposition the patient in their bed. Both programs are based on proper body mechanics and the concept of not lifting to reposition patients. METHODSTwenty-six university aged students were recruited. The exclusion criteria for this study were that participants must not suffer from low back pain or shoulder disorder during the study period (or 3 months prior) and they must be between 19 and 35 years old. The BIF program has two techniques for turning a patient in their bed and are referred to as Turn-to-side 1-Caregiver andTurn-to-Side 2-Caregiver, respectively. The ATRM program also has two

techniques referred to as Turn-1 and Turn-2, where each technique is completed by one caregiver. Participants performed each of the techniques twice while neuromuscular activity was monitored bilaterally on eight muscles using a Bortec Octopus AMT-8. The eight muscles of interest were: anterior deltoid [AD], trapezius descendens [TD], biceps brachii [BB], thoracic erector spinae [TES] located at the level of the T9 spinous process, lumbar erector spinae [LES] located at the level of the L3 spinous process, external oblique [EO], rectus femoris [RF], and biceps femoris [BF]. Results and ConclusionThe raw EMG signal was rectified, and Butterworth low passed filtered (RMS converted) using MATLAB. Peak activity was determined for each muscle during a maximum voluntary contraction protocol (MVC) and used to normalize all subsequent EMG data. The Peak muscle activity was determined for two phases: 1) the preparation for patient turning (PPT); and 2) the patient turning (PT). A series of ANOVAs with corrections were used to determine the difference in peak muscle activity. In the PPT phase, significant differences in peak muscle activity on the right were observed: TD, AD, BB exhibited higher activity for the Turn-2 technique, while the TES showed increased activity in Turn-to-side 1-Caregiver technique, and the LES showed higher activity for Turn-1 technique. On the left side, differences were found for BB during the Turn-2 technique and for the RF during the Turn-to-side 1-Caregiver technique. During the PT phase, significant differences on the right were found: AD showed higher activity in the Turn-to-side 1-Caregiver technique, and higher activity was found for TES and LES in the Turn-1 technique. On the left side, differences were found for the AD in the Turn-1 technique and for the RF in the Turn-to-side 1-Caregiver technique. Overall, it was observed that lower neuromuscular activity occurred when two caregivers performed the task, compared to only one, regardless of which program used.

P2.11-D: Combining measures of central (functional MRI) and peripheral (surface electromyography) correlates of movement control

Monika Jasenská, Faculty of Medicine and Dentistry Palacky University Olomouc; Martin Kojan, Masaryk University Brno, Central European Institute of Technology; Ales Holobar, University of Maribor, Faculty of Electrical Engineering and Computer Science; Ondrej Burkot, University Hospital Olomouc; Klara Balazova, University Hospital Olomouc; Barbora Kolarova, University Hospital Olomouc; Petr Hlustik, Faculty of Medicine and Dentistry Palacký University Olomouc

Introduction: Whereas functional magnetic resonance imaging (fMRI) has been extensively used to describe the central correlates of real and imagined movement [2], surface electromyography (sEMG) provides complementary information about muscle engagement and synergies [1]. The combination of both will facilitate the exploration of quantitative relationships between brain and peripheral muscle activations during overt movement and motor imagery. Methods: This study involved 19 healthy subjects (31.1±7.3 years; 8 females, 11 males). MRI data were acquired on 3 Tesla scanners (Prisma, Siemens Medical, Germany). A multimodal whole-brain MRI protocol included a high-resolution T1-weighted anatomical scan and a 10-minute fMRI scan with multi-band T2*-weighted gradient echo (BOLD) EPI acquisition during a block paradigm consisting of two active (paced dorsi-/plantarflexion of the ankle and gait imagery) and two resting (with and without beeps) 30-second conditions, each repeated five times. sEMG and kinematic data were recorded (Brain Products GmbH, Germany) during BOLD scanning. The bipolar sensors for sEMG were located on the left lower limb at tibialis anterior (TA) and

gastrocnemius medialis (GM). Accelerometric data were acquired from the dorsal side of the foot to verify the presence or absence of motion.Analysis of fMRI data was conducted in FSL software, and physiological data was analysed in MATLAB R2023b. Data processing began with a gradient artifact correction algorithm, followed by signal processing involving frequency filtering and RMS (root mean square) calculations. Results: The pilot study revealed activation in all relevant cortical areas (M1, S1, SMA) during execution of the movement task. During imagination, active cortical areas included SMA, pre-SMA, S1, SPL/IPS (superior parietal lobule / intraparietal sulcus), CMA (cingulate motor area) and the cerebellum. Active movement measurements revealed increased sEMG activity in the TA (48.9±5.5 μV) and GM (20.2±4.8 μV), gait imagery revealed sEMG activity in TA (4.7±1.3 μV) and GM (2.8±0.7 μV). CONCLUSIONS: The combination of sEMG-fMRI with accelerometer recordings offers a more precise understanding of the brain's motor system activation than using fMRI alone. Additionally, we have complementary information about muscle activation and their interplay, including tracking the kinematics of the movement performed.Acknowledgment: We acknowledge the core facility MAFIL supported by MEYS CR (LM2023050 Czech-BioImaging), part of the Euro-BioImaging (www.eurobioimaging.eu) ALM and Medical Imaging Node (Brno, CZ). AH was supported by Slovenian Research and Innovation Agency (P2-0041).References: 1. Kolářová et al. Effect of Gait Imagery Tasks on Lower Limb Muscle Activity with Respect to Body Posture. Percept Mot Skills. 2016. 2. Boyne et al. Functional magnetic resonance brain imaging of imagined walking to study locomotor function after stroke. 2021.

P2.12-E: Post-Activation Depression is Attenuated in Individuals following Spinal Cord Injury with and without Spasticity

Mitsuhiro Nito, Yamagata Prefectural University of Health Sciences; Bing Chen, Shirley Ryan AbilityLab; Jens Nielsen, University of Copenhagen; Monica Perez, Shirley Ryan AbilityLab

Post-activation depression (PAD) is thought to be one of the mechanisms altered after spinal cord injury (SCI) that might contribute to spasticity. However, limited information is available on how PAD differs between humans with SCI with and without spasticity. To address this question, we tested the soleus H-reflex at interstimulus intervals of 1, 2, 4, and 10 s using half of the maximal H-reflex (half H-max) and the maximal H-reflex (H-max) size in 34 individuals with chronic (≥6 month) SCI and 17 aged-matched control subjects. Spasticity in the soleus muscle was assessed by the stretch reflex (elicited by rapid >300°/s passive dorsiflexion of the ankle) and the Modified Ashworth Scale (MAS). The presence or absence of spasticity in individuals with SCI was classified based on the highest amplitude of stretch reflex obtained in control subjects. We found that the H-max was similar in individuals with SCI with and without spasticity and control subjects, whereas the M-max was smaller in both groups of individuals with SCI compared with control subjects. PAD was stronger at shorter interstimulus intervals at half H-max compared with H-max in individuals with SCI with and without spasticity and control subjects. Notably, PAD was attenuated to a lesser extent in individuals with SCI compared with control subjects but no differences were found in individuals with SCI with and without spasticity. In addition, the magnitude of PAD was not correlated with the stretch reflex and the MAS. Our findings demonstrate that PAD is attenuated following SCI regardless of the presence

of spasticity, suggesting that it is less likely that PAD plays a role in the pathophysiology of spasticity.

P2.13-E: Central and peripheral somatosensory characteristics of the ankle joint: an exploratory study

Chang Yu-Tung, National Yang Ming Chiao Tung University; Yi Fen Shih, Department of Physical Therapy and Assistive Technology, National Yang Ming Chiao Tung University

Background: Previous research in somatosensory dysfunction has predominantly focused on neurological disorders. Recently, some emerging evidence showed alterations in somatosensory regions in individuals with chronic musculoskeletal conditions, such as anterior cruciate ligament injury. However, little was known regarding the central somatosensory characteristics of the ankle joint. The purpose of this study aims to explore the central and peripheral somatosensory characteristics including the evoked potentials (SEP), corticomuscular coherence (CMC), joint position sense, and two-point discrimination (TPD) of the ankle joint. Methods: In this exploratory study,10 asymptomatic healthy adults between 20-30 y/o were recruited. SEP and CMC were collected using the 64-chanel electroencephalogram (EEG) and surface electromyography (EMG). The stimulus site was on the tibial nerve, and target muscles were the peroneal longus (PL), soleus, and tibilalis anterior (TA). Joint position sense of ankle joint was measured using the Active movement extent discrimination assessment (AMEDA) with a self-made device. TPD was measured using a caliper on the 1st and 5th metatarsal bone and heel. The within-day measurement reliability was assessed using the intra-class correlation coefficients (ICC) for CMC, TPD, and joint position sense. RESULTS: The SEP testing showed a significant increase in amplitude between 30 to 100 milliseconds following a sensory level electrical stimulation on Cz and C1 electrodes. The range of CMC ranged from 0.074 to 0.259 for the PL, from 0.0743 to 0.2558 for the soleus, and from 0.074 to 0.2198 for the TA. The measurement reliability was moderate for the C3 electrode and PL muscle at the alpha band (ICC3,2=0.428), for the C1 electrode and PL muscle at the beta band (ICC3,2=0.601), and for the C1 electrode and soleus muscle at the gamma band (ICC3,2=0.645). As for the remaining electrode-muscle pairs in the three frequency bands, their reliability is poor. The measurement of TPD had excellent reliability on the 1st and 5th metatarsal bone and moderate reliability on the heel (1st : TPD=12.77±2.4 mm, ICC3,1=0.905, standard error of measurement (SEM)=0.743; 5th : TPD=14.51±2.3 mm, ICC3,1=0.866, SEM=0.855; heel: TPD=14.09 mm, ICC3,1=0.558, SEM=2.194). The AMEDA had moderate to excellent measuring reliability (ICC3,1= 0.697 to 0.891) and the accuracy rate is between 47.5% to 82.5% in forty trials. CONCLUSIONS: This research established the measurement method for further investigations of central and peripheral somatosensory characteristics in musculoskeletal conditions related to the ankle joint. Our data indicated that with good practice and standardization, measurement of SEP, CMC, AMEDA, and TPD offers reasonable reliability for clinical investigation.

P2.14-E: Changing the position of the stimulating electrode reduces the pain when recording the F-waves from the vastus lateralis muscle

Masataka Kurobe, Kobe College of Rehabilitation and Health; Naoki Kado, Kobe College of Rehabilitation and Health; Toshiaki Suzuki, Graduate School of Kansai University of Health Sciences

Introduction: F-waves are compound muscle action potentials produced by the reciprocal excitation of motor neuron axons and back-firing in anterior horn cells upon electrical stimulation. F-wave latency measures the nerve conduction velocity, and F-wave persistence is a measure of the excitability of the anterior horn cells. Conventional recording of F-waves from the vastus lateralis muscle (VL) causes severe pain in some subjects. We aimed to investigate the effects of stimulation position on pain when recording F-waves from the VL and to develop a method for recording F-waves from the VL that causes minimal pain. Methods: A total of 15 healthy subjects participated in the study. The active electrode was placed distal to the VL. The reference and ground electrodes were placed on the patella and the anterior surface of the lower leg, respectively. The anode of the stimulating electrode was placed at the lateral aspect of the thigh. In the conventional trial, the cathode of the stimulating electrode was located 80% of the distance along a line extending from the groin proximally to the patella. In the new trial, the cathode of the stimulating electrode was placed 80% along a line extending from the greater trochanter to the patella and at a point where a large M-wave could be recorded even with weak electrical stimulation. The stimulation intensity was at 1.2-fold the maximum M-wave amplitude obtained by gradually increasing the voltage. The stimulus duration was 0.2 milliseconds, the stimulus frequency was 0.2 Hz, and the number of stimuli was 30. The filters were set from 20 Hz to 3000 Hz. The examiners electrically stimulated each site of the distal thigh at random and recorded the F-waves from the VL. A visual analog scale was used to evaluate pain intensity. The participants were asked to indicate the pain intensity of the electrical stimulation immediately after the F-waves recording. The stimulation intensity, visual analog scale score, M-wave amplitude, F-wave latency, F-wave average amplitude, and F-wave persistence were analyzed at each trial. RESULTS: In the new trial, the stimulation intensity, visual analog scale score, M-wave amplitude, and F-wave persistence decreased, and F-wave average amplitude increased compared with the conventional trial.Discussion: In the conventional trial, it is presumed that the cathode of the stimulating electrode was far from the motor branch of the VL, potentially resulting in stimulation of both the VL and non-VL muscles. Conversely, in the new trial, the cathode of the stimulating electrode was probably closer to the motor branch of the VL, thus selectively stimulating only the VL. Consequently, in the new trial, both stimulation intensity and pain were decreased. Furthermore, we inferred that the exclusive excitation of the VL contributed to the reduction in M-wave amplitude and F-wave persistence, alongside an increase in the F-wave average amplitude.

P2.15-E: Exploring spinal reflex modulation in the pelvic floor muscles through tibial nerve stimulation

Yao Sun, University of British Columbia; E. Paul Zehr, University of Victoria; Jaynie Yang, University of Alberta; Tania Lam, University of British Columbia

Background: Urinary dysfunctions are often experienced in older adults and people with neurological injuries. The spinal segments mediating lower urinary tract function overlap with those controlling lower limb sensorimotor function at the lumbosacral region. Studies in

animals indicate that activating one system affects the other. However, the interaction between the somatic nervous system and autonomic function is less studied in human participants. Spinally-mediated reflexes, such as Hoffmann (H-) reflex and cutaneous reflexes, show task-dependent modulation in the leg muscles indicating sensory inputs from the muscles and skin regulate motoneuron excitability based on the functional goal of the tasks. The pelvic floor muscles (PFM) play critical roles in maintaining continence during different physical activities. Our recent studies in healthy adults show that PFM is activated during walking and jogging with greater activity seen during the stance phase. Emerging evidence also shows that gait training may be accompanied by improved bladder function in people with spinal cord injury. Furthermore, electrical stimulation of the posterior tibial nerve at the ankle is a target for treating overactive bladder. These lines of evidence indicate potential modulatory effects of peripheral sensory inputs from the leg on PFM activity. The purpose of this study is to explore: 1) the feasibility of measuring tibial nerved evoked spinal reflexes in PFM and 2) whether this reflex response is modulated by posture and task. Methods: Five healthy young adults have been recruited for this study so far. Soleus and pelvic floor muscle electromyography were measured using surface electrodes. Soleus H-reflex and M-wave were evoked through electrical stimulation of the tibial nerve at the popliteal fossa. Reflex responses in the pelvic floor muscle were concurrently measured when obtaining the recruitment curve of soleus H-reflex in sitting and standing positions, with the soleus muscle relaxed and contracted to different levels. RESULTS: Tibial nerve stimulation evoked a reflex response in PFM at a latency around 15ms. The amplitude of this response is modulated task-dependently and enhanced during soleus muscle contraction. Conclusion: Peripheral sensory input from the tibial nerve has a modulatory effect on the activity in PFM. This study indicates that the neural circuits that control the sensorimotor function of the leg muscles interact with those that control urinary function. It shows the potential of using exercise-based rehabilitation approaches such as walking exercises and transcutaneous stimulation to manage neurogenic dysfunction.

P2.16-F: Exercise combined with electrical stimulation for the treatment of chronic ankle instability – a randomized controlled trial

Uri Gottlieb, Ariel University; Roee Hayek, Ariel University; Jay Hoffman, Ariel University; Shmuel Springer, Ariel University

Purpose: Chronic ankle instability (CAI) is a common condition that can lead to significant functional impairment and reduced quality of life. One of the factors contributing to CAI is arthrogenic muscle inhibition (AMI), which is characterized by decreased activation of the muscles surrounding the ankle joint. Both Transcutaneous Electrical Nerve Stimulation (TENS) and Neuro-Muscular Electrical stimulation (NMES) have been shown to improve muscle activation in conditions involving AMI. This study aimed to compare the short, medium, and long-term effects of balance exercises combined with either peroneal NMES or peroneal TENS on dynamic postural control and patient-reported outcomes (PROMs) in subjects with CAI. Methods: Thirty-four participants with CAI were randomly assigned to a 12-session home-based exercise program combined with NMES (Ex-NMES) or TENS (Ex- TENS). Both the participants and the investigator were blinded to group assignment. Postural control was tested with the modified Star Excursion Balance Test (mSEBT) and time to stabilization (TTS) after a

single-leg drop-jump. Self-reported function was measured using the Cumberland Ankle Instability Tool (CAIT), the Identification of Functional Ankle Instability (IdFAI), and the Sports subscale of the Foot and Ankle Ability Measure (FAAMSport). Subjects were assessed at baseline, before and after treatment, and PROMs were also measured at 6 and 12 months. RESULTS: Both groups showed significant improvements in all self-reported outcome measures at 12-month follow-up. Subjects in the Ex-NMES group had significantly better IdFAI (-4.2 [95% CI -8.1, -0.2]) and FAAMSport (13.7 [95% CI 2.2, 25.2]) scores than those in the ex-TENS group at 6- and 12-month follow-up, respectively. Medium to large between-group effect sizes were observed for self-reported functional outcomes and mSEBT. Yet, there were no improvements in mSEBT and TTS immediately after training with either TENS or NMES. CONCLUSIONS: The consistent trend for long-term improvement in self-reported functional outcomes when training is combined with NMES compared to training with TENS may indicate a potential benefit that should prompt clinicians to consider the use of NMES when prescribing balance training for individuals with CAI.

P2.17-F: Effect of electrolyte amount and concentration on Neuromuscular Electrical Stimulation (NMES) stimulation – Towards near-dry textile electrodes

Yohann Opolka, University of Borås; Luisa Euler, Science Park Borås, University of Borås, Allégatan 1, 501 90 Borås; Robin Juthberg, Karolinska Institute, Department of Molecular Medicine and Surgery, Solna, 171 76 Stockholm; Li Guo, University of Borås; Paul W. Ackermann, Karolinska University Hospital, Solna, 171 76 Stockholm; Nils-Krister Persson, University of Borås

BackgroundIn recent years, textile electrodes have gained recognition for medical applications pertaining to both sensorics and stimulation, particularly in a home-based setting. Some of these applications, such as Neuromuscular Electrical Stimulation (NMES), involve current intensities that can be high enough to be perceived as painful, and therefore require the addition of an electrolyte in the form of a conductive gel or saline solution. However, little is known about the minimum requirements in terms of electrolyte volume and concentration. AimThis exploratory study investigates the lower limit of electrolyte volume and the effect of saline concentration in an NMES modality using two motor points on the calf. In doing so, it aims to deepen the understanding of the painfulness of electrostimulation with near-dry textile electrodes, to improve the safety of home-based electrostimulation. METHODSDifferent pairs of 3×3cm textile electrodes, knitted with silver-coated yarns, were wetted with different combinations of electrolyte volume (ranging from 0µL to 320µL) and saline concentration (0%, 0.9%, 5%). These pairs of electrodes were then tested on 21 volunteers for their propensity to evoke pain (rated on a 101-item Numerical Rating Scale) at increasing stimulation intensity levels, following the first clear observation of plantar flexion. Participants were also asked to fill in a short survey about factors thought to have an impact on the quality of electrostimulation (use of moisturizer, frequency of physical activities, etc.). Results were analyzed using nonparametric statistics and ordinal regression. ResultsPlantar flexion could be obtained in an NMES modality with textile electrodes and very low electrolyte volumes (<1mL). Unsurprisingly, higher electrolyte volumes were associated with lower pain ratings. Pain ratings were more strongly correlated with electrolyte volume than with saline concentration. Moreover,

sigmoid curve fitting, and comparisons based on Wilcoxon-Mann-Whitney Odds seem to suggest the existence of “painfulness thresholds”, in current intensity and electrolyte volume. CONCLUSION: The findings indicate that NMES can be effectively performed using very small electrolyte volumes (<1mL), with reasonable levels of evoked pain or discomfort. Short-term applications of these results could include the creation of safety guidelines for home-based products. In the more distant future, textile-based electrostimulation devices could be designed to store and/or transport enough electrolyte, to allow for safe electrostimulation with less complexity for the end-user. These considerations are especially important in a home-based setting, where ease of use and minimal need for supervision are key factors of treatment adherence.

P2.18-G: Effects of Prolonged Mouse Aiming on Forearm Muscle Fatigue and Motor Performance in Gamers and Non-Gamers

Garrick Forman, Brock University; Sophia Nikitin, Brock University; Cameron Lang, Brock University; Mike Holmes, Brock University

Introduction: Esports are becoming increasingly popular; however, little research exists on the physical demands of the sport. Many individuals become injured (McGee and Ho, 2021) or experience pain and discomfort in their upper limbs while gaming (Forman and Holmes, 2023). Investigating changes in forearm muscle activity and fatigue while gaming could provide critical insight into how muscular demands change during extended periods of gaming and how those changes may impact the performance and health of gamers. Therefore, the purpose of this study was to evaluate muscle fatigue and performance impairments during an extended mouse aiming fatigue protocol.Methodology: Twenty participants were recruited for this study (8F, 12M), separated into gaming and non-gaming groups. Surface electromyography was measured from eight muscles of the right upper limb. Participants performed a 30-second aiming task using aim training software (AimLab, State Space Labs, Inc., New York, New York, USA). The fatiguing protocol involved six, 5-minute bouts of clicking targets in AimLab. To assess muscle fatigue, reference contractions of radial and ulnar deviation (30% of maximum) were performed throughout the experiment. Participants also provided ratings of perceived fatigue (RPF) throughout the experiment. Performance and fatigue assessments were performed after each bout of AimLab fatigue. Mean power frequency (MnPF) and RMS amplitude were calculated and spike shape analysis was performed during reference contractions to quantify muscle fatigue. Performance measures were calculated in AimLab and included total targets hit, accuracy, and error size. RESULTS: While gamers outperformed non-gamers, no changes in performance measures were observed throughout the experiment. Extensor digitorum (ED) and extensor carpi ulnaris (ECU) produced the greatest levels of muscle activity at 9.3% and 8.2% of MVC, respectively. RPF increased in a linear fashion during the fatiguing protocol, reaching a maximum rating of 4.2/10 after 30-minutes. MnPF of the wrist extensors significantly decreased due to the fatiguing protocol, with a maximum decrease of 25.7%. Spike shape characteristics of the wrist extensors showed a decrease in spike frequency, peaks per spike, spike slope, and zero crossings following the fatigue protocol.Discussion: Changes in performance metrics indicate no impairments caused by the fatigue protocol. RPF ratings reached 4.2/10 after 30-minutes, indicating participants experienced muscle fatigue. Changes in fatigue metrics

indicate that ED and ECU were fatigued following prolonged mouse aiming, which could suggest that the wrist extensors are prone to gaming related fatigue and injury.References: [1] McGee and Ho. (2021). Tendinopathies in Video Gaming and Esports. Front. Sports Act. Living.[2] Forman and Holmes. (2023). Upper-Body Pain in Gamers: An Analysis of Demographics and Gaming Habits on Gaming-Related Pain and Discomfort. Journal of Electronic Gaming and Esports.

P2.19-G: The Impact of Joint Angle on Muscle Fatigue in Concentric Contractions using sEMG: Assessing Muscle Fiber Conduction Velocity-Amplitude Relationship

Aya Shirai, Aoyama Gakuin University; Kazuyuki Mito, The University of Electro-Communications

IntroductionSurface electromyogram (sEMG) stands as a non-invasive and objective method for evaluating muscle function, showing potential applications in sports training and rehabilitation. This study aimed to assess muscle fatigue based on the relationship between MFCV (Muscle Fiber Conduction Velocity) and sEMG amplitude differences at varying elbow joint angles.MethodTwenties males were participated, and they performed repetitive elbow flexion and extension exercise from 40 to 140 degrees of elbow joint angle at a speed of 10 degree/s in a seated position until reaching a state of fatigue. sEMG signals of the right biceps brachii muscle were recorded using array electrodes (with an electrode distance of 5mm). the signals were derived bipolarly from adjacent wires, filtered by a band-pass from 5 Hz to 1 kHz, and digitized with sampling frequency of 10 kHz. In the data, the signals were sampled 1 second at 50, 90, 130 degrees during each cycle. MFCV and the root mean square (RMS) of the amplitude were calculated every 20 ms. The distributions of RMS and MFCV were analyzed to examine the relationship between RMS and MFCV with muscle fatigue. Results and discussionsIn some subjects, there was a tendency for the average MFCV and RMS to increase with an increasing elbow joint angle during each cycle. Additionally, MFCV decreased and RMS increased during muscle fatigue. However, the variabilities of the average value were significant, and the trends were not clearly observed in other subjects. The figure shows a heatmap illustrating the relationship between MFCV and RMS during muscle fatigue across various elbow joint angles in subject A. Regarding the muscle fatigue, there tended to be a shift in the mode positions of MFCV and RMS towards higher values with increasing elbow joint angle, and the distribution variability increased. In addition, there was a larger variance in distribution at 130 degrees compared to 50 degrees. During muscle fatigue, the position of RMS mode consistently shifted towards higher across all elbow joint angles, and the distribution variability increased with the muscle fatigue. From the relationship between MFCV and RMS, it was suggested that the size of motor units participating in activity varies with elbow joint angles and fatigue. CONCLUSION: This study investigated muscle fatigue assessment based on the relationship between MFCV and sEMG amplitude differences across varied elbow joint angles. As the result, MFCV and the amplitude increased with increasing elbow joint angle. Additionally, motor units of various sizes were involved in the activity at 130 degrees compared to 50 degrees, regardless of the muscle fatigue.

P2.73-G: Can task-specific training mitigate the effects of fatigue?

Jean-Sebastien Roy, Université Laval; Catherine Mercier, Université Laval; Frederique Dupuis, Université Laval

Introduction: Fatigue has the potential to impact both physical and cognitive functions, causing disruptions in muscle function and hindering the central nervous system's capacity to coordinate voluntary movements. Ultimately, fatigue heightens the risk of injuries by altering the mechanical stress on musculoskeletal structures. Considering the detrimental effects of fatigue, it is imperative to develop prevention strategies to mitigate its negative consequences. Optimizing motor control through practice holds promise as a preventive measure. This could be achieved through targeted motor training interventions that promote motor learning, involving the repeated practice of context-specific motor tasks. Such practice is thought to enhance movement planning, strengthen internal representation, and reinforce feedforward control. The objective of this study was to examine the effects of task-specific training on upper limb motor performance and kinematics during a reaching task performed in a fatigued state. Methods: Thirty young and healthy participants, free from self-reported pain or disabilities, were recruited and assigned to either the Training group (n=15) or the Control group (n=15). Both groups participated in two evaluation sessions (Day 1 and Day 5), performing an upper limb reaching task under two conditions: rested and fatigued. Motor performance (accuracy and speed) and joint kinematics were assessed during the reaching task. The Training group participated in three task-specific training sessions on Day 2, 3, and 4, practicing the same task as in the evaluation sessions (five times each training day, totaling 375 reaching movements). The Control group did not undergo any training. Non-parametric ANOVA for repeated measures (Nonparametric Analysis of Longitudinal Data) was used to assess the impact of the condition (rested vs fatigued) and the training (Training vs Control group) on motor performance and joint kinematics. RESULTS: There was no statistically significant between-group difference (p>.05) in participants' characteristics. There was a significant condition effect (p<.01) on both motor performance and kinematics. Fatigue led to a reduction of accuracy and speed, coupled with an increase in sternoclavicular elevation, trunk contralateral trunk rotation and trunk extension during reaching. Following the training period, the Training group demonstrated a significant increase in reaching speed compared to the Control group (Group x Day interaction effect; p<.01). No significant between-group difference was observed in terms of accuracy (p>.44). The Training group exhibited a reduction in contralateral trunk rotation and lateral trunk flexion on Day 5 under the fatigue condition (Group x Day interaction effect, p<.04). Discussion: Task-specific training mitigated certain compensations linked to upper-limb reaching in a fatigued state. After the 3-day training, participants exhibited improved performance and demonstrated reduced reliance on trunk compensations to complete the task under fatigue. Engaging in task-specific training may prove beneficial in alleviating some of the negative effects of fatigue.

P2.20-H: Highly configurable model for the simulation of muscle superficial electromyography

Alvaro Costa Garcia, National Institute of Advanced Industrial Science and Technology

The objective of this study is to propose a versatile framework for simulating muscle activity, with a primary focus on the muscle fiber as a fundamental unit of activation. Our methodology treats the muscle fiber as an autonomous programmable entity, complete with defined characteristics, enabling a broad spectrum of potential configurations. Parameters like fiber radius, length, intracellular conductivity, conduction velocity, spatial distribution, force generation properties, etc., can be tailored to suit the precise demands of the task or the muscle under simulation. Additionally, the proposed muscle fibers can be dynamically organized into motor units and muscles. Furthermore, higher-level control strategies, such as the selection of motor units to engage and the timing of impulses received by each unit, are also subject to customization.Recent strides in artificial intelligence and machine learning introduce thrilling possibilities for exploring and optimizing our model's extensive parameter range. By harnessing these technologies, this approach holds promise for shedding fresh insight on the intricate interplay among muscle fibers, motor neurons, and higher-level motor control systems. It has the potential to unlock new revelations in the realm of human movement.

P2.21-H: Consensus for experimental design in electromyography (CEDE) project: Checklist for reporting and critically appraising studies using EMG (CEDE-Check)

Manuela Besomi, The University of Queensland; Valter Devecchi, Centre of Precision Rehabilitation for Spinal Pain (CPR Spine), School of Sport, Exercise and Rehab; Deborah Falla, University of Birmingham; Kevin McGill, VA Palo Alto Health Care System; Matthew Kiernan, Brain and Mind Centre, University of Sydney, Sydney, Australia; Department of Neurology, Royal Prin; Roberto Merletti, 5LISiN, Department of Electronics and Telecommunications, Politecnico di Torino, Torino, Italy.; Paul Hodges, The University of Queensland

Background: The diversity in electromyography (EMG) techniques and their reporting present significant challenges across multiple disciplines, including neurology, neuroscience, electrodiagnostic medicine, physiology, sleep medicine, sports science, ergonomics and rehabilitation, biofeedback, and control of artificial limbs, where EMG is commonly needed. To address these challenges and enhance the consistency and replicability of studies using EMG, the Consensus for Experimental Design in Electromyography (CEDE) project has developed a checklist (CEDE-Check) through a multi-stage Delphi process. Methods: The method used for the development of this checklist followed a similar process employed in previous CEDE matrices. We followed a three-step process: 1) initial listing and rating of potential items via an online survey; 2) development of the checklist draft; 3) Delphi process for consensus. Consensus was defined as 70% or more of the respondents indicating that an item should be reported ‘most of the time’ or ‘always’; fewer than 15% scoring it as ‘unsure’ or ‘never’; and an interquartile range <2 points. RESULTS: From the 17 CEDE experts who agreed to participate in the Delphi process, 16 (94%) replied to the first- and second-round questionnaires, and consensus was achieved afterwards. A few additional amendments were made to the checklist after a pilot test assessment. The final CEDE-Check consists of 40 selected items covering four critical areas in EMG recording and reporting – the task investigated (10 items), electrode placement (6 items), characteristics of recording electrodes (13 items), acquisition and pre-processing of EMG signals (11 items). Conclusion: The CEDE-Check aims to guide researchers in accurately reporting and critically appraising EMG studies, thereby promoting a standardised

critical evaluation, and ensuring scientific rigor in EMG-based research. This approach not only aims to facilitate comparisons between studies but will also contribute to the advancement of research quality and its clinical application. We encourage researchers to adopt and adhere to the checklist in their future EMG studies and advocate for journal editors to endorse the checklist as a reporting guideline.

P2.22-H: Evaluation of Accuracy and Precision for Low-Frequency Oculometers: A Preliminary Study Prior to Cervical Torsion Testing

Min Hsu, Kaohsiung Medical University; Lan-Yuen Guo, Kaohsiung Medical University

Introduction: Cervicogenic dizziness is a condition that impairs postural control. It is associated with sensitization of the neck muscles. It is caused by abnormal proprioceptive signals or sympathetic control due to cervical pathology. The cervical torsion test and cervical joint localization test are frequently used in clinical evaluation. An effective diagnostic model for cervicogenic dizziness has not yet been developed due to the high cost of the evaluation system and failing to consider the sensorimotor and oculomotor characteristics of the head planes. The aim of this study is to improve the accuracy of the instruments that are required for the development of a measurement system.Method: Ten study participants collected data using the instruments to determine the accuracy of the rating system instruments. Data were collected using the Stuart platform and two low-frequency eye trackers: the Tobii 5 and the Gazepoint GP3. The study was carried out in a two-phase design. In Phase 1, seven participants conducted repeated reliability tests on the Tobii 5 and made correction of translations on the Stuart platform. The participants received instructions to focus on the target displayed on the monitor. Eye movements recorded from five different screen positions while the participants were securely attached to a chair for safety. The study examined seven head positions, including a neutral position, 20 degrees of rotation to each side, 5 degrees of forward and backward tilt, and 5 degrees of lateral flexion to each side. In the second stage, data were gathered from three participants with different visual fitness, comparing the accuracy and precision of the Tobii 5 and the GP3. The accuracy and precision of the oculometers used for the task were analyzed by calibration and processing of physiological parameters of eye movements. RESULTS: In the early stage of the study, Tobii 5 reliability with the Stewart platform was tested in various positions, but performance was unsatisfactory due to data errors from head movement and high blink frequency (mean of ICC: 0.07±1.19, range: -6.01~0.98). Reliability test performance can be improved to a medium level by controlling environmental variables and processing data signals (mean of ICC: 0.50±0.26, range: 0.01~0.86). The second phase of the study was a comparison of the accuracy and precision of the Tobii 5 and the GP3. The results indicated that the Tobii 5 performed better in the center position with better accuracy (mean: 0.71±0.28°) and precision (0.22±0.18°) after data filtering, but accuracy decreased as visual fitness declined. In contrast, the GP3 showed a less accuracy (mean: 1.36±0.82°) and precision (0.73±0.15°) but a similar performance across visual fitness level, with a smaller change in angle after filtering. Conclusion: Confirmed by precise head rotation control and low-sampling rate dynamometer-recorded eye tracking parameters, output data accuracy and precision revealed gaze points within the 0.5-1.5° range. This study lays the foundation for cervicogenic dizziness diagnostic system development, emphasizing the need

for controlling head movement, addressing blinking factors, and implementing post-processing to enhance low-cost eye-tracking device data quality.

P2.23-I: Neural mechanisms underlying task dependency of inter-limb reflexes during bimanual postural maintenance task

Hirotaka Sugino, Keio University; Daichi Nozaki, The University of Tokyo; Junichi Ushiyama, Keio University

Our daily activities demand versatile control of our upper limbs, ranging from independent movements like using knife and fork to coordinated movements such as carrying a tray. Remarkably, this adaptability extends to reflexive response. For instance, during tasks like carrying a tray, stretch reflexes emerge in both limbs even when one side limb is perturbed. This phenomenon is known as inter-limb reflexes. However, the neural mechanisms underlying this task dependent reflex modulation remain unclear. To clarify this point, we have conducted two experiments.In Experiment 1, we initially examined the presence of reflexive interaction between limbs during a task requiring independent control of each limb. Twenty-two participants performed a bimanual postural maintenance task. They tried to control two cursors representing their left and right fingertip positions under background load and align them within the target . Elbow flexion torque was randomly applied to either the right or left limb, while they were required to maintain the unperturbed limb within its target. Electromyograms (EMGs) from both biceps brachii and triceps brachii muscles (TB) were recorded. Stretch reflexes were divided into three segments (R1, 20-50 ms; R2, 51-75 ms; R3, 76-105 ms) aligned with perturbation timing . Results from Experiment 1 demonstrated that stretch reflex was elicited in the TB of perturbed limb in all tasks, while TB activity in the unperturbed side decreased in the R2 compared to the baseline, even though they did not need to change its activity to maintain its target (fig. 1a). To investigate the mechanism behind the inhibited activity in the unperturbed limb, transcranial magnetic stimulation (TMS) was applied to the primary motor cortex corresponding to the hotspot of TB in unperturbed limb during the inhibited activity phase. The active motor threshold intensity was set for stimulation. As a result, motor evoked potentials (MEPs) of the unperturbed limb TB were smaller than linear prediction. This prediction value was derived from the summation of MEPs when TMS given alone and EMG activity of the unperturbed side during perturbation alone (fig. 1b). This indicates that corticospinal excitability of the unperturbed limb was inhibited in R2 by perturbation.In Experiment 2, we examined the presence of reflexive interaction between limbs during a task requiring coordinated control of upper limbs. Twenty-two participants performed a task similar to Experiment 1 by controlling a bar at the midpoint between both fingertips, necessitating bimanual coordination. As a result, the inhibitory activity in R2 seen in Experiment 1 was not observed, while reflexive response of unperturbed limb appeared in R3 (fig. 1c). Furthermore, in contrast to Experiment 1, even by adding TMS to the hotspot of TB in unperturbed limb, MEPs showed no difference from linear prediction (fig. 1d). These findings suggested the adaptation of inter-limb reflexes depending on task demands by modulating the corticospinal excitability of the unperturbed limb. This modulation is probably caused by interhemispheric inhibition . In independent control tasks, a hemisphere controlling unperturbed limb was inhibited by signals from the opposite

hemisphere, while in coordinated tasks, it may be disinhibited to generate simultaneous bimanual reflexes.

P2.24-I: The force steadiness of the middle finger and variability of motor unit discharge frequency are affected by the position of the ring finger.

Momoka Nakamura, Graduate School of Science and Technology, Shinshu University; Moeka Samoto, Graduate School of Science and Technology, Shinshu University; Yasuhide Yoshitake, Shinshu University

[Introduction]Humans have an extremely ability to flex digits of the hand independently, compared with other non-human primates, but this independence is not perfect. Notably, voluntary flexion of the metacarpophalangeal joint in the middle finger can lead to involuntary flexion in the ring finger, suggesting potential mechanical linkages between the compartments of the extrinsic muscle controlling each finger. Since a shortening of the muscle compartment controlling one finger in the extrinsic muscle would be forced to cause a change in muscle length in the muscle compartment of the other finger, mechanical linkages would thus interfere with the shortening of the muscle compartment to achieve the required force. In other words, additional neural input to motor units (MUs) in the muscle compartment should be required to produce the desired force output. Hence, it is possible that the mechanical linkages between the muscle compartment of one finger and the adjacent muscle compartment of another finger may reduce the ability to perform steady force output due to alterations in MU activity. The current study aimed to examine whether the position of the ring finger (metacarpophalangeal joint angle), which may determine the stiffness of mechanical linkages between muscle compartments, influences the force steadiness and MU activity during steady isometric finger flexion with the middle finger. Mechanical linkages can be stiffer when the muscle length is longer. Therefore, the length of the ring finger muscle compartment was varied by flexion and extension of the ring finger metacarpophalangeal joint. [Methods]Eleven healthy young male adults were sheated in a chair with their right elbow joint and wrist fixed at 150° (full extension = 180°) and 60° dorsiflexion (natural position = 0°), respectively. The metacarpophalangeal joint of the middle finger was flexed at 90° and a force transducer was attached to the skin surface of the metacarpophalangeal joint to measure the isometric flexion force. The ring finger was placed in two conditions: full extension (EXT) and 90° flexion (FLX) of the metacarpophalangeal joint. A target force was 20% of maximal voluntary contraction (MVC) that was obtained during isometric flexion with the middle finger with maximum effort while the ring finger was at FLX. The target force and the actual middle finger flexion force were displayed as lines on a monitor in real time. The participants attempted to match the lines as steady as possible for approximately 10 s. A 64-channel high-density surface EMG from the flexor digitorum superficialis muscle was measured to detect MU discharge timing using the CKC method. The analysis interval was 8 s, during which the force was stable. Force steadiness was assessed by the standard deviation (SD) of the force. After extracting MU that can be assessed as the same across two conditions, MU activity was evaluated as the mean discharge frequency and the coefficient of variation (CV) of the discharge frequency. All calculated parameters were compared between EXT and FLX conditions using a paired t-test. If there were no statistical differences between conditions, the intraclass correlation coefficient (ICC) was calculated to

check whether the values were similar between conditions. [Results]The SD of the middle finger force was 58% greater in EXT than in FLX (P < 0.05). The mean discharge frequency of a total of 34 MUs did not differ between conditions (P > 0.05, ICC = 0.83, mean 13.9 ± 2.4 Hz in both conditions), but the CV of discharge frequency was greater in EXT (20.1 ± 2.5%) than in FLX (17.9 ± 2.5%, P < 0.05). [Conclusion]These results suggest that when the ring finger is passively extended, which may increase the stiffness of the mechanical linkages between muscle compartments, force fluctuations are increased, accompanied by an increase in variability of MU discharge frequency during steady isometric finger flexion with the middle finger. This sheds light on the intricate interplay between muscle compartments during finger movements, highlighting the importance of considering mechanical linkages in understanding precise force control.

P2.25-I: The force steadiness of the middle finger and variability of motor unit discharge frequency are affected by the position of the ring finger

Yasuhide Yoshitake, Shinshu University; Momoka Nakamura, Graduate School of Science and Technology, Shinshu University; Moeka Samoto, Graduate School of Science and Technology, Shinshu University

[Introduction] Humans have an extremely ability to flex digits of the hand independently, compared with other non-human primates, but this independence is not perfect. Notably, voluntary flexion of the metacarpophalangeal joint in the middle finger can lead to involuntary flexion in the ring finger, suggesting potential mechanical linkages between the compartments of the extrinsic muscle controlling each finger. Since a shortening of the muscle compartment controlling one finger in the extrinsic muscle would be forced to cause a change in muscle length in the muscle compartment of the other finger, mechanical linkages would thus interfere with the shortening of the muscle compartment to achieve the required force. In other words, additional neural input to motor units (MUs) in the muscle compartment should be required to produce the desired force output. Hence, it is possible that the mechanical linkages between the muscle compartment of one finger and the adjacent muscle compartment of another finger may reduce the ability to perform steady force output due to alterations in MU activity. The current study aimed to examine whether the position of the ring finger (metacarpophalangeal joint angle), which may determine the stiffness of mechanical linkages between muscle compartments, influences the force steadiness and MU activity during steady isometric finger flexion with the middle finger. Mechanical linkages can be stiffer when the muscle length is longer. Therefore, the length of the ring finger muscle compartment was varied by flexion and extension of the ring finger metacarpophalangeal joint.[Methods] Eleven healthy young male adults were seated in a chair with their right elbow joint and wrist fixed at 150° (full extension = 180°) and 60° dorsiflexion (natural position = 0°), respectively. The metacarpophalangeal joint of the middle finger was flexed at 90° and a force transducer was attached to the skin surface of the metacarpophalangeal joint to measure the isometric flexion force. The ring finger was placed in two conditions: full extension (EXT) and 90° flexion (FLX) of the metacarpophalangeal joint. A target force was 20% of maximal voluntary contraction (MVC) that was obtained during isometric flexion with the middle finger with maximum effort while the ring finger was at FLX. The target force and the actual middle finger flexion force were displayed as lines on a monitor

in real time. The participants attempted to match the lines as steady as possible for approximately 10 s. A 64-channel high-density surface EMG from the flexor digitorum superficialis muscle was measured to detect MU discharge timing using the CKC method. The analysis interval was 8 s, during which the force was stable. Force steadiness was assessed by the standard deviation (SD) of the force. After extracting MU that can be assessed as the same across two conditions, MU activity was evaluated as the mean discharge frequency and the coefficient of variation (CV) of the discharge frequency. All calculated parameters were compared between EXT and FLX conditions using a paired t-test. If there were no statistical differences between conditions, the intraclass correlation coefficient (ICC) was calculated to check whether the values were similar between conditions.[Results] The SD of the middle finger force was 58% greater in EXT than in FLX (P < 0.05). The mean discharge frequency of a total of 34 MUs did not differ between conditions (P > 0.05, ICC = 0.83, mean 13.9 ± 2.4 Hz in both conditions), but the CV of discharge frequency was greater in EXT (20.1 ± 2.5%) than in FLX (17.9 ± 2.5%, P < 0.05). [Conclusion] These results suggest that when the ring finger is passively extended, which may increase the stiffness of the mechanical linkages between muscle compartments, force fluctuations are increased, accompanied by an increase in variability of MU discharge frequency during steady isometric finger flexion with the middle finger. This sheds light on the intricate interplay between muscle compartments during finger movements, highlighting the importance of considering mechanical linkages in understanding precise force control.

P2.26-I: Antagonism of 5-HT2 receptors effects the excitability of intracortical motor circuits in humans

Liana Laughton, Griffith University; Tyler Henderson, Griffith University; Justin Kavanagh, Griffith University

Introduction: In recent times the monoamine serotonin (5-HT) has been heavily studied as a key neuromodulator of human movement. Serotonergic pathways from the raphe-nuclei of the brainstem project to the spinal cord to regulate motoneuron firing via 5-HT2 receptors located on the soma and dendrites. However, the raphe-nuclei also ascend to cortical areas associated with motor activity. Although 5-HT2 receptors have been suggested to affect cortical inhibition associated with γ–amino butyric acid (GABA) activity within motor cortical areas (Henderson et al., 2023; Thorstensen et al., 2021), the mechanisms by which 5-HT2 receptors regulate corticospinal excitability remain unknown. Thus, the purpose of this study was to investigate the effects of 5-HT2 receptor antagonism on the excitability of motor cortical circuits.Method: This project was a human double-blind, placebo-controlled crossover design with 10 healthy participants (23 ± 4 years, 7 female). Participants attended two testing sessions where neurophysiological measurements were obtained pre- and post-administration of either a 5-HT2 antagonist (cyproheptadine, 8 mg) or a placebo. During each session, Transcranial Magnetic Stimulation (TMS) was applied to the motor cortex to produce motor evoked potentials (MEP) in the resting first dorsal interosseus muscle of the right hand. Single- and paired-pulse TMS paradigms were used to produce unconditioned and conditioned MEPs as a measure of corticospinal excitability and intracortical excitability. Paired-pulse TMS was used at interstimulus intervals of 3 ms to measure short-interval intracortical inhibition (SICI), 100 ms to

measure long-interval intracortical inhibition (LICI), and 10 ms to measure intracortical facilitation (ICF). RESULTS: Change scores were calculated as the difference in the outcome measure from pre- pill to post-pill. There was no difference in the change in MEP amplitude between the drug condition and the placebo condition ($p = 0.250$). However, the amplitude of SICI ($p = 0.043$) and ICF ($p = 0.024$) increased following the administration of cyproheptadine compared to the administration of placebo. There were no drug differences identified for LICI ($p = 0.089$) responses. Conclusion: While 5-HT2 receptors are involved in the modulation of intracortical motor circuits, the same receptors do not affect the overall excitability of the corticospinal pathway. Drug-related changes to SICI and ICF suggest that the serotonergic system can regulate GABA and glutamate activity within cortical circuits. Overall, this study provides evidence that 5-HT2 receptors modulate motor cortical circuits even without voluntary drive to the muscle, since all measurements were made at rest.

P2.27-I: Modulation of corticomuscular coherence by changes in the visuomotor environment

Mariko Ichikawa, Keio University; Junichi Ushiyama, Keio University

When using surgery robots and computers, we can deal with the changes in visuomotor environments (i.e., the correspondence relationship between actual movements and how they are reflected visually in the system) and control their movements at the time. Such flexible control of our bodily movements can be accomplished through the neural interaction between the brain and the body. Corticomuscular coherence (CMC) is known as a physiological indicator that evaluates synchrony between activities of the motor cortex and the contracting muscles (Conway et al. 1995). Recently, our laboratory reported CMC is modulated depending on the motor context, which is a combination of some parameters about motor tasks, such as muscle contraction type (sustained or intermittent contraction), contraction intensity, trial randomization, and how to output force initially (Suzuki & Ushiyama 2020). However, no CMC studies have examined whether visual information could become a crucial motor context that affects CMC.Here, the present study investigated whether and how CMC was modulated in the change of visual feedback gain (i.e., how visual information of contracting force was provided to participants through a monitor) within a task in 31 healthy young adults. Within experiments, when visual feedback gain was changed, the relation between a cursor movement on the monitor and the contraction intensity was changed.We conducted 2 experiments with the intermittent contraction task using two types of visual feedback gain (i.e., High- and Low-gain conditions). Specifically, when a certain force output, the movement of a cursor was larger in the High-gain trials, and smaller in the Low-gain trials. Therefore, participants received more detailed feedback of their movement in the High-gain trials than Low-gain trials. We recorded the ankle dorsiflexion force, electroencephalogram (EEG) over the motor cortex of the lower limb, and electromyogram (EMG) from the tibialis anterior muscle during visuomotor tasks (Fig. 1a). In Experiment 1 (Fig. 1b), we provided two visual feedback gains randomly within a set, where the visually needed intensity was the same, but the required intensity was different (10% and 25% of maximal force). In Experiment 2 (Fig. 1c), we also provided two visual feedback gains randomly within a set, where the visually needed intensity was different, but the required intensity was the same (10% of maximal force).The results showed that the magnitude of CMC

was significantly greater in the High-gain trials than in Low-gain trials in only Experiment 1. On the other hand, Experiment 2 didn't show a significant difference in CMC between visual feedback gains.These results suggested even in the visuomotor environment where visual feedback gain changed within the task, our nervous system deals with it online by modulating neural interaction between the motor cortex and muscle depending on a difference in the motor output exhibited, rather than how it is visual feedback.

P2.28-I: Modulation of triceps surae cutaneous reflexes to non-noxious stimuli during walking and running in humans

Alan Phipps, Medical University of South Carolina; Aiko Thompson, Medical University of South Carolina

Background: Cutaneous reflexes (CRs) to non-noxious stimuli are task-dependently modulated between standing and running (Brain Res. 1993: 613: 230-238), and the modulation pattern is nerve-specific during walking (J. Neurophysiol 1997: 6: 3311-3325). Because different modes of locomotion are typically associated with different speed (i.e., speed of locomotion is faster during running than during walking), whether CRs are speed or mode (task) dependently modulated during locomotion is currently not known. Are cutaneous reflexes modulated between different modes of locomotion and/or between different speeds of locomotion? To address this question, this study examined the triceps surae CRs during two modes (i.e., walking and running) of locomotion at two different speeds each, with the speed of faster walking matching the speed of slower running speed. Methods: 18 individuals with no known neurological conditions participated in this study. CRs were elicited by stimulating the sural (SRn), superficial peroneal (SPn), and distal tibial nerve (DTn) near the left ankle. For each stimulation, a 5 x 1-ms pulse train (200 Hz) at ~1.9 x radiating threshold was delivered while the participant walked at 3 or 4 km/h (WalkSlow) and 6 or 7 km/h (WalkFast) and ran at 6 or 7 km/h (RunSlow) and 9 or 10 km/h (RunFast). EMG was recorded from the soleus, medial (MG), and lateral gastrocnemius (LG) ipsilateral to the stimulation site. For three distinctive phases (early stance, mid-late stance, end swing) of each locomotion condition, short (50-80ms post-stimulus onset, SLR) and medium (80-120ms, MLR) latency CRs were quantified as the difference between stimulated and non-stimulated EMG in early stance, mid-to-late stance, and end swing phase, and expressed in % maximum M-wave (%Mmax). Results and Discussion: Soleus, MG, and LG SLRs showed mode- (i.e., WalkFast vs. RunSlow) and speed- (i.e., different speeds within the mode of walking or running) dependent modulation during early and mid-to-late stance phases but only speed-dependent modulation during end swing. For instance, in the soleus, early stance SLR was inhibitory and greater during RunSlow than WalkFast with all three nerve stimulation conditions: SPn (-3.4%Mmax vs. -1.7%, p=0.002), SRn (-3.8% vs. -1.3%, p=0.002), and DTn (-3.7% vs. -0.8%, p=0.004) while inhibitory SLRs were greater during WalkFast than WalkSlow (-1.3% vs. -0.6%, p=0.036) to SRn stimulation; during end swing, SLRs to SPn stimulation was less excitatory during WalkFast than Walkslow (0.01% vs. 0.4%, p=0.046). MLRs were modulated similarly to SLRs but appeared less robust in all three phases studied. The facts that triceps CRs are mode- and speed-dependently modulated in early stance but only speed-dependently modulated in end swing may suggest phase-dependent roles of cutaneous

afferent input in human locomotion. Spinal processing of cutaneous afferent activity appears to be complex and dynamically modulation across the locomotion cycle in humans.

P2.29-I: Co-modulation of the stress response and motor activation during adaptation to split-belt walking

Beier Lin, University of British Columbia; Kaya Yoshida, Rehabilitation Research Program; Jayne Garland, Western University; Tanya Ivanova, Western University; Janice J. Eng, University of British Columbia; Lara Boyd, University of British Columbia; Amy Schneeberg, University of British Columbia; Courtney Pollock, University of British Columbia

Introduction: When individuals encounter unexpected perturbations to gait, the central nervous system actively recognizes error and rapidly recalibrates sensorimotor control to accommodate the altered walking conditions. Neurophysiological changes associated with the autonomic nervous system (ANS) and its stress response to perturbations may contribute to adaptation of motor control strategies when standing balance is challenged. However, the interaction between motor adaptation and the stress response associated with challenge to gait remains unknown. The purpose of this study was to investigate the co-modulation of the physiological stress response as measured by electrodermal activation (EDA) and the motor activation of muscles about the ankle during a repeated block split-belt treadmill walking protocol. Methods: Twelve healthy young adults (28.5 ± 5.5 years, 8 males) participated in a single session of split-belt treadmill walking. The belt speeds were individualized. The fast belt speed was set at 90% of a person's fast walking speed measured during a 10m over ground walking test and, the slow belt speed was set at 50% of the fast speed to achieve a 2: 1 ratio between belts. Participants were familiarized with the fast and slow speed of tied-belt treadmill walking, then were exposed to 3 blocks of split-belt walking (3.5 mins, 2: 1 belt-speed) alternated with 3 blocks of tied-belt walking (3.5 mins, slow speed). EDA measured the ANS stress response and electromyography (EMG) recorded bilateral tibialis anterior (TA) and gastrocnemius medialis (MG) muscle activation. Step length symmetry (SLS) was measured with embedded force plates. Linear mixed models were conducted to test changes in EMG amplitude, EDA and SLS across blocks, and within blocks during the initial 10s (early) and final 10s (late) phases. RESULTS: Both EDA and bilateral ankle muscle activation showed similar patterns of adaptation during the first exposure (block 1) to split-belt treadmill walking only. There was a decrease in muscle activation in the late phase compared to the early phase of block 1 in bilateral TA and MG muscles (p<0.05). EDA was also decreased in the late phase compared to the early phase of block 1 (p<0.05). SLS was increased in the late phase compared to the early phase of block 1 (p<0.05). There were no significant differences found between the late and early phases of blocks 2 and 3 in any variables. CONCLUSIONS: Our results are consistent with an established pattern of adaptation to split-belt treadmill walking whereby participants demonstrate the greatest amount of improvement in SLS early in a practice session. Importantly, these results extend our understanding of the co-modulation of the stress response and motor activation of muscles during adaptation of motor performance of walking when gait is challenged.

P2.30-I: Differential Changes in Short-latency SEP Peaks and Motor Performance Following a Visuomotor Tracing Task in Healthy Adults

Alexandre Kalogerakis, Ontario Tech Univeristy; Hailey Tabbert, Ontario Tech Univeristy; Ushani Ambalavanar, Ontario Tech Univeristy; Bernadette Murphy, Ontario Tech Univeristy; Paul Yielder, Ontario Tech Univeristy

Neck muscle vibration has been shown to alter neural processing and upper limb proprioception in healthy adults. Previous research has demonstrated significant differential changes in the N18 and N24 SEP peaks coupled with altered motor learning following acquisition of force matching task, reliant on proprioceptive inputs while under the influence of vibration. The current research aims at discovering if neck muscle vibration impacts motor learning of a visuomotor tracking task in addition to force matching.14 right-handed, healthy participants (aged: 21.4 ± 2.3) were divided into vibration (V, n=8) and no vibration control (NV, n=6) groups. All had the vibration device affixed over the right sternocleidomastoid and left cervical extensor muscles. Participants underwent right median nerve stimulation at 2.47Hz and 4.98Hz to elicit short and middle latency somatosensory evoked potentials (SEPs). 1000 sweeps were recorded and averaged using a 64 lead EEG cap pre- and post-acquisition of a novel visuomotor tracing task (MTT). After the pre-acquisition trials, the NV group was given 10 minutes rest, and the V group received 10 minutes of vibration at 60Hz before performing the motor acquisition task. Task performance was assessed immediately post-acquisition and at retention 24 hours after. Motor Tracing Results: Trends from the motor tracing data indicate that accuracy in the NV group improved by 30% from pre to post and by 6% from post to retention. Accuracy in the V group improved by 28% from pre to post and by 3% from post to retention. SEPs Results: The N18 SEP peak amplitude increased by 13% in the V group and decreased by 33% in the NV group. Similarly, the N20 amplitude increased by 13% in the V group and decreased by 33% in NV group. The N24 SEP peak increased by 20% in the V group while decreasing by 8% in the NV group. Discussion: The preliminary data suggests that neck muscle vibration resulted in differential SEP changes induced by motor learning as compared to no vibration for the N18, N20 and N24 SEP peaks. Both groups appeared to learn the task, with the V group showing a trend towards less retention than NV. When compared to previously published work which used a proprioceptive-based force matching task (FMT), the V group had opposite effects on the N18 which increased in this study but decreased in the previous FMT study. The N24 had similar findings with increases after both tasks. Interestingly, the N20 which reflects processing in primary somatosensory cortex, showed differential changes in this study, while showing no significant differences in the previous FMT study. Conclusion: Preliminary trends in the neurophysiological and motor performance data indicate that vibration may have differential effects on processing of olivo-cerebellar and primary somatosensory cortex SEPs for a visuomotor tracking task as compared to a proprioceptive-based force matching task. Additional data is being collected to confirm these findings.

P2.31-J: Possibility of early Parkinson's disease detection by support vector machine classifier

Yuichi Nishikawa, Kanazawa University

Parkinson's disease (PD) is one of the most common neurodegenerative diseases. Early treatment relies on early diagnosis of PD. This study was to investigate characteristics of motor unit firing behavior of first dorsal interosseous (FDI) muscle between people with PD and healthy control subjects using high-density surface electromyography (HD-sEMG), and to distinguish PD patients from healthy control subjects according to the HD-sEMG information using a support vector machine (SVM) classifier. Twelve people with PD and 14 healthy control subjects were enrolled in this study. Healthy control subjects were targeted on the dominant hand and people with PD were targeted on the less-affected side. The participants performed ramp-up and sustained contractions at 30% of their maximal voluntary contraction. HD-sEMG signals were recorded in the FDI muscle and decomposed into individual motor unit firing behavior using a convolution blind source separation method. Discharge rate, coefficient of variation (CV) of the inter-spike interval, and persistent inward currents (PIC) were used in the analysis. The ΔF obtained from the paired-motor unit analysis was used to estimate PIC. CV of ISI and ΔF were found to be significantly different between the people with PD and healthy control subjects. This information was subsequently used to distinguish people with PD from healthy control subjects using the SVM classifier to obtain a mean accuracy of 93.79%. Although it targeted the less-affected side, which has fewer or no symptoms, this study was able to distinguish PD with a high degree of accuracy. Identification of people with PD by SVM classifier is useful for early detection of people with PD.

P2.32-J: Motor unit properties in human movement disorders

Vishal Rawji, Imperial College London; Dario Farina, Imperial College London

Movement disorders encompass a wide range of neurological conditions that affect the normal execution of voluntary movements as well as producing additional involuntary movements. These disorders, which include parkinsonian disorders, dystonia, ataxias, myoclonus, and tremors, have a profound impact on the quality of life for millions of individuals worldwide. Despite extensive research efforts, the underlying pathophysiology of these disorders remains elusive, making it challenging to develop targeted and effective treatments. We believe that understanding the behaviour of motor units, the basic functional units of motor control, is crucial for elucidating the mechanisms underlying movement disorders. Motor units, composed of motor neurons from the spinal cord and the corresponding muscle fibres, play a crucial role in muscle contraction and movement execution. As the final common output for generating movement, studying motor units provides valuable insights into the motor system's functioning. High-density electromyography (HD-EMG) systems, allow simultaneous recording of electrical signals from multiple motor units non-invasively. HD-EMG, coupled with advanced signal processing techniques, enables the extraction and analysis of individual motor unit action potentials. Through HD-EMG decomposition, spinal cord motor neuron activity can be inferred, offering a non-invasive method to study human motor unit behaviour. This approach provides insights into firing patterns, recruitment properties, and synchronisation of motor units, contributing to our understanding of human motor control. Combining HD-EMG with neurophysiological techniques like electroencephalography (EEG), transcranial magnetic stimulation (TMS) and peripheral nerve stimulation reveals the causal drivers of motor unit activity. We present work that showcases how motor unit estimation can be used to inform

about the pathophysiology of several human movement disorders. Simply, we show that patterns of motor unit activity will be different in muscles affected by movement disorders versus those muscles that are not (i.e., motor units in a dystonic muscle behave differently to motor units in a non-dystonic muscle). We also show that the patterns of activity are specific to the movement disorder in question (i.e., the motor unit patterns during dystonia are different to those during tremor, ataxia, myoclonus, and bradykinesia). By combining HD-EMG with TMS, EEG and peripheral nerve stimulation, we reveal the causal drivers behind changes that we find in these movement disorders.

P2.34-K: Towards the Identification of Neural and Biomechanical Constraints on Motor Unit Control

Ciara Gibbs, Imperial College London; Simon Avrillon, Imperial College London; Vishal Rawji, Imperial College London; Dario Farina, Imperial College London; Juan Gallego, Imperial College London

The repertoire of human movement is made possible by control of the elementary actuators of our neuromuscular system – the 'motor units'. A motor unit comprises an alpha motor neuron and the muscle fibres it innervates. Motor unit behaviour is thought to be subject to neural constraint by 1) common synaptic inputs that prevent their selective recruitment, and 2) Henneman's size principle. Whilst these descriptions have helped conceptualise the coordination of motor units for control, ultimately, our understanding has been hindered by difficulties disambiguating neural and biomechanical constraints. Depending on the task demands, functional correlations are imposed on motor unit activity. This may in part justify differences between canonical motor unit descriptions, and recent works hinting at more flexible motor unit control. For instance, Bräcklein et.al (eLife 2020)demonstrated some volitional decorrelation of two motor units during de-recruitment, whilst Marshall et.al (Nature Neurosci 2022) showed selective modulation of motor unit activity during targeted electrical stimulation of motor cortex. Accordingly, the field is yet to clearly identify the fundamental principles of motor unit control. An abridging perspective that would remain consistent with all observations is the notion of 'motor unit modules'. Here, motor units are grouped by their synaptic inputs, leading to an anatomically unrestricted definition in which modules span parts of a muscle, or even multiple muscles. To disentangle the contributions of neural and biomechanical constraints on motor unit control and explore the existence of motor unit modules, our first study will focus on muscles partitioned by compartments. Compartments are relevant candidates for possessing motor unit modules, given earlier reports on less common synaptic inputs to motor units across muscle compartments, compared to within. With such partitioning in synaptic input, the functions of different compartments may be effectively decoupled, as observed previously for compartments controlling different effectors or actions. However, not all compartmentalised muscles appear to be structured under the same incentive. One example may be the human Flexor Carpi Ulnaris (FCU), a forearm flexor with two distinct compartments. Unlike muscles of prior studies, each compartment is not associated with a unique function; rather ,they work cooperatively in achieving wrist flexion and adduction. With intramuscular and high-density surface EMG recordings, we will study the activity of motor unit populations in each FCU compartment, comparing motor unit co-modulation metrics

within and across compartments. Concurrently, we will detect the motor unit activity of neighbouring synergistic and antagonist muscles that harbour either a similar neural (innervation), or mechanical (muscle origin) constraint. Combined with the study of several contraction types and forearm configurations, we will begin to decouple the influences of task-related (biomechanical) and neural constraints on motor unit control. In turn, this will help us to establish whether motor unit modules exist at the most coarse, compartmental level within muscle, and their stability across behaviours. Overall, our experiment will aid in defining what constitutes the smallest functional unit of the motor system, shedding light into a fundamental question in systems neuroscience whilst also informing the design of muscle-machine interfaces.

P2.36-K: Considerations for determining 'gold standard' methods for analyzing motor unit firing behavior

Nathan Wages, Rutgers University; Jongsang Son, New Jersey Institute of Technology; Jean-Francois Daneault, Rutgers University; Christopher Thompson, Temple University

Presently, there are no ‘gold standard’ methods to analyze estimated motor unit firing behavior (MUFB) due to theoretical and practical limitations of varying decomposition-based technologies. This barrier increases the difficulty to objectively assess the accuracy of MUFB. Current methods to assay MUFB vary from collapsing data for an individual or a group of individuals at a particular contraction intensity, collapsing data across multiple intensities, or analyzing data on a subject-by-subject or group-by-group basis before collapsing the data. Additionally, there are a variety of methods to report MUFB data, ranging from listing the traditional absolute values to listing values in a relative way, such as normalizing data by ‘recruitment, frequency, or time bins’, or by averaging data across certain phases of a contraction. Moreover, the time at which data is extracted for analysis also influences the information that is gleaned. For instance, data has been reported via extraction rates of a few milliseconds to rates that exceed a few minutes. Finally, it’s important to highlight that visual real-time feedback provided to the subject, whether it be force or an EMG-derived index such as root mean square, dictates the underlying motor control scheme for the MUs used during that contraction. For example, a 60% maximum voluntary contraction (MVC) force matching task doesn’t imply each synergistic muscle uses 60% of its MUs, but rather the combined effort of all MUs recruited across the synergistic muscles equates to a 60% force output. Thus, individual percent contributions for MUs from synergistic muscles remain unknown. While each approach has advantages and limitations, the clinical significance of that data lies in the data’s interpretation. To illustrate this point, when estimating motoneuron intrinsic excitability (delta F) the identification of when a MU is recruited and decruited is paramount to determining whether a pool of MNs is considered hyper or hypo-excitable. Taken together, these points underscore the need to develop universal analysis standards for accurate clinically meaningful interpretations of MUFB.

P2.37-K: Assessment of motor unit activity in patients with post-COVID-19 syndrome

Camila Castro Vergasta, Universidade Estadual de Campinas; Emilia Frigerio Cremasco, Universidade Estadual de Campinas; Ellen Pereira Zambalde, Universidade Estadual de Campinas; Carina Germer, Universidade Estadual de Campinas; Leonardo Abdala Elias, Universidade Estadual de Campinas

A significant number of individuals infected by SARS-CoV-2 report persistent symptoms lasting weeks or months after the acute phase of COVID-19. This condition, not yet fully understood, characterizes the post-COVID-19 syndrome (PCS), whose prevalent symptom is fatigue. Fatigue encompasses a wide range of physiological manifestations, including cognitive, neuromuscular, and psychological, precluding a precise definition and assessment. In the present study, we design an experimental protocol to assess the fatigability in individuals affected by PCS by measuring muscle force and motor unit activities. Participants were divided into two groups: COVID and Control. The COVID group consisted of 18 volunteers (16 women, 40.6 ± 7.5 yr.), while the Control group comprised 17 participants (14 women, 41.6 ± 9.5 yr.). Participants performed isometric abduction of the index finger of the dominant hand in four different motor tasks. The experimental protocol consisted of three blocks: pre-fatigue, post-fatigue, and post-rest, with a 30-minute interval between the last two blocks. Maximum voluntary contraction (MVC), reaction time, trapezoidal force, and time to task failure motor tasks were performed. Throughout the tasks, surface electromyography signals were collected and subsequently decomposed using the software NeuroMap (Delsys) to analyze motor unit activities. The main results of this study highlighted notable differences between COVID and Control groups in both motor unit activity and force metrics. MVC was significantly lower in COVID when compared to Control participants (13.79 ± 1.81 N vs. 20.03 ± 2.42 N, p = 0.02). In the reaction time task, significant differences were observed in the maximum discharge rate (COVID: 15.41 ± 1.33 Hz vs. Control: 18.42 ± 1.43 Hz, p = 0.037) and in the rate of force development (COVID: 182.92 ± 18.84 %MVC/s vs. Control: 236.74 ± 29.92 %MVC/s, p = 0.007). In the trapezoidal force task, there were significant differences in the force variability, quantified by the coefficient of variation (COVID: 4.25 ± 0.49 % vs. Control: 2.86 ± 0.32 %, p = 0.001), as well as in the coefficient of variation of smoothed cumulative spike train (sCST) (COVID: 17.58 ± 1.82 % vs. Control: 13.48 ± 1.10 %, p = 0.005) and the relative power spectral density of sCST in the 5-10 Hz frequency band (COVID: 8.76 ± 1.42 % vs. Control: 5.96 ± 0.86 %, p = 0.012). Furthermore, significant differences were observed in motor unit action potential (MUAP) amplitude (COVID: 177.18 ± 10.96 mV vs. Control 212.37 ± 11.57 mV, p < 0.001) and duration (COVID: 20.28 ± 0.49 ms vs. Control: 18.96 ± 0.42 ms, p < 0.001), assessed in the plateau phase of trapezoidal force task. These findings show that infection by SARS-CoV-2 modifies both discharge (central) and MUAP (peripheral) properties of motor units with a detrimental influence on performance of the neuromuscular system of patients with PCS. The specific causes of these changes should be further investigated.

P2.38-K: Acute changes in motor unit recruitment threshold following resistance exercise with various exercise intensities [Poster Award]

Rii Shinoda, Chukyo University; Taichi Nishikawa, Chukyo university; Ryosuke Takeda, CU; Kohei Watanabe, Chukyo University

Purpose: The number and/or types of motor units recruited during exercise is primarily determined by exercise intensity. Also, repeated contraction-induced neuromuscular fatigue can change motor unit recruitment pattern due to a decrease in the recruitment threshold. In the actual scenes of resistance exercise session, the number of repetitions is determined by exercise intensity, so motor unit recruitment pattern could be determined by exercise intensity and number of repetitions. The purpose of this study was to clarify acute changes in motor unit recruitment threshold (MURT) following single session resistance exercise with various combinations of exercise intensity and number of repetitions. Methods: Eleven healthy men were recruited for the study. Isometric knee extension exercises were performed at 40%, 60%, and 80% of maximal voluntary contraction (MVC). In order to match the total work among different exercise intensities, three sets of 14, 9, and 7 repetitions were conducted for 40%, 60%, and 80% of exercise intensity. The participants completed three exercise sessions with different exercise intensities on separate days and the order of the given exercise intensities were randomized. Before and after the exercise sessions, MVC of isometric knee extension and high-density surface electromyography (EMG) of the vastus lateralis was recorded during submaximal ramp-up isometric knee extension. MURTs of motor units that could be tracked before and after the exercise session was then calculated. RESULTS: MVCs were decreased 16.8±6.1%, 16.5±5.0%, and 19.0±6.1% for 40%, 60%, and 80% of exercise intensities (p < 0.05). Degrees of decrease in MVC were not significantly different among three exercise intensities (p > 0.05). Numbers of detected and tracked motor units for 40%, 60%, and 80% of exercise intensities were 91, 79, and 85. MURTs were significantly decreased following single resistance exercise sessions with 40% and 60% of exercise intensities, i.e. -1.3±4.3%MVC and -2.4±3.9%MVC (p < 0.05), but not with 80% of exercise intensity (-0.3±4.8%MVC, p > 0.05). Conclusion: The present study suggests that additional recruitment of motor units can be induced during a single session of resistance exercise with middle exercise intensities (≤ 60%), but not with higher exercise intensities (≥ 80%) when total work are matched. Acknowledgement: The authors appreciate Prof. Aleš Holobar of the University of Maribor, Slovenia, for supporting the analyses of motor unit firing properties using the DEMUSE tool.

P2.39-K: Short-term strength training does not affect motor unit recruitment threshold and discharge frequency during isometric dorsiflexion at a submaximal level in the tibialis anterior muscle [Poster Award]

Gaku Shinohara, Shinshu University; Patricio Pincheira, The University of Queensland; Glen Lichtwark, Queensland University of Technology; Andrew Cresswell, The University of Queensland; Yasuhide Yoshitake, Shinshu University

A classical study conducted by Moritani and deVries (1979) revealed that, following several weeks of strength training, the amplitude of surface EMG remained unaltered during submaximal contractions at a given level while maximal voluntary contraction (MVC) force and the corresponding amplitude of surface EMG increased without muscle hypertrophy. The intricate nature of surface EMG signals, composed of a summation of motor unit (MU) action potentials presents a significant challenge in identifying adaptations in MU recruitment and discharge patterns induced by strength training during submaximal contractions. Using recent advances in high-density EMG (HDEMG), Del Vecchio and colleagues (2019) showed that a 4-

week of strength training decreased MU recruitment threshold and increased MU discharge frequency during isometric contractions at a given submaximal level. Assuming identical twitch force characteristics such as contraction time, relaxation time and peak force, an increase in discharge frequency and the number of recruited MU may lead to a greater exerted force. Based on this notion, the finding by Del Vecchio et al. (2019) implies that a 4-week of strength training may reduce electro-mechanical efficiency concerning force exertion at a submaximal identical level. This study aims to re-investigate whether a 4-week strength training intervention induces changes in MU recruitment threshold and discharge frequency concerning isometric force exertion at a submaximal level.[Methods]Thirteen healthy young males participated in a 4-week training session, with the same content as that conducted by Del Vecchio et al. (2019). Before and after the training intervention, participants were seated in a chair with their right ankle angle at 10° of plantarflexion. Participants performed trapezoidal isometric dorsiflexion contractions while following visual guidance that involved a linear-increase in force to a 35% MVC (obtained before training) at a rate of 5% MVC per sec and 10 s of constant force at 35% MVC. A 64-channel HDEMG from the tibialis anterior muscle was recorded to identify MU discharge timing using the CKC method (Holobar & Zazula 2007). MUs were tracked across the training intervention based on the cross-correlation analysis of the MU action potential, which was extracted by spike-triggered averaging from HDEMG. MU activity was evaluated in terms of MU recruitment threshold during the ascending phase and mean discharge frequency during the steady phase.[Results]Following four weeks of strength training, a 14.2% increase in maximal strength was observed (P < 0.05), which was a very similar increase (13.8%) to the results of Del Vecchio et al. (2019). In 74 trackable MUs before and after training, there was no change (P > 0.05) in the MU recruitment threshold between before (20.7 %MVC) and after (22.5 %MVC) strength training. Similarly, there was no change (P > 0.05) in mean MU discharge frequency between before (17.0 Hz) and after (16.7 Hz) strength training.[Conclusion]These results suggest that four weeks of strength training do not alter the recruitment threshold and discharge frequency of MUs during isometric submaximal dorsiflexion. It is implied that the number of recruited MUs and their discharge frequency during submaximal isometric contractions at a given level may remain unchanged after training intervention. The inconsistency with the findings by Del Vecchio et al. (2019) remains unclear.

P2.40-K: Motor Unit Activity and Active Area Changes in the Gastrocnemius Muscle During Single Joint Movement

Koyo Nogi, Saitama Prefectural University

Movement is achieved through an intricate motor control system regulated by the central nervous. Despite the potential of motor unit: MU analysis in understanding movement control, MU measurements during dynamic tasks are scarce because of hampering their application. This study aimed to elucidate the relationship between MU activity and biomechanics in dynamic tasks, using gastrocnemius muscle MU activity and joint torque data during single-joint movements while tracking MU spatial position coordinates. Five healthy adult male subjects were used as subjects, and the target muscle was the medial head of the gastrocnemius muscle: MGAS. The multi-mode dynamometer, BIODEX, and High-density surface EMG: HDEMG were used. The target torque was set at 10 and 25% MVC. The task was

isokinetic contraction at each target torque. The joint motion was controlled using BIODEX so that the joint angular velocity was 5 and 10 degrees per second. MUs decomposed were analyzed using DEMUSE, and only MUs with a PNR of 28 dB or higher were included. In the analysis, the activity position coordinations were calculated from the increase/decrease rate of MU discharge rate: DR and MUAP of grid electrodes, and the changes in MU activity during the dynamic task were followed. The rate of increase in MUDR during concentric contraction was significantly higher than the rate of decrease in DR during eccentric contraction during the task. The rate of increase in MU activity during concentric contraction at the target torque of 10% MVC increased significantly with increasing joint angular velocity. The MU activity position during the task varied greatly at each MU spike timing, and the activity position distribution was wide, with no differences depending on the muscle contraction style. The rate of increase or decrease in MU activity has been reported to vary with contraction mode and rate of contraction. The rate of change in MUDR was smaller in centrifugal contractions than in concentric contractions. This may be due to the involvement of non-contractile tissues with high tension, such as tendon tissue, in force generation. Because of the shortening of muscle length in concentric contractions, it is difficult to utilize tension outside the muscle. Therefore, neuromuscular activity may flexibly adjust the contractile force and velocity changes. These results suggest that MU activity can be efficiently regulated by considering the tension caused by non-contractile tissues and that the amount of activity is regulated according to the velocity and force. In addition, the change in spatial position coordinates of MU activity during a task may be greatly affected by the anatomical structure of the muscle and waveform propagation during contraction. Therefore, it is difficult to extract the same MUAP waveform from EMG, and it is difficult to calculate and track the MU position coordinates for each activity.

P2.41-L: Muscle synergy from changes in subjective effort in table tennis service.

Yuki Sato, National Institute of Technology, Oyama College; Kengo Wakui, Niigata University; Shuhei Kameyama, Niigata University; Yukihiko Ushiyama, Niigata University

In competitive sports, the ability to subjectively control the exertion of force is considered crucial. The focus of this study is on the service action in table tennis, where players often vary their force to confuse their opponents – sometimes applying a strong spin with considerable force, and at other times hitting the ball with less force. This variability highlights the essential nature of being able to control force exertion subjectively. However, the impact of this subjective force exertion ability on muscle synergy in the table tennis service action is not yet clearly understood. This study aims to investigate the relationship between subjective effort levels in the forehand backspin serve in table tennis and muscle synergy, using muscle synergy analysis.For the experimental trials, the forehand backspin serve was selected. This was chosen because it is one of the most common services used in table tennis matches by a wide range of players. The subjective effort levels were divided into five stages (60%, 70%, 80%, 90%, and 100%), with each level performed consecutively five times. The order of these trials was randomized. During these trials, surface electromyography (sEMG) was recorded for ten upper limb muscles involved in the forehand backspin serve. The movement was captured using five motion capture cameras, which facilitated the extraction of analysis segments. The sEMG data were then filtered and used to calculate the Average Rectified Value (ARV). Subsequently, the

data from the five trials were averaged, and non-negative matrix factorization was applied to derive muscle synergy vectors and synergy activation coefficients.The results revealed that several muscle synergies were identified in the forehand backspin serve across the five levels of force exertion. This indicates that muscle synergies in table tennis backspin serves change in response to variations in subjective effort levels. This study thus sheds light on how subjective control of force influences muscle coordination and synergy, particularly in the context of table tennis serving techniques. The findings contribute to a broader understanding of the role of subjective force control in sports performance, with potential implications for training and technique optimization in table tennis and other sports.

P2.42-L: Center of pressure change and lower limb muscles activities during single leg stance

Hyun Kyoon Lim, Korea Research Institute of Standards and Science; Jooyeon Ko, Daegu Health College

INTRODUCTIONPostural stability is an important ability to maneuver many daily life movements. Especially good balance helps kids and the senior people from falling or getting injured. It is an important to measure the stability ability of a person, especially children and old adults, with proper tools. In this study, we used a plate equipped with the load cells as well as multi-electromygraphy electrodes (n= 14 places) during single leg stance (SLS). METHODSMultiple surface electromyography (sEMG) electrodes (Ultium, Noraxon, USA) were used for both legs: tibialis anterior, soleus, rectus femoris, rectus abdominus, peroneus, lumbar erector spinae, and biceps femoris. Participants were 15 children (age = 8.9 +/- 1.5 years, 10 females), 14 young adults (age = 22.2 +/- 1.9 years, 14 females), and the old adults (age = 71.6 +/- 3.7 years, 5 females) during SLS. Tests were made after taking signed consent forms from all participants before participation (IRB no. KRISS-IRB-2023-01 and DHCIRB-2022-06-0008). The measurement device (Bertec force plate) was used to measure the center of gravity (COP). Authors finished the calibration and calculation of the uncertainty of the device. We employed Brain Motor Control Analysis (BMCA) protocol for sEMG analysis composing of an amplitude and a similarity index for the analysis. We built prototype vector using young adults and then compared with the other groups. <Performance time>, <95% confidence ellipse area>, <COP path length>, and <COP average velocity> were evaluated using COP data. RESULTS AND DISCUSSIONAll three groups were showing significant difference in <Performance time> and <COP average velocity> (p<0.05). <95% confidence ellipse area> showed significant difference between Children and young adults groups (p<0.05). <COP path length> showed significant difference between children and old adults, and between young adults and old adults (p<0.05). BMCA analysis showed similarity index from 0.34 to 0.99. Average similarity index of children were 0.91, 0.93 for young adults, and 0.82 for old adults. Total magnitude of EMG from all muscles was 902, 950, and 831 (uV) for each groups during SLS. EMG patterns showed similar patterns in children and young adults. Abnormal EMG patterns were observed from one young adult and one old adults. BMCA protocol showed the strong point that it may pick one abnormal behavior out of ten muscle activities involved during the SLS. <COP path length> and <COP average velocity> could be a good index for evaluate aging effect on stability (Fig. 1). Fig. 1. COP path length,

average velocity, and BMCA analysis results CONCLUSIONS Inthisstudy, we evaluated the center of pressure and muscle activities during single leg stance. It may be a reliable quantitative index to evaluate the stability ability of children and old adults. ACKNOWLEDGEMENTSThis study was financially supported by the Ministry of Trade, Industry, and Energy (MOTIE), Korea, under the Korean Reference Data Center ProgramsupervisedbytheKoreaResearchInstituteofStandardsandScience(KRISS). REFERENCES[1] Lim, H.K. et al. 2005, J Rehabbil Res Dev 42, 413-22. [2] Sozzi, S. et al. 2013, Clinical Neurophsisology 124, 1175-1186.

P2.44-M: Modelling surface EMG signals during voluntary movements with neuromechanical and deep network models

Shihan Ma, Imperial College London; Irene Mendez Guerra, Imperial College London; Arnault Caillet, Imperial College London; Jiamin Zhao, Shanghai Jiao Tong University; Alexander Clarke, Imperial College London; Kostiantyn Maksymenko, Neurodec; Samuel Deslauriers-Gauthier, Neurodec, Inria Centre at Université Côte d'Azur; Xinjun Sheng, Shanghai Jiao Tong University; Xiangyang Zhu, Shanghai Jiao Tong University; Dario Farina, Imperial College London,

BACKGROUND AND AIM: Neuromechanical studies investigate how the nervous system interacts with the musculoskeletal (MSK) system to generate volitional movements. Such studies require an integrated understanding of the dynamic systems, which are complicated to understand from experimental measurements alone. Simulations play a complementary role by providing insights into the variables that cannot be directly measured and a test platform for iterating if-then scenarios before experimental implementations. However, current simulation methods of surface electromyogram (EMG), a core physiological signal in neuromechanical studies, are mainly limited to static conditions. Here, we address this limitation by proposing NeuroMotion, an integrated open-source simulator that can be used to simulate surface EMG signals during hand, wrist, and forearm dynamic movements. METHODS NeuroMotion is comprised of three modules. The first is a neuro-biomechanical module that uses an upper-limb MSK model and OpenSim API to estimate the muscle activations and fibre lengths during movement. We used the ARMs Wrist and Hand Model, which includes 23 degrees-of freedoms (DoFs) that cover the finger movement and the flexion/extension and the radial/ulnar deviation of the wrist. The estimated muscle fibre lengths are then utilised by the second module, BioMime, which is a deep generative model that takes in the physiological parameters and outputs the dynamic motor unit action potentials (MUAPs) during the movement. The third module is a motoneuron pool model that simulates motor unit spike trains given the muscle activations. Lastly, surface EMG signals during the movement are generated by convolving the dynamic MUAPs and the motor unit spike trains with some additive noise. The three modules are implemented in Python and integrated into a single package available here https: //github.com/shihan-ma/NeuroMotion. RESULTS We first show how simulated MUAPs change during different levels of physiological parameter changes and different movements. Then, we show that the synthetic data during two-DoF hand and wrist movement can be used to augment the experimental dataset for improving joint angle regression. Ridge regressors trained on the synthetic data can be directly applied to predict the joint angles from two subjects' experimental data with Pearson correlation coefficient > 0.5. The regression accuracy can be

further improved for two subjects when the experimental data are combined with the synthetic data. CONCLUSIONS With NeuroMotion, users can generate plausible surface EMG signals given the kinematics during a voluntary human hand, wrist, and forearm movement. The synthetic dataset is useful to fast iterate regression algorithms and validate information extraction algorithms.

P2.45-M: Quantum sensor-based magnetomyography for contactless measurement of muscle fiber conduction velocity [Poster Award]

Lukas Baier, Hertie-Institute for Clinical Brain Research, University of Tübingen, Tübingen; Dogukan Keles, Institute for Modelling and Simulation of Biomechanical Systems, University of Stuttgart; Markus Siegel, Hertie-Institute for Clinical Brain Research, University of Tübingen, Tübingen, Germany; Oliver Röhrle, University of Stuttgart; Thomas Klotz, University of Stuttgart; Tim Brümmer, Hertie-Institute for Clinical Brain Research, University of Tübingen, Tübingen, Germany; Justus Marquetand, Department of neural dynamics and Magnetoencephalography, University of Tuebingen

Abstract: Muscle fiber conduction velocity (MFCV) is the speed at which electrical activity propagates along muscle fibers and can be measured using high-density electromyography (HD-EMG). With the development of miniaturised quantum sensors (so-called optical pumped magnetometers, OPM), contactless MFCV can now also be measured using the magnetic counterpart of EMG, magnetomyography (MMG). However, this claim remains to be proven experimentally in-vivo.Therefore, the right abductor digiti minimi muscle of 12 healthy volunteers was measured using simultaneous non-magnetic high-density(HD)-EMG (64 channels) and -MMG (15 OPM sensors) after electrical stimulation of the ulnar nerve at the cubital tunnel. Post-hoc synchronisation of the two data sets was used to compare the peak-to-peak latencies of evoked muscle activity per electrode pair with the spatially matched OPM.The electrically evoked muscle activity was measurable In all 12 healthy subjects, both in HD-EMG and MMG. After preprocessing (30-120Hz, 50Hz notch filter), and the application of a peak detection algorithm, it became evident that in both modalities the delay of the respective evoked peak-to-peak muscular activity was already visually apparent. Both modalities showed comparable results of 3-4 m/s of MFCV. Of note, measuring simultaneous HD-EMG and -MMG was not straight-forward, since MMG requires magnetic shielding and is clearly susceptible to artefacts whose origin can be traced back to movements, electromagnetic signals or vulnerabilities of the measuring system. Therefore, all used materials must be tested aforehead for magnetism, i.e. if the materials inherit ferromagnetic metals like iron, nickel or cobalt.Despite the practical difficulties and considering the explorative, partly pioneering nature of measuring MMG using OPM, we firstly were able to prove that MCFV is measurable contactless. This study paves the way towards the further employment and development of quantum sensors for clinical neurophysiology.

P2.46-M: Muscle activation between individuals with anterior cruciate ligament reconstruction and matched healthy controls during 30-min running

Jaewook Lee, Kyung Hee University; Kanghun Lee, Kyung Hee University; Hyeonjun You, Kyung Hee University; Young-Seong Lee, Korea National Sport University; Sang-Kyoon Park, Korea National Sport University; Jihong Park, Kyung Hee University

Background: Since neuromuscular alterations during dynamic tasks (e.g., running) vary, monitoring electromyographic (EMG) activity during a bout of exercise would yield insights into neuromuscular activation profiles in response to sports activities.Objectives: To compare muscle activation in the lower extremity between individuals with anterior cruciate ligament reconstruction (ACLR) and matched healthy controls during 30-min self-paced running. Methods: Twenty physically active individuals with ACLR (25.2 years; 171.4 cm; 73.1 kg; 24.7 kg/m2; month after surgery: 50.0 months; exercise duration: 320.6-min per week) and twenty matched healthy controls (24.7 years; 169.6 cm; 67.0 kg; 23.2 kg/m2; exercise duration: 310.5-min per week) were volunteered. A total of three surface EMG (sampled at 2,000 Hz) electrodes were attached to the rectus femoris (RF), semitendinosus (ST), and medial gastrocnemius (MG) on their involved limb (defined as the limb that had undergone ACLR or dominant limb in healthy control). Participants were asked to run at a self-paced speed for 30-min on a force plate instrumented treadmill (sampled at 1,000 Hz). The average speed was recorded as 8.3 km/h. The EMG signals were recorded for a minute at the 5th and 25th minute during running. Recorded signals during the five successful stance phases (0% being heel strike and 100% being toe off, distinguished by the heel marker) were filtered and smoothed through a 4th order Butterworth filter (cutoff frequency: 10 to 500 Hz and 20 Hz). Afterward, smoothed data were normalised by the peak amplitude value recorded during the knee extension phase of countermovement jumps. The amplitude-normalised EMG data were analysed using 2 (group: ACLR vs. control) × 2 (time: 5th-min vs. 25th-min) functional data analysis (α=0.05). Cohen's d effect sizes (d) were calculated where the statistical differences exist. RESULTS: Regardless of time, activation of the RF (1% to 12%; 39% to 50% of the stance phase), ST (83% to 100% of the stance phase), and MG (84% to 90% of the stance phase) were greater (RF: < 61%, d=0.45; ST: < 68%, d=0.65; MG: < 16%, d=0.36) while activation of the ST (2% to 7% of the stance phase) and MG (1% to 70% of the stance phase; Figure 1) were less (ST: < 5%, d=0.39; MG: < 64 %, d=0.64) in individuals with ACLR than those with the control. Regardless of group, activation of the RF (13% to 24% and 38% to 91% of the stance phase) was greater (< 114%, d=0.41) at the 25th-min time point than the 5th-min. CONCLUSION: : Individuals with ACLR showed different neuromuscular patterns during 30-min running compared to healthy controls. Except for the RF, these altered neuromuscular activation patterns were consistent during running in individuals with ACLR. For the RF, neuromuscular activation increased at 25th-min regardless of the group.

P2.47-M: Neuromuscular activity of the lower extremities during walking in ACL reconstructed individuals and healthy controls

Kanghun Lee, Kyung Hee University; Jaewook Lee, Kyung Hee University; Yunji Park, Kyung Hee University; Young-Seong Lee, Korea National Sport University; Sang-Kyoon Park, Korea National Sport University; Jihong Park, Kyung Hee University

Background: Anterior cruciate ligament reconstruction (ACLR) may lead to alterations in muscular activation of the lower extremities during walking, yet the neuromuscular activity after

a bout of exercise (e.g., 30-min running) is unclear.Purpose: We asked two research questions: (1) Will neuromuscular activation patterns in the lower extremity be different between individuals with ACLR and healthy individuals during walking? (2) Will lower extremity neuromuscular activation during walking be altered after 30-min running in both groups? Methods: Twenty individuals with ACLR (25.2 years; 171.4 cm; 73.1 kg; 24.7 kg/m2; 50.0 months from surgery) and twenty matched healthy controls (24.7 years; 169.6 cm; 67.0 kg; 23.2 kg/m2) who self-reported exercising at least 150-min per week were recruited. Three surface electromyography (EMG; sampled at 2,000 Hz) electrodes were attached to medial gastrocnemius (MG), rectus femoris (RF), semitendinosus (ST) on their involved limb (defined as the limb that had ACLR or the matched limb in healthy control). Subjects walked for 1-min with a habitual walking speed (an average of 4.6 km/h) before and after 30-min of self-paced running (an average of 8.3 km/h). The EMG signals during the consecutive three stance phase (SP; from heel strike to toe off; 1%=heel strike, 100%=toe off) were cropped and filtered through a 4th order Butterworth band-pass filter (cutoff frequency: 20 to 350 Hz), full-wave rectified, and smoothed through low-pass filter (cutoff frequency: 20 Hz). Afterwards, smoothed EMG data was normalised with the peak amplitude value recorded during the knee extension phase of countermovement jumps. Amplitude-normalised EMG data was analysed using two factor (group by time) functional linear models (p<0.05). Cohen's d effect sizes (ES) were calculated to determine practical significances. RESULTS: Regardless of time, RF activation was greater (1 to 7% of the SP, ES=0.44; 18 to 27% of the SP, ES=0.36; 62 to 66% of the SP, ES=0.33; 84 to 86% of the SP, ES=0.33) and ST activation was less (1 to 16% of the SP, ES=0.39; 21 to 27% of the SP, ES=0.34); Decreased (59 to 80% of the SP, ES=0.57; Fig. 1) and increased (91 to 100% of the SP, ES=0.53; Fig. 1) MG activation were observed in individuals with ACLR relative to healthy controls. Regardless of group, MG (26% of the SP, ES=0.32; 37 to 38% of the SP, ES=0.32; 50 to 54% of the SP, ES=0.35; 68 to 73% of the SP, ES=0.37) and ST (44 to 48% of the SP, ES=0.34; 71 to 73% of The SP, ES=0.32) activation were decreased while RF was increased (23 to 26% of the SP, ES=0.32) after 30-min running. CONCLUSION: : We answered the research questions: (1) Individuals with ACLR have different MG, RF and ST neuromuscular activation pattern compared to healthy controls during walking. (2) 30-min running changed MG, RF and ST neuromuscular activation patterns during walking individuals with ACLR.

P2.48-M: Differences in gait electromyographic activity in stroke and healthy subjects using Discrete Wavelet Transform

Marina Algaba Vidoy, Cajal Institute (CSIC) and E.T.S. Ingenieros de Telecomunicación (Universidad Politécnica de Madrid); Jorge Andrés Gómez García, Neural Rehabilitation Group, Cajal Institute, Spanish National Research Council (CSIC). 28006 Madrid; Filipe Barroso, Cajal Institute - CSIC; Francisco Molina Rueda, Department of Physical Therapy, Physical Medicine & Rehabilitation,Rey Juan Carlos University Madrid; Enrique Navarro Cabello, Department of Health and Human Performance. Technical University of Madrid, Madrid, Spain; Diego Torricelli, Neural Rehabilitation Group, Cajal Institute, Spanish National Research Council (CSIC). 28006 Madrid; Juan C. Moreno, Neural Rehabilitation Group, Cajal Institute, Spanish National Research Council (CSIC). 28006 Madrid

Hemiplegic gait is a common outcome of stroke. Hence, to assess asymmetric control of poststroke gait, this work analyzed time-frequency domain (TFD) of surface electromyography (sEMG). Methodology: 9 chronic stroke patients (SP) and 10 healthy controls (HC) were compared using Discrete Wavelet Transform (DWT) to study the electrophysiology underlying tibialis anterior (TA) activity. DWT was applied to filtered sEMG signals during 10 walking trials. Percent of energy within frequency bands (25Hz bandwidth, 25 to 300Hz) was compared in stance (ST) and swing (SW) phases using Wilcoxon's test (dominant vs. nondominant in HC, paretic vs. nonparetic in SP) and Mann-Whitney U-test (paretic, nonparetic vs. HC). RESULTS: The energy at each frequency band may reflect the number and type of recruited motor units (MUs). For dominant vs. nondominant HC, a marked distribution along gait was found: low-frequency MUs prevailed in ST (25-50Hz), while slow (50-75Hz) and fast (200-225Hz) did in SW for effective foot clearance. Yet, differences in HC were observed, probably due to subjects' variability or other effects (i.e., nondominant required more energy for the same task in ST). This physiological distribution was altered in SP. For paretic vs. HC, paretic ST had lower energy. In SW, it increased at 25-50Hz, but decreased at 75-100 and 150-300Hz. This overall reduction explains the typical TA weakness in stroke. Energy changes in bands suggest alterations in MUs recruitment: 50-75Hz MUs that sustain HC ST were replaced by slower MUs in paretic (25-50Hz). Also, faster MUs were reduced in paretic ST (75-125, 175-275Hz) and SW (75-100, 150-300Hz). For nonparetic vs. HC, energy was lower in 25-50Hz, but it increased in 75-99, 125-150 and 175-200Hz, likely because of nonparetic mechanisms that compensate the inability to activate the affected TA. During SW, nonparetic showed a rise in low frequencies (25-50, 50-75Hz) and a reduction in 175-250Hz, contrary to the HC pattern of MUs during SW. For paretic vs. nonparetic, energy in paretic was lower in all bands. In SW, energy in paretic increased in 25-50 and 225-300Hz bands and was reduced in 50-75 and 150-200Hz. Thus, paretic relies on the slowest (25-50Hz) and fastest (225-300Hz) MUs, rather than the 50-75Hz (HC and nonparetic) or 200-225Hz (HC) and 150-174Hz (nonparetic) ones. Conclusion: DWT of TA showed altered spectral attributes in stroke gait. The energy distribution in HC was modified in paretic and nonparetic, which may indicate a pathological alteration in the ratio of recruited MUs of each class during gait. In paretic SW this change is pronounced, possibly due to the occurrence of foot drop. Energy distribution characterized poststroke gait and asymmetries of dominant vs. nondominant and paretic vs. nonparetic. In the future, these findings will be compared with Continuous Wavelet Transform and new features will be extracted from TFD to provide a deeper description of neuromuscular altered mechanisms.

P2.49-M: Force Fluctuations (Steadiness) in patients undergoing Anterior Cruciate Ligament Reconstruction.

Rony Silvestre, meds; Macarena Soldan, MEDS Clinic

Introduction: Anterior Cruciate Ligament (ACL) rupture is one of the most common knee injuries in physically active individuals. After the injury patients undergo surgery which has a very deleterious effect on the quadriceps muscle. It has been reported that approximately 30% of the patients who undergo surgery will develop persistent muscle atrophy, and consequently won't be able to regain muscle strength. Steadiness has been described as a variable that results from the variability in motor unit discharge, providing insight into altered muscle control

mechanisms. Methods: This study was approved by the ethics committee of Clínica MEDS. 13 controls and 13 patients were assessed before surgery and 1, 2, and 3 months after ACLR. Clinical and demographic data was assessed before surgery, maximal voluntary force (MVC), and a trapezoidal force profile at 30% of the MVC was captured in each period to calculate steadiness as the Coefficient of Variation expressed as a percentage (CoV %) as previously described in the literature. The Shapiro-Wilk test was used to assess the data's normality, and then descriptive statistics and data inference using ANOVA were described.Preliminary Results: Nine males and four women with ages 34 ±9 years, weight 75 ± 11 Kg, height 1.72 ± 0.084 m and Body Mass Index 25.23 ± 2.67Kg/m2. There are significant differences in the force variable between the first month after surgery (F1=286 ± 117.4 N) and all the other periods of assessment (F0=467 ± 243 N, F2=387.87 ± 167.83 N and F3=420 ± 157.15 N). The steadiness (CoV, %) at 30% of the MVC didn't show significant differences between periods of assessment. CONCLUSION: : As previously reported in the literature, MVC exhibits a major decrease immediately after surgery but after 2-3 months it returns to pre-surgery levels. Steadiness at 30% of the MVC didn´t show significant differences as we expected.

P2.50-O: Associations between impaired dynamic trunk muscle control in people with chronic low back pain and altered spatial EMG-torque correlations

Michail Arvanitidis, Centre of Precision Rehabilitation for Spinal Pain (CPR Spine), University of Birmingham, UK; David Jiménez-Grande, Centre of Precision Rehabilitation for Spinal Pain (CPR Spine), University of Birmingham, UK; Nadège Haouidji-Javaux, Centre of Precision Rehabilitation for Spinal Pain (CPR Spine), University of Birmingham, UK; Deborah Falla, University of Birmingham; Eduardo Martinez-Valdes, University of Birmingham

Background: Torque fluctuations depend mainly on the amplitude of the low-frequency component of the neural command. Surface electromyographic (sEMG)/torque relationships provide insights into the association between muscle activity and the generated force, which is useful for muscles/muscle groups such as the lumbar erector spinae (ES), where sEMG signal decomposition is challenging. Applying principal component analysis (PCA) further refines these estimations. People with chronic low back pain (CLBP) show reduced isometric torque steadiness and altered HDsEMG-torque relationships compared to controls, likely due to regional adjustments in ES sEMG oscillatory activity, as assessed by topographical δ band coherence maps. However, the neuromuscular control during dynamic contractions, particularly eccentric and flexion movements, and the mechanisms of force control impairments in people with CLBP are yet to be fully understood.Purpose: To quantify the relationship between HDsEMG-torque oscillations in both time and frequency domains during concentric/eccentric trunk extension/flexion contractions in individuals with and without CLBP and evaluate and compare regional variations in HDsEMG amplitude and HDsEMG-torque cross-correlation and coherence for the ES, rectus abdominis (RA), and external oblique (EO) muscles. Methods: Twenty people with CLBP and 20 asymptomatic controls participated. HDsEMG signals were recorded unilaterally from the thoracolumbar ES using two grids, each containing 64 electrodes and from the RA and EO muscles using a single 64-electrode grid for each muscle. Torque was recorded using an isokinetic dynamometer during submaximal trunk flexion/extension contractions. The relationship between HDsEMG signals and torque was

investigated using coherence (δ-band, 0–5 Hz) and cross-correlation analysis. Topographical maps of HDsEMG amplitude and HDsEMG-torque cross-correlation and coherence maps were also generated for each muscle to assess regional between-group differences in muscle activation. PCA was used to reduce HDsEMG data dimensionality. RESULTS: People with CLBP had reduced torque steadiness during trunk flexion/extension concentric/eccentric contractions. For trunk extension, they showed greater HDsEMG-torque coherence in the upper region of the thoracolumbar ES and a higher HDsEMG cross-correlation than asymptomatic participants. For trunk flexion, they demonstrated increased HDsEMG amplitude in their abdominal muscles, with a higher cranial centre of activation and a higher contribution of these muscles, particularly of the EO, to the resultant torque. CONCLUSIONS: This study revealed notable differences in muscle activation patterns in the thoracolumbar ES and EO between people with and without CLBP during trunk flexion/extension contractions and poorer trunk muscle force control in people with CLBP, highlighting the importance of assessing torque steadiness in this patient group.Keywords: chronic low back pain, torque steadiness, coherence, cross-correlation, PCA

P2.51-O: Concurrent validity and reliability of a novel algometer for measuring pressure pain thresholds in healthy volunteers.

Marco Barbero, University of Applied Sciences and Arts of Southern Switzerland; Corrado Cescon, University of Applied Sciences and Arts of Southern Switzerland; David Evans, Independent Consultant; Deborah Falla, University of Birmingham

Background: Assessment of the response of the body to an applied load is a fundamental component of a clinical examination. Obtaining pain responses to such loads is particularly useful for diagnosis, management and monitoring recovery of musculoskeletal conditions. The Pressure Pain Threshold (PPT) is defined as the minimum pressure applied to body tissues required to evoke pain. Renowned for its simplicity, speed of application, and objectivity, lower PPT values are typically recorded in those with pain conditions, indicating altered pain sensitivity and possible central sensitization. Traditional commercial algometers, such as the Somedic, are validated tools but are limited by their cost and lack of visual feedback. The eAlgo algometer, with its lower cost and user-friendly interface, offers a viable alternative for PPT assessment in clinical settings. The objective of this study was to evaluate the concurrent validity and reliability of PPT measurements performed using eAlgo across multiple testing sites, compared with a commonly used commercial digital algometer (Somedic). Methods: Two novice raters received training to perform PPT measurements. Twenty-two healthy volunteers from the University of Birmingham were invited to participate in three experimental sessions (two with the same rater, and one with the second rater). Two digital algometers (eAlgo and Somedic) were used to record bilateral repeated PPT measurements, in a controlled environment, at the upper trapezius, tibialis anterior, dorsal first interosseous, and erector spinae (C5, T5, and L3 spinal levels). Participants reported their PPT in response to a gradual increase in pressure (30 kPa/s). A minimum of 30-seconds interval between PPT measurements was used to prevent sensory adaptation. Each site was initially assessed using eAlgo, followed by the Somedic device. Real-time visual feedback was used to control load in both devices. Customized software installed on a 7” tablet was used to wirelessly monitor pressure applied

using the eAlgo, via a Bluetooth connection. The LCD screen of the Somedic algometer provided visual feedback. For statistical analysis, Pearson's correlation coefficient r was determined to measure the linear relationship between PPT measured with the two algometers. The means of the two measurements per site were calculated and a Bland-Altman plot was used to visualize the mean differences and limits of agreement between eAlgo and Somedic measurements. Intraclass correlation (ICC) and respective 95% confidence intervals were calculated to evaluate the intra- and inter-rater reliability of eAlgo. RESULTS: The analysis demonstrated strong concurrent validity between the eAlgo and Somedic algometers (r=0.883, p<0.001). The Bland-Altman plot indicated minimal bias with an average PPT difference of +82.9 kPa, underscoring the validity of eAlgo. Excellent to good intra-rater reliability (ICC: 0.81-0.96) and excellent to moderate inter-rater reliability (ICC: 0.62-0.91) were established for PPT measurements with eAlgo. Conclusion: The eAlgo algometer exhibits robust concurrent validity in comparison with the Somedic for PPT assessment within a healthy population. Moreover, eAlgo demonstrated excellent to good intra-rater reliability and excellent to moderate inter-rater reliability. Its cost-effectiveness, clear real-time feedback and user-friendliness support its potential adoption in broader research and clinical practice.

P2.52-P: Pronounced limb size asymmetries after post-anterior cruciate ligament reconstruction rehabilitation clearance

Ashley Herda, University of Kansas; Christopher Cleary, Univeristy of Kansas; Christopher Bernard, University of Kansas Medical Center; Bryan Vopat, University of Kansas Medical Center

Current recovery from anterior cruciate ligament (ACL) reconstruction or repair can take six to nine months and results in severely decreased strength and muscle mass (atrophy) of the quadriceps muscles in the effected leg.The primary aim of this study is to determine the extent of the muscle asymmetry after an athlete incurs any knee-related injury.Fourteen athletes (female=3) aged 18.6 +/- 5.6 years that had experienced ACL reconstruction consented to participate in this study. The participants' operative (OP) and non-operative (NOP) limbs were assessed for differences in muscle size (muscle cross-sectional area: mCSA; cm2) by ultrasound image analysis and thigh circumference (Tcirc). Additional segmental body composition was collected for OP and NOP leg lean mass (LLM). Maximal isometric extension and flexion were also recorded for each limb using a handheld dynamometer. Analyses included paired t-tests with a predetermined level of significance at p<0.05 and were completed using IBM SPSS Statistics version 28.0.1.1. The results of the OP vs NOP comparisons revealed significant differences in quadriceps mCSA (OP>NOP; mean difference = 9.32 cm2; p<0.001; d=1.368) and total thigh circumference (OP>NOP; mean difference = 1.64 cm; p=0.005; d=0.898). There were no differences indicated for hamstrings mCSA (p=0.223), LLM (p=0.326), isometric maximal extension strength (p=0.053), nor isometric maximal flexion strength (p=0.217).The primary indicators practitioners use to clear an athlete to safely return to sport are performance metrics of the OP being within (or greater than) 90% of the function of NOP. In many cases muscular size is overlooked or it is measured indirectly using circumference and not used as an indicator of potential performance. The present results

demonstrate that despite the muscular size difference in the quadriceps, no differences existed between the limbs at return to sport clearance testing.

P2.53-P: Comparison of gait asymmetry between groups with longer and shorter time since amputation in unilateral transfemoral amputees

Takeshi Hara, Tokyo University of Science; Genki Hisano, Arts et Metiers Sciences et Technologies; Hiroaki Hobara, Tokyo University of Science; Toshiki Kobayashi, Department of Biomedical Engineering

【Background/Aim】Time since amputation (TSAmp) is one of the non-modifiable predisposing parameters and influences social reintegration or mobility. For example, clinical outcome and mobility score were reported to improve with longer TSAmp (Puhalski et al., 2008; Seth et al., 2022). Hence, the TSAmp is one of the factors that can predict mobility in individuals with lower limb amputation. However, little is known about how the TSAmp affects gait mechanics in transfemoral amputees from a long-term perspective. Therefore, the aim of this study was to investigate the effect of TSAmp on gait asymmetry in individuals with unilateral transfemoral amputation over a wide range of walking speeds. 【Method】Thirty individuals with transfemoral amputation (7 females and 23 males, K-3 or K-4 levels, average TSAmp 11.5 ± 8.6 years) were recruited. All participants were asked to walk on an instrumented treadmill (FTMH-1244WA, Tec Gihan, Kyoto, Japan) at 8 speeds from 2.0 to 5.5 km/h in 0.5 km/h increments. Based on previous studies (Puhalski et al., 2008; Gailey et al, 2002), the participants were allocated into two TSAmp groups (shorter and longer than 11 years). From the ground reaction forces (GRFs), the spatiotemporal parameters (stance time, swing time, double limb stance time, cadence, step time, and step length) and GRF peaks (anteroposterior, mediolateral, and vertical GRFs) were determined. The asymmetry ratio for each parameter was calculated by prosthetic value/intact value (Patterson et al., 2008). When the data were normally distributed, a two-way mixed analysis of variance (ANOVA) was performed (within-subject; speeds, between-subject; groups). If the asymmetry ratios were not normally distributed, the Friedman tests and Mann-Whitney U test were used to investigate the main effects of groups and speeds, respectively. Statistical significance was set to P < 0.05. 【Results】There were no significant main effects of group on the asymmetry of all parameters. On the other hand, significant main effects of speeds were found on the asymmetry ratio of all parameters, except for 2nd peak of anteroposterior GRF. As walking speed increased, the asymmetry ratio of contact time, step time, and step length increased. However, the asymmetry ratio decreased in other gait parameters. Further, there were no significant interaction effects of the groups and speeds on the asymmetry ratio of all parameters. 【Conclusion】The results of the present study suggest that gait asymmetry in individuals with unilateral transfemoral amputation is not solely determined by the TSAmp. And social reintegration and/or higher levels of mobility are likely influenced by other factors as well. 【References】Gailey et al. The Amputee Mobility Predictor: A instrument to access determinants of the lower-limb amputee's ability to ambulate, Arch Phys Med Rehabil. 83 (2002) 613-627Puhalski et al., How are transfemoral amputees using their prosthesis in northwestern Ontario? J prosthet Orthot. 20 (2008) 53-60Seth et al. Time since lower-limb amputation an important consideration in mobility outcomes, Am J Phys Med Rehabil. 101 (2022) 32-39

P2.54-P: Effects of Diagonal Exercise with Resistance Training in Traumatic Brachial Plexus Injury Patients after Nerve Reconstruction

靜玉 陳, National Sun Yat-Sen University; Yuan-Kun Tu, E-Da Hospital; Yi-Jung Tsai, E-Da Hospital

Background Traumatic brachial plexus injuries (BPI) would cause severe damage and affect the functional activities. Recovery of shoulder stability and elbow movements are primary goals of surgical treatments and post-surgical rehabilitation. Diagonal exercise with resistance training might increase the stability of shoulder and trunk, and it is worth to investigate the training effects in BPI patients after reconstruction. Methods Eight (1 female and 7 males, age=35.9±8.3) upper arm type BPI patients (C5-C6 / C5-C7 = 7/1) received nerve transfer were recruited in our study. Subjects were required to perform the diagonal movement in sitting position with isokinetic dynamometer (Biodex system 4, Biodex Medical System Inc., New York) as fast as possible. They needed to perform 5 repetitions per set and 3 sets at the speeds at 60°/sec and 120°/sec. Muscle activities of biceps, serratus anterior, and latissimus dorsi were collected synchronously by surface EMG system (Noraxon, USA Inc.) at sampling rate of 1200 Hz. After 1st evaluation, subjects had 12-week training program of diagonal exercise with resistance by the theraband. They needed to perform 30 reps / day and 5 days/week. The normalized peak torque of shoulder flexion/extension and muscle activities level were conducted for further analysis. The differences between pre-training and post-training were examined by paired-t test with SPSS software. Significant level was set at p<0.05. Results At the first evaluation, the normalized peak torque of shoulder flexion and extension at 60°/sec were 51.2±22.4 Nm/BW and 30.3±19.4 Nm/BW, respectively. At the speed of 120°/sec, the peak shoulder flexion torque was 54.1±17.6 Nm/BW and the peak extension torque was 38.1±24.0 Nm/BW. After training, subjects showed trends of increased torque in shoulder extension at 60°/sec (34.2±20.0 Nm/BW) and significant improvement shoulder flexion torque at 120°/sec (62.9±17.7 Nm/BW, p=0.02). In muscle activities, subjects showed trends of higher activation in serratus anterior and latissimus dorsi muscles after training. However, no significant differences of muscle activation level were found (p=0.09 for serratus anterior, p=0.8 for latissimus dorsi). Discussion & Conclusions Based on our results, resistance training in diagonal direction could improve the shoulder stability and muscle strength. Shoulder movement in diagonal plane is a functional activity in our daily life. Though the small sample size and large variation between subjects might cause non-significance after training, diagonal exercise still could be the rehabilitation protocol in BPI patients after surgery.

P2.55-P: Comparison of electromyographic activity of the gluteal muscles and tensor fascia lata between persons with and without patellofemoral pain during a step-down activity, using indwelling fine-wire electrodes

David Selkowitz, MGH Institute of Health Professions; George Beneck, California State University, Long Beach; Christopher Powers, University of Southern California; Junsu Kim, TBC (please enter); Geordon Smith, TBC; Lisa Stone, TBC (please enter); Jason Tan, TBC (please enter)

Introduction: Persons with patellofemoral pain (PFP) have been shown to activate the tensor fascia lata (TFL) muscle greater than, and the gluteus medius (GMED) and superior gluteus maximus (SUP-GMAX) muscles less than, uninjured persons in selected, hip-focused therapeutic exercises. In addition, it has been shown that persons with PFP activate the TFL greater than the GMED and SUP-GMAX in numerous exercises, with the clam exercise as a notable exception. However, this has not been assessed in the step-down task, which is commonly used in both examination and intervention in persons with PFP. Excessive hip internal rotation and adduction have been associated with PFP, hence, the interest in studying electromyographic (EMG) activity in hip muscles contributing to and/or opposing these motions. Thus, the purpose of our study was to compare activation of the TFL (hip abductor and internal rotator), SUP-GMAX (hip abductor and external rotator) and GMED (hip abductor) between persons with and without PFP, during the step-down task. Methods: Participants comprised 12 persons with PFP and 19 persons without PFP between the ages of 18-50. EMG signals were collected from the TFL, SUP-GMAX, and GMED using indwelling fine-wire electrodes during performance of the step-down task. EMG activity (mean root-mean-square) for each muscle during the step-down was normalized to maximum voluntary isometric contraction. Independent t-tests were used to compare EMG activity between groups for each muscle. RESULTS: There was significantly lower activation of the GMED in persons with PFP compared to those without PFP (p=.025). There were no significant differences between groups for the TFL (p=.555) and SUP-GMAX (p=.555). CONCLUSIONS: Based on the lower EMG activity of the GMED in persons with PFP, it appears that the step-down task can differentiate between persons with and without PFP. We recommend that the step-down not be used as an intervention without prior facilitation exercises to enhance activation of the GMED.

P2.56-P: WEIGHT BEARING ASYMMETRY DURING STANDING IN INDIVIDUALS WITH UNILATERAL TRANSFEMORAL AMPUTATION

Ryota Morishima, Tokyo Univercity of Science; Genki Hisano, Arts et Metiers Sciences et Technologies; Hiroaki Hobara, Tokyo University of Science

・IntroductionSince excessive loading on one leg could increase the risk of knee degenerative disorder [1], weight bearing is important parameter in gait rehabilitation and clinical settings [2]. Despite that the patients with hemiparesis showed asymmetric weight bearing during standing, little is known about the weight bearing individuals with unilateral transfemoral amputation. The aim of this study was to investigate the relationship between weight bearing and demographic data in individuals with unilateral transfemoral amputation. ・MethodsWe recruited active 34 individuals with unilateral transfemoral amputation (K2-K4). All patients walked independently without a walking aid at the time of testing. They were asked to stand comfortably for five seconds using their conventional transfemoral prosthesis on the two force platforms (FTMH-1244WA, Tec Gihan, Kyoto, Japan). As shown in Figure 1, we collected the vertical grand reaction force (vGRF), and then determined the weight-bearing over one second during the stable time-course vGRF. We also calculated the weight-bearing ratio (WBR), which was calculated as the prosthetic limb divided by the intact limb. Correlation analysis was performed to investigate the relationships between the WBR and demographic data, such as age, height, body mass and time since amputation, respectively. Further, we compared the WBR

between sexes and prosthetic knee units (microprocessor vs. non-microprocessor knee) by allocating whole population into the two groups. WBR was also compared among different residual limb length levels (short, middle, long and knee disarticulation). Finally, we compared the WBR between exercise histories (Athletes vs. Non-Athletes). IBM SPSS statistics (Ver. 28.0.1.1(15)) was used for statistical analysis. ・ResultsOverall, the WBR of the current population was 1.36. There were no linear correlations between the WBR and all demographic data. Further, we also found no significant differences in the WBR between sexes and prosthetic knee units. Furthermore, despite there was a significant main effect of residual limb length on the WBR, no significant differences were found for the post-hoc comparisons among the groups. On the other hand, the WBR was significantly smaller in Athletes group than Non-Athletes group (p<0.05). ・DiscussionThe aim of this study was to investigate the relationship between weight bearing and demographic data. The WBR was 1.36, which was smaller than that of hemiparesis (1.46) [3], indicating that weight bearing may be symmetric in active individuals with transfemoral amputation than patients with hemiparesis. Further, we found that the WBR of Athletes group was significantly smaller than that of Non-athletes group. Therefore, the result of the present study suggests that training history and functionality could affect the weight bearing asymmetry during standing. ・References[1] Highsmith et al., Gait & Posture, 34: 86-91, 2011[2] Eng and Chu, Arch Phys Med Rehab, 83: 1138-1144, 2002[3] Bohannon and Larkin, Phys Ther, 65: 1323-1325,1985

P2.57-P: Unstable Subject's Characteristics of Center of Pressure Changes During the Transition from Bilateral to Unilateral

Ayako Hisari, Osaka Kawasaki Rehabilitation University; Naoko TAKEUCHI, Graduate school of Science, Osaka Prefecture University; Iori Arisue, Kansai University of Welfare Sciences; Sunghyun Kim, Kaeru LLC; Masaaki Yoneda, Kaeru LLC

In the initial phase of gait, there is a critical transition from a bilateral to a unilateral stance, a juncture notoriously susceptible to falls. Consequently, accurate fall prediction and specialized training in this specific postural transition from a bilateral to a unilateral stance are imperative in the context of fall prevention strategies. The disparity in balance strategies between subjects who are unstable during the transition from bilateral to unilateral stance and those who are not, aids in forecasting falls at the onset of walking and in developing specific training to reduce fall risk for individuals. The objective of this study is to define the characteristics of the center of pressure (CoP) changes during the postural transition from bilateral to unilateral stance in both unstable and stable subjects as quantitative indicators, thereby enhancing fall predictability and formulating training protocols aimed at reducing fall risk. The subjects were informed about the purpose and methods of the study, and their consent was obtained. Subjects performed the task under instruction to transition from a bilateral to a unilateral left leg stance. We simultaneously collected the 2 types of data during the task; the medial-lateral center of pressure (CoP) and the position of the right lateral malleolus. Also, we determined the starting point of the change in the medial-lateral CoP position (C1) and the vertical position of the right lateral malleolus (M1) and defined C1M1 as the value obtained by subtracting C1 from M1. Our study found that unstable subjects in the transition to a unilateral stance had a shorter C1M1 compared to stable ones. This implies that subjects with instability during the bilateral to

unilateral postural transition are prone to delayed weight shift. For subjects who are unstable and at a higher risk of falling during the transition to a one-legged stance, a key training component could be conscious weight shift training to the stance leg before lifting the other leg. Further research is needed to define more precise quantitative indicators and to verify the effectiveness of training.

P2.58-P: Scapular muscle activity including rhomboid major during arm raising and lowering without loading in healthy participants —Examination using fine-wire and surface electrodes—

Gen Adachi, Toyo University; Tomoki Oshikawa, Waseda University; Hiroshi Akuzawa, Niigata University of Health and Welfare; Koji Kaneoka, Waseda University

Background and Aims: Coordinated activity of muscles attached to the scapula play an important role in scapular motor control. Rhomboid major (RM) and Serratus anterior (SA) share an attachment site at the medial border of the scapula and are thought to contribute to scapular motor control. Inman et al. reported that RM and middle trapezius (MT) are functionally similar. (Inman et al., 1944) However, no studies have quantitatively compared their muscle activity and clarified functional differences between RM and MT during arm raising and lowering. The purpose of this study was to clarify the scapular muscle activity including RM during arm raising and lowering without loading in healthy participants using fine-wire and surface electrodes.Method: Thirteen healthy men (age: 21⍰2 years) participated in this study. RM activity was measured using bipolar intramuscular fine-wire electrodes, upper trapezius (UT), MT, lower trapezius (LT), and SA activity was measured using surface electrodes. Participants performed raising and lowering of dominant arm without loading five times each in two directions of shoulder flexion and abduction in random order. The speed of motion in trials was controlled with a metronome set at 60 beats per minute for 3 s of raising (from the starting limb position to the maximum raising position) and 3 s of lowering (from maximum raising position to the starting limb position). The raising and lowering phases in 3 s were subdivided into 1 s early, middle, and late phases, respectively. The muscle activity was represented as percent MVIC (%MVIC). Two-way analysis of variance (ANOVA) on two factors (directions, phases) was used to compare the %MVIC of each muscle between each trial. Additionally, two-way ANOVA on two factor (muscles, phases) was used to compare the %MVIC of each phase between RM and MT. The significance level was set at 0.05. RESULTS: All muscles measured in this study had a significant main effect in the phases, with a unimodal activity pattern with the highest activity in the late raising phase for both flexion and abduction trials. RM (flexion; 23.7±16.5%MVIC, abduction; 23.1±14.7%MVIC) and SA (flexion; 45.8±32.2%MVIC, abduction; 45.8±28.1%MVIC) activity in the late raising phase was significantly higher than all other phases. MT also had a significant main effect in the directions, with abduction (7.9±6.6%MVIC) showing a higher activity pattern throughout the entire phase than flexion (2.9±4.3%MVIC). In comparing activity of RM and MT, significant main effects were found in the muscles and phases, and RM (flexion: 13.4±11.5%MVIC, abduction: 11.9±10.2%MVIC) was greater throughout the entire phase than MT (flexion: 2.9±4.3%MVIC, abduction: 7.9±6.6%MVIC). CONCLUSION: : In arm raising and lowering without loading, RM showed coordinated activity

with SA, suggesting a contribution to scapular motor control. RM and MT showed different muscle activity patterns, suggesting that they have functional differences.

P2.59-P: Isometric co-contraction training effects on muscle torque and muscle thickness in patients undergoing chemotherapy for colorectal cancer (The CoConTract Study) – Preliminary results

Rafael Fujita, University of São Paulo; Fernanda Peria, University of São Paulo – Faculty of Medicine, Department of Clinical Oncology; Mucio Cirino, University of São Paulo – Faculty of Medicine, Department of Medical Sciences; Marina Villalba, University of Sao Paulo - Ribeirao Preto College of Nursing; Kristin Campbell, The University of British Columbia – Faculty of Medicine, Department of Physical Therapy; Daniela Tirapelli, University of São Paulo – Faculty of Medicine, Department of Surgery and Anatomy; Matheus Gomes, Universiy of São Paulo

BACKGROUND AND AIM: Chemotherapy induces fatigue and muscle strength reduction in 80% of patients living with cancer, which negatively impacts quality of life. While traditional strength training has positive outcomes on muscle strength and self-reported fatigue, adherence to supervised programs during chemotherapy is typically low (<60%). Co-contraction training, which involves the simultaneous activation of agonist and antagonist muscles without the need for external equipment, emerges as a potential alternative. We aim to analyze the effects of co-contraction training of elbow and knee flexors and extensors muscles on strength (muscle torque) and morphology (muscle thickness) in patients living with and beyond colorectal cancer undergoing chemotherapy. Methods: The CoConTract study (Trial Registration: RBR-7hh489b) is an ongoing randomized-controlled double-arm study. To be able to participate, individuals must have completed surgery, be enrolled in chemotherapy treatment, be at I-III colorectal cancer stage, and have access to an electronic device as well as reliable internet connection. The exercise program runs for 8-weeks, with participants attending virtual supervised exercise sessions twice weekly. The virtual supervised exercise sessions are composed by 10 sets of 10 voluntary co-contractions (five sets for elbow and five sets for knee flexor and extensor muscles). Each co-contraction is composed by four second effort followed by four second rest. Between each set there is a 90-second interval. Data collection occurs pre and post-exercise program. Muscle torque is assessed by isokinetic dynamometer (Biodex, System 4 Pro) and muscle thickness is assessed by ultrasound B-mode (Saevo FP 102) for the elbow and knee flexors and extensors muscles. RESULTS: To date, one participant (59 years old, 173.0cm, 58.0kg, body mass index 19.4 kg/m^2) completed the supervised exercise program with 100% attendance. The elbow peak torque increased for both extension (+9%, pre: 28.6 vs. post: 31.2 N·m) and flexion (+11%, pre: 48.8 vs. post: 54.0 N·m) after intervention. Regarding knee peak torque, there was an increase for extension (+1%, pre: 134.1 vs. post: 135.4 N·m) but a decrease for flexion (–4 %, pre: 65.7 vs. post: 63.3 N·m). Regarding muscle thickness, all muscles presented increases after intervention: rectus femoris (+40.0%, pre: 7.5 vs. post: 10.5mm); vastus intermedius (+7.5% pre: 10.6 vs. post: 11.4mm); vastus lateralis (+3.9%, pre: 18.0 vs. post: 18.7mm); elbow flexors (+43.6%, pre: 14.0 vs. post: 20.1mm); elbow extensors (+102.1%, pre: 9.4 vs. post: 19.0mm). CONCLUSIONS: Co-contraction training appears to be a promising alternative for preventing muscle impairments in patients undergoing chemotherapy

for colorectal cancer, as evidenced by the increased muscle mass and torque observed in the majority of analyzed muscles.

P2.60-P: Analysis of Injury Incidences and Risk Factors in Korean Female Professional Soccer Players

Jae Min Lee, Miraebone hospital; Hyung Gyu Jeon, Yonsei university; Seon Hee Im, Miraebone hospital; Sae Yong Lee, Yonsei university

Background: The purpose of this study is to monitor injuries that occur during the 2020 WK (Korea Women's Football) League season in Korean female professional soccer players to identify the epidemiological characteristics of injuries and to identify risk factors for observed injuries. The assumed internal risk factors are hip joint flexibility, ankle joint flexibility, hamstring flexibility and past injury history, and external risk factors are soccer position, climate and playing surface. Methods: This survey was conducted on 138 players from six Korean women's professional soccer teams. All players are officially registered with the KFA (Korea Football Association). And the 2020 WK League injury surveillance system included injury date, location, type, mechanism, severity, recurrence, activity, ground condition, and climate. We calculated injury rates per 1000 hours of exposure and rate ratio. The logistic regression was used to analyze the risk factors of injury. It examined how flexibility in the hip joint and ankle joint affects injury of the lower extremity, how the flexibility of the hamstring affects the injury, and how previous injuries in the sprained ankle and knee affect the recurrence of injury. RESULTS: In 2020 WKLeague injury surveillance, lower extremity injuries accounted for more than 80% of all injuries, and most of them were joint, ligament, and muscle injuries. And the overall injury incidence rate in the 2020 WK League was 5.86, and the injury rate was about 11.5 times higher in the competition (35.70) based on practice (3.10). As a risk factors for injury, the lower the internal rotation flexibility of the hip joint and the eversion flexibility of the ankle joint, the lower extremity injury increased. And the players who had suffered grade 1 and 3 previous knee sprain injury were more likely to appear again as new knee sprain injury. In addition, it was confirmed that the characteristics of injuries vary depending on the soccer position, and severe and moderate injuries occurred in artificial turf compared to natural grass. CONCLUSION: : With regard to injury risk, the results of this study suggest that it is desirable to identify injury-prone players with respect to playing surfaces, playing positions, flexibility, previous injuries and so on. A continuous injury surveillance system can inform the development of interventions to help reduce the severity and frequency of injuries suffered by players, and it may be appropriate to provide injury prevention programs tailored to individual characteristics.

P2.61-Q: A novel methodology utilizing nonnormalized surface EMG with a minimal number of sensors in the development of powered ankle prosthesis control algorithm.

Dogukan Keles, Institute for Modelling and Simulation of Biomechanical Systems, University of Stuttgart; Tarık Turksoy, Bogazici University

Lower limb amputation is partial or complete removal of the limb due to disease, accident or trauma. Advancements in motion assistive device technologies and robotic rehabilitation

instrumentation support improved powered ankle prostheses hardware development for amputees. However, control algorithms have limitations regarding number and type of sensors utilized and achieving autonomous adaptation, which is key to a natural ambulation. Surface electromyogram (sEMG) sensors are promising for this purpose. Previously, sEMG of a large number of muscles and force sensors have been used to develop control algorithms for lower limb powered prostheses. Therefore, minimizing the use of solely sEMG muscle inputs will make the powered prosthesis control algorithm economic. On the other hand, unlike ankle disarticulation, transtranstibial amputation yields less intact lower leg muscle mass in the lower leg. Taking this into account, limiting the use of specifically the lower leg muscles will make the control algorithm flexible. With those definitions in place, in order to determine appropriate sensor combinations, a systematic assessment of the predictive success of variations of multiple sEMG inputs in estimating ankle position and moment has to be conducted. More importantly, tackling the use of nonnormalized sEMG data in such algorithm development to overcome processing complexities in real-time is essential, but lacking. We used healthy population level walking data to (1) develop sagittal ankle position and moment predicting algorithms using nonnormalized sEMG, and (2) rank all muscle combinations based on success to determine economic and practical algorithms. Eight lower extremity muscles were studied as sEMG inputs to a long-short-term memory (LSTM) neural network architecture: tibialis anterior (TA), soleus (SO), medial gastrocnemius (MG), peroneus longus (PL), rectus femoris (RF), vastus medialis (VM), biceps femoris (BF) and gluteus maximus (GMax). Five features extracted from nonnormalized sEMG amplitudes were used: integrated EMG (IEMG), mean absolute value (MAV), Willison amplitude (WAMP), root mean square (RMS) and waveform length (WL). Muscle and feature combination variations were ranked using Pearson's correlation coefficient (r > 0.90 indicates successful correlations), the root-mean-square error and one-dimensional statistical parametric mapping between the original data and LSTM response. The results showed that IEMG+WL yields the best feature combination performance. The best performing variation was MG + RF + VM (rposition = 0.9099 and rmoment = 0.9707) whereas, PL (rposition = 0.9001, rmoment = 0.9703) and GMax+VM (rposition = 0.9010, rmoment = 0.9718) were distinguished as the economic and practical variations, respectively. The study showed for the first time the plausibility of the use of nonnormalized sEMG signals in control algorithm development for powered ankle prostheses in level walking.

P2.62-Q: Effects of an ankle-assist robot on spinal reciprocal inhibition and voluntary ankle dorsiflexion movements.

Ai Watanabe, Hiroshima University; Akari Ikeda, Hiroshima University; Sotaro Sato, Hiroshima University; Ayaka Hanaki, Hiroshima University Graduate School of Biomedical and Health Sciences; Nozomi Maeda, Hiroshima University Graduate School of Biomedical and Health Sciences; Makoto Takahashi, Hiroshima University; Shinro Matsushita, Nishi-Hiroshima Rehabilitation Hospital; Shinro Matsushita, Nishi-Hiroshima Rehabilitation Hospital; Eiichiro Tanaka, Waseda University; Louis Yuge, Hiroshima University; Kei Nakagawa, Hiroshima University,

Post-stroke hemiplegic patients often have difficulties in walking due to their ankle dorsiflexion limitation. One of the possible reasons for this issue is the modulation of spinal reciprocal

inhibition (RI), which includes reciprocal Ia inhibition and presynaptic short (D1) and long (D2) inhibition. These RI pathways can control coordinated movements of the antagonist muscle. RE-Gait® is a robotic-controlled ankle foot orthosis that can repeatedly induce appropriate plantar and dorsiflexion of the ankle joint. A previous study reported that the RE-Gait® intervention resulted in an immediate improvement in reciprocal Ia inhibition in post-stroke hemiplegic patients. However, the changes of D1 inhibition and dynamic muscle tone after the intervention have not been evaluated. Therefore, this study assessed the effectiveness of RE-Gait® in detail by examining these parameters. Twelve healthy adults and one post-stroke hemiplegic patient (male, age: 40s, BRS V) participated in this study. They engaged in a 20-minute session of robotic-assisted gait training (RAGT) using the RE-Gait® at their comfortable speed. RI was assessed before and after RAGT. The test stimulus was administered to the tibial nerve and conditioning stimulus to the common peroneal nerve, and EMG potentials were recorded from the soleus (SOL) and tibialis anterior (TA) muscles. The intensity of the conditioning stimulus was set to 0.1 μV, and that of the test stimulus was set to induce an H-reflex of 20% of the maximum amplitude value of the M-wave. The conditioning-test stimulation interval (CTI) was set at 0-4 ms in the measurements of reciprocal Ia inhibition, and at 0 and 20 ms in the measurements of D1 inhibition. The number of stimuli administered was randomly set to 12 stimuli in each CTIs. Moreover, the subjects performed 10 repetitions of the ankle voluntary dorsiflexion task from 20°of ankle plantar flexion to maximum dorsiflexion at the fastest speed. The task was recorded with slow motion video (120 fps). As a result, in healthy adults, the reciprocal Ia inhibition ratio with 1ms-CTI was significantly enhanced after the intervention (p < 0.05), while the D1 inhibition ratio with 20ms-CTI was not significantly changed after the intervention (p = 0.14). The duration of ankle dorsiflexion voluntary movement was significantly reduced after the intervention (p < 0.05). In post-stroke hemiplegic patients, both the reciprocal Ia and D1 inhibition ratio were increased after the intervention. In addition, the duration of the ankle voluntary dorsiflexion task was reduced. These findings suggest that ankle joint assistance by a robotic-controlled ankle foot orthosis may influence the RI and the improvement of ankle voluntary dorsiflexion movements.

P2.63-Q: Effects of Robotic Ankle Joint Control on the Hip Joint during the Stance Phase

Sotaro Sato, Hiroshima University; Ai Watanabe, Hiroshima University; Tomoki Moriya, Hiroshima University Graduate School of Biomedical and Health Science; Shunpei Kishida, Hiroshima University Graduate School of Biomedical and Health Sciences; Makoto Takahashi, Hiroshima University; Eiichiro Tanaka, Waseda University; Louis Yuge, Hiroshima University; Kei Nakagawa, Hiroshima University

RE-Gait® is one of the robots used for rehabilitation of walking impairments in Post-stroke hemiplegic patients. RE-Gait® is an ankle-foot orthosis exoskeleton-type walking assistive robot designed to assist ankle joint movements during gait specifically dorsal flexion and planter flexion. Just as RE-Gait® controls the ankle joint and acts on the ascending kinetic chain of gait, robot-assisted control of the ankle joint also affects the knee joint, suggesting that it is effective not only for ankle disorders but also for problems occurring in the knee joint. However, the specific changes in the hip joint refusing from ankle joint control remain unclear. Therefore, this study investigated the detailed examination of the influence of ankle joint control on the hip

joint and aims to contribute to the intervention of robot-assisted rehabilitation for hemiplegic patients. The study recruited 15 healthy young adults. The task involved attaching RE-Gait® to the right lower limb and performing level ground walking at a comfortable speed. The settings of RE-Gait® were determined based on the measurement of the subject's gait cycles, specifically from heel contact (HC) to 30% of the stance phase, corresponding to the midstance (MSt). Three conditions were established: no setting from HC to MSt (FLAT condition), dorsiflexion setting (DF condition), and plantarflexion assistance setting (PF condition). After MSt, the settings were same for each condition, and no control was applied from MSt to heel off (HO). From HO, plantarflexion assistance was provided during the pre-swing phase, and dorsiflexion assistance was provided during initial swing phase. Kinematic and kinetic data ware obtained using a three-dimensional motion analysis system and force plates. Joint angles and moments at the hip and knee joints were calculated. Additionally, hip joint angles were separated into three stance phases based on the vertical ground reaction force, and changes in hip joint angles during each phase were computed. In the PF condition, the knee joint angle exhibited a significantly larger extension angle during the stance phase compared to the other conditions (p<0.01). While no significant difference was observed in the maximum hip joint extension angle during stance phase, the PF condition demonstrated a larger extension angle from the loading response (LR) to MSt (p<0.05) and a smaller from MSt to the terminal stance (TSt) compared to the FLAT condition (P<0.05). In terms of hip joint moments, the maximum flexion moment in the PF condition was significantly smaller than that in the FLAT condition (p<0.01). The robotic control of ankle dorsiflexion during the stance phase significantly influenced the angular changes and peak moments at the hip joint. The ankle joint control by RE-Gait® not only affects the ankle and knee joint but also has an impact on the hip joint, suggesting the potential for adaptability to various walking impairments.

P2.64-R: Comparison of knee strengthening combined with hip or ankle joint exercises on clinical symptoms and muscle strength in women with patellofemoral pain syndrome

Wan-Chi Hou, No.100, Shih-Chuan 1st Road, Sanmin Dist., Kaohsiung City,80708, Taiwan; NAI-JEN CHANG, Kaohsiung Medical University

Patellofemoral pain syndrome(PFPS) reduces exercise performance and quality of life. Currently, the inconclusive strategy of the rehabilitation process remains challenging. Although PFPS leads to anterior knee pain, the cause of pain does not only originate from the knee. The pain may also come from other surrounding joints, such as the hip and ankle joints. Therefore, the treatment appears to be complicated. Among them, is used to describe the combined kinetic movement of the ankle, knee, and hip joints during weight-bearing. When the dynamic knee valgus (DKV) angle becomes excessive, it is one of the risk factors for lower limb injuries. However, most researches focus on the knee joint intervention alone while there is still a lack of further high-level evidence to compare the comprehensive benefits of knee joint strength training combined with hip or ankle joint exercises in women with PFPS. PURPOSE: To compare the effects of knee strengthening combined with hip or ankle joint exercise on intensity of pain, muscle strength, and DKV angle in women with PFPS. Methods: This study was a randomized controlled trial. Eligible 9 female recreational players (age: 24.9 ± 5.7 years, height: 160.4 ± 5.7 cm, weight: 55.0 ± 5.4 Kg) diagnosed by the physicians with PFPS were recruited. The

participants had symptoms for 3 months at least. participants were randomized to hip and knee combined exercise group (n = 3), knee and ankle combined exercise group (n = 3), or non-intervention control group (n = 3). A physical therapist instructed the exercise. Each exercise consists of 30 minutes, once a day, 3 times a week, for periods of 8 weeks. The primary outcome was Visual Analogue Scale (VAS) for the intensity of pain during activity. Secondary outcomes were single leg landing test to assess DKV angle and maximal isometric strength. RESULTS: After an 8-week intervention, significant improvements in VAS scores during activities were observed after the intervention in both the hip + knee group (3.0 ± 0.58; p = 0.04) and ankle + knee group (4.33 ± 0.67; p=0.02), but not in the control group. No significant differences between interventional groups were found in all outcomes. CONCLUSION: Both the hip + knee group and the ankle + knee group showed a significant clinical effect in reducing pain during activities. A larger sample size warrants verifying the clinical effectiveness of the combined exercise treatment for this population.

P2.65-R: Effect of tasks on intramuscular regional differences in rectus femoris elasticity during isometric contraction: an ultrasound shear wave elastography study

Taiki Kodesho, Japan Institute of Sports Sciences (JISS); Kazuma Yamagata, Sapporo Medical University; Gakuto Nakao, Sapporo Medical University; Masaki Katayose, Sapporo Medical University; Keigo Taniguchi, Sapporo Medical University

Background: Based on various research, regional differences exist within the rectus femoris (RF) muscle. In particular, RF muscle strains are known to occur more frequently in the proximal region during hip flexion motions. However, intramuscular regional differences and task specificity of mechanical stress associated with contraction related to injury development remain unknown. Ultrasound shear wave elastography (SWE) can quantify the elasticity of specific muscular regions. The elasticity measured by SWE has been shown to reflect the change in force associated with contraction. This study aimed to investigate intramuscular regional differences and task specificity of RF elasticity during isometric contraction. Methods: Sixteen healthy males (aged 24.3 ± 4.1 years) participated in this study. Subjects were seated at 50˚ hip flexion and 90˚ knee flexion, with the distal leg and distal thigh fixed to the force sensors. The tasks included isometric hip flexion (HF) and knee extension (KE), and the contractions were maintained at 0%, 30%, and 60% of their respective maximum voluntary isometric contraction (MVC) forces for 5 seconds each. RF elasticity was measured in two regions, proximal (33%) and distal (66%). The shear modulus (kPa) measured by SWE was used for RF elasticity. A three-way ANOVA with repeated measures was used to compare the changes in shear modulus with increasing contraction intensity among regions and tasks. RESULTS: A significant interaction was observed (intensity × region × task) (P = 0.01). In the KE task, the RF shear modulus increased with increasing contraction intensity in each region, while in the HF task, the RF shear modulus in the proximal region was higher than that in the distal region at 0% MVC (Mean ± SD, proximal: 12.18 ± 3.02, distal: 6.21 ± 1.35) and 60% MVC (proximal: 70.63 ± 14.36, distal: 51.66 ± 21.62). In the proximal region, the RF shear modulus of the KE task was higher than that of the HF task only in the 30% MVC (30% MVC KE: 55.05 ± 18.24, HF: 38.45 ± 21.72; 60% MVC KE: 74.87 ± 19.05, HF: 70.63 ± 14.36). In the distal region, the RF shear modulus of the KE task was higher than that of the HF task at 30% MVC (KE: 52.83 ± 18.52, HF:

30.98 ± 19.67) and 60% MVC (KE: 77.75 ± 17.98, HF: 51.66 ± 21.62).Discussion: The present results indicate that the trends of intramuscular regional differences in RF elasticity differ depending on the exercise task. No interregional differences were observed in the KE task. However, in the HF task, the proximal region had higher elasticity at 60% MVC. Since muscle elasticity during contraction as measured by SWE reflects mechanical force, there will be proximal-specific heterogeneity in mechanical stress during contraction of moderate to high intensity in the HF in RF. In addition, the KE may generate more mechanical stress in the distal region than the HF since the distal region showed higher RF elasticity in the KE than in the HF at contraction.

P2.66-R: The effects of EMG waveforms on the availability of EMG threshold detection

Kengo Wakui, Niigata University; Shuhei Kameyama, Niigata University; Yuki Sato, National Institute of Technology, Oyama College; Yukihiko Ushiyama, Niigata University

<Introduction> It has been reported that the rapid increase of the EMG amplitude in the lower limb, especially the anterior thigh muscles is observed during incremental pedaling exercise. The exercise intensity where it occurs is equivalent to the lactate threshold (LT), which is one of the anaerobic threshold (AT) estimation indices. In the previous studies, this point is called EMG threshold (EMGT), and its usefulness of EMGT as an index estimating AT noninvasively and relatively inexpensively is claimed. On the other hand, some previous studies reported that, during incremental exercise, EMGT is not observed, the detection rate is not stable depending on subjects or tested muscle, and EMGT is inconsistent with other AT estimation indices and is not practical. As above, there is no unanimous view on EMGT. In the previous studies on EMGT, the average amplitude of EMG is calculated using EMG data extracted from relatively long intervals, such as several seconds or one crank cycle, so it is not clear which factor of the EMG waveform changes during one single crank cycle to cause the rapid increase in EMG average amplitude. Therefore, in this study, we investigate the differences in EMG waveform changes during one crank cycle between subjects whose EMGT is detected and those whose EMGT is not detected and try to obtain that will contribute to the practical use of EMGT. <Methods> Male cyclists performed incremental pedaling exercise (90rpm, start at 110W, add 10W every 30 seconds) and EMG measured from lower limb muscles which are considered suitable for EMGT detection in previous studies. At the same time, the acceleration and angular velocity of the crank arm were measured to synchronize the EMG and crank motion. The ARV was calculated from lowpass-filtered EMG and divided into each workload. Then, averaged ARV during one crank cycle was calculated using stable EMG data in each workload, and they are normalized to the maximum value in the muscle overall workloads. We calculated the EMG activation interval and peak value and compared their changes between EMGT detectable group and EMGT undetectable group. <Results> The EMG activation interval length gradually increased from the start of incremental exercise in the EMGT detectable group and the final increase in the EMG activation interval length with increasing workload tended to be larger than in the EMGT undetectable group. Referring to the peak value in each workload, continuous increases during exercise are observed in both groups.

P2.67-R: Biomechanical characteristics of trunk muscles and sagittal alignment of basic posture in ballet

Mao Hayashi, Ochanomizu University; Mayumi Kuno-Mizumura, Ochanomizu University

Purpose In ballet, teachers often encourage their students to keep good posture by the words "pull-up". Sueyoshi et al.(2016) reported that the curvature of the spine decreased by changing from a relaxed posture to a ballet posture in people with ballet experience the cross-sectional area of their core muscles was significantly larger than those of the non-dance group. It was also found that there was a significant negative correlation between changes in the spinal alignment angle, the amount of change in the lumbar kyphosis angle, and the cross-sectional area of the psoas major and transversus abdominis muscles. McMeeken et al. (2004) investigated the relationship between changes in the thickness of the transversus abdominis muscle and electromyogram and reported that electromyogram activity increased in proportion to the increase in muscle thickness, and there was a high correlation. However, few studies have examined the biomechanical difference between basic posture in ballet and natural standing posture. Therefore, the purpose of this study was to examine the basic posture of ballet in terms of the trunk muscles' structure and sagittal skeletal alignment. METHODS17 Japanese female students with more than 10 years of ballet experience participated in this study. From the ultrasound images, the thickness of rectus abdominis, right and left external oblique abdominal muscles, internal oblique abdominal muscles, and transversus abdominis muscles were measured in both supine and standing position at rest, during maximal inhalation, maximal exhalation, and basic posture in ballet. For skeletal alignment, six markers were fixed to the subcostal, 10th and 12th thoracic vertebrae, left ASIS, PSIS, and greater trochanter for evaluating sagittal skeletal alignment. The video images were recorded 2.5 m away from the side of the subject. The lumbar spine angle, pelvic angle, the angle between the PSIS and the greater trochanter on the axis of ASIS, and the angle between the lower ribs and the PSIS were measured by the images using ImageJ. Results and DiscussionNo significant difference in the rectus abdominis muscle in the supine position among four different posture conditions. In basic ballet posture, the muscle thickness of the left and right external oblique muscles, transversus abdominis muscles, and the left internal oblique muscle were significantly greater compared to the other three conditions. No significant differences were observed in sagittal skeleton alignment. Conclusion From the results of this study, greater muscle thickness during basic ballet posture compared to at rest or during maximal inhalation/exhalation would indicate that structural changes would occur especially in deeper trunk muscles. In addition, no significant changes in skeletal alignment were observed among four different conditions related to sagittal alignment of the posture.

P2.68-R: Neural and morphologic changes in calf muscles during five-week of session-adjusted calf-raise training in untrained males: a preliminary study

Yoonseo Ki, Kyung Hee University; Jaewook Lee, Kyung Hee University; Yoongwan Choi, Kyung Hee University; Hyeonkon Choi, Kyung Hee University; Hoon Kim, Soonchunhyang University; Jihong Park, Kyung Hee University

Purpose: The study aimed to test how a session-adjusted resistance exercise protocol is effective in gaining strength and to observe neural and morphologic changes in the medial gastrocnemius (MG) and tibialis anterior (TA) during and after five-week calf-raise training in untrained males. Methods: Five healthy untrained males (21 years; 177.2 cm; 67.5 kg) performed five weeks of resistance exercises (two sessions per week). Participants who had been engaged in aerobic or resistance exercises for the last six months or a history of musculoskeletal surgery in their lives were excluded. In each session, participants performed three sets of calf-raise exercises on a Smith machine with a workload of 10-repetition maximum and a rest period of 2-min between sets. The workload of each set was controlled by the session-adjusted protocol with the cut-off range (e.g., from 9 to 11 repetitions). Specifically, if the number of repetitions were > 12 or < 8, the workload was increased or decreased by 2.5 kg. Dependent measurements were the workload, neuromuscular activity, and muscle morphology at week 1, 3 (1st session), and 5 (2nd session). The average workloads at each time point (week 1, 3, and 5) were recorded. Two surface electromyography (EMG) electrodes (2,000 Hz) on the MG and TA on the dominant leg were used to record neural changes in the 2nd set. The EMG signals during the concentric (raise up) and eccentric (raise down) phases were separately cropped and filtered through a 4th order Butterworth band-pass filter (cutoff frequency: 20 to 450 Hz). Filtered data was wavelet-transformed in the time-frequency domain with 11 morlet wavelets to get intensities. After that, principal component analysis was used to extract the principal components (PCs) and PC scores. Before the first set, three ultrasonographic images (frequency: 12 MHz; depth: 6 cm) of MG and TA were obtained and averaged to test morphologic changes. One-way analysis of variances with Tukey's tests were performed to test a time effect on workload and muscle morphology (p<0.05). A two-way analysis of variances was performed to test differences in PC scores between the contraction type over time. RESULTS: The workload was different (F4,16=11.33, p<0.0001) that there was a 23% increase at week 3 (81.2 kg to 99.8 kg, p=0.009) but there was no further increase at week 5 (110.2 kg, p=0.24). Although PCs captured amplitude shift and frequency shift, respectively, there was no interaction and main effect on PC scores were observed between contraction type over time (p>0.05). The muscle morphology was not different in the MG (F2,8=0.78, p=0.49) and the TA (F2,8=0.15, p=0.86). Conclusion: Our study resulted in a 36% increase in workloads after five-weeks of training. Despite the strength gain, neither neural nor morphologic change was observed. A larger sample size would be needed to detect the relative contribution of each factor.

P2.69-S: Development of a self-adhesive, reusable sEMG electrode designed for independent application by the patient

Elmar Junker, RWTH Aachen; Catherine Disselhorst-Klug, Institute for Applied Medical Engineering, RWTH Aachen University; Elisa Romero Avila, Institute of Applied Medical Engineering

BACKGROUND: Information about muscular coordination during everyday activities is becoming increasingly important in rehabilitation. From a clinical perspective, it is desirable to monitor muscle activation preferably in the patient's home environment and over longer periods. This approach presupposes that the recording surface electrode (sEMG electrode) can

be placed autonomously by the patient and remain in this position all day. The quality of the derived signals should neither be impaired by inaccurate positioning nor by time. METHOD: Silicone rubber was chosen as the carrier material. To achieve the adhesive properties of the carrier material, the mixed silicone components were poured into a rectangular mold with the underside coated with a porous material. In this way, the silicone adheres to the small pores, enabling the carrier material to adapt to irregularities of the human skin. This results in an adhesion effect. Additionally, a curved shape of the silicone carrier leads to a better adaptation to the shape of the human body and, thus, to even better adhesion. A total of 7 gold contacts were integrated into the carrier material to form regions with high conductivity. The gold contacts used have a hemi spherically curved surface, a diameter of 8 mm, and a spacing of 10 mm. By differential amplification close to the electrodes, two sEMG leads were created from 3 gold contacts (lead electrodes) arranged in line. The individual components of the amplifier circuit were adapted to the high contact impedances between the gold contact and the skin. The required ground electrode was formed from the remaining 4 gold contacts, arranged symmetrically around the center lead electrode and short-circuited to each other. This results in an active sEMG electrode that provides 2 sEMG channels and adheres to the skin surface on its own. RESULTS: The newly developed sEMG electrode was tested for adhesion strength, adhesion duration, and reusability on 7 subjects. The adhesive sEMG electrode could be reused up to 5 times without any problems and was worn by the test subjects for an average of 14 hours daily. In terms of wearing comfort, all test subjects found the electrode acceptable and comfortable to wear. Skin irritation did not occur. In addition, the signal quality was analysed in terms of the signal-to-noise ratio, long-term stability, and interference from movement artifacts. The signal quality achieved was comparable to conventional wet electrodes and stable over several hours. Only minor movement artifacts occurred even with strong movements. CONCLUSION: The carrier material with integrated gold contacts represents an adhesive electrode material with which an sEMG electrode can be realised that adheres to the skin surface like a plaster and is reusable. The sEMG electrode can be attached autonomously by the patient. Its signal quality is sufficient to use it for long-term recording of muscular activation.

P2.70-S: Development of a Surface EMG E-Textile

Emmanuel Moncada, Universidad de Guadalajara; Abhishek Prasad, IISER Bhopal; Timothy Green, Andrew and Marjorie McCain Human Performance Laboratory, University of New Brunswick; Usha Kuruganti, University of New Brunswick

Background: In recent years, the incorporation of electronics into clothing has become more common, particularly in the healthcare sector. These wearable systems allow researchers and clinicians to monitor patients outside of a laboratory setting. This advancement addresses the dissatisfaction with current market systems and offers features such as comfort, washing resistance, and flexibility in usage. Surface electromyography (sEMG) is commonly used to measure the muscular activity of athletes and patients, aiding in diagnosis and rehabilitation. Although wireless systems capable of transmitting signals to computers currently exist and have become standard, implementing them outside the laboratory remains challenging. Purpose: The purpose of this study was to design and test a custom-built 8-channel e-textile

sEMG system to analyze signals obtained from two materials: conductive thread and dry electrodes, to achieve an e-textile grid that is easily replaceable, low-cost, reusable, and can be used outside of a laboratory setting. Methods: Four male subjects (mean age 21 ± 0.43 years) participated in the study. Participants completed isometric and isotonic contractions while wearing the two different EMG e-textile grids. In the isometric protocol, participants were given a handheld dynamometer and asked to reach 25 kg of force for a period of 4 seconds twice within ten second period. The signals were obtained from the participant's dominant forearm. In the isotonic protocol, a 2.5-pound weight was positioned in the subject's hand. They rested their elbow on a flat platform and fully extended their forearm, forming a 110° angle at the elbow joint. The subject was asked to flex their arm within a 4-second period twice within a ten second window. During the isotonic contractions, sEMG signals were collected from the biceps brachii muscle. The signals were acquired using a Sessantaquattro+ (OTBioelettronica, Turin, Italy) and power spectrum densities, signal-to-noise ratios, coefficient of variations, and root mean squares were compared between the conductive thread and dry electrodes. RESULTS: Both materials met the expectations of an electrode for (sEMG) data collection. The frequency distribution is as expected for an sEMG signal, as shown in Figure 1. Both materials are sensitive to electromyographic activity, and the signal-to-noise ratio is significant, indicating that the signal stands out and is detectable in relation to the noise. When comparing individual values between material groups, the differences between the dry electrodes and the conductive thread are evident. The conductive thread shows better performance in the power spectral density (PSD) as it exhibits fewer artifacts, resulting in a lower amount of noise. Additionally, the conductive thread obtains a higher signal-to-noise ratio (SNR) in the isotonic contraction (+10 dB). Conclusion: In summary, the conductive thread material displayed clear advantages in metrics such as PSD and SNR. Successfully embedding electrodes into fabric is the first step in creating a robust and practical e-textile system which presents possibilities in the fields of wearable technology and biomedical monitoring. While preliminary, these results are promising, and future work will include a greater sample size as well as different contractions to test the robustness of the materials.

P2.71-S: Exploring the impact of including activity when walking when quantifying daily upper limb use in people with sub-acute stroke

Aishwarya Shenoy, University of British Columbia; Kyle S Weber, University of Waterloo; Kit B. Beyer, University of Waterloo; Janice J. Eng, University of British Columbia; William McIlroy, University of Waterloo; Sean Dukelow, University of Calgary; Courtney Pollock, University of British Columbia

Introduction: Incorporating the use of the arm and hand in daily life is the ultimate goal of upper extremity rehabilitation. Objectively measuring UE activity during free-living can provide clinicians with essential information regarding performance and functional use of the paretic UE. Inertial measurement units (IMUs) have been used post-stroke to objectively measure UE activity during free living. Bilateral magnitude (BM) and magnitude ratio (MR) are metrics used to quantify intensity of activity across both arms and symmetry of arm use, respectively. Use of these metrics to quantify UE activity during free-living have been studied in stroke; however, how arm swing during walking compared to non-walking UE use (i.e., activities of daily living)

contributes to measurement of UE use is not known. Aim: This study aims to evaluate the impact of removing UE activity that occurs during walking on the measurement of UE use during free-living. BM and MR were used as measures of UE activity and were compared when including UE activity during walking vs. UE activity without walking. Methods: Participants (< 6 months post-stroke) wore bilateral wrist and ankle Axivity AX6 IMUs for 24 hours/day for 7 days. Data was collected at 50 Hz. A 20 Hz low pass 4th order Butterworth filter was applied to the raw data and average vector magnitude was calculated using 1-second epochs. The mean BM and MR were calculated for UE activity with walking included and without walking included for each participant. Statistical Analysis: We used Lin's Concordance Correlation Coefficient (CCC) to 1) explore agreement between BM with and without walking and 2) explore agreement between MR with walking and without walking. Bland Altman analysis was conducted between 1) BM with and without walking and 2) MR with and without walking. RESULTS: Eight (2 females) participants (66.25± 11.65 years) were included in the preliminary analysis. Participants ranged from severe to marked impairment for the hemi-paretic side (Fugl Meyer Assessment: 56.75± 22.89). There was moderate agreement (CCC= 0.93, 95% CI 0.74– 0.98) between BM with walking and without walking. Bland Altman plots showed that inclusion of walking activity tended to increase BM reported (95% Limit of Agreement -5.6 – 14.9) compared to without walking. Substantial agreement (CCC=0.994, 95% CI 0.971– 0.998) was found between MR with walking and without walking. Bland Atlman plots showed no systematic bias between MR with walking and without walking (95% Limit of Agreement -0.09– 0.06)Conclusion: Results suggest that inclusion of arm swing during walking in free-living data may increase the reported BM as a reflection of the intensity of UE activity. However, it may not impact MR to a similar extent. Agreement between measurements of MR suggest that symmetry of arm swing in walking reflects symmetry of UE use in non-walking tasks such as activities of daily living.

P2.72-S: Extended reality for physical performance enhancement

Pascal Madeleine, Aalborg University; Dan Eisenhardt, Aalborg University; Mathias Kristiansen, Aalborg University

BACKGROUND AND AIM: Physical performances are of utmost importance in sports and at work to obtain optimal efficiency without increasing the risk of musculoskeletal injuries. The development of modern electronics and computer enables to feed the users with metrics that inform about their current level of physical performance. Sensory information using audio, tactile or visual feedback can be added to the input an athlete, or a worker receive while performing sports or while working. This places the athlete or the worker in a setup called augmented or extended reality. The aim of this abstract is to showcase a few applications impacting the future of sports and work. Methods: Augmented or extended reality is defined as the combination of real environment complemented by additional sensory information. Augmented reality covers a large spectrum that e.g., mix real and virtual environment being depicted as either augmented or mixed reality where the athlete or the worker is provided with additional feedback using visual, auditive or tactile sense. The additional feedback is based on data collected using inertial measurement units and/or optic sensors. Inertial measurement units combine accelerometer, inclinometer, and gyroscope data and are getting more and more integrated in equipment like watches and goggles feeding the user with information concerning

e.g., running or swimming style, heart rate, and effort level. Further these sensors also open a new era for gamification that can also been used in real-life settings to improve e.g., head pitch angle in swimming. RESULTS: The current approaches offer a vast number of possibilities found to (i) be reliable and possible, (ii) improve physical performance during for example penalty kicks in soccer. Still feeding the sportsmen or the worker with additional sensory information can also have negative effect especially if the added information increases the cognitive load or changes the focus of attention that could have a negative effect and increase the risk of injuries. CONCLUSIONS: Augmented or extended reality is and will be become an integral part of our life during sports and at work. This opens a large number of possibilities to improve physical capacity even if longitudinal studies are needed to clearly demonstrate the real benefit of extended reality.

Poster Session 3

P3.1-B: Exploring Lower Body Action Recognition Through Distance-Based Time Series Analysis and Template Matching

Po-Hsien Jiang, National Taiwan University; Yu-Ting Chen, National Taiwan University; Kuei-Yuan Chan, National Taiwan University

Human motion recognition technology has significant applications in various fields, such as rehabilitation, long-term care, monitoring, entertainment, and human-computer interaction. These technologies primarily process data in the form of time series and are categorized based on the data source into two main types: image-based and wearable sensor-based. This is a widely researched topic in the realms of big data and artificial intelligence. Our study aims to analyze human motion in an intuitive manner that does not rely on traditional neural networks or machine learning techniques. We understand the mechanics of motion by analyzing the changes in human joint angles, focusing on similarity measurement and time series alignment, employing various time series distance metrics such as Euclidean distance, Dynamic Time Warping, Move-Split-Merge, and Fisher-Rao Metric.The research is divided into three main parts: First, we collect motion data using the Vicon motion capture system to obtain movement data and build a human model in OpenSim software to calculate the rotational angles of the lower limb joints. This time series data of angles is used to describe lower limb motions. Second, we create and analyze motion templates, covering ten common lower limb movements, adjusting the motion samples through time series alignment techniques and various distance metrics to align the main features in the samples. We then use these aligned samples to establish motion templates and analyze the distance distribution among different sample categories. Lastly, we conduct template matching experiments, proposing a similarity scoring method based on time series distance measurement, integrating the softmax and bell-shaped functions for motion classification, effectively eliminating outliers. We designed three motion scenarios for testing, including artificially generated scenarios. The results show that our similarity scoring method is effective, particularly when using the Dynamic Time Warping method, maintaining good performance even in data with noise.

P3.2-B: Error Movement Detection System for Baseball Pitching Using MediaPipe and LSTM-based Deep Learning

Wen-Lan Wu, Kaohsiung Medical University; Jing-Min Laing, Kaohsiung Medical University; Hung-Chun Huang, Kaohsiung Medical University; Pei-Hsi Chou, Kaohsiung Medical University; Wen-Hsien Ho, Kaohsiung Medical University

In recent years, artificial intelligence and computer vision technology have been developing rapidly and have been widely applied in various research fields, such as medical rehabilitation, motion-sensing games, and sports quality monitoring. The focus of this study was to utilize human body pose recognition technology for error detection in baseball pitching movements. Seven college baseball players were recruited into this study, and each player performed 10 pitches in an outdoor setting. The camera was fixed at 2 meters to the side of the players for

video recording. This study aimed to detect errors in the shoulder, torso, and lower limb positions from the foot contact to the arm cocking phase of the pitching process. Coaches evaluated four types of errors based on the players' motion videos, including: insufficient trunk rotation, the throwing elbow is not level with the line of the shoulders, the throwing arm is not level with or slightly behind the body, and insufficient stride length. In this study, Python programming language and MediaPipe's Python API was employed for images RGB color conversion and changed the images into a fixed resolution (1280*720) and frame (30 fps). Subsequently, the three-axis coordinate data of 12 landmarks on the body, such as the both side shoulder, elbow, wrist, hip, knee, and ankle, were extracted by using a pre-trained deep neural network model in MediaPipe. Before training and testing the model, the pose data were divided into 80% for training data and 20% for testing data. Finally, the long short-term memory (LSTM) was used to establish a pitch style classification model. The classification accuracy for the four types of error movements was 81.48%, 85.71%, 85.19%, and 88.89%, respectively. The results of this study showcase the viability of employing Human Pose Estimation and Machine Learning algorithms to automatically detect the players' error pitching movements. In conclusions, the findings of this study hold the promise of benefiting players, coaches, and researchers, thereby making a meaningful contribution to the instruction of baseball skills.

P3.3-C: Visually induced vection leads to sensory reweighting in postural control- A preliminary study-

Takuya Yada, Tokyo Metropolitan Rehabilitation Hospital; Wataru Kuwahara, Tokyo Metropolitan University; Kouta Kuramochi, Human health Sciences, Tokyo Metropolitan University; Megumi Okawada, Keio University School of Medicine; Kenya Tanamachi, Tokyo Metropolitan University; Fuminari Kaneko, Tokyo Metropolitan University

【Introduction】Vection, a form of whole-body kinesthetic illusion induced by visual stimulation, is a phenomenon where subjects perceive motion despite their stationary position due to the presented visual input. Vection results in an augmented vestibular and somatosensory influence during postural control in conjunction with visual stimulation. Thus, vection-inducing video is possible to be effective as balance training for subjects such as elderly individuals who are considered to have higher vision weighting. However, sensory reweighting in postural control when subjects are asked to watch a video for a relatively long period (i.e. period of balance training) have not been shown. The purpose of this study was to demonstrate the effect of sensory reweighting in postural control after visually induced vection in healthy subjects as a preliminary study.【Methods】Eight healthy adults (four males and four females, age: 21.5±0.5 years) participated in this study. Subjects were applied to the intervention to watch the vection-inducing video using by Head-Mounted Display (HMD: Meta Quest pro, Meta Inc.). This intervention was roll circular vection in which random dots rotates around anti-clockwise. Video rotated random dots was presented for 10 seconds, and static dots image was presented for 20 seconds, and the videos were repeated for 10 minutes. Subjects were asked to stand in side-by-side stance during this intervention. Outcomes were center of pressure (COP) of side-by-side stance in 30 sec using a force plate. COP data were acquired before and after the intervention. COP parameters were total trajectory length, rectangular area, and power spectrum density (PSD) in the lateral direction of COP using the

fast fourier transform. PSD was then divided into three frequency intervals: the low-frequency (LF: 0–0.3 Hz), the medium-frequency (MF: 0.3–1 Hz), and the high-frequency (HF: 1–3 Hz) band. The PSD of each band was thereafter normalized by the sum of three bands and is presented as percentages. 【Results】 There were no significant different in total trajectory length and rectangular area. After intervention, LF band was significantly decreased and MF band was significantly increased compared to before intervention. 【Discussion】 Our results indicated that the sensory reweighting in postural control was led by visually induced vection. Previous studies have reported that the LF band reflects visual weighting, and the MF band reflects vestibular and somatosensory weighting in postural control. Increasing the MF band after the intervention in this study might contribute to lead reweighting of vestibular and somatosensory in postural control by vection. Vection may be effective as the intervention methods of balance training for the elderly who are considered to have higher vision weighting.

P3.4-C: Temporal muscle activation during gait post-Achilles surgery: A longitudinal analysis using surface electromyography.

Oscar Valencia, LIBFE, Escuela de Kinesiología, Universidad de los Andes, Chile; Kylie Tucker, The University of Queensland; Taylor Dick, University of Queensland; Rodrigo Guzmán-Venegas, LIBFE, Escuela de Kinesiología, Universidad de los Andes, Chile.; Manuel Pellegrini, Clinica Universidad de los Andes, Chile; Giovanni Carcuro, Clinica Universidad de los Andes, Chile; Diego Silva, Clinica Universidad de los Andes, Chile; Rafael Rossi, Clinica Universidad de los Andes, Chile

Introduction. Advancements in Achilles tendon reconstruction have led to significant improvements for patients, expediting the return to routine activities. Minimally invasive techniques, such as PARS-Dresden, have notably reduced recovery times, enabling patients to walk without crutches by postoperative week five. However, it remains unclear whether alterations in the triceps surae muscle activation patterns occur during recovery. This study aims to compare the onset-offset activation intervals in the triceps surae during gait following Achilles reconstruction.Material and methods. Eight patients (age: 35.37±4.74 years; height: 172.12±6.37cm; weight: 70.50±13.90kg, eight males) were recruited after Achilles surgery (PARS-Dresden) and followed for one year. Three-dimensional motion capture was used to identify the different gait cycles while each person walked on the treadmill (evaluated at 8, 12, 24, and 48 weeks). Each volunteer walked at a self-selected speed, determined in the first session (8 weeks) and maintained during the follow-up sessions. Surface electromyography (sEMG) was utilised to measure muscle activation of the triceps surae (soleus [SOL], medial [MG], lateral [LG] gastrocnemius). Each sEMG signal was processed with the Teager-Kaiser energy operator and filtered with a low pass of 50Hz. The onset, offset, and duration of each burst of muscle activation in the operated limb were determined on ten gait cycles and then averaged. The results were represented in milliseconds (ms). Activation outcomes were compared between sessions using a one-way ANOVA and Bonferroni's post-hoc test. All statistical analyses were calculated with a p-value<0.05. Results. There was a main effect of session for each outcome. Post-hoc analysis showed changes for the onset and burst duration of the MG between 8 weeks (onset=475±185ms, burst duration=280±203ms) versus 24 weeks (onset=208±99ms, p=0.001; burst duration=538±147ms, p<0.01) and 48 weeks

(onset=139±35ms, p<0.01; burst duration=625±86ms, p<0.01). LG onset and burst duration changed similarly over time from 8 weeks (onset=399±121ms, burst duration=349±176ms) versus 24 weeks (onset=191±167ms, p=0.01; burst duration=562±211ms, p=0.04) and 48 weeks (onset=160±74ms, p<0.01; burst duration=603±137, p=0.01). For SOL onset and burst duration also differed from 8 weeks (onset=445±100ms; burst duration=222±109ms) versus 24 weeks (onset=211±150ms, p<0.01; burst duration=554±197ms, p<0.01) and 48 weeks (onset=142±50ms, p<0.01; burst duration=639±127ms, p<0.01). The SOL offset also differed between 8 weeks (668±103ms) versus 48 weeks (781±97ms, p=0.02),Conclusions. The activation timing of the triceps surae muscles differed over time from 8 to 24 weeks post-Achilles tendon reconstruction. Notably, there was an earlier onset and a marked increase in the duration of activation at both 24 and 48 weeks. These findings advance our understanding of alterations in neuromuscular control during post-surgery recovery.

P3.5-C: Neurophysiological factors associated with performance parameters in elementary school students

Akane Yoshimura, Waseda University; Shun Kunugi, Aichi Institute of Technology; Tetsuya Hirono, Kyoto University; Kohei Watanabe, Chukyo University

Background: It is known that both neural and muscular adaptations develop with growth; however, their contribution to performance parameters in children remains unclear. The present study aimed to clarify: 1) the association of muscular and neural factors with performance parameters (maximal voluntary isometric contraction (MVC) and vertical jump (VJ)), and 2) the effects of growth on them in elementary school-age children. Methods: 68 (52 boys and 16 girls) elementary school students (chronological age (CA): 8.71 ± 1.63 years) participated in this cross-sectional study. We measured MVC, VJ, muscle thickness (MT) and the motor unit firing rate (MUFR) of knee extensor muscles. MT and MUFR were measured using an ultrasound device and high-density surface electromyography, respectively. Age of peak height velocity (PHVA) was calculated to consider individual maturity level by using the BTT model. A non-parametric partial correlation analysis was performed to investigate the association of muscular/neural factors (MT, MUFR) with performance parameters (MVC, VJ), controlling for maturation level assessed by subtracting PHVA from CA. In addition, Kruskal-Wallis test and Mann-Whiteney test were used to compare all data (MVC, VJ, MT, MUFR) among the three groups classified by the following maturity levels: young (CA-PHVA < -5 years), middle (-5 years ≤ CA-PHVA < -3 years), old (CA-PHVA ≥ -3 years). RESULTS: Average of PHVA and CA-PHVA were 12.41 ± 1.05 years and -3.70 ± 2.12 years, respectively. 60 motor units detected from 27 participants were used in analysis for MUFR. A partial correlation analysis showed that there were no significant correlations with MVC for MT (r = .33, p = .09) and MUFR (r = .21, p = .30). No significant correlations with VJ for MT (r = -.11, p = .57) and MUFR (r = .13, p = .50) were also found. In comparison among groups, MVC and VJ values were significantly higher with increasing maturity levels (MVC: young vs middle, p < .01; young vs old, p < .01; middle vs old, p < .05; VJ: young vs middle, p < .01; young vs old, p < .01; middle vs old, p < .05). Moreover, the MT value in old group was significantly higher than that in young group (p < .05) although no significant difference in MUFR values among groups was found. CONCLUSION: : The findings of the present study suggested that performance parameters such as MVC and VJ

of elementary school-age children are influenced by both of muscular and neural parameters. On the other hand, it was suggested that MUFR is not affect by maturation level although MVC, VJ, and MT improve with maturation.

P3.6-C: Relationship between forelimbs and head/neck movements and muscle activity during cantering on the treadmill in Thoroughbreds

Yuji Ohgi, Keio University; Takumi Omura, Keio University; Tatsuro Ishizuka, Keio University; Yuji Takahashi, Equine Research Institute, Japan Racing Association; Toshinobu Yoshida, Equine Research Institute, Japan Racing Association

(Background and Purpose)When thoroughbreds in their high-speed locomotion such as canter and gallop, they move with asymmetry gait patterns. The limbs on the side that contact first in time between left and right is called the trail limb, and those on the side that contact last is called the lead limb in horses. When the forelimb is in protraction, the brachiocephalic muscles, which has its origin and insertion at the cranial surface of the humerus and dorsal surface of the neck, contracts, causing the neck to rotate downward theoretically. The head and neck parts which have almost 10% weight show up and down oscillation during one single complete stride. However, it is an interesting question whether the head and neck parts, whose downward rotation is initiated and controlled by trail or lead front limb. The purpose of this study was to clarify the relationship between the protraction/retraction motion of the forelimbs and the head/neck rotating motion and the muscle activities controlling them. (Methods)Four thoroughbreds cantered on the treadmill at the speed of 12m/s with 0% slope condition. Two of subject horses were left leading limbs and others were right leading limbs. Their sEMG was obtained from left and right brachiocephalic, infraspinatus and deltoid muscles with 1000Hz sampling rate. For the kinematical analysis, 14 optical motion capture cameras were settled to capture 32 reflective markers on the anatomical landmarks of horses. The obtained marker trajectories were smoothed by IIR Butterworth low pass digital filter at the cut off frequency of 15Hz. The sEMGs were also smoothed by the band pass filter with between 15 to 500Hz, then rectified and calculated iEMG. The activation period was identified with 30% threshold level of each muscle's maximum amplitude of iEMG. (Results)The infraspinatus muscle, which is thought to support the forelimb, activated immediately before the forelimb landed, a trend similar to that observed in previous studies. We observed that changes in the angular velocity of forelimb swinging were synchronized with the timing of activation of the brachiocephalic muscle. However, there was no synchronization between the activation of the brachiocephalic muscle and the movement of the head and neck. In addition, the activation of trailing front limb's brachiocephalic muscles initiated, then leading side followed, i.e., asymmetrical motion on the left and right sides muscular activity was observed. It suggested that the head/neck motion was controlled by not only the brachiocephalic muscle, but also the cervical ligaments and the splenius muscles, which might anchor their neck part from the dorsal side. Also, it suggested that an alternating left-right bending moment always acts in the rotating neck motion during the single complete stride.

P3.7-C: Changes in pregnancy-related hormones, neuromechanical adaptations and clinical pain status throughout pregnancy: a prospective cohort study

Catherine Daneau, Université du Québec à Trois-Rivières; François Nougarou, Université du Québec à Trois-Rivières; Jacques Abboud, Université du Québec à Trois-Rivières; Stephanie-May Ruchat, Université du Québec à Trois-Rivières; Martin Descarreaux, Université du Québec à Trois-Rivières

BACKGROUND AND AIM: More than half of pregnant women will experience lumbopelvic pain during their pregnancy. During this period, women undergo hormonal, neuromechanical and clinical adaptations, which may contribute to the development of lumbopelvic pain. For instance, increased relaxin, estrogen and progesterone levels contribute to ligament laxity in the pelvic girdle, potentially leading to joint instability and predisposing pregnant women to lumbopelvic pain. Various changes observed in a woman's posture can also lead to neuromuscular adaptations, such as increased muscle activation of the lumbar muscles. The flexion-relaxation phenomenon has been used to evaluate neuromuscular adaptations since silencing of myoelectric activity during a full trunk flexion is lacking in individuals with low back pain. Although hormonal changes might be involved in lumbopelvic joint instability causing pain in pregnant women, their influence is not yet clearly determined.The main objective of this study was to assess changes in pregnancy-related hormones, neuromechanical adaptations and clinical pain status throughout pregnancy. An exploratory objective was to examine the possible association between those variables. Methods: Twenty-eight pregnant women completed, at each trimester, clinical questionnaires to assess functional disability, risk of poor prognosis, avoidance behaviors, catastrophizing and pain, and realized a flexion-relaxation task. Blood samples were taken to assess the levels of relaxin, estrogen and progesterone. During the flexion-relaxation task, surface electromyography over the right and left lumbar paraspinal muscles was assessed. Also, lumbar and pelvic angles during the task were collected using a motion capture system (flexion-relaxation phenomenon onset and cessation). RESULTS: Results showed that nocturnal and diurnal pain intensity, disability, risk of poor pain prognosis and avoidance behaviors increased, while pain catastrophizing decreased throughout pregnancy. Neuromechanical characteristics of the flexion-relaxation phenomenon, including EMG and kinematics, were similar throughout the three trimesters.Positive associations were found between estrogen levels and disability (changes between first and second trimester, r=0.46), and between estrogen levels and diurnal lumbo-pelvic pain intensity (change between second and third trimester, r=0.53). CONCLUSIONS: Our result showed moderate correlations between pregnancy hormone levels and clinical pain status. In pregnant women with and without lumbopelvic pain, estrogen was the only hormone associated with clinical features such as physical disability and the diurnal intensity of lumbopelvic pain. If the woman develops this type of pain during pregnancy, another physical test could be more appropriated to provide associations between the variables.

P3.8-C: Thoracic spine and shoulder kinematics and muscle activation of rock climbers with shoulder pain

Guan-Xuan Wu, National Yang Ming Chiao Tung University; Yin-Liang Lin, National Yang Ming Chiao Tung University

Background: Rock climbing has been a popular sport in recent years, involving a variety of arm movements, such as overhead reaching and pull-up. Overhead reaching and pull-up during climbing may be accompanied by trunk movement due to various wall inclinations. Among rock climbing injuries, shoulder injuries are about 17%, the second most common. Individuals with shoulder impingement syndrome have shown decreased upward and externally rotation during arm elevation and have limited thoracic extension range of motion and greater kyphotic posture. However, a previous study found no difference in the scapular kinematics and scapular muscle activation during pull-up between rock climbers with shoulder pain and healthy climbers, possibly due to no inclination during the pull-up task. Therefore, this study aimed to investigate kinematics and muscle activation of the shoulder and thoracic spine in rock climbers with shoulder pain during tasks designed to mimic climbing tasks. Methods: Thirteen rock climbers with shoulder pain and 13 healthy climbers matched with gender, age, and dominant hand have been recruited. Testing tasks included arm elevation in the scapular plane and climbing tasks. The climbing task was pull-up in backward inclination with overhead reaching upward and backward. Thoracic and shoulder kinematics were collected using an electromagnetic tracking system. The upper trapezius, lower trapezius, serratus anterior and latissimus dorsi were collected with surface electromyography (EMG). RESULTS: Compared to healthy climbers, climbers with shoulder pain exhibited more serratus anterior muscle activation during arm elevation from 90 to 120 degrees ($p = 0.03$) with no other difference in scapular and thoracic kinematics between groups. Additionally, climbers with shoulder pain demonstrated greater scapular posterior tilt during pull-up with overhead reaching upward ($p=0.027$) and backward ($p=0.023$), and less activation of the latissimus dorsi at 90 degrees of pull-up with reaching upward ($p=0.032$), as compared to controls. Furthermore, climbers with shoulder pain exhibited less thoracic extension range of motion compared to controls ($p=0.03$), with no differences in thoracic posture between groups. Conclusion: During arm elevation, climbers with shoulder pain may increase the serratus anterior activation to maintain normal scapular kinematics. Greater scapular posterior tilt during pull-up shown in climbers with shoulder pain may be a compensatory movement to increase subacromial space. Furthermore, lower activation of the latissimus dorsi in climbers with shoulder pain suggests potential muscle imbalance issues that hinder the latissimus dorsi muscle from serving as the primary mover to provide the necessary force during pull-up. Additionally, assessing thoracic extension range of motion may be more important than assessing posture in climbers with shoulder pain.

P3.9-C: Validation of Using Markerless Motion Capture System to Measure Functional Test in Patients with Degenerative Lumbar Disease: A Pilot Study

Yi-Ting Huang, National Taiwan University; Po-Jung Chen, National Taiwan University; Wei-Li Hsu, National Taiwan University; Pei-Yuan Wu, National Taiwan University

Introduction: Degenerative lumbar disease (DLD) is a common geriatric condition that leads to lumbar degeneration and lower extremity dysfunction. Previous studies have shown that these patients exhibit significant abnormalities in lower extremity kinematics when performing functional tests, such as the five times sit-to-stand test, clinically. In the past, these kinematic changes were mainly detected using marker-based motion capture systems, which are not readily adaptable to clinical settings. With advances in technology, markerless motion capture

systems have become popular.The purpose of this study was to investigate the validation of MediaPipe, a markerless motion capture system, compared to that of a gold standard motion capture system for the functional test in DLD. We hypothesized that there is a strong correlation for the five times sit-to-stand test in DLD between the markerless motion capture system and the marker-based motion capture system. Materials and Methods: DLD patients aged 50 to 80 with no surgical history were recruited. Data was captured using: 1) 11-camera VICON system (ver. 2.5, Oxford Metrics Ltd., Oxford, UK) with 45 reflective markers, 2) Markerless system with two iPhone 14 cameras - 2D poses estimated via MediaPipe (ver. 0.10.3, Google, California, USA), then lifted to 3D using 2D-to-3D approach. The pipeline is illustrated in Figure 1. To enhance the feasibility of rapid 3D human pose reconstruction, two calibrated cameras were placed in front of the participant with 40 cm apart, which is illustrated in Figure 2.The joint positions of the lower extremities in the anterior-posterior (A-P), medio-lateral (M-L), and vertical axes while performing the five times sit-to-stand test were analyzed using the Pearson correlation coefficient and 95% confidence intervals (95% CIs) and a p-value < 0.05 was considered statistically significant. Statistical analysis for this study was conducted using PASW Statistics 25. Results: Three DLD patients were recruited (age: 61.00 ± 8.19 years; height: 157.33 ± 55.51 cm; weight: 56.33 ± 1.53 kg). Validity data of the MediaPipe compared to the VICON were presented in Table 1. Discussions: The results supported our hypothesis of a strong correlation between the MediaPipe and VICON systems for the five times sit-to-stand test in DLD. Markerless systems can aid in assessing lower limb kinematics, providing objective data for DLD clinical intervention and facilitating telemedicine evaluation. Acknowledgement: This work was supported by National Science and Technology Council (MOST 111-2223-E-002-004-MY3) and National Taiwan University (NTU-113L7854) awarded to Dr. Wei-Li Hsu.

P3.10-E: Oscillatory transcranial direct current stimulation targeting corticoreticular pathway increases common neural drives to thigh muscles during gait

Ryosuke Kitatani, Niigata University of Health and Welfare; Haruki Hoshi, Niigata University of Health and Welfare; Runa Sorimachi, Niigata University of Health and Welfare; Rina Numata, Niigata University of Health and Welfare; Shiori Hirano, Niigata University of Health and Welfare; Naofumi Osturu, Niigata University of Health and Welfare; Hideaki Onishi, Niigata University of Health and Welfare

BACKGROUND AND AIM: Human gait depends on the integrated neural action of supraspinal and spinal levels, within which the corticospinal tract has important contribution. Recently, corticoreticular pathway (CRP), which is derived from the secondary motor areas such as pre-supplementary motor area (pre-SMA) to reticulospinal tract, has also been proposed to have an important role in human gait because CRP has a crucial role for bilateral activation of axial and proximal muscles during postural control. However, there is little evidence that non-invasive brain stimulation targeting CRP during gait can modulate the neural control of human gait. Therefore, we investigated the effects of oscillatory transcranial direct current stimulation (otDCS), which can modulate the potential and oscillation activity of brain neuronal membranes, targeting CRP on common neural drives to lower limb muscles during gait using coherence analysis of paired surface electromyography (EMG). Methods: Sixteen healthy young adults were subjected to following treadmill gait measurements: pre-stimulation gait for 5 min,

gait with otDCS over the pre-SMA for 11 min, and post-stimulation gait for 5 min. Subjects randomly experienced following 3 stimulation conditions on 3 different days apart from about 1 week: 10 Hz otDCS, 30 Hz otDCS, and sham stimulation. otDCS with a current intensity of 1.5 mA (ranging from 0 to 1.5 mA) was applied for 10 min with each 30 s fade in/out stimulation, and sham stimulation was applied only for 30 s. EMG-EMG coherence was calculated from following muscle pairs: the proximal and distal parts of the tibialis anterior muscle (TA-TA), medialis and lateralis gastrocnemius muscles (MG-LG), vastus medialis and lateralis muscles (VM-VL), and semitendinosus and biceps femoris muscles (ST-BF). The average coherence values in the 7.5 to 12.5 Hz (alpha) and 20 to 40 Hz (beta to low-gamma) frequency bands were calculated during the pre- and post-stimulation gait using each 200 gait cycles. RESULTS: Only one subject was excluded from statistical analyses because this subject had high coherence over 0.3–0.4 across a broad range of frequency bands, which might have been attributable to crosstalk, volume conduction, and/or current noise. In the 30 Hz otDCS condition, the average VM-VL coherence in the beta to low-gamma bands was significantly increased during the post-stimulation gait compared to the pre-stimulation gait. There were no significant differences between the pre- and post-stimulation gait in all paired EMG-EMG coherence in the alpha and beta to low-gamma bands in the 10 Hz otDCS and sham stimulation conditions. CONCLUSIONS: Since 30 Hz otDCS over the pre-SMA targeting the CRP increased the common neural drives to quadriceps muscles around stimulation frequency, otDCS targeting CRP during gait may be an effective rehabilitation tool in patients after stroke, who have low motor function in the proximal lower limb muscles.

P3.11-E: Larnygeal magnetomyography using an array of optically pumped magnetometer

Justus Marquetand, Department of neural dynamics and Magnetoencephalography, University of Tuebingen

Objective: This feasibility study investigated whether and to what extent laryngeal muscle activity can be recorded and functionally mapped contactless using magnetomyography (MMG) with optically pumped magnetometers (OPM). Methods: Five healthy subjects vocalized a high-, normal- and low-pitched A-schwa ("Aaa...") several times for 5 seconds each in a total duration of 90 seconds with a loud and a soft voice while a 3x5 array of OPM recorded the magnetic muscle activity of the larynx and the neighboring cervical muscles. The root-mean-square (RMS) average of each pitch per individual subject was calculated, color-scaled, and mapped to a general cervical anatomy. In addition, the individual amplitude per pitch was calculated. RESULTS: Although little consideration could be given to individual anatomical differences in the placement of the OPM and the subjects had not been trained beforehand, it was possible to identify an individual activity pattern for each subject that made it possible to distinguish between low and high pitches. The amplitude per pitch varied considerably between subjects (Min.: 0.4, Max.: 2.5 pT) and also the baseline noise between 0.2-0.5pT, which had to be taken into account for the analysis. CONCLUSIONS: Laryngeal MMG using an array of OPM is possible, but sensor positioning is crucial. In comparison to other skeletal muscles, the signal amplitude of laryngeal and neighboring muscles during vocalization is low.Significance: Functional, contactless muscle mapping of vocalization is feasible and might pose a new application of miniaturized quantum sensors for linguistic studies and speech rehabilitation.

P3.12-E: Facial magnetomyography

Justus Marquetand, Department of neural dynamics and Magnetoencephalography, University of Tuebingen

Objective: This feasibility study investigated whether and to what extent facial muscle activity can be recorded and imaged using non-invasive magnetomyography (MMG) with optically pumped magnetometers (OPM). Methods: Five healthy subjects performed 12 different standardized facial expressions (repetitive 2-second expression-trials during 90 seconds recording), while an array of 11 OPM of the right side of the face was utilized to measure the MMG of the respective facial muscles. The root-mean-square (RMS) average of each facial expression-trial per OPM and individual subject was calculated, color-scaled, and mapped to the individual face per facial expression to prove that an array of OPM can image facial muscle activity across facial expressions. In addition, the maximum average muscle activity and signal-to-noise ratio (SNR) per facial expression were calculated. RESULTS: Facial muscle activity could be mapped individually per facial expression, but the positioning of the OPM revealed to be a crucial factor for mapping accurately muscle activity. The SNR ranged from 1 to 8, the maximal observed average muscle activity reached almost 25pT in one subject and was on average 1±0.57pT. CONCLUSIONS: Imaging facial MMG with an array of OPM is possible, but sensor positioning is crucial. In comparison to other skeletal muscles, the signal amplitude of facial muscles is low.Significance: As imaging of facial MMG is feasible, this study paves the way for future studies for using quantum sensors diagnostics, monitoring and rehabilitation of facial muscles.

P3.13-F: Spatial-temporal transcutaneous spinal cord stimulation improves walking in humans with SCI

Ming Wu, University of Illinois at Chicago; Shijun Yan, Shirley Ryan AbilityLab; Hyosok Lim, Shirely Ryan AbilityLab; Iram Hameeduddin, University of Illinois at Chicago; Jack Snodgrass, Northwestern University; Weena Dee, Shirley Ryan AbilityLab; Velarie Pech, Shirley Ryan AbilityLab; Renee Keefer, Shirley Ryan AbilityLab

The goal of this study was to determine whether the application of spatial-temporal transcutaneous spinal cord electrical stimulation will facilitate walking in humans with SCI. Ten subjects with chronic (>1 year) SCI were recruited in this study. They were tested in 3 different spinal stimulation conditions: swing phase, stance phase, and combined stance and swing phases. For the swing phase condition, two self-adhesive round electrodes (5cm diameter) were placed at ~2 cm laterally from the midline over L1 and L4 spinous processes of the weaker leg as active electrodes. The stimulation waveform used was monophasic, rectangular, 100 us pulses at a frequency of 80 Hz filled with a carrier frequency of 9.5 kHz. Each participant was tested in 4 sessions, i.e., L1, L4 phasic, and L1, L4 continuous. Participants walked on a treadmill with the stimulation was applied to L1 or L4 segment and each session was lasted for ~2 minutes. For the stance phase condition, a protocol that was comparable to the swing phase condition was used except that the active electrodes were placed at 2cm laterally from the midline over L3 and S1 spinous process and the stimulation

frequency was 30 Hz. Each participant was tested in 4 sessions, S1, L3 phasic, and S1, L3 continuous. For the phasic stimulation sessions, the stimulation was delivered only during the swing or stance phases of the weaker leg for the swing and stance phase sessions, respectively. For the combined condition, a protocol that was comparable to the swing phase condition was used except that the stimulation was applied to S1 during stance phase with frequency of 30 Hz, and to L4 during swing phase with frequency of 80 Hz. For the control condition, no electrical stimulation was applied. Kinematics of pelvis and ankle, and muscle activity of the weaker legs were recorded. RESULTS: For the swing phase stimulation condition, the step height of the weaker leg was significantly greater for the phasic stimulation at L4 ($p = 0.02$) and L1 ($p = 0.045$) compared to the control. The step height of the weaker leg tended to be greater for the phasic stimulation at L4 ($p = 0.058$) and L1 ($p = 0.05$) than that of the continuous stimulation. For the stance phase stimulation condition, step height of the weaker leg was significantly greater for the phasic stimulation at S1 than the control ($p = 0.0498$), and than that of the continuous stimulation ($p = 0.038$). The application of stimulation at L3 had no significant impact on the step height of the weaker leg ($p = 0.16$). For the combined condition, the step height of the weaker leg was significantly greater for the combined condition that the control ($p = 0.04$). Conclusion: The application of spatial-temporal spinal cord stimulation through non-invasive transcutaneous electrodes may facilitate walking in people with SCI. Results from this study may be used to develop a new intervention approaches for improving locomotor function in people with SCI through targeted non-invasive spinal cord neuro-modulation.

P3.14-F: Does acute electrical muscle stimulation induce stress responses?

Hiroki Terada, The University of Electro-Communications; Wataru Ninomiya, The University of Electro-Communications; Kosuke Kano, The University of Electro-Communications; Mizuki Sudo, Meiji Yasuda Life Foundation of Health and Welfare; Soichi Ando, The University of Electro-Communications

Introduction: Recent studies suggest that electrical muscle stimulation (EMS) applied to lower limb muscles can be used as an alternative modality to voluntary exercise. Despite this, EMS often induces pain sensation, which may induce stress responses. However, it remains unclear whether EMS induces stress responses. The purpose of this study was to identify stress responses in response to a single bout of EMS in healthy participants.Method: Eleven male participants (age: 23.1 ± 0.9 yr., height: 172.2 ± 4.6 cm, weight: 65.2 ± 5.0 kg) were recruited for the experiment. Subjective pain was assessed using visual analogue scale (VAS) score at the end of EMS. Electroencephalogram (EEG), heart rate (HR), and salivary cortisol concentration were measured before and after acute EMS. EMS was applied bilaterally to the abdomen, glutes, thighs, and lower legs with an electrical stimulator while lying supine (Auto Tens Pro; Homerion laboratory Co., Ltd, Tokyo, Japan). The stimulator current waveform was set at a frequency of 4 Hz with a pulse width of 0.25 ms. Stimulus intensity was set at the maximal tolerable level. A power spectrum was calculated from the EEG signal using a fast Fourier transformation, and percentage of relative power of theta (4-8 Hz), alpha (8-13 Hz), and beta (13-30 Hz) bands was calculated. Inter-beat (R-R) interval data was used to assess autonomic modulation of HR, and LF to HF ratio (LF/HF) was calculated as an index of autonomic balance. RESULTS: Percentage of relative power of theta, alpha, and beta bands did not change after

EMS at Fz, Cz, and Pz (all p > 0.05), whereas LF/HF ratio decreased after EMS (p = 0.008). EMS did not affect salivary cortisol level (p = 0.489). However, there was a negative correlation between VAS score and changes in relative percentage of theta band (Spearman's rho = -0.691, p = 0.023), suggesting that relative percentage of theta band was reduced with individuals who experienced stronger pain sensation. CONCLUSION: : The present results suggest that EMS does not induce stress responses. However, stimulus intensity should be carefully set for each individual to minimize stress responses.

P3.15-G: Effects of blood flow restriction on muscle fatigue during isometric contractions

Corrado Cescon, University of Applied Sciences and Arts of Southern Switzerland; Alessandro Schneebeli, University of Applied Sciences and Arts of Southern Switzerland; Edoardo Muscionico, University of Applied Sciences and Arts of Southern Switzerland, 2rLab, Manno, Switzerland; Edoardo Muscionico, University of Applied Sciences and Arts of Southern Switzerland, 2rLab, Manno, Switzerland; Marco Barbero, University of Applied Sciences and Arts of Southern Switzerland

Blood Flow Restriction (BFR) is a training method that partially restricts arterial blood flow and completely restricts venous return by applying a cuff proximally on the target limb, exerting pressure (Scott et al., 2015). This acute reduction of blood flow, decreases oxygen supply, leading to muscle hypoxia, and blood pooling in occluded capillaries (Patterson et al., 2019). Originating from Japan's KAATSU (meaning "training with added pressure") proposed by Yoshiaki Sato in 1966, BFR was inspired by Sato's observation of muscle discomfort during prolonged kneeling. BFR induces muscle hypoxia during voluntary muscle contraction, affecting ATP rephosphorylation, reactive oxygen species production, and energy processes (Manini & Clark, 2009). Muscle tissue under BFR experiences greater oxygen depletion, switching to anaerobic metabolism, increasing blood lactate, and reducing pH. The higher AMP-activated protein kinase (AMPK) production in regular BFR training may explain increased muscle glycogen content (Manini & Clark, 2009).The aim of the present study is to observe the acute effects of blood flow restriction on muscle fatigue during isometric contraction in healthy subjects. The hypothesis is that higher percentages of blood occlusion lead to higher muscle fatigue, thus higher slope values for EMG variables such as mean power spectral frequency (MNF).The experiment was conducted on quadriceps muscles of five healthy volunteers. Participants were sitting with the knee joint of the dominant leg at 90° and were asked to exert knee extension againss a strap fixed to the ankle with a constant torque of 50 Nm (provided by a visual feedback) until failure. Tests were administered in three different conditions: at 0%, 40%, and 80% of arterial occlusion pressure (AOP). For the restriction of blood flow, we used AirBands (AirBandsBFR, Newstead, Queensland), while EMG measurements were performed with bipolar electrodes positioned over vastus medialis and lateralis muscles using a wireless amplifier (Due, OT-Bioelettronica). ARV and MNF were computed using epochs of 1s to evaluate changes of amplitude and frequency during the endurance contraction. Perceived exertion was asked to the subject using the Borg CR10 scale, and individual discomfort was assessed through a modified VAS every 30s. A higher restriction percentage showed higher slopes of heart rate, as well as higher slope values for MNF. Higher percentages of BFR were also associatede with slighly higher ARV slopes during the contractions suggesting higher neuromuscular

recruitment. Additionally, we observed that in 4 out of 5 participants, BFR resulted in higher values of perceived fatigue (Borg CR10). Given the limitations of the study and the nature of the sample, further in-depth research is necessary to determine which among the available percentage options may be most suitable for achieving greater neuromuscular fatigue and, therefore, establishing a more effective dosage for rehabilitative purposes.The preliminary findings underscore BFR's capacity to amplify muscular fatigue, hinting at its utility for endurance training. However, robust empirical support is necessary to confirm its clinical value.

P3.16-H: Detection volume simulation of diaphragm bilateral sEMG electrodes using an MRI-based finite element model

Andra Oltmann, Fraunhofer IMTE; Amelie Schulz, Institute for Electrical Engineering in Medicine, Universität zu Lübeck; Franz Wegner, Institute for Interventional Radiology, Universitätsklinikum Schleswig-Holstein; Alex Frydrychowicz, Clinic for Radiology and Nuclear Medicine, Universitätsklinikum Schleswig-Holstein; Philipp Rostalski, Fraunhofer IMTE / Institute for Electrical Engineering in Medicine, Universität zu Lübeck

Surface electromyography (sEMG) of respiratory muscles is applied in assisted mechanical ventilation to analyze both respiratory effort and patient-ventilator-interactions. A variety of research projects used a differential electrode pair positioned bilaterally on the midclavicular lines on the costal margin for recording the diaphragm as the main respiratory muscle. However, no widely accepted standard has been established yet. Due to the diaphragm’s shape, the area of the costal part detected by these electrodes and contributing to the signal is non-obvious. The objective of this research project is to develop a numerical electrophysiological simulation of the diaphragm enabling the investigation of the detection volume. To implement an anatomical model, an MRI T1w sequence (Dixon) of the torso in the end-expiratory phase for one subject was acquired. Data were segmented into the lung, heart, rib cage, and diaphragm with Materialise Mimics 24.0 (Materialise NV, Leuven, Belgium). A size-principle motor unit (MU) pool was implemented. To reproduce the physiological fiber pathways, a curvilinear vector field in both hemidiaphragms was simulated using the curvilinear coordinates system simulation in COMSOL Multiphysics® v. 6.1 (COMSOL AB, Stockholm, Sweden). The homogeneously distributed fibers follow the vector field, and motor end plates as well as fiber ends were uniformly placed. MUs were assigned to fibers using a probability function depending on the MU size and proximity. To calculate single fiber action potentials (SFAPs), a reciprocal approach was used, which determines the fiber's transfer behavior by solving the Poisson equation in COMSOL Multiphysics® v. 6.1. The obtained transfer function per fiber was convolved with the propagating signal component and static signal components were added. To visualize the detection volume the SFAP peak-to-peak amplitude is calculated. The MU pool was simulated for five stochastic seeds to account for the unknown physiological parameters. The MU pool resulted in approximately 16000 simulated muscle fibers. Due to the electrode positions bilaterally on the midclavicular line above the costal margin, the end-of-fiber effect is dominant in most SFAPs. The different stochastic seeds provide comparable peak-to-peak amplitudes of SFAPs. The visualization of the mean detection volume clearly shows the contribution of fibers in both diaphragm domes. However, only a limited area of the costal diaphragm on the ventral torso will make a substantial impact on the resulting sEMG signal. The anatomically and

physiologically based simulation of the diaphragm provides useful information to enhance the understanding of respiratory sEMG. It enables the visualization of SFAPs and the resulting detection volume in the diaphragm. By considering further electrode positions and extension to the end-inspiratory breathing phase, the work has the potential to contribute to the standardization of electrode positions.

P3.17-H: A biophysical model of the motoneuron pool to understand the role of neuromodulation in motor control

Natalia Torres-Cónsul, Imperial College London; Simon Avrillon, Université Côte d'Azur; Dario Farina, Imperial College London; Juan Gallego, Imperial College London

Supraspinal regions control motoneuron activity by modulating their firing patterns to produce the desired muscle force. A substantial portion of these descending synaptic inputs project to multiple motoneurons within a pool, imposing a rigid constraint on their behaviour. Common synaptic input thus leads to the orderly recruitment — from smallest to largest — of motoneurons, and mediates force control through the modulation of motoneuron firing rate. Recent studies, however, have challenged this longstanding view of motoneuron control, suggesting that it may be more flexible. For example, Marshall et al. (Nature Neurosci, 2022), reported that the responses of motoneuron pairs evoked by intracortical microstimulation changed in relatively latency and magnitude depending on the stimulation site. Besides, Bräcklein et al. observed patterns of inversion of derecruitment, consistent with activity-dependent changes in motoneuron excitability (eLife, 2022). These observations conflict with the most rigid view of motoneuron control, and can be potentially explained by neuromodulatory processes.Neuromodulation refers to the alteration of motoneuron excitability that occurs due to neurotransmitter release — primarily, serotonin — from descending brainstem axons. The most significant neuromodulatory effects in the spinal cord are persistent inward currents (PICs). PICs impact motoneuron function via amplification, which accelerates the initial phase of motoneuron firing, and hysteresis, which sustains motoneuron firing activity even after the cessation of synaptic input. In this work, we aim to understand how neuromodulation leads to a more flexible control of motoneurons. Our first objective is to characterise the mechanisms that facilitate the inversion of motoneuron derecruitment. To better understand the distribution and interplay of PICs and inhibitory mechanisms with synaptic input, we are developing a biophysical model of a motoneuron pool that builds upon the Hodgkin-Huxley model. In our model, all motoneurons receive the same common synaptic input as well as different combinations of neuromodulatory and inhibitory signals; together, they drive the firing activity of single motoneurons. The parameters of the biophysical model will be optimised based on recordings from large populations (n~130 per participant) of motoneurons from the Tibialis Anterior and Vastus Lateralis muscles from 16 participants performing trapezoidal contractions during. Our model will also implement a feedback controller, to simulate motor control tasks. First, we will model the experiments by Bräcklein et al., in which participants had to control the movement of a cursor in two dimensions to acquire different targets by modulating the activity of two motoneurons from the same muscle. We will compare the results from simulations with different combinations of neuromodulatory and synaptic input to establish potential biophysical mechanisms underlying

the reversion in motoneuron derecruitment order reported there.By replicating these and other experimental results, we expect our model to clarify the contributions of neuromodulatory inputs to motoneuron control, in particular in enabling a degree of flexibility that was unsuspected until very recently. Besides, by comparing across alternative implementations, we will be able to define potential mechanisms by which neuromodulation may achieve this additional flexibility.

P3.18-H: A neuromorphic approach to decoding motor intentions from intraneural recordings of a trans-radial amputee

Farah Baracat, Univeristy of Zurich and ETH Zurich; Alberto Mazzoni, The BioRobotics Institute and Department of Excellence in Robotics and AI; Silvestro Micera, The BioRobotics Institute and Department of Excellence in Robotics and AI; Giacomo Indiveri, University of Zurich and ETH Zurich; Elisa Donati, Univeristy of Zurich and ETH Zurich

Advanced prosthetic devices hold the promise of restoring dexterity for upper-limb amputees by decoding the user's motor intentions and delivering tactile sensory feedback during object manipulation. These bidirectional interfaces operate by recording and processing neural signals from multiple electrodes while concurrently stimulating the afferent pathway to elicit sensations. Crucially, both the decoding and encoding systems must unfold in real-time within a closed-loop framework, and continuously adapt to a changing neural signal. Furthermore, considering the wearability constraint of prostheses, processing of neural signals and stimulation modules should be implemented on low-power, low-latency, compact hardware placed in close proximity to the recording site. Consequently, careful consideration of algorithms and processing techniques alongside their hardware implementation is essential for the system realization.In this poster, we depart from conventional machine learning-based approach and adopt a neuromorphic, event-based computing paradigm for the processing of the recorded neural signals. Our primary focus is on the decoding pathway of the bidirectional prosthesis. We present the stages within a neuromorphic pipeline and demonstrate their advantages, in terms of pre-processing computation requirements, accuracy, and linearity on gesture decoding from nerve recordings, electroneurography (ENG), of a trans-radial amputee acquired using Transverse Intrafascicular Multichannel Electrodes (TIMEs). Neuromorphic computing is a computational paradigm that stands in stark contrast to conventional processing. By emulating the biophysical properties of biological neurons and synapses, neuromorphic systems adopts key biological features such as fault-tolerance, robust computation and event-driven, low-power processing. A neuromorphic pipeline starts with the encoding of recorded signals into a stream of events. The encoding stage should be carefully crafted to extract key features from the signal. Our findings demonstrate that using leaky-integrate-and-fire neuron model effectively converts the power of each ENG channel into a sequence of spike trains and further increases the linear separability of the gestures. Next, a spiking neural network is trained to predict the intended motor task based on the firing rates of output neurons.We show that this event-based approach can decode 4 gestures of a trans-radial amputee. Furthermore, it enhances the overall robustness of the system, achieving an accuracy improvement from 62 % +/- 8 % to 67 % +/- 1.8 % compared to a traditional machine learning pipeline. These results suggest that neuromorphic processing holds significant value

for the field of neuroprosthesis, particularly in addressing key constraints such as accuracy, latency, and power efficiency.

P3.19-I: Modulation of bilateral motor learning by the order and timing of right and left upper limb movements

Yoshiki Zaitsu, Keio University; Hirotaka Sugino, Keio University; Daichi Nozaki, The University of Tokyo; Junichi Ushiyama, Keio University

When learning upper limbs movement in our daily life, it is common to start practicing with each limb individually, and then combine both limbs together. It is known that acquired skills through unimanual motor learning can only be partially transferred to bimanual movement (Nozaki el al., Nature Neuroscience 2006), which means that a specific practice is required to master a bimanual movement. In the bimanual task used in the previous study, participants only moved both limbs at the same time. However, in our daily life, we move both limbs in the certain order depending on the task (i.e., one-two punch in boxing). To expand the understanding of bimanual motor learning, therefore, the present study compared bimanual motor learnings where both limbs move in different order and timing. We used exoskeleton robot manipulandum to replicate a protocol from the previous study. Participants performed bimanual reaching task with forcefield perturbation on right limb. We altered the order and timing of limbs' movements as follows: 1) Perturbed limb and non-perturbed limb moved at the same timing (PTB-sync); 2) Non-perturbed limb moved first then perturbed limb followed after 0.1s (PTB-later-0.1s) or 1s (PTB-later-1s); 3) Perturbed limb moved first then non-perturbed limb followed after 0.1s (PTB-first-0.1s) or 1s (PTB-first-1s). By repeating the trials with forcefield perturbation, they gradually learned to reach straight to the target with the opposing force to the perturbation. Subsequently, we prepared two washout phases. First, in unimanual washout, they performed unimanual reaching with their right limb without the forcefield to forget the motor memory. Next, in bimanual washout, they performed bimanual reaching without the forcefield to confirm how much memory is remained. We evaluated the aftereffect by measuring lateral deviation of right limb's trajectory, with the first trial of unimanual and bimanual washouts. In PTB-sync condition, unimanual aftereffect was observed and bimanual aftereffect was also observed even after the unimanual washout (fig1. a). In PTB-later-0.1s condition, bimanual aftereffect was significantly larger than unimanual aftereffect (fig1. b). In contrast, in PTB-first-0.1s condition, unimanual aftereffect was significantly larger than bimanual aftereffect (fig1. c). In PTB-later-1s and PTB-first-1s conditions, unimanual aftereffect were larger, and bimanual aftereffect were smaller compared to 0.1s conditions (fig1. d, e). These results suggest the exhibition of two discrete nature of bimanual motor learning, such as "a single bimanual movement" or "two separate unimanual movements." PTB-later-0.1s condition with significantly greater bimanual aftereffect would mean that motor learning proceeded as a single bimanual movement. On the other hand, PTB-first-0.1s and PTB-first-1s conditions with significantly greater unimanual aftereffect would mean that motor learning proceeded as two separate unimanual movements.

P3.20-I: Rhythmic Galvanic Vestibular Stimulation Modulates Sensorimotor Synchronization to Auditory Syncopation

a

P3.21-I: Temporal Relation Between Corticomuscular Coherence and Event-related Desynchronization is Associated with Force Output Strategies

Jing Zhou, Keio University; Junichi Ushiyama, Keio University

"Corticomuscular coherence (CMC)" is a synchronized phenomenon between the electroencephalogram (EEG) activity over the sensorimotor cortex and the electromyogram (EMG) activity of voluntary contracted muscle within the β-band (15-35Hz). However, there is a desynchronization in the β-band EEG activity known as "event-related desynchronization (ERD)", starting from motor preparation and leading to reduced EEG β-power. Our purpose is to clarify the temporal relation between the synchronized (CMC) and the desynchronized phenomena within the β-band during voluntary muscle contraction.In Experiment 1, 30 healthy young adults performed intermittent ballistic-and-hold contractions of the tibialis anterior muscle at 10% of maximal voluntary contraction (MVC). EEG β-power decreased before EMG activity onset and rebounded during force maintenance. The magnitude of β-rebound following ERD varied among individuals (Figure 1). Moreover, the CMC occurred after the muscle contraction onset and increased coincided with the dynamic β-rebound following the ERD (Figure 1A-C). Notably, participants with continuous ERD during force maintenance showed no significant CMC, whereas participants with clear β-rebound showed significant CMC (Figure 1D). Linear regression analysis revealed a positive correlation between β-rebound magnitude and CMC ($r = 0.54$, $p=0.0021$). Based on Experiment 1, we hypothesized that participants with continuous ERD and less CMC might make a greater effort to actively adjust their force even during the force-maintenance period, while those with clear β-rebound and greater CMC performed force maintenance with lower energy cost by using efficient sensorimotor integration. To test this hypothesis and investigate the individual differences in β-power rebound after ERD, we conducted experiment 2. In experiment 2, we compared the difference in temporal relation between ERD and CMC across tasks with different difficulties in controlling force output.In experiment 2, 9 participants with significant CMC from experiment 1 were involved in three tasks: 10% MVC straight-line task (identical to experiment 1), sin task (target line consisted of a sine wave with 10% MVC average and 2% MVC amplitude), and 3sin task (target line consisted of 3 sine waves with 10% MVC average and 2% MVC amplitude). Results aligned with our predictions with the highest β-rebound and CMC in the 10% MVC straight-line task and the lowest in the 3sin task (Figure 2).In summary, our studies clarified the temporal relation between ERD and CMC and demonstrated that the individual CMC difference was positively correlated with the extent of β-rebound. Furthermore, increased task difficulty in force adjustment resulted in lower β-rebound and CMC. Therefore, β-rebound variations suggested different strategies of force output: ongoing active adjustment of motor output in those with continuous ERD versus efficient adjustment after initially reaching the target in those with β-rebound. This distinction also correlated with CMC variations, indicating various extents of sensorimotor integration.

P3.22-I: Discovering the occupational profiles and occupational performance of children with handwriting difficulties: A parent's perspective

Dini Fajariani, Tokyo Metropolitan University; Yuko Ito, Tokyo Metropolitan University

Background and aimHandwriting is a complex perceptual-motor skill that involves visual-motor coordination, motor planning, cognitive and perceptual skills, and tactile and kinesthetic sensitivity to effectively complete a writing task. The occupational profile and occupational performance analysis are combined in the evaluation to inform the occupational therapy intervention plan. The occupational therapist considers all aspects of the domain and assesses their impact on the others, both individually and collectively. The purpose of this research is to identify and analyze factors that support and hinder children's handwriting improvement. METHODSThis study conducted semi-structured individual interviews through purposive sampling with parents who have children with handwriting difficulties in Indonesia. In order to recruit participants, the researcher will ask teachers at the school where the study will take place to select parents who meet the criteria. Parents were asked about their perspectives on handwriting difficulties, the child's learning environment, and the child's learning process at home. This study was ethically approved by the ethics committee of the university where the authors are affiliated and conducted from September to November 2023. All participants gave informed consent before their participation. ResultsFive parents participated in the study. The interview lasted 45 to 60 minutes. A qualitative study with inductive content analysis was used to analyze the data, and two themes emerged: supportive factors and inhibiting factors. Details of the results are shown in result table. From the parents' perspective, they realized that their child has a difficulty with handwriting and they need to seek advice from professionals. At home, they provide a special place for practicing and also accompany their child while practicing. Even though they already set up an environment to study, the child often gets easily tired and have short attention span during practice. In addition, sometimes their siblings also distract while the child is practicing. CONCLUSION: Handwriting is a complex skill that is not only related to the child's personal factors, but also related to the child's environmental factors. Most of the child's time during a day is spent at home. With a better understanding of the supporting and hindering factors of handwriting difficulties, OTs can provide appropriate practice to improve children's handwriting skills at home. From this study, it clearly stated that supportive family members, supportive environment and parent-child attachment could be considered while designing handwriting practice in child's natural environment.

P3.23-I: Evaluation of neck force control and neck muscle activation in Astronauts post-spaceflight

Michail Arvanitidis, Centre of Precision Rehabilitation for Spinal Pain (CPR Spine), University of Birmingham, UK; Eduardo Martinez-Valdes, University of Birmingham; Deborah Falla, University of Birmingham

Background: Astronauts have an increased risk of cervical intervertebral disc herniation (IVD) post-spaceflight, yet the cause of this heightened risk remains elusive. People with neck pain commonly exhibit changes in neck muscle strength and altered neck muscle activity, which can contribute to the persistence of their symptoms. Whether astronauts experience similar

alterations post-flight and if these are linked to the higher prevalence of IVD in this population is yet to be determined. Purpose: This project aimed to explore potential alterations in the behaviour of the neck flexor and extensor muscles in astronauts after extended time (>120 days) at the International Space Station by utilising high-density surface electromyography (HDsEMG) and hand-held dynamometry. Methods: This study is ongoing, and to date, three astronauts have been measured at two measurement sessions (pre-flight and five days post-spaceflight). Neck flexor and extensor muscle isometric strength was recorded with a handheld dynamometer. Then, submaximal isometric neck flexor/extensor force steadiness was measured during force target-tracking contractions at 25% and 50% of their maximal voluntary contraction. Visual trapezoidal feedback of their force trace was provided on a monitor. HDsEMG signals were acquired bilaterally from the sternocleidomastoid (SCM) and splenius capitis (SCap) muscles in monopolar mode, using four grids of 64 equally spaced (4mm) electrodes. The monopolar signals were differentiated longitudinally in the direction of the muscle fibres for each muscle to form adjacent bipolar channels. Topographical HDsEMG amplitude maps were created to investigate regional changes in muscle activation across all electrode pairs, and modified entropy was calculated based on the root mean square values. Force steadiness was characterised by the force signal's standard deviation (SD) and coefficient of variation (CoV). RESULTS: A consistent trend of reduced neck flexor and extensor muscle strength (19.37%), in addition to a decline in neck flexor and extensor muscle force steadiness (CoV: 61.39%; SD: 59.65%), was observed for all astronauts, five days after returning to Earth. Additionally, alterations were observed in the distribution and uniformity (modified entropy) of neck flexor and extensor muscle activation during the submaximal contractions. Conclusions: This study offers preliminary insights into changes in neck flexor and extensor muscle behaviour immediately after spaceflight. The reduction in muscle strength and force control, together with changes in neck muscle activation, could be relevant factors in understanding the increased risk of IVD in astronauts. Given the preliminary nature of this work, these findings should be interpreted with caution. All additional data collected by the time of the presentation will be incorporated to strengthen these findings.Keywords: Neck muscles, Force steadiness, High-density EMG, Regional Activation This study is funded by the UK Space Agency (ST/X002233/1).

P3.24-I: Effects of Stochastic Resonance-Based Mechanical Stimulation Intervention in the Abdominal Core Muscle on Static Balance: A Pilot Study

Yi Ting Lin, Tzu Chi university; Chich-Haung Yang, Tzu Chi University; Unpisith Jeamsupakorn, PhD student

Background: Young people have been exercising less due to lifestyle changes. This has resulted in poor muscle endurance and postural stability, increasing the risk of exercise injury or falls in exercise. Poor core stability has been identified as a risk factor for athletes' lower back and extremity injuries. Sensory Augmentation (SA) has proposed a potential positive intervention on postural control in people during standing. A novel design of vibrotactile mechanical stimulation system over the torso still not be confirmed experimentally. Aim: This study aimed to discuss whether the stochastic resonance-based mechanical stimulation intervention in the abdominal core muscle can improve changes in postural stability during static balance. Method: Ten volunteers (2 men and eight women) participated in this study. All participants had

no injuries in their lower limbs, did not experience any balance impairment, and were without any surgical history of lower limbs. Our outcome measures were the forefoot force, the midfoot force, the rear foot force, the total force in lateral and medial, and overall COP. Statistical analysis was performed using the Wilcoxon rank sum test, with a significance level defined at P <0.05. Result: After the intervention, significant differences in the decrease in pressure in medial total foot pressure (p=0.022) and lateral total foot pressure (p=0.022) were found during standing on the dominant side, significant differences in the subject's center of pressure (COP) the medial-lateral direction demonstrated the Sharped Romberg test with an open eye(p=0.022). However, the Romberg test with closed eyes condition reduced sway from the medial-lateral(MD=7.06) and anterior-posterior direction(MD=11.97) but no significant difference (p>0.05). Conclusion: The stochastic resonance-based mechanical stimulation intervention may improve our stability during single-leg standing.

P3.25-I: Dynamic Taping Improves Scapular Neuromuscular Control in Individuals with Impingement Syndrome

Kai-Ling Wang, National Yang Ming Chiao Tung University; Yin-Liang Lin, National Yang Ming Chiao Tung University

IntroductionSubacromial Impingement Syndrome (SIS) is the commonest disorder of the shoulder, accounting for 44%–65% of all complaints of shoulder pain [1]. Previous studies have found changes in scapular kinematics and muscle activation patterns [2,3]. To restore altered scapular kinematics and muscle activation in individuals with SIS, treatments for SIS commonly include scapula-focused exercises or/and taping. Recently, a newly developed biomechanical taping technique, dynamic tape, has been used in clinical practice to provide load absorption, force contribution and modify movement. However, only few studies have investigated the effect of dynamic tape in individuals with musculoskeletal injuries and no research has investigated the effect of dynamic tape in combination with exercises, in individuals with SIS. The purpose of this study was to investigate the immediate effects of dynamic taping in combination with scapula-focused exercise, compared to exercise alone on scapular kinematic and muscle activity in individuals with subacromial impingement syndrome. METHODSThis was a randomized control trial. We plan to recruit 30 individuals with SIS and randomly assign them into either an exercise group (Control group) or a dynamic taping with exercise group (Taping group). Both groups received one 30-minute treatment protocol of scapula-focused exercise. The taping group performed exercise with dynamic taping, which was applied to increase scapular upward rotation, posterior tilt and external rotation (Figure1). Outcome measures were collected at baseline and right after the treatment protocol. Outcome measures included scapular kinematics and scapular muscle activation (upper trapezius, lower trapezius and serratus anterior) during arm elevation with an electromagnetic device (ViperTM, Polhemus, Colchester, VT, USA) and surface electromyography (myoMotionTM, Noraxon, Scottdale, Ariz , USA). Scapular kinematics and muscle activation were calculated at 30° 60° 90° and 120° of the humerothoracic elevation. Changes from baseline to post-treatment were calculated to compare between groups. ResultsThis is an ongoing study. Ten individuals have been recruited (four individuals (4M/0F) in the taping group with average age of 28y, height of 1.8m, and weight of 79kg and six (5M/1F) in the control group individuals with average age of 29y, height of 1.7m,

and weight of 75kg). The individuals in the taping group demonstrated significant increases in scapular external rotation at all elevation angles (p = 0.01 – 0.02), compared to control group (Figure 2).DiscussionCompared to those receiving only scapular motor control exercise, subjects having scapular motor control exercise with dynamic taping demonstrated increased scapular external rotation. These findings suggest that scapular exercise protocols for patients with SIS could include dynamic tape to improve scapular kinematics.References1. Bhattacharyya, Rahul et al. “Does arthroscopic sub- acromial decompression really work for sub-acromial impingement syndrome: a cohort study.” BMC musculoskeletal disorders vol. 15 324. 29, 20142. Ludewig, Paula M, and Jonathan P Braman. “Shoulder impingement: biomechanical considerations in rehabilitation.” Manual therapy vol. 16,1, 20113. Phadke, V et al. “Scapular and rotator cuff muscle activity during arm elevation: A review of normal function and alterations with shoulder impingement.” Revista brasileira de fisioterapia vol. 13,1, 2009

P3.26-I: What is optimally updated in split-belt treadmill adaptation?

Yuki Ishida, Tokyo University of Agriculture and Technology; Ken Takiyama, Tokyo University of Agriculture and Technology; Hikaru Yokoyama, Tokyo University of Agriculture and Technology; Naotsugu Kaneko, University of Tokyo; Tatsuya Kato, Sony Computer Science Laboratories Inc; Keiichi Ishikawa, The University of Tokyo; Kimitaka Nakazawa, The University of Tokyo

The human motion involves redundancy, where movements to achieve a goal are not uniquely determined. In particular, it is unclear how to modify the redundant motion features in minimizing objective functions, e.g., movement error. A possible solution is to decompose motion features into task-relevant and task-irrelevant features and modify only the task-relevant features.However, there are few frameworks to evaluate how we modify redundant motion features when objective function is not evident. Split-belt treadmill adaptation is an example where objective function is not yet clearly defined. Although several studies assumed the asymmetry of step length as a modified motion feature (Vasudevan+, 2010, Jnp), recent studies reported a contradictory result against the assumption (Sanchez+, 2021, Jnp).Here, we propose a novel objective function in split-belt adaptation based on optimality of learning direction in redundant motion features. We assume that asymmetries of some kind of step parameters can be candidates of objective functions in split-belt adaptation. Under this assumption, the equilibrium state is “x_fast–x_slow=const”. The optimal learning direction, in the two-dimensional plane consisting of “x_fast“ and “x_slow”, is a vector “v” parallel to “v=(-1,1)”. By utilizing goal-equivalent manifold, we quantified variability along with the direction of “v”, optimality-relevant dimension, and that along with the orthogonal vector of “v”, optimality-irrelevant dimension. If some motion features are modified in an optimal manner, the variability in optimality-relevant dimension is larger than the variability in optimality-irrelevant dimension.In adaptation, assuming the objective function to be the minimization of step length asymmetry did not lead to optimal learning directions. Conversely, assuming the objective function to be the minimization of step velocity asymmetry resulted in learning towards the optimal direction. Within the framework of minimization of step velocity asymmetry, we can explain the change of sign in step length asymmetry in some cases.Furthermore, upon investigating the adaptive muscle activity, it became evident that muscles such as peroneus longus and medial gastrocnemius exhibited adaptive patterns in the fast leg. This is associated

with the acceleration component of the Ground Reaction Force (GRF), indicating acceleration of gait due to left ankle plantarflexion. Conversely, in the slow leg, muscles like rectus femoris and vastus lateralis depicted adaptive patterns. This is linked to the deceleration component of GRF, signifying deceleration of gait due to right knee extension. These muscle activity components are implicated in the correction of walking speed asymmetry between both sides, suggesting a potential role in resolving asymmetry in step velocity.

P3.27-I: Impact of perturbation type on muscle activation: insights from medial gastrocnemius responses to split-belt treadmill perturbations

Jayne Garland, Western University; Joshua Cohen, Durham College; Dominique Arsenault, Western University; Tanya Ivanova, Western University

High Density surface Electromyography (HDs-EMG) has allowed the investigation of regionally-specific muscle activation during functional tasks. This study examined the impact of standing balance perturbation type on spatial muscle activity in the right medial gastrocnemius (MG). Eleven participants (22±3 yrs; 5 female, 6 male) experienced three perturbation types whilst standing on a split-belt treadmill: unilateral (left belt) and bilateral (both belts) backward translations and unilateral (left belt) forward translations. Each translation was 300 ms in duration and delivered at the maximal perturbation intensity without needing to take a step. HDs-EMG, using a 64-channel grid with 8 mm interelectrode distance, was employed to record spatial muscle activity within the MG of the right (stance) leg. Spatial activity analysis utilized the barycenter of the HDs-EMG, characterized as the weighted mean of maximal average rectified values across columns and rows, and assessed the medio-lateral and proximo-distal shifts in MG muscle activity. Perturbation type exerted a discernible influence on the barycenter location. Specifically, unilateral forward translations elicited a proximal shift (F=7.87, p<0.0001), while unilateral (F=6.91, p<0.0001) and bilateral backward translations (F=2.72, p= 0.008) resulted in a distal shift of the MG barycenter. Additionally, a medial shift of the barycenter was observed (F=1.91, p<0.04) in the unilateral forward translations. Analysis further revealed an association between perturbation type and muscle burst amplitude, with unilateral (F=5.33, p<0.001) and bilateral (F=8.54, p<0.001) backward translations eliciting larger HDs-EMG bursts compared to unilateral forward translations. There was no statistically significant difference in barycenter location or burst amplitude between the unilateral and bilateral backward translation perturbation types. Collectively, these findings revealed that the stance leg experiencing maximal standing perturbations activated different regions of medial gastrocnemius muscle, highlighting unique adaptive strategies contingent upon the direction of the perturbation.

P3.28-K: Proximo-distal modulation of biceps femoris long head motor units during knee flexion and hip extension isometric tasks

Liliam De Oliveira, Federal University of Rio de Janeiro; Helio Cabral, Università degli Studi di Brescia; José Albarello, UNIVERSIDADE FEDERAL DO RIO DE JANEIRO

BACKGROUND AND AIM: Regionalized neuromuscular responses have consistently been reported for the rectus femoris and gastrocnemius [1,2], suggesting task-dependent activation in biarticular muscles. However, evidence regarding the biceps femoris long head (BFlh) is controversial, showing both homogeneous [3] and non-uniform patterns [4] when comparing knee flexion and hip extension movements. These discrepancies may be attributed to methodological issues in surface electromyography (EMG), especially amplitude cancellation [5]. To overcome these issues, in this study we decomposed high-density surface EMGs from the BFlh muscle to investigate whether the discharge rate of motor units located in distinct proximo-distal regions could be modulated differently during knee flexion and hip extension tasks. Methods: Seventeen healthy men performed isometric knee flexions and hip extensions with trapezoidal ramp feedback set at 20% and 40% of maximal voluntary isometric contraction (MVC). Tasks were performed with the knee and hip in a neutral position. High-density surface EMGs (2 grids of 32 channels) were acquired from the proximal and distal regions of the BFlh. EMGs were decomposed into motor unit spike trains using a convolutive blind-source separation algorithm [6], and the mean discharge rate (MDR) was calculated during the plateau (30s), separately for each region. Linear mixed models (LMM) were applied to compare the effect of the two contractions intensities and the two BFlh regions on the MDR. Bonferroni's post-hoc test was used for paired comparisons. RESULTS: For both tasks, a significant main effect was observed (LMM; F > 6.021; P < 0.001 for both). In the knee flexion task, pairwise comparisons revealed a significant increase in MDR between 20% and 40% MVC in the distal region, but not in the proximal region (panel A). In the hip extension task, significant increases in MDR across contraction intensities were found for both proximal and distal regions (panel B). Conversely, for both tasks, no differences were observed in the MDR between proximal and distal regions, regardless of the contraction intensity. CONCLUSIONS: Our results revealed that proximal and distal regions of the BFlh exhibit a similar motor unit discharge rate pattern, regardless of the joint involved in the task. Moreover, this homogeneous pattern remained unchanged across different contraction intensities. These findings suggest that the motor units located in different proximo-distal regions of the BFlh are modulated similarly during isolated knee flexion or hip extension isometric tasks.REFERENCES: [1] Miyamoto et al. 2012; PLoS ONE 7(3)[2] Cohen et al. 2020; Experimental Brain Research, 238(1)[3] Watanabe et al. 2016; Journal of Applied Biomechanics, 32(1)[4] Hegyi et al. 2019; Scandinavian Journal of Medicine and Science in Sports, 29(1) [5] Keenan et al. 2005; Journal of Applied Physiology, 98(1)[6] Negro et al. 2016; Journal of neural engineering, 13(2)

P3.29-K: Underlying Changes in Motor Units Properties in Presence of Epidural Spinal Cord Stimulation in Individuals Affected by Spinal Muscular Atrophy

Luigi Borda, Carnegie Mellon University

Spinal Muscular Atrophy (SMA) is the most common genetic disease of the spinal motor neurons (MN) and the most common cause of death in infants [1]. The disease causes motor neurons death and consequently muscle atrophy and motor impairment [2] as well as pulmonary and gastrointestinal complications [1]. Lefebvre et al. [3] identified the homozygous deletion of the SMN1 gene as the cause of SMA already in 1995, however, as of today, there are no effective disease-modifying treatments for SMA [1]. Moreover, Fletcher et al. [4],

hypothesized that the effects of SMA on motor neurons may progressively expand to proprioceptive synaptic inputs, intensifying disease progression. Specifically, they have shown how the blockade of proprioceptive synaptic drive led to decreased MN firing rate and consequently motor behavior impairments.Here we hypothesized that epidural Spinal Cord Stimulation (SCS) could increase the MNs firing rate resulting in greater muscle strength and potentially reverse maladaptive changes in the spinal motor neurons. Over the past 20+ years, SCS has been applied to treat motor recovery after SCI, Stroke and Parkinson disease revealing striking motor improvements both at the lower and upper limb level. SCS preferentially recruit large diameter sensory afferents in the dorsal column and dorsal roots which in turn deliver synchronous volleys of excitatory inputs to α-motor neurons innervating the muscles. We hypothesized that the increased synaptic input mediated by SCS would increase the firing rate of MNs during active movements.In this study, two 8-contact SCS leads were implanted percutaneously in the dorsal epidural space of the lumbar spinal cord targeting bilateral lower extremity muscles in three participants affected by SMA. Participants kept the SCS leads implanted for 29 days to test immediate and long-term effects of SCS. To assess changes in the motor units' properties, we recorded HDsEMG signals from both knee extensor (i.e., rectus femoris) and flexor (i.e., hamstring) muscles. Participants were asked to perform two sets of three Maximum Voluntary Contractions (MVC) of knee extension and flexion in isometric condition using Humac Norm Isokinetic Machine. One 8x8 channel flexible HDsEMG grid was placed over the Rectus Femoris and Bicep Femoris muscles and signals were acquired using the TMSi SAGA 64 high density amplifier. HDsEMG recordings were then decomposed using the convolution kernel compensation (CKC) method.The MN spiking data show immediate increases in the firing rate in presence of SCS targeting lower limb muscles. Similarly, long-term effects on MNs population reveal increased firing rate after 4 weeks of testing with respect to the pre-implant even in absence of SCS. These results therefore support the hypothesis that SCS can compensate for MNs deficits such as decreased firing rate in people affected by SMA, potentially reversing maladaptive changes in spinal motor neurons. [1] Arnold, W. David, "Spinal muscular atrophy: diagnosis and management in a new therapeutic era." Muscle & nerve 51.2 (2015)[2] Montes, Jacqueline, et al. "Clinical outcome measures in spinal muscular atrophy." Journal of child neurology . Cell(1995)[3] Lefebvre, Suzie, et al. "Identification and characterization of a spinal muscular atrophy-determining gene." [4] Fletcher, Emily V., et al. "Reduced sensory synaptic excitation impairs motor neuron function via Kv2. 1 in spinal muscular atrophy." Nature neuroscience 20.7 (2017)

P3.30-K: The influence of maturation on muscle strength, muscle size, and motor unit firing rate in soccer players.

Masamichi Okudaira, Iwate University; Ryosuke Takeda, CU; Taichi Nishikawa, Chukyo university; Tetsuya Hirono, Kyoto University; Shun Kunugi, Aichi Institute of Technology; Yukiko Mita, Sugiyama Jogakuen University; Kohei Watanabe, Chukyo University

[Introduction and Purpose] It is believed that rapid muscle hypertrophy occurs during puberty with the increase in sex hormone secretion, while the development of the neural system is accelerated before puberty. However, the changes in muscle size and neural function associated with the development of muscle strength before and after pubescent are still

unclear. Based on the peak height velocity (PHV), a key reference marker of maturation, this study aimed to clarify the developmental process of maximal strength, muscle size, and motor unit (MU) activity in children aged from pre- to post-PHV. [Methods] Ninety-eight soccer players aged 6 to 18 years participated in this study. They performed maximal voluntary isometric contraction with knee extensor (MVC, Nm). Muscle thickness of the quadriceps muscles (MT, cm) was measured. High-density surface electromyography (HDsEMG) was collected from the vastus lateralis during a submaximal ramp-up contraction to 70 %MVC. All HDsEMG signals were decomposed into individual MU activity. MU firing rate (FR) was calculated during the plateau phase of the 70%MVC ramp-up contraction. Input-output gain (pps/%MVC) was calculated from the relationship between the change in FR (ΔFR) and the change in exerted force (Δ%MVC) from recruitment to the plateau phase. All MUs were categorized into two groups based on their recruitment threshold: low-threshold MU (LT MU, MUs recruited at <30%MVC) and high-threshold MU (HT MU, MUs recruited at 30%MVC to <60%MVC). Estimated PHV age was calculated from body height history with AUXAL software. Participants ranging from three years before PHV to three years after PHV were included for further analysis. They were classified into three maturity groups according to their maturity status: pre-PHV (-3 years to > -1 years from PHV), circa-PHV (-1 to +1 years from PHV), and post-PHV (>1 to +3 years from PHV), respectively (n=18, 15, 13).[Results and Discussion] Circa-PHV and post-PHV showed significantly greater MVC and MT than pre-PHV (p < 0.05), and no significant difference was observed between circa-PHV and post-PHV. No significant group differences were observed in MU FR and input-output gain both in LT MU and HT MU. These findings suggested that developmental change in MU FR and the input-output gain were limited around PHV age. The gap in maximal strength between pre-PHV, circa-PHV, and post-PHV would be explained by the difference in muscle size.[Conclusion] Circa-PHV and post-PHV showed greater MVC and MT but not MU FR and input-output gain compared to pre-PHV. Maturation affects maximal strength and muscle size but does not neural function.

P3.31-K: A multi-site analysis of female motor unit discharge behavior across the menstrual cycle [Poster Award]

Sophie Jenz, Northwestern University; Padraig Spillane, Northumbria University, Newcastle, UK; Mollie O'hanlon, Nottingham Trent University; James Beauchamp, Carnegie Mellon University; Alex Benedetto, Northwestern University; Melissa Fajardo, Northwestern Unversity; Stuart Goodall, Northumbria University; Colin Franz, Northwestern University; CJ Heckman, Northwestern University; Kirsty M Hicks, Washington Spirit Soccer Club; Tom Inns, Nottingham Trent University; Tea Lulic-Kuryllo, University of Brescia, University of Brescia

Biological studies have historically excluded females, resulting in a strong understanding of the neural control of movement in males, but a poor understanding in females. Furthermore, studies across the female menstrual cycle are often underpowered. There is a great need to study female motor physiology because many aspects of neurological disease and human performance differ between the sexes. Sex-related differences in neuromuscular fatigue and motor unit discharge patterns have been observed in recent work, including variations across the female menstrual cycle, but the underlying mechanisms remain unknown. One possible mechanism is the magnitude of motoneuronal persistent inward currents (PICs), which are

facilitated by descending monoaminergic inputs. PICs modulate motor unit discharge patterns and estimates of their magnitude are greater in females. Endogenous levels of estradiol and progesterone fluctuate across the menstrual cycle in females not using hormonal contraception, and these hormones have known effects on monoaminergic signaling throughout the central nervous system. Therefore, fluctuations in female sex hormones are likely to influence PICs and, subsequently, motor unit discharge. The purpose of this collaborative, multi-site research effort is to explore the mechanisms behind sex-related differences in motor unit discharge by quantifying discharge properties across the female menstrual cycle.At four different universities, motor unit discharge properties and hormone levels were examined across the menstrual cycle. At each session, venous blood samples were taken, and high-density surface electromyograms were sampled from the tibialis anterior during isometric dorsiflexion contractions. Plasma levels of estradiol and progesterone were subsequently quantified, and blind source separation algorithms were used to identify motor unit spike times. PIC magnitudes were estimated using the paired motor unit analysis technique, which quantifies discharge rate hysteresis (ΔF) by obtaining the discharge rate of a lower-threshold motor unit (reporter unit) at the onset and offset of a higher-threshold motor unit (test unit).Preliminary data revealed during the late follicular phase, when estradiol levels were elevated, estimates of PIC magnitude were lower (4.36 ± 0.60 pps) compared to the early follicular (5.15 ± 0.59 pps) and mid luteal (5.21 ± 0.60 pps; $\chi 2 = 6.19$, $p = 0.045$) phases. These findings suggest that fluctuating sex hormones have a substantial impact on motor unit discharge behavior, and that elevated estradiol levels might either reduce descending monoaminergic drive to motor units, alter patterns of inhibition, and/or have direct effects on intrinsic motoneuron excitability. These novel findings underscore the necessity of studies focusing on female participants both to ensure a comprehensive understanding of motor physiology and to strive towards scientific equity.

P3.32-K: Effects of vibrotactile stimulation on motor unit recruitment and firing behavior

Pedro L. G. Nogueira, Federal University of Pernambuco; Carina Germer, Universidade Estadual de Campinas

BACKGROUND AND AIM: The effect of cutaneous afferents on motor unit recruitment remains inconclusive, with some evidence of inhibitory and excitatory effects on low and high threshold motor units, respectively. However, previous studies primarily utilized electrical stimulation, therefore bypassing the skin's mechanoreceptors. This study aims at evaluating the effect of vibrotactile stimulation on motor unit recruitment and firing behavior during low-force contractions. Methods: Eleven healthy young adults (7 men) participated in a trapezoidal force task involving the dominant first dorsal interosseus muscle. The task consisted of a 2.5-s ramp-up, a 5-s plateau sustained at 10 % of the maximal voluntary contraction (MVC) and a 2.5-s ramp-down. Participants executed three repetitions without cutaneous stimulation (CTR) and three with vibrotactile stimulation (VIB) in a randomized order. Vibrotactile stimuli, delivered by a linear resonant actuator (1.5 G) at a center frequency of 175 Hz, targeted the Paccini cutaneous receptors on the radial surface of the first metacarpophalangeal joint. In the VIB tasks, the stimulus was delivered 2 seconds before force onset and persisted throughout the trial. High-density surface electromyography recorded muscle activity, and a decomposition

algorithm extracted motor unit (MU) spike trains. MUs were tracked for all VIB and CTR trials, and the recruitment threshold (RecTh), discharge rates at recruitment (RecDR), plateau (PlateauDR), and derecruitment (DerecDR), and discharge rate variability (PlateauDRCoV) were compared. Statistical analysis included dependent t-test for parametric distributions and Wilcoxon signed-rank tests for non-parametric distributions. Linear regression assessed the potential differential effects of VIB based on MU RecTh (during CTR). RESULTS: Vibrotactile stimulation significantly reduced RecTh ($Z = -3.447$, $p = 0.001$), particularly affecting the later recruited MUs (Fig. 1A). The linear regression between RecTh at VIB and CTR revealed a slope smaller than one (slope = 0.827, confidence interval [0.733, 0.922], p < 0.001). VIB also increased PlateauDR ($t(81) = -2.47$, $p = 0.016$), with a slightly stronger effect on the later recruited MUs (Fig. 1B). Linear regression between RecTh at CTR and the difference between PlateauDR at CTR and VIB demonstrated a slope smaller than zero (slope = -0.188, [-0.318, -0.058], $p = 0.005$). However, no statistically significant differences were observed between CTR and VIB for RecDR ($Z = -0.423$, $p = 0.672$), DerecDR ($Z = -0.996$, $p = 0.319$) and PlateauDRCoV ($Z = -1.167$, $p = 0.243$). CONCLUSIONS: Vibrotactile stimulation increased the excitability of motor units with recruitment thresholds up to 10% MVC, exhibiting a more pronounced effect on the later recruited units.

P3.34-K: The Neuromuscular Functions in Stroke Patients Were Changing Depending on the Post-Onset Phases

Mio Ito, Graduate School of Health, Medicine, and Welfare, Saitama Prefectural University, Saitama, Japan; Takanori Kokubun, Department of Physical Therapy, School of Health and Social Services, Saitama Prefectural University

Stroke impaired voluntary motor function in patients. Paralysis post-stroke is a complex neuro-muscular condition because patients have primary neurological impairment and secondary disused dependent dysfunction. The aim of this study was to clarify the neuromuscular features, such as motor unit (MU) recruitment patterns in stroke patients at different phases.Eight subacute stroke patients and eight chronic stroke patients were recruited. We attached wireless surface EMG (Trigno Galileo; 2,222Hz) sensors on each biceps brachii muscle on the affected side and the less affected side to record muscle activity. Subjects performed a maximum voluntary contraction (MVC) followed by a force control task. The acquired muscle activity was decomposed into motor unit action potential (MUAP). From the obtained MUAP spike trains, the timing at each MU started firing (First firing timing) was detected. The quartile range and median of the First firing timing for all MUs recruited were then calculated and used as the Recruitment range and Recruitment threshold, respectively. We performed a two-way ANOVA on the phases factor and test side factor for MVC Force, Recruitment range, and Recruitment threshold. We also performed an unpaired t-test on the clinical score of the affected side in each group.MVC Force was a significant difference in the test side factor (p < 0.00), while there were no significant differences in the phases factor ($p = 0.05$). There was no significant difference in the recruitment range in the test side factor ($p = 0.59$) while there was a significant difference in the phases factor ($p = 0.03$). The recruitment threshold showed no significant difference in the test side factor ($p = 0.99$) while there was a significant difference in the phases factor ($p = 0.02$). The clinical score of the subacute stroke group showed no

significant difference between the groups (p = 0.29).There were no significant differences in clinical scores and no significant difference in the phases factor in MVC Force. This indicates that the subacute stroke group and chronic stroke group had similar levels of paralysis. Nevertheless, neuromuscular functions such as the recruitment range and the recruitment threshold had a significant difference chronologically. Thus, the neuromuscular functions in stroke patients change depending on the phases. We should not only evaluate post-stroke paralysis with existing clinical scores but also investigate the neuromuscular functions of each phase in detail.

P3.35-K: Selection of Optimal Multidimensional Feature Sets for Tracking Motor Unit Action Potentials

Jérémy Liegey, UCD; Lara Mcmanus, Trinity College Dublin; Madeleine Lowery, University College Dublin

Surface EMG decomposition enables the non-invasive detection of a relatively large number of concurrently active motor units. Reliably track the activity of the same motor unit across different trials, however, can be challenging when compared with traditional intramuscular recordings. The most commonly used methods of tracking motor units recorded using high-density arrays are based on the two-dimensional cross-correlation (Martinez-Valdes et al., 2017). Cross-correlation based methods, however, are highly sensitive to changes in motor unit action potential (MUAP) shape, which can occur with fatigue or MUAP superposition. An alternative approach proposed utilizes multidimensional representation of MUAP trajectories to characterize the waveform representation across multiple channels . Features extracted from the MUAP trajectories can be clustered, enabling MUAPs corresponding to the same motor unit to be identified and those with different spatial representations, originating from different motor units, to be distinguished. A number of different features are available to characterize the multidimensional motor unit trajectories , however, it is not clear which subset of features is optimal for representing the unique features of each motor unit, or whether this varies with muscle type. To address this, in this study we systematically examine the efficacy of different features in quantifying the similarity between pairs of MUAP trajectories using simulated and experimentally obtained MUAPs from the first dorsal interosseous muscle. The robustness of the feature set to perturbations in waveform shape, typical of those that can occur experimentally, was examined by distorting MUAPs waveforms through alterations in MUAP amplitude, the introduction of noise, and changes in muscle fiber conduction velocity. A total of 11 features were identified and tested. To measure the robustness of the features, the accuracy, sensitivity, specificity and clustering metrics including the Dunn index were used. Every possible combination of features was computed and given a score based on the metrics, the set of features that performed best among all the tested data sets was deemed to be the most robust for tracking MUAPs from the same motor unit. The original set of features was thus reduced to 4 final features: the standard Euclidian distance, the minimum projected distance and the Procrustes distance between trajectories as well as the instantaneous angle between velocity vectors. In conclusion, novel tracking methods using multi-dimensional representations of MUAP trajectories were used and the most robust features to consistently track motor units across trials were identified. Future work will investigate the optimal features

in other muscles with different muscle fiber architecture and surrounding tissue properties to investigate the sensitivity of the optimal feature set to factors such as spatial filtering, fiber pinnation and muscle size.

P3.37-L: Characteristics of muscle synergy in upper limb for reaching movement to different body locations

Hiroshi Kurumadani, Hiroshima University; Shota Date, Hiroshima University; Toshiyuki Fukushima, Hiroshima University; Toru Sunagawa, Hiroshima University

Introduction: The upper limb muscles have intermuscular coordination during upper limb movements. It has been reported that intermuscular coordination is also exhibited during reaching movements and can be represented by a small number of muscle synergies. The muscle synergies are shared between subjects or between movements, and a shared muscle synergy may be the basis of intermuscular coordination. The shared muscle synergy during reaching movements has not been widely examined; thus, its characteristics still need clarification. This study examined the characteristics of muscle synergy during reaching movements to a body segment, focusing on shared muscle synergy. Methods: Muscle activities of upper limb muscles were measured while seven healthy adults performed reaching movements to the body location (head, lower back, contralateral shoulder, and ipsilateral ankle joint) with their dominant hand. Surface electromyographic signals were recorded from 17 muscles (4 shoulder girdle muscles, six shoulder joint muscles, three elbow/forearm muscles, and four wrist muscles). Root mean square waveforms were calculated from the electromyographic signals and were extracted during reaching movement as the muscle activity waveforms. Global muscle synergies were extracted from the non-negative matrix factorization for the muscle activity waveforms of all subjects during all movements, and task-specific muscle synergies were extracted from the non-negative matrix factorization for the muscle activity waveforms of all subjects during each reaching movement. For examining shared muscle synergies, muscle synergies were classified based on the cosine similarity between global and task-specific synergies. RESULTS: Six global muscle synergies were extracted, which consisted of the coordinated pattern between the shoulder girdle and shoulder joint muscles and between the shoulder joint muscles and between shoulder girdle muscles. The coordinated pattern between the shoulder girdle and shoulder joint muscles was shared in all reaching movements. The shoulder girdle muscle pattern was similar in the three locations of reaching movement. The coordinated pattern between shoulder joint muscles was similar in the two locations of reaching movement. CONCLUSIONS: The coordination pattern between the shoulder girdle and shoulder joint muscles results in motor coordination between the scapula and humerus, which may provide the basis of body part reach. In addition, the coordination pattern between shoulder joint muscles, depending on the direction of reaching movement, is considered an activity specific to the direction of reach. These results suggest that upper limb muscles during reaching movements may be controlled by both intermuscular coordination underlying reaching movements and direction-specific intermuscular coordination.

P3.38-L: Variations of lower limb muscle synergies during single leg squat depending on dynamic knee valgus.

Kaho Yamamoto, Hiroshima university; Yoshitaka Iwamoto, Hiroshima University Hospital; Masanosuke Mizutani, Hiroshima university; Hikaru Yokoyama, Tokyo University of Agriculture and Technology; Yosuke Ishii, Hiroshima university; Makoto Takahashi, Hiroshima University

Background and Aim: Dynamic knee valgus (DKV) is a dynamic alignment that can be assessed through movements such as single leg squat (SLS). The ideal movement pattern is one in which the knee is not displaced medially, and a larger valgus is a risk factor for musculoskeletal disease of lower limb. Characteristics of people with larger DKV include larger trunk tilt and smaller dorsiflexion angle of the ankle joint. In addition, it has been reported that muscles such as the gluteus muscles and quadriceps are less active than in people with good dynamic alignment. However, coordinated muscle activity is still unclear. Therefore, this study focused on the relationship between kinematic differences that can be observed from outside the body and the coordination of muscle activity created inside the body. The purpose of this study was to investigate whether specificity is expressed in muscle synergy during single leg squat depending on the amount of DKV. METHODSTwenty-four healthy young adults (12 males, 12 females, age: 21.8 ± 0.7 years) participated in this study. The task was SLS with 60° of knee flexion at a comfortable speed on the dominant leg. DKV was calculated using frontal plane projection angle (FPPA) and subjects were divided into two groups (Large group and Small group) according to the median of the FPPA value. Muscle synergies were extracted from surface electromyography data of 12 dominant lower limb muscles using non-negative matrix factorization. The extracted muscle synergies were classified using the k-mean method based on synergy vectors to ensure that all data fell into one of the clusters. Statistical analysis for the FPPA and synergy number was performed by applying the Shapiro-Wilk test, followed by the t-test or Mann-Whitney U test. The significance level was set at 0.05. ResultsThe median of the FPPA was 8.26°, used as a grouping criterion. The mean values for each group were Large group: 15.9 ± 4.6° and the Small group: 4.5 ± 2.3° (p < 0.05). There were no significant differences in the number of muscle synergies between groups. Considering the average number, three muscle synergies were extracted from each subject and clustered using the k-mean method and divided into five groups. Each subject displayed distinct combinations, with the most frequent combination was Synergy1, 2, and 4. (Large group: 8/12 subjects, Small group: 5/12 subjects). CONCLUSIONSThe percentage of subjects showing the most combinations differed between the groups. While similarity existed within the Large group, the Small group showcased diverse muscle synergy combinations. This implies that kinematic characteristics influence extracted muscle synergy patterns, even during the same task movement. It highlights the importance of flexibility in exercise performance rather than adhering rigidly to specific patterns for optimal outcomes.

P3.39-L: Functional coordination of multiple muscles depends on time-frequency characteristics of target tracking movements

Shota Hagio, Kyoto University

When riding bicycles, one must steer the handlebars along the road while occasionally making swift adjustments in response to unexpected obstacles or pedestrians. This process involves generating movements towards a goal across different frequencies over time. Previous research on target tracking tasks, where movements were produced to follow a continuously moving visual target, demonstrated that the movements were flexibly controlled based on changes in goals and environmental conditions, as observed through various frequencies in the time-frequency domain (Yang et al., 2021, eLife). However, it remains unclear how the activity of multiple muscles is coordinated to produce movements with diverse time-frequency characteristics. This study aimed to elucidate the control of muscle activity for generating movements with a variety of time-frequency characteristics.Participants performed a task where they exerted force on a fixed handle in front of them while seated, gripping the handle with one hand. The force exerted in the horizontal plane was measured by a force sensor embedded in the handle, and a cursor corresponding to the measured force was displayed in real-time on a monitor. Additionally, the monitor showed a tracking target, synthesized from 14 different sine waves, with frequencies ranging from 0.1 to 2.15Hz, varied amplitudes, and phase shifts. The participants aimed to align the cursor with the moving target as accurately as possible. The required force for tracking was set below 5% of the participant's maximum exerted force. The tracking task consisted of 48 trials, each lasting approximately 50 seconds. Surface electromyography (EMG) was recorded from 8 upper limb muscles. Coherence among activities of individual muscle pairs was initially calculated for 28 different combinations. Subsequently, non-negative matrix factorization was applied to these coherence functions to identify groups of muscles exhibiting shared time-frequency characteristics (Boonstra et al., 2015, Sci Rep).The study demonstrated several muscle control modules responsible for generating target-tracking movements across a broad range of time frequencies. The module activating distal arm muscles was associated with movements at relatively high time frequencies, whereas the module involving muscles closer to the trunk was linked to lower frequency movements. These results indicate that different muscle groups are recruited according to the frequency of movements. Furthermore, the other module was identified that involved muscle activity across a mixture of various frequency bands. These findings suggest the functional coordination of muscle activity to accommodate movements over a range of time frequencies. The modular control system, dependent on time-frequency, would allow for flexible adaptation and precise control over a diverse array of movements, from those requiring rapid adjustments to those demanding slower, more sustained changes.

P3.40-L: Mechanomyography of Biceps Brachii Using the Microphones Array

Pilkee Min, student

According to the evaluation of muscle function during static exercise using an accelerometer and microphone, the accelerometer was reported to be less likely to introduce motion artifacts than the microphone [1], and muscle function was also evaluated using an accelerometer and a microphone during dynamic exercise in the biceps brachii muscle, and the microphone was reported to be less likely to introduce motion artifacts than the accelerometer [2]. It was reported that motion artifacts were less likely to be introduced by the microphone than by the accelerometer [2].However, this was due to the fact that muscle function was evaluated using

Microphones Array at a single location on the muscle fiber,In this study, muscle function is evaluated in the biceps brachii muscle by Mechanomyography using an array of microphones to evaluate muscle function at different locations on the muscle fibers.Concentric and isometric contractions were performed on five healthy male subjects with three microphones attached over the right biceps brachii muscle at elbow joint angles ranging from 40° to 140°. Concentric contractions were performed at speeds of 10°/sec and 20°/sec, while isometric contractions were performed at 0°/sec. The contractile forces used were 20% and 40% of the maximum voluntary contraction (MVC) measured at 90° elbow angle during isometric contractions. The central frequency was used for analysis. The results showed that separate signals were obtained from the microphones at each position, so the Mechanomyography had different signals when the same muscle was applied in different positions.

P3.41-M: Deltoid muscle and cortical complexity: a task-based analysis

Giacomo Nardese, Queensland University of Technology; Yuyao Ma, The University of Queensland; Wolbert Van Den Hoorn, Queensland University of Technology; Patricio Pincheira, The University of Queensland; Graham Kerr, Queensland University of Technology; Paul Hodges, The University of Queensland

Introduction: How the M1 provides neural drive(ND) to specific motoneuron pools (MN) or if this is rigidly or flexibly wired depending on task constraints remains unclear. Classic M1 mapping methods enable the exploration of motor evoked potentials(MEP) with limited spatial resolution. High-density electromyography(HDsEMG) might gain extensive insights into muscle activity patterns and their organization over M1, especially in muscles with complex functions[e.g., deltoid muscle(DM)]. We hypothesized that certain M1 regions may steadily trigger MEPs irrespective of tasks, suggesting shared functions. Conversely, distinct areas might evoke task-specific responses, reflecting specialized roles of M1. Methods: Anterior(AD), Middle(MD) and Posterior(PD) DM regions were mapped with transcranial magnetic stimulation(TMS) in 4 right-handed healthy adults. They performed isometric shoulder abduction(ABD) in 90° at 5% of MVC. In separate trials, they were provided with feedback from each DM regions. Hotspot, Active and Resting motor threshold(aMT/rMT) for each region were identified. Three rounds x 42 stimuli were delivered over a 7x6cm grid at 120% aMT/rMT of the target portion. We generated a HDsEMG muscle map for each grid site. After normalisation to MVC, we explored 1)the difference between Rest and Active HDsEMG muscle maps(as % of sites with increased, decreased, and unchanged values in respect of the total sites) and 2)the differences between trials with feedback from each DM region(as % of the overlapped and non-overlapped area, in respect the total area). RESULTS: Initial analysis shows how HDsEMG MEP distribution is M1-sites and task-dependent(Figure 1). Collectively, in ~63% of the map, the MEPs amplitude rises during Active from Rest[AD: 61(21)%; MD: 65(22)%; PD: 64(25)%], in ~33% MEPs amplitude doesn't change [AD: 33(18)%; MD: 29(16)%; PD: 29(20)%] and in ~4% MEPs amplitude falls[AD: 3(5)%; MD: 4(6)%; PD: 5(5)%]. When compared across feedback, 67(18)% of the maps overlap between AD and MD, 76(11)% overlap between AD and PD and 67(20)% overlap between PD and MD. Discussions: Initial findings suggest that MEP in the Active state differ between M1 sites of TMS. Changes in MEP amplitude from Rest to Active states are uneven across the HDsEMG grid. Although the proportion of HDEMG grid sites with

amplitude changes is fairly consistent across the 3 feedback tasks, the distributions for AD, MD and PD don't fully overlap – some HDEMG grids sites are consistent between pairs of feedback tasks, but other change in a feedback-specific way. This suggests some independence of connections between M1 and MN for the 3 regions of the DM. Greater common responses between AD and PD suggest a greater common ND between the two, than MD. MD has the greatest mechanical advantage for pure ABD. The shared role of AD and PD to generate ABD, but with antagonistic functions (i.e., sagittal/transversal plane), might highlight coordinate action to prevent these motions.

P3.42-M: Neuromuscular Mechanisms during Squatting Movement by Electroencephalogram and Electromyogram Coherence Changes in Healthy Young People

Kana Mori, Juntendo University; Reona Arai, Juntendo University; Shinji Onuki, Juntendo University; Hitoshi Makabe, Juntendo University; Eizaburou Suzuki, Yamagata Prefectural University of Health Sciences; Kenichi Kaneko, Fuji University

Background and Aim: Squatting movements have been shown to improve balance function and prevent falls in older adults, but the neuromuscular mechanism still needs to be elucidated. Therefore, this study aimed to investigate the neuromuscular mechanisms during the squatting movement by examining Electroencephalogram and Electromyogram (EEG-EMG) coherence, and Electroencephalogram and Electroencephalogram (EEG-EEG) coherence changes. Methods: Thirty healthy young people (male15, female15, age: 21.9 ± 0.7) participated in this study. The squatting movement was performed from standing position to a squatting posture with hip and knee joints at 90 degrees for 5 seconds and then to a standing position for 5 seconds after holding the squatting posture for 5 seconds. The squatting movement was divided into four phases according to the contraction pattern of the quadriceps muscle: (1) static phase, (2) eccentric phase, (3) isometric phase, and (4) concentric phase. A wireless biometric device (MP208, Miyuki Giken) measured electroencephalogram (EEG) and electromyogram (EMG) at 1000 Hz sampling frequency during squatting. EEG activity was recorded through unipolar silver electrodes placed at Fp1, Cz, and P3 by the international 10-20 system. Ag/AgCl surface EMG electrodes (Kendal H124SG, 30mm×24mm, interelectrode distance between electrodes 2 cm) were placed in the vastus medialis of quadriceps femoris muscle (Quad) and medial head of gastrocnemius (Gas) of the right leg. The impedances of the EEG and EMG electrodes were kept below 10k Ohm. The Welch algorithm calculated EEG-EMG coherence (Fp1-Quad, Fp1-Gas, Cz-Quad, Cz-Gas, P3-Quad, P3-Gas) and EEG-EEG coherence (Fp1-Cz, Fp1-P3, Cz-P3) in beta (13-30Hz) bands (window width: 1024 points, overlap 512 points, resolution 1Hz). Differences in EEG-EMG coherence and EEG-EEG coherence in the four phases of the squat movement were examined using ANOVA. RESULTS: The EEG-EMG coherence between P3 and Quad in the beta band was significantly higher in the concentric phase than in the static phase. The EEG-EEG coherence between P3 and Cz was significantly higher than the coherence of EEG-EMG between P3 and Quad in all phases. Discussion: The brain-muscle network function was more facilitated in the concentric phase of squatting movement because the EEG-EMG coherence between P3 and Quad was significantly higher in the concentric phase. In addition to that, the network function between brain regions, especially between the frontal and parietal lobes, was promoted during the squatting movement. These

results suggest that squatting movement may promote the network function between the brain and muscle and between brain regions.

P3.43-M: Neuromuscular Mechanisms during Squatting Movement by Electroencephalogram and Electromyogram Coherence Changes in Healthy Young People

Kana Mori, Juntendo University; Reona Arai, Juntendo University; Shinji Onuki, Juntendo University; Hitoshi Makabe, Juntendo University; Eizaburou Suzuki, Yamagata Prefectural University of Health Sciences; Kenichi Kaneko, Fuji University

Background and Aim: Squatting movements have been shown to improve balance function and prevent falls in older adults, but the neuromuscular mechanism still needs to be elucidated. Therefore, this study aimed to investigate the neuromuscular mechanisms during the squatting movement by examining Electroencephalogram and Electromyogram (EEG-EMG) coherence, and Electroencephalogram and Electroencephalogram (EEG-EEG) coherence changes. Methods: Thirty healthy young people (male15, female15, age: 21.9 ± 0.7) participated in this study. The squatting movement was performed from standing position to a squatting posture with hip and knee joints at 90 degrees for 5 seconds and then to a standing position for 5 seconds after holding the squatting posture for 5 seconds. The squatting movement was divided into four phases according to the contraction pattern of the quadriceps muscle: (1) static phase, (2) eccentric phase, (3) isometric phase, and (4) concentric phase. A wireless biometric device (MP208, Miyuki Giken) measured electroencephalogram (EEG) and electromyogram (EMG) at 1000 Hz sampling frequency during squatting. EEG activity was recorded through unipolar silver electrodes placed at Fp1, Cz, and P3 by the international 10-20 system. Ag/AgCl surface EMG electrodes (Kendal H124SG, 30mm×24mm, interelectrode distance between electrodes 2 cm) were placed in the vastus medialis of quadriceps femoris muscle (Quad) and medial head of gastrocnemius (Gas) of the right leg. The impedances of the EEG and EMG electrodes were kept below 10k Ohm. The Welch algorithm calculated EEG-EMG coherence (Fp1-Quad, Fp1-Gas, Cz-Quad, Cz-Gas, P3-Quad, P3-Gas) and EEG-EEG coherence (Fp1-Cz, Fp1-P3, Cz-P3) in beta (13-30Hz) bands (window width: 1024 points, overlap 512 points, resolution 1Hz). Differences in EEG-EMG coherence and EEG-EEG coherence in the four phases of the squat movement were examined using ANOVA. RESULTS: The EEG-EMG coherence between P3 and Quad in the beta band was significantly higher in the concentric phase than in the static phase. The EEG-EEG coherence between P3 and Cz was significantly higher than the coherence of EEG-EMG between P3 and Quad in all phases. Discussion: The brain-muscle network function was more facilitated in the concentric phase of squatting movement because the EEG-EMG coherence between P3 and Quad was significantly higher in the concentric phase. In addition to that, the network function between brain regions, especially between the frontal and parietal lobes, was promoted during the squatting movement. These results suggest that squatting movement may promote the network function between the brain and muscle and between brain regions.

P3.44-M: Distinguishing the neural origins of the anticipatory postural adjustment

Cassandra Russell, University of Wollongong; Jonathan Shemmell, University of Wollongong

Background: Anticipatory Postural Adjustments (APAs) are crucial for postural stabilisation during voluntary perturbations[1]. The location of generation and execution of APAs in the brain is speculated to be cortical[1], however startreact (SR) studies using startling acoustic stimuli (SAS), a brainstem probe[2], released APAs at shorter latencies than voluntary APAs[3], suggesting the brainstem may release the APA. However, studies using Transcranial Magnetic Stimulation (TMS) and SAS simultaneously, and found the silent period induced by TMS delays SAS-induced movement onsets in a wrist extension task[4], suggesting cortical involvement. It remains unclear whether posturally-related APAs are dependent upon cortical or subcortical motor pathways.Objectives: We investigate APAs in the postural lower limb muscles, using SAS and TMS-induced cortical inhibition to assess the impact of cortical state on APA latency. Design: The onset of the APA from a stepping task was recorded with electromyography (EMG) from right tibialis anterior and soleus muscles. An auditory warning and Go cue initiated the APA. TMS was applied 200 ms prior to the Go cue and SAS were placed 30ms prior to, simultaneous with and 30ms after TMS firing, and alone. Results/Discussion: The average APA latency following a 'Go' cue was 90 ms in the tibialis anterior (TA) (N=3), and 126ms in the soleus, due to its initial inhibition in the APA. A SAS applied 200 ms prior to the Go cue, changed the onset latency to 50 ms (p<0.001, t-test). This was also significant in the soleus (p <0.001). In the TA activation was then significantly delayed (p= 0.002) when SAS and TMS stimuli were applied synchronously relative to SAS alone. TMS applied alone 200 ms prior to the Go cue increased TA latency by a further 40 ms, suggesting that APA expression can occur during cortical inhibition. In the soleus synchronous TMS+SAS resulted in a significantly shorter response than with SAS alone (p= 0.049), possibly due to the different role of the soleus in the APA, or the small sample. The APA delay then was significantly longer when TMS was applied at 200 ms prior to the Go cue alone (p= 0.040). CONCLUSION: : TMS contributes to delayed APA onset when paired with SAS akin to previous work[7], alluding to cortical control, but the brainstem cannot be ruled out due to the advancement of APA onset when TMS is paired with SAS vs alone.1.Gahéry, Y. and J. Massion,Co-ordination between posture and movement. Trends in Neurosciences,1981.4(C): p.199-2022.Brown, P, et al, New observations on the normal auditory startle reflex in man. Brain, 1991.114(4): p.1891-19023.MacKinnon,CD, et al,Preparation of anticipatory postural adjustments prior to stepping. Journal of Neurophysiology, 2007.97(6): p.4368-43794.Alibiglou,L. and CD.Mackinnon,The early release of planned movement by acoustic startle can be delayed by transcranial magnetic stimulation over the motor cortex. Journal of Physiology,2012.590(4): p.919-936

P3.46-M: Neuromuscular adaptations after isometric knee extension training performed at the knee flexed (muscle lengthened) versus at the optimal joint angle

Sumiaki Maeo, Ritsumeikan University; Hikaru Sakurai, Ritsumiekan University; Yuuri Eihara, Ritsumeikan University; Yuuto Kobayashi, Ritsumeikan University; Takashi Sugiyama, Ritsumeikan University; Jonathan P Folland, Loughborough University; Hiroaki Kanehisa, National Institute of Fitness and Sports in Kanoya; Tadao Isaka, Ritsumeikan University

Introduction: Growing evidence suggests that training at long muscle lengths produces greater hypertrophy than training at short muscle lengths. However, it is unknown whether this superiority holds true when compared to training at the optimal joint angle for maximum torque production. We therefore compared the effects of isometric knee extension training performed at the knee flexed (muscle lengthened) versus at the optimal joint angle on the changes in

quadriceps muscle size and strength. Methods: Nineteen healthy males performed isometric knee extension training in a seated position unilaterally with each leg (randomly allocated to the following conditions): one leg at the knee flexed angle (FLEX: 135° of knee flexion) where the knee extensors are at long muscle lengths, and the other leg at the individually assessed optimal knee joint angle for knee extension torque (OPT: 75 ± 7°). Both legs completed 5 sets of 10 repetitions (5-s isometric contraction and 5-s relaxation per rep) at the same relative torque (70% of maximum voluntary torque) during each training session, and 2 sessions/week for 12 weeks. Another 11 healthy males served as controls (CON). Isometric maximum knee extensor torque and electromyogram (TQ and EMG: at 20, 50, 65, 75, 85, 105, 135° of knee flexion) as well as MRI-derived muscle volume of the individual and whole quadriceps were assessed before and after the intervention for each leg in all participants. Additionally, hypoxic state (tissue oxygen saturation, StO2) of the quadriceps during exercise was measured at the first training session. Results: Throughout the intervention period, absolute torque output was always greater for the OPT than FLEX (+73% on average, P < 0.001) as expected. On the other hand, StO2 during exercise was lower for FLEX than OPT (45 ± 8% vs 53 ± 7% on average across muscles/sets, P < 0.001). There were significant increases in individual and whole quadriceps muscle volumes after FLEX (+13.6 – 17.1%, all P < 0.001), but no changes after OPT (+1.1 – 2.1%, P = 0.141 – 0.339) or CON (-0.4 – +0.4%, P = 0.622 – 0.981). Changes in TQ and EMG demonstrated joint-angle specificity in both training conditions (i.e. pronounced increases of TQ and EMG around the training angle, P ≤ 0.001), with no such changes found in CON (P = 0.058 – 0.956). CONCLUSIONS: Training at a long muscle length produced greater hypertrophy than training at the optimal joint angle. This suggests that muscle length (joint angle) rather than absolute torque output is a more influential factor, and even the necessary stimulus, for inducing quadriceps muscle hypertrophy during resistance exercise.

P3.47-N: Morphologic characteristics in femoral cartilage in collegiate athletes for 11 sports and non-athletic males: a cross-sectional study

Junhyeong Lim, Kyung Hee University; Seunghun Lee, Kyung Hee University; Seonggyu Jeon, Kyung Hee University; Jaewon Kim, Kyung Hee University; Jinwoo Lee, Kyung Hee University; Sanghyup Park, Kyung Hee University; Dongkyun Seo, Kyung Hee University; Jihong Park, Kyung Hee University

BACKGROUND: Long-term high-intensity exercises with insufficient recovery can lead to deterioration of the structural integrity in articular cartilage. Comparisons of the femoral cartilage morphology across athletes for various sports and non-athletic individuals would be an early detection and a surrogate assessment of knee joint and cartilage health. PURPOSE: To cross-sectionally compare the femoral cartilage cross-sectional area (CSA) in collegiate athletes for 11 sports and non-athletic males. Methods: A total of 589 males (34 Archery, 46 Badminton, 69 Baseball, 56 Basketball, 65 Judo, 54 SsiReum, 47 Taekwondo, 20 Tennis, 40 Track and Field, 48 Volleyball, and 66 Wrestling athletes, and 44 non-athletic individuals) volunteered. After a 20-min unloading period (seated with their knees fully extended), ultrasonographic images (frequency: 10 MHz, gain: 20 dB, frame rate: 30 fps, and depth: 3.0 cm) of the femoral cartilage on each side were obtained and manually segmented to calculate the CSA using ImageJ software. Femoral cartilage CSA values (mm2) were normalised by body mass index

(BMI; kg/m2). Age, sex, height, weight, BMI, career, knee injury and osteoarthritis score (KOOS), a history of knee injury (none, left, right, and both sides) and a history of knee surgery (history or non-history), and pain perception were collected via questionnaire. After performing a variable selection using Multivariate Regression, 'group', 'a history of injury', and 'a history of surgery' were selected as the independent variables. Therefore, two-way analysis of variance with Tukey tests as post-hoc comparisons (α = 0.05) were performed to assess group (group by side; 12 × 2), a history of injury (injury history by side; 4 × 2), and a history of surgery effects (surgical history by side; 2 × 2). Cohen's d effect size (ES) with 95% confidence intervals was calculated. RESULTS: There was no group by side interaction (F11,1177=0.50, p=0.91). There was a group effect (F11,1177=36.24, p<0.0001; Table 1) that Volleyball and Archery showed the largest and smallest femoral cartilage CSA (left: p<0.0001, ES=1.80; right: p<0.0001, ES=2.31). There was no injury history by side (F3,1177=0.20, p=0.90). There was an injury history effect (F3,1177=6.82, p<0.0001) that subjects who had a history of injury on both sides had a larger femoral cartilage CSA compared with subjects who had a history of injury on the left side (p=0.01, ES=0.29) and did not have an injury history (p=0.0002, ES=0.41). In addition, subjects who had a history of injury on the right side had a larger femoral cartilage CSA than the subjects who did not have experience of an injury (p=0.03, ES=0.23). There was no surgical history and side effect (F1,1177=0.07, p=0.93). CONCLUSIONS: Joint loading patterns from sports-specific movements and a history of lower-extremity injuries appear to be responsible for a long-term adaptation of the femoral cartilage morphology. Volleyball athletes showed the largest femoral cartilage CSA and Archery was the smallest. Subjects who had a history of injury to both sides had a larger femoral cartilage CSA than those who did not have an injury history.

P3.48-N: The effect of measurement conditions on thigh muscles' size in vivo

Hiroto Shiotani, Waseda University; Yusaku Nishino, Waseda University; Hoshizora Ichinose, Nihon University; Yasuo Kawakami, Waseda University

Background: Postural conditions during measurements of muscle size using magnetic resonance imaging (MRI) have not been well standardized across studies, and in the case of the thigh musculature there are studies employing supine or prone positions with the thigh compressed on an examination table, or suspended between the hip and knee secured high above the table. In each case, the thigh under compression or being sagged with gravity, can result in deformation of muscles which can change muscles' shape thereby affecting anatomical cross-sectional area (ACSA). Moreover, thigh compression can increase the external and intramuscular pressure in the thigh which may pump the existing water out of muscles and decrease muscle volume (MV). This study aimed to investigate the effect of postural conditions on muscle ACSA and MV. Methods: Twenty male participants (10 Olympic-style weightlifters and 10 untrained controls) underwent 3-T MRI scans in the supine and prone positions with the thigh compressed and suspended conditions, respectively, in a randomized and counterbalanced order. From the obtained axial images, the maximal ACSA (ACSAmax) and MV of 11 individual thigh muscles/muscle groups were assessed. As it was difficult to identify the boundaries between the adductor magnus, brevis, and longus, the sum of these muscles was assessed as the adductors. Four postural conditions were compared using a one-way repeated measures analysis of variance followed by multiple comparisons with a Bonferroni correction.

RESULTS: Upon the thigh compression, ACSAmax of vastus medialis (-3.3±1.6%, p < 0.001, d = 2.910) and vastus intermedius (-4.3±3.8%, p < 0.001, d = 1.307) and MV of semitendinosus (-2.9±1.9%, p < 0.001, d = 1.624) and semimembranosus (-3.7±2.9%, p < 0.001, d = 1.617) were significantly smaller in prone than in the supine position. In the supine position, ACSAmax of rectus femoris (-5.5±4.3%, p < 0.001, d = 1.337) and adductors (-4.3±2.9%, p < 0.001, d = 0.753) and MV of rectus femoris (-3.6±3.7%, p < 0.001, d = 0.889), vastus medialis (-2.5±2.9%, p < 0.001, d = 0.951), and adductors (-2.8±3.0%, p < 0.001, d = 0.991) were significantly smaller in compressed than in the suspended condition. CONCLUSION: : In this study, we found significant, inhomogeneous, and large-sized effects of the measurement positions (supine versus prone) and conditions (compressed versus suspended) on the thigh muscles' ACSAmax and MV. These results may reflect the effects of deformations due to muscle compression/suspension and fluid shifts due to changes in external and intramuscular pressure. Our findings suggest the need to standardize the postural conditions for thigh muscle MRI and to take into account differences in postural conditions when summarizing results between studies (e.g., examining muscle-specific hypertrophy/atrophy and intervention effects).

P3.49-P: Effects of an augmented neuromechanical rehabilitation program on an acute phase after Achilles tenorrhaphy.

Macarena Soldan, MEDS Clinic; Rony Silvestre, meds

Introduction: Achilles tendon rupture is one of the most common tendinous injuries of the lower extremity. To date, little is known about the effects of neuromechanical rehabilitation protocols that begin during the first week after surgery. This study aims to assess mechanical and electrophysiological variables before and after an augmented neuromechanical rehabilitation protocol during the acute phase of an Achilles tenorrhaphy. Methods: This study was approved by the ethics committee of Clínica MEDS. 5 participants who meet the eligibility criteria were selected for this study. All patients were assessed during the first week after surgery and a second evaluation was performed 5 weeks after surgery. Variables assessed were, medial gastrocnemius stiffness using a Myoton PRO device, plantar flexor steadiness (% CoV) on the injured leg was quantified at 10% of the maximal voluntary contraction (MVC) and 20% of the MVC on the non-injured leg using a feedback trace as previously described in the literature, Achilles tendon length was assessed through ultrasonography. The rehabilitation protocol included 2 to 3 days a week of training for 5 weeks, during which EMGs feedback of the gastrocnemius medialis activity was provided to patients, also through ultrasonography feedback of the Posterior Tibialis, Flexor Hallucis Longus and Flexor Digitorum Longus muscle contraction was provided. The Shapiro Wilk test was used to assess the data's normality, then the Mann–Whitney U test was used to compare medians. RESULTS: There were significant differences (p < 0.05) in the plantar flexor steadiness of the operated limb between the before-protocol (17.00% CoV) and after-protocol (13.40% CoV) periods. Also, there were significant differences (p < 0.05) in the Gastrocnemius Medialis EMG signal amplitude of the operated limb between the before-protocol (0.50 mV) and after-protocol (0.89 mV) periods. There weren´t significant differences in the other variables measured. Conclusion: Augmented Neuromechanical Rehabilitation programs during an acute phase after Achilles tenorrhaphy

have positive effects on plantar flexor steadiness and gastrocnemius medialis EMG amplitude of the operated limb. Steadiness improvement and an increase in EMG amplitude have been associated with better functional performance and an increase in intermuscle coordination respectively, providing evidence that miofeedback through EMG or ultrasonography feedback are promising tools to implement in rehabilitation programs.

P3.50-P: Design, development, and experimental validation of an Augmented Reality Biofeedback system providing information about muscle activation through HD-sEMG

Giacinto Luigi Cerone, Politecnico di Torino; Michail Arvanitidis, Centre of Precision Rehabilitation for Spinal Pain (CPR Spine), University of Birmingham, UK; Martina Sergi, Politecnico di Torino; Marco Gazzoni, Politecnico di Torino; Deborah Falla, University of Birmingham

BACKGROUND AND AIM. The use of electromyography-based biofeedback (BF) in sport and rehabilitation contexts has been widely investigated to improve voluntary muscle activation; BF has been demonstrated to have a remarkable potential in the treatment of a broad range of musculoskeletal conditions[1]. Augmented Reality (AR) allows to superimpose virtual contents over real-world scenes. Although AR has been proven to be effective in several biomedical applications[2], in rehabilitation settings it is mainly used to show virtual objects that patients have to interact with overlayed in the real world. The use of AR to provide biofeedback of electrophysiological signals is largely unexplored. This work aims to describe the design, development, and experimental validation of an AR-based BF framework for the monitoring of muscle activity from high-density surface electromyography (HD-sEMG). METHODS. Figure 1a shows the System Architecture. A wireless Body Sensor Network of HD-sEMG acquisition systems (Sensor Unit-SU) transmits EMG signals detected with one or more electrode grids to a PC or Mobile Device (Signal Processing Unit-SPU). The SPU calculates a muscle activation index for each grid (e.g. EMG RMS) and transmits this to one or more Feedback Units (FUs, e.g., tablet or Microsoft HoloLens). A monochromatic marker is attached over each electrode grid. The FUs recognize the markers and provide the augmented BF by coloring the electrode detection area according to the muscle activation level. The system was tested in an experimental study. Twenty-three healthy individuals and nine diagnosed with Patellofemoral Pain Syndrome were recruited. Both groups underwent two randomized measurement sessions performing isometric sub-maximal and fatiguing knee extensions with and without the AR BF. HD-sEMG signals were collected from Vastus Medialis (VM) and Lateralis (VL) muscles using two 8x4 electrodes grids (10mm inter-electrode distance). During the fatiguing contraction with the AR BF, the participants were required to modify their muscle activity, alternating the activation between VM and VL (Figure 1b). Endurance time, root mean square, and mean frequency normalized slopes were computed from the single-differential EMG signals and compared between the two conditions. Ongoing experiments on the symptomatic group are underway to increase the sample size. RESULTS AND CONCLUSIONS. The asymptomatic group exhibited a notably higher mean endurance time compared to the symptomatic group in both sessions, increasing when the AR BF was used. Further analyses on myoelectric manifestations of muscle fatigue and differences between the tested groups are in progress. The developed system was successfully tested in a rehabilitation scenario from a technological point of view. The demonstration of its

effectiveness and advantage with respect to standard BF requires further research.REFERENCES[1] O. M. Giggins et al., JNER, 2013.[2] D. J. Im et al., Ann. Rehabil. Med., 2015. This collaborative work is partly funded by a Royal Society International Exchange Award (ES\R3\223137).

P3.51-P: The immediate effects of Vibrotexture insoles on quiet standing balance and lower limb neuromuscular responses in healthy young adults

Megan Trotman, University of Queensland; Avni Hurkat, University of Queensland; Kylie Tucker, The University of Queensland; Thomas Cattagni, Nantes University; Anna Hatton, University of Queensland

Sensory-stimulating footwear devices are an emerging rehabilitation tool, which are designed to optimize balance control by providing enhanced sensory input to the plantar surface of the feet. Prior work has shown that insoles delivering a single source of sensory stimulus (vibration or texture) can improve clinical and laboratory measures of balance in young and old, healthy and disease populations. We propose that a hybrid insole design, delivering vibration and texture stimuli ('Vibrotexture') will offer greater benefits to balance control than insoles with a single stimulus. This study aimed to investigate the immediate effects of wearing Vibrotexture insoles (compared to vibrating, textured, and control [no stimulation] insoles) on standing balance and lower limb neuromuscular responses in healthy young adults. Thirteen participants (9 females; 26.1±7.1 years; 65.6±8.8kg; 166.3±7.9cm) stood on a force plate with standardised foot and body position. Participants performed tests of quiet standing balance over 30 seconds with eyes open and closed, on a firm and foam surface, whilst wearing each of the four insoles (2 trials/condition) within standard shoes. Balance measures were centre of pressure (COP) velocity and COP anteroposterior (AP) and mediolateral (ML) excursion. Amplitude of lower limb muscle activity was examined using surface electromyography at the medial gastrocnemius, soleus, peroneus longus (PL), rectus femoris, biceps femoris, and gluteus medius (dominant leg only). Data were analyzed using a two-way (surface and eye condition vs insole) repeated measures analysis of variance. Post-hoc tests were performed using pairwise comparisons with a Bonferroni adjustment.Analysis of COP velocity revealed main effects for insoles (p=0.01) and conditions (p<0.001). Pairwise comparisons showed greater COP velocity when wearing vibrating insoles compared to textured insoles (p=0.02). For COP AP excursion, there were main effects for insoles (p=0.01) and conditions (p<0.001). COP AP excursion was greater when wearing vibrating insoles versus Vibrotexture (p=0.01) and textured (p=0.02) insoles. For COP ML excursion, there were main effects for insoles (p=0.04) and conditions (p<0.001), with no post-hoc differences between insoles (p>0.09). Greater PL amplitude was observed when wearing Vibrotexture insoles compared to vibrating insoles (p=0.02). Wearing Vibrotexture insoles for the first time does not appear to have a superior benefit on standing balance, over and above vibrating or textured insoles. However, our results suggest Vibrotexture insoles may have the capacity to alter underlying neuromuscular responses, specifically the amplitude of lower limb muscle activity, for balance control. The effects of Vibrotexture insoles may become apparent during more challenging balance tasks or on other measures of neuromuscular control (e.g., timing of muscle activity) in healthy and patient groups; this requires further investigation.

P3.52-P: Relationship between fibula motion characteristics and knee joint during walking.

Akihiro Yamashita, The University of Electro-Communications

INTRODUCTIONDue to its position and structure in the body, the fibula has almost no role in compressive stress on the physiological axis and is said to be unrelated to load. It constitutes a joint with the tibia and displaces its position in the distal tibial joint for continuous adaptation of the distance between the inner and outer malleolus in the ankle joint. As mentioned above, the fibula does not have a load function, but the lower leg transmits the impact of ground reaction above the knee joint. Since the shock-absorbing role occurs throughout the lower limb when grounded, part of them may contain same function between the tibia and fibula. The position of the fibula relative to the tibia affects the knee joint and ankle joint, which I have strongly felt from my clinical experience, but its dynamics are still largely unknown. Therefore, in this study, by measuring the fibular dynamics during walking in relation to the tibia, we will elucidate a part of the fibula function by examining the movement of the fibula relative to the tibia during walking and examine whether intervention on the fibula is useful for knee joint treatment because of the influence of the fibula function on the joint movement for the knee joint. METHODSThe subjects were 16 healthy adult males aged 18 to 40 who had a history of lower limb surgery, orthopedic problems within the past one year, and no pain. The measurement operation was a stationary standing and walking, and the subject was instructed to step on the force platform on the fourth step on a 10 m walking way. The measurement instrument used a 3D motion capture system consisting of 12 MX cameras, and the measurement sampling frequency was 100 Hz. A total of 45 infrared reflective markers with a diameter of 14 mm were affixed to the subjects' bodies. Three segments were created using the Body Builder, the femur, the tibia and the fibula. The relative angles to others e were calculated. Correlation analysis was performed using the amount of angular change of the fibula with respect to the tibia and the amount of angular change of the tibia relative to the femur as output variables. Results AND DISCUSSIONThe fibula changed position relative to the tibia when walking. We also found that the phenomenon during the Lording Response correlated with the knee joint at the same time. Since the fibula movement is coincident the ankle sagittal behaviors, it is expected to be affected by the morphology of the pulley of talus. Previous studies have shown that when the peroneus brevis muscle was resected and then dorsiflexed from the neutral position with a load applied, the malleolus was displaced backwards. The movement of the fibula is thought to change its position due to joint structure and muscle contraction because the anterior displacement of the outer malleolus was observed in this experiment. CONCLUSIONSIt was predicted that the fibula moves independently of the tibia to absorb the impact applied to the knee joint by performing a combination of coronal, sagittal, and horizontal planes. These results suggest that the observation of peroneal dynamics can be used as an index to predict knee joint rotation during walking.

P3.53-P: Prosthesis Users Demonstrate Similar HD-EMG Spatial Parameters of the Upper Limb during Slow, Moderate and Fast Isokinetic Contractions Compared to Controls

Alexandria Irvine, University of New Brunswick; Madison Melvin, University of New Brunswick; Prashanth Jonna, International Institute of Information Technology Bangalore; Timothy Green, Andrew and Marjorie McCain Human Performance Laboratory, University of New Brunswick; Usha Kuruganti, University of New Brunswick

Introduction: Upper limb function is critical for efficient movement during activities of daily living (ADLs) and can be impacted by injury, disease and disuse. Surface electromyography (sEMG) has been used to examine upper limb musculature to aid in muscle assessment, in particular for upper limb prosthetics. High density sEMG (HDsEMG) uses two-dimensional electrode grids to estimate spatial muscle activity and can provide insight regarding muscle function during common upper limb tasks. Aim: The purpose of this study was to examine HDsEMG activity of the biceps and triceps during slow, moderate, and fast isokinetic flexion and extension contractions in those with intact upper limbs and upper limb prosthesis users. Spatial features of the HDsEMG were compared to determine the effect of speed on muscle activity. Methods: Thirty-one males (n=16) and females (n=15) (mean age= 24.33 +/- 10.43) completed three maximal isometric ramped elbow flexion and extension contractions followed by three isokinetic dynamometer (HUMAC Norm) elbow flexion and extension contractions at 60, 90 and 120 degrees/second. Two prosthesis users (1 male, 1 female) also completed the testing protocol. High density sEMG signals were collected (OT Bioeelettronica, Turin, Italy) with a 32-channel electrode grid placed over the short head of the biceps brachii and the lateral head of the triceps brachii (HD10MM0804). Spatial distribution was estimated using the Root Mean Square (RMS) EMG signals for each of the electrode grid locations from which 2D maps were developed (Figure 1). Amplitude and frequency features of the HDsEMG signal were compared across speeds for all contractions (flexion and extension) and each arm. Entropy was used to represent the increased variety of signals (heterogeneity) of the HDsEMG distribution. Significant differences were determined using an analysis of variance (ANOVA) with an alpha level set to 0.05 and post hoc tests (Tukey) conducted when p<0.05. RESULTS: No significant differences were detected in HDsEMG features in the control group due to speed. Both prosthesis users demonstrated lower amplitude and frequency features compared to the control group on their amputated side, however entropy was similar, regardless of arm side. In addition, prosthesis users did not show differences in HDsEMG features due to contraction speed. Both clinical patients demonstrated lower amplitude and frequency HDsEMG features in their affected limb compared to their intact limb, except for entropy, which remained similar regardless of limb side. CONCLUSIONS: In this limited work, upper limb prosthesis users demonstrated similar muscle activity compared to a control group during isokinetic upper limb contractions in their unaffected side. While prosthesis users demonstrated lower HDsEMG amplitude on their amputated side, entropy was similar between control and clinical participants regardless of speed or side suggesting that muscle activity differences may be due to training status of the clinical participants rather than muscle fibre type. Data collection is ongoing and more clinical participants are needed. This preliminary work demonstrates that when designing training and rehabilitation programs for prosthesis users, it is important to recognize that while reduced muscle mass (may result in lower HDsEMG amplitude, muscle heterogeneity (estimated with entropy) may be similar to controls.

P3.54-P: Relationship between finger dexterity and anterior horn cells of the spinal cord - Investigation by waveform analysis of F wave-

真理奈 東藤, Graduated School of Kansai University of Health Sciences; Yuki Fukumoto, Graduated School of Kansai University of Health Sciences; Toshiaki Suzuki, Graduate School of Kansai University of Health Sciences

F waves are used in many situations as an indicator of the excitability of spinal anterior horn cells. F waves from normal muscles are known to show a diversity of waveforms, but F waves from patients with spasticity result in the appearance of repeater F, which show the same waveforms. However, there are no standard values for waveform diversity, and no valid analysis method has yet been established. Analyzing the waveform of the F wave provides clues to the state of the spinal cord anterior horn cells that make up the F wave. It could also be used as an evaluation of spasticity and voluntary movement due to spasticity. In this study, as a preliminary study in applying waveform analysis of F wave in spastic patients, we would like to analyze waveforms from F waves during isometric contractions in healthy subjects because spastic muscles are almost in a hypertonic state and examine the relationship with motor skills. 〔Methods〕 F waves were recorded from the abductor pollicis brevis muscle during isometric contractions at 20% and 50% maximal voluntary contraction of the opposing movements of the thumb and the index finger in 20 healthy subjects. In the analysis section, coefficients of variation for three parameters; amplitude value, onset latency, and coefficient of variation of peak latency, were calculated to reflect the diversity of the F wave. In addition, Chronodispersion, which indicates the difference between the shortest and longest latencies, and ORF (occupancy rate of repeater F-waves), which indicates the ratio of repeater F to the number of waveforms that appeared using cluster analysis, were calculated. The fingertip dexterity evaluation was a task in which the participants had to demonstrate individually defined strength for 30 seconds in a sustained manner. The evaluation method was established 5% before and after the specified value, and the percentage of correct responses within the time was calculated. 〔Results〕 The coefficient of variation of peak latency showed a decrease in negative peak at 50% MVC compared to resting, and a decrease in positive peak at 20% and 50% MVC, respectively, compared to resting. The relationship between hand dexterity and F-wave diversity was examined with coefficients of variation for negative and positive peaks below 0.03 in more than half of the cases with less than 50% correct responses. ORF was 0 in 18/20 cases, regardless of contraction strength, and the appearance of repeater F wave was extremely small. 〔Discussion〕 In this study, we investigated the relationship between finger dexterity and spinal cord anterior horn cell excitability during isometric contraction. With isometric contraction, negative and positive peak latencies appear at a constant latency, but the ORF values are extremely close to zero. Therefore, even though similar waveforms appear, various anterior horn cells of the spinal cord fire and are thought to be involved in muscle output.

P3.55-P: The motor imagery content as a reflective report and the skill gains brought about by motor imagery may be consistent

Yuki Fukumoto, Graduated School of Kansai University of Health Sciences; 真理奈 東藤, Graduated School of Kansai University of Health Sciences; Toshiaki Suzuki, Graduate School of Kansai University of Health Sciences

[Introduction]Motor imagery is a cognitive process that utilizes working memory and is defined as the reproduction of motor-related memories. Motor imagery content is often interpreted using the results of the subject's introspective reporting. Therefore, we examined whether introspective reports on the motor imagery content were consistent with subsequent changes in motor performance due to motor imagery. In addition, we recorded F waves during motor imagery to confirm whether the degree of excitation of spinal motor neurons varied with the motor imagery content.[Methods]25 right-handed healthy participants were included (13 males and 12 females, mean age 23.8 ± 6.1 years). Fingertip dexterity was assessed with a pinch task using the thumb and index finger of the left hand to determine baseline performance (Pre-BP). The motor task was an alternating force adjustment task in which the participants adjusted the pinch force to 50% and 10% MVC at 2-s intervals, and the index of fingertip dexterity was calculated as the absolute error (kgf) from the specified value. First, changes in the excitability of spinal motoneurons were measured during 30 s of rest (Rest). Next, six sets of repetitions of combined motor practice and motor imagery were performed. The excitability of spinal motoneurons was also assessed during motor imagery. Fingertip dexterity was again assessed with a pinch task using the left thumb and index finger (Post-BP). After the experiment, the visual analog scale was used to evaluate whether the participants were more enthusiastic about 50% or 10% MVC as the motor imagery content. The visual analog scale was marked with 10% MVC at 0 mm and 50% MVC at 100 mm from the left end. Absolute errors were compared to the Pre and Post-BP periods. In addition, Cosine similarity refers to the cosine value of the angle between two vectors in vector space (total performance and 50% MVC performance / total performance and 10% MVC performance). Cosine similarity and Euclidean distance were calculated. And, the pattern of change in total performance over time was strongly influenced by changes in either 50% or 10% MVC performance. We performed multiple comparisons of the F/M amplitude ratio during 6 repetitive motor imagery for changes in spinal motoneuron excitability, using Rest as a control. This study was approved by the Research Ethics Committee at Kansai University of Health Sciences (Approval No. 22-04).[RESULTS]The absolute error decreased for Post-BP compared to Pre-BP. Changes over time in performance were influenced by changes in the ability to adjust to 50% MVC performance in both cosine similarity and Euclidean distance. The mean value of the visual analog scale was 60.7 mm, and there was a trend toward 50% MVC. The F/M amplitude ratio was no difference between each motor imagery session with Rest as a control[Discussion]When force-regulation tasks with different intensity are given, the force-regulation skills corresponding to the contraction intensity of the motor imagery content improve. However, no difference in the degree of increase in spinal motor neuron excitability appears regardless of the contraction intensity of the motor imagery content, and it is possible that the increase in spinal motor neuron excitability during motor imagery is not consistently observed.

P3.56-P: Effects of functional performance in professional athletes after ACL reconstruction on muscle fiber conduction velocity

Eduard Kurz, Martin-Luther-University Halle-Wittenberg; Stefan Pröger, Sports Clinic Halle, Center of Joint Surgery; Leonardo Gizzi, University of Stuttgart; Rene Schwesig, Martin-Luther-University Halle-Wittenberg; Karl-Stefan Delank, Martin-Luther-University Halle-Wittenberg; Thomas Bartels, Sports Clinic Halle, Center of Joint Surgery

Background: After rupture of the anterior cruciate ligament (ACL), surgical reconstruction is the main treatment option, particularly for professional athletes aiming to return to their pre-injury level of activity. Even after a successful return to sport, neuromuscular impairments may persist in athletes after ACL reconstruction. Because positive correlations were found between training status and muscle fiber conduction velocities (MFCV), we expected lower MFCV values in athletes who scored lower in functional performance tests. This study was designed to examine the link between overall lower extremity performance at the time of return to sport and the MFCV of vastus medialis (VM) and lateralis (VL) muscles at different contraction intensities. Methods: Twenty professional team-sport athletes (soccer: 16, handball: 3, ice hockey: 1; age: 18-35 years) were recruited 6-12 months after primary ACL reconstruction. Participants performed four isometric ramp contractions at 20%, 40%, 60% and 80% maximum voluntary torque (MVT). Activity of the VM and VL was recorded in monopolar mode using a linear electrode array concurrently with the isometric force. From the raw signals, MFCV was calculated. In addition to the MVT, participants executed the drop jump and the vertical alternating foot tapping test. Outcomes of both functional tests were converted into z-scores. The latter were summed-up, resulting in the overall performance score (PS), with higher values indicating better performance. According to the PS, athletes were equally divided into lower (LPS) and higher (HPS) performers. Possible subgroup effects were verified using mixed-design ANOVAs separately on each contraction intensity. Practical relevance was estimated calculating partial eta-squared (ES) with values 0.01, 0.06, 0.14 indicating small, moderate, or large effects, respectively. RESULTS: Independent from subgroup, on average, higher MFCV were found for the VM (20%: 5.0 (0.6), 40%: 5.6 (0.8), 60%: 6.0 (0.9), 80%: 6.2 (0.9) m/s) as compared with the VL (20%: 4.8 (0.7), 40%: 5.2 (0.8), 60%: 5.7 (0.9), 80%: 6.0 (0.8) m/s) muscle. The ANOVA results for the 20% MVT indicated no effect of subgroup (ES < 0.01), a moderate effect of muscle (ES = 0.07) and a moderate interaction effect (ES = 0.13). For the 40% MVT, no effect of subgroup (ES < 0.01), a large effect of muscle (ES = 0.20) and a large interaction effect (ES = 0.01) were found. For the higher contraction intensities, small effects of subgroup (60%: ES < 0.01, 80%: ES = 0.01), moderate effects of muscle (60%: ES = 0.08, 80%: ES = 0.04) and large interaction effects (60%: ES = 0.22, 80%: ES = 0.15) were found. CONCLUSION: : The MFCV increased with higher contraction intensities consistently for both muscles. The large interaction effects found consistently over higher contraction intensities indicate that LPS athletes compensate with higher MFCV of the VM, whereas in HPS athletes higher MFCV of the VL muscle can be expected.

P3.57-P: Operant conditioning of the H-reflex: can down-conditioning hyperactive H-reflexes help to improve motor functional recovery in people with chronic incomplete spinal cord injury?

Krista Fjeld, Medical University of South Carolina; Blair Dellenbach, Medical University of South Carolina; Alli Lewis, Medical University of South Carolina; Alan Phipps, Medical University of South Carolina; Aiko Thompson, Medical University of South Carolina

Through operant conditioning, modification of a behavior is brought about by the consequence of that behavior. In both animals and humans, operant down-conditioning of the H-reflex (a partial electrical analog of spinal stretch reflex) can decrease H-reflex size, which further

induces CNS multi-site plasticity beyond the plasticity in the targeted H-reflex pathway (Front Integr Neurosci 2014;8: 25). Thus, targeting beneficial plasticity to a specific spinal pathway (e.g., reducing the excitability of a hyperactive H-reflex pathway) may be used as a therapeutic tool. For example, in people with incomplete spinal cord injury (SCI) hyperexcitable excitatory spinal reflexes may be associated with function-limiting spasticity. Previously studies demonstrated that operant down-conditioning can decrease the soleus H-reflex size and can improve locomotion in people with chronic incomplete SCI (J Neurosci 2013;33: 2365-2375; J Physiol 2021;599: 2453-69). Our working hypothesis is that decreasing H-reflex size in spastic muscles not limited to the soleus is possible through operant down-conditioning, and that decreasing the H-reflex size can lead to motor function improvements in people with chronic incomplete SCI. Towards testing this hypothesis, we are currently applying H-reflex down-conditioning in the upper and lower extremity muscles of individuals with spasticity due to chronic incomplete spinal cord injury. Methods: The H-reflex down-conditioning protocol consist of 6 baseline sessions and 24 (in upper extremity) or 30 (in lower extremity) conditioning sessions (all at a pace of 3/week). In each baseline session, 225 control H-reflexes were elicited without any feedback on H-reflex size. In each conditioning session, 225 conditioned H-reflexes were elicited while the participant was asked to decrease H-reflex size and was given visual feedback as to whether the resulting H-reflex was smaller than a criterion value. Before and after H-reflex down-conditioning, EMG and kinematic measurements during dynamic motion, and functional assessments are performed. Results and Implications: In the lower extremity, we are currently conducting a clinical trial of the soleus H-reflex down-conditioning in individuals with chronic incomplete SCI, in order to capture the range and extent of sensorimotor function improvements associated with this approach (NCT05094362).In upper extremity, the first participant chronic C5 SCI has completed the flexor carpi radialis (FCR) H-reflex down-conditioning protocol. His FCR H-reflex decreased steadily over the course of 24 down-conditioning sessions, to the final reflex size (average of the last 3 conditioning sessions) of 30%. This offers the promising interpretation that H-reflex down-conditioning is not limited to the soleus muscle, and indeed has the potential to be effective in any muscle where an H-reflex can be elicited.

P3.58-P: Transcutaneous spinal cord stimulation phase-dependently modulates spinal reciprocal inhibition induced by pedaling in healthy individuals

Keita Takano, Juntendo University Graduate School of Medicine; Tomofumi Yamaguchi, Juntendo University; Kano Kikuma, Tokyo Bay Rehabilitation Hospital; Kohei Okuyama, Tokyo Bay Rehabilitation Hospital; Natsuki Katagiri, Juntendo University Graduate School of Medicine; Takatsugu Sato, Tokyo Bay Rehabilitation Hospital; Shigeo Tanabe, Fujita Health University; Kunitsugu Kondo, Tokyo Bay Rehabilitation Hospital; Toshiyuki Fujiwara, Juntendo University Graduate School of Medicine,

Reciprocal inhibition (RI) plays an essential role in the smooth movement. RI is often impaired in patients with stroke, and impaired RI contributes to abnormal muscle co-activation during locomotion. Pedaling is a rhythmic movement that can increase RI in healthy individuals but not in patients with severe stroke. Transcutaneous spinal cord stimulation (tSCS) stimulates spinal neural circuits by targeting afferent fibers. Pedaling with simultaneous tSCS may modulate the

plasticity of the spinal neural circuit, altering neural activity based on movement and muscle engagement. This study investigated the RI changes after pedaling combined with tSCS and determined the phase of pedaling in which tSCS should be applied for optimal RI modulation in healthy individuals. Twelve healthy men participated in Experiment 1, 11 of whom also participated in Experiment 2. In Experiment 1, the subjects underwent three interventions on different days: pedaling combined with tSCS in the early phase of lower extension (phase 1) of the pedaling cycle, pedaling combined with sham tSCS, and tSCS alone. In Experiment 2, the subjects performed pedaling combined with tSCS applied in the late phase of lower flexion (phase 4). The results were compared with those of phase 1. Active pedaling was performed at a comfortable speed for 7 minutes. The parameters of pedaling were set at a low level to accommodate patients with severe hemiplegia. For tSCS, a monophasic 100 Hz current (1 ms pulse width) was applied at the stimulation intensity of the motor thresholds of the trunk muscles for the activation of afferent fibers. The cathodal electrode was placed on the skin over the Th11–Th12 spinous processes and an anodal electrode was placed on the trunk above the umbilicus. At the assessment of RI, disynaptic reciprocal Ia inhibition from the tibialis anterior to the soleus muscle was assessed before and after the intervention. A two-way repeated measures analysis of variance of the factors of the interventions and time, and t-tests with Bonferroni adjustments for multiple comparisons were performed in Experiments 1 and 2. In the results, there was a significant interaction in Experiments 1 and 2. In Experiment 1, post hoc analyses revealed that pedaling combined with sham tSCS significantly increased RI after the intervention compared to before the intervention (P = 0.01), whereas pedaling combined with tSCS at phase 1 and tSCS alone did not significantly affect RI (P > 0.05). In Experiment 2, pedaling combined with tSCS at phase 4 significantly increased RI after the intervention compared to before the intervention (P = 0.02). And, there was a significant difference after the intervention between pedaling combined with tSCS at phases 4 and 1 (P < 0.01). The results demonstrate that tSCS modulates RI changes induced by pedaling in a stimulus phase-dependent manner in healthy individuals. Thus, pedaling combined with tSCS may modulate impaired RI in patients with severe stroke.

P3.59-P: Eccentric cycling is more time-efficient than functional rehabilitation in recovering post-intensive care syndrome patients after Covid-19

Luis Penailillo, Universidad Andres Bello; Maria Fernanda Miranda, Universidad Andres Bello

The recently experienced COVID pandemic left numerous patients with post-intensive care syndrome (PICS), which affected all aspects of the lives of the survivors. Eccentric training is a simple option, requiring less metabolic demand, and it could be ideal for these patients. Aim: to compare the effects of eight weeks of eccentric cycling rehabilitation versus a standard functional rehabilitation protocol on functional performance and quality of life of the patients. Methods: twenty survivors of the COVID infection (age= 50.8 ± 8.8 years old) who were recruited in critical units after hospitalization (14.5 ± 11.5 days). Both groups performed an eight-week control period. Participants were divided into a functional rehabilitation group (FUNCTIONAL) and an eccentric training group (arm and leg cycle ergometer; ECC). Both groups trained for a period of 8 weeks, then rested for two weeks and performed the control condition (no exercise) as a crossover design study. Body composition, functional performance, grip muscle strength,

functional post-covid scale (FPCS), and quality of life (Patient Health Questionnaire; PHQ) were measured before and after interventions. RESULTS: Muscle mass increased 1.2±3.4% and 0.1±2.5%, functional performance increased 20.4±8.1% and 16.2±10.7%, grip strength increased 35.4±28.0% and 28.0±19.4%, FPCS decreased 36.7±18.0% and 29.6±23.2%, and PHQ decreased 40.1±44.6% and 41.6±32.0% after ECC and FUNCTIONAL, respectively. No differences between FUNCTIONAL and ECC were observed in the main outcomes, while metabolic and psychological demand during training was lesser during ECC. Furthermore, training time per session was much lesser during ECC. Conclusion: Both interventions improve the functional performance of patients after hospitalization for COVID. ECC obtained improvements in functional performance at a lower cardiopulmonary demand, which may be desirable in patients with PICS.

P3.60-Q: The Effects of Intensive Rehabilitation Using an Ankle Assistance Robot on push-off Motion in Stroke Patients

Nozomi Maeda, Hiroshima University Graduate School of Biomedical and Health Sciences; Keita Higashi, Inoshima Medical Association Hospital; Ayaka Hanaki, Hiroshima University Graduate School of Biomedical and Health Sciences; Makoto Takahashi, Hiroshima University; Eiichiro Tanaka, Waseda University; Louis Yuge, Hiroshima University; Kei Nakagawa, Hiroshima University

Gait impairments, such as an insufficient ankle dorsiflexion angle during the swing phase and decreased push-off motion during the pre-swing phase, are often observed in stroke patients. These impairments have been reported to result in a reduction in propulsive force. In recent years, numerous robotic walking rehabilitation devices have been developed and researched. They can adjust assistance during the entire gait cycle, allowing detailed settings based on individual walking functions. This makes it possible to reproduce movement patterns as close to normal as possible in terms of temporal and spatial parameters, enabling repetitive practice. In particular, walking assistance robots specialized in ankle joint assistance have been reported to support improvements in foot clearance, push-off assistance, and heel contact during walking, aiming to enhance walking function. Therefore, this study aimed to investigate the long-term effects of using a robot specialized in ankle joint assistance on push-off motion in stroke patients. Ten stroke patients who agreed to participate and could walk under supervision participated in this study. They underwent 20 minutes of robot-assisted gait training in addition to their regular rehabilitation for two weeks. The robot used in this study was RE-Gait®, a close-fitting walking assistance device that electrically assists ankle dorsi-and planter-flexion. The settings were tailored to the participant's gait, including plantar flexion assistance during the pre-swing phase, dorsiflexion assistance during the swing phase, and dorsiflexion assistance during the stance phase to achieve smooth weight shifting. The gait performance was assessed by performing a 10-meter walking test at a comfortable speed on the first day and after two weeks. Participants wore Inertial Measurement Unit (ULTIUM EMG, NORAXON Inc.) at four locations: midpoints of the left and right PSIS, right heel, left heel, and the paralyzed side's toe. The foot pressure distribution was measured using a myo PRESSURE device (NORAXON Inc.). The outcomes were heel clearance, knee joint angle, gait speed and stride length. Heel clearance was calculated using a inertial Measurement Unit attached to the heel. Knee joint

angle was calculated using a markerless motion capture system. No significant differences were observed in gait speed and stride length. However, changes in the ankle and knee joints were found after two weeks of intervention, with a significant increase in heel clearance. From the above, it is suggested that continuous intervention with a robot specialized in ankle joint assistance may lead to improvement in push-off motion, resulting in increased propulsive force and potentially contributing to the improvement of gait.

P3.61-Q: Changes in Knee Kinematics after Exoskeleton-Type Wearable Robotics Training in Individuals with and Without Reconstruction of Anterior Cruciate Ligament: A Pilot Study

Chang Yu Hsin, 983057806; Chich-Haung Yang, Tzu Chi University; Mei-Hui He, Tzu Chi University; Kuan-Lin Liu, Department of Orthopedics, Hualien Tzu Chi Hospital

Background: The rupture of anterior cruciate ligaments commonly affects knee joints, impacting patients' daily life activities such as walking. A decrease in knee flexion is one of the problems after ACL Reconstruction (ACLR) during walking. Sit-to-stand is effective for measuring functional deficits in post-ACLR. Post-ACLR, patients display reduced specific angles and moments due to muscle weakness. Exoskeleton-type robot training alters motion ranges initially for nerve and muscle impairment. This intervention may reduce the risk of secondary ACL injuries. Aim: This study assessed the change in knee flexion angle after exoskeleton robotics training in individuals with and without ACL surgery in knee flexion during walking and sit-to-stand tasks. Method: Four participants were recruited for this experiment and separated into control without any lower-limb injury and ACLR groups (one male and one female in each group). The experiment used the OPENCAP program to record the data before and after the training sessions with the KEEOGO exoskeleton robot. The analysis focused on the peak knee flexion angle change before and post-intervention as a mean difference during walking and sitting-to-stand. Result: The results involved comparing peak knee flexion angles before and after KEEOGO exoskeleton robot training in control and ACLR groups. The control group showed a 1.63° increase in walking; the ACLR group demonstrated a 6.46° improvement. Similarly, in sitting-to-stand, the control group increased by 1.09°, while the ACLR group improved by 1.08°. Findings highlight the positive impact of KEEOGO training on knee joint mobility in both groups. Conclusion: KEEGO intervention immediately affects walking and sitting-to-stand (STS) tasks to improve the peak values of knee joint mobility.

P3.62-Q: Controlling detached robotic hand with synergistic torso muscles to induce finger neuromotor adaptation in individuals with and without stroke

Joshua Posen, Georgia Institute of Technology; Stephen Housley, Georgia Institute of Technology; Andrew Butler, University of Alabama at Birmingham; Minoru Shinohara, Georgia Institute of Technology

Damage to neuromotor pathways due to stroke alters neuromotor activity and impairs hand function. While most robotic rehabilitation systems provide mechanical force to the impaired limb peripherally, we have invented a detached robotic rehabilitation system that focuses on

the central nervous system without involving the impaired hand. To intervene the neuromotor system beyond standard mental practice, we have adopted the neuromechanical synergy of reaching and grasping to enable the active embodiment of a detached robotic hand. Our unique idea was to control the robotic hand by activating the corresponding torso muscles (external abdominal oblique and latissimus dorsi) for synergistic movements for reaching (trunk rotating inward and hand opening) and retrieving (hand closing and trunk rotating back), respectively. We aimed to clarify acute neuromotor adaptations during this intervention in eighteen healthy adults and to investigate the feasibility and trend in four post-stroke adults with mild impairment in their right hand. They were tested on their embodiment of the detached robot, right-hand motor function, and neuromotor excitability during various background tasks: visual motor imagery, torso muscle interaction with the developed robotic system with (RoboMI) and without motor imagery (RoboNoMI), observation of robotic hand movements, and resting. In healthy subjects, the embodiment score in RoboMI (5.09 ± 1.59) was higher compared with RoboNoMI (3.96 ± 1.80, p = 0.04) and observation (2.47 ± 1.99, p < 0.001). The score in RoboNoMI was higher compared with observation (p = 0.046). During the reaction time test with the biological finger, the reaction time was longer in all dual-task conditions compared with resting. Interestingly, the maximal rate of force development was greater for finger flexion in RoboNoMI for retrieving compared with resting (by 51%, p = 0.024). The maximal rate of force development was also greater for finger extension in RoboMI for reaching compared with resting (by 40%, p = 0.004) and motor imagery (by 36%, p = 0.046). Corticospinal excitability was not affected significantly by the background task. The increased maximal rate of force development without a change in corticospinal excitability suggests an improvement in premotor planning. In all four post-stroke adults, RoboMI was feasible with the embodiment score being 3.3-8.2 (Mean: 5.88), and RoboMI for retrieving showed a faster reaction time for finger flexion compared with motor imagery (by 67-366 ms, Mean: 144 ms) and a higher maximal rate of force development for finger flexion compared with motor imagery (by 57-114%, Mean: 73%) and resting (by 7-48%, Mean: 23%). RoboMI also showed a higher maximal voluntary contraction force compared with motor imagery in all four post-stroke subjects (by 27-361%, Mean: 121%). These findings and observations support the efficacy of the developed robotic system. Supported by NIH/NINDS (1R21NS118435-01A1).

P3.63-R: Muscular activity of upper limbs during rapid unique arm movement of pop dance in street dance

Hinari Nakashima, Ochanomizu University; Mayumi Kuno-Mizumura, Ochanomizu University

PurposeWhile previous studies of street dance have been conducted in hip-hop on injury and motion analysis (Olga Tjukov's, 2004, Sato, 2016), scientific studies focusing on Pop dance movements which is one of the street dances are still limited. In Pop dance, dancers perform unique movement called “hit” which the observer could perceive the hitting during this movement. The instruction by dance teachers is also likely provided without scientific knowledge. Therefore, the aim of this study was to clarify the muscular activity of the upper limb which is imitated this unique arm movement in Pop dance using surface electromyography in dance students with and without street dance experiences. Methods: Twenty-six healthy adult women participated in this study. They were divided into three groups: pop dancers(P)(n=9);

women with more than two years of pop dance experience; other dancers(D)(n=11); women with dance experience other than pop dance; and non-dancers(N) (n=6); group of women with no dance experience. The participants were asked to sit in front of the box and place their right arms on the box with the right shoulder joint flexed at 90 degrees. They were instructed to perform rapid arm pronation which is imitated unique arm movement in pop dance as soon as they saw the light signal. Surface electromyography was used to measure muscle activity of the triceps brachialis, biceps brachialis and brachioradial muscles. A data logger system (BioLog, S&ME, Japan) was used to record surface EMG signals. Six EMG electrodes were applied to the participant's right arm. The Data were sampled at 1,000 Hz, with high and low pass filters of 20 and 500 Hz. EMG data were full-wave rectified and root-mean-square smoothed. Maximum voluntary EMG force was the 3-second average of stable values, and movements mimicking the hit were normalized by dividing by this maximum voluntary EMG force Mean values of EMG activity across the three trials were assessed for each participant. The time from optical signal to the first 5%MVC detected was analyzed (T1), from the first 5%MVC to the maximum within the trial (T2), from the maximum within the trial to the last 5%MVC (T3), and from the first 5%MVC to the last 5%MVC as the. Total muscle contraction time (ToT). Co-contraction index was calculated by the equation from previous study (Falconer and Winter, 1985)Results and DiscussionA significant difference (p<0.05) was detected in T1 with 0.43±0.18(s) in group P and 0.14±0.05(s) in group D and in ToT was 0.44±0.18(s) in group P and 0.91±0.33(s) in group N in the brachialis triceps brachialis muscle. No significant differences in co-contraction index were observed. CONCLUSION: From the results of this study, it is suggested that the unique arm movement observed in experienced pop dancers would be performed with longer reaction time to the onset of muscle contraction and shorter duration of muscle contraction of the arms.

P3.65-R: Electromyographic activity and perceived exertion during the performance of a training protocol with internal focus direction in the bench press exercise.

Pedro Nascimento, Federal University of Minas Gerais; Marcel Lanza, University of Maryland Baltimore; Andre Gustavo Pereira Andrade, Federal University of Minas Gerais; Camila Caldeira, Federal University of Minas Gerais; Rodrigo Cesar Ribeiro Diniz, Federal University of Minas Gerais; Mauro Heleno Chagas, Federal University of Minas Gerais; Fernando Vitor Lima, Federal University of Minas Gerais

Background & Aim: Strategies that enhance neuromuscular adaptations through training are of interest to healthcare professionals. The use of verbal instruction aimed at directing the focus of attention to a muscle or muscle group during strength training may represent a strategy to increase neuromuscular responses. Thus, obtaining data on the impact of adopting a strategy to direct the focus of attention to a specific muscle (e.g., pectoralis major), with the intention of promoting a greater activation response in the muscle during the performance of an exercise (e.g., bench press), could show selective manipulation of muscle activation. The aim of this study was to analyze the electromyographic (EMG) activity of the pectoralis major (PM) and anterior deltoid (AD) muscles during the performance of the flat bench press exercise with (IF) or without (WIF) internal focus for the PM muscle. Methods: Thirteen strength-trained volunteers were subjected to three experimental sessions (48-hour interval). The first session consisted of familiarization with the one-repetition maximum (1RM) test, associated with the

anchoring of the local subjective perception of effort (PE) for the PM and AD muscles. The second session involved performing the 1RM test and the PE anchoring procedure. After 10 minutes, a maximum voluntary isometric contraction (MVIC) test was performed and EMG recorded for normalizing the EMG data. Subsequently, after 10 minutes, the IF training protocol was performed. Finally, the third session consisted of the MVIC procedure, followed by the execution of the WIF training protocol. The IF and WIF conditions were performed with the following protocol: 3 sets of 8 repetitions, 50% of 1RM, with a 90-second rest interval between sets, differentiated only by the inclusion or not of verbal instruction for the direction of focus of attention. A two-way repeated measures ANOVA test was used to compare the normalized EMG signal during the protocols. The analysis of local PE was performed with the Friedman test. The significance level was α < 0.05, and Bonferroni post hoc test was applied when necessary. RESULTS: No significant time x muscle interaction was found, indicating that there were no changes between the EMG activities of the PM and AD muscles between the IF and WIF conditions. However, a main effect of muscle was identified, demonstrating that the EMG activity of the PM was higher than that of the AD. We also identified no differences between the muscles for PE, or between the IF and WIF conditions. Conclusion: In conclusion verbal instruction aimed at directing the focus of attention to a specific muscle was not an effective strategy to increase the activation of the PM muscle during the performance of a strength training protocol. Also, the adoption of verbal instruction for focus direction did not increase the PE response associated with the PM muscle.

P3.66-R: Enhancing Speed Skating Performance: A Comprehensive Analysis of IMU-based Motion Phase Identification Reliability

Yosuke Tomita, Takasaki University of Health and Welfare; Tomoki Iizuka, Kurosawa Hospital; Koichi Irisawa, Department of Physical Therapy, Graduate School of Health Care, Takasaki University of Health and We

This research examines the reliability of Inertial Measurement Units (IMUs) for motion phase identification in long-track speed skating. Fifteen skaters of varying levels participated in 500m trials, where IMUs provided real-time data. The study focuses on the reliability of IMU-based event identification using Intraclass Correlation Coefficients (ICCs) and Bland-Altman analysis to assess systematic and chance errors. Results show high intra-rater reliability with ICC(11) values ranging from 0.86 to 0.99, and inter-rater reliability with ICC(21) values between 0.81 to 0.99. The percentage of Standard Error of Measurement (%SEM) varied from 1 to 5%, and the Minimal Detectable Change (%MDC95) ranged from 2 to 15%. These findings validate the high reliability of IMUs in event identification, offering a valuable tool for enhancing skating techniques and contributing to sports biomechanics. The study's insights into IMU application in sports contexts highlight their potential for broader adoption in various sports.

P3.67-R: Biomechanical analysis of wheelchair propulsion in a variety of disability and competition level of para athletics wheelchair racing

Mikito Hikosaka, Research Institute, National Rehabilitation Center for Persons with Disabilities; Nadaka Hakariya, The University of Tokyo; Noritaka Kawashima, Research Institute, National Rehabilitation Center for Persons with Disabilities

Highly trained para-athletes in wheelchair racing exhibit unique modalities and extraordinarily enhanced upper limb motor functions that far exceed the daily use of wheelchair propulsion (Vanlandewijck et al., 2001). Although a classification system based on an individual's residual function exists for the fairness of competition (World Para Athletics, 2023), purposive performance differs depending on their disability and/or competition levels. For example, athletes with spinal cord injury for wheelchair racing are categorized as T51-T54: T51 has paralysis in both upper arm and trunk, T52 has partial paralysis and limited trunk function, T53 has limited trunk function, and T54 has intact upper arm and trunk functions. Elucidating the principles behind racing wheelchair propulsion as fast as possible with limited function is not only scientifically significant in understanding motor control strategies but also crucial in promoting athletic competitiveness. Therefore, this study aimed to characterize racing wheelchair propulsion using comprehensive biomechanical measurements. Fourteen wheelchair racers with diverse disabilities and competition levels participated in this study. Participants performed 30 strokes of wheelchair propulsion at approximately 80% of their maximum effort. We recorded wheel torque/velocity and trajectories of body landmarks using a custom-developed wheelchair simulator and motion capture system. We analyzed spatiotemporal parameters including total torque during the push phase, angle at the timing of hand contact with the hand-rim (contact angle), release angle, and angle at the timing of maximum torque exertion. In addition, electromyography in the upper limb and trunk, including the paralyzed area, were recorded during wheelchair propulsion. We observed that the maximum torque angle was deeper in the elite level of athletes, and also in moderate level of disability. Moreover, a moderate correlation was found between scores corrected from personal best records for 100m/400m races for classifications and the maximum torque angle ($r = -0.530$, $p = 0.005$), indicating that competition level largely affects the wheelchair propulsion strategy. The backward shift in maximum torque exertion with disability/competitive level implies the potential importance of the racer's propulsive force generation and its tangential force transfer. Specifically focusing on the erector spinae muscle activity, higher cross-correlation coefficients (0.781 ± 0.090) and minimal lag (-0.032 ± 0.086 s) with wheel velocity were observed. The larger contribution of erector spinae muscle activity on wheelchair propulsion clearly suggests that involvement of trunk function affect to contribute the wheelchair racing performance. The above-mentioned comprehensive biomechanical analysis might suitably characterize the purposive performance of wheelchair racers in relation to disability/competition level.

P3.68-R: Diurnal variations of neuromuscular system and inter-individual differences

Kaito Igawa, Chukyo University; Tetsuya Hirono, Kyoto University; Taichi Nishikawa, Chukyo university; Ryosuke Takeda, CU; Kohei Watanabe, Chukyo University

Introduction: Diurnal variations in maximal muscle strength are reported (ex. Knaier et al. 2022), but not in some studies (ex. Raphael et al. 2019). Muscle strength is determined by central and peripheral components of the neuromuscular system, i.e., central nervous excitability and muscle contractile properties. These components might be influenced by

diurnal variations, independently, due to fluctuations in motoneuron pool excitations, core temperature and muscle temperature. Also, these fluctuations would have inter-individual differences due to chrono type. Understanding of diurnal variations and its inter-individual differences of central and peripheral components of the neuromuscular system would assist in establishing training strategy focusing on individual components of the neuromuscular system. This study aimed to investigate diurnal variations of the neuromuscular system and its individual difference. Methods: Ten healthy young men participated in the present study (age: 22.9±4.9years). At 10: 00 (morning),13: 30 (noon), 17: 00 (evening), and 20: 30 (night), the knee extensor maximal isometric voluntary contraction (MVC) torque, motor unit firing properties by high-density surface electromyography (HDsEMG) of vastus lateralis, electrically evoked twitch torque of knee extensor were measured. HDsEMG was recorded during 50%MVC ramp-up task. Individual motor unit was tracked among four times, and firing rate (FR) during 35-45%MVC was calculated. RESULTS: MVC and twitch torque did not reveal significance change for time of day ($p = 0.681$ and 0.135, respectively). FR revealed a main effect for time-of-day ($p < 0.001$), and FR in the evening and night was significantly greater than that in the morning ($p = 0.002$ and $p < 0.001$, respectively). Inter-individual difference which was assessed by coefficient variation (CV) in diurnal variations of the neuromuscular system did not reveal significance among MVC, FR, and twitch torque ($p = 0.085$). Inter-individual CV on each time of MVC were 15.2, 17.1, 13.0, and 15.4%, those of FR were 14.2, 15.8, 14.3, and 14.1%, those of twitch torque were 17.7, 23.4, 19.3, and 19.6% at morning, noon, evening, and night. Discussion: Motor unit firing rate had diurnal variations, while electrically evoked twitch torque was unchanged during a day. These results suggest that the effects/adaptations of exercises such as resistance training, would be influenced by a time of day for central components of neuromuscular system. While intra-individual differences in diurnal variations were not difference between motor unit firing rate and twitch force, greater inter-individual difference was found in twitch force at noon. Exercise training focusing on peripheral muscle components might give different outcomes to each individual when the exercise is performed at noon. (2856/3000 characters)

P3.69-R: The Relationship Between Ground Reaction Forces and Subjective Evaluations in Table Tennis Players' Forehand Drives: A Focus on Weight Transfer

Koichiro Miyazaki, Graduate School of Niigata University; Masaaki Oba, Niigata University; Kengo Wakui, Niigata University; Yuki Sato, National Institute of Technology, Oyama College; Yukihiko Ushiyama, Niigata University

Table tennis is characterized by its rapid rally tempo and diverse techniques, performed in a relatively small area compared to other sports. This makes it challenging for players to objectively assess their own movements during a rally. Table tennis players heavily rely on their subjective sensations during play, but these sensations do not always correspond to their objective movements. Studies investigating the relationship between athletes' subjective perceptions and objective data, such as grading studies comparing athletes' subjective evaluations of force output to objective measurement data, have demonstrated their usefulness in coaching. Therefore, investigating how table tennis players' actual movements correspond with their subjective evaluations is crucial for enhancing player performance and providing effective coaching. In top-level table tennis matches, forehand drives account for 36%

of all shots and are more frequently used by winning players, indicating their essential role in securing match victories. An important element in executing a powerful forehand drive is weight transfer. Instructional books and coaching practices often emphasize that for right-handed players, transferring weight from the right to the left foot significantly affects racket swing speed. From a kinetic chain perspective, the energy generated in the lower limbs is commonly transferred continuously to the racket, making lower limb weight transfer a critical component. Therefore, this study aimed to focus on the weight transfer during the forehand drive of table tennis players and examine the relationship between ground reaction force values and subjective evaluations. This research could provide insights for improving player performance and effective coaching. The participants were 20 university table tennis players. In the experiment, participants performed multiple forehand drives on a force plate to measure ground reaction force (GRF) during their trials. A motion capture system was used to measure movements and divide them into different phases, allowing for the calculation of GRF in each phase. The Visual Analogue Scale (VAS) was used for subjective evaluation of weight transfer. After completing their trials, participants used the VAS to rate, on a scale from 0 to 100, how much weight was on their pivot and stepping feet in each phase. To explore the relationship between GRF and VAS ratings, Pearson's correlation coefficient was calculated. Additionally, linear regression analysis was conducted with GRF as the independent variable and VAS ratings as the dependent variable to investigate how GRF influences VAS ratings.

P3.70-R: Development of a novel training tool for sitting balance in chair ski athletes

Nadaka Hakariya, The University of Tokyo; Mikito Hikosaka, Research Institute, National Rehabilitation Center for Persons with Disabilities; Noritaka Kawashima, Research Institute, National Rehabilitation Center for Persons with Disabilities

BACKGROUND AND AIM: Chair ski is a highly unique paralympic sports category and enjoyable activity for individuals with lower limb dysfunction. Under the sitting posture, player could ski even on the same course as healthy skiers. Specifically for the athlete level of skier, it is necessary to take trial-and-error actual on-snow practice to acquire chair balance and turning skills, but the total amount of practice is limited within ski season and it is not easy to take practice many times due to transportation issue. In my presentation, we introduce our attempts on the development of a novel training tool for sitting balance in elite athlete chair skiers with the comparison of beginner level of skiers. Methods: An elite Paralympic level and a beginner level of skier participated in this study. Both subjects were patients with chronic thoracic level of complete spinal cord injury. In order to realize a roll direction of whole chair tilting due to slope change in the real ski environment, their chair settled on a 65cm-diameter hemispherical balance board (BOSU® NexGen Pro, BOSU) with the placement based on pre-estimated the center of gravity (CoG) of whole body and chair skis. With the precise adjustment of chair and balance board setting, the roll angle was identical to the situation under gentle slope when sliding on snow while maintaining the regular sitting position. Under such a novel environment, the participants were asked to shift CoG toward left and right to simulate the turning motion, and then added forward and backward motion that imitate/simulate the “bending turn” skill. The center of pressure (CoP) was calculated by the data obtained from the ground reaction force (Kistler Inc.), and the absolute coordinate of the whole-body reference points was

captured by the three-dimensional motion measurement system (Mac3D system, Motion Analysis Inc.). Surface electromyography was also recorded from five key muscles (Upper Rectus Abdominis, Lower Rectus Abdominis, External Oblique, Upper Trapezius, and Rhomboid). RESULTS: In the stationary position of the elite skier, the ski angle was 14.4º, which was similar to that of the gentle slope. On the other hand, the beginner skiers' ski angle was 8.1º, which was smaller than that of the elite skiers. In addition, the amount of COP movement to the left and right during the execution of the bending turn was greater for the elite skier. CONCLUSIONS: It is noteworthy that both of participants told us that the balance adjustment on the developed tool is quite similar to that during real skiing on-snow. One of the advantages of imitating skiing performance would be the capability of precise measurement during chair balance skills. Our custom build tool enable us not only to evaluate differences between elite and beginner skiers but also to deeply focus on certain aspect of chair balance skills to achieve more high level of technique even during off-days and seasons.

P3.72-R: Effects of core muscle training in knee cartilage and sports performance of the soccer players

Hwai-Ting Lin, Kaohsiung Medical University; Yi-Jou Lin, Kaohsiung Medical University

Introduction: Soccer is one of the most popular games in the world, requiring high-intensity and long-term training. The risk of knee cartilage damage is extremely high, and injured cartilage has limited spontaneous healing ability due to age and other factors. In the past decade, the concept of core stability has been ubiquitous in various sports training. It is responsible for stabilizing the trunk and transferring the strength of the body's core area to the limbs during sports actions such as running, batting, or throwing movements to increase jumping, sprinting, and shooting ability, as well as asymmetric movements of the lower limbs. The purpose of this study was to investigate through routine training and 6-week core stabilization training intervention, whether the thickness of abdominal muscles and knee cartilage thickness of the female professional soccer players would be related to functional performance. Moreover, it further explores whether core training can improve articular cartilage thickness. It was hypothesized that specific core stabilization training can increase cartilage thickness and functional performance. Methods: Thirty-eight healthy female soccer players aged 18 to 40 were recruited and randomly divided into two groups. All subjects received routine training as usual. The experimental group required an additional six weeks of core training. All subjects underwent ultrasound knee scans before and after training. The thickness of articular cartilage (the cartilage of the medial femoral condyle, intercondyle, and lateral condyle) and the thickness of abdominal muscles (internal oblique, external oblique, transversus abdominis) are measured. Moreover, T-shaped agility, triple jump on one foot, and 10-meter sprint were tested. Paired T tests was used to test the differences of the testing parameters before and after training, and the significance level was set at p<0.05. RESULTS: Compared to the control group, the 10-meter sprint and triple jumps on both sides of the experimental group were increased compared with before intervention (P < 0.05), and the knee cartilage thickness at the right medial condyle, both lateral condyle, and both The lateral condylar spaces were all increased compared with those before intervention (P≤0.05). CONCLUSION: : Core stability training is associated with changes in the thickness of lower limb knee cartilage and improved

functional performance in female professional soccer players. This may imply that core training has the potential effect to reduce the risk of injury to lower limb cartilage and also has the ability to improve functional performance.

P3.73-S: Intelligent upper-limb exoskeleton using deep learning to predict human intention for sensory-feedback augmentation

Jin Woo Lee, Dongguk University

The age and stroke-associated decline in musculoskeletal strength degrades the ability to perform daily human tasks using the upper extremities. Although there are a few examples of exoskeletons, they need manual operations due to the absence of sensor feedback and no intention prediction of movements. Here, we introduce an intelligent upper-limb exoskeleton system that uses cloud-based deep learning to predict human intention for strength augmentation. The embedded soft wearable sensors provide sensory feedback by collecting real-time muscle signals, which are simultaneously computed to determine the user's intended movement. The cloud-based deep-learning predicts four upper-limb joint motions with an average accuracy of 96.2% at a 200-250 millisecond response rate, suggesting that the exoskeleroaafton operates just by human intention. In addition, an array of soft pneumatics assists the intended movements by providing 897 newton of force and 78.7 millimeter of displacement at maximum. Collectively, the intent-driven exoskeleton can augment human strength by 5.15 times on average compared to the unassisted exoskeleton.

P3.74-S: Changes in Upper Limb Usage 6 Months After Arthroscopic Rotator Cuff Repair and Its Relationship to Range of Motion, Muscle Strength, and Pain: A Study Using a Triaxial Accelerometer

Toshiyuki Fukushima, Hiroshima University; Hiroshi Kurumadani, Hiroshima University; Shota Date, Hiroshima University; Yoshihiro Nakamura, Chugoku Rosai Hospital; Toru Sunagawa, Hiroshima University

Introduction: Although arthroscopic rotator cuff repair (ARCR) has reported promising outcomes, changes in postoperative upper limb use in daily life and factors related to upper limb use remain unclear. Three-axis accelerometry enables an objective evaluation of upper limb usage in daily life. This study aims to examine changes in upper limb usage during daily life up to 6 months postoperatively and investigate their associations with range of motion, muscle strength, and pain. Methods: The study included 21 participants (mean age 68.7 ± 7.1 years) who underwent ARCR and rehabilitation between June 2022 and June 2023 and 12 healthy adults (mean age 64.8 ± 6.6 years) without a history of upper limb disorders. Participants who had difficulty wearing the accelerometer, had difficulty with continuous assessment up to 6 months postoperatively, and experienced retears postoperatively were excluded. Two three-axis accelerometers (wGT3X-BT, ActiGraph) were worn on both upper arms for three days, excluding bathing and sleep. From accelerometer data, upper limb usage was calculated as activity intensity, frequency, and symmetry. The activity intensity and frequency ratio were also calculated on the operated and non-operated sides. Clinical assessments included active

range of motion (AROM), muscle strength, and visual analog scale (VAS) for pain during movement and nighttime. AROM and muscle strength were calculated as the operative and nonoperative side ratio. Accelerometry and clinical assessments were performed preoperatively and at 2, 3, and 6 months postoperatively. The Kruskal-Wallis test was used to compare activity intensity ratio, frequency ratio, and symmetry between postoperative volume and healthy adults. Spearman's correlation coefficient was used to examine associations between accelerometer data and six-month clinical assessments. RESULTS: Activity intensity ratio and symmetry of ARCR patients showed significantly lower values than those of healthy adults at 2 and 3 months postoperatively and improved to comparable levels at six months. The frequency ratio of ARCR patients was significantly lower than those of healthy adults at two months and normalized at three months postoperatively. Regarding the correlation with clinical evaluation, flexion AROM showed significant positive correlations with intensity ratio, frequency ratio, and symmetry. In addition, external rotation AROM and flexion muscle strength showed significant positive correlations with frequency ratio and symmetry, while nighttime pain showed a significant negative correlation. Abduction AROM and muscle strength had significant positive correlations only for symmetry. Conclusion: The results of this study suggest that more time is needed to improve the activity intensity ratio and symmetry in upper limb usage in daily life after ARCR. Furthermore, it was considered that the flexion AROM was particularly relevant to the actual upper limb usage.

P3.75-S: An innovative magneto-inertial measurement units-based method for accurate upper limb and shoulder kinematics assessment

Arthur Fabre, Queensland University of Technology; Wolbert Van Den Hoorn, School of Biomedical Sciences, The University of Queensland, Australia; Peter Pivonka, Queensland University of Technology; Glen Lichtwark, Queensland University of Technology; Ashish Gupta, Queensland Unit for Advanced Shoulder Research, Queensland University of Technology, Australia; Kenneth Cutbush, Queensland University of Technology; Graham Kerr, Queensland University of Technology

Introduction: Clinical methods to estimate active range motion such as a universal goniometer or visual estimation lack reliability and are limited to thoracohumeral shoulder angle. Magneto-Inertial Measurement Units (MIMU) present a potential alternative as sensors are small, relatively easy to use, can track the glenohumeral joint and can be used in the clinic. However, extracting meaningful anatomically relevant angles from sensors that are placed on the skin is challenging. Some of the issues are related to sensor-to-segment alignment and ability to account for skin movement artefacts. Overall Aim: to develop an MIMU-based method to obtain clinically meaningful shoulder joint angles. The specific aims were to determine the accuracy of a new method that aligns the sensor orientations to the actual orientation of the underlying bone using bony landmarks (i.e., sensor-to-segment calibration procedure). Methods: 5 participants volunteered with normal shoulder function (age (mean (SD)) = 27 (2.4) years, height 1.64 (0.08) m, weight = 68.1 (15.5) kg, sex = 4M/1F). Shoulder movements were concurrently recorded using 3D motion capture (Vicon) based on International Society of Biomechanics recommendations and MIMUs (ImeasureU) to track the thorax, scapula and upper arm movements. The MIMUs were aligned to the underlying bony segment using a manual sensor-

to-segment alignment of the MIMUs. A calliper and scapula locator tools were used to point and estimate the orientation between palpable anatomical landmarks for the different segments. A gradient descent-based algorithm estimated MIMU orientation. Participants performed 3 repetitions of clinical range of motion assessments (e.g. thoracohumeral abduction, shoulder girdle elevation and depression, elbow flexion and extension) and functional movements (e.g. jogging, lifting a box). Differences between 3D motion capture and MIMUs were determined as the error quaternion which represents a rotation global space from one segment orientation to another as define by q_error = q_3dMoCap * conj(q_MIMUs). The rms error is expressed from each ZYX cardan sequence. RESULTS: Across all tasks and axes, the errors between 3D motion capture and MIMUs were 4.2° [3.9°, 4.6°], 3.4° [3.1°, 3.8°], 3.8° [3.4°, 4.1°] for the humerus, scapula and thorax, respectively. Discussion: Preliminary findings suggest that the proposed system exhibits acceptable levels of accuracy in capturing joint angles for all segments across both clinical and functional movements. These findings suggest that the proposed MIMU-based method has the potential to provide accurate objective measurements of shoulder kinematics, thereby overcoming some of the challenges associated with traditional assessment methods.

P3.76-S: Wearable capacitive tactile sensor based on porous dielectric composite of polyurethane and silver nanowire for physiological signal monitoring

Gen-Wen Hsieh, National Yang Ming Chiao Tung University; Chih-Yang Chien, National Yang Ming Chiao Tung University

Flexible tactile sensors that can convert physiological stimuli into electronic signals have garnered significant attention for their potential use in electronic skin, healthcare monitoring, and human–machine interaction. The implementation of wearable and biocompatible tactile sensing elements with sufficient response is particularly intriguing but still challenging. Recently, capacitive tactile sensors possessing elastomeric dielectric rubbers/polymers have been intensively studied owing to their simple geometry, superior flexibility, inexpensive material cost, and low power consumption. Though, the sensing ability of these elastomer based capacitive tactile sensors is restricted by their compressibility. These elastomers cannot produce enough deformation, upon a small amount of applied pressure. Additionally, after the removal of pressure, the time required for restoration to their initial status is excessively long due to the viscoelastic property of the unstructured films. Hence, finding an augmentative means by comprehensively combining two or more aspects is very much key for high performance capacitive tactile sensing. Here, we propose a wearable all-polyurethane capacitive tactile sensor that utilizes a salt crystal-templated porous elastomeric framework filling with one-dimensional silver nanowire as the composite dielectric material. The former, holding unique conducting and dielectric polarization properties, has received widespread attention for optoelectronic, sensing, and energy harvesting applications; the latter has recently been adopted as a biomimetic membrane for artificial skin because of its good dimensional stability, air permeability, bio-safe property, and low-cost processability. With the aids of these cubic air pores and conducting nanowires, the fabricated capacitive tactile sensor provides pronounced enhancement of both sensor compressibility and effective relative dielectric permittivity across a broad pressure regime (from a few Pa to tens of thousands of Pa). The fabricated silver nanowire–porous polyurethane sensor presents a sensitivity improvement of

up to 4–60 times as compared to a flat polyurethane device. An ultrasmall external stimulus as light as 3 mg, equivalent to an applied pressure of ∼0.3 Pa, can also be clearly recognized. Our all-polyurethane capacitive tactile sensor based on a porous dielectric framework hybrid with conducting nanowire displays the versatility required for use in various human activities, such as contactless airflow, finer bending, and spatial pressure distribution. Furthermore, the proposed sensor integrated with a data acquisition and Bluetooth transmission module can achieve wireless monitoring for radial arterial pulse, making it a promising candidate for artificial skin and healthcare electronics.